

Sheffield Hallam University

Effect of pomegranate extracts on apoptosis and cell cycle in haematological malignancies.

DAHLAWI, Haytham.

Available from the Sheffield Hallam University Research Archive (SHURA) at:

<https://shura.shu.ac.uk/19527/>

A Sheffield Hallam University thesis

This thesis is protected by copyright which belongs to the author.

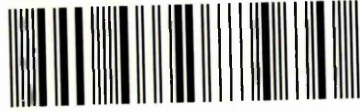
The content must not be changed in any way or sold commercially in any format or medium without the formal permission of the author.

When referring to this work, full bibliographic details including the author, title, awarding institution and date of the thesis must be given.

Please visit <https://shura.shu.ac.uk/19527/> and <http://shura.shu.ac.uk/information.html> for further details about copyright and re-use permissions.

Learning and Information Services
Adsets Centre, City Campus
Sheffield S1 1WD

102 019 792 7



Sheffield Hallam University
Learning and Information Services
Adsets Centre, City Campus
Sheffield S1 1WB

REFERENCE

ProQuest Number: 10694408

All rights reserved

INFORMATION TO ALL USERS

The quality of this reproduction is dependent upon the quality of the copy submitted.

In the unlikely event that the author did not send a complete manuscript and there are missing pages, these will be noted. Also, if material had to be removed, a note will indicate the deletion.



ProQuest 10694408

Published by ProQuest LLC (2017). Copyright of the Dissertation is held by the Author.

All rights reserved.

This work is protected against unauthorized copying under Title 17, United States Code
Microform Edition © ProQuest LLC.

ProQuest LLC.
789 East Eisenhower Parkway
P.O. Box 1346
Ann Arbor, MI 48106 – 1346

Effect of Pomegranate Extracts on
Apoptosis and Cell Cycle in
Haematological Malignancies

Haytham Dahlawi

A Thesis submitted in partial fulfilment of the requirements of Sheffield
Hallam University for the degree of Doctor of Philosophy

September 2013

Dedications

This thesis is lovingly dedicated to my wife, Rana, who supported me each step of the way of my research

To my parents

For their love, endless support and prayers, here's to the first Dr. in the family

To my brother,

Ismail

Whose words of encouragement and push for insistence ring in my ears especially this past year

To my lovely daughters,

Sarah and Lara

For being my inspiration

Acknowledgement

Foremost, I would like to express my honest gratitude to my supervisors Dr. Christine Le Maitre and Dr. Nikki Jordan-Mahy for the continuous support throughout my PhD study and research, for their patience, motivation, enthusiasm, and immense knowledge. Their guidance helped me in all the time of research and writing of this thesis.

My sincere thanks also go to all my colleagues and friends in the BMRC.

Abstract

Leukaemia is a complex form of blood malignancy characterized by the uncontrolled proliferation of haematopoietic cells and progressive accumulation of these cells within the bone marrow (BM) and secondary lymphoid tissues. The exact cause of leukaemia remains unknown. Leukaemia is a major problem worldwide affecting many people each year. However, current treatment options still have several limitations not least, the cytotoxicity of these therapies to normal cells and the fact that certain chemotherapy agents may cause bone marrow toxicity and organ damage.

Several epidemiological studies have shown that high intake of fruit and vegetables are associated with low incidence of a number of human cancers. Researchers suggest that pomegranates contain bioactive chemicals with potential for treatment and prevention of cancer. Pomegranate juice (PJ) have been shown to inhibit cellular proliferation and tumor growth and induce cell death via apoptosis in a number of cancer cell lines. However, to date, few studies have investigated the potential of PJ in the treatment of Leukaemia.

Here, PJ significantly induced apoptosis in 8 leukaemia cell lines and non tumour control cells although the lymphoid and 2 myeloid cell lines were affected to a greater extent than non-tumour control cells and 2 of the myeloid cell lines. Furthermore, PJ induced cell cycle arrest. These results provide evidence that PJ contain bioactive compounds that could be used in the treatment of Leukaemia.

Treatment of four Leukaemia cell lines with five fractions obtained from PJ by solid phase extraction demonstrated that only the acetonitrile fractions decreased adenosine triphosphate (ATP) levels in all Leukaemia cell lines. Acetonitrile fractions also significantly activated caspase-3 and induced nuclear morphology characteristic of apoptosis. S phase arrest was induced by acetonitrile fractions which matched S phase arrest seen previously following whole PJ treatments. The acetonitrile fractions contained higher phenol content than whole PJ whereas only low levels of phenols were seen in any other fraction. Liquid chromatography mass spectrometry (LC-MS)

analysis demonstrated that acetonitrile fractions were enriched in ellagitannins, ellagic acid, and hydroxycinnamic acid derivatives but depleted in anthocyanins.

The potential protective effect of a number of pure compounds that were either identified in the acetonitrile fraction of PJ were present in the other fractions of PJ or have been identified as PJ components in previous studies were studied on ATP levels in four human leukaemia cell lines. Among the 26 naturally occurring pomegranate compounds investigated, only seven compounds: delphinidin; cyanidin; pelargonidin; EGCG; gallic acid; ellagic acid; quercetin; and punicalagin induced 50% decrease in ATP levels in the studied leukaemia cell lines.

To compare the chemoprotective properties of anthocyanins found in PJ and to understand the relationship between anthocyanin chemical structure and chemoprotective activity, the inhibition of cell proliferation and induction of apoptosis in leukaemia cell lines was measured. Anthocyanins activity was found to be dependent on the ortho-hydroxyphenyl structure and the most potent glycosidic form of the anthocyanins with proliferation and apoptosis effects seen in anthocyanins with greatest hydroxyl groups and least glycosidic form, namely delphinidin. Delphinidin induced apoptosis through intrinsic and extrinsic pathways. Suggesting that delphinidin may have potential for use as a chemotherapeutic agent against leukaemia. Furthermore, EGCG, gallic acid, quercetin, and punicalagin induced apoptosis and resulted in cell cycle arrest in the majority of the leukaemia cell lines.

Together this study has shown that PJ is a rich source of bioactive compounds which could hold promise for treatment of leukaemia. The most promising compounds found within PJ were delphinidin, gallic acid, and punicalagin. Further investigation into these agents in the treatment and prevention of leukaemia are essential to develop these potential agents as future treatments.

Dissemination

Published papers

1. Dahlawi H, Jordan-Mahy N, Clench M, Le Maitre CL (2011). Bioactive Actions of Pomegranate Fruit Extracts on Leukaemia Cell lines *in vitro* Hold Promise for New Therapeutic Agent for Leukaemia. *Nutrition and Cancer*, 7(1): 13-18.
2. Dahlawi H, Jordan-Mahy N, Clench M, McDougall G, Le Maitre CL (2013). Polyphenol are responsible for proapoptotic properties of pomegranate juice on leukaemia cell lines. *Food Science and Nutrition*, 1(2): 196-208

Papers in Preparation:

1. Dahlawi H, Jordan-Mahy N, Clench M, Le Maitre CL. Impact of Anthocyanin Chemical Structure Found in Pomegranate Juice on Leukaemia Treatment.
2. Dahlawi H, Jordan-Mahy N, Clench M, Le Maitre CL. Effect of different compounds found in pomegranate juice extracts on the inhibition of cell proliferation and induction of apoptosis leukaemia cell lines.

Conference Presentations

1. 4th International Congress on Leukaemia Lymphoma Myeloma: 22-25 May (2013): Effect of pomegranate anthocyanidins (delphinidin, cyanidin and pelargonidin) on inhibition of proliferation and induction of apoptosis in human leukaemia cell lines. Istanbul, Turkey.
2. The BMRC/MERI Winter Poster Event: 19 December (2012): Impact of Anthocyanin Chemical Structure Found in Pomegranate Juice on Leukaemia Treatment. Liverpool, UK.
3. National Cancer Research Institution (NCRI): 5 November (2012): Effect of different compounds found in pomegranate juice extracts on the inhibition of cell proliferation and induction of apoptosis leukaemia cell lines. Liverpool, UK.
4. National Cancer Research Institution (NCRI): 5 November (2012): Impact of Anthocyanin Chemical Structure Found in Pomegranate Juice on Leukaemia Treatment. Liverpool, UK.
5. The Pathological Society Meeting: 3-5 July (2012): Impact of Anthocyanin Chemical Structure Found in Pomegranate Juice on Leukaemia Treatment. Sheffield, UK.

6. BMRC's Summer Conference: 9th July (2012): Impact of Anthocyanin Chemical Structure Found in Pomegranate Juice on Leukaemia Treatment. Sheffield, UK.
7. 6th Paris Polyphenols: 7 & 8, June (2012): Impact of Anthocyanin Chemical Structure Found in Pomegranate Juice on Leukaemia Treatment. Paris, France.
8. BMRC/MERI Winter Poster Session: 16 December (2011): Impact of Anthocyanin Chemical Structure Found in Pomegranate Juice on Leukaemia Treatment. Sheffield, UK.
9. National Cancer Research Institution (NCRI): 8 November (2011): Effect of bioactive compounds found in pomegranate juice extract on treatment of leukaemia. Liverpool, UK.
10. The 5th International Conference on Polyphenols and Health (ICPH): 17-20 October (2011): Bioactive chemicals from carrots (*Daucus carota*), polyacetylenes and carotenoids for the treatment of lymphoid leukaemia. Barcelona, Spain.
11. Multiple Sclerosis and cancer user group at Sheffield Hallam University: June (2011): Pomegranate and its potential for treatment of leukaemia. Sheffield, UK.
12. Health and Wellbeing (Sheffield Hallam University) Faculty day: June (2011): Pomegranate and its potential for treatment of leukaemia. Sheffield, UK.
13. Health and Wellbeing (Sheffield Hallam University) Faculty Day: May (2010): Pomegranate and its potential for treatment of leukaemia. Sheffield, UK.
14. World Cancer Research Fund (WCRF): 11-13 September (2010). Royal College of Physicians, London, UK: Pomegranate and its potential for treatment of leukaemia. London, UK.
15. National Cancer Research Institution (NCRI): 4-7 November (2010). BT Convention Centre, Liverpool, UK: Pomegranate and its potential for treatment of leukaemia. Liverpool, UK.

Abbreviations

Abbreviation	Definition
μM	Micro molar
ABC	Avidin-Biotin-peroxidase Complex
Abs	Antibodies
ADP	Adenosine diphosphate
AIF	Apoptosis inducing factor
AIP	Apoptosis inducing protein
ALL	Acute lymphoid leukaemia
AML	Acute myeloid leukaemia
AMP	Adenosine monophosphate
Apaf-1	Apoptosis protease activation factor-1
Apo2L	Apoptosis ligand 2L
Apo3L	Apoptosis ligand 3L
ATP	Adenosine triphosphate
Bad	Bcl-2-antagonist of cell death
Bak	Bcl-2-antagonist/killer
Bax	Bcl-2-antagonist X protein
BB	Binding buffer
Bcl-2	B-cell leukaemia/lymphoma 2
Bcl-xl	B-cell lymphoma extra large
BH-3	Bcl-2 homology domain 3
Bid	BH3 interacting domain death agonist
BM	Bone marrow
CAD	Caspase activated DNase
Caspase	Cysteine-aspartic-acid-protease
CDKIs	Cyclin-dependent kinases inhibitors
CDKs	Cyclin-dependent kinases
cDNA	Complementary DNA
c-FLIP	Caspase-FLICE like inhibitor protein
ciAP2	Baculoviral IAP repeat-containing protein 3
Cip/Kip	Kinase inhibitor protein
CLL	Chronic lymphoid leukaemia
CML	Chronic myeloid leukaemia
Ct	Cycle threshold
DAB	3,3'-Diaminobenzidine
DAF	DNA fragmentation factor
DAPI	4, 6-Diamidino-2-phenylindole
DISC	Death inducing signaling complex
DNA	Deoxy ribo nucleic acid
dNTPs	Deoxynucleotide triphosphates
DPBS	Dulbecco's phosphate buffered saline
DPPH	Free radical scavenging capacity by 2,2-diphenyl-1-picrylhydrazyl
DR4	Death receptor 4
DR5	Death receptor 5
EGCG	Epigallocatechin 3-gallate
FAB	French-American-British
FADD	Fas-associated death domain

Table (continued)	
FITC	Fluorescein isothiocyanate
FRAP	Ferric reducing antioxidant power
g	Gravity
GAPDH	Glyceradehyde 3-phosphate dehydrogenase
G-CSF	Granulocyte colony stimulating factor
h	Hour
HSCs	Haematopoietic stem cells
HtrA2/Omi	High temperature requirement protein A2 (Omi)
IC₅₀	Median inhibition concentration or inhibit cellular proliferation by 50%
ICC	Immunocytochemistry
INK4	Inhibitor of CDK4
LC-MS	Liquid chromatography mass spectrometry
μl	Microliter
MDR	Development of multidrug resistance
ml	Milliliter
MMLV	Moloney Murine Leukaemia Virus
MPT	Mitochondrial permeability transition
mRNA	Messenger RNA
MS	Mass spectrometry
MTS	3-(4,5-dimethylthiazol-2-yl)-5-(3-carboxymethoxyphenyl)-2-(4-sulfophenyl)-2H-tetrazolium, inner salt
NK	natural killer
nm	Nanometer
p53	Tumour suppressor protein
PARP	Nuclear enzyme poly ADP-ribose polymerase
PB	Peripheral blood
PCR	Polymerase chain reaction
PDAD	Pump and photo diode array detector
PI	Propidium iodide
PJ	Pomegranate juice extract
PS	Phospholipid phosphatidylserine
qRT-PCR	Quantitative real Time polymerase chain reaction
Rb	Retinoblastoma
REAL	Revised European-American Lymphoma
ROS	Reactive oxygen species
rpm	Revolution per minute
RT	Reverse transcription
Smac/Diablo	Second mitochondria-derived activator of caspase/Direct IAP binding protein
SPE	Solid phase extraction
TEAC	Trolox equivalent antioxidant activity
TNF	Tumour necrosis factor
TNFR	TNF receptor
TORC	Total oxygen radical absorbance capacity
TRAIL	Tumour necrosis related apoptois inducing ligand
UV	Ultra violet
WHO	World Health Organisation
WM	Waldenstrom macroglobulinemia
XIPA	X-linked inhibitor of apoptosis protein

Table of contents

1. General Introduction:	30
1.1 Normal Regulatory Cellular Pathways	31
1.1.1 Normal Haematopoiesis	31
1.1.2 Cell Cycle	32
1.1.3 Programmed Cell Death (Apoptosis)	37
1.2 Hallmarks of Cancer	44
1.2.1 Resisting Cell Death	45
1.2.2 Evading Growth Suppressors	45
1.2.3 Sustaining Proliferation Signalling	45
1.3 Leukaemia	46
1.3.1 Causes of Leukaemia.....	46
1.3.2 Incidence of Leukaemia	48
1.3.3 Leukaemia Classification.....	49
1.3.4 Leukaemia Treatment.....	50
1.3.5 Complications associated with common leukaemia therapy	53
1.4 Potential for Naturally Sourced Bioactive Compounds	55
1.4.1 Dietary compound overview.....	55
1.8.2 Targeting cell cycle.....	56
Table 1.7: Effect of Natural dietary bioactive compounds on cell cycle.....	58
1.8.3 Targeting apoptotic cell death.....	59
1.9 Aim and objective:	63
2. Standard Materials and Methods	64
2.1 Preparation of Pomegranate Juice Extracts (PJ)	65
2.2 Cell lines and Culture	65
2.2.1 Cell Lines	65

CD133 (Lonza: 2M-102A):	69
2.2.2 Culture	69
2.2.3 Mycoplasma Testing	70
2.3 Assays of Cell Proliferation	71
2.3.1 Trypan Blue Exclusion Assay	71
2.3.2 CellTiter-Glo [®] Luminescent Cell Viability Assay	73
2.3.3 MTS Assay	74
2.4 Assays of Apoptosis.....	76
2.4.1 Annexin V/PI FITC Flow Cytometry Assay	76
2.4.2 DAPI Staining.....	79
2.4.3 Caspase-3 Activity	81
2.5 Cell cycle Analysis by Flow Cytometry	83
2.5.1 Method	84
2.5.2 Analysis	84
2.5.3 Statistical Analysis.....	85
3. Bioactive Actions of Pomegranate Juice Extracts on Leukaemia Cell Lines <i>In vitro</i>	86
3.1 Introduction	87
3.1.1 Pomegranate.....	87
3.2 Objective	95
3.3 Experimental Design	95
3.3.1 Treatment	95
3.3.2 Assessment of Apoptosis	96
3.3.3 Cell viability Assay	96
3.3.4 Cell Cycle Analysis	97
3.3.5 Statistical Analysis.....	97
3.4 Results.....	98

3.4.1 Effect of PJ on Induction of Apoptosis Using Annexin V-FITC/PI based on Flow Cytometry.....	98
3.4.2 Effect of PJ on Induction of Apoptosis Using DAPI for Morphology Assessment	109
3.4.3 Effect of PJ on Cell Viability.....	119
3.4.4 Effect of PJ on Cell Cycle Using Flow Cytometry.....	125
3.4.5 Effect of Isotonic/Osmolarity and pH Changes on Induction of Apoptosis	130
3.5 Discussion	136
3.6 Conclusion.....	139
4. Identification of potential active compounds within PJ	140
4.1 Introduction	141
4.2 Materials and Methods.....	142
4.2.1 Sample Preparation and Fraction Separation from PJ.....	142
4.2.2 Cell lines and Culture	143
4.2.3 Cell Viability	144
4.2.4 Annexin V- FITC /PI Flow Cytometry assay	144
4.2.5 Caspase-3 Activity.....	144
4.2.6 Hoechst 33342 and Propidium Iodide (PI) staining	144
4.2.6 Cell Cycle	146
4.2.7 Liquid Chromatography Mass Spectrometry (LC-MS)	146
4.2.8 Determination of Total Phenolics.....	147
4.2.9 Statistical analysis:.....	148
4.3. Results:.....	149
4.3.1 Differential Effects of Pomegranate Fractions on ATP Levels	149
4.3.2 Effect of Acetonitrile Fraction from Pomegranate Juice on Cell Cycle Arrest Within Leukaemia Cell Lines.....	151
4.3.3 Induction of Apoptosis by Acetonitrile SPE Fraction from Pomegranate Extracts within Leukaemia Cell Lines	153

4.3.4 Phenolic Content of SPE Fractions.....	160
4.3.5 LC–MS of Whole PJ and SPE Fractions.....	161
4.4 Discussion	166
5. Anti-proliferative activity of pomegranate pure compounds in leukaemia cell lines	169
5.1 Introduction	170
5.2 Objective	170
5.3 Material and Methods	175
5.3.1 Cell Culture.....	175
5.3.2 Treatment of Cells.....	175
5.4 Results:.....	176
5.4.1 Effect of Pomegranate Compounds in Leukaemia Cell Lines; on ATP Levels as an Indicator of Total Viable Cells.....	176
5.4.1.6 Ellagitannins.....	196
5.4.2 Summary of Results	207
5.4.3 Anti-proliferative effect of Pomegranate Compounds in Non-Tumour CD133+ HSCs.....	208
5.4 Discussion	210
5.4.1 Phenolic Acids	210
5.4.2 Flavan-3-ols.....	211
5.4.3 Flavanoids	212
5.4.4 Ellagitannins.....	213
5.4.5 Anthocyanins	213
5.4.6 Tumour Cell Selectively.....	214
5.5 Conclusion.....	215
6. Impact of Anthocyanin Chemical Structure on Leukaemia Treatment	216
6.1 Introduction	217
6.1.1 Chemistry of Anthocyanins.....	217

6.1.2 Anthocyanins Found in Pomegranate Juice	219
6.1.3 Anthocyanins Bioactivity.....	219
6.2 Objective	223
6.3 Material and Methods	223
6.3.1 Cell Culture.....	223
6.3.2 Treatment of Cells.....	223
6.3.3 Cell Viability	225
6.3.4 Annexin V- FITC /PI Flow Cytometry Assay.....	225
6.3.5 Caspase-3 Activity	225
6.3.6 DAPI Stain.....	225
6.3.7 Cell Cycle	226
6.3.8 Caspase-8 and -9.....	226
6.3.9 Immunocytochemistry.....	227
6.3.10 Quantitative Real Time Polymerase Chain Reaction (qRT-PCR)	230
6.3.10.3 Statistical Analysis.....	235
6.4 Results.....	236
6.4.1 Effect of Anthocyanidins and Anthocyanins on ATP Levels as an Indicator of Total Viable Cells	236
6.4.2 Effect of anthocyanidins and anthocyanins found in PJ on induction of cell death	248
6.4.3 Effect of Anthocyanidins (Delphinidin, Cyanidin, and Pelargonidin) on Caspase-3 Activity.....	255
6.4.4 Effect of Delphinidin on Induction of Apoptosis Using DAPI for Morphology Assessment.....	257
6.4.5 Effect of Delphinidin on Cell Cycle Arrest within Leukaemia Cell Lines.....	262
6.4.6 Effect of Delphinidin on Activities of Caspase-8 and -9 in HL-60 and MOLT-3..	264
6.4.7 Effect of Delphinidin on Expression of Cytochrome C in HL-60 and MOLT-3 Cells	267

6.4.8 Effect of Delphinidin on Expression of Smac/Diablo in HL-60 and MOLT-3 Cells	267
6.4.9 Effect of Delphinidin on the Expression of Pro-Apoptotic Proteins (BAX and BAD) and Anti-Apoptotic Proteins (Bcl-2 and Bcl-xl).....	273
6.5 Discussion:	275
6.5.1 Delphinidin is the most active Anthocyanin on Leukaemia Cells	275
6.5.2 Effect of Sugar Molecules	276
6.5.3 Regulation of Cell Cycle by Delphinidin	277
6.5.4 Molecular Mechanism of Apoptosis Induction by Delphinidin	277
6.6 Conclusion.....	278
7. Induction of apoptosis and cell cycle arrest following stimulation ith EGCG, Gallic acid, querticin and punicalagin.	279
7.1 Introduction	280
7.2 Materials and Methods.....	281
7.2.1 Cell Culture.....	281
7.2.2 Treatment of Cells.....	281
7.2.3 Annexin V- FITC /PI Flow Cytometry Assay	282
7.2.4 Caspase-3 Activity	282
7.2.5 DAPI Stain.....	282
7.2.6 Cell Cycle	283
7.3 Results.....	284
7.3.1 EGCG	284
7.3.1.2 Effect of EGCG on Cell Cycle:	290
7.3.2 Gallic acid	292
7.3.3 Quercetin	300
7.3.3.2 Effect of Quercetin on Cell Cycle	306
7.3.4 Punicalagin.....	308
7.4 Discussion	316

7.4.1 EGCG	316
7.4.2 Gallic Acid.....	317
7.4.3 Quercetin	318
7.4.4 Punicalagin.....	319
7.5 Conclusion.....	319
8. General discussion	321
8.1 Key Findings	322
8.2 Future Directions	323
8.2.1 <i>In vitro</i> Studies	324
8.2.2 <i>In vivo</i> Studies	326
8.2.3 Clinical Trials	327
8.3 Final Conclusions.....	327

List of Figures

Figure 1.1 Haematopoiesis and differentiation of myeloid stem cells and lymphoid stem cell.	32
Figure 1.2 The four separate phases of cell cycle process; G ₁ phase, S (synthesis) phase, G ₂ phase and M phase (mitosis).	33
Figure 1.3: The positive and negative regulatory proteins that are involved in cell cycle progression. Modified from Dai and Grant, 2003	36
Figure 1.4 Morphological changes of apoptotic cells at different stages.	38
Figure 1.5 The intrinsic and extrinsic pathways of apoptosis.	39
Figure 1.6 The ten hallmarks of cancer.	44
Figure 2.1: Luminescent reaction to detect ATP in mycoplasma test.	70
Figure 2.2: Cell countess analysis image comparing live and dead cells.	72
Figure 2.3: The luciferase reaction. Mono-oxygenation of luciferin is catalyzed by luciferase in the presence of Mg ²⁺ , ATP and molecular oxygen.	73
Figure 2.4: Schematic representation of phospholipid phosphatidylserine (PS) translocate to outside leaflet of the membrane	78
Figure 2.5: Flow cytometry analysis of Annexin V-FITC/PI.	79
Figure 2.6: Analysis of apoptosis of HL-60 cell line using DAPI staining.	81
Figure 2.7: Schematic showing the principle of intracellular caspase-3 detection using NucView™ 488 caspase-3 substrate.	82
Figure 2.8: Flow cytometry histograms of caspase-3 activation using FlowJo software.	83
Figure 2.9: Cell cycle analysis based on flow cytometry using flowJo software.	87
Figure 3.1: Pomegranate in coats of arms of the British medical society and three royal colleges.	88
Figure 3.2: Illustrated pomegranate fruit and tree.	88
Figure 3.3: Illustrates pomegranate fruit parts (peel, arils and seeds).	90
Figure 3.4: Increase in the number of scientific papers on pomegranate and its constituents from 2000 to 2012.	92
Figure 3.5: Functional and medicinal effect of pomegranate.	94
Figure 3.6: Annexin V-FITC/ PI of live cell populations normalized to untreated controls in 4 lymphoid leukaemia cell lines (CCRF-CEM, JURKAT, MOLT-3, SUP-B15), 4 myeloid leukaemia cell lines (KG-1a, HL-60, K562, THP-1), and non-tumour hematopoietic stem cells (CD133) following treatment PJ for 24 h.	99
Figure 3.7: Annexin V-FITC/ PI of live cell populations normalized to untreated controls in 4 lymphoid leukaemia cell lines (CCRF-CEM, JURKAT, MOLT-3, SUP-B15), 4 myeloid leukaemia cell lines (KG-1a, HL-60, K562, THP-1), and non-tumour hematopoietic stem cells (CD133) following treatment PJ for 48 h.	99
Figure 3.8: Annexin V-FITC/ PI based on flow cytometry following treatment with PJ (0%, 6.25%, 12.5% and 25%) for 24 and 48 h on CCRF-CEM.	100
Figure 3.9: Annexin V-FITC/ PI based on flow cytometry following treatment with PJ (0%, 6.25%, 12.5% and 25%) for 24 and 48 h on Jurkat.	101
Figure 3.10: Annexin V-FITC/ PI based on flow cytometry following treatment with PJ (0%, 6.25%, 12.5% and 25%) for 24 and 48 h on MOLT-3.	102
Figure 3.11: Annexin V-FITC/ PI based on flow cytometry following treatment with PJ (0%, 6.25%, 12.5% and 25%) for 24 and 48 h on SUP-B15.	103

Figure 3.12: Annexin V-FITC/ PI based on flow cytometry following treatment with PJ (0%, 6.25%, 12.5% and 25%) for 24 and 48 h on KG1a.	104
Figure 3.13: Annexin V-FITC/ PI based on flow cytometry following treatment with PJ (0%, 6.25%, 12.5% and 25%) for 24 and 48 h on HL-60. Mean \pm SEM. * indicates significant difference ($P \leq 0.05$) vs. untreated control. n= 3.	105
Figure 3.14: Annexin V-FITC/ PI based on flow cytometry following treatment with PJ (0%, 6.25%, 12.5% and 25%) for 24 and 48 h on K562.	106
Figure 3.15: Annexin V-FITC/ PI based on flow cytometry following treatment with PJ (0%, 6.25%, 12.5% and 25%) for 24 and 48 h on THP-1.	107
Figure 3.16: Annexin V-FITC/ PI based on flow cytometry following treatment with PJ (0%, 6.25%, 12.5% and 25%) for 24 and 48 h on CD133 positive hematopoietic stem cells (non-tumour HSC).	108
Figure 3.17: (1) Morphological staining analysis of CCRF-CEM with DAPI treated with PJ at concentrations 0%, 6.25%, 12.5% and 25% for 24 h.	110
Figure 3.18: (1) Morphological staining analysis of Junket with DAPI treated with PJ at concentrations 0%, 6.25%, 12.5% and 25% for 24 h.	111
Figure 3.19: (1) Morphological staining analysis of MOLT-3 with DAPI treated with PJ at concentrations 0%, 6.25%, 12.5% and 25% for 24 h.	112
Figure 3.20: (1) Morphological staining analysis of SUP-B15 with DAPI treated with PJ at concentrations 0%, 6.25%, 12.5% and 25% for 24 h.	113
Figure 3.21: (1) Morphological staining analysis of KG-1a with DAPI treated with PJ at concentrations 0%, 6.25%, 12.5% and 25% for 24 h.	114
Figure 3.22: (1) Morphological staining analysis of HL-60 with DAPI treated with PJ at concentrations 0%, 6.25%, 12.5% and 25% for 24 h.	115
Figure 3.23: (1) Morphological staining analysis of K562 with DAPI treated with PJ at concentrations 0%, 6.25%, 12.5% and 25% for 24 h.	116
Figure 3.24: (1) Morphological staining analysis of K562 with DAPI treated with PJ at concentrations 0%, 6.25%, 12.5% and 25% for 24 h.	117
Figure 3.25: Analysis of DAPI staining of apoptotic cell populations normalized to untreated controls in 4 lymphoid leukaemia cell lines (CCRF-CEM, JURKAT, MOLT-3, SUP-B15), 4 myeloid leukaemia cell lines (KG-1a, HL-60, K562, THP-1), and non-tumour hematopoietic stem cells (CD133) following treatment PJ for 24 h.	118
Figure 3.26: Analysis of DAPI staining of apoptotic cell populations normalized to untreated controls in 4 lymphoid leukaemia cell lines (CCRF-CEM, JURKAT, MOLT-3, SUP-B15), 4 myeloid leukaemia cell lines (KG-1a, HL-60, K562, THP-1), and non-tumour hematopoietic stem cells (CD133) following treatment PJ for 48 h.	118
Figure 3.27: Effect of pomegranate juice extract (PJ) on cell viability using trypan exclusion assay following 24 and 48 h incubation at 6.25%, 12.5%, and 25% on CCRF-CEM.	120
Figure 3.28: Effect of pomegranate juice extract (PJ) on cell viability using trypan exclusion assay following 24 and 48 h incubation at 6.25%, 12.5%, and 25% on CCRF-CEM.	120
Figure 3.29: Effect of PJ on cell viability using trypan exclusion assay following 24 and 48 h incubation at 6.25%, 12.5%, and 25% on MOLT-3.	121
Figure 3.30: Effect of PJ on cell viability using trypan exclusion assay following 24 and 48 h incubation at 6.25%, 12.5%, and 25% on SUP-B15.	121
Figure 3.31: Effect of PJ on cell viability using trypan exclusion assay following 24 and 48 h incubation at 6.25%, 12.5%, and 25% on KG-1a.	122

Figure 3.32: Effect of PJ on cell viability using trypan exclusion assay following 24 and 48 h incubation at 6.25%, 12.5%, and 25% on HL-60.....	122
Figure 3.33: Effect of PJ on cell viability using trypan exclusion assay following 24 and 48 h incubation at 6.25%, 12.5%, and 25% on K562.....	123
Figure 3.34: Effect of PJ on cell viability using trypan exclusion assay following 24 and 48 h incubation at 6.25%, 12.5%, and 25% on K562.....	123
Figure 3.35: Effect of PJ on cell viability using trypan exclusion assay following 24 and 48 h incubation at 6.25%, 12.5%, and 25% on K562.....	124
Figure 3.36: Cell cycle based on flow cytometry using FlowJo software following treatment with PJ at concentration 0%, 6.25%, and 12.5% for 24 h incubation on CCRF-CEM.....	126
Figure 3.37: Cell cycle based on flow cytometry using FlowJo software following treatment with PJ at concentration 0%, 6.25%, and 12.5% for 24 h incubation on Jurkat.....	126
Figure 3.38: Cell cycle based on flow cytometry using FlowJo software following treatment with PJ at concentration 0%, 6.25%, and 12.5% for 24 h incubation on MOLT-3.....	127
Figure 3.39: Cell cycle based on flow cytometry using FlowJo software following treatment with PJ at concentration 0%, 6.25%, and 12.5% for 24 h incubation on SUP-B15.....	127
Figure 3.40: Cell cycle based on flow cytometry using FlowJo software following treatment with PJ at concentration 0%, 6.25%, and 12.5% for 24 h incubation on KG-1a.....	128
Figure 3.41: Cell cycle based on flow cytometry using FlowJo software following treatment with PJ at concentration 0%, 6.25%, and 12.5% for 24 h incubation on HL-60.....	128
Figure 3.42: Cell cycle based on flow cytometry using FlowJo software following treatment with PJ at concentration 0%, 6.25%, and 12.5% for 24 h incubation on K562.....	129
Figure 3.43: Cell cycle based on flow cytometry using FlowJo software following treatment with PJ at concentration 0%, 6.25%, and 12.5% for 24 h incubation on THP-1.....	129
Figure 3.44: Annexin V-FITC/PI g based on flow cytometry. CCRF-CEM treated in pH adjusted media for 48 h.....	131
Figure 3.45: Annexin V-FITC/PI based on flow cytometry. MOLT-3 treated in pH adjusted media for 48 h.....	131
Figure 3.46: Annexin V-FITC/PI based on flow cytometry. HL-60 treated in pH adjusted media for 48 h.....	132
Figure 3.47: Annexin V-FITC/PI based on flow cyotmetry. THP-1 treated in pH adjusted media for 48 h.....	132
Figure 3.48: Annexin V-FITC/PI based on flow cyotmetry. CD133 treated in pH adjusted media for 48 h.....	133
Figure 3.49: Annexin V-FITC/PI based on flow cytometry. CCRF-CEM treated in equivalent concentration of water for 48 h.....	133
Figure 3.50: Annexin V-FITC/PI based on flow cytometry. MOLT-3 treated in with equivalent concentration of water for 48 h. Mean \pm SEM. * indicates significant difference ($P \leq 0.05$) vs. untreated control. n= 3.....	134
Figure 3.51: Annexin V-FITC/PI based on flow cytometry. HL-60 treated in equivalent concentration of water for 48 h. Mean \pm SEM. * indicates significant difference ($P \leq 0.05$) vs. untreated control. n= 3.....	134
Figure 3.52: Annexin V-FITC/PI based on flow cytometry. THP-1 treated in equivalent concentration of water for 48 h. Mean \pm SEM. * indicates significant difference ($P \leq 0.05$) vs. untreated control. n= 3.....	135

Figure 3.53: Annexin V-FITC/PI based on flow cytometry. CD133 treated in equivalent concentration of water for 48 h.....	135
Figure 4.1: Illustrates fractions generated from PJ using SPE. A: Unbound fraction, B: water fraction, C: acetonitrile fraction, D: acetone fraction, and D: ethyl acetate fraction.	142
Figure 4.2: Analysis of apoptosis of HL-60 cell line using Hoechst and PI staining. Live cells indicated by blue arrow, early apoptotic cells indicated by green arrows, dead and late apoptotic cell indicated by red arrows, and necrotic cell indicated by purple arrow.	146
Figure 4.3: Effect of water, unbound, acetonitrile, acetone, and ethyl acetate fractions generated by SPE of PJ together with whole PJ in four leukaemia cell lines (CCRF-CEM, MOLT-3, HL-60, and THP-1). Cells were treated for 48 h with all fractions at concentrations equivalent to the concentration of compounds within 6.25%, 12.5%, and 25% whole PJ. ATP levels were investigated using the Cell Titer-Glo [®] Luminescent Cell Viability Assay to provide indication of live cell numbers.	150
Figure 4.4: Effect of acetonitrile fraction generated by SPE of PJ on cell cycle phase distribution in four leukaemia cell lines (CCRF-CEM, MOLT-3, HL-60, and THP-1). Cells treated for 48 h with acetonitrile fraction at concentrations equivalent to those found in 6.25%, 12.5%, and 25% whole PJs.	152
Figure 4.5: Effect of acetonitrile fraction generated by SPE of PJ on induction of apoptosis in leukaemia cell lines CCRF-CEM and MOLT-3. Cells treated for 24, 48, and 72 h with acetonitrile fraction at concentration equivalent to the concentrations of compounds found in 6.25%, 12.5%, and 25% whole PJ. Induction of apoptosis was determined by Annexin V-FITC/PI based on flow cytometry analysis.....	154
Figure 4.6: Effect of acetonitrile fraction generated by SPE of PJ on induction of apoptosis in leukaemia cell lines HL-60 and THP-1. Cells treated for 24, 48, and 72 h with acetonitrile fraction at concentration equivalent to the concentrations of compounds found in 6.25%, 12.5%, and 25% whole PJ. Induction of apoptosis was determined by Annexin V-FITC/PI based on flow cytometry analysis.....	155
Figure 4.7: Effect of acetonitrile fraction generated by SPE of PJ on caspase-3 activation in four leukaemia cell lines (CCRF-CEM, MOLT-3, HL-60, and THP-1). Cells treated for 24, 48, and 72 h with acetonitrile fraction equivalent to the concentrations of compounds found in 6.25%, 12.5%, and 25% whole PJ. Caspase-3 activation was determined by NucView™ 488 Caspase-3 substrate based on flow cytometry analysis.....	156
Figure 4.8: Effect of acetonitrile fraction generated by SFE of PJ on morphology of apoptotic cells in HL-60. Cells treated for 48h at concentration 6.25%, 12.5% and 25%. Apoptotic morphology was determined by Hoechst 33258 and PI staining using fluorescence microscope at magnification of x40.....	157
Figure 4.9: Percentage of Live, apoptotic, and necrotic in CCRF-CEM and MOLT-3 cells determined from Hoechst 33258 and PI morphological assessment following treatment with acetonitrile fraction generated by SPE of PJ at concentration 6.25%, 12.5% and 25% for 24	158
Figure 4.10: Percentage of Live, apoptotic, and necrotic in HL-60 and THP-1 cells determined from Hoechst 33258 and PI morphological assessment following treatment with acetonitrile fraction generated by SPE of PJ at concentration 6.25%, 12.5% and 25% for 24.....	159
Figure 4.11: Estimated total level of phenolic compounds of PJ fractions (unbound, water, acetonitrile, acetone, and ethyl acetate) generated by SPE and whole PJ.....	160
Figure 4.12: LC–MS chromatographs of whole PJ (A) and acetonitrile (B), acetone (C) and ethyl acetate fractions (D) from solid phase extraction of PJ LC–MS performed on samples containing	

20 µg GAE/mL by follin assay. LC–MS, liquid chromatography mass spectrometry; PJ, pomegranate juice extract; GAE, gallic acid equivalent.....	162
Figure 4.13: LC–MS chromatographs of whole PJ (Black) and acetonitrile solid phase fraction from PJ (Blue) demonstrating peak differences within negative ion mode.....	163
Figure 4.14: LC–MS chromatographs of whole PJ (Black) and acetonitrile solid phase fraction from PJ (Blue) demonstrating peak differences within positive ion mode.....	164
Figure 5.1: Effect of citric acid on cell proliferation at concentrations 0, 10, 25, 50, and 100 µM in CCRF-CEM, MOLT-3, HL-60, and THP-1 leukaemia cell lines following 24 and 48 h. ATP levels investigated using Cell Titer-Glo® Luminescent Cell Viability Assay to provide indication of live cell numbers.	177
Figure 5.2: Effect of malic acid on cell proliferation at concentrations 0, 10, 25, 50, and 100 µM in CCRF-CEM, MOLT-3, HL-60, and THP-1 leukaemia cell lines following 24 and 48 h. ATP levels investigated using Cell Titer-Glo® Luminescent Cell Viability Assay to provide indication of live cell numbers.	178
Figure 5.3: Effect of Tartaric acid on cell proliferation at concentrations 0, 10, 25, 50, and 100 µM in CCRF-CEM, MOLT-3, HL-60, and THP-1 leukaemia cell lines following 24 and 48 h. ATP levels investigated using Cell Titer-Glo® Luminescent Cell Viability Assay to provide indication of live cell numbers.	179
Figure 5.4: Effect of Fumaric acid on cell proliferation at concentrations 0, 10, 25, 50, and 100 µM in CCRF-CEM, MOLT-3, HL-60, and THP-1 leukaemia cell lines following 24 and 48 h. ATP levels investigated using Cell Titer-Glo® Luminescent Cell Viability Assay to provide indication of live cell numbers..	180
Figure 5.5: Effect of succinic acid on cell proliferation at concentrations 0, 10, 25, 50, and 100 µM in CCRF-CEM, MOLT-3, HL-60, and THP-1 leukaemia cell lines following 24 and 48 h. ATP levels investigated using Cell Titer-Glo® Luminescent Cell Viability Assay to provide indication of live cell numbers..	181
Figure 5.6: Effect of ascorbic acid on cell proliferation at concentrations 0, 10, 25, 50, and 100 µM in CCRF-CEM, MOLT-3, HL-60, and THP-1 leukaemia cell lines following 24 and 48 h. ATP levels investigated using Cell Titer-Glo® Luminescent Cell Viability Assay to provide indication of live cell numbers.	182
Figure 5.7: Effect of gallic acid on cell proliferation at concentrations 0, 10, 25, 50, and 100 µM in CCRF-CEM, MOLT-3, HL-60, and THP-1 leukaemia cell lines following 24 and 48 h. ATP levels investigated using Cell Titer-Glo® Luminescent Cell Viability Assay to provide indication of live cell numbers.	184
Figure 5.8: Effect of ellagic acid on cell proliferation at concentrations 0, 10, 25, 50, and 100 µM in CCRF-CEM, MOLT-3, HL-60, and THP-1 leukaemia cell lines following 24 and 48 h. ATP levels investigated using Cell Titer-Glo® Luminescent Cell Viability Assay to provide indication of live cell numbers.	185
Figure 5.9: Effect of caffeic acid on cell proliferation at concentrations 0, 10, 25, 50, and 100 µM in CCRF-CEM, MOLT-3, HL-60, and THP-1 leukaemia cell lines following 24 and 48 h. ATP levels investigated using Cell Titer-Glo® Luminescent Cell Viability Assay to provide indication of live cell numbers..	186
Figure 5.10: Effect of <i>p</i> -cuanmic acid on cell proliferation at concentrations 0, 10, 25, 50, and 100µM in CCRF-CEM, MOLT-3, HL-60, and THP-1 leukaemia cell lines following 24 and 48 h. ATP levels investigated using Cell Titer-Glo® Luminescent Cell Viability Assay to provide indication of live cell numbers.	187

Figure 5.11: Effect of quinic acid on cell proliferation at concentrations 0, 10, 25, 50, and 100 μM in CCRF-CEM, MOLT-3, HL-60, and THP-1 leukaemia cell lines following 24 and 48 h. ATP levels investigated using Cell Titer-Glo[®] Luminescent Cell Viability Assay to provide indication of live cell numbers.. 188

Figure 5.12: Effect of catechin on cell proliferation at concentrations 0, 10, 25, 50, and 100 μM in CCRF-CEM, MOLT-3, HL-60, and THP-1 leukaemia cell lines following 24 and 48 h. ATP levels investigated using Cell Titer-Glo[®] Luminescent Cell Viability Assay to provide indication of live cell numbers..... 190

Figure 5.13: Effect of epicatechin on cell proliferation at concentrations 10, 25, 50, and 100 μM in CCRF-CEM, MOLT-3, HL-60, and THP-1 leukaemia cell lines following 24 and 48 h. ATP levels investigated using Cell Titer-Glo[®] Luminescent Cell Viability Assay to provide indication of live cell numbers..... 191

Figure 5.14: Effect of EGCG on cell proliferation at concentrations 10, 25, 50, and 100 μM in CCRF-CEM, MOLT-3, HL-60, and THP-1 leukaemia cell lines following 24 and 48 h. ATP levels investigated using Cell Titer-Glo[®] Luminescent Cell Viability Assay to provide indication of live cell numbers..... 192

Figure 5.15: Effect of quercetin on cell proliferation at concentrations 0, 10, 25, 50, and 100 μM in CCRF-CEM, MOLT-3, HL-60, and THP-1 leukaemia cell lines following 24 and 48 h. ATP levels investigated using Cell Titer-Glo[®] Luminescent Cell Viability Assay to provide indication of live cell numbers.. 194

Figure 5.16: Effect of rutin on cell proliferation at concentrations 0, 10, 25, 50, and 100 μM in CCRF-CEM, MOLT-3, HL-60, and THP-1 leukaemia cell lines following 24 and 48 h. ATP levels investigated using Cell Titer-Glo[®] Luminescent Cell Viability Assay to provide indication of live cell numbers..... 195

Figure 5.17: Effect of punicalagin on cell proliferation at concentrations 0, 10, 25, 50, and 100 μM in CCRF-CEM, MOLT-3, HL-60, and THP-1 leukaemia cell lines following 24 and 48 h. ATP levels investigated using Cell Titer-Glo[®] Luminescent Cell Viability Assay to provide indication of live cell numbers.. 197

Figure 5.18: Effect of proline on cell proliferation at concentrations 0, 10, 25, 50, and 100 μM in CCRF-CEM, MOLT-3, HL-60, and THP-1 leukaemia cell lines following 24 and 48 h. ATP levels investigated using Cell Titer-Glo[®] Luminescent Cell Viability Assay to provide indication of live cell numbers. ATP levels normalized to controls and presented as means \pm standard error. * indicates significant difference ($P \leq 0.05$) vs. untreated control. n= 3. 198

Figure 5.19: Effect of valine on cell proliferation at concentrations 0, 10, 25, 50, and 100 μM in CCRF-CEM, MOLT-3, HL-60, and THP-1 leukaemia cell lines following 24 and 48 h. ATP levels investigated using Cell Titer-Glo[®] Luminescent Cell Viability Assay to provide indication of live cell numbers..... 199

Figure 5.20: Effect of methionine on cell proliferation at concentrations 0, 10, 25, 50, and 100 μM in CCRF-CEM, MOLT-3, HL-60, and THP-1 leukaemia cell lines following 24 and 48 h. ATP levels investigated using Cell Titer-Glo[®] Luminescent Cell Viability Assay to provide indication of live cell numbers.. 200

Figure 5.21: Effect of tryptamine on cell proliferation at concentrations 0, 10, 25, 50, and 100 μM in CCRF-CEM, MOLT-3, HL-60, and THP-1 leukaemia cell lines following 24 and 48 h. ATP levels investigated using Cell Titer-Glo[®] Luminescent Cell Viability Assay to provide indication of live cell numbers.. 201

Figure 5.22: Effect of serotonin on cell proliferation at concentrations 0, 10, 25, 50, and 100 μ M in CCRF-CEM, MOLT-3, HL-60, and THP-1 leukaemia cell lines following 24 and 48 h. ATP levels investigated using Cell Titer-Glo [®] Luminescent Cell Viability Assay to provide indication of live cell numbers..	202
Figure 5.23: Effect of melatonin on cell proliferation at concentrations 0, 10, 25, 50, and 100 μ M in CCRF-CEM, MOLT-3, HL-60, and THP-1 leukaemia cell lines following 24 and 48 h. ATP levels investigated using Cell Titer-Glo [®] Luminescent Cell Viability Assay to provide indication of live cell numbers..	203
Figure 5.24: Effect of delphinidin on cell proliferation at concentrations 0, 10, 25, 50, and 100 μ M in CCRF-CEM, MOLT-3, HL-60, and THP-1 leukaemia cell lines following 24 and 48 h. ATP levels investigated using Cell Titer-Glo [®] Luminescent Cell Viability Assay to provide indication of live cell numbers..	204
Figure 5.25: Effect of cyanidin on cell proliferation at concentrations 0, 10, 25, 50, and 100 μ M in CCRF-CEM, MOLT-3, HL-60, and THP-1 leukaemia cell lines following 24 and 48 h. ATP levels investigated using Cell Titer-Glo [®] Luminescent Cell Viability Assay to provide indication of live cell numbers..	205
Figure 5.26: Effect of pelargonidin on cell proliferation at concentrations 0, 10, 25, 50, and 100 μ M in CCRF-CEM, MOLT-3, HL-60, and THP-1 leukaemia cell lines following 24 and 48 h. ATP levels investigated using Cell Titer-Glo [®] Luminescent Cell Viability Assay to provide indication of live cell numbers..	206
Figure 5.27: Effect of delphinidin, cyanidin, pelargonidin, gallic acid, quercetin, EGCG, and punicalagin on cell proliferation at concentrations 0, 10, 25, 50, and 100 μ M in non-tumour HSC (CD133) following 24 and 48 h. ATP levels investigated using Cell Titer-Glo [®] Luminescent Cell Viability Assay to provide indication of live cell numbers.....	209
Figure 6.1: Basic chemical structure of common anthocyanidins.	218
Figure 6.2: Caspase-8 or -9 cleavage of the proapoptogenic substrates containing LETD or LEHD, respectively. Following caspase cleavage, a substrate for luciferase (aminoluciferin) is released, resulting in the luciferase reaction and production of light.	226
Figure 6.3: Illustration of the indirect method of immunocytochemistry.....	228
Figure 6.4: Illustrates analysis of cytochrome C expression in HL-60 cells following treatment with delphinidin for 3 h using Olympus light microscope (X100)..	230
Figure 6.5: Illustration of how TaqMan reagent works. Modified from Applied Biosystems.	231
Figure 6.6: Illustrates qRT-PCR amplification plot.	232
Figure 6.7: Effect of Delphinidin, Delphinidin-3-O-glucoside, and delphinidin-3,5-di-O-glucose on ATP levels proliferation at concentrations 10, 25, 50, and 100 μ M on CCRF-CEM leukaemia cell line. ATP levels investigated using Cell Titer-Glo [®] Luminescent Cell Viability Assay to provide indication of live cell numbers..	236
Figure 6.8: Effect of Delphinidin, Delphinidin-3-O-glucoside, and delphinidin-3,5-di-O-glucose on ATP levels at concentrations 10, 25, 50, and 100 μ M on MOLT-3 leukaemia cell line. ATP levels investigated using Cell Titer-Glo [®] Luminescent Cell Viability Assay to provide indication of live cell numbers.	237
Figure 6.9: Effect of Delphinidin, Delphinidin-3-O-glucoside, and delphinidin-3,5-di-O-glucose on ATP levels at concentrations 10, 25, 50, and 100 μ M on HL-60 leukaemia cell line. ATP levels investigated using Cell Titer-Glo [®] Luminescent Cell Viability Assay to provide indication of live cell numbers.....	238

Figure 6.10: Effect of Delphinidin, Delphinidin-3- <i>O</i> -glucoside, and delphinidin-3,5-di- <i>O</i> -glucose on ATP levels at concentrations 10, 25, 50, and 100 μ M on THP-1 leukaemia cell line. ATP levels investigated using Cell Titer-Glo [®] Luminescent Cell Viability Assay to provide indication of live cell numbers.....	239
Figure 6.11: Effect of cyanidin, cyanidin-3- <i>O</i> -glucoside, and cyanidin -3,5-di- <i>O</i> -glucose on ATP levels at concentrations 10, 25, 50, and 100 μ M on CCRF-CEM leukaemia cell line. ATP levels investigated using Cell Titer-Glo [®] Luminescent Cell Viability Assay to provide indication of live cell numbers.....	240
Figure 6.12: Effect of cyanidin, cyanidin-3- <i>O</i> -glucoside, and cyanidin -3,5-di- <i>O</i> -glucose on ATP levels at concentrations 10, 25, 50, and 100 μ M on MOLT-3 leukaemia cell line. ATP levels investigated using Cell Titer-Glo [®] Luminescent Cell Viability Assay to provide indication of live cell numbers.....	241
Figure 6.13: Effect of cyanidin, cyanidin-3- <i>O</i> -glucoside, and cyanidin -3,5-di- <i>O</i> -glucose on ATP levels at concentrations 10, 25, 50, and 100 μ M on HL-60 leukaemia cell line. ATP levels investigated using Cell Titer-Glo [®] Luminescent Cell Viability Assay to provide indication of live cell numbers.....	242
Figure 6.14: Effect of cyanidin, cyanidin-3- <i>O</i> -glucoside, and cyanidin -3,5-di- <i>O</i> -glucose on ATP levels at concentrations 10, 25, 50, and 100 μ M on THP-1 leukaemia cell line. ATP levels investigated using Cell Titer-Glo [®] Luminescent Cell Viability Assay to provide indication of live cell numbers.....	243
Figure 6.15: Effect of pelargonidin, pelargonidin-3- <i>O</i> -glucoside, and pelargonidin -3,5-di- <i>O</i> -glucose on ATP levels at concentrations 10, 25, 50, and 100 μ M on CCRF-CEM leukaemia cell line. ATP levels investigated using Cell Titer-Glo [®] Luminescent Cell Viability Assay to provide indication of live cell numbers.	244
Figure 6.16: Effect of pelargonidin, pelargonidin-3- <i>O</i> -glucoside, and pelargonidin -3,5-di- <i>O</i> -glucose on ATP levels at concentrations 10, 25, 50, and 100 μ M on MOLT-3 leukaemia cell line. ATP levels investigated using Cell Titer-Glo [®] Luminescent Cell Viability Assay to provide indication of live cell numbers..	245
Figure 6.17: Effect of pelargonidin, pelargonidin-3- <i>O</i> -glucoside, and pelargonidin -3,5-di- <i>O</i> -glucose on ATP levels at concentrations 10, 25, 50, and 100 μ M on HL-60 leukaemia cell line. ATP levels investigated using Cell Titer-Glo [®] Luminescent Cell Viability Assay to provide indication of live cell numbers..	246
Figure 6.18: Effect of pelargonidin, pelargonidin-3- <i>O</i> -glucoside, and pelargonidin -3,5-di- <i>O</i> -glucose on ATP levels at concentrations 10, 25, 50, and 100 μ M on THP-1 leukaemia cell line. ATP levels investigated using Cell Titer-Glo [®] Luminescent Cell Viability Assay to provide indication of live cell numbers. ATP levels normalized to controls and presented as means \pm standard error. * indicates significant difference ($P \leq 0.05$) vs. untreated control. n= 3.	247
Figure 6.19: Annexin V-FITC/ PI based on flow cytometry following treatment with delphinidin, delphinidin-3- <i>O</i> -glucoside, and delphinidin-3,5-di- <i>O</i> -glucose (0, 10, 25, 50, 75, and 100 μ M) for 24 h on CCRF-CEM and MOLT-3.	249
Figure 6.20: Annexin V-FITC/ PI based on flow cytometry following treatment with delphinidin, delphinidin-3- <i>O</i> -glucoside, and delphinidin-3,5-di- <i>O</i> -glucose (0, 10, 25, 50, 75, and 100 μ M) for 24 h on HL-60 and THP-1.....	250
Figure 6.21: Annexin V-FITC/ PI based on flow cytometry following treatment with cyanidin, cyanidin-3- <i>O</i> -glucoside, and cyanidin-3,5-di- <i>O</i> -glucose (0, 10, 25, 50, 75, and 100 μ M) for 24 h on CCRF-CEM and MOLT-3.....	251

Figure 6.22: Analysis of Annexin V-FITC/ PI based on flow cytometry following treatment with cyanidin, cyanidin-3- <i>O</i> -glucoside, and cyanidin-3,5-di- <i>O</i> -glucose (0, 10, 25, 50, 75, and 100 μ M) for 24 h on HL-60 and THP-1.	252
Figure 6.23: Annexin V-FITC/ PI based on flow cytometry following treatment with pelargonidin, pelargonidin -3- <i>O</i> -glucoside, and pelargonidin-3,5-di- <i>O</i> -glucose (0, 10, 25, 50, 75, and 100 μ M) for 24 h on CCRF-CEM and MOLT-3.	253
Figure 6.24: Annexin V-FITC/ PI based on flow cytometry following treatment with pelargonidin, pelargonidin -3- <i>O</i> -glucoside, and pelargonidin-3,5-di- <i>O</i> -glucose (0, 10, 25, 50, 75, and 100 μ M) for 24 h on HL-60 and THP-1.	254
Figure 6.25: Effect of delphinidin, cyanidin, and pelargonidin on caspase-3 activation in four leukaemia cell lines (CCRF-CEM, MOLT-3, HL-60, and THP-1). Cells treated for 24 at concentrations 10, 25, 50 and 100 μ M. Caspase-3 activation was determined by NucView™ 488 Caspase-3 substrate based on flow cytometry analysis.....	256
Figure 6.26: (1) Morphological staining analysis of HL-60 with DAPI treated with delphinidin 25, 50, and 100 μ M for 24 h. Live cells are indicated by the green arrows, and apoptotic cells are indicated by the red arrows. (2) Percentage of apoptotic cells determined from DAPI morphological assessment following treatment with delphinidin at concentration 25, 50, and 100 μ M for 24 h.....	258
Figure 6.27: (1) Morphological staining analysis of MOLT-3 with DAPI treated with delphinidin 25, 50, and 100 μ M for 24 h. Live cells are indicated by the green arrows, and apoptotic cells are indicated by the red arrows. (2) Percentage of apoptotic cells determined from DAPI morphological assessment following treatment with delphinidin at concentration 25, 50, and 100 μ M for 24 h.....	259
Figure 6.28: (1) Morphological staining analysis of HL-60 with DAPI treated with delphinidin 25, 50, and 100 μ M for 24 h. Live cells are indicated by the green arrows, and apoptotic cells are indicated by the red arrows. (2) Percentage of apoptotic cells determined from DAPI morphological assessment following treatment with delphinidin at concentration 25, 50, and 100 μ M for 24 h.....	260
Figure 6.29: (1) Morphological staining analysis of THP-1 with DAPI treated with delphinidin 25, 50, and 100 μ M for 24 h. Live cells are indicated by the green arrows, and apoptotic cells are indicated by the red arrows. (2) Percentage of apoptotic cells determined from DAPI morphological assessment following treatment with delphinidin at concentration 25, 50, and 100 μ M for 24 h.....	261
Figure 6.30: Analysis of cell cycle based on flow cytometry using FlowJo software following treatment with delphinidin at concentration 25, 50, and 100 μ M for 24 h incubation on four leukaemia cell lines (CCRF-CEM, MOLT-3, HL-60, and THP-1)..	263
Figure 6.31: Effect of delphinidin on activation of caspase-8 (A) and caspase-9 (B). HL-60 cells were treated with delphinidin at concentration 25 and 50 μ M for 3, 6, and 24 h. Caspase-8 and -9 activities were investigated using Caspase-Glo™ 8 and 9 Assays.....	265
Figure 6.32: Effect of delphinidin on activation of caspase-8 (A) and caspase-9 (B). MOLT-3 cells were treated with delphinidin at concentration 25 and 50 μ M for 3, 6, and 24 h. Caspase-8 and -9 activities were investigated using Caspase-Glo™ 8 and 9 Assays.	266
Figure 6.33: Effect of delphinidin (50 μ M) on the expression of cytochrome C on HL-60 leukaemia cells following 3, 6, and 24 h treatment.	
Figure 6.34: Effect of delphinidin (50 μ M) on the expression of cytochrome C on MOLT-3 leukaemia cells following 3, 6, and 24 h treatment.	

Figure 6.35: Morphological analysis of effect of delphinidin (50 μ M) on the expression of SMAC/DIABLO on HL-60 leukaemia cells following 3,6, and 24 h treatment.	270
Figure 6.36: Effect of delphinidin (50 μ M) on the expression of Smac/DIABLO on MOLT-3 leukaemia cells following 3, 6, and 24 h treatment. The result of untreated cells was normalized to 1.	
Figure 6.37: Percentage of active cytochrome C in HL-60 and MOLT-3 cells determined from ICC morphological assessment following treatment with delphinidin at 50 μ M for 3, 6, and 24 h normalized to untreated controls.	272
Figure 6.38: Percentage of active Smac/DIABLO in HL-60 and MOLT-3 cells determined from ICC morphological assessment following treatment with delphinidin at 50 μ M for 3, 6, and 24 h normalized to untreated controls.	272
Figure 6.39: Effect of delphinidin (50 μ M) on the mRNA expression of pro-apoptotic protein (BAX and BAD) and anti-apoptotic proteins (Bcl-2 and Bcl-xl) on HL-60 leukaemia cells following 6 h treatment.	274
Figure 6.40: Effect of delphinidin (50 μ M) on the mRNA expression of pro-apoptotic protein (BAX and BAD) and anti-apoptotic proteins (Bcl-2 and Bcl-xl) on MOLT-3 leukaemia cells following 6 h treatment.	274
Figure 7.1: Annexin V-FITC/ PI based on flow cytometry following treatment with EGCG (0, 10, 25, 50, 75, and 100 μ M) for 24 h on CCRF-CEM, MOLT-3, HL-60, and THP-1.	284
Figure 7.2: Effect of EGCG on caspase-3 activation in four leukaemia cell lines (CCRF-CEM, MOLT-3, HL-60, and THP-1). Cells treated for 24 at concentrations 10, 25, 50, 75 and 100 μ M. Caspase-3 activation was determined by NucView™ 488 Caspase-3 substrate based on flow cytometry analysis.	285
Figure 7.3: (1) DAPI Morphological staining analysis of CCRF-CEM with DAPI treated with EGCG at concentrations 25, 50, and 100 μ M for 24 h. Live cells are indicated by the green arrows, and apoptotic cells are indicated by the red arrows. (2) Percentage of apoptotic cells determined from DAPI morphological assessment following treatment with delphinidin at 25, 50, and 100 μ M for 24 h.	286
Figure 7.4: (1) Morphological staining analysis of MOLT-3 with DAPI treated with EGCG at concentrations 25, 50, and 100 μ M for 24 h. Live cells are indicated by the green arrows, and apoptotic cells are indicated by the red arrows. (2) Percentage of apoptotic cells determined from DAPI morphological assessment following treatment with delphinidin at 25, 50, and 100 μ M for 24 h.	287
Figure 7.5: (1) Morphological staining analysis of HL-60 with DAPI treated with EGCG at concentrations 25, 50, and 100 μ M for 24 h. Live cells are indicated by the green arrows, and apoptotic cells are indicated by the red arrows. (2) Percentage of apoptotic cells determined from DAPI morphological assessment following treatment with delphinidin at 25, 50, and 100 μ M for 24 h.	288
Figure 7.6: (1) Morphological staining analysis of THP-1 with DAPI treated with EGCG at concentrations 25, 50, and 100 μ M for 24 h. Live cells are indicated by the green arrows, and apoptotic cells are indicated by the red arrows. (2) Percentage of apoptotic cells determined from DAPI morphological assessment following treatment with delphinidin at 25, 50, and 100 μ M for 24 h.	289
Figure 7.7: Cell cycle based on flow cytometry using FlowJo software following treatment with EGCG at concentration 25, 50, and 100 μ M for 24 h incubation on four leukaemia cell lines (CCRF-CEM, MOLT-3, HL-60, AND THP-1.	291

Figure 7.8: Annexin V-FITC/ PI based on flow cytometry following treatment with gallic acid (0, 10, 25, 50, 75, and 100 μ M) for 24 h on CCRF-CEM, MOLT-3, HL-60, and THP-1. Mean \pm SEM. * indicates significant difference ($P \leq 0.05$) vs. untreated control. n= 3. 292

Figure 7.9: Effect of gallic acid on caspase-3 activation in four leukaemia cell lines (CCRF-CEM, MOLT-3, HL-60, and THP-1). Cells treated for 24 at concentrations of 10, 25, 50, 75 and 100 μ M. Caspase-3 activation was determined by NucView™ 488 Caspase-3 substrate assay based on flow cytometry analysis..... 293

Figure 7.10: (1) Morphological staining analysis of CCRF-CEM with DAPI treated with gallic acid at concentrations 25, 50, and 100 μ M for 24 h. Live cells are indicated by the green arrows, and apoptotic cells are indicated by the red arrows. (2) Percentage of apoptotic cells determined from DAPI morphological assessment following treatment with delphinidin at 25, 50, and 100 μ M for 24 h..... 294

Figure 7.11: (1) Morphological staining analysis of MOLT-3 with DAPI treated with gallic acid at concentrations 25, 50, and 100 μ M for 24 h. Live cells are indicated by the green arrows, and apoptotic cells are indicated by the red arrows. (2) Percentage of apoptotic cells determined from DAPI morphological assessment following treatment with delphinidin at 25, 50, and 100 μ M for 24 h..... 295

Figure 7.12: (1) Morphological staining analysis of HL-60 with DAPI treated with gallic acid at concentrations 25, 50, and 100 μ M for 24 h. Live cells are indicated by the green arrows, and apoptotic cells are indicated by the red arrows. (2) Percentage of apoptotic cells determined from DAPI morphological assessment following treatment with delphinidin at 25, 50, and 100 μ M for 24 h..... 296

Figure 7.13: (1) Morphological staining analysis of THP-1 with DAPI treated with gallic acid at concentrations 25, 50, and 100 μ M for 24 h. Live cells are indicated by the green arrows, and apoptotic cells are indicated by the red arrows. (2) Percentage of apoptotic cells determined from DAPI morphological assessment following treatment with delphinidin at 25, 50, and 100 μ M for 24 h..... 297

Figure 7.14: Cell cycle based on flow cytometry using FlowJo software following treatment with gallic acid at concentration 25, 50, and 100 μ M for 24 h incubation in four leukaemia cell lines (CCRF-CEM, MOLT-3, HL-60, AND THP-1).. 299

Figure 7.15: Annexin V-FITC/ PI based on flow cytometry following treatment with quercetin (0, 10, 25, 50, 75, and 100 μ M) for 24 h on CCRF-CEM and MOLT-3..... 300

Figure 7.16: Effect of punicalagin on caspase-3 activation in four leukaemia cell lines (CCRF-CEM, MOLT-3, HL-60, and THP-1). Cells treated for 24at concentrations 10, 25, 50, 75 and 100 μ M. Caspase-3 activation was determined by NucView™ 488 Caspase-3 substrate based on flow cytometry analysis..... 301

Figure 7.17: (1) Morphological staining analysis of CCRF-CEM with DAPI treated with quercetin at concentrations 25, 50, and 100 μ M for 24 h. Live cells are indicated by the green arrows, and apoptotic cells are indicated by the red arrows. (2) Percentage of apoptotic cells determined from DAPI morphological assessment following treatment with delphinidin at 25, 50, and 100 μ M for 24 h..... 302

Figure 7.18: (1) Morphological staining analysis of MOLT-3 with DAPI treated with quercetin at concentrations 25, 50, and 100 μ M for 24 h. Live cells are indicated by the green arrows, and apoptotic cells are indicated by the red arrows. (2) Percentage of apoptotic cells determined from DAPI morphological assessment following treatment with delphinidin at 25, 50, and 100 μ M for 24 h..... 303

Figure 7.19: (1) Morphological staining analysis of HL-60 with DAPI treated with quercetin at concentrations 25, 50, and 100 μ M for 24 h. Live cells are indicated by the green arrows, and apoptotic cells are indicated by the red arrows. (2) Percentage of apoptotic cells determined from DAPI morphological assessment following treatment with delphinidin at 25, 50, and 100 μ M for 24 h.....	304
Figure 7.20: (1) Morphological staining analysis of THP-1 with DAPI treated with quercetin at concentrations 25, 50, and 100 μ M for 24 h. Live cells are indicated by the green arrows, and apoptotic cells are indicated by the red arrows. (2) Percentage of apoptotic cells determined from DAPI morphological assessment following treatment with delphinidin at 25, 50, and 100 μ M for 24 h.....	305
Figure 7.21: Cell cycle based on flow cytometry using FlowJo software following treatment with quercetin at concentration 25, 50, and 100 μ M for 24 h incubation on four leukaemia cell lines (CCRF-CEM, MOLT-3, HL-60, AND THP-1).....	307
Figure 7.22: Annexin V-FITC/ PI based on flow cytometry following treatment with punicalagin (0, 10, 25, 50, 75, and 100 μ M) for 24 h on CCRF-CEM and MOLT-3.....	308
Figure 7.23: Effect of punicalagin on caspase-3 activation in four leukaemia cell lines (CCRF-CEM, MOLT-3, HL-60, and THP-1). Cells treated for 24at concentrations of 10, 25, 50, 75 and 100 μ M. Caspase-3 activation was determined by NucView™ 488 Caspase-3 substrate based on flow cytometry analysis.....	309
Figure 7.24: (1) Morphological staining analysis of CCRF-CEM with DAPI treated with punicalagin at concentrations 25, 50, and 100 μ M for 24 h. Live cells are indicated by the green arrows, and apoptotic cells are indicated by the red arrows. (2) Percentage of apoptotic cells determined from DAPI morphological assessment following treatment with delphinidin at 25, 50, and 100 μ M for 24 h.....	310
Figure 7.25: (1) Morphological staining analysis of MOLT-3 with DAPI treated with punicalagin at concentrations 25, 50, and 100 μ M for 24 h. Live cells are indicated by the green arrows, and apoptotic cells are indicated by the red arrows. (2) Percentage of apoptotic cells determined from DAPI morphological assessment following treatment with delphinidin at 25, 50, and 100 μ M for 24 h.....	311
Figure 7.26: (1) Morphological staining analysis of HL-60 with DAPI treated with punicalagin at concentrations 25, 50, and 100 μ M for 24 h. Live cells are indicated by the green arrows, and apoptotic cells are indicated by the red arrows. (2) Percentage of apoptotic cells determined from DAPI morphological assessment following treatment with delphinidin at 25, 50, and 100 μ M for 24 h.....	312
Figure 7.27: (1) Morphological staining analysis of THP-1 with DAPI treated with punicalagin at concentrations 25, 50, and 100 μ M for 24 h. Live cells are indicated by the green arrows, and apoptotic cells are indicated by the red arrows. (2) Percentage of apoptotic cells determined from DAPI morphological assessment following treatment with delphinidin at 25, 50, and 100 μ M for 24 h.....	313
Figure 7.28: Cell cycle based on flow cytometry using FlowJo software following treatment with punicalagin at concentration 25, 50, and 100 μ M for 24 h incubation on four leukaemia cell lines (CCRF-CEM, MOLT-3, HL-60, AND THP-1).....	315

List of Tables

Table 1.1: Cell cycle progression is promoted by Cyclins binding to CDKs at different stages...	35
Table 1.2: Summary of proteins involved in apoptosis.....	43
Table 1.3: Genetic abnormalities associated with certain types of leukaemia.	47
Table 1.4: UK leukaemia incidence (2009) and mortality (2010).....	49
Table 1.5: Apoptosis drugs targets	52
Table 1.6: Cell cycle drugs targets.....	53
Table 1.7: Effect of Natural dietary bioactive compounds on cell cycle.....	58
Table 1.8: Effect of natural dietary bioactive compounds on induction of apoptosis.....	62
Table 2.1: CCRF-CEM cell line description.....	65
Table 2.2: SUP-B15 cell line description.....	66
Table 2.3: MOLT-3 cell line description..	66
Table 2.4: Jurkat cell line description.....	67
Table 2.5: HL-60 cell line description.	67
Table 2.6: KG-1a cell line description.....	68
Table 2.7: THP-1 cell line description.....	68
Table 2.8: K562 cell line description..	69
Table 2.9: CD133 cell line description.....	69
Table 2.10: Comparison of cell proliferation assay; Trypan blue exclusion assay, CellTiter-Glo [®] Luminescent Cell Viability Assay and CellTiter 96 [®] Aqueous One solution Cell Proliferation Assay.....	76
Table 3.1: Summary of studies of pomegranate different cancers.	95
Table 3.2: Experimental design for Chapter 3.	96
Table 4.1: Experimental design for Chapter 4.	143
Table 4.2: The IC ₅₀ of PJ and acetonitrile fractions on leukaemia cell lines (CCRF-CEM, MOLT-3, HL-60, and THP-1) following 24 h treatment.	149
Table 4.3: Putative identification of phenolic components.....	165
Table 5.1: Summarised pomegranate compounds found in PJ and their chemical structure..	174
Table 5.2: Experimental design for Chapter 5.	175
Table 5.3: IC ₅₀ values of compounds found in PJ in CCRF-CEM, MOLT-3, HL-60, and THP-1 leukaemia cells following 24 and 48 h treatments. NR= IC ₅₀ not reached.....	208
Table 6.1: Illustrates distribution of the six most common anthocyanidins in edible parts of plants.	219
Table 6.2: Impact of anthocyanins in different cancer models in term of induction of apoptosis inhibition of cell proliferation and cell cycle	223
Table 6.3: Experimental design for chapter 6.....	224
Table 6.4: The source and dilution factors used for the primary antibodies.	228
Table 6.5: The source and dilution factors used for the secondary antibodies.....	229
Table 6.6: RT Mastermix	233
Table 6.7: Real-Time PCR Mastermix.	234
Table 6.8: The IC ₅₀ of anthocyanins and anthocyanidins on leukaemia cell lines (CCRF-CEM, MOLT-3, HL-60, and THP-1) following 24 h treatment.	248
Table 7.1: Experimental design for chapter 7.	282

1. General Introduction:

1.1 Normal Regulatory Cellular Pathways

1.1.1 Normal Haematopoiesis

Haematopoietic stem cells (HSCs) are found in abundance within the bone marrow (BM) and have the ability to proliferate and differentiate into a variety of lineages (Congdon, 2008; Kondo, 2009). HSCs can generate lymphoid and myeloid precursors (Figure 1.8) (Kendo *et al*, 2003; Kondo, 2010). The lymphoid lineage produces T cells, B cells and natural killer (NK) cells. While the myeloid lineage produces red blood cells (erythrocytes), mast cells, megakaryocytes, granulocytes (neutrophils, eosinophils and basophils) and monocytes which go on to form macrophages (Figure 1.1). In addition HSC have been shown to give rise to cell types not directly associated with the haematopoietic system, such as osteoclasts (Kendo *et al*, 2003; Gabilovich and Nagaraj, 2009; Kondo, 2010).

T lymphocytes play an essential part in antigen-recognition in the body's immunity (Alegre *et al*, 2001). The proliferation, differentiation and acquisition of effector functions of T cells requires the recognition of specific antigens, this is also important to provide help to other cell types which participate in the immune response, such as B cells and NK cells (Alegre *et al*, 2001). B lymphocytes respond to foreign particles, which are recognised by membrane bound IgM, upon binding they divide and differentiate into plasma cells (also called plasma B cells, effector B cells and plasmocytes), which produce large volumes of antibodies (Abs) with the same specificity as the original B-cell (Bernasconi *et al*, 2002) (Figure 1.1). B-cells are synthesized in the BM prior to release into the circulation where they migrate to secondary tissues such as the lymph nodes where differentiation to terminally differentiated plasma cells takes place (Calame, 2001). In healthy individuals, the proliferation, differentiation and release of cells from the BM is highly controlled, if defects arise in these processes this can lead to a number of human diseases such as leukaemia (Zone, 2001).

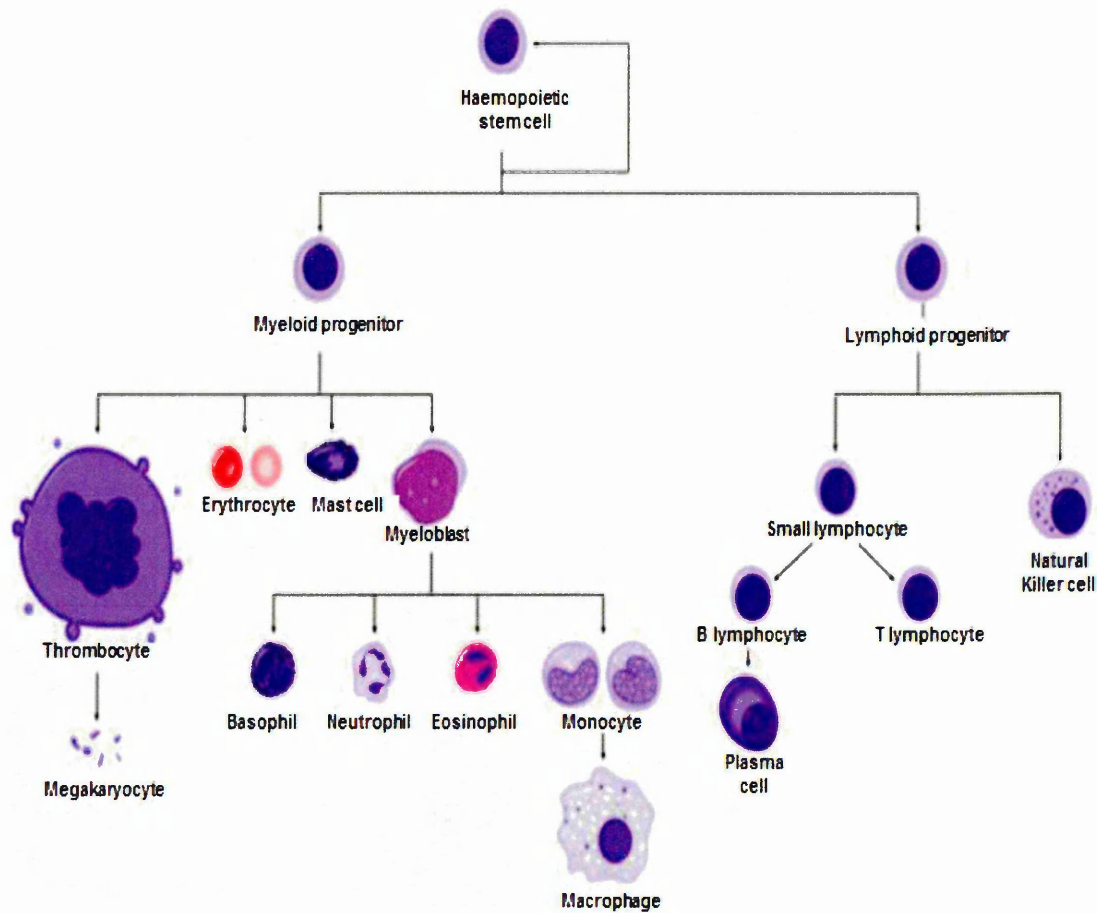


Figure 1.1 Haematopoiesis and differentiation of myeloid stem cells and lymphoid stem cell. Modified from Nielsen *et al*, 1998

1.1.2 Cell Cycle

The cell cycle is the process by which a cell replicates its DNA and divides in a tightly control process that involves five separate phases: G_0 , G_1 , S (DNA synthesis), G_2 and M (mitosis) (Figure 1.2) (Nurse, 2000). Firstly, in the G_0 phase (quiescence cellular arrest) the cell arrests leaving the cell cycle and stops growing. However, even after long period of quiescence, cells are able to re-enter the cell cycle and proliferate (Heinrichs, 2008). Cyclins and cyclin-dependent kinases are not expressed during this phase (Nurse, 2000; Blagosklonny, 2011). Growth phase 1 (G_1) is the first stage of interphase and during this stage proteins and enzymes are synthesized preparing cells for DNA synthesis in S phase (Park and Lee, 2003). During S phase the quantity of chromosomal DNA is replicated to create exactly two identical chromosomes. Synthesis is completed as quickly as possible, because during synthesis the exposed base pairs are sensitive to

external factors, and hence carcinogenic agents can induce mutation in the DNA (Figure 1.1) (Roger and King, 2006). Finally, during M phase the cell splits into two identical daughter cells (Vermeulen *et al*, 2003; Gwyneth *et al*, 2003) (Figure 1.1). The process of mitosis is fast, complicated and involves two processes; mitosis and cytokinesis. During mitosis the cellular chromosomes are divided between the two daughter cells in a highly controlled manner. Mitosis consists of four stages: prophase, metaphase, anaphase, and telophase (Figure 1.2). In contrast, cytokinesis is a separate process which starts at the same time as telophase in this stage the cells cytoplasm divides into half between two daughter cells (Vermeulen *et al*, 2003).

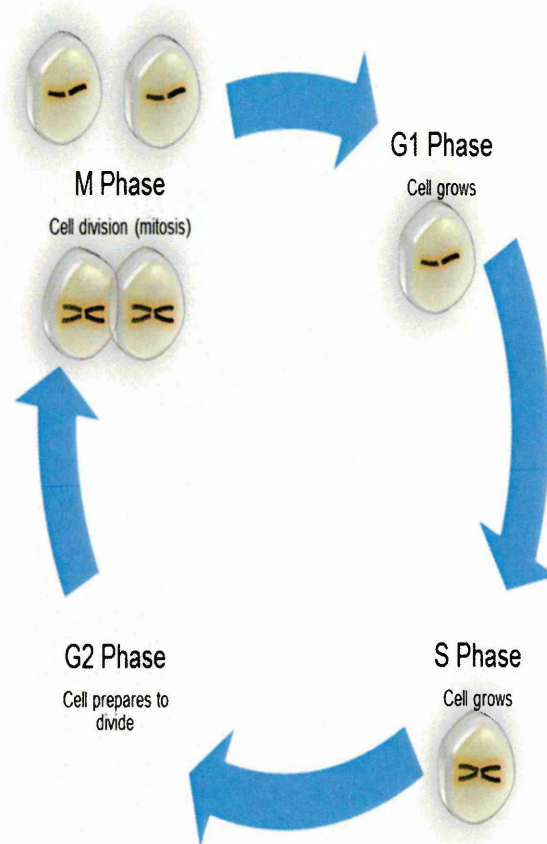


Figure 1.2 The four separate phases of cell cycle process; G₁ phase, S (synthesis) phase, G₂ phase and M phase (mitosis).

1.1.2.1 Regulation of Cell Cycle

The regulation of cell cycle is critical to ensure faithful segregation of genetic material and thus allow normal development and maintenance of multicellular organisms (Vermeulin *et al*, 2003). Failure to coordinate such process can result in genomic instability, which may lead to cancer. Therefore, during the cell cycle there are a number of checkpoints which monitor and regulate the timing and progression through cell cycle, these take place at the G₁/S phase boundary, in S phase, and during G₂/M phases. These checkpoints ensure that the correct sequence of events in particular the phase of cell cycle is completed successfully before a new phase is initiated (Harbour and Douglas, 2000; Meeran and Katiyar, 2008). The regulation of cell cycle involves two main protein families; the cyclin-dependent kinases (CDK) and the cyclins (Figure 1.3)

1.1.2.1.1 Cyclin-Cyclin-Dependent Kinases (Cyclin-CDKs)

The cyclin-dependent kinases (CDKs) are small serine/threonine protein kinases that play a critical role in triggering cell cycle events (Meeran and Katiyar, 2008). CDKs consist of a conserved catalytic kinase core of about 34 kDa, which is inactive by itself. Their activation requires association with regulatory subunits known as cyclins which lead to CDKs phosphorylation providing decisions for the cell to proceed through G₁ into S phase, and from G₂ to M phases (Table 1.1) (Schwartz and Shah, 2005; Meeran and Katiyar, 2008). CDK4 or CDK6 regulate events in the early G₁ phase of the cell cycle; CDK2 triggers entry into S phase when phosphorylated with cyclin E; CDK2 binding to cyclin A and CDK1 to cyclin A regulate the completion of the S phase while CDK1 binds to its specific cyclin partners cyclin B and is responsible for mitosis (Table 1.1) (Boxem *et al*, 1999; Boxem and van den Heuvel, 2001). However, CDK-4 activity has a limited effect on the G₁/S phase of the cell cycle (Van den Heuvel, 2005; Meeran and Katiyar, 2008). CDK-4 is also responsible for the phosphorylation of retinoblastoma gene product (Rb), which is a tumour suppressor protein (See section 1.1.2.1.3). A number of other CDKs are found to work indirectly to regulate the cell cycle including CDK-5, (Cruz and Tasi, 2004) and two other CDKs: CDK-8 and -9 which are involved specifically in regulating transcription (Shim *et al*, 2002 ; Schwartz and Shah, 2005; Meeran and Katiyar, 2008).

CDKs	Cyclins	Cell cycle phase
CDK4	Cyclin D1, D2, D3	G ₁ - phase
CDK6	Cyclin D1, D2, D3	G ₁ - phase
CDK2	Cyclin E	G ₁ -S phase transition
CDK2	Cyclin A	S phase
CDK1	Cyclin A	G ₂ -M phase transition
CDK1	Cyclin B	M phase
CDK7	Cyclin H	All cell cycle phases

Table 1.1 Cell cycle progression is promoted by Cyclins binding to CDKs at different stages. Modified from Meeran and Katiyar, 2008

1.1.2.1.2 Cyclin-Dependent Kinase Inhibitors (CDKIs)

Cell cycle is negatively regulated by cyclin-dependent kinases inhibitors (CDKIs) which are small inhibitory proteins (Meeran and Katiyar, 2008). There are two major families of CDKIs: the INK4 (inhibitor of CDK4) family and the Cip/Kip (kinase inhibitor protein) family (Vermeulen *et al*, 2003; Dai and Grant, 2003; Meeran and Katiyar, 2008). The INK4 family consists of four members including: p15^{ink4b}; p16^{ink4a}; p18^{ink4c} and p19^{ink4d} which specifically bind to CDK4 and CDK6 and inhibit their activity. Each member of the INK4 family is encoded by a unique gene and there are 15- to 19-kDa polypeptides that share approximately 40% homology with one another (Vermeulen *et al*, 2003). The Cip/Kip family, includes; p21^{cip1/waf1}, p27^{Kip1} and p57^{Kip2}, which inhibit the activities of most CDKs (Vermeulen *et al*, 2003). Dis-regulation of molecules controlling the cell cycle plays an important role in tumour pathogenesis (Meeran and Katiyar, 2008). For example, alterations within CDKIs (e.g. p16 and p21) have also been found in many human cancers (Dai and Grant, 2003; Vos *et al*, 2006). Because CDK dis-regulation is reported in most human tumour cells, pharmacological CDK inhibition has become an attractive approach regarding non-genotoxic and mechanism-based therapies in oncology (Figure 1.3) (Fischer and Gianella, 2003).

1.1.2.1.3 Retinoblastoma (Rb)

Retinoblastoma is an essential tumour suppressor protein, which inhibits cell cycle progression and blocks cell growth via preventing their entry to S phase, and is often referred to as the gatekeeper of the cell cycle (Giacinti and Giordano, 2006; Burkhart and Sage, 2008). There are three members of the Rb family including; Rb/p105, p107

and Rb2/p130, collectively referred to as 'pocket proteins'. The negative regulation of cellular transition from G₁ to S phase can be inhibited when Rb protein is hypophosphorylated and then directly binds to the transactivation domain of E2F (group of genes of transcription factors that are involved in cell cycle regulation) (Qian *et al*, 1992; Stevaux and Dyson, 2002; Dimova *et al*, 2003; Burkhardt and Sage, 2008). However, when it's a time for the cell to enter S phase the phosphorylation of Rb by CDK2/cyclin 2, preventing their inhibitory action and binding to the E2F domain. Thus, loss of Rb function may induce cell cycle dis-regulation and so lead to a tumour phenotype. Chromosomal mutations and inactivation of Rb is often considered a crucial component in the development of cancer (Giacinti and Giordano, 2006). Indeed alterations of the Rb gene are common in human cancers including; lung (Wikenheiser-Brokamp, 2006), brain (Jacks, *et al*, 1992), liver (Hui *et al*, 1999) and leukaemia (Krug *et al*, 2002). Interestingly Rb inactivation is more frequently seen in acute myeloid leukaemia than in acute lymphocytic leukaemia (Tang *et al*, 1992).

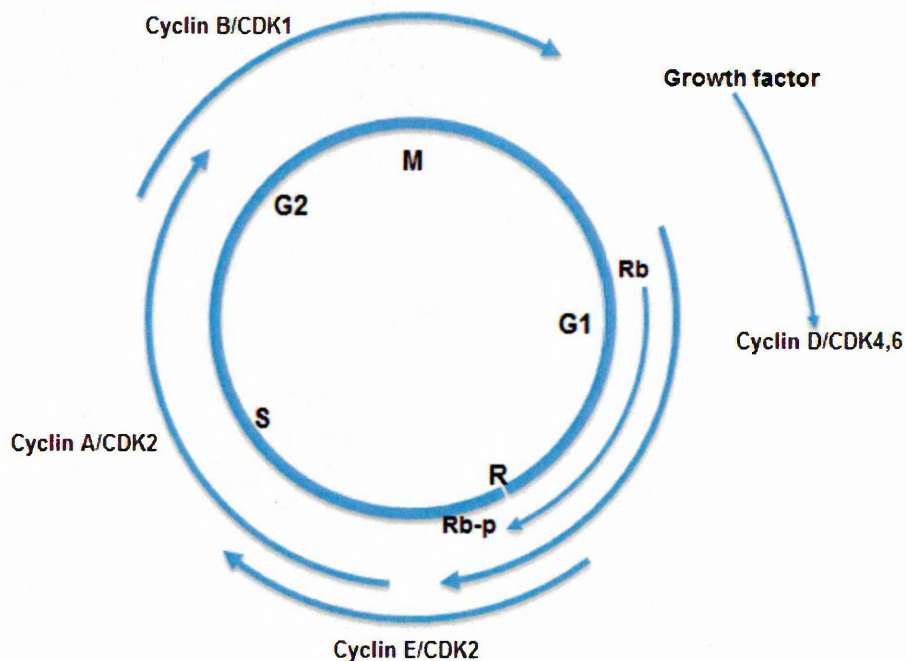


Figure 1.3 The positive and negative regulatory proteins that are involved in cell cycle progression. Modified from Dai and Grant, 2003

1.1.3 Programmed Cell Death (Apoptosis)

Apoptotic cell death occurs as a homeostatic mechanism to maintain cell populations in tissues throughout development and aging (Elmore, 2007). Apoptosis also takes place as a protective process when cells are damaged by disease or during immune reactions (Norbury and Hickson, 2001). There are a number of different conditions which are able to initiate apoptosis, including: cell stress and DNA damage, however, not all cells will undergo apoptosis in response to these stimuli (Elmore, 2007). A number of classical morphological changes characterise the stages of apoptosis (Figure 1.4) (Hacker, 2000). These changes include: cell shrinkage; membrane blebbing; nuclear DNA fragmentation; chromatin condensation and formation of apoptotic bodies (Figure 1.4) (Saraste and Pulkki, 2000). Apoptotic bodies then are rapidly phagocytosed by neighbouring macrophages, providing non-inflammatory clearance of cancerous and pre-cancerous cells, which reduces the chance of tissue damage resulting from inappropriate autoimmune responses (Ren and Savill, 1998; Hoffmann *et al*, 2001).

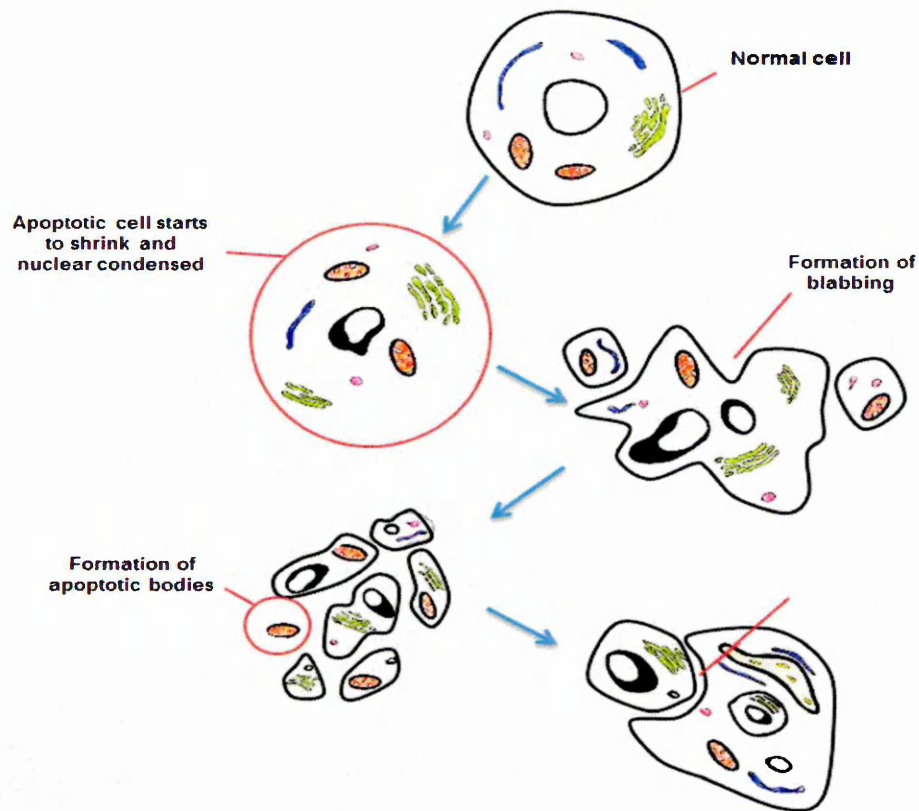


Figure 1.4 Morphological changes of apoptotic cells at different stages. Modified from Vaskivuo, 2002.

There are two major molecular signalling pathways for apoptosis which are highly complex, sophisticated and involve an energy-dependent cascade of molecular events, known as the extrinsic and intrinsic pathways (Figure 1.5). Both pathways are associated with enzymatic caspase activation (Brady, 2003; Martin, 2006; Ashkenazi, 2008).

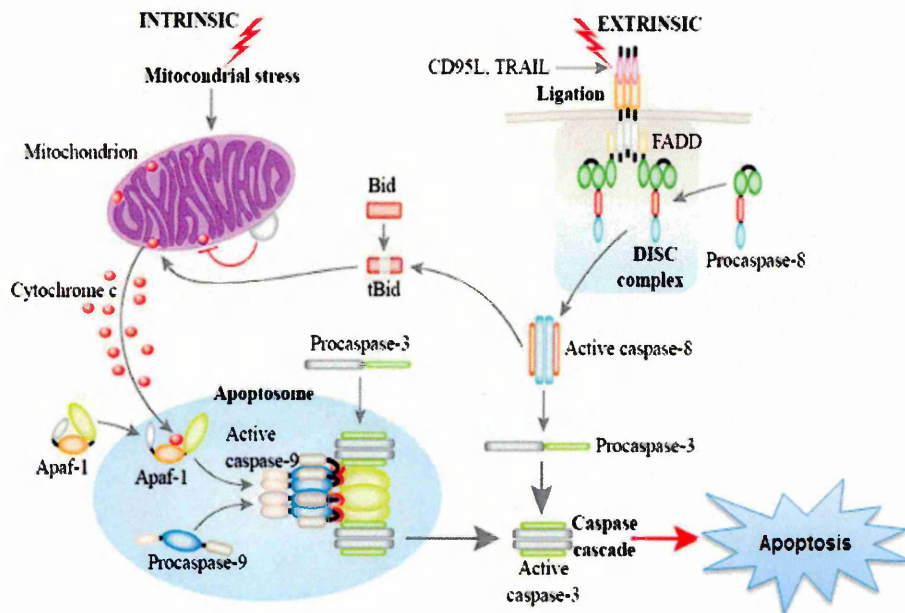


Figure 1.5 The intrinsic and extrinsic pathways of apoptosis. This figure has been modified from Fernandez *et al*, 2010.

1.1.3.1 The Intrinsic Pathway

In the intrinsic pathway, apoptosis is initiated from inside the cell when pro-apoptotic stimuli, such as the absence of certain growth factors; cytokines; hormones; hypoxia or infections lead to initiation of death programs, this in turn causes activation of apoptosis (Saelens *et al*, 2004; Elmore, 2007; Yip and Reed, 2008). Commonly, these stimuli activate the expression of pro-apoptotic members of Bcl-2 family, such as Bax, leading to their transportation to the outer membrane of mitochondria. Alterations in the inner mitochondrial membrane lead to changes in the mitochondrial permeability transition (MPT) pore; loss of the mitochondrial transmembrane potential and release of mitochondrial pro-apoptotic proteins such as: cytochrome C; Second mitochondria-derived activator of capsase/Direct IAP binding protein SMAC/Diablo and the serine protease HtrA2/Omi from the intermembrane space into the cytosol (Hill *et al*, 2004; Saelens *et al*, 2004; Garrido *et al*, 2006) (Figure 1.5). These proteins activate the caspase-dependent mitochondrial pathway. Upon the release of cytochrome C, it binds and activates Apoptotic protease activating factor 1 (APAF-1) as well as procaspase-9, forming an “apoptosome” (Figure 1.5) (Hill *et al*, 2004; Khan (1) *et al*, 2006). The

procaspase-9 cluster causes caspase-9 activation by self-cleavage which in turn activates the executioner caspase-3 (Figure 1.5).

1. 1.3.1.1 Regulation of the Intrinsic Pathway

1.1.3.1.1.1 Bcl-2-Family

The Bcl-2-family includes a group of structurally similar proteins which play an important role in the regulation of the intrinsic pathway by controlling mitochondria membrane permeability and the release of pro-apoptotic factor: cytochrome *c*. Bcl-2 proteins can be divided into three groups: those that promote apoptosis (Bak, Bax, Bcl-2, Bcl-x_s, Bcl-x_l, Bcl-w, Mcl-1, Bcl-10, and Bcl-2 related protein A1); those that inhibit apoptosis (Bcl-2, Bcl-x_l, Bcl-w, Mcl-1, Bcl-10, and Bcl-2 related protein A1); and the pro-apoptotic BH-3, the proteins which bind to and regulate the anti-apoptotic Bcl-2 proteins (Bad, Bid, Bik/Nbk, Bim, Blk, Bmf, Hk/DP5) (Table 1.2) (Cory and Adams, 2002; Elmore, 2007; Yip and Reed, 2008). The ratio between anti- and pro-apoptotic family members controls whether or not cells will undergo apoptosis (Elmore, 2007).

1.1.3.1.1.2 Non-Bcl2 Family Proteins

In addition to the Bcl-2 family proteins, Apoptotic inducing factor (AIF), endonuclease G and caspase-activated DNase (CAD) are other proteins which have a pro-apoptotic function and are released from the mitochondria during the late stages of apoptosis (Table 1.3). AIF and endonuclease G translocate from the mitochondria and move to the nucleus and to induce DNA fragmentation and chromatin condensation (Joza *et al*, 2001; Li *et al*, 2001). AIF and endonuclease G both function in a caspase-independent manner (Enari *et al*, 1998). In addition, caspase 3 is able to cleave the inhibitor of caspase activated DNase (CAD) and allows CAD to cleave the DNA at random points between individual nucleosomes (Larsen *et al*, 2010). In contrast, there are some proteins which act as inhibitors including intracellular apoptosis inhibitor proteins (IAP) which regulate caspase activity by binding and inhibiting the activation of pro-caspases and the activity of mature caspases (Khan (1) *et al*, 2006) (Table 1.3). Some of these inhibitors are X-linked inhibitor of apoptosis protein (XIAP), Baculoviral IAP repeat-containing protein 3 (CIAP2) and Survivin (van Loo *et al*, 2002). SMAC/Diablo and

HtrA2/Omi are described to stimulate apoptosis by inhibiting the activity of IAP (Table 1.3) (van Loo *et al*, 2002). SMAC/Diablo proteins are activated by the effect of apoptosis inducing factor (AIF) (Khan (1) *et al*, 2006; Martin, 2006).

1.1.3.2 The extrinsic Pathway

Extrinsic apoptosis is initiated from outside the cell, when an apoptotic signal is received by binding of pro-apoptotic ligands such as: Apo2L (apoptosis ligand 2); Apo3L (apoptosis ligand 3); TRAIL (tumour necrosis factor-related apoptosis-inducing ligand); Fas Ligand and TNF α to their specific pro-apoptotic membrane death receptors such as DR4 (death receptor 4); DR5 (death receptor 5); Fas and TNF RII (Figure 1.5) (Rodriguez *et al*, 2005; Martin, 2006; Ashkenazi, 2008). Upon binding, the death domain of each receptor (which is cytoplasmic domain of about 80 amino acids) react with Fas-associated death domain (FADD) (cytoplasmic domain which works as a bridge between the receptor and pro-caspase8) leading to recruitment and formation of the death-inducing signalling complex (DISC) (Figure 1.6) (Ashkenazi and Dixit, 1998; Locksley *et al*, 2001). Formation of the DISC can be initiated by each receptor independently by recruiting the adapter FADD and activates the initiator caspases-8 and -10 (Figure 1.5) (Kischkel *et al*, 2000; Rodriguez *et al*, 2005; Elmore, 2007; Ashkenazi, 2008). Activated caspase 8 then in turn activates the executioner caspase 3. The activation of this effector caspase is essential for DNA fragmentation and chromosomal condensation. The cross linking between extrinsic and intrinsic pathway occurs when the active caspase 8 activates the pro-apoptotic member Bid (Bcl-2 interacting domain), to trigger the release of cytochrome C (Fadeel and Orrenius, 2005; Martin, 2006; Elmore, 2007). This pathway can be inhibited by cellular FADD-like interleukin-1 β -converting enzyme inhibitory protein (c-FLIP) (Figure 1.5).

1.1.3.3 The Tumour Suppressor Protein p53

Additionally, the tumour suppressor protein p53 can directly or indirectly regulate the expression and/or release of pro-apoptotic and anti- apoptotic proteins and proteins that control mitochondrial membrane permeability and therefore, can modulate the release of mitochondrial proteins within intrinsic apoptosis (Hofseth *et al*, 2004; Elmore, 2007). In addition, within the intrinsic pathway p53 increasing the expression

of APAF-1, a crucial component of the apoptosome. Interestingly, p53 is also involved in regulation of extrinsic apoptosis through increasing the expression of cellular death receptors such as DR5. p53 can be induced as a result of many signals including; telomere shortening; DNA damage; oncogene activation and over expression of tumour suppressor genes (Miura *et al*, 2004). Thus, it is apparent that p53 is a key tumour suppressor protein at the crossroads of cellular stress response pathways. Though these pathways, it can initiate cell-cycle arrest, DNA repair, chromosomal segregation, cellular senescence and differentiation (Hofseth *et al*, 2004). The different functions of activated p53 are complex and highly dependent on co-expression of other factors which vary by cell type as well as by the severity and persistence of conditions of cell stress and genomic damage (Hanahan and Weinberg, 2011). It has been shown that the loss of p53 in myeloid progenitor cells is associated with a high risk of developing AML, since p53 has a role in controlling cell proliferation though limiting self-renewal of normal HSCs (Zhao *et al*, 2010). Apoptosis mechanisms are highly complex and associated by complex cascades of intracellular events that include activation of pro-apoptotic Bcl-2 family, member of the caspase family and several nucleases. Table 1.2 summarizes important proteins that involve in apoptosis.

Apoptotic proteins	Function	References
Death receptors (Fas, TNFR1, DR3, DR4, DR5)	These are effective in the extrinsic pathway of apoptosis. The extrinsic pathway is initiated by interaction be	Elmore, 2007; Reuter <i>et al</i> , 2008.
Death ligand (FasL, TNFα, TRAIL)		
Caspase family (e.g. caspase 2, 3, 6, 7, 8, 9, 10)	Caspases are a family of cytosolic aspartate-specific cysteine protease, play an important role in the initiation and execution of apoptosis.	Holdenrieder and Stieber, 2004.
Inhibitor of apoptosis (IAP) (e.g. Survivin, XIAP)	IAPs are inhibit apoptosis though inhibition pro-apoptotic members of the caspase family	Debatin <i>et al</i> , 2004; Duberz Daloz <i>et al</i> , 2008.

Table (continued)		
Bcl-2 family (e.g. Bcl-2, Bcl-xl, Bax, Bad, Bak, Bid)	Bcl-2 family proteins regulate the intrinsic pathway by controlling mitochondria permeability and release of the pro-apoptotic factor cytochrome c	Cory and Adams, 2002; Debatin et al, 2004; Elmore, 2007)
Cytochrome c	Cytochrome c is released from the mitochondria into cytosol in response to pro-apoptotic stimuli and act as a cofactor in initiating the activation of the APAF-1/caspase-9 complex.	Debatin et al, 2004; Elmore, 2007
Apoptosis inducing factor (AIF)	AIF release from mitochondria into cytosol, and triggers chromatin condensation as part of the intrinsic caspase-9 mediated apoptosis	Joza et al, 2001;
SMAC/Diablo	Sequesters IAPs and hence favours caspase activation	Van Loo et al, 2002; Debatin et al, 2004; Elmore; 2007
Caspase-activated DNase (CAD)	CAD degrades chromosomal DNA	Enari et al, 1998
Apaf-1	Apaf-1 is a cytosolic protein that participates in the cytochrome c-dependent activation of caspase-3.	Debatin et al, 2004; Elmore, 2007
p53	P53 is a tumour suppressor protein, play role in many cellular process including apoptosis	Debatin et al, 2004; Garwal and Shishodia, 2006; Elmore, 2007

Table 1.2: Summary of proteins involved in apoptosis.

Deregulation within one or more of the normal regulatory pathways including; cell proliferation, differentiation, and apoptosis could result in cancerous cells developing, proliferating and evade death which can lead to the formation of cancer. These aspects are components of the hallmarks of cancers which are required for malignant transformation. Here the key hallmarks, which this study targets for potential treatments for leukaemia will be discussed further.

1.2 Hallmarks of Cancer

Hanahan and Weinberg (2011) initially defined six essential hallmarks of cancer, required for cells to become malignant and these included: (1) evading growth suppressors; (2) resisting cell death (apoptosis); (3) sustaining proliferative signalling; (4) inducing angiogenesis; (5) enabling replicative immortality and (6) activating invasion and metastasis (Pietras and Östman, 2010; Hanahan and Weinberg, 2011). In 2011, they added four new hallmarks: (1) abnormal metabolic pathways; (2) evading the immune system; (3) chromosome abnormalities and unstable DNA, and (4) inflammation (Figure 1.6). Hallmarks which act as targets for new leukaemia therapies will be discussed further here. These include: resisting cell death, evading growth suppressors, and sustain proliferation signalling.



Figure 1.6 The ten hallmarks of cancer. Modified from Hanahan and Weinberg, 2011.

1.2.1 Resisting Cell Death

Resisting programmed cell death plays a key role in cancer cell survival. The most common mechanism by which cancer cells resist apoptosis is by modulation of p53 either through gene deletions or mutations (Bouillet and Strasser, 2002; Juntila *et al*, 2009). Alternative mechanisms include the over expression of anti-apoptotic proteins such as Bcl-2, and Bcl-x_L or by down regulating pro-apoptotic proteins such as Bax. Modulation of extrinsic apoptosis is also seen via decreased expression of death receptors (Hanahan and Weinberg, 2011).

1.2.2 Evading Growth Suppressors

Within normal healthy cells proliferation is tightly controlled by the CDK and CDKI. Particularly during G₁ stage which is an essential checkpoint where the anti-proliferation signals produce their activity to prevent further cell proliferation such as Rb. The Rb protein (see section 1.1.1.1.3) actively inhibits cell passage through the restriction (R) point in the G₁ phase and decides whether or not a cell should proceed (Sherr and McCormick, 2002; Burkhardt and Sage, 2008). Thus, cancer cells with mutated Rb remove this gatekeeper and allow ongoing cell proliferation. On the other hand, p53 functions to arrest the cell cycle once DNA damage is detected and acts as a central regulator of apoptosis (Hanahan and Weinberg, 2011; Hofseth *et al*, 2004). p53 mutation is important in a number of cancers and is linked to poor prognosis in chronic lymphocytic leukaemia (CLL) patients (Zenz *et al*, 2010), and associated with the aggressive forms of Acute myeloid Leukaemia (AML) (Zaho *et al*, 2010).

1.2.3 Sustaining Proliferation Signalling

In normal cells, cell signalling is a highly controlled process; however this regulation is compromised during cancer (Hanahan and Weinberg, 2011). One of the important behaviours of tumour cells is their ability to proliferate uncontrolled. This can be achieved through; stimulating and sending signals to normal cells in the microenvironment to provide cancer cells with additional growth factors; increasing growth factor production by the cancerous cells and increasing the number of growth factor receptors expressed on the cell surface leading to auto proliferation stimulation (Korpal and Kang, 2010; Hanahan and Weinberg, 2011).

1.3 Leukaemia

Leukaemia is a complex form of blood malignancy characterized by the uncontrolled proliferation of haematopoietic cells and progressive accumulation of these cells within the BM and secondary lymphoid tissues, which can spill over into the peripheral blood and other organs. This accumulation prevents the production of other vital normal blood cells such as red blood cells and platelets resulting in anaemia, bleeding and immunodeficiency (Buffler and Kwan, 2005; Alitheen *et al*, 2011).

1.3.1 Causes of Leukaemia

The exact cause of leukaemia remains unknown (Greaves, 1997; Buffler and Kwan, 2005; Buffler *et al*, 2005; Eden, 2010). Leukaemia is thought to have multifactorial causes which involve interaction between different aspects originating from the environmental as well as human genetics (Buffler *et al*, 2005). However there are a number of factors involved which increase the chance of leukaemia developing.

Exposure to Certain Chemicals: The risk of leukaemia may be increased by exposure to certain chemicals. For example long-term exposure to high levels of benzene is a risk factor for AML (Weng *et al*, 2004; Buffler and Kwan, 2005; Rossi *et al*, 2000). In addition, Smoking is known to be linked to cancers of the mouth, lung, and throat, but studies have shown that it can also affect cells which do not come into direct contact with smoke (Weng *et al*, 2004; Buffler and Kwan, 2005).

Age and Gender: Leukaemia is more common in men than women and the risk of getting leukaemia increases with age, but the reasons for this are not clear (Weng *et al*, 2004).

Family History: Most cases of leukaemia are not thought to have a strong genetic linkage; however having a close relative in some types of leukaemia enhances the risk of getting the disease. For example, in identical twins, where one developed AML before they were a year old increased the risk of the second twin developing AML demonstrating a genetic linkage (Amigou *et al*, 2011).

High-Dose Radiation Exposure: Exposure to high-dose radiation (for example as being a survivor exposed to the Hiroshima and Nagasaki atomic bombs or nuclear factor

accident) is known to be associated with increased risk of leukaemia such as CLL (Weng *et al*, 2004; Buffler and Kwan, 2005; Rossi *et al*, 2000).

Viral infection: Epstein-Bar virus (EBV) and human T-cell lymphoma leukemia virus (HTLV-1) have been implicated in the development of leukaemia. The EBV is a herpesvirus that can inhibit B-lymphocytes and nasopharyngeal cells. The HTLV-1 virus is closely associated with T-cell lymphocytic leukemia found in Japan, Africa (Lackritz, 2000)

Genetic abnormalities: Genetic defects and abnormalities are key risk factors associated with the incidence of certain types of leukaemia (Table 1.3) (Buffler and Kwan, 2005; Rossi *et al*, 2000; Amigou *et al*, 2011). A number of syndromes that result from genetic mutations present at birth seem to increase the risk of leukaemia. These include; bloom syndrome, blackfan-diamond syndrome, and fanconi anaemia. Down syndrome and trisomy 8 which are caused by chromosome problem present at birth are also linked to raise the risk of leukaemia (Weng *et al*, 2004; Buffler and Kwan, 2005; Rossi *et al*, 2000).

Genetic abnormalities	Disease group	References
Exportin 1 (XPO1) mutation	CLL	Puente <i>et al</i> , 2011
JAK2 mutation	Acute leukaemia	Biondi <i>et al</i> , 2000; Peacock, 2000; Deschle <i>et al</i> , 2006; Deschler and Lübbert, 2006; Malinge <i>et al</i> , 2007
Loss or deletion of chromosome 5, 7, Y, and 9, translocations	AML	Deschler and Lübbert, 2006
Notch1 mutation	ALL	Weng <i>et al</i> , 2004; Mansour <i>et al</i> , 2007
PAX5 mutation	ALL	Mullighan <i>et al</i> , 2007
Philadelphia (Ph) chromosome translocation between chromosome 9 and 22	90% CML 30% ALL	Fainstein, <i>et al</i> , 1987
t (15; 17) translocation	AML	Kakizuka <i>et al</i> , 1991

Table 1.3 Genetic abnormalities associated with certain types of leukaemia.

1.3.2 Incidence of Leukaemia

Leukaemia is a major problem worldwide affecting many people each year. It is estimated that more than a quarter of million people died from leukaemia in 2008. Leukaemia is the ninth most common cancer death in the UK (Table 1.4) and the fifth in the USA. About 4,500 people died from leukaemia in the UK in 2010 and 23,540 in USA in 2012 (Cancer Research UK, 2013; Leukaemia & Lymphoma Research, 2013). In France, during the period 2000 to 2004, leukaemia and lymphoma was the most frequent cancer accounting for 41% of the total diagnosed malignancies (Lacour *et al*, 2010). In 2013, around 4,800 people are expected to be diagnosed with leukaemia and more than 23,000 people expected to die from leukaemia in USA (Siegel *et al*, 2012)

Generally leukaemia occurs with varying frequencies at different ages and is more common in adults than children. Overall leukaemia is more common in males than females (Table 1.4). Leukaemia causes about one-third of all cancer deaths in children. Acute lymphoblastic leukaemia (ALL) is the most common type in children. More than 50% of all leukaemia diagnosed in children are ALL and the risk for getting it, is highest in children under 5 years old (Cancer Research UK, 2013). In the USA, ALL accounted for 74% of new leukaemia cases in children (Leukaemia & Lymphoma Research, 2013). AML and CLL are the most common type in adults (Table 1.4) (Cancer Research UK, 2013; Leukaemia & Lymphoma Research, 2013). In USA, more than 14,500 new cases of AML were reported in adult and 10,370 deaths from this blood malignancy (American cancer society, 2013). Moreover, according to Leukaemia & Lymphoma Research around 2200 people are diagnosed with AML in the UK annually.

In Leukaemic relative survival rate vary according to patient's age at diagnosis, gender, and type of leukaemia (Leukaemia & Lymphoma Research, 2013). The death rates from leukaemia are very low in people under age of 50 years old, but rise dramatically in the over 60's (Cancer Research UK, 2012). In the USA, the mortality rate from chronic myeloid leukaemia (CML) showed a decrease in 2005 comparing to the five years before while the AML showed a significant increase in the same period of time (Radich, 2010). In the UK, between 2005 and 2009, 44% of people survived from leukaemia for at least five years post diagnosis (Cancer Research UK, 2013). Moreover, mortality rates for both men and women from leukaemia shows a very gradual decline between

the late 1970's and 2008 in the UK (Leukaemia & Lymphoma Research, 2012). Therefore an improved understanding of the pathogenesis of leukaemia and the development of novel drugs is essential to improve the prognosis of leukaemia patients.

Type of leukaemia	Number of cases			Number of deaths		
	Male	Female	Persons	Male	Female	Persons
ALL	391	311	702	125	93	218
CLL	1931	1206	3137	673	463	1136
AML	1399	1164	2563	1253	1057	2310
CML	364	274	638	113	115	248

Table 1.4: UK leukaemia incidence (2009) and mortality (2010). Modified from Cancer Research UK.

1.3.3 Leukaemia Classification

A number of classifications for hematopoietic blood malignancies have been identified such as French–American–British (FAB), Revised European-American Lymphoma (REAL) and 2001 and 2008 World Health Organization (WHO) classifications. These classification systems were based on the identification of distinct tumours using clinical features, immunophenotype, genetic information, molecular and morphological investigation of the peripheral blood (PB) and BM specimens (Gralnick *et al*, 1977; Neame *et al*, 1989 and Vardiman *et al*, 2009). In addition, these classification have some similarity, for example the diagnosis of AML is usually dependant on the level of blast cells as in the blood or bone marrow smears, however, the most important difference between the 2001 WHO system and FAB classifications for the diagnosis of this disorder was the lowering of the blast threshold from 30% to 20% in the PB or BM smears (Vardiman *et al*, 2002). According to the 2008 WHO classification, the name myeloid includes all granulocytic cells (neutrophil, eosinophil, basophil), monocytic/macrophage, erythroid, megakaryocytic and mast cell lineages, while the lymphoid malignancies include T-cell and B-cell lineages (Figure 1.1) (Vardiman, 2010). Moreover, within the updated WHO classification the definitions of some well-established disorders such as CLL, plasma cell neoplasm's and Waldenstrom macroglobulinemia (WM) were improved (Morgan, 2003; Owen *et al*, 2003; Hallek *et*

al, 2008; Vardiman, 2010) and tumour location and age groups, such as the elderly and children were linked to the incidence of certain types of leukaemia (Campo *et al*, 2011). Leukaemia classification is important to determine the cellular maturation degree and origin of the leukaemia cells from where they were originated which is an important tool to determine therapeutic choices and patient's survival.

However in this thesis the four main classification of leukaemia were used to describe the types of cells studied as most research studies related to leukaemia treatment are based on this classification and by using such classification we can identify stage of cellular maturation and the origin of the leukaemic cells. Within this thesis the classification system divides leukaemia into four large groups, including: *acute*, which is a rapidly progressing disease that results in the accumulation of immature cells in the bone marrow and blood, or *Chronic*, which progresses more slowly and allows partially mature cells to form. These can be either myeloid or lymphoid origin (Peacock, 2000; Leukaemia & Lymphoma Research, 2012). If leukaemia begins in early forms of myeloid cells including red blood cells, platelets or white blood cells (but not T, B, lymphocytes, or NK cells) this is considered as myeloid leukaemia. Conversely, in lymphoblastic leukaemia the cancer starts in early form of lymphocytes in bone marrow. Therefore, there are generally four types of leukaemia commonly termed: AML, ALL, CML and CLL (Peacock, 2000). The first three of these types arise from HSCs whilst CLL is derived from mature B lymphocytes.

1.3.4 Leukaemia Treatment

The goal of current leukaemia treatments is to kill the leukaemic cells and allow normal cells to form in the BM. The treatment depends on a number of factors such as histologic type of leukemia, its stage, and prognostic features (patient's age and overall health) (Appelbaum *et al*, 2006). Chemotherapy is the most common treatment for most types of leukaemia and their side effects vary depending on the type of therapy. Bone marrow transplantation is a relatively straightforward medical procedure. Diseased or damaged bone marrow can be replaced by donated bone marrow from healthy patient, which helps treat, and often cure, many serious, life-threatening conditions, including leukaemia (Laughlin *et al*, 2004). This choice of leukaemia treatment provides a very high rate of success (Laughlin *et al*, 2004).

Radiotherapy can be used as part of the preparation for BM transplantation to destroy the cancerous BM with the leukaemia cells using very high level of energy (Walch *et al*, 2013). Radiation may also use as single therapy for different types of malignant diseases such as breast cancer (Radiation *et al*, 2006). In addition, growth factor treatments such as granulocyte colony stimulating factor (G-CSF) may be used to stimulate the BM to synthesis more blood cells to decrease the risk of infection that is generated as a result of low level of WBC following the chemotherapy (Dombret *et al*, 1995; Löwenberg *et al*, 2003). The survival rate in patients with AML was about 9% higher following the treatment with chemotherapy plus G-CSF than patients who did not receive G-CSF (Löwenberg *et al*, 2003).

Targeted cancer therapy is a type of medical treatment designed to treat cancer by blocking the growth and spread of cancer by interfering with specific target molecules involved in tumour growth and progression rather than simply interfering with rapidly dividing cells (e.g. chemotherapy). Targeted therapies can cause cancer cell death by inducing apoptois or arresting cell cycle.

1.3.4.1 Targeting Apoptosis

To date, many of the crucial players in the system of apoptosis regulation are identified and can be targeted by therapeutic strategies which include Bcl-2 proteins, caspases, and death receptors. Therefore, identification of the major regulators increases research into developing therapeutic approaches to intervene either in a pro- or anti-apoptotic direction (Ghobrial *et al*, 2005). Another approach is to classify the agents as those that target the extrinsic pathway, intrinsic pathway, or the proteins regulating apoptosis (Ghobrial *et al*, 2005). In addition some drugs aimed to control apoptosis indirectly by targeting protein kinases, transcriptional factors, phosphatases, proteasomes and cell surface receptors (Ghobrial *et al*, 2005) (Table 1.5).

Pathway	Agents	Target	
Extrinsic pathway	TRAIL	DR4 and DR5	Havell <i>et al</i> , 1988
	Monoclonal antibodies agonist to Dr4 and Dr5 (HGS-ETR1, HGS-ETR2, and HGS-TR2J)	DR4 and DR5	Ghobrial <i>et al</i> , 2005
Intrinsic pathway	Arensic trioxide	Direct effect on the mitochondria inner membrane	Zangemeister-Wittke <i>et al</i> , 2000
	Lonidamine	Direct effect on the mitochondria inner membrane	Oudard <i>et al</i> , 2003
	G3139	Bcl-2	O'Brein <i>et al</i> , 2007
	Antisense Bcl-xl	Bcl-xl	Zangemeister-Wittke <i>et al</i> , 2000
The common pathway	Apoptin	Caspases	Van der <i>et al</i> , 2002
	Survivin	IAP	Zaffaroni and Diadone <i>et al</i> , 2000

Table 1.5: Apoptosis drugs targets

1.3.4.2 Targeting Cell Cycle

The cell cycle is a series of events which allow the cell to grow and proliferate. Important parts of the cell cycle mechanism are the CDKs which, when activated, provide a means for the cell to move from one phase of the cell cycle to the next (Section 1.1.2.1) (Schwartz and Shah 2005). The CDKs are regulated positively by cyclins and regulated negatively by naturally occurring CDKIs (Section 1.1.2.1.1 and 1.1.2.1.2). Cancer is characterised by a dysregulation of the cell cycle such that cells overexpress cyclins or do not express CDKIs and thus, continue to undergo unregulated cell growth (Section 1.1.2.1). The cell cycle also works to protect the cell from DNA damage. Therefore, cell cycle arrest is a survival mechanism which gives the cancer cells the opportunity to repair their damaged DNA. Recently, in clinical trials are a series of targeted agents that directly in inhibit CDKs, inhibit unrestricted cell growth, and induce growth arrest (Schwartz and Shah 2005). In addition the aim of a number of studies has focused on these drugs as inhibitor transcriptions. A number of targeting cell cycle cancer therapies are summarise in table 1.6.

Targeted agents	Function	References
Flavopiridol	classified as CDKI because of its high affinity for CDKs and its ability to induce cell cycle arrest. It has been shown to inhibit CDK1, CDK2, CDK4, and CDK6.	Losiewicz <i>et al</i> , 1994; Carlson <i>et al</i> , 1996
UCN-01	Associated with G ₁ /S cell cycle arrest, associated with induction of p21 ^{CIP} /Waf1, and desphosphorylation of CDK2.	Kawakami <i>et al</i> , 1996
CYC202	a potent inhibitory of CDK2 Affect the cell cycle at G ₁ and G ₂ /M phases	NcClue <i>et al</i> , 2002
N-acyl-2-aminothiazole analog	Is selective inhibitory for CDK2/cyclin E	Shapiro <i>et al</i> , 2003
E7070	Targets the G ₁ phase of the cell cycle by depleting cyclin E and inducing p53 and p21.	Terret <i>et al</i> , 2003
Imidazopyridines	Is selective inhibitory for CDK2	Byth <i>et al</i> , 2003
Bryostatins-1	Produces transient induction of p21 and subsequent dephosphorylation, inactivation of CDK2, and inhibition of tumour cell growth	Asiedu <i>et al</i> , 1995

Table 1.6: Cell cycle drugs targets

1.3.5 Complications associated with common leukaemia therapy

1.3.5.1 Cancer recurrence

Recurrence of cancer, is when tumour comes back again commonly when the therapy is completed. Moreover, no signs or symptoms for the disease are seen during a period of weeks, months or years. In some types of tumour the recurrence is expected and considered as a part of the disease cycle such as CML (Kantarjian *et al*, 2002). Remission, a state in which no cancerous cells can be found in the body, can be either temporary or permanent. Sometimes remission is temporary, and patients relapse and cancer recurs in the same place where the disease first began (primary site) or in different places in the body (secondary site). Unfortunately, the most frequent causes of treatment failure and drug resistance are associated with relapse where curing the cancer becomes more difficult (Giralt *et al*, 1994; Leukaemia and Lymphoma Research, 2013). Moreover, patient's survival after relapse is poor and ranges from 21% to 33%

(Rubintz *et al*, 2006). The rate of complete remission (CR) is related to patient age, for example patients with AML younger than 60 years have remission rates of 60–80% (Lowenberg *et al*, 1999), whereas remission rates of 40–65% was seen in those 60 years and older, who represent the majority of the AML population (Hiddemann *et al*, 1999; Leopold *et al*, 2002). A number of studies have shown that combination therapies between two chemotherapies agents induced higher rates of CR, for example, more than 40% of patients with AML achieved a CR and long-term survival following the treatment with cytosine arabinoside and an anthracyclin (Juliusson *et al*, 2005).

1.3.5.2 Resistance to chemotherapy

Development of multidrug resistance (MDR) against anti-cancer drugs is a serious problem during the treatment of leukaemia and other cancers (Gottesman, 2002; Luqmani, 2008). Once MDR develops, using high doses of chemotherapy agents to overcome resistance is ineffective and may lead to further toxic effects and resistance are more stimulated (Ozben, 2006). Multidrug resistance severely limits the effectiveness and inhibits cytotoxic effects of chemotherapy in a number of common tumours and is responsible for the overall poor efficacy of cancer chemotherapy (Liscovitch *et al*, 2002; Akan *et al*, 2005). The resistance can be either acquired as a cellular response to drug exposure or inherited in some cancerous cells leading to altered target enzyme; increased drug degradation, decrease drug absorption and/ or enhanced DNA repair (Luqmani, 2008). Mutations within some vital genes such as p53 (tumour suppression gene) have been reported to play an important role in multidrug resistance via inhibiting apoptotic production within tumour cells (Gottesman *et al*, 2002).

1.3.5.3 Side effects

It is very common for patients to experience side effects as a direct result of cancer treatments. The occurrence of side effects following the anti-cancer agent treatment are varies depending on different factors such as patient's age, overall health, type of cancer, its size and how close the cancer to other important organ such as the brain (Cancer Research UK, 2013). However, there are a number of common side effects associated with the majority of chemotherapies including; nausea, sickness, vomiting,

feeling weak, tiredness, hair loss, depression and Low white blood cell count (Cancer Research UK, 2013). In addition, high dose chemotherapy or radiotherapy is associated with ovarian failure and infertility as a result of ovarian damage following the treatment; however, this depends on patient's age and treatment protocol (Meirow and Nugent, 2001). Some side effects are serious medical conditions that need to be treated whereas; many side effects are inconvenient or upsetting but are not harmful to the patient's health and disappear when the treatment finished (Leukaemia and Lymphoma Research, 2013).

Because blood cancer treatments have become more aggressive during the last 20 years (Redd *et al*, 2001), the need for new treatments for leukaemia to improve patient's health and reduce the side effects associated with such therapy has become essential.

1.4 Potential for Naturally Sourced Bioactive Compounds

1.4.1 Dietary compound overview

Cancer is a complex disease, in which there is genetic variability among not only different types of cancer but also among different patients with the same type of cancer, and even among different cells within same tumor. As a consequence, the targeting of a single molecular target for therapeutic purposes might not be sufficient to elicit the desired outcome. Different nutrients, specifically dietary botanicals, can play a role in the regulation of both normal and pathologic process (Aggarwal and Shishodia, 2006). An improved understanding of the regulatory role of these nutrients may help in the prevention and treatment of various cancers. For more than a decade, there has been considerable interest in the use of naturally occurring botanicals for prevention of disease including prevention of various cancers (Aggarwal and Shishodia, 2006). Several epidemiological studies have shown that high intake of fruit and vegetables are associated with low incidence of a number of human cancers (Neuhouser, 2004; Pavia *et al*, 2006; Boffetta *et al*, 2010; Key, 2010). Fruits and vegetables are excellent source of fibre, vitamins, and minerals, but they also contain bioactive compounds including polyphenols. Polyphenols are an integral part of human diet flavonoids and phenolic acids representing the majority of polyphenols present in fruits and vegetables such as pomegranate. These compounds have been shown to

have anti-carcinogenic effects *in vitro* and in *in vivo* models by modulating important cellular and molecular mechanisms related to carcinogenesis such as modulation cell cycle and induction of apoptosis (Ahn *et al*, 2003; Brusselmans *et al*, 2003; Miyoshi *et al*, 2003; Roy *et al*, 2005; Hafeez *et al*, 2008; Zaini *et al*, 2011). Therefore, apoptotic induction and cell cycle arrest within tumour cells has become excellent targets for potential cancer treatments and are proposed to decrease mortality from malignancy (Paschka *et al*, 1998; Brady, 2003; Dorai and Aggarwal, 2004).

1.8.2 Targeting cell cycle

Disruption of the normal regulation of cell cycle progression and division are important events in the development of cancer. For more than a decade, there has been significant interest in the use of naturally occurring botanical agents for the prevention of disease including preventing of cancers. Several dietary agents or nutrients have been shown to affect the cell cycle regulation on the treatment of cancer (Table 1.7).

Bioactive compound	Source	Phase of cell cycle arrest	Cell line	References
Apigenin	Cereals and herbs	G ₂ /M phase	Human colon carcinoma cell lines (SW480, HT-29, and Caco-2)	Wang <i>et al</i> , 2000
		S phase	Leukaemia cell lines (Jurkat and MOLT-3)	Mahbub <i>et al</i> , 2013
		G ₀ /G ₁	Leukaemia cell lines (HL-60 and CCRF-CEM)	Mahbub <i>et al</i> , 2013
Chrysin	Passion flowers	G ₀ /G ₁	Leukaemia cell lines (Jurkat, CCRF-CEM, THP-1, U937, KG-1a, and K562)	Mahbub <i>et al</i> , 2013
Cis- Stilbene		G ₀ /G ₁	Leukaemia cell lines (Jurkat, CCRF-CEM, THP-1, and U937)	Mahbub <i>et al</i> , 2013
Acidic bogs	Cranberry	G ₁ phase	Human breast cancer cells (MCF-7)	Sun and Liu, 2006
Curcumin	Turmeric, curry and mustard	G ₂ /M and S phase	Glioma cell line (U251)	Liu <i>et al</i> , 2007

Table (continued)				
EGCG	Green tea	G ₁ phase	Human Ovarian Carcinoma Cell Line(SKOV-3 and OVCAR-3)	Huh <i>et al</i> , 2004
Ellagic acid	Avocado, red berries, grapes, strawberries, raspberries	G ₁ phase	Human bladder cancer Cells (T24) and cervical carcinoma (CaSki)	Li <i>et al</i> , 2005; Narayanan <i>et al</i> , 1999.
Emodin	Rhubarb	G ₂ /M phase	Human promyelocytic leukaemia cells (HL-60)	Chen <i>et al</i> , 2004
		G ₀ /G ₁ phase	Leukaemia cell lines (Jurkat, CCRF-CEM, and THP-1)	Mahbub <i>et al</i> , 2013
Falcarinol	Carrots	S phase	Leukaemia cell lines (CCRF-CEM and MOLT-3)	Zaini <i>et al.</i> , 2013
Flavones and flavonols	green tea, chocolate, red wine	G ₂ /M phase	Human esophageal squamous carcinoma cell line (KYSE-510)	Zhang <i>et al</i> , 2009
Gallic acid	Guava, geraniaceae	G ₂ /M	Human prostate carcinoma cell (DU145)	Agarwal (1) <i>et al</i> , 2006
Glycyrrhetic acid	Licorice root	G ₀ /G ₁ phase	Human hepatoma cell (HepG2)	Satomi <i>et al</i> , 2005
Hydroxytyrosol	Virgin olive oil	G ₀ /G ₁ phase	Human promyelocytic leukaemia cells (HL-60)	Fabiani <i>et al</i> , 2002
Luteolin	Celery and green pepper	G ₀ /G ₁ phase	Human colon cancer cell line (HT-29)	Lim <i>et al</i> , 2007
Lycopene	Tomatoes and tomato products	G ₂ /M phase	Human prostate cancer cells (LCNaP)	Hwang and Bowen, 2004
Parthenolide	Feverfew	G ₀ /G ₁	Hepatocellular carcinoma lines (Hep3B, HepG2,)	Ralstin <i>et al</i> , 2006

Table (continued)				
Proanthocyanidins	Grape seeds	G ₁ phase	Human epidermoid carcinoma (A431)	Meeran and Katiyar, 2007
Quercetin	Apple, onion, black and green tea and cranberry	S phase and G ₂ /M phase	Human acute lymphoblastic leukaemia T precursor (MOLT-4) and Human lung cancer cell line (NCI-H20)	Mertens-Talcott and Percival, 2005; Yang <i>et al</i> , 2006
Resveratrol	grapes and red wine	S phase	Human prostate cancer cells (LCNaP)	Benitez <i>et al</i> , 2007
	Rhubarb	G ₀ /G ₁ phase	Leukaemia cell lines (CCRF-CEM, MOLT-3, and HL-60)	Mahbub <i>et al</i> , 2013
		S phase	Leukaemia cell lines (Jurkat and K562)	Mahbub <i>et al</i> , 2013
Silymarin/silibinin	Plant flavonoid from milk thistle	G ₂ /M phase	Human prostate carcinoma cell (DU145)	Deep and Agarwal (2), 2006
Sulforaphane	Cauliflower, broccoli, and Brussels sprouts	M phase	Human pancreatic cancer cell lines (MIA PaCa-2 and PANC-1)	Pham <i>et al</i> , 2004
Tannic acid	Oak park and leaves	G ₀ /G ₁ phase	Human leukaemia cell (Jurkat)	Nam <i>et al</i> , 2001

Table 1.7: Effect of Natural dietary bioactive compounds on cell cycle

1.8.3 Targeting apoptotic cell death

Apoptosis helps to establish a natural balance between cell death and cell renewal in mature animals by destroying excess, damaged, or abnormal cells. However, the balance between survival and apoptosis often tips towards the former in cancer cells. Dis-regulation in pro-apoptotic or anti-apoptotic proteins can inhibit the apoptotic process and allow cells to proliferate. Leukaemia cells could cause this imbalance and evade apoptosis through numerous mechanisms (see section 1.2.1) (Lessene *et al*, 2008; Hanahan & Weinberg, 2011). Several naturally occurring bioactive chemicals have been shown to induce apoptosis (Table 1.8) through both intrinsic and extrinsic pathways (Vermeulen *et al*, 2005; Khan (1) *et al*, 2006).

Dietary Compound	Sources	Cells cell type	Apoptosis effect	References
Apigenin	Plant seeds fruits and vegetables	Breast cancer cells (MDA-MB453, SK-BR-3)	Induced apoptosis, triggered caspase activation.	Choi and Kim, 2009; Chung <i>et al</i> , 2007.
		Colon cancer cells (HT-29, APC, HT-29-GAL)	Release cytochrome <i>c</i> , up-regulation Bax	Choi and Kim, 2009; Shukla and Gupta, 2008
		Prostate cancer cells (22Rv1, PC-3)	Induced apoptosis, decrease levels of Bcl-xl, Bcl-2	Choi and Kim, 2009; Shukla and Gupta, 2008
Acidic bogs	Cranberry	Human breast cancer cells (MCF-7)	Cell cycle arrest and apoptosis	Sun and Liu, 2006
Chrysin	Passion flowers, Rhubarb	Leukaemia cell lines (Jurkat, CCRF-CEM, THP-1, U937, KG-1a, and K562)	Induced apoptosis	Mahbub <i>et al</i> , 2013
Curcumin	Turmeric, curry, mustard	Lung cancer cell line (H1299)	Induce Bax, inhibit NF- κ B and activation of caspases	Dorai and Aggarwal, 2004; Phillai <i>et al</i> , 2004

Table (continued)				
Capsaicin	Red peppers	Breast cancer cells (MCF-7, SKBR-3, MDA-MB231) and	Induced apoptosis,	Thoennissen <i>et al</i> , 2010, Chou <i>et al</i> , 2009.
		Colon cancer cells (HCT116, HT-29, Colo320DM)	Induced apoptosis via Reactive oxygen species (ROS) generation, activated caspase-3	Sanchez <i>et al</i> , 2007, Yang <i>et al</i> , 2009.
Daidzein	Soybean	Breast cancer cells (MCF-7, MDA-MB-453)	Down-regulation of Bcl-2, up-regulation of Bax, and release of cytochrome C from the mitochondria into the cytosol, Activation caspase-3,-9,-7	Jin <i>et al</i> , 2010; Hsu <i>et al</i> , 2010; Choi and Kim , 2008
		Colon cancer cells (Lovo)	Release Cytochrome c	Jin <i>et al</i> , 2010
		Prostate cancer cells (LnCap, PC3)	Induced apoptosis	Choi and Kim, 2008; Guo <i>et al</i> , 2004
Delphinidin	Strawberry and pomegranate	Human prostate cancer cells (PC3)	Activation of caspases, increase in Bax, decrease in Bcl-2, nuclear condensation and fragmentation.	Lazze <i>et al</i> , 2004 ; Hafeez <i>et al</i> , 2008
EGCG	Green tea	Cervical cancer cell line (CaSki) Human cervical cancer cell line (HeLa)	Induced apoptosis by TRAIL sensitization	Ahn <i>et al</i> , 2003; Brusselmans <i>et al</i> , 2003; Zou <i>et al</i> , 2010
Falcarinol	Carrots	Leukaemia cell lines (CCRF_CEM and MOLT-3)	Induced apoptosis, increase caspase 3,8 and 9 activity, release cytochrome c from mitochondria	Zaini <i>et al</i> , 2013
Flavones	Green tea, chocolate, red wine	Human esophageal squamous cell carcinoma cell line (KYSE-510)	Cleavage of caspase-9 and caspase-3	Zhang <i>et al</i> , 2009

Table (continued)

Flavonols	Green tea, chocolate, red wine	Human esophageal squamous cell carcinoma cell line (KYSE-510)	Cleavage of caspase-9 and caspase-3	Zhang <i>et al</i> , 2009
Gingerol	Ginger	Human T lymphoma cells (Jurkat)	Release of cytochrome C from mitochondria, down regulation of Bcl-2 and enhancement of Bax.	Miyoshi <i>et al</i> , 2003
Genistein	Soy beans, Chickpea	Breast cancer (MDA-MB-231, MCF-7) and colon cancer (SW480, HT-29)	Induced apoptosis, induced caspase-3 activity, increased cytochrome c release; down-regulation of Bcl-2 and up regulation of Bax	Hsu <i>et al</i> , 2010; Li <i>et al</i> , 2008; Ferene <i>et al</i> , 2010
	Rhubarb	Leukaemia cell lines (CCRF-CEM, MOLT-3, and HL-60)	Induced apoptosis	Mahbub <i>et al</i> , 2013
Liquiritigenin	Licorice	Human cervical cancer cell line (HeLa)	Up-regulation of p53 and Bax, along with down-regulation of Bcl-2 and survivin.	Liu <i>et al</i> , 2010
Luteolin	Tea, fruits, vegetables, celery,	Colon cancer cells (HT-29, HCT116)	Induced apoptosis	Do Lim <i>et al</i> , 2007; Chiu and Lin, 2008
Lycopene	Tomatoes and tomato products	Breast cancer cells (MCF-7 and MDA-MB-231)	Induced apoptosis, down-regulation of Bcl-2, up regulation of Bax	Wan and Zhang; 2007 Chalabi <i>et al</i> , 2006;
lycopene phytocomplex (Lycoc)	Tomatoes and tomato products	Human promyelocytic leukaemia cells (HL-60)	Loss of mitochondrial transmembrane potential	Ettore <i>et al</i> , 2010
Quercetin	Apple, onion, black and green tea and cranberry	Human lung cancer cell line (NCI-H209)	Decrease of the mitochondrial membrane potential, release of cytochrome C, up-regulation of Bax, down-regulation of Bcl-2	Yang <i>et al</i> , 2006

Table (continued)				
Resveratrol	Grapes	Human pancreatic cancer cells (PANC-1 and AsPC-1). Human breast cancer cell line (MCF-7)	Induced apoptosis by TRAIL sensitization and release of cytochrome C from mitochondria, activation of caspases, and induction of p53-dependent transcriptional activation.	Clement <i>et al.</i> , 1998& Ding and Adrian, 2002; Pozo-Guisado <i>et al.</i> , 2005
Sulforaphane	Cauliflower, broccoli, and Brussels sprouts	Transformed mouse (SV40-)	Increase in the protein levels of both Bax and Bak	Choi and Singh, 2005

Table 1.8: Effect of natural dietary bioactive compounds on induction of apoptosis.

1.9 Aim and objective:

The aim of this study was to test the hypothesis that extracts from pomegranate contain bioactive compounds with strong anti-proliferative effects, and induce apoptosis in human leukaemia cell lines. The specific objectives for this study were to:

A) Investigate the effect of whole PJ on human myeloid and lymphoid leukaemia cell lines and non-tumour control cells in terms of induction of apoptosis and inhibition of cell cycle.

B) Identify active compounds within PJ which are inducers of apoptosis and/or inhibitors of cell cycle.

2. Standard Materials and Methods

2.1 Preparation of Pomegranate Juice Extracts (PJ)

Fresh pomegranates were purchased from Sainsbury's (Sainsbury's, Sheffield, UK) which were originally cultivated in India. Pomegranates were washed, peeled and edible parts separated from the pith. Edible parts were juiced using a pulp ejector juicer (L'EQUIP). The pomegranate juice extract (PJ) was then centrifuge at 1000 g for 35 minutes and filtered through 0.22µm sterile syringe filters (Invitrogen, Paisley, UK) to remove any fibre. The filtered juice was stored at -80°C. Before treatment PJ was diluted (1:1) with complete media and recentrifuged at 1000g for 15 minutes to remove any precipitate.

2.2 Cell lines and Culture

2.2.1 Cell Lines

In this study, four human lymphoid cell lines; CCRF-CEM (Table: 2.1), SUP-B15 (Table: 2.2), MOLT-3 (Table: 2.3), Jurkat (Table: 2.4) and four myeloid human leukaemia cell lines; HL-60 (Table: 2.5), KG1a (Table: 2.6), THP-1 (Table: 2.7), and K562 (Table: 2.8) together with non-tumour CD133 positive haematopoietic stem cells (Table: 2.9) (LONZA) were used.

CCRF-CEM (ATCC: CCL-119)	
Organism:	<i>Homo sapiens</i> (Human)
Organ:	Peripheral blood
Disease:	Acute lymphoblastic leukaemia
Morphology	Lymphoblast
Cell type:	T lymphoblast
Tumour source:	Primary
Age :	4 years juvenile
Gender	Female
Growth properties	Suspension
Expression of p53:	Null
Comment:	CCRF-CEM is a lymphoblast cell line derived by G.E. Foley, <i>et al.</i> Cells were derived from peripheral blood buffy coat of a child (CEM) with acute lymphoblastic leukaemia who had originally presented with lymphosarcoma in 1964 (Foley <i>et al</i> , 1965).

Table 2.1: CCRF-CEM cell line description. LGC Standards, 2013.

SUP-B15 (ATCC: CRL-1929)	
Organism:	<i>Homo sapiens</i> (Human)
Organ:	Bone marrow
Disease:	Acute lymphoblastic leukaemia
Morphology	Lymphoblast
Cell type:	B lymphoblast
Tumour source:	Primary
Age :	8 years
Gender	Male
Growth properties	Suspension
Expression of p53:	Null
Comment:	SUP-B15 cell line was derived from malignant cells collected from a bone marrow of an 8 year old child with Philadelphia chromosome positive B cell ALL. The cells express multiple B lineage markers, but do not express T cell marker (Fainstein. <i>et al</i> , 1987).

Table 2.2: SUP-B15 cell line description. LGC Standards, 2013.

MOLT-3 (ATCC: CRL-1552):	
Organism:	<i>Homo sapiens</i> (Human)
Organ:	Peripheral blood
Disease:	Acute lymphoblastic leukaemia
Morphology	Lymphoblast
Cell type:	T lymphoblast
Tumour source:	Primary
Age :	19 years
Gender	Male
Growth properties	Suspension
Expression of p53:	Wild
comment:	MOLT-3 was derived from the same patient as the MOLT-4 cell line (ATCC: CRL-152). The MOLT-4 cell line was established from cells taken from a patient in relapse who had received multidrug chemotherapy (Minowada <i>et al</i> , 1972).

Table 2.3:MOLT-3 cell line description. LGC Standards, 2013.

JURKAT (ATCC: TIB-152):	
Organism:	<i>Homo sapiens</i> (Human)
Organ:	Peripheral blood
Disease:	Acute T cell leukaemia
Morphology	Lymphoblast
Cell type:	T lymphocyte
Age :	14 years
Gender	Male
Growth properties	Suspension
Doubling time	24 h
Expression of p53:	Null
comment:	This is a clone of the Jurkat-FHCRC cell line, a derivative of Jurkat cell line. The Jurkat cell line was established from the peripheral blood of a 14 year old boy by Schneider, <i>et al</i> (1972) and was originally designated JM (Schneider <i>et al</i> , 1977).

Table 2.4: Jurkat cell line description. LGC Standards, 2013.

HL-60 (ATCC: CCL-240):	
Organism:	<i>Homo sapiens</i> (Human)
Organ:	Peripheral blood
Disease:	Acute promyelocytic leukaemia
Morphology	Myeloblastic
Cell type:	Promyeloblast
Tumour source:	Primary
Age :	36 years
Gender	Female
Growth properties	Suspension
Expression of p53:	Null
Comments	HL-60 is a promyelocytic cell line derived by Collins, <i>et al.</i> (1978). HL-60 cells spontaneously differentiate.

Table 2.5: HL-60 cell line description. LGC Standards, 2013.

KG-1a (ATCC: CCL-246.1):	
Organism	<i>Homo sapiens</i> (Human)
Organ	Bone marrow
Disease	Acute myelogenous leukaemia
Morphology	Myeloblast
Age:	59 years
Gender:	Male
Growth properties:	Suspension
Expression of p53:	Null
Comment:	The KG-1a cell line is derived from the KG-1(ATCC: CCL-246) and is almost identical. The variant subline was isolated by Koeffler <i>et al</i> , 1980 and was composed of undifferentiated promyeloblast

Table 2.6: KG-1a cell line description. LGC Standards, 2013.

THP-1 (ATCC: TIB-202):	
Organism:	<i>Homo sapiens</i> (Human)
Organ:	Peripheral blood
Disease:	Acute monocytic leukaemia
Morphology	Monocyte
Cell type:	Monocyte
Tumour source:	Primary
Age :	1 year infant
Gender	Male
Growth properties	Suspension
Doubling time	Approximately 26 hr
Expression of p53:	Null
Comment:	THP-1 cells are phagocytic and have Fc and C3b receptors and lack surface and cytoplasmic immunoglobins (Tsuchiya <i>et al</i> , 1980, Skubitz <i>et al</i> , 1983).

Table 2.7 THP-1 cell line description. LGC Standards, 2013.

K-562 (ATCC: CCL-243):	
Organism:	<i>Homo sapiens</i> (Human)
Organ:	Bone marrow
Disease:	Chronic myelogenous leukaemia (CML)
Morphology	lymphoblast
Cell type:	B lymphoblast
Tumour source:	Primary
Age :	53 years
Gender	Female
Ethnicity:	Caucasian
Comment:	K562 established from pleural effusion of 53 year old female with chronic myelogenous leukaemia (Lozzio, 1975). Studies have shown the K562 blasts are multipotential, hematopoietic malignant cells that spontaneously differentiate into recognisable progenitors of the erythrocyte, granulocyte and monocytic series Andersson <i>et al</i> , 1979).

Table 2.8: K562 cell line description. LGC Standards, 2013.

CD133 (Lonza: 2M-102A):	
Organism:	<i>Homo sapiens</i> (Human)
Organ:	Bone marrow, cord blood, and fetal liver
Disease:	Normal
Cell type:	Haematopoietic stem cell
Cell source:	Primary
Growth properties	Suspension
Comment:	These cells were used as a control population of non-carcinogenic primary cells to investigate the effects on hematopoietic stem cells, which are often the cell types affected by leukaemia therapies.

Table 2.9: CD133 cell line description. Lonza, 2013.

2.2.2 Culture

All cells were cultured in 75cm² flasks (Invitrogen, Paisley, UK) at a density of 2×10^6 cells/ml in RPMI 1640 medium (Invitrogen) supplemented with 10% (v/v) foetal bovine serum, 1.5 mM Glutamine and 100µg/ml penicillin/streptomycin (complete RPMI) and incubated at 37°C in a 5% CO₂ atmosphere. Cultures were maintained by the addition of fresh complete RPMI every 2 to 3 days.

2.2.3 Mycoplasma Testing

Mycoplasma are a class of Mollicutes that represent a large group of specialized bacteria, which are characterized by their lack of rigid cell wall. Mycoplasma are small and flexible, which make them able to pass through conventional microbiological filters (0.2 μM). Mycoplasma compete with the cells for the nutrients in culture media which results in reduction in the rate of cell proliferation and changes in cellular responses including gene expression (Drexler *et al*, 2002). The degree of infection is varied and depends on the mycoplasma species, cell type and culture condition (Dvorakova *et al*, 2005).

Here, the MycoAlertTM assay (Lonza) was used to ensure cultures were mycoplasma negative every two months. MycoAlertTM assay is a selective biochemical assay that exploits the activity of certain mycoplasma enzymes. The presence of these enzymes allows a rapid screening procedure which provides sensitive detection of contaminating mycoplasma in a test sample. The viable mycoplasma are lysed and the enzymes react with MycoAlertTM substrate catalyzing the conversion of adenosine diphosphate ADP to adenosine triphosphate ATP. The presence or absence of mycoplasma can be detected by measuring the level of ATP in a sample both before and after the addition of MycoAlertTM substrate. If no mycoplasma enzymes are present the second reading shows no increase for the first reading, in contrast reaction of mycoplasma enzymes with their specific substrate in the MycoAlertTM substrate causes raised ATP levels. The ATP is detected via a bioluminescent reaction (Figure 2.1). The light intensity emitted is directly proportional to the ATP concentration and was measured using a luminometer.

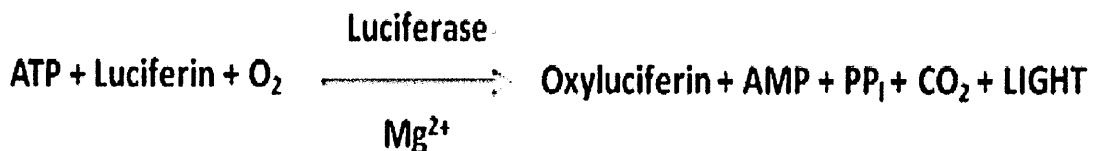


Figure 2.1: Luminescent reaction to detect ATP in mycoplasma test. Modified from Promega.

2.2.3.1 Methodology

MycoAlert™ reagent and MycoAlert™ substrate were reconstituted in MycoAlert™ assay buffer. Two millilitres of cell culture supernatant of each tested sample was transferred into a centrifuge tube, and spun at 400 g for 5 minutes. One hundred microlitres of cleared supernatant was transferred into white 96 well plates (Fisher Scientific), and 100 µl MycoAlert™ reagent was added to each sample and incubated for 5 minutes at room temperature. Following incubation time the plate was placed in a Wallac Victor 2 1420 luminescence detector to measure luminescence (Reading A). Finally 100 µl of MycoAlert™ substrate was added to each sample and incubated for a further 10 minutes before remeasuring the luminescence using the Wallac Victor 2 1420 luminescence detector (Reading B). This shows the increased to determine increased detection of ATP (Reading B).

2.2.3.2 Analysis

The ratio was calculated for each well using a luminometer reading A (before adding the MycoAlert™ Substrate) and luminometer reading B (after adding the MycoAlert™ Substrate). The increase in ATP levels over 10 minutes were calculated using the following equation

$$\text{Ratio} = \frac{\text{Reading A}}{\text{Reading B}}$$

All cultures were negative for mycoplasma for the full duration of the project.

2.3 Assays of Cell Proliferation

2.3.1 Trypan Blue Exclusion Assay

Trypan blue exclusion assay was used to quantify the number of live and dead cells in suspension culture (Strober, 2001). Trypan blue is a vital dye which is only able to enter dead cells, staining them blue. Live cells have an intact cell membrane; therefore do not take in the dye from surrounding medium. In contrast dead cells do not have an intact and functional membrane and therefore do take up the dye from their surroundings. This results in the ability to easily distinguish between live and dead cells (Strober, 2001).

Here the countess™ automated cell counter (Invitrogen) was used which uses state of the art optics and image analysis to automate cell counting. The countess™ automated cell counter is used to determine cell count and viability (live, dead and total cells) following trypan blue staining technique.

2.3.1.1 Methods

Following treatments, suspended cells were mixed to minimize clumping of the cells. Then cell suspension was mixed 1:1 with 0.4% trypan blue solution (Sigma) and incubated at room temperature for 5 minutes. Following incubation 10 µl of stained cells was added into the countess™ chamber slide. Then the countess™ chamber slide was inserted into the instrument and the image of cells was adjusted to focus for analysis.

2.3.1.2 .Analysis

Live cells have bright centres and dark edges and dead cells have a uniform blue colour throughout the cell with no bright centre. The average number of live and dead cells was calculated and all treated samples were normalized to controls (Figure 2.2).

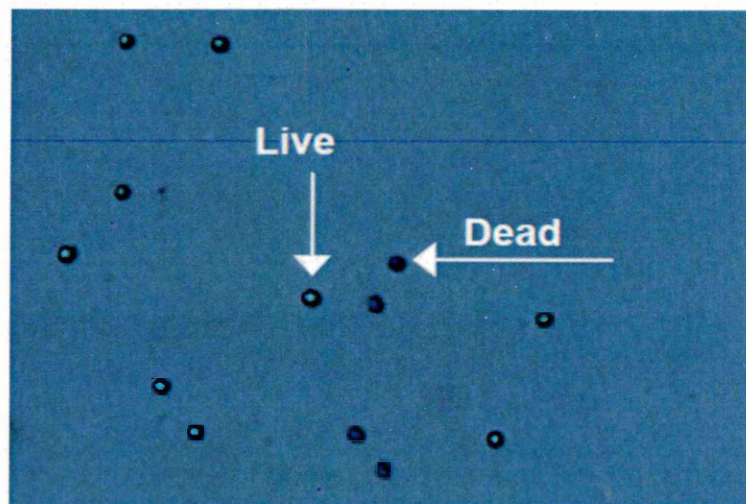


Figure 2.2: Cell countess analysis image comparing live and dead cells. Live cells: have bright centres and dark edges. Dead cells: have a uniform blue colour throughout the cell with no bright centre.

2.3.1.3 Statistical Analysis

Data are presented as the mean \pm SEM and were analyzed by Stats Direct using a Shapiro Wilke test to check for normality. Data were shown to be non-parametric, and thus a Kruskal-Wallis and Conover-Inman post-hoc test was used to test for significance. $P \leq 0.05$ was considered significant.

2.3.2 CellTiter-Glo[®] Luminescent Cell Viability Assay

The nucleotide adenosine triphosphate (ATP) is the primary energy source for all metabolic reactions and is found in all intact cells. It serves as a tool for the functional integrity of living cells as all cells need ATP to remain alive and carry out their specialized functions (Crouch *et al*, 1993). Interruption of cellular processes due to chemical effects, cell injury and physical damage, or depletion of essential nutrients or oxygen results in a decrease in ATP levels (Matthew *et al*, 2009, Crouch *et al*, 1984). Therefore measurement of ATP is essential to the study of cell viability. The use of ATP bioluminescence to measure cell proliferation has been shown with leukaemic cell lines (MOLT-4 and HL-60) where significant correlations between increased cell number and ATP levels were observed (Crouch *et al*, 1993).

The CellTiter-Glo[®] Luminescent Cell Viability Assay (Promega) is a homogeneous method used to identify the number of live cells in culture based on quantification of the level of ATP present that signals the presence of metabolically active cells. The homogeneous format results in cell lysis and generation of a luminescent signal proportional to the amount of ATP present (Kangas *et al*, 1984). The amount of ATP is directly proportional to the number of cells. The CellTiter-Glo[®] Luminescent Cell Viability Assay relies on the production of light caused by the reaction of ATP with luciferase. The emitted light is proportional to ATP concentration inside the cell. The luciferase reaction is summarized in figure 2.3.

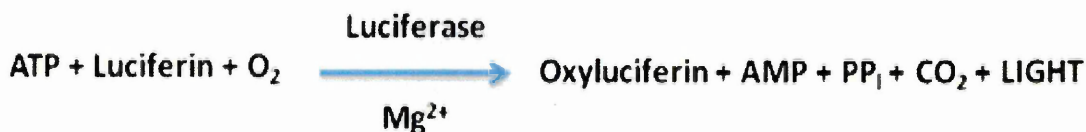


Figure 2.3: The luciferase reaction. Mono-oxygenation of luciferin is catalyzed by luciferase in the presence of Mg^{2+} , ATP and molecular oxygen. Modified d from Promega.

2.3.2.1 Methods

Ten millimetres of CellTiter-Glo[®] Buffer was transferred to the bottle containing CellTiter-Glo[®] Substrate to reconstitute the lyophilized enzyme/substrate mixture which forms the CellTiter-Glo[®] Reagent. Then the reagent was mixed by gently vortexing for 10 minutes. Following treatment, cell culture white-96 well plate and its contents were equilibrated at room temperature for 30 minutes. A hundred microliters of Cell Titer-Glo[®] Reagent was added to each well, mixed well for 2 minutes on an orbital shaker at 400 rpm to induce cell lysis. The plate was allowed to incubate at RT for 10 minutes prior to luminescence detection using the Wallac 1420 luminescence detector (PerkinElmer, Waltham, USA). Control wells were prepared containing medium and treatments without cells to obtain a value for background luminescence.

2.3.2.2 Analysis

Background readings were subtracted from all test measurements. The average from the luminescence readings was calculated and all treated samples were normalized to controls.

2.3.2.3 Statistical Analysis

Averages and Standard error of the means (SEM) were calculated and Stats Direct was used to test whether data followed a normal distribution using a Shapiro Wilke test. As the data did not follow a normal distribution, a Kruskal-Wallis and Conover-Inman post hoc tests were used to investigate significant differences. Results were considered statistically significant when $P \leq 0.05$.

2.3.3 MTS Assay

The CellTiter 96[®] Aqueous One solution Cell Proliferation Assay (Promega) is a colourmetric method for determining the number of live cells in proliferation assays. The celltiter 96[®] Aqueous One Solution Reagent contains a novel tetrazolium compound [3-(4,5-dimethylthiazol-2-yl)-5-(3-arboxymethoxyphenyl)-2-(4-sulfophenyl)-2H-tetrazolium, inner salt; MTS] and electron coupling reagent (phenazineethosulfate; PES). PES has enhanced chemical stability, which allows it to be combined with MTS to form a stable solution. The MTS tetrazolium compound is bio-reduced by cells into a coloured formazan product that is soluble in culture medium (Figure 2.4). This conversion is presumably accomplished by NADH or NADH produced by

dehydrogenase enzymes in metabolically active cells. The quantity of formazan is directly proportional to the number of living cells in culture.

2.3.3.1 Methodology

Following treatment, 20 µl of CellTiter 96[®]Aqueous One Solution Reagent was pipetted into each well of the 96 well plate containing the samples in 100 µl of culture medium. The plate was allowed to incubate at 37°C for 2 hours in a humidified, 5% CO₂ atmosphere prior to recording absorbance at 490nm using Wallac 1420 colourmetric detector. Control wells were prepared containing medium without cells to obtain a value for background.

2.3.3.2 Analysis

The absorption values for the background readings in the wells with complete medium were subtracted from the control and treated samples. Then the average for control and treated cells was calculated and the result of treated samples was normalized to the average of control cells.

2.3.3.3 Statistical Analysis

Average and Standard error of the mean (SEM) was calculated and Stats Direct was used to test whether data followed a normal distribution using a Shapiro Wilke test. Data did not follow a normal distribution, thus Kruskal-Wallis and Conover-Inman post-hoc tests were used to investigate significant differences. Results were considered statistically significant when $P \leq 0.05$.

Here, results of cell viability using trypan blue exclusion assay and CellTiter-Glo[®]Luminescent Cell Viability Assay were shown to be more reliable. CellTiter-Glo[®]Luminescent Cell Viability Assay required only few minutes to generate a measurable signal and providing an advantage over MTS assay that requires 2 h incubation to develop a signal. CellTiter-Glo[®]Luminescent Cell Viability Assay was also more suitable enumerating low cell counts due to high sensitivity. In addition the MTS assay showed high background levels, which may have been due to the fact that most of compounds used here were coloured and interfere in the assay (Table 2.10).

Characteristics	Trypan blue exclusion assay	CellTiter-Glo [®] Luminescent Cell Viability Assay	CellTiter 96 [®] Aqueous One solution Cell Proliferation Assay
Incubation	5 minutes	10 minutes	2 h
Parameter measured	Cell counting	ATP	MTS reduction
Sensitivity	1x10 ⁴ cells/ml	50 cells in a 96 well plate	800 cells in a 96 well plate
Detection	Optics and image analysis	luminescence	Colourmetric

Table 2.10: Comparison of cell proliferation assay; Trypan blue exclusion assay, CellTiter-Glo[®] Luminescent Cell Viability Assay and CellTiter 96[®] Aqueous One solution Cell Proliferation Assay.

2.4 Assays of Apoptosis

2.4.1 Annexin V/PI FITC Flow Cytometry Assay

The asymmetric distribution of plasma membrane phospholipids between inner and outer leaflets is a characteristic feature of healthy cells. Under physiological conditions, choline phospholipids (phosphatidylcholine, sphingomyelin) are exposed on the external surface of the plasma membrane while amino phospholipids (phosphatidylserine, phosphatidylethanolamine) are located on the internal surface of plasma membrane (Fadok *et al*, 1992, Koopman *et al*, 1994, van Engeland *et al*, 1998). During apoptosis the membrane phospholipid phosphatidylserine (PS) translocates to the outside leaflet of the membrane. Exposition of PS to the external cellular environment provides signals to macrophages, which then become attracted and initiate phagocytosis of the apoptotic cells (Figure 2.5).

Since detection of exposed PS provides an early quantification of apoptosis, here fluorochole-tagged 36-kDa anticoagulant protein Annexin V was used. Annexin V is a 35-36 kDa Ca²⁺ dependent phospholipids-binding protein which has a high affinity to bind to cells with exposed PS (van Engeland *et al*, 1998). Annexin V conjugated to fluorocholes including FITC, which retains its high affinity for PS and thus serves as a sensitive probe for flow cytometric analysis of apoptotic cells. Annexin V-FITC staining can identify apoptosis at earlier stages of apoptosis when PS is exposed on the external surface of plasma membrane. Annexin V-FITC staining precedes the loss of membrane

integrity that accompanies the latest stages of cell death resulting from either apoptosis or necrosis. Thus, here Annexin V-FITC (Beckton-Dickinson) was used in conjunction with propidium iodide (PI) (Sigma), a plasma membrane permeability marker, to distinguish between live, early apoptotic, late apoptotic and dead cells (Figure 2.5). Viable cells have minimal Annexin V and PI fluorescence. Cells that are in an early stage of apoptosis stain brightly with Annexin V-FITC but exclude PI. Finally, cells that are in late stages of apoptosis or are already dead stain intensely with both markers (Figure 2.4).

2.4.1.1 Methodology

Following treatment, cells were harvested into 1.5 ml Eppendorf tubes and centrifuged at 400 *g*, 4°C for 5 min. Supernatant was removed and cells washed once in 100 μ l cold Dulbecco's phosphate buffered saline (DPBS) (Invitrogen). Following washing, supernatant was removed and cells resuspended in 100 μ l binding buffer (BB) (10 mM HEPES/NaOH, pH7.4, 140 mM NaCl, 2.5 mM CaCl₂) (Beckton-Dickinson). After washing with BB twice, cells were resuspended in 50 μ l of BB and 5 μ l of Annexin V-FITC. Cells were gently mixed and incubated for 15 min in the dark. Labelled cells were transferred to FACS tubes, and 300 μ l of PI (50 μ g/ml) (Sigma) was added and mixed gently; samples were then read directly on the flow cytometer (FACS Calibur cytometer (Becton-Dickinson, UK)) measuring fluorescence for FITC and PI. Control samples (unstained cells, cells stained with Annexin V-FITC only and cells stained with PI only) were prepared within each experiment to set up compensation and quadrants.

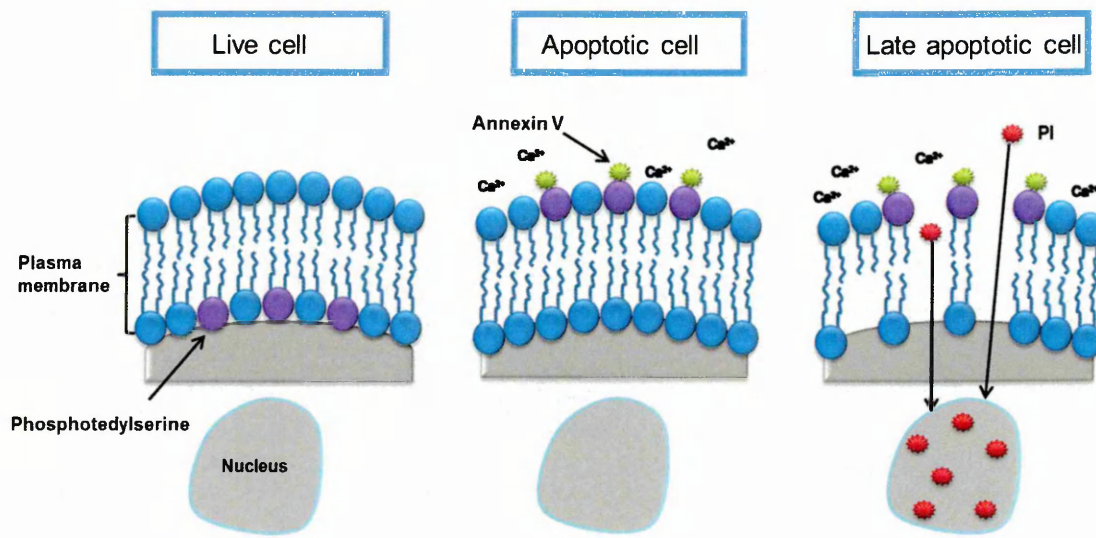


Figure 2.4: Schematic representation of phospholipid phosphatidylserine (PS) translocate to outside leaflet of the membrane

2.4.1.2 Analysis

Data were recorded from 10,000 cells per sample and analyzed using FlowJo software (Tree Star, Ashland, OR). A dot plot was used to provide a two-parameter display of FITC and PI. Control samples (unstained cells, cells stained with Annexin V-FITC only and cells stained with PI only) were prepared within each experiment to set up compensation and quadrant makers. Quadrant markers were applied to distinguish populations that are considered negative, single positive, or double positive. The dot plot in Figure 2.6 shows the lower left quadrant (live cells) displays events that are negative for both annexin V and PI. The lower right quadrant (early apoptotic cells) contains events that are positive for the Annexin V but negative for the PI. The upper-right quadrant (late apoptotic and dead cells) contains events that are positive for both annexin V-FITC and PI (Figure 2.5).

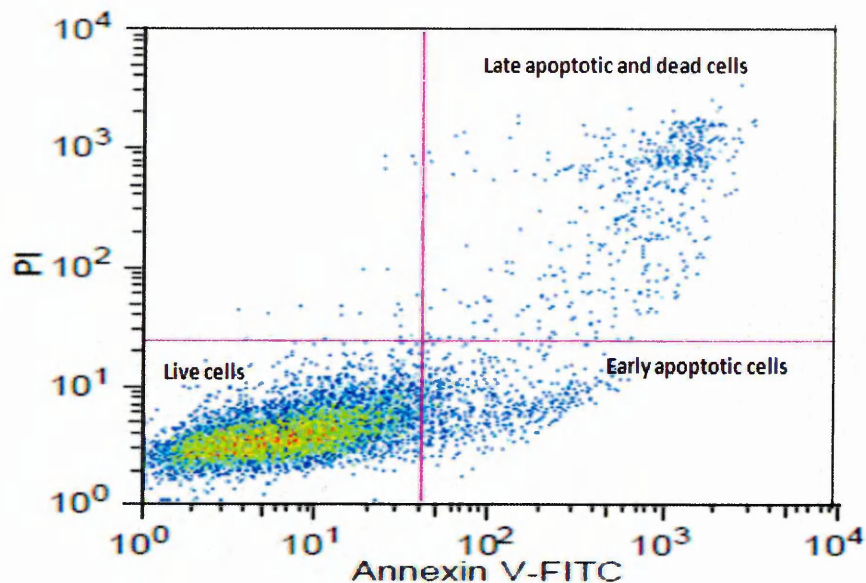


Figure 2.5: Flow cytometry analysis of Annexin V-FITC/PI. Live cells (lower left quadrant) are Annexin V and PI negative, early apoptotic cell (lower right quadrant) are Annexin V-FITC positive and PI negative and cells that are in late apoptosis or already dead (upper right quadrant) are both Annexin V-FITC and PI positive.

2.4.1.3 Statistics

Data was presented as the means \pm SEM and were analyzed by Stats Direct using Shapiro Wilke test to check for normality. Data was shown to be non-parametric, and thus a Kruskal-Wallis and Conover-Inman post hoc test was used to test for significance. $P \leq 0.05$ was considered significant.

2.4.2 DAPI Staining

Apoptotic cells can be distinguished from healthy and necrotic cells by classic morphological changes which are an important tool in apoptosis research. These features include cell shrinkage, membrane blebbing, chromatin condensation and nuclear fragmentation (Kerr *et al*, 1972, Wyllie *et al*, 1980, Galluzi *et al*, 2007). Such features can be observed under a fluorescence microscope using a DNA specific dye.

Here 4, 6-Diamidino-2-phenylindole (DAPI) was used. DAPI (Sigma) nucleic acid stain preferentially stains dsDNA; strongly binding to AT clusters in the minor groove (Gonzalez-Juanatey *et al*, 2004). Binding of DAPI stain to dsDNA results in approximately 20-fold increase in fluorescence, due to displacement of water

molecules from both DAPI and the minor groove (Barcellona *et al*, 1990). However the DAPI stain is not completely permeable, thus cells must be fixed and permabilised to enable it to pass through normal cell membranes and the blue fluorescence is then observed by fluorescent microscope via excitation by UV light at 350 nm. In cells undergoing apoptosis, the DNA has condensed and thus apoptotic nuclei will produce higher fluorescence intensity than live cells.

2.4.2.1 Methodology

Following treatment, cells were transferred to Eppendorf tubes, and centrifuged for 5 min at 400 *g*, at 4°C. The cells were then washed twice in 100 μ l of cold DPBS. Cells were then resuspended in 100 μ l of 4% (v/v) paraformaldehyde/DPBS for 10 minutes. Following fixation, cells were transferred to slides via a 20-min cytospin at 1,000 rpm (Shandon Cytospin 3 Centrifuge). Slides were then dried at room temperature and 100 μ l of DAPI stain (10 μ g/ml) (Sigma) applied to cells for 10 min in the dark at room temperature. Excess DAPI stain was removed and slides mounted in 90% glycerol and coverslips applied and sealed with nail varnish. An Olympus BX60 fluorescence microscope was used to assess the morphology of cell nuclei using UV light at excitation wavelength of 350 nm.

2.4.2.2 Analysis

Quantitative analysis of cell populations was performed based on counting of 200 randomly-selected cells and the percentage of apoptotic features determined for each sample. DAPI nuclear morphological analysis demonstrated apoptotic cells with irregular edges around the nucleus, intense staining, and chromatin concentration in the nucleus and an increased number of nuclear body fragments in late apoptotic cells. Live cells demonstrated clear-edged, round and uniformly stained with DAPI (Figure 2.6).

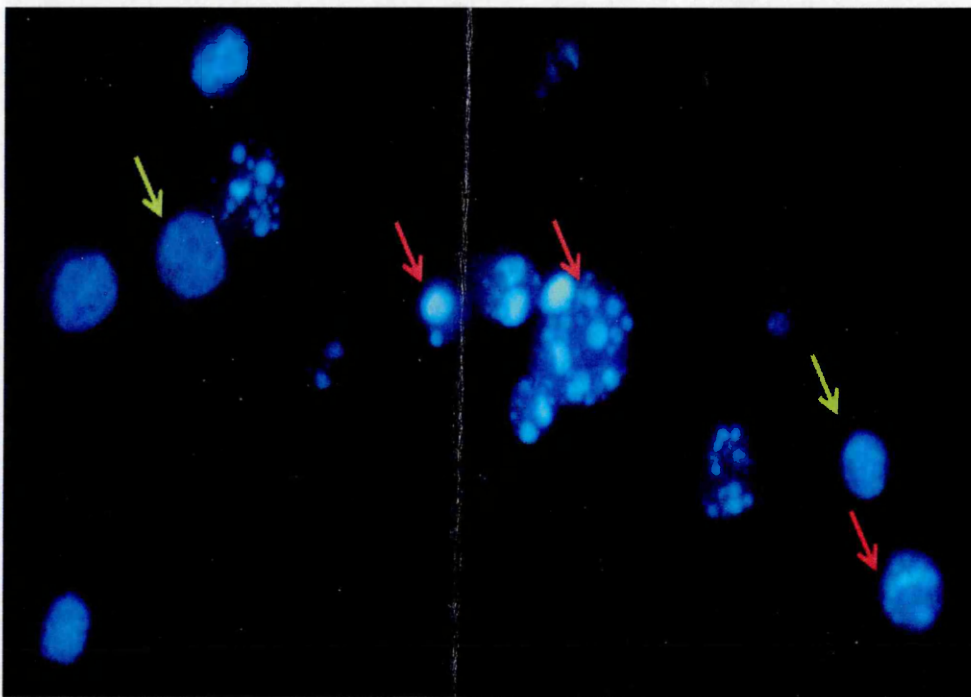


Figure 2.6: Analysis of apoptosis of HL-60 cell line using DAPI staining. Live cells are indicated by the **green arrows**, and apoptotic cells are indicated by the **red arrows**.

2.4.3 Caspase-3 Activity

Caspase-3 activation plays a central role during the apoptotic process. Caspase 3 is expressed by most leukaemic cells as a 32kDa proenzyme (Estrov *et al*, 1998). In response to several stimuli, caspase-3 is cleaved and generates two subunits of 17 and 12 kDa that fit together in a double heterodimer showing activity (Nicholson *et al*, 1995). This enzyme is activated by caspase-8 and caspase-9 and serves a convergence point for different signalling pathways. The active enzyme cleaves and activates other caspases such as caspase-6 and-7 as well as other targets such as nuclear enzyme poly ADP-ribose polymerase (PARP) and DNA fragmentation factor (DFF) (Fernandes-Alnemri *et al*, 1994). Because active caspase 3 is considered as a common effector in several apoptotic pathways, it can be a good marker to detect early apoptotic cells.

Here, the DEVD-NucView™ 488 caspase-3 substrate (Cambridge Bioscience) was used which is a fluorescence probe that allows detection of caspase-3 activity in living cells in real time. NucView 488 DNA dye is attached to caspase-3 substrate peptide sequence DEVD. When linked to the substrate peptide, the dye is unable to bind to DNA and remains non-fluorescent. The substrate crosses the plasma membrane to

enter the cytoplasm, where it can be cleaved by caspase-3 to release the high affinity DNA dye that migrates to the cell nucleus to stain the nucleus with bright green fluorescence (Figure 2.7).

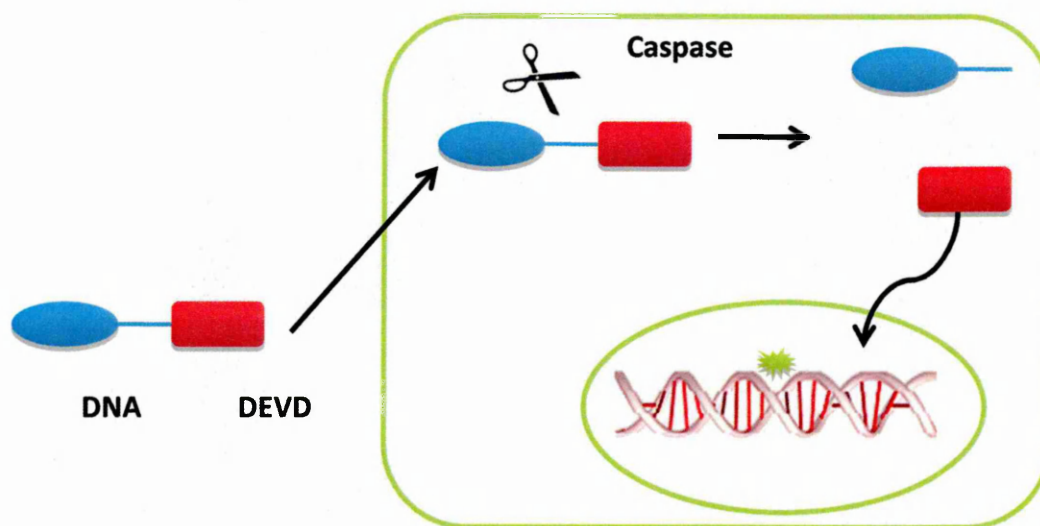


Figure 2.7: Schematic showing the principle of intracellular caspase-3 detection using NucView™ 488 caspase-3 substrate. Modified from Biotium.

2.4.3.1 Methodology

Following treatment, 200 μL of cell suspension was added to flow cytometry tubes, and 5 μL of NucView™ 488 Caspase-3 substrate added directly into the cell suspension and mixed well, cells were incubated for 20 minutes at room temperature protected from the light. Following incubation 300 μL of Dulbecco's Phosphate-Buffered Saline (DPBS) (Invitrogen, Paisley, UK) was added and samples analyzed directly on FACS Calibur Cytometer (Becton- Dickinson, UK) measuring fluorescence in the green detection channel FL-1 for FITC.

2.4.3.2 Analysis

Data was recorded from 10,000 cells per sample and analysed using FlowJo software (Tree Star, Ashland, OR, USA). Data were displayed as a single parameter histogram, showing FITC signal value against the number of events. A negative control was used to determine where the markers will be placed in the histogram. Histogram markers were used to specify a range of events for FITC. On the first histogram, marker M1 placed around the caspase-3 negative cells (live cells). Marker M2 was placed to the right of M1 to assign caspase-3 positive cells (apoptotic cells) (Figure 2.8).

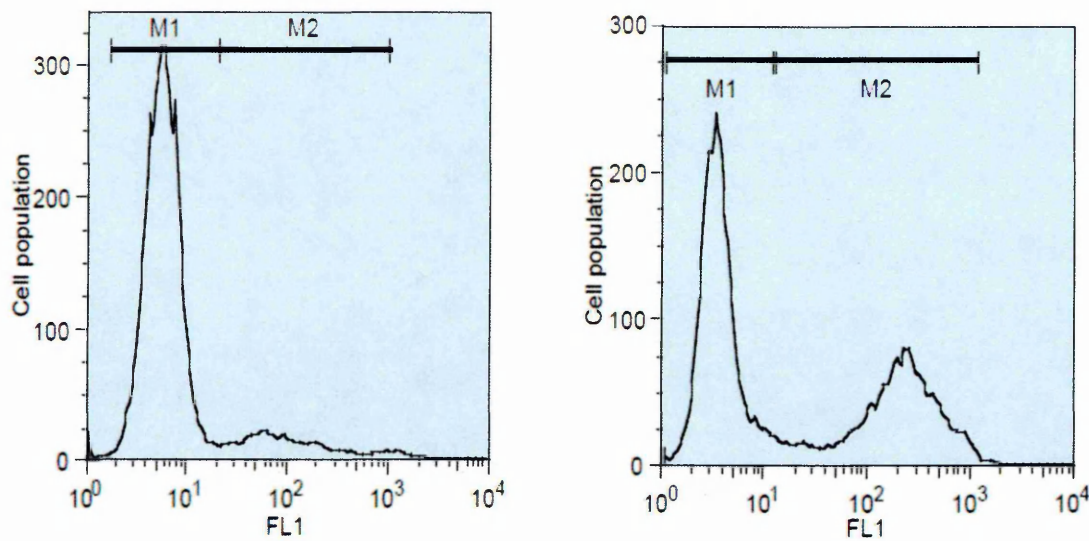


Figure 2.8: Flow cytometry histograms of caspase-3 activation using **FlowJo software**. Histogram (A): negative control of Jurkat cell line. Histogram (B) Jurkat cell line treated with PJ for 24 h. M1 indicate population negative for caspase-3 and M2 indicates population positive for caspase-3.

2.4.3.3 Statistical Analysis

Averages and Standard error of the mean (SEM) were calculated for both control and treated samples were calculated. Stats Direct was used to test whether data followed a normal distribution using a Shapiro Wilke test, the majority of data was non-parametric thus a Kruskal-Wallis and Conover-Inman post hoc test was used to investigate statistical significance. Results were considered statistically significant when $P < 0.05$.

2.5 Cell cycle Analysis by Flow Cytometry

The cell cycle consists of four distinct phases G_1 , S, G_2 and M phases. Cells in the G_0/G_1 phase have a defined amount (2x) of DNA (a diploid chromosomal DNA content). During S phase, cells contain between (2x and 4x DNA levels. Within the G_2 or M phases (G_2/M), cells have twice the amount of DNA (tetraploid chromosomal 4x DNA content) (Figure 1.2).

Based on measuring the DNA content of individual cells with a DNA binding fluorescence dye, one is able to obtain information about their distribution across cell cycle by using flow cytometry. A dye which intercalates with DNA and then becomes fluorescent such as propidium iodide (PI) is used, where DNA content is directly

proportional to the amount of fluorescent signal (Nunez, 2001). A variety of fluorescent probes have been developed for the flow cytometric analysis of cycling cells such as PI and 7-aminoactinomycin D (7-AAD), Hoechst 33342 and 33258 and 4'6'-diamidino-2-phenylindole (DAPI) (Nunez, 2001). Here, PI the most widely used fluorescent dye to stain the total cellular DNA was used. PI has red fluorescence and is excited at 488-nm wavelength of light. As PI can stain both double stranded RNA (dsRNA) and DNA (dsDNA), cells must be incubated with RNase to remove any double stranded RNA and ensure that PI staining is DNA specific. Additionally as PI is excluded by the plasma membrane of live cells, cells are fixed and permeabilized prior to adding the dye.

2.5.1 Method

Following treatment, cells were centrifuged for 5 min at 400 *g*, at 4 °C, and washed twice in 100 μ l ice-cold DPBS. Following washing, cells were stored at -20°C in 80% ethanol overnight. Fixed cells were then washed twice with 100 μ l cold DPBS and resuspended in 50 μ l of RNaseA (0.1 unit/ml) (Sigma) and 300 μ l of PI (50 μ g/ml) (Sigma). Cells were incubated at 4°C overnight prior to analysis with the FACS Calibur with excitation at 488 nm and emission at 585 nm using the FL2 channel.

2.5.2 Analysis

Data was recorded from 10,000 cells per sample and processed using FlowJo software (Tree Star, Ashland, OR, USA). Firstly, the forward scatter (FS) and side scatter (SS) were used to identify single cells (Figure 2.9 A). Then, a dot plot was applied showing pulse width vs. pulse area to gate out doublets and clumps (Figure 2.9 B). The gated single cells were plotted in a histogram, as the populations that represent PI histogram (G_0/G_1 , S, and G_2/M) are not discrete (Figure 2.9 C). The Waston Pragmatic mathematical model was used to define the population and assign percentage values in each phase. The Waston model fits G_1 and G_2 with Gaussian curves and makes no assumptions about the shape of the S phase distribution. It fits the region between the identified G_0/G_1 populations exactly by first subtracting the G_0/G_1 and G_2/M portions of the data and then builds a function that fits what remains. Because both G_2 and M phases have an identical DNA content they cannot be discriminated based on their differences in DNA content.

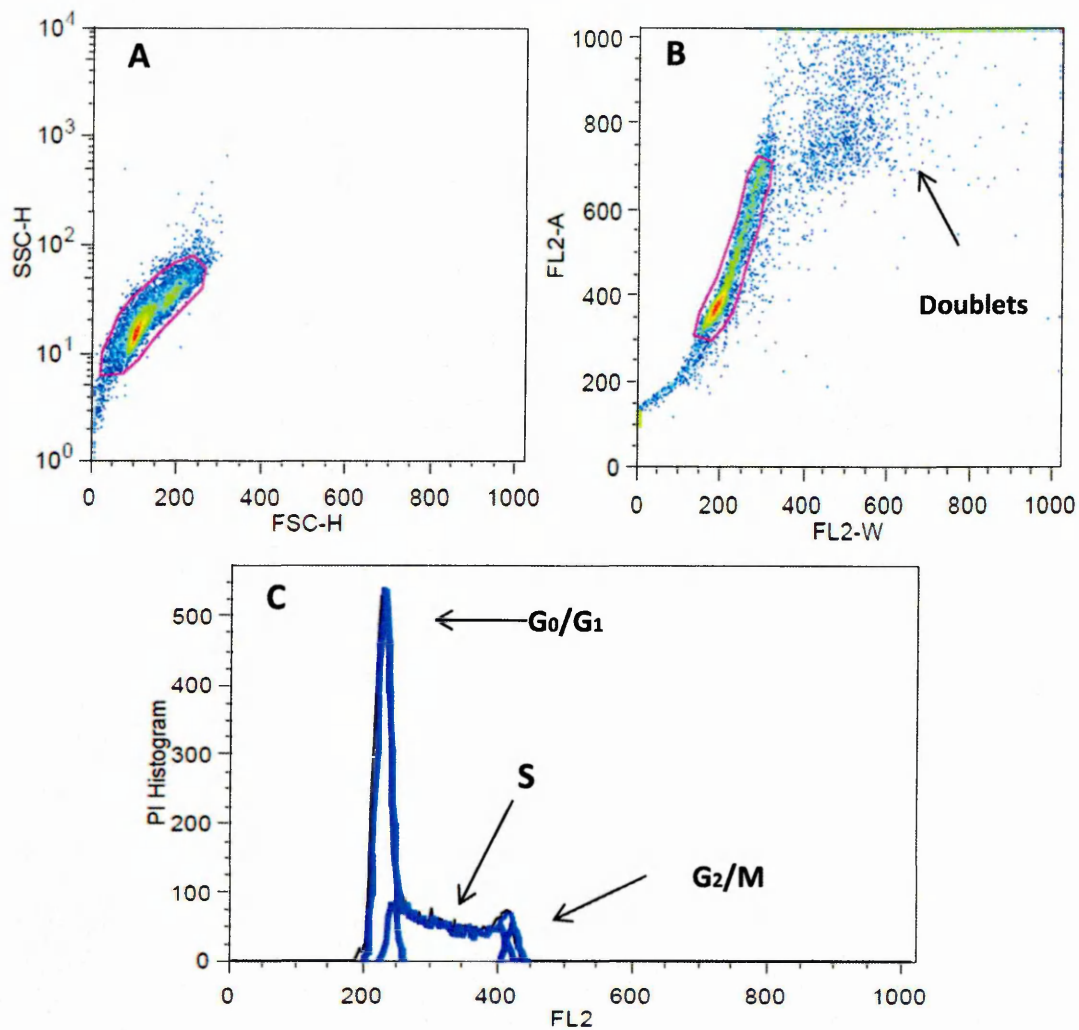


Figure 2.9: Cell cycle analysis based on flow cytometry using flowJo software. A: forward scatter (FS) and side scatter (SS). B: pulse width vs. pulse area to gate out doublets and clumps. C: PI histogram.

2.5.3 Statistical Analysis

Averages and Standard error of the mean (SEM) were calculated and Stats Direct was used to test whether data followed a normal distribution using a Shapiro Wilke test. Data did not follow a normal distribution, thus Kruskal-Wallis and Conover-Inman post hoc tests were used to investigate significant differences. Results were considered statistically significant when $P \leq 0.05$.

3. Bioactive Actions of whole
Pomegranate Juice Extract on Leukaemia
Cell Lines In vitro

3.1 Introduction

3.1.1 Pomegranate

3.1.1.2 Pomegranate History

Pomegranate is one of the oldest known edible fruits. Its history dates to very ancient times (Mars, 2000). Pomegranate cultivation and usage are greatly embedded in human history and its utilization has been found in many ancient cultures as food as well as medical remedies (Longtin, 2003). In Greek mythology it represents life generation and marriage. Sculpture representations of the fruit are found on ancient monuments of Egypt and the Assyrian ruins (Longtin, 2003; Jurenka, 2008). Thus fruit that has featured prominently by many of the major religions of the world such as Islam, Christianity, Buddhism and Zoroastrianism. In Islam for example, the Koran describes four gardens with shade, springs, and fruits-including the pomegranate. Legend holds that each pomegranate contains a seed that comes down from paradise (Langley, 2000; Longtin, 2003).

Pomegranate trees are native to the region of Persia and the Himalayan ranges of India. There are over thousands of cultivars of pomegranate which are spreading throughout the Mediterranean, China, India, as well as the American Southwest (California and Arizona) and Mexico (Levin, 1994; Langley, 2000).

Pomegranates are used in several systems of medicine for a variety of diseases. In the Indian Ayurvedic system of medicine, the pomegranate is considered “a pharmacy unto itself” and is used as a general tonic and to treat diarrhoea, ulcers and parasitic infections (Frawely, 1986; Khan, 1991; Jurenka, 2008). Pomegranate are also considered an important part of the Unani system of medicine practice in the Middle East and India where it is popularly served as a remedy for diabetes mellitus (Jurenka, 2008). Pomegranate termed “*super fruit*” has long been a symbol of life, longevity, and health (Mahdihassan, 1984). It was also chosen as a logo for the Millennium Festival of Medicine and features in the coat of arms of the British Medical Society and three royal colleges (Figure 3.1) (Langley, 2000).



Royal College of
Midwife



Royal College of
Physicians



British Medical
Association



Royal college of
Obstetricians and
Gynaecologists

Figure 3.1: Pomegranate in coats of arms of the British medical society and three royal colleges. Modified from Langley, 2000

3.1.2.2 Botanical Description

Pomegranate (*Punica granatum* L.) belongs to the family puniceaceae which consists of only two species, *Punica granatum* and *Punica protpunica*. Pomegranate grows as a small tree or a large shrub reaching 12-16 ft tall, and can live over 20 years. It has spiny branches, glossy lance shaped leaves, with bark turning grey with age (Lansky and Newman, 2007; Jurenka, 2008).

The tree bears large, red, white or variegated flowers that eventually become the fruit. Its fruit is classified as a large berry, growing up to 5 inches in diameter, delimited by a leathery peel, contained within are numerous arils, each a single seed surrounded by a translucent juice containing sac. Thin acid-tasting membranes extended into interior of the fruit from the peel, giving a latticework for suspending the arils (Lansky and Newman, 2007; Jurenka, 2008).



Figure 3.2: Illustrated pomegranate fruit and tree.

3.1.2.3 Pomegranate Chemical Constitutes

Different types of phytochemicals have been identified within the different parts of the pomegranate tree, including fruits and seeds. The major class of pomegranate phytochemicals is the polyphenols (phenolic rings bearing multiple hydroxyl groups) that predominant in the fruit (Viuda-Marrots *et al*, 2010). Pomegranate fruit polyphenols include flavonoids (flavonols, flavanols, and anthocyanins), condensed tannins and hydrolysable tannins (ellagitannins and gallotannins). Other phytochemicals identified from pomegranate are organic and phenolic acids, sterols, and titerpenoids and alkaloids (Artik, 1998; Halvorsen *et al*, 2002; Afaq *et al*, 2005; Lansky and Newman, 2007).

The major source of dietary pomegranate phytochemicals is the fruit. The fruit can be divided to three parts, the seeds, the arils and the peel including the interior network of membranes (Figure 3.3). Edible part of the fruit (50%) represents 40% arils (juice obtain from arils) and 10% seeds. The juice contain 85% water, 10% total sugar mainly fructose and glucose, and 1.5% pectin (Aviram *et al*, 2000; Tezcan *et al*, 2009)

Minerals in pomegranate juice include iron, calcium, cerium, chloride, copper, chromium, caesium, potassium, magnesium, manganese, molybdenum, sodium, rubidium, selenium, scandium, tin, strontium, and zinc (Waheed *et al*, 2004). Alkaloids were mainly found in the juice as well as in the bark of the both stem and the root. There are two main types of alkaloids involving piperidines and pyrrolinidines identified in pomegranate plants (Badria, 2000). Organic acids in pomegranate juice are mainly straight chain fatty acids, of which citric acid and malic acid are the major compounds with content up to 4.5 and 1.75 g/L, respectively. In addition, tartaric acid and succinic acid were also identified in the juice of pomegranate (Poyrazoglu *et al*, 2002; Tezcan *et al*, 2009).

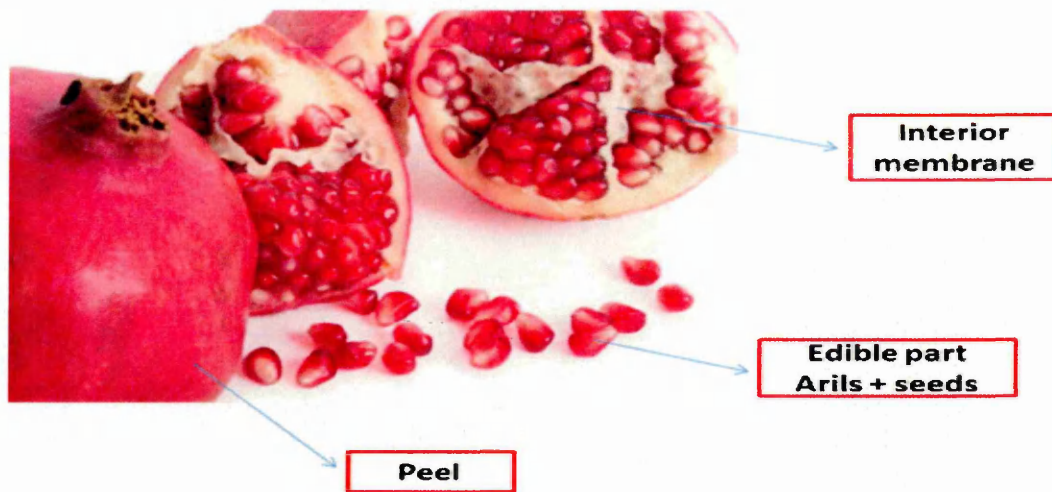


Figure 3.3: Illustrates pomegranate fruit parts (peel, arils and seeds).

The main classes of polyphenols found in pomegranate juice are the flavonoids, phenolic acids, and hydrolysable tannins. The soluble polyphenol content in pomegranate juice has been identified to vary within the limits of 0.2% to 1.0% (Ben Nasr *et al*, 1996).

The flavonoids in pomegranate juice include flavonols flavan-3-ols and anthocyanins. Flavonols that have been identified in pomegranate juice include quercetin and rutin (Artik, 1998), and flavan-3-ols such as catechin, epicatechin, and epigallocatechin 3-gallate (EGCG) (De Pascuala-Teresa *et al*, 2000). Anthocyanins are the largest and most important group of flavonoids present in the juice. They are responsible for the red colour of pomegranate juice (Hernandez *et al*, 1999). The main anthocyanins identified in pomegranate juice are cyanidin-3-glucoside, Cyanidin-3,5-diglucoside, pelargonidin-3-glucoside, pelargonidin-3,5-diglucoside, delphinidin-3-glucoside, delphinidin-3,5-diglucoside (Hernandez *et al*, 1999; Reed *et al*, 2005).

Phenolic acid are non-flavonoids polyphenols. They can be divided into two main types: (1) hydroxycinnamic acid, principally caffeic acid, *p*-cumaric acid, and chlorogenic acid; and (2) hydrobenzoic acid, mainly ellagic acid and gallic acid.

Hydrolysable tannins are high molecular weight plant polyphenols. They are found in the arils and account for 92% of the antioxidant activity of pomegranate fruit (Gil *et al*,

2000). The predominant hydrolysable tannins in pomegranate juice is punicalagin, which is responsible for about 50% of its antioxidant capacity (Gil *et al*, 2000).

The chemical composition of pomegranates can vary depending on the cultivar, growing region, climate, maturity and storage conditions and part of the plant (Poyrazoglu *et al*, 2002; Barzegar *et al*, 2004; Fadvi *et al*, 2005). It has been reported over the years by different researches significant variations in organic acids, phenolic compounds, sugar, and minerals found in pomegranates (Aviram *et al*, 2000; Mirdehghan and Rahemi, 2007). Gozlekci and his colleagues (2011) investigated the total phenolic distribution of peel, juice, and seed extracts of four Turkish pomegranate cultivars using Folin-Ciocalteu colourmetric method, demonstrating the phenolic compounds altered depending on cultivars and fruit parts.

3.1.2.4 Bioavailability and Toxicity of Pomegranate

Despite the evidence in favour of pomegranate use, extensive studies are needed to fully understand its possible contribution to human health before recommending its regular consumption. The absorption, bio-availability, bio-distribution, and metabolism profile of pomegranate compounds has not yet been completely characterized. A small number of clinical studies have tested the metabolic profile of certain pomegranate derived compounds, such as ellagic acid. Seeram *et al*, 2006 reported that healthy subjects who consumed 10 ml of concentrated PJ exhibited presence of ellagic acid metabolites in plasma as well as in urine. It has been proposed that dimethylellagic acid glucuronide in human plasma and urine samples after consumption of the fruit juice concentrate is a reliable biomarker of pomegranate intake (Seeram *et al*, 2006). In general, the metabolites present in humans following PJ consumption matches those found in rats fed with pomegranate extracts (Cerdeja *et al*, 2003a).

Pomegranate and its constituents have safely been consumed for centuries across the world without any adverse effects. Toxicity of punicalagin, an abundant antioxidant polyphenol in PJ, was investigated in rats (Jurenka, 2008). Demonstrating no toxic effects or significant differences were detected in the treatment group compared to controls (Cerdeja *et al*, 2003b). In another study, no toxic effect on blood chemistry analysis for kidney, liver and heart was observed in patients with carotid artery

stenosis who consumed PJ for up to three years. However, a number of studies have shown toxic effect after intake of pomegranate products (Lansky and Newman, 2007) and Hedge *et al*, (2002) reported allergic reactions after consumption of pomegranate fruit.

3.1.2.5 Pomegranate and Health

Recent years, have seen a great interest on the part of consumers, researchers, and the food industry into how food products may help maintain health and the role that diet plays in the prevention and treatment of many illnesses has become widely accepted (Johanningsmeier and Harris, 2011). At the present time, considerable importance is given to functional foods that provide physiological benefits and are useful in disease prevention or slowing the progression of chronic diseases in a manner beyond their basic nutritional functions (Johanningsmeier and Harris, 2011).

This fruit, which has been consumed and used as medicinal food in Middle East for thousands of years, has recently gained popularity in various parts of the world (Johanningsmeier and Harris, 2011). The current explosion of research into pomegranates is evidenced by a science direct search from 2000 to 2012, revealing a significant increase in new scientific papers concerning pomegranate (Figure 3.4).

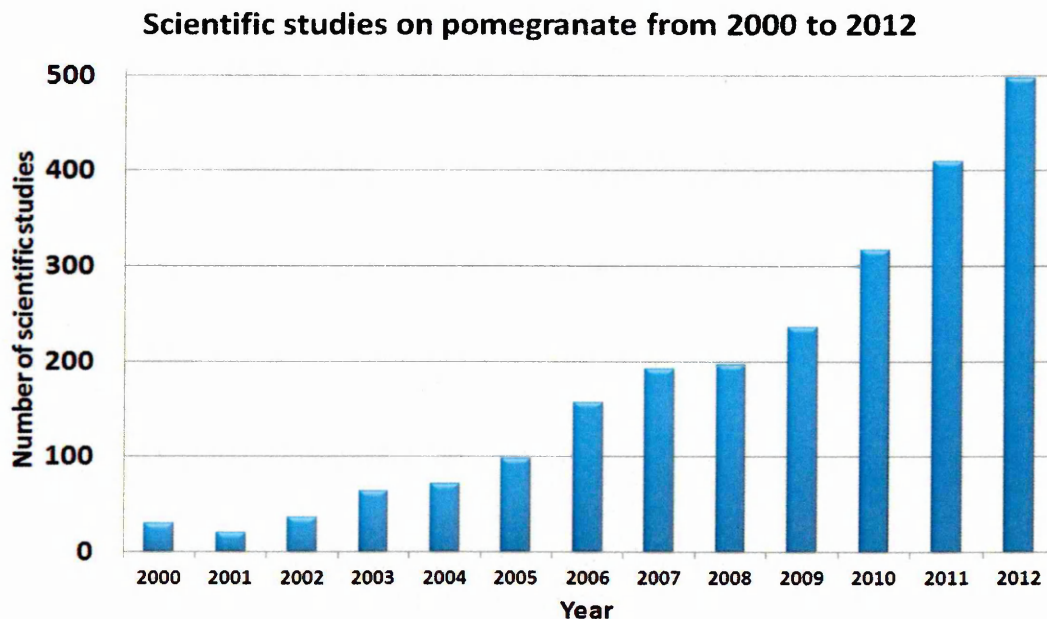


Figure 3.4: Increase in the number of scientific papers on pomegranate and its constituents from 2000 to 2012.

The high antioxidant content of pomegranate the fruit and juice as compared with other fruits and antioxidant beverages has been the basis for much of proposed health benefits and has stimulated interest in research on potential nutraceutical and functional food applications. Seeram *et al*, 2008b have reported that PJ had a higher antioxidant potency composite index and total polyphenol content in comparison to common fruit juices (orange, grape-fruit, grape, cranberry, pear, pineapple, apple, red wines, iced tea and black cherry); as demonstrated by using four antioxidant tests (Trolox equivalent antioxidant activity (TEAC), total oxygen radical absorbance capacity (ORAC), free radical scavenging capacity by 2,2-diphenyl-1-picrylhydrazyl (DPPH), and ferric reducing antioxidant power (FRAP); and the antioxidant activity was at least 20% higher than any of the other juices tested. In addition, pomegranate juice was shown to have a 3-fold higher antioxidant activity than that of red wine and green tea (Gil *et al*, 2000) and 2-, 6- and 8-fold higher levels than those identified in grape, grapefruit, and orange juices, respectively (Azadzoi *et al*, 2005; Rosenblat and Avriam, 2006). The high antioxidant activity may relate to the variety of phenolic compounds present in pomegranate, including punicalagin, ellagic acid derivatives and anthocyanins. Such compounds are identified for their properties to scavenge free radicals and to inhibit lipid oxidation *in vitro* (Gil *et al*, 2007; Noda *et al*, 2002).

The functional and medicinal effect of pomegranate fruits and its derivatives have shown to act as anti-diabetic (Katz *et al*, 2007), anti-viral (Neurath *et al*, 2005), anti-tumour and anti-inflammatory (Ahmed *et al*, 2005) and improve cardiovascular diseases such as atherosclerosis, hyperlipidemia and hypertension (Aviram *et al*, 2000; Fuhman *et al*, 2010). They also help to prevent Alzheimer's disease (Singh *et al*, 200) and improve sperm quality (Turk *et al*, 2010) and they can improve skin (Pachco-Palencia *et al*, 2000; Afaq *et al*, 2009) and oral health (Vasconcelos *et al*, 2003) (Figure 3.5).

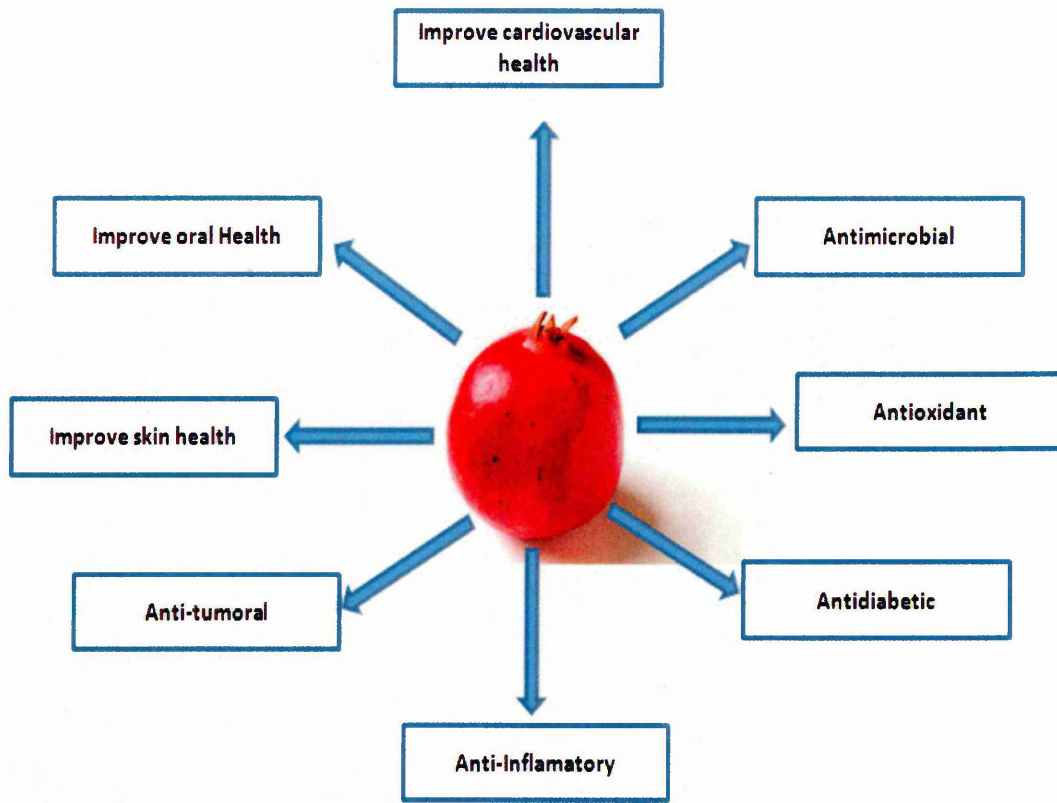


Figure 3.5: Functional and medicinal effect of pomegranate. Modified from E Mendoza *et al*, 2011

In terms of anti-tumour properties pomegranate has shown potential in the treatment of solid tumour as anti-proliferative, and pro-apoptotic agents in many cancer cell lines and animal models of colon, breast, prostate, skin and lung cancers (Table 3.1). Of these, prostate cancer has been the most well studied, and it has made significant progress in assessment of the chemo preventive and therapeutic potential of pomegranate derived phytochemicals in prostate cancer with an initial phase II clinical trial reporting a significant prolongation of prostate cancer antigen doubling time in patients with prostate cancer (Pantuck *et al*, 2006). However, few studies have investigated the potential of pomegranate juice extract (PJ) in the treatment of leukaemia. Kawaii and Lansky (2004) evaluated the effect of fresh and fermented pomegranate juice on HL-60 human leukaemia cell line differentiation. Their study demonstrated that treatment with PJs induced differentiation of HL-60 cells and inhibition of cellular proliferation (Kawaii and Lansky, 2004). No studies to date have

investigated the effects of PJs on non-tumour cells, and thus selective toxicity to cancer cells has not previously been investigated.

Cancer type	Pomegranate fraction	References
Breast	Juice, seed-oil, fermented juice polyphenols, extract	Kim <i>et al.</i> (2002) Mehta and Lansky (2004), Toi <i>et al.</i> (2003), Jeune <i>et al.</i> (2005), Khan <i>et al.</i> (2009), Grossmann <i>et al.</i> (2010), Adams <i>et al.</i> (2010), Tran <i>et al.</i> (2010).
Prostate	Seed-oil, fermented juice polyphenols, extract, juice	Seeram <i>et al.</i> (2005), Lansky (2) <i>et al.</i> (2005), Albrecht <i>et al.</i> (2004), Seeram <i>et al.</i> (2007), Sartippour <i>et al.</i> (2008), Malik <i>et al.</i> (2005), Hong <i>et al.</i> (2008), Rettig <i>et al.</i> (2008), Koyoma <i>et al.</i> (2010), Kasimsetty <i>et al.</i> (2009), Pantuck <i>et al.</i> (2006)
Lung	Fruit extract	Khan <i>et al.</i> (2006a)
Colon	Seed-oil, juice	Kohono <i>et al.</i> (2004), Adams <i>et al.</i> (2006), Saruwatari <i>et al.</i> (2008), Sharma (2010)
Skin	Seed-oil, fruit extract	Hora <i>et al.</i> (2003), Pacheco-Palencia <i>et al.</i> (2008). Zaid <i>et al.</i> (2007), Syed <i>et al.</i> (2006)
Leukaemia	Fresh and fermented juice	Mertens-Talcott and Percival (2005), Kawaii and Lansky (2004)

Table 3.1: Summary of studies of pomegranate different cancers.

3.2 Objective

This study investigated the hypothesis that PJ can induce cell death and prevent cellular replication to a greater extent in leukaemia cells than non tumour control cells.

3.3 Experimental Design

3.3.1 Treatment

Eight leukaemia cell lines 4 lymphoid (Jurkat, SUP-B15, MOLT-3 and CCRF-CEM) and 4 myeloid (HL-60, THP-1, K562, KG1a) in addition to CD133 (Normal human HSCs) were maintained as described in section 2.2.2. PJ was prepared as mentioned in section 2.1 and used for the treatment of cells at concentrations: 0%; 6.25; 12.5 and 25% for 24

and 48 h following treatment induction of apoptosis and cell cycle arrest were investigated (Table 3.2).

Techniques	Treatment	Concentration	Cell lines	Time point
Trypan blue	PJ	6.25%, 12.5%, and 25%	8 leukaemia cell lines + non-tumour HSsc	24 and 48 hr
Annexin V-FITC/PI	PJ	6.25%, 12.5%, and 25%	8 leukaemia cell lines + non	24 and 48 hr
DAPI Staining	PJ	6.25%, 12.5%, and 25%	8 leukaemia cell lines + non	24 and 48 hr
Cell cycle	PJ	6.25%, 12.5%, and 25%	8 leukaemia cell lines	24 and 48 hr

Table 3.2: Experimental design for Chapter 3.

3.3.2 Assessment of Apoptosis

We investigated the effect of PJ in terms of induction of apoptosis by using two techniques; Annexin V-FITC/PI and DAPI staining.

3.3.2.1 Annexin V-FITC /PI Stain Assay

Cells were plated in 12 well plate at cell density 5×10^5 per well and incubated with PJ at different concentrations (6.25%, 12.5% and 25%) for 24 and 48 h. Annexin V/PI FITC stains were used to detect apoptosis based on flow cytometry as described previously 2.4.1. Data was recorded from 10,000 cells per sample and analysed using FlowJo software (Tree Star).

3.3.2.2 DAPI Stain

Following treatment with PJ at concentrations 6.25%, 12.5% and 25% for 24 and 48 h at cell density 5×10^4 , cells were stained with DAPI to observe apoptotic morphology as explained before in section 2.4.2. Cells were investigated using Olympus BX60 fluorescence microscope using UV light at excitation wavelength 350 nm.

3.3.3 Cell viability Assay

All cell lines in addition to normal HSCs were seeded in 12 well plates and at concentration 5×10^5 per well and treated with PJ at concentration 6.5%, 12.5% and 25% PJ for 24 and 48 h. Cell viability was measured by trypan blue exclusion using the countess™ automated cell counter as described in section 2.3.1. All experiments were

performed in quadruplicate. Percentage of cell viability was calculated by normalizing to untreated samples.

3.3.4 Cell Cycle Analysis

The effect of PJ on cell cycle of all leukaemia cell lines and normal HSCs were investigated using a PI stain, and analyzed using flow cytometry as describe in section 2.5 following treatment with PJ at concentration 6.25%, 12.5% and 25% for 24 h at cell density 5×10^5 . Data from 10,000 cells per sample were recorded and percentages of cells within G_0/G_1 , S and G_2/M cell cycle phase were determined with FlowJo software and Waston (pragmatic) analysis of cell cycle (Tree Star).

3.3.5 Statistical Analysis

Average and Standard error of the mean (SEM) was calculated and Stats Direct was used to test whether data followed a normal distribution using a Shapiro Wilke test. Data did not follow a normal distribution, thus Kruskal-Wallis and Conover-Inman post hoc tests were used to investigate significant differences. Results were considered statistically significant when $P \leq 0.05$.

3.4 Results

3.4.1 Effect of PJ on Induction of Apoptosis Using Annexin V-FITC/PI based on Flow Cytometry

A significant ($P \leq 0.05$) decrease in the number of live cells and increase in the number of apoptotic and dead cells when assessed at 24 and 48 h post treatment with PJ was seen in all leukaemia cell lines (Figure 3.6 and 3.7). However, within the leukaemia cell lines and non-tumour primary HSCs different levels of sensitivity were observed, where was the most affected of all the leukaemia cell lines while THP-1 was the least affected leukaemia cell lines. In myeloid cell lines KG-1a was the affected cells comparing with the same lineage of cells. Interestingly, CD133 (non-tumour primary HSCs) was the least affected cells compared to all leukaemia cell lines (Figure 3.6 and 3.7).

Live Cells Following Treatment with PJE for 24 h

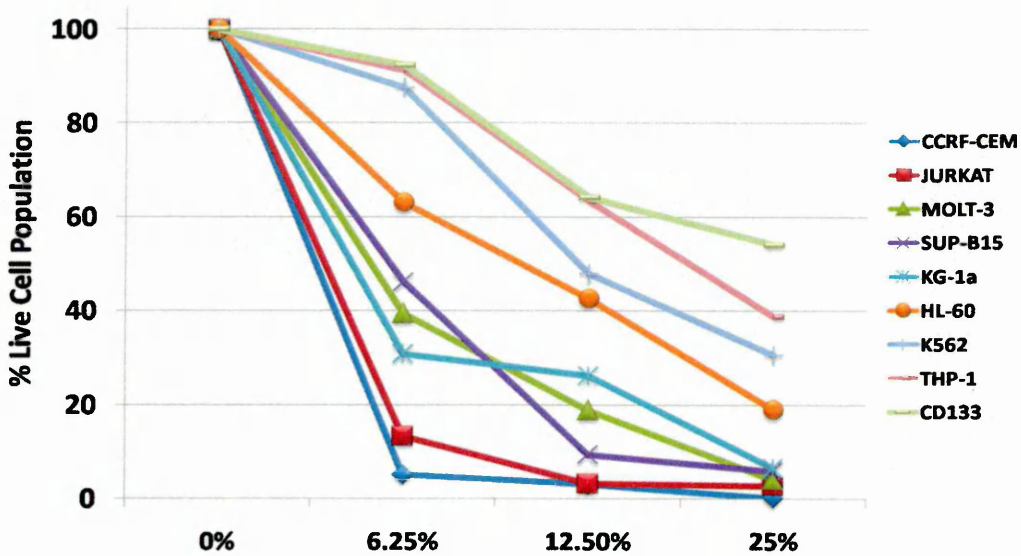


Figure 3.6: Annexin V-FITC/ PI of live cell populations normalized to untreated controls in 4 lymphoid leukaemia cell lines (CCRF-CEM, JURKAT, MOLT-3, SUP-B15), 4 myeloid leukaemia cell lines (KG-1a, HL-60, K562, THP-1), and non-tumour hematopoietic stem cells (CD133) following treatment PJ for 24 h. n=3.

Live Cells Following Treatment with PJE for 48 h

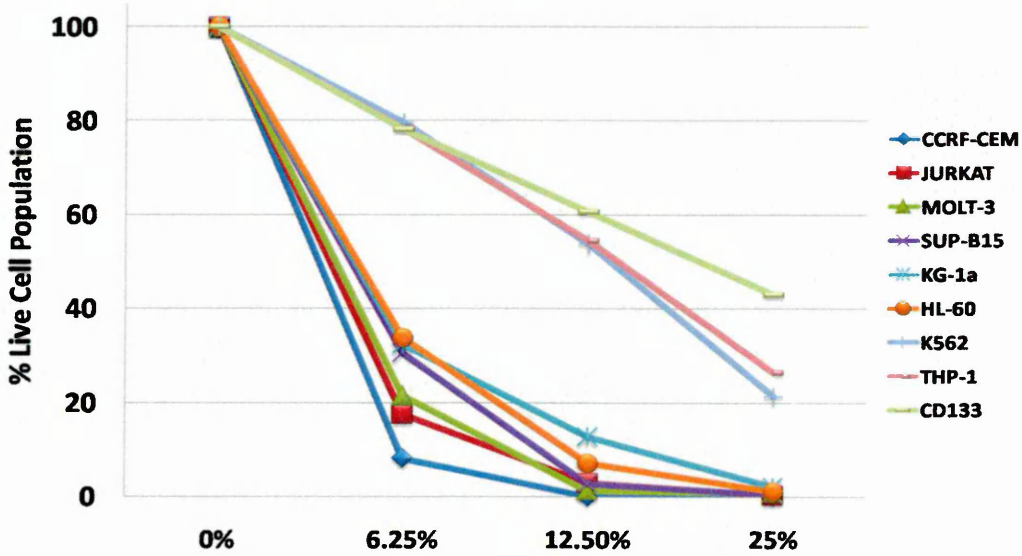


Figure 3.7: Annexin V-FITC/ PI of live cell populations normalized to untreated controls in 4 lymphoid leukaemia cell lines (CCRF-CEM, JURKAT, MOLT-3, SUP-B15), 4 myeloid leukaemia cell lines (KG-1a, HL-60, K562, THP-1), and non-tumour hematopoietic stem cells (CD133) following treatment PJ for 48 h. n=3.

CCRF-CEM the most affected cell line and showed a significant ($P \leq 0.05$) decrease in viable cells following 24 and 48h treatment with 6.25%, 12.5% and 25% of PJ (Fig 3.8). At low concentration (6.25%) of PJ approximately 90% decrease in the number of live cells was observed following 24 and 48 h. Treatment with high concentration of PJ (25%) showed no live cells remaining after 24 or 48h. Both early apoptotic and dead cells were significantly ($P \leq 0.05$) increased following treatment with all concentrations of PJ after 24 and 48 h incubation (Fig 3.8).

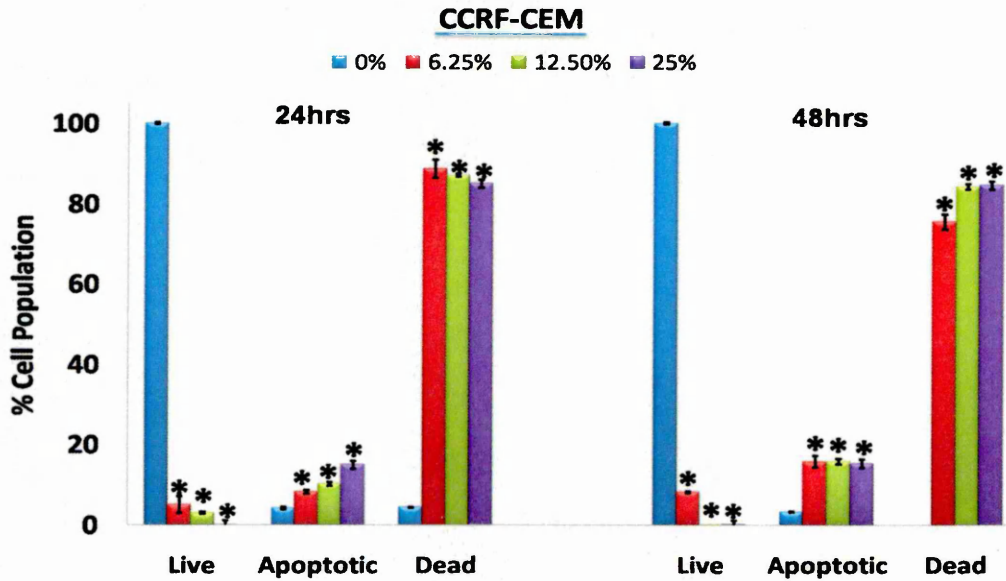


Figure 3.8: Annexin V-FITC/ PI based on flow cytometry following treatment with PJ (0%, 6.25%, 12.5% and 25%) for 24 and 48 h on CCRF-CEM. Mean \pm SEM. * indicates significant difference ($P \leq 0.05$) vs. untreated control. n= 3.

Jurkat cell lines following treatment with PJ after 24 and 48 h incubation showed a significant ($P \leq 0.05$) decrease in the number of live cells in a dose dependent manner at 6.25%, 12.5% and 25% (Figure 3.9). More than 80% decrease in the number of live cells was detected at low concentrations (6.25%) of PJ following incubation times. At high concentration (25%) of PJ approximately 97% and 99% decrease in live cells was observed after 24 and 48 h incubation respectively. Apoptotic and dead cells showed a significant ($P \leq 0.05$) increase at all concentrations following 24 and 48 h (Figure 3.9).

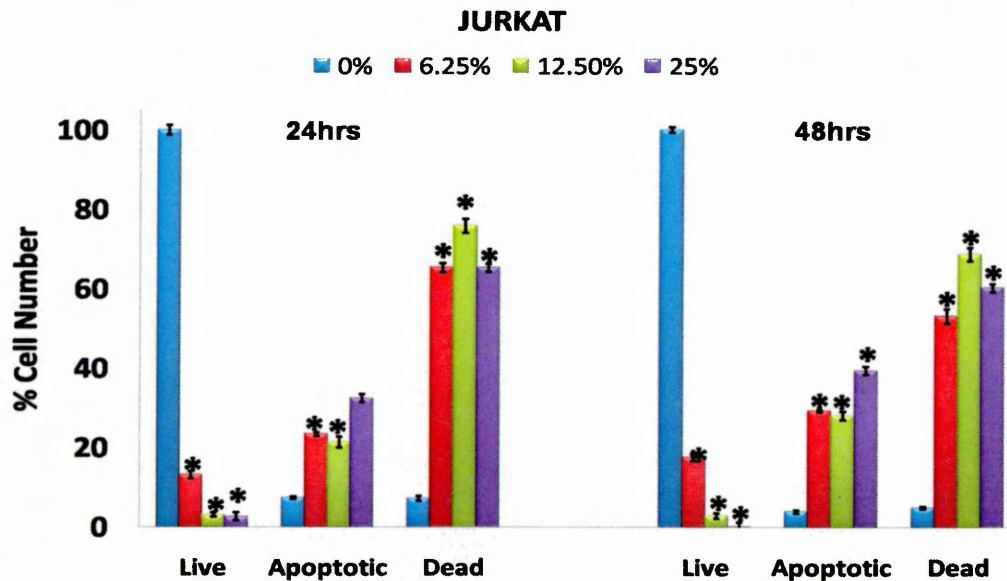


Figure 3.9: Annexin V-FITC/ PI based on flow cytometry following treatment with PJ (0%, 6.25%, 12.5% and 25%) for 24 and 48 h on Jurkat. Mean \pm SEM, * indicates significant difference ($P \leq 0.05$) vs. untreated control. n= 3.

MOLT-3 cell lines illustrated a significant ($P \leq 0.05$) decrease in the number of live cells following treatment with PJ at concentration 6.25%, 12.5% and 25% (v/v) following 24 and 48 h incubation (Figure 3.10). At concentration 12.5% and 25% following 48 h treatment with PJ more than 99% decreased in the number of live cells was detected. The number of apoptotic and dead cells significantly ($P \leq 0.05$) increased following treatment with PJ at all concentrations following 24 and 48 h incubation times (Figure 3.10).

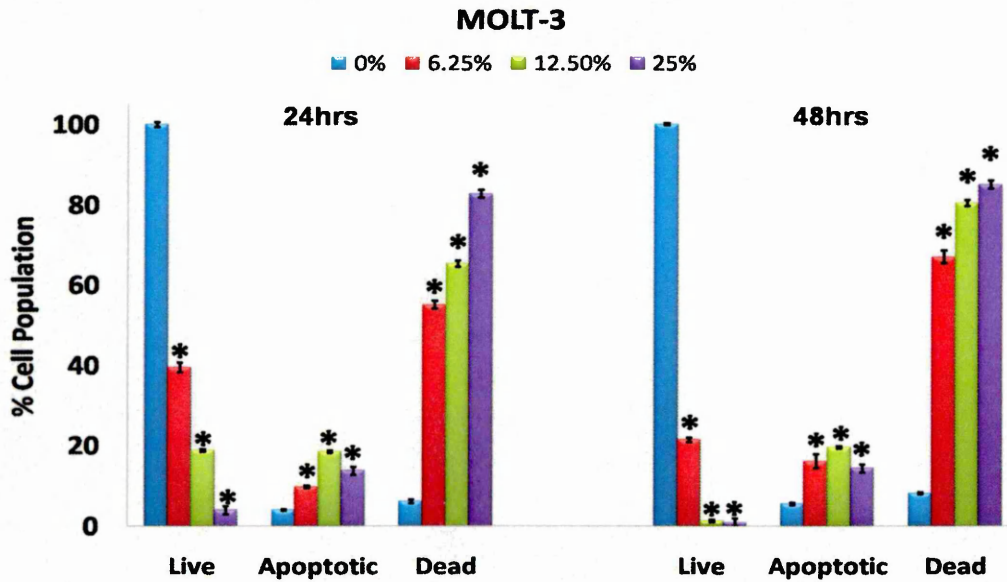


Figure 3.10: Annexin V-FITC/ PI based on flow cytometry following treatment with PJ (0%, 6.25%, 12.5% and 25%) for 24 and 48 h on MOLT-3. Mean \pm SEM. * indicates significant difference ($P \leq 0.05$) vs. untreated control. n= 3.

SUP-B15 cells also showed a significant ($P \leq 0.05$) decrease in the number of live cells and significant increase in the number of apoptotic and dead cells after treatment with PJ following 24 and 48 h incubation (Figure 3.11). Treatment with lowest concentration (6.25%) of PJ showed the smallest decrease in the number of live cells compared with other lymphoid cell lines with 46% and 30% decrease following 24 and 48 h respectively (Figure 3.11).

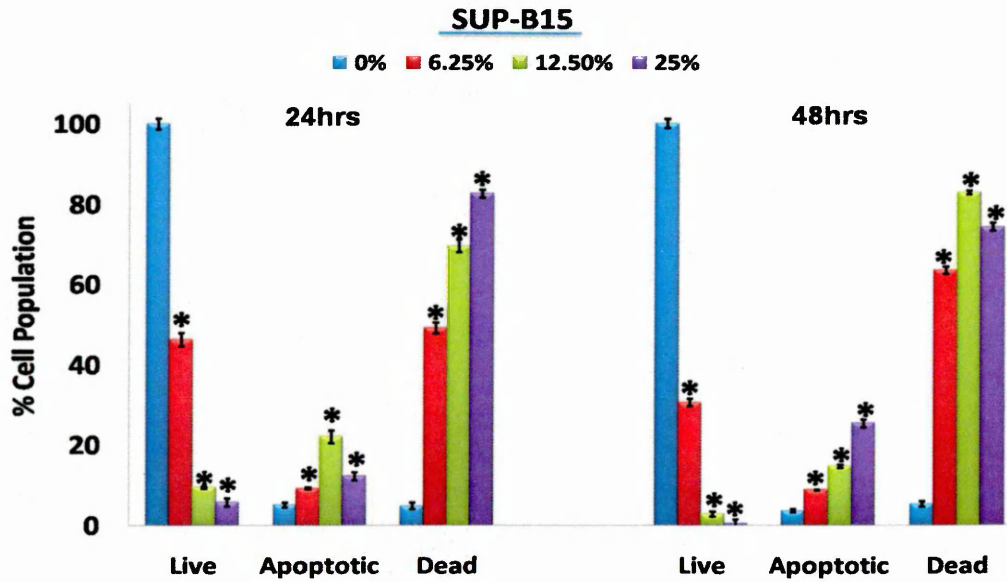


Figure 3.11: Annexin V-FITC/ PI based on flow cytometry following treatment with PJ (0%, 6.25%, 12.5% and 25%) for 24 and 48 h on SUP-B15. Mean \pm SEM * indicates significant difference ($P \leq 0.05$) vs. untreated control. n= 3.

KG-1a showed the greatest sensitivity to PJ than the other myeloid leukaemia cell lines. Live cells showed a significant ($P \leq 0.05$) decrease when treated with 6.25%, 12.5% and 25% after 24 and 48 h when compared to control (Figure 3.12). Percentage of live cell population was not significantly different between time points when treated with 6.25% of PJ. The number of live cells decreased by half after 48 h compared with 24 h incubation following treatment with 12.5% of PJ ($P \leq 0.05$). At highest concentration 25% of PJ caused 98% decrease in the number of live cells. Significant increase in the number of apoptotic and dead cells was shown after treatment with all concentrations of PJ (Figure 3.12).

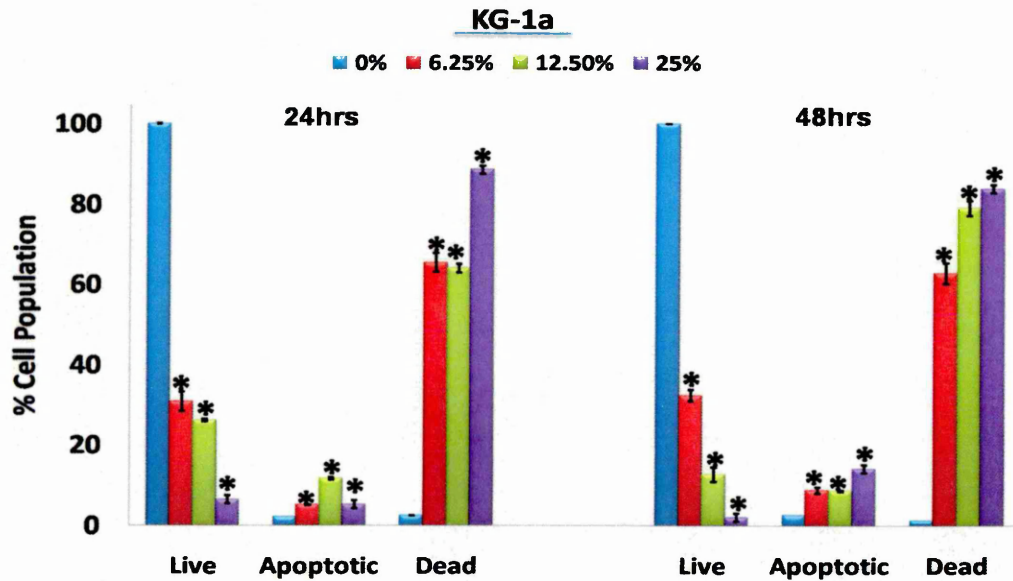


Figure 3.12: Annexin V-FITC/ PI based on flow cytometry following treatment with PJ (0%, 6.25%, 12.5% and 25%) for 24 and 48 h on KG1a. Mean \pm SEM. * indicates significant difference ($P \leq 0.05$) vs. untreated control. n= 3.

Treatment HL-60 cell lines with PJ also showed a significant decrease in the number of live cells and increase in the number of apoptotic cells at all concentrations (6.25%, 12.5% and 25%) after 24 and 48 h ($P \leq 0.05$) (Figure 3.13). Following 24 h the number of live cells decreased to 17% compared to control and following 48 h only 1% of cells remained alive (Figure 3.13).

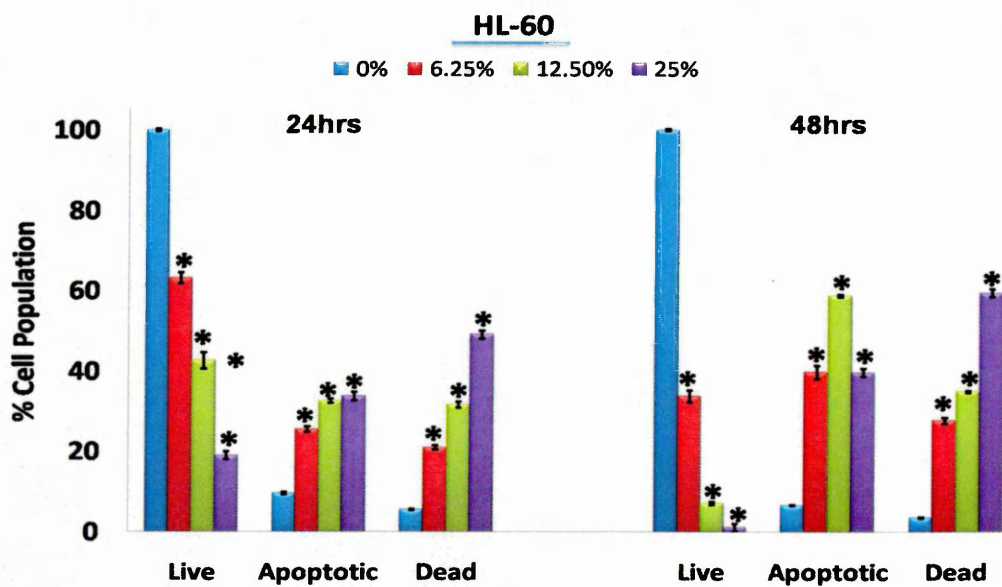


Figure 3.13: Annexin V-FITC/ PI based on flow cytometry following treatment with PJ (0%, 6.25%, 12.5% and 25%) for 24 and 48 h on HL-60. Mean \pm SEM. * indicates significant difference ($P \leq 0.05$) vs. untreated control. n= 3.

Treatment of K562 cell lines with PJ showed a significant decrease in the number of live cells and increase in the number of apoptotic cells at all concentrations (6.25%, 12.5% and 25%) after 24 and 48 h ($P \leq 0.05$) (Figure 3.14).

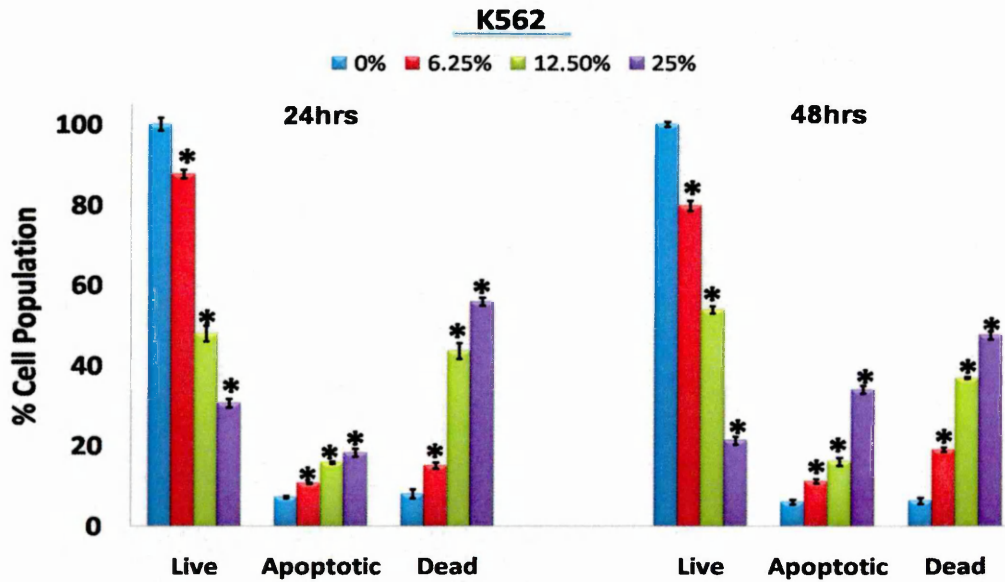


Figure 3.14: Annexin V-FITC/ PI based on flow cytometry following treatment with PJ (0%, 6.25%, 12.5% and 25%) for 24 and 48 h on K562. Mean \pm SEM. * indicates significant difference ($P \leq 0.05$) vs. untreated control. n= 3.

THP-1 cells were the most resistant leukaemia cell line, they showed a significant decrease in the number of live cells and increase in the number of apoptotic and dead cells after all time points ($P \leq 0.05$). Less than 10% decrease in the number of live cells was observed following 6.25% PJ treatment for 24 h which increased to 22% following 48 h (Figure 3.15). Apoptotic cells did not show an increase in the number of cells comparing to control when treated with PJ at concentration 6.25% after 24 h incubation, although all other treatments induced significant increases in apoptotic and dead cell populations ($P \leq 0.05$) (Figure 3.15).

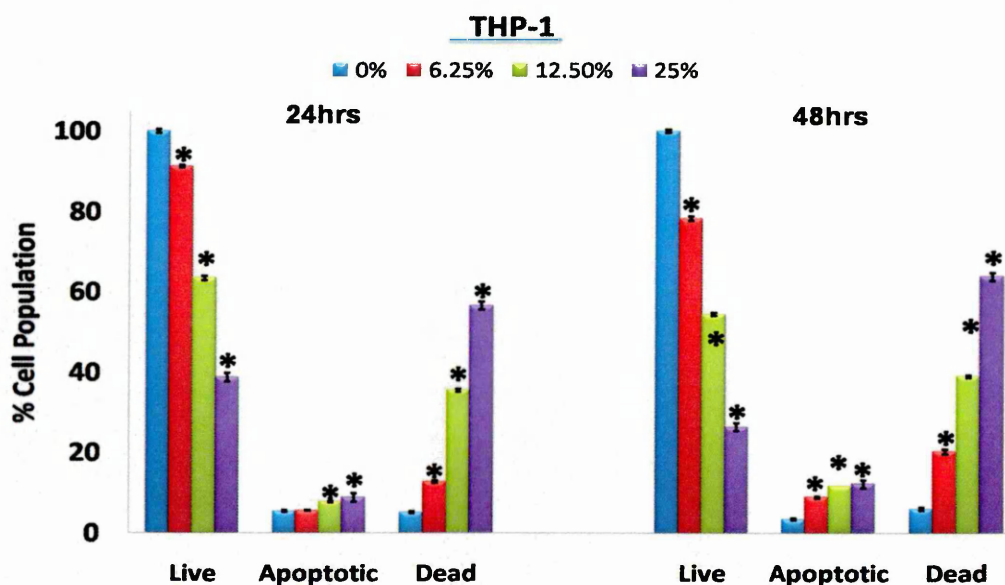


Figure 3.15: Annexin V-FITC/ PI based on flow cytometry following treatment with PJ (0%, 6.25%, 12.5% and 25%) for 24 and 48 h on THP-1. Mean \pm SEM. * indicates significant difference ($P \leq 0.05$) vs. untreated control. n = 3.

The non-tumour CD133+ HSCs were less sensitive to PJ treatment than the majority of the leukemia cell lines (Figure 3.16). Treatment with 6.25% PJ did not show a significant decrease in the number of live cell and increase in the number of apoptotic and dead cells after 24 h ($P > 0.05$). The highest dose of PJ (25%) failed to induce 50% cell death even after 48 h (Figure 3.16).

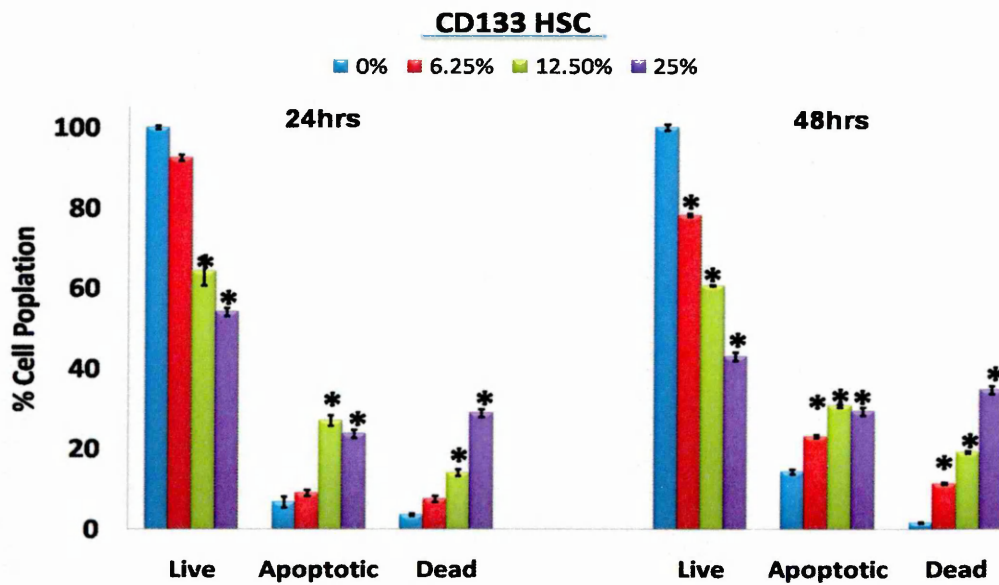


Figure 3.16: Annexin V-FITC/ PI based on flow cytometry following treatment with PJ (0%, 6.25%, 12.5% and 25%) for 24 and 48 h on CD133 positive hematopoietic stem cells (non-tumour HSC). Mean \pm SEM. * indicates significant difference ($P \leq 0.05$) vs. untreated control. n= 3.

3.4.2 Effect of PJ on Induction of Apoptosis Using DAPI for Morphology Assessment

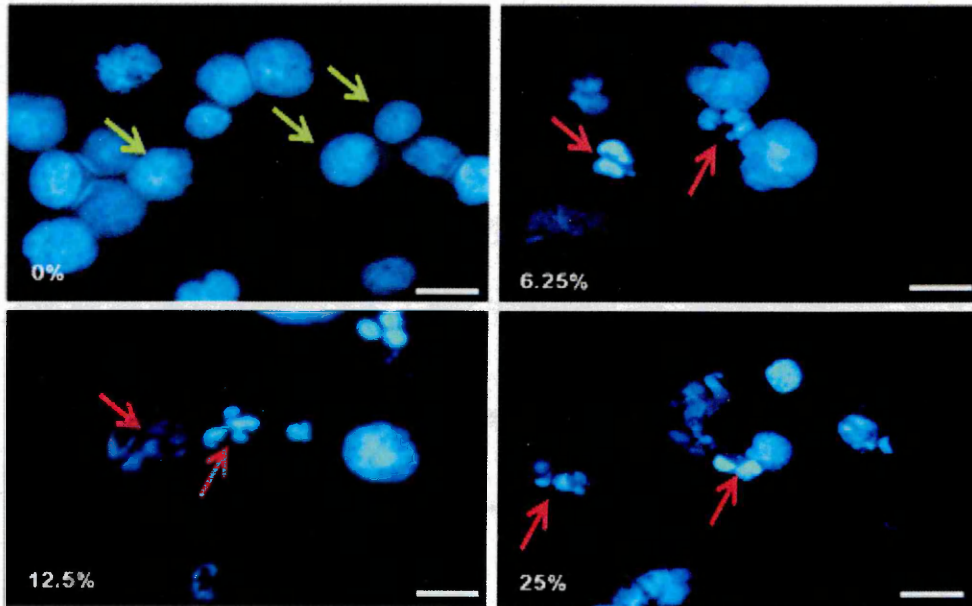
DAPI nuclear stain exhibits normal cells with round, clear edged and uniformly stained. In contrast it demonstrates apoptotic cells with irregular edges around the nucleus, chromatin condensation in the nucleus, intense staining and with pyknosis increase number of nuclear body fragments (Figure 2.6). DAPI morphological analysis showed a significant ($P \leq 0.05$) increase in the number of apoptotic cells in all 4 lymphoid and 4 myeloid human leukaemia cell lines in a dose dependent manner following treatment with PJ at concentration 6.25%, 12.5% and 25% compared to control with patterns confirming the annexin V/PI results (Figure 3.17 to 27). In addition, the percentage of apoptotic cells was significantly higher within lymphoid than the myeloid cell lines.

CCRF-CEM cells showed a significant increase in apoptotic population at all doses of PJ after 24 and 48 h incubation (Figure 3.17). Similarly, Jurkat cells showed a significant ($*P \leq 0.05$) rise in the number of apoptotic population at all three PJ concentrations following 24 and 48 h. The lowest dose (6.25%) and highest dose (25%) of PJ have shown a 10% increase in the apoptotic cell number following 48 h incubation compared with 24 h incubation time (Figure 3.18). Similarly MOLT-3 and SUP-B15 also showed significant ($P \leq 0.05$) increase in apoptosis following 24 and 48 h incubation with PJ (Fig 3.19 and 3.20)

KG-1 cells were the most affected myeloid cell line with 57, 71 and 82 apoptotic cell number following 24 h incubation and 71%, 82% and 92% apoptotic cell population following 48 h at concentration of PJ 6.25%, 12.5% and 25% respectively (Figure 3.21). THP-1 was least affected lymphoid cell lines with maximum apoptotic cells of 46% and 64% at highest dose of PJ following 24 and 48 h incubation respectively (Figure 3.22). CD133 demonstrated a significant ($P \leq 0.05$) increase in the number of apoptotic cells, but it was less than all leukaemia cell lines (Figure 3.23).

CCRF-CEM

(1)



(2)

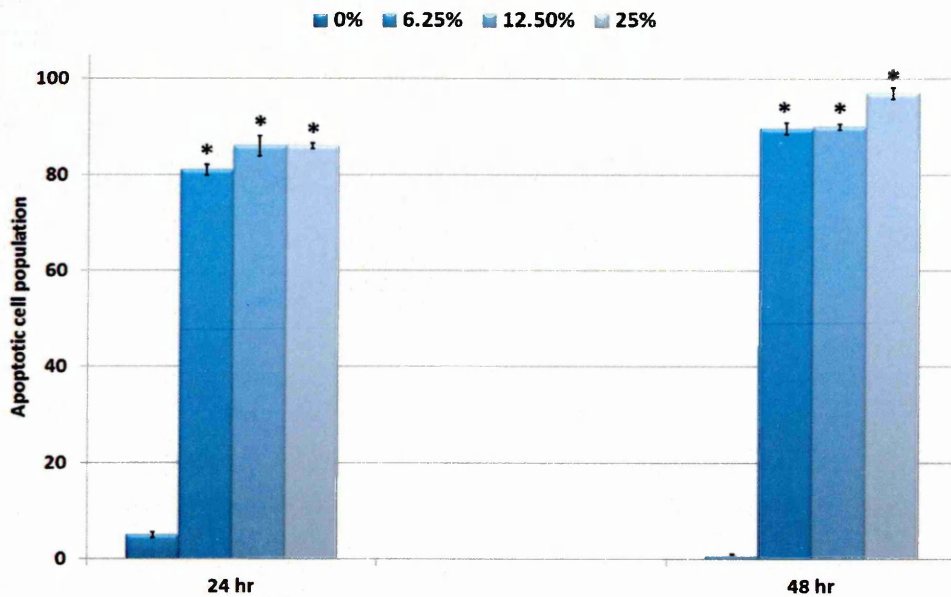
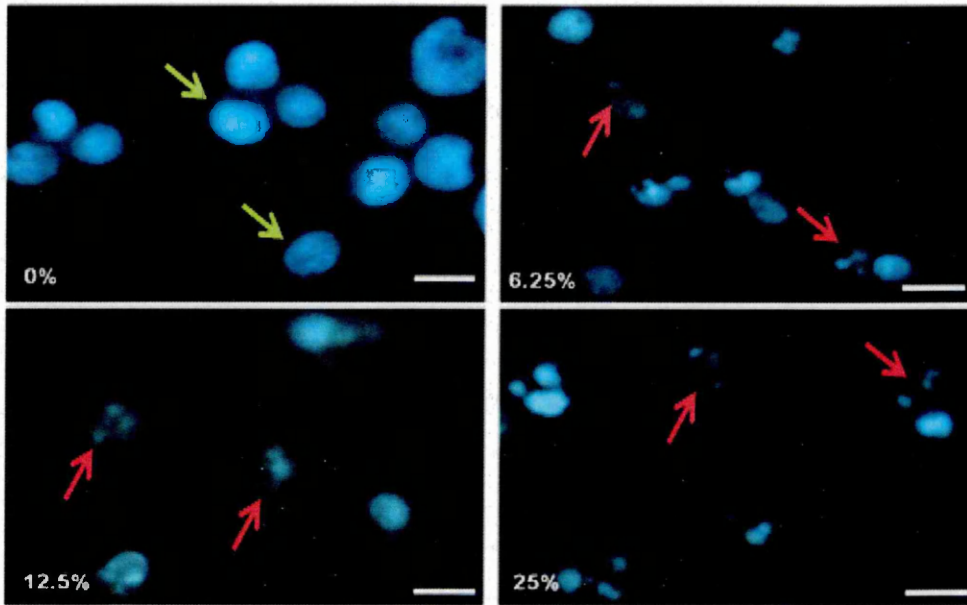


Figure 3.17: (1) Morphological staining analysis of CCRF-CEM with DAPI treated with PJ at concentrations 0%, 6.25%, 12.5% and 25% for 24 h. Live cells are indicated by the **green arrows**, and apoptotic cells are indicated by the **red arrows**. **(2)** Percentage of apoptotic cells determined from DAPI morphological assessment following treatment with PJ at concentration 0%, 6.25%, 12.5% and 25% for 24 and 48 h. Mean \pm SEM. * indicates significant difference ($P < 0.05$) vs. untreated control. Scale bar= 25 μ m. n= 3.

Jurkat

(1)



(2)

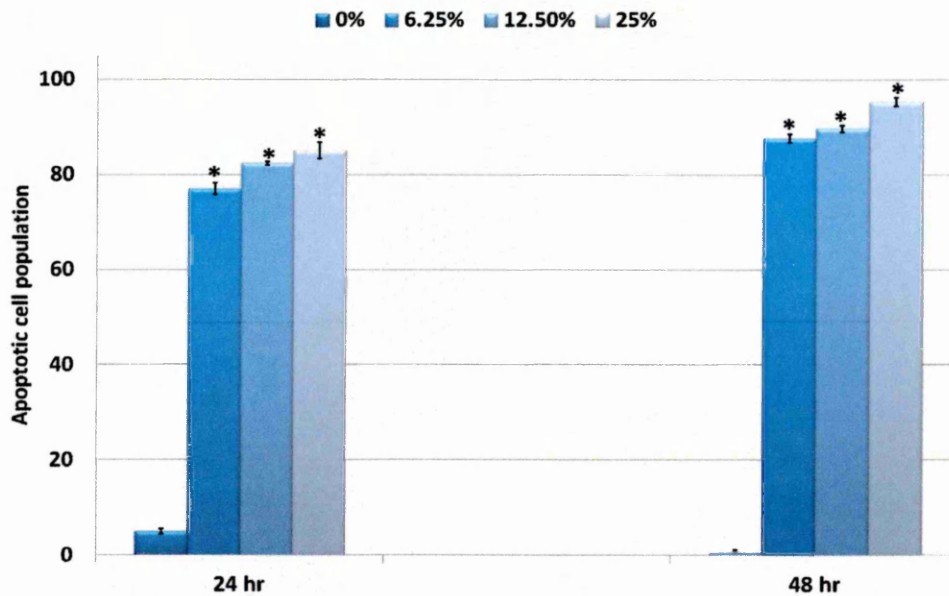


Figure 3.18: (1) Morphological staining analysis of Jurkat with DAPI treated with PJ at concentrations 0%, 6.25%, 12.5% and 25% for 24 h. Live cells are indicated by the green arrows, and apoptotic cells are indicated by the red arrows. **(2)** Percentage of apoptotic cells determined from DAPI morphological assessment following treatment with PJ at concentration 0%, 6.25%, 12.5% and 25% for 24 and 48 h. Mean \pm SEM. * indicates significant difference ($P \leq 0.05$) vs. untreated control. Scale bar= 25 μ m. n= 3.

MOLT-3

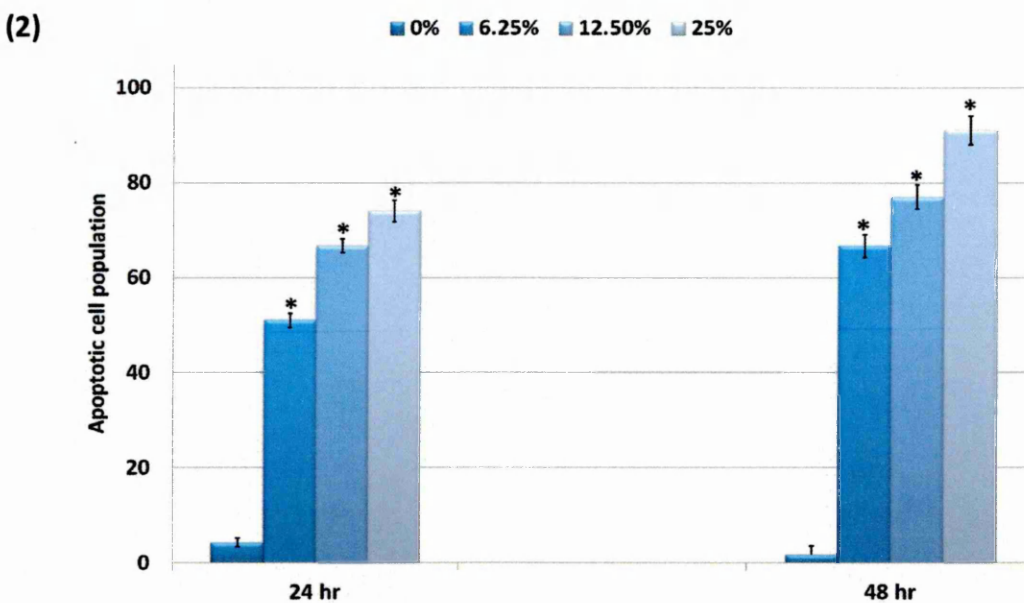
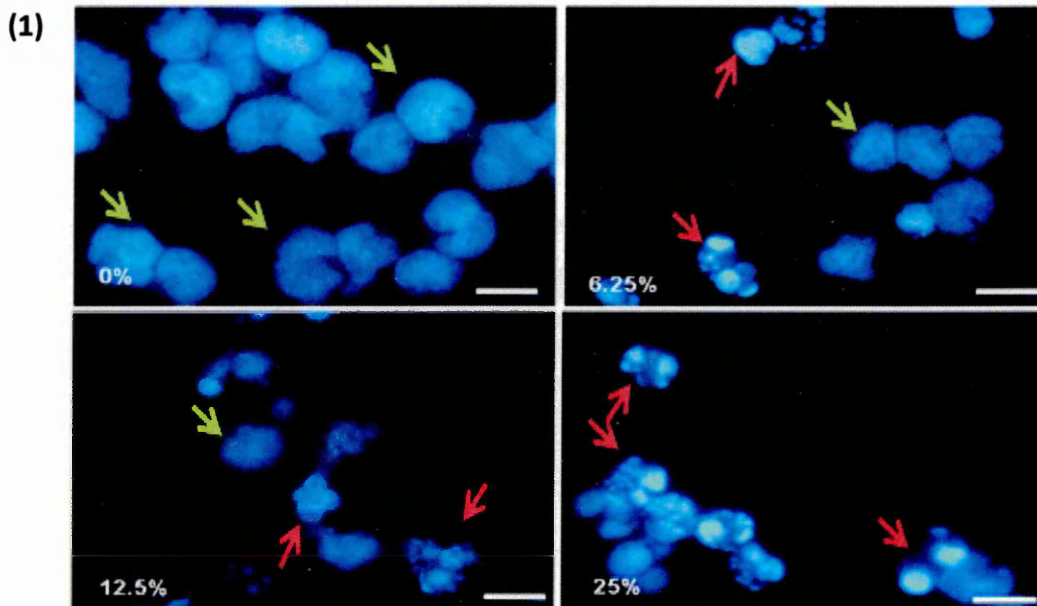


Figure 3.19: (1) Morphological staining analysis of MOLT-3 with DAPI treated with PJ at concentrations 0%, 6.25%, 12.5% and 25% for 24 h. Live cells are indicated by the green arrows, and apoptotic cells are indicated by the red arrows. **(2)** Percentage of apoptotic cells determined from DAPI morphological assessment following treatment with PJ at concentration 0%, 6.25%, 12.5% and 25% for 24 and 48 h. Mean \pm SEM. * indicates significant difference ($P \leq 0.05$) vs. untreated control. Scale bar= 25 μ m. n= 3.

SUP-B15

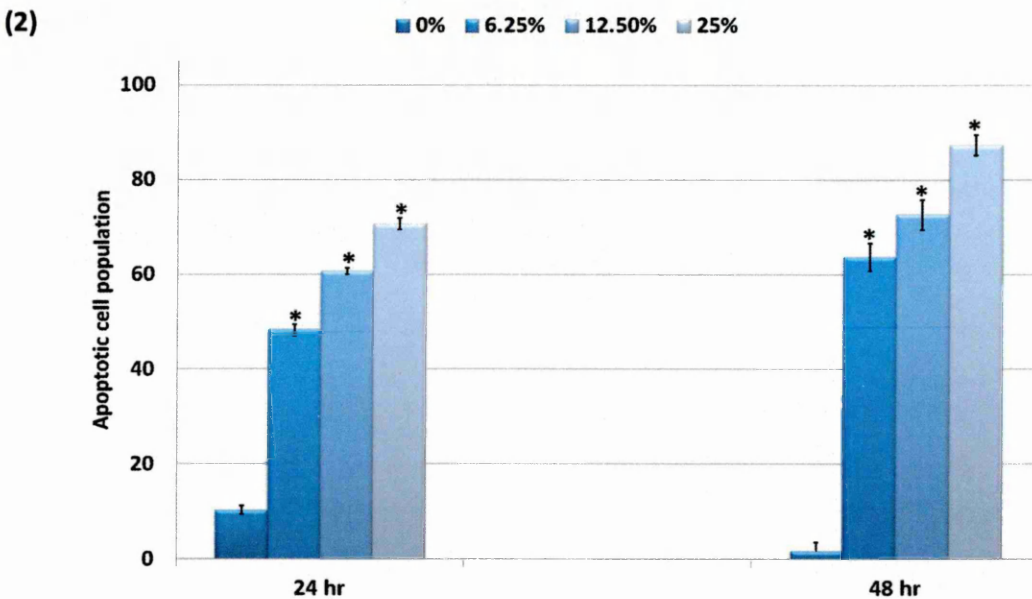
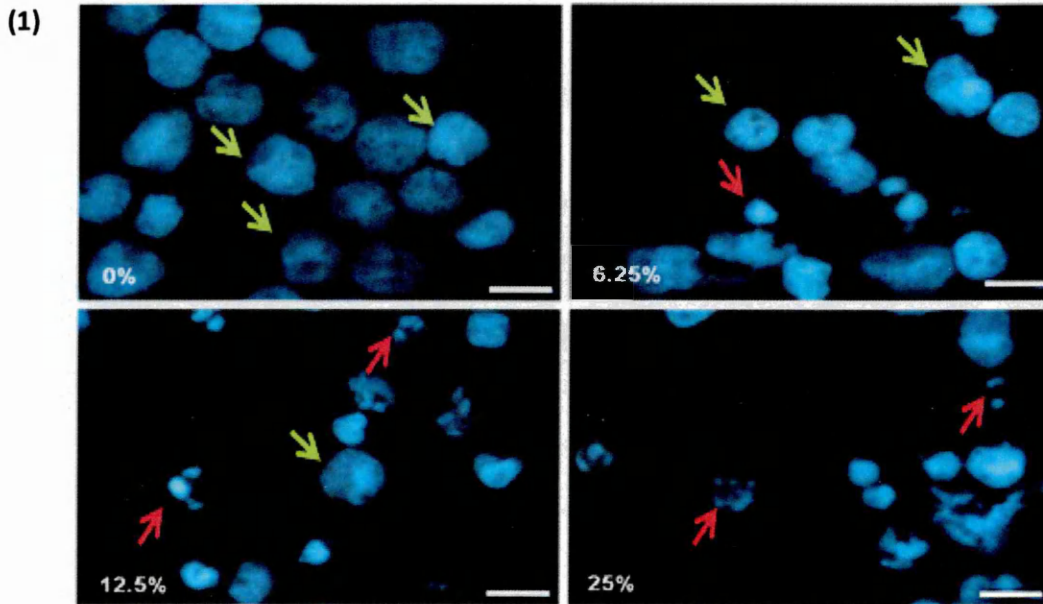


Figure 3.20: (1) Morphological staining analysis of SUP-B15 with DAPI treated with PJ at concentrations 0%, 6.25%, 12.5% and 25% for 24 h. Live cells are indicated by the green arrows, and apoptotic cells are indicated by the red arrows. (2) Percentage of apoptotic cells determined from DAPI morphological assessment following treatment with PJ at concentration 0%, 6.25%, 12.5% and 25% for 24 and 48 h. Mean \pm SEM. * indicates significant difference ($P \leq 0.05$) vs. untreated control. Scale bar = 25 μ m. n = 3.

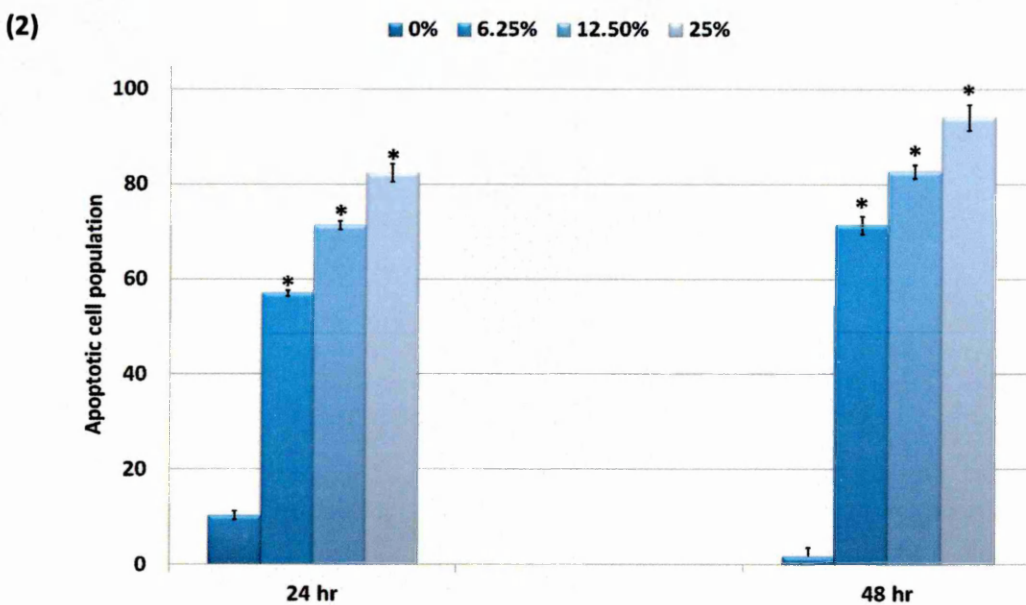
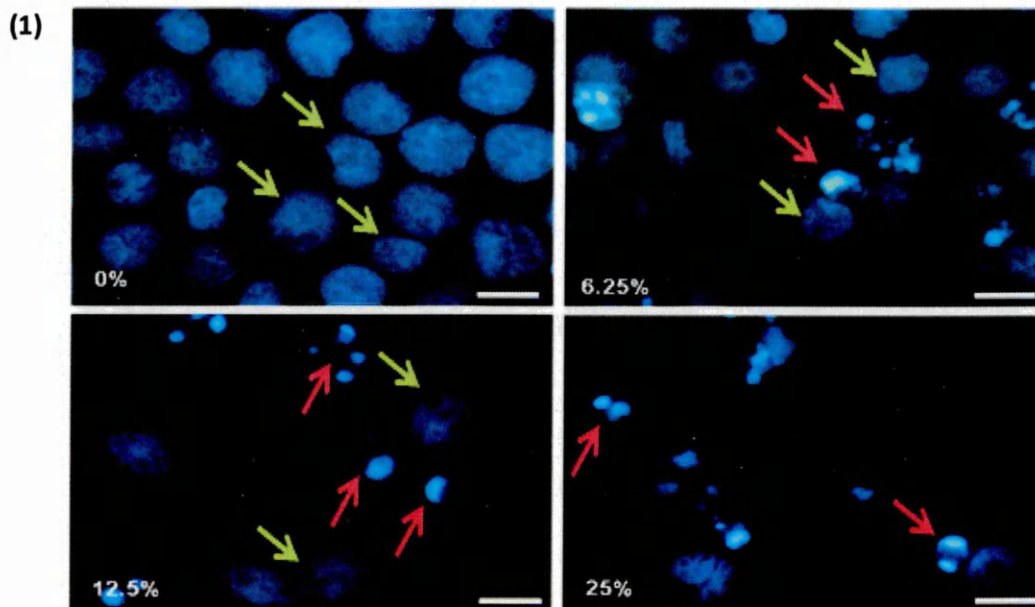


Figure 3.21: (1) Morphological staining analysis of KG-1a with DAPI treated with PJ at concentrations 0%, 6.25%, 12.5% and 25% for 24 h. Live cells are indicated by the green arrows, and apoptotic cells are indicated by the red arrows. **(2)** Percentage of apoptotic cells determined from DAPI morphological assessment following treatment with PJ at concentration 0%, 6.25%, 12.5% and 25% for 24 and 48 h. Mean \pm SEM. * indicates significant difference ($P \leq 0.05$) vs. untreated control. Scale bar= 25 μ m. n= 3.

HL-60

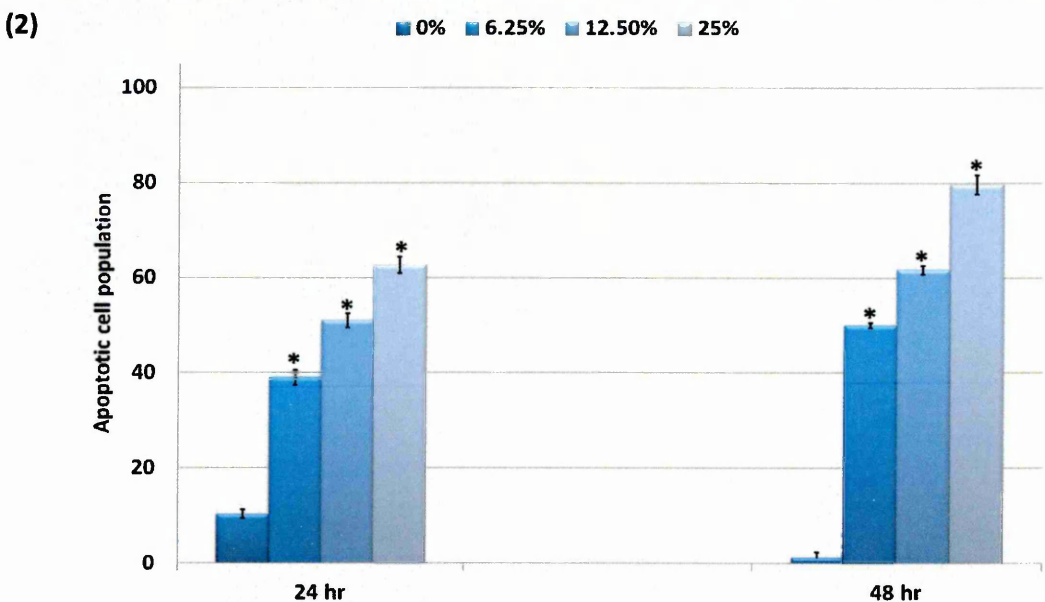
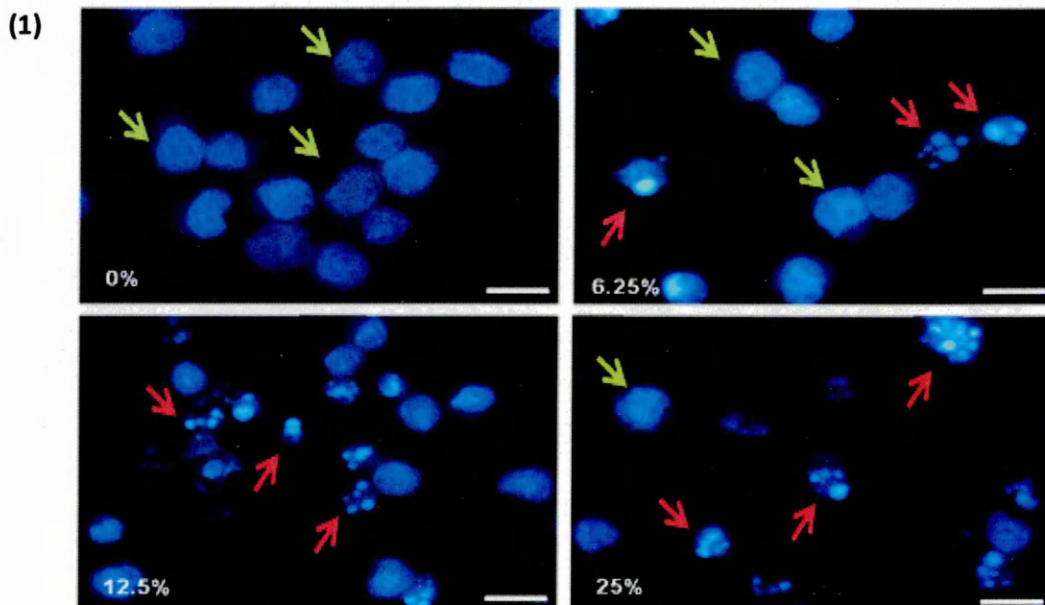


Figure 3.22: (1) Morphological staining analysis of HL-60 with DAPI treated with PJ at concentrations 0%, 6.25%, 12.5% and 25% for 24 h. Live cells are indicated by the **green arrows**, and apoptotic cells are indicated by the **red arrows**. **(2)** Percentage of apoptotic cells determined from DAPI morphological assessment following treatment with PJ at concentration 0%, 6.25%, 12.5% and 25% for 24 and 48 h. Mean \pm SEM. * indicates significant difference ($P \leq 0.05$) vs. untreated control. Scale bar= 25 μ m. n= 3.

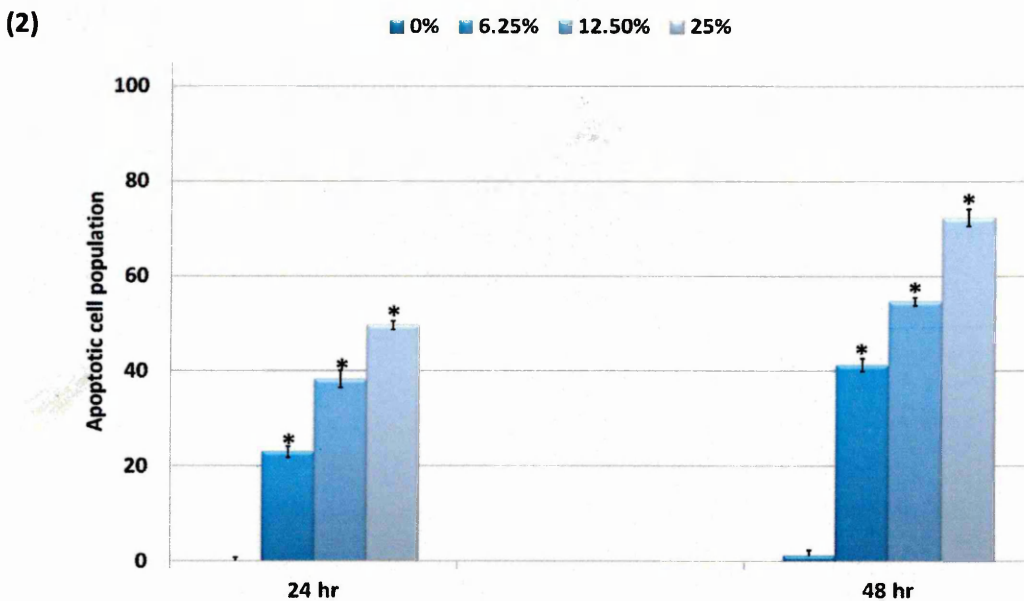
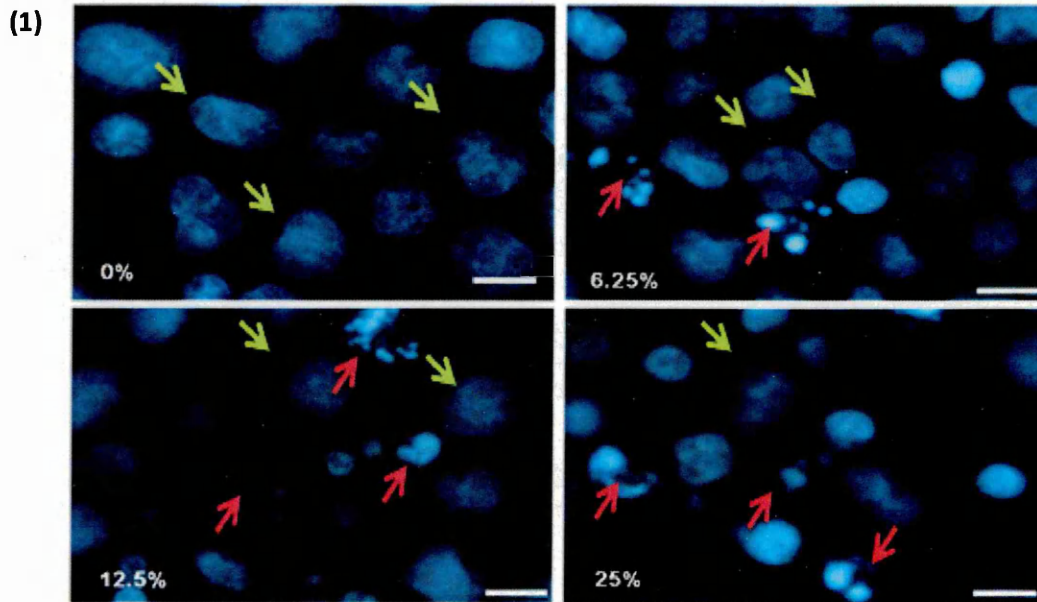
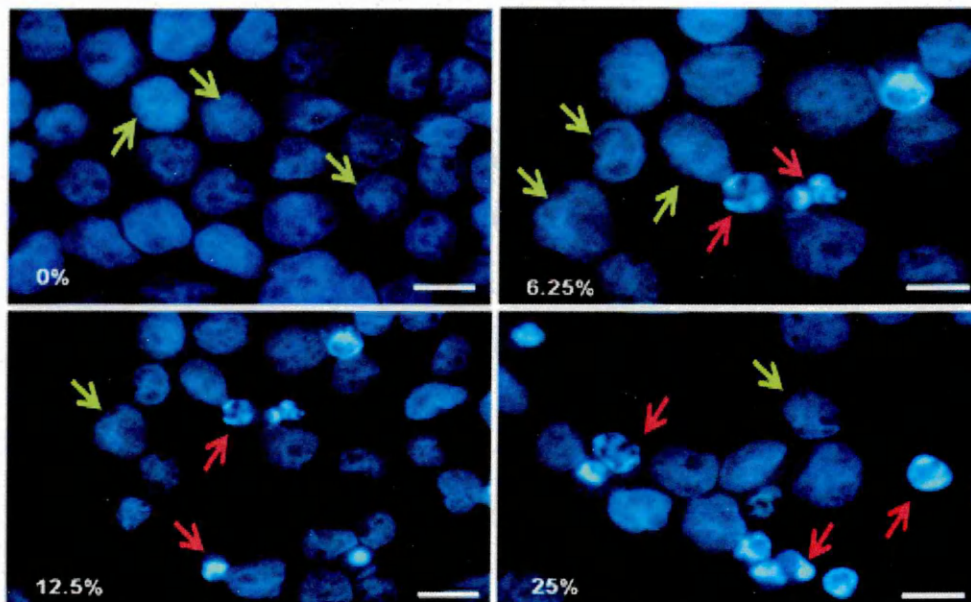


Figure 3.23: (1) Morphological staining analysis of K562 with DAPI treated with PJ at concentrations 0%, 6.25%, 12.5% and 25% for 24 h. Live cells are indicated by the green arrows, and apoptotic cells are indicated by the red arrows. **(2)** Percentage of apoptotic cells determined from DAPI morphological assessment following treatment with PJ at concentration 0%, 6.25%, 12.5% and 25% for 24 and 48 h. Mean \pm SEM. * indicates significant difference ($P \leq 0.05$) vs. untreated control. Scale bar= 25 μ m. n= 3.

(1)



(2)

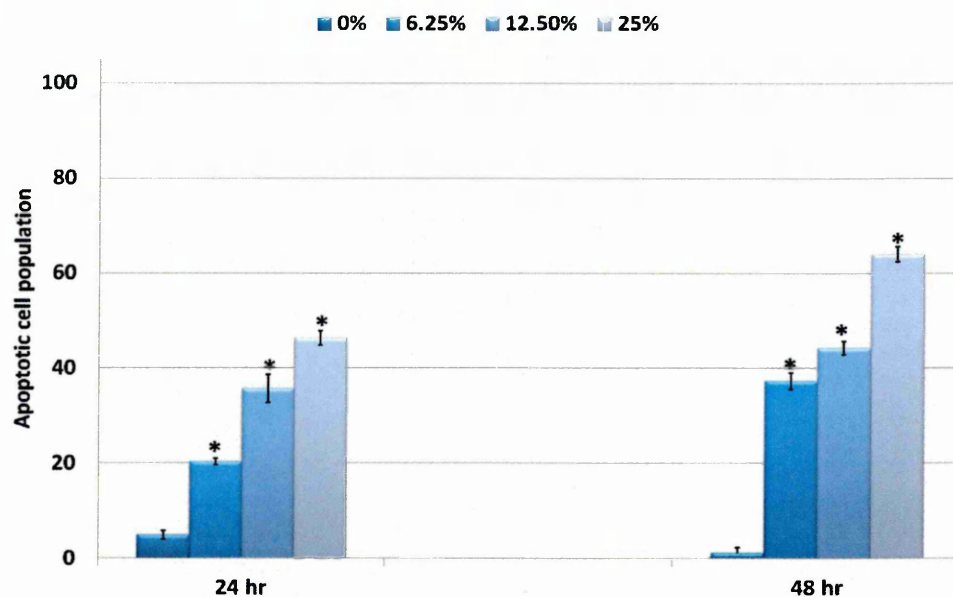


Figure 3.24: (1) Morphological staining analysis of K562 with DAPI treated with PJ at concentrations 0%, 6.25%, 12.5% and 25% for 24 h. Live cells are indicated by the green arrows, and apoptotic cells are indicated by the red arrows. **(2)** Percentage of apoptotic cells determined from DAPI morphological assessment following treatment with PJ at concentration 0%, 6.25%, 12.5% and 25% for 24 and 48 h. Mean \pm SEM. * indicates significant difference ($P \leq 0.05$) vs. untreated control. Scale bar= 25 μ m. n= 3.

Effect of PJE on induction of apoptosis using DAPI staining following 24 hr incubation

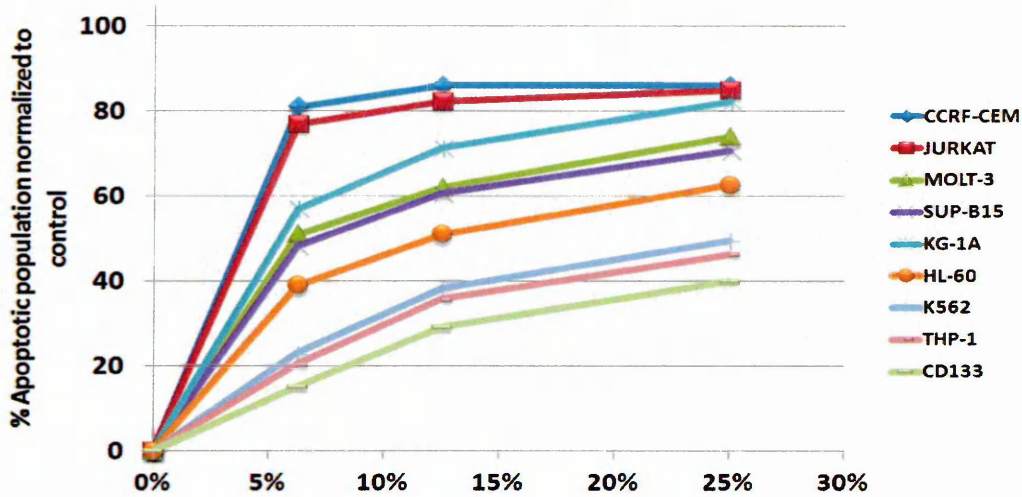


Figure 3.25: Analysis of DAPI staining of apoptotic cell populations normalized to untreated controls in 4 lymphoid leukaemia cell lines (CCRF-CEM, JURKAT, MOLT-3, SUP-B15), 4 myeloid leukaemia cell lines (KG-1a, HL-60, K562, THP-1), and non-tumour hematopoietic stem cells (CD133) following treatment PJ for 24 h.

Effect of PJE on induction of apoptosis using DAPI staining following 48 hr incubation

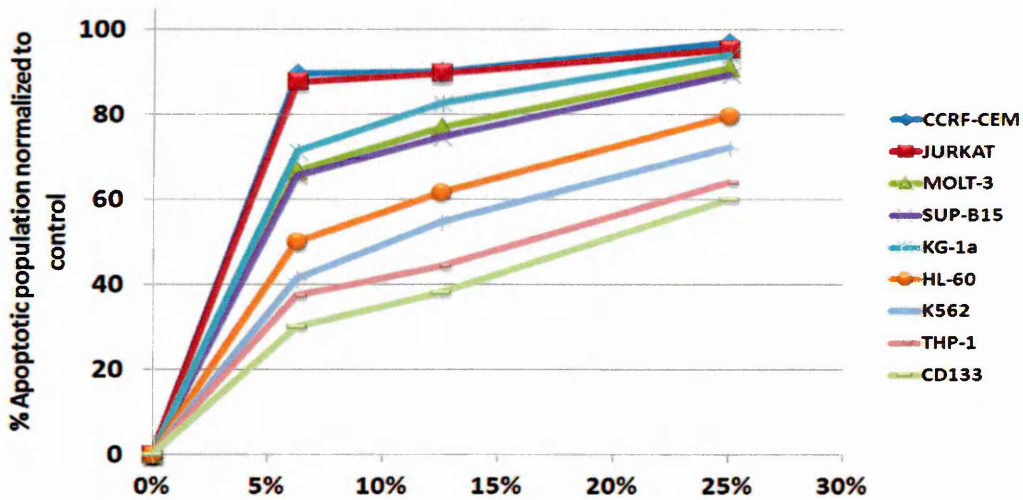


Figure 3.26: Analysis of DAPI staining of apoptotic cell populations normalized to untreated controls in 4 lymphoid leukaemia cell lines (CCRF-CEM, JURKAT, MOLT-3, SUP-B15), 4 myeloid leukaemia cell lines (KG-1a, HL-60, K562, THP-1), and non-tumour hematopoietic stem cells (CD133) following treatment PJ for 48 h.

3.4.3 Effect of PJ on Cell Viability

To investigate whether PJ treatment imparts anti-proliferative effects against leukaemia cells, the effect of PJ on the growth of these cells was evaluated by the trypan blue exclusion assay.

Trypan blue exclusion assay was used based on the countess™ automated cell counter to measure the effect of PJ on all leukaemia cell lines and non-tumour haematopoietic stem cells on cell viability following 24 and 48 h incubation. In this case the dye is normally taken up by viable cells but non-viable cells.

Treatment with PJ at concentrations 6.25%, 12.5% and 25% resulted in a significant decrease in the number of viable cells in a dose dependent manner compared to untreated cells (0%) following 24h and 48 h incubation in all four human lymphoid leukaemia cells (CCRF-CEM, MOLT-3, Jurkat and SUP-B15) and four myeloid leukaemia cells (HL-60, THP-1, K562 and KG1a) ($P \leq 0.05$) (Figure 3.28 to 3.36).

CCRF-CEM and Jurkat showed less than 2% viable cells post treatment with 12.5% and 25% PJ after only 24 h incubation and there was no significant difference between 24 and 48 h in the same concentration (Figure 3.27). Other lymphoid cell lines (MOLT-3 and SUP-B15) were less affected than CCRF-CEM and Jurkat with about 10% of cells remaining viable following 25% PJ treatment for 48 h (Figure 3.28, 3.29, and 3.30).

KG-1a was the most affected myeloid cell line with 96% decrease in the number of live cells following 48 h treatment with 25% PJ (Figure 3.31). In contrast THP-1 was the least affected cell lines since it only showed less than 10% decrease in the number of live cells at 6.25% PJ following 24 and at highest concentration of PJ 25% following 48 h demonstrated less than 80% decrease in the number of live cells compared to control (Figure 3.34). 25% PJ failed to inhibit more than 50% of CD133 after 24 h incubation, while following 48 h incubation the number of live cells for CD133 showed a decrease with about 80% reduction following 25% PJ (Figure 3.35).

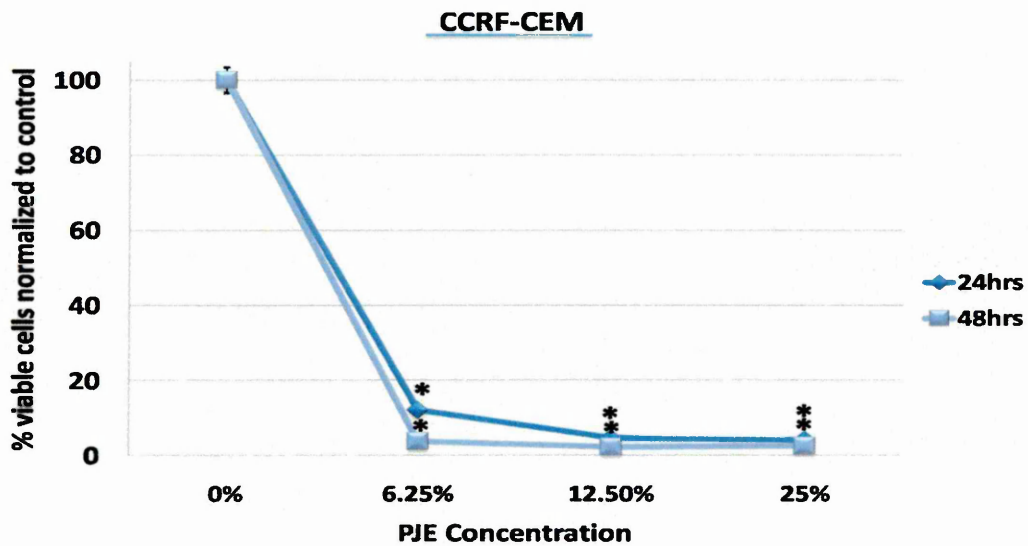


Figure 3.27: Effect of pomegranate juice extract (PJ) on cell viability using trypan exclusion assay following 24 and 48 h incubation at 6.25%, 12.5%, and 25% on CCRF-CEM. Average cell number of untreated cells was set at 100% and relative number of cells calculated accordingly. Mean \pm SEM. * indicates significant difference ($P \leq 0.05$) vs. untreated control. n= 3.

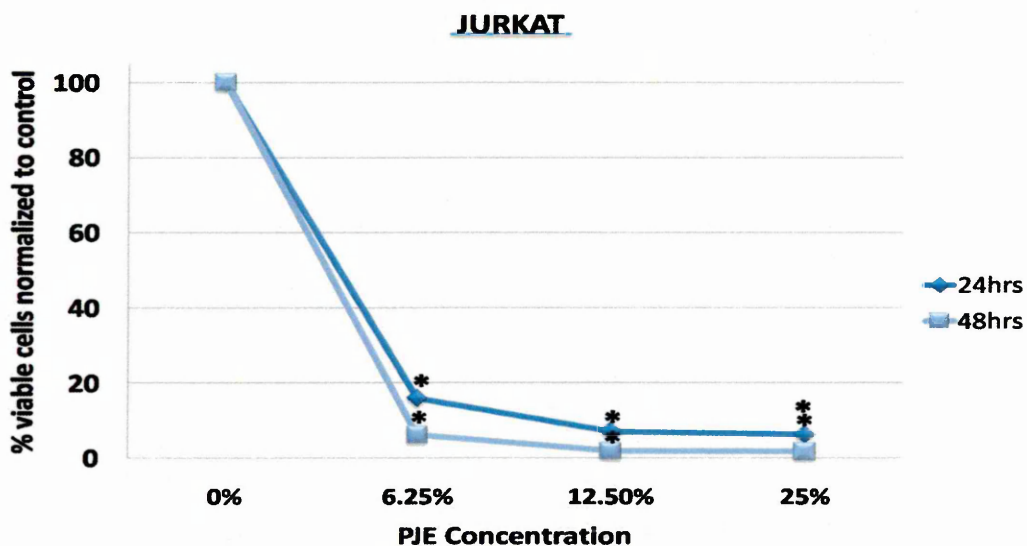


Figure 3.28: Effect of pomegranate juice extract (PJ) on cell viability using trypan exclusion assay following 24 and 48 h incubation at 6.25%, 12.5%, and 25% on CCRF-CEM. Average cell number of untreated cells was set at 100% and relative number of cells calculated accordingly. Mean \pm SEM. * indicates significant difference ($P \leq 0.05$) vs. untreated control. n= 3.

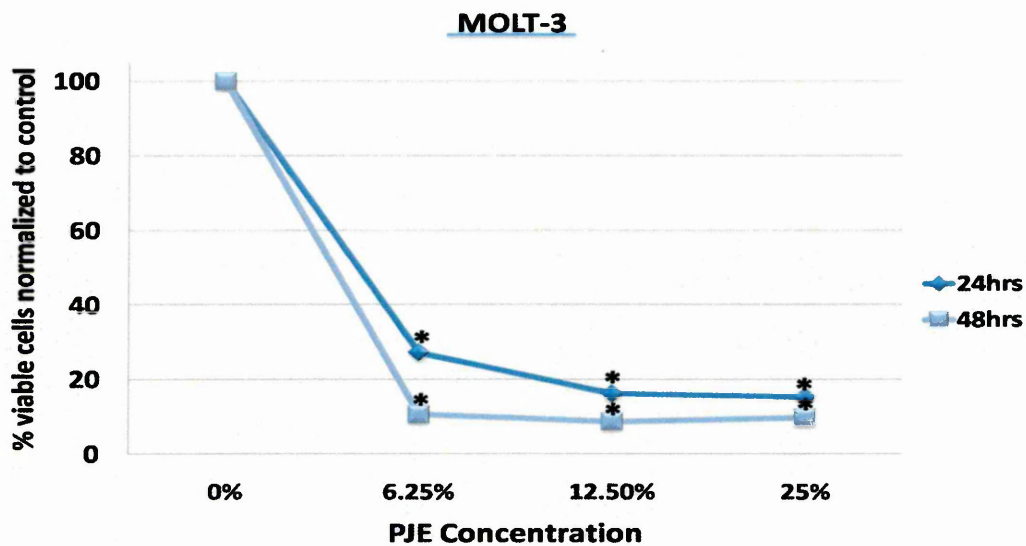


Figure 3.29: Effect of PJ on cell viability using trypan exclusion assay following 24 and 48 h incubation at 6.25%, 12.5%, and 25% on MOLT-3. Average cell number of untreated cells was set at 100% and relative number of cells calculated accordingly. Mean \pm SEM. * indicates significant difference ($P \leq 0.05$) vs. untreated control. n= 3.

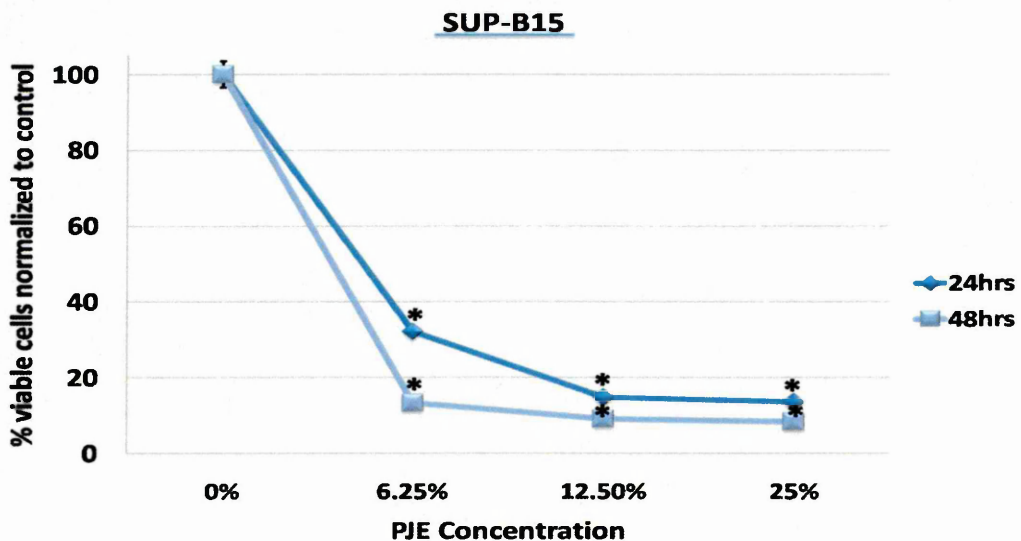


Figure 3.30: Effect of PJ on cell viability using trypan exclusion assay following 24 and 48 h incubation at 6.25%, 12.5%, and 25% on SUP-B15. Average cell number of untreated cells was set at 100% and relative number of cells calculated accordingly. Mean \pm SEM. * indicates significant difference ($P \leq 0.05$) vs. untreated control. n= 3.

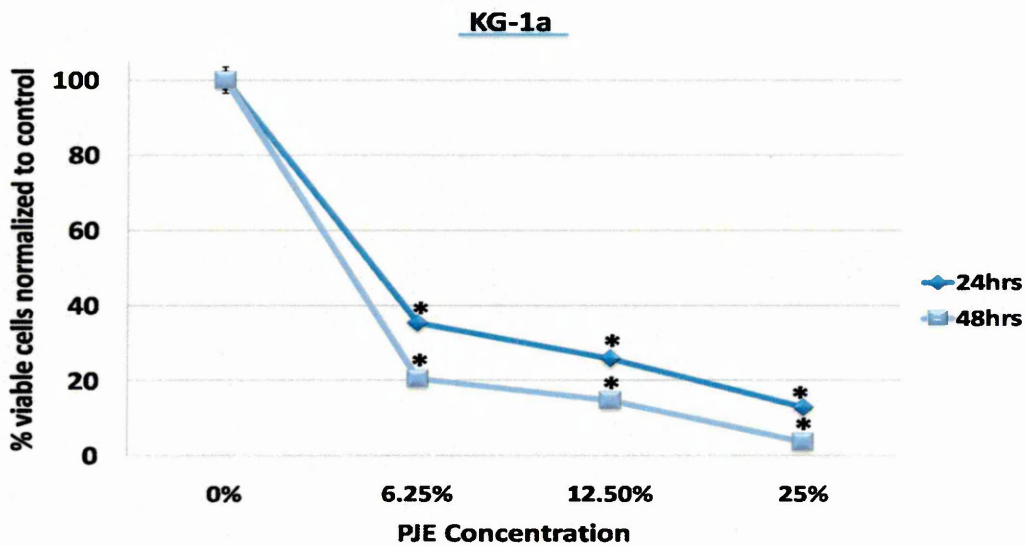


Figure 3.31: Effect of PJ on cell viability using trypan exclusion assay following 24 and 48 h incubation at 6.25%, 12.5%, and 25% on KG-1a. Average cell number of untreated cells was set at 100% and relative number of cells calculated accordingly. Mean \pm SEM* indicates significant difference ($P \leq 0.05$) vs. untreated control. n= 3.

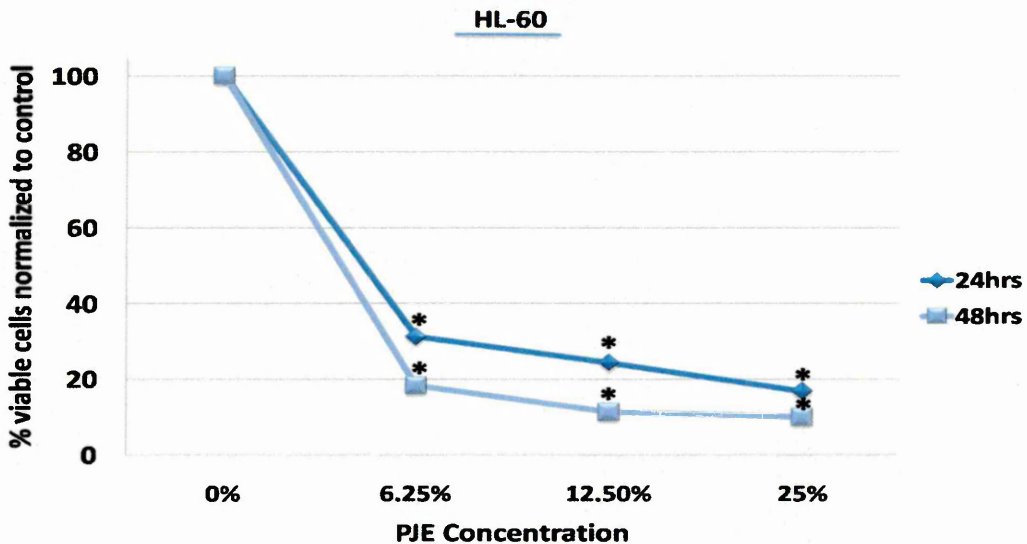


Figure 3.32: Effect of PJ on cell viability using trypan exclusion assay following 24 and 48 h incubation at 6.25%, 12.5%, and 25% on HL-60. Average cell number of untreated cells was set at 100% and relative number of cells calculated accordingly. Mean \pm SEM. * indicates significant difference ($P \leq 0.05$) vs. untreated control. n= 3.

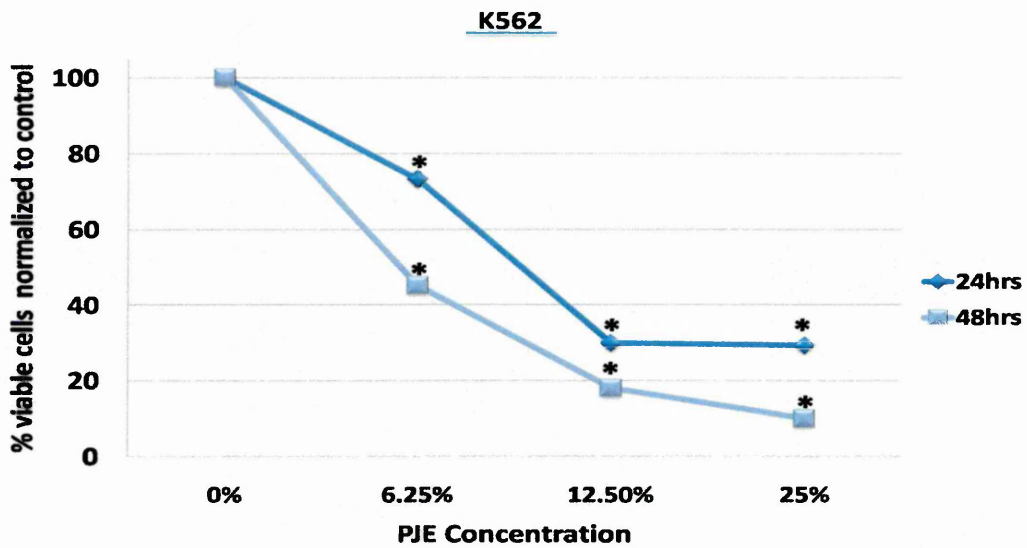


Figure 3.33: Effect of PJ on cell viability using trypan exclusion assay following 24 and 48 h incubation at 6.25%, 12.5%, and 25% on K562. Average cell number of untreated cells was set at 100% and relative number of cells calculated accordingly. Mean \pm SEM. * indicates significant difference ($P \leq 0.05$) vs. untreated control. n= 3.

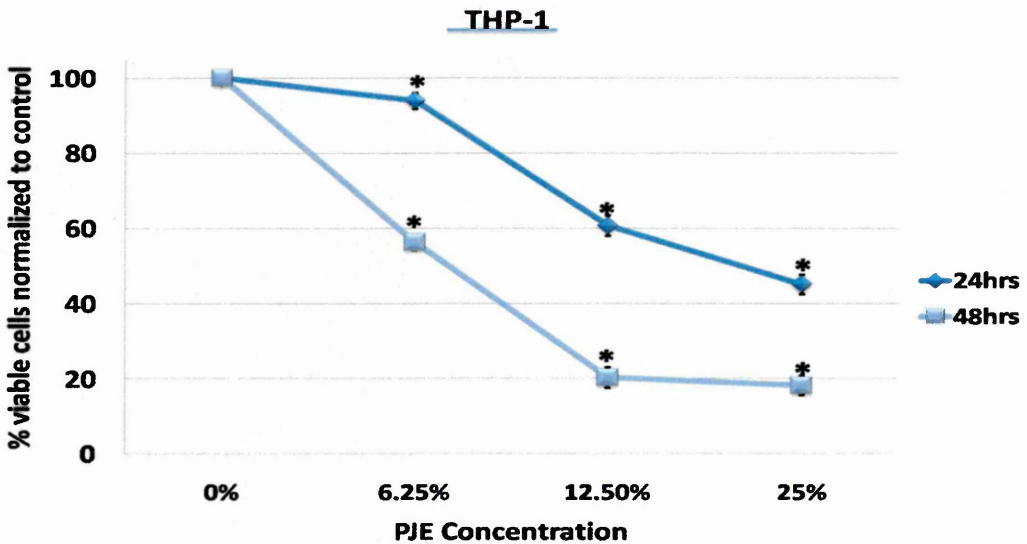


Figure 3.34: Effect of PJ on cell viability using trypan exclusion assay following 24 and 48 h incubation at 6.25%, 12.5%, and 25% on K562. Average cell number of untreated cells was set at 100% and relative number of cells calculated accordingly. Mean \pm SEM.* indicates significant difference ($P \leq 0.05$) vs. untreated control. n= 3.

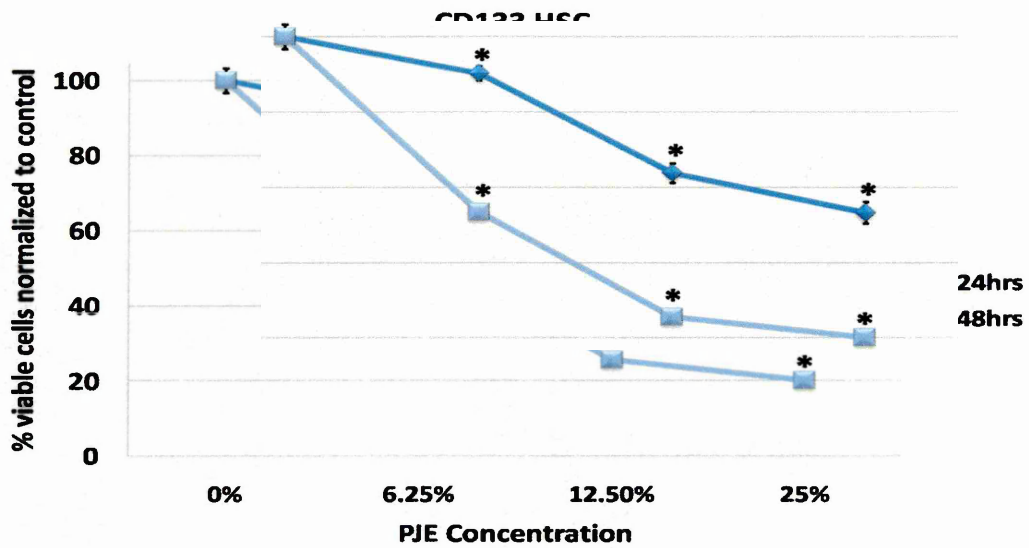


Figure 3.35: Effect of PJ on cell viability using trypan exclusion assay following 24 and 48 h incubation at 6.25%, 12.5%, and 25% on K562. Average cell number of untreated cells was set at 100% and relative number of cells calculated accordingly. Mean \pm SEM. * indicates significant difference ($P \leq 0.05$) vs. untreated control. n= 3.

3.4.4 Effect of PJ on Cell Cycle Using Flow Cytometry

Differential effects on cell cycle stage following PJ treatment were observed dependent on cell type investigated and dose and duration of PJ treatments (Table 3.3). CCRF-CEM cells displayed cell cycle accumulation in S phase, which was significant following 6.25% and 25% treatments with PJ (Figure 3.36) ($P \leq 0.05$). MOLT-3 and SUP-B15 cells showed a significant ($P \leq 0.05$) S phase accumulation at all concentrations of PJ (Figure 3.37 and 3.38). Jurkat cells displayed a significant G_0/G_1 phase accumulation at 6.25% of PJ and significant ($P \leq 0.05$) S phase accumulation at 12.5% and 25% of PJ (Figure 3.37). Myeloid cells (K562 and THP-1) displayed a significant ($P \leq 0.05$) S phase accumulation at the higher doses of PJ (Figure 3.42 and 3.43), while KG-1a and HL-60 cells were the only two cell lines which displayed a G_0/G_1 phase accumulation at all doses (Figure 3.40 and 3.41).

Cell lines	PJ concentration		
	6.25%	12.5%	25%
CCRF-CEM	S	S*	S*
JURKAT	G_0/G_1^*	S*	S*
MOLT-3	S*	S*	S*
SUP-B15	S*	S*	S*
KG-1a	G_0/G_1	G_0/G_1^*	G_0/G_1^*
HL-60	G_0/G_1^*	G_0/G_1^*	S*
K562	G_0/G_1	S*	S*
THP-1	S	S*	S*

Table 3.3: Summary of cell cycle results.

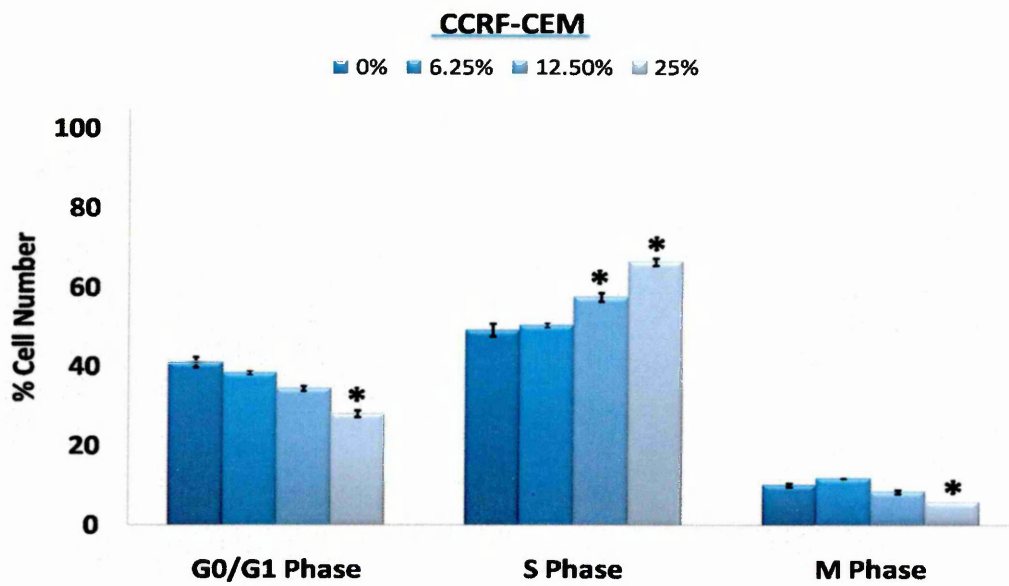


Figure 3.36: Cell cycle based on flow cytometry using FlowJo software following treatment with PJ at concentration 0%, 6.25%, and 12.5% for 24 h incubation on CCRF-CEM. Mean \pm SEM. * indicates significant difference ($P \leq 0.05$) vs. untreated control. n= 3.

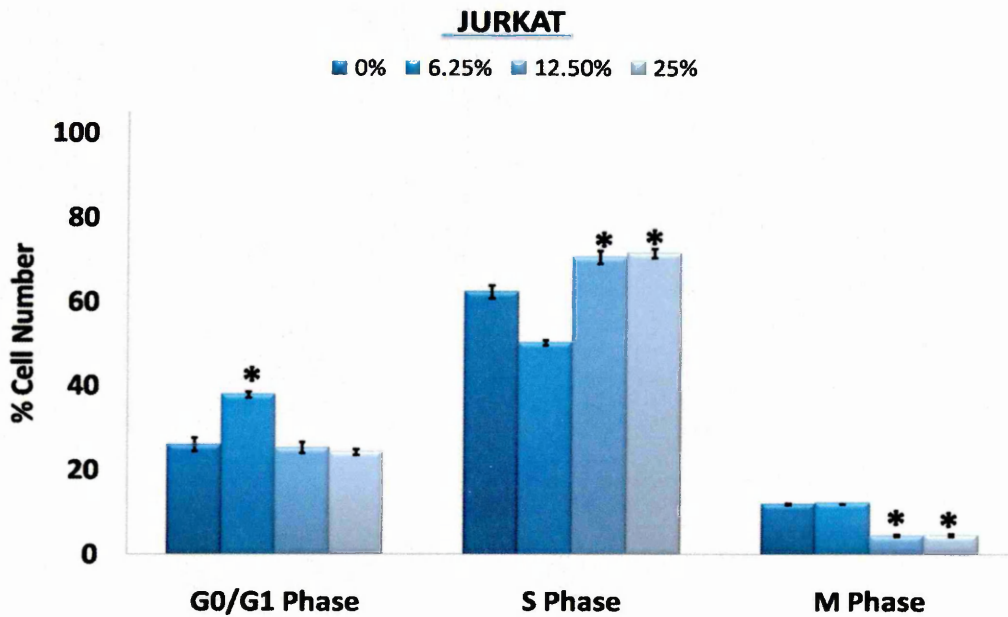


Figure 3.37: Cell cycle based on flow cytometry using FlowJo software following treatment with PJ at concentration 0%, 6.25%, and 12.5% for 24 h incubation on Jurkat. Mean \pm SEM* indicates significant difference ($P \leq 0.05$) vs. untreated control. n= 3.

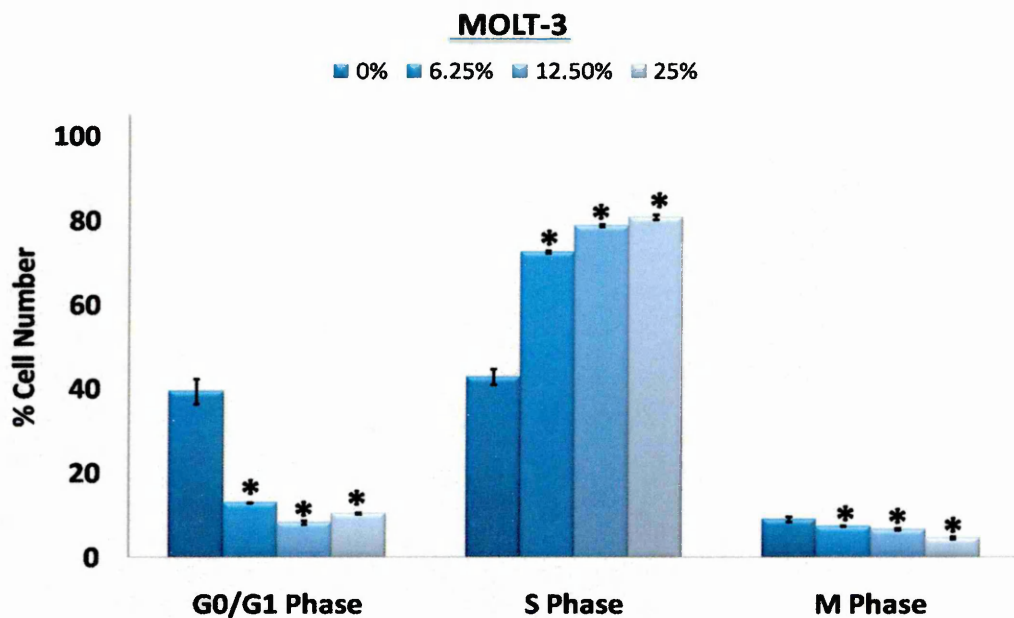


Figure 3.38: Cell cycle based on flow cytometry using FlowJo software following treatment with PJ at concentration 0%, 6.25%, and 12.5% for 24 h incubation on MOLT-3. Mean \pm SEM. * indicates significant difference ($P \leq 0.05$) vs. untreated control. n= 3.

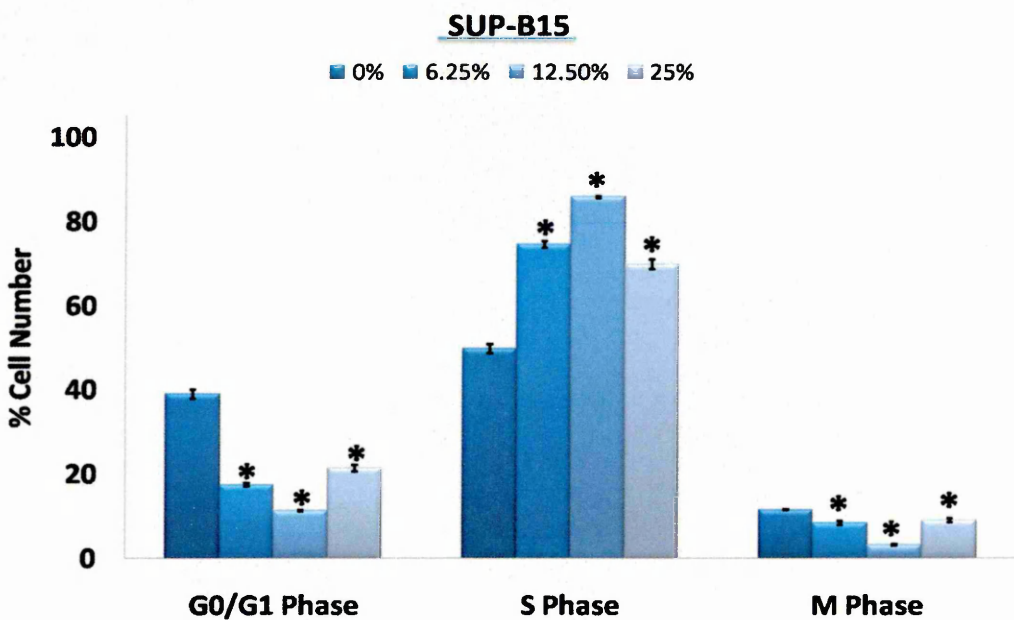


Figure 3.39: Cell cycle based on flow cytometry using FlowJo software following treatment with PJ at concentration 0%, 6.25%, and 12.5% for 24 h incubation on SUP-B15. Mean \pm SEM. * indicates significant difference ($P \leq 0.05$) vs. untreated control. n= 3.

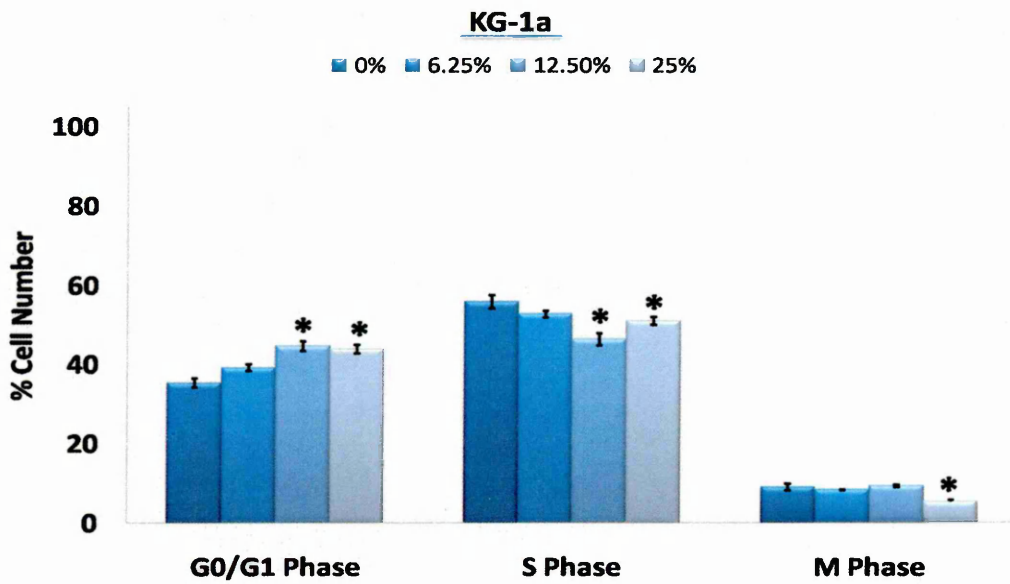


Figure 3.40: Cell cycle based on flow cytometry using FlowJo software following treatment with PJ at concentration 0%, 6.25%, and 12.5% for 24 h incubation on KG-1a. Mean \pm SEM. * indicates significant difference ($P \leq 0.05$) vs. untreated control. n= 3.

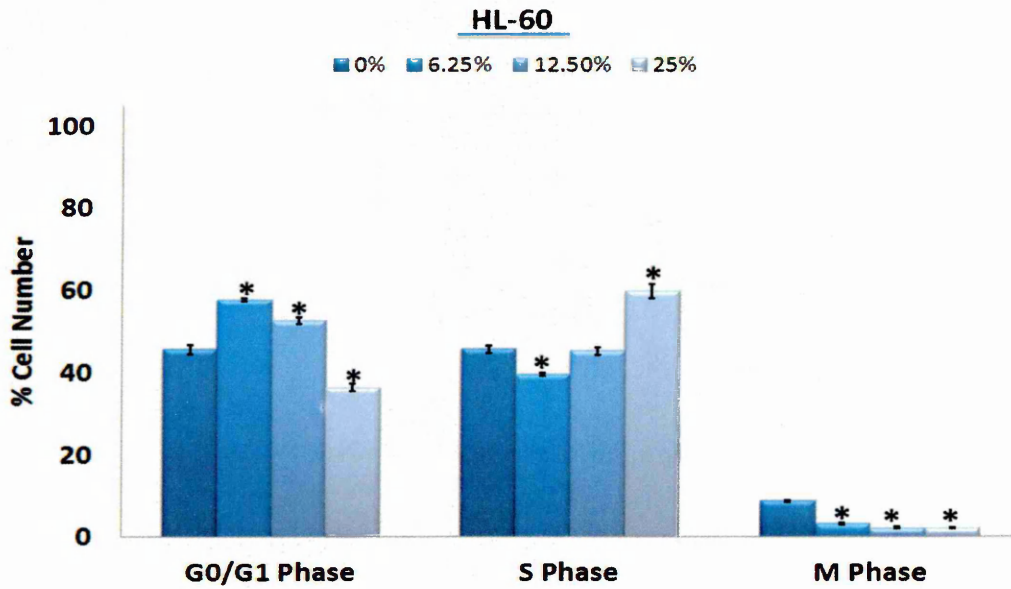


Figure 3.41: Cell cycle based on flow cytometry using FlowJo software following treatment with PJ at concentration 0%, 6.25%, and 12.5% for 24 h incubation on HL-60. Mean \pm SEM. *Significant difference ($P \leq 0.05$) vs. untreated control. n=3.

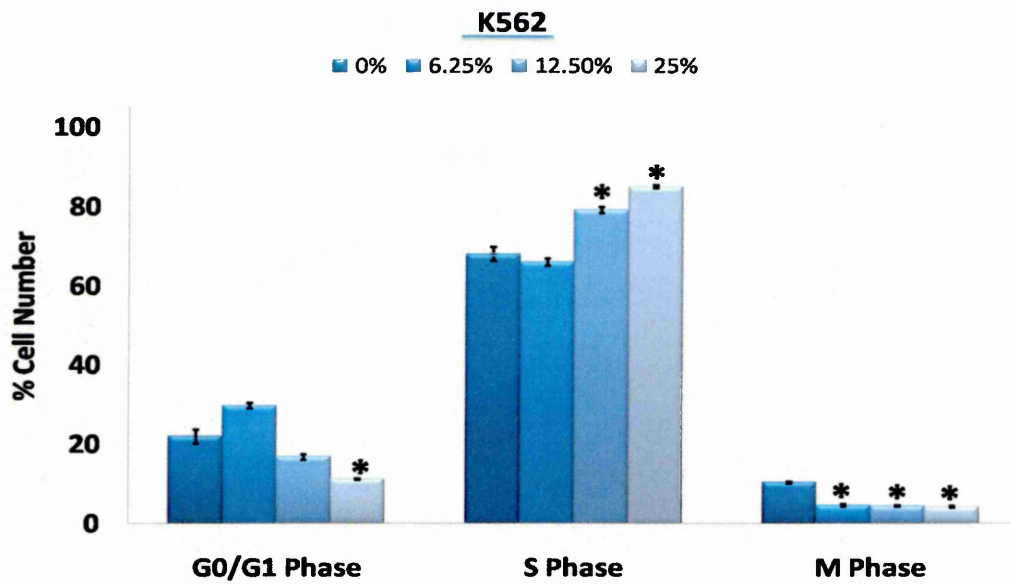


Figure 3.42: Cell cycle based on flow cytometry using FlowJo software following treatment with PJ at concentration 0%, 6.25%, and 12.5% for 24 h incubation on K562. Mean \pm SEM. * indicates significant difference ($P \leq 0.05$) vs. untreated control. n= 3.

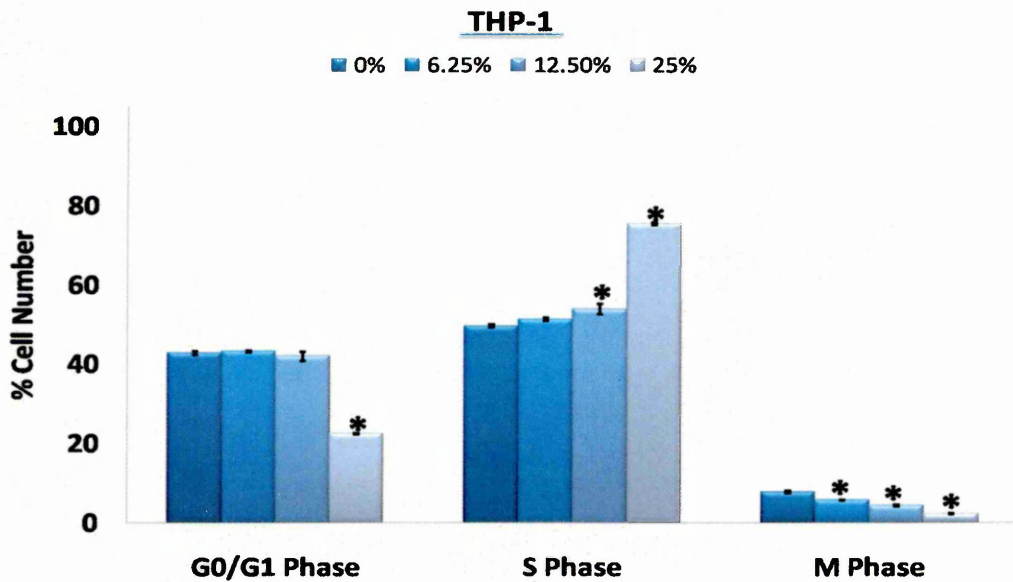


Figure 3.43: Cell cycle based on flow cytometry using FlowJo software following treatment with PJ at concentration 0%, 6.25%, and 12.5% for 24 h incubation on THP-1. Mean \pm SEM. * indicates significant difference ($P \leq 0.05$) vs. untreated control. n= 3.

3.4.5 Effect of Isotonic/Osmolarity and pH Changes on Induction of Apoptosis

To ensure the toxic effects observed were due to bioactive agents in the PJ and not as a result of altered isotonic or osmolarity or decreased pH induced by PJ inclusions, cells were treated with equivalent concentrations of distilled water (0%, 6.25%, 12.5% and 25%) or in adjusted media [pH of control media = 7.5; pH of PJ at 6.25% = 7.42; pH of PJ at 12.5% = 7.42; pH of PJ at 25% = 6.52] on two lymphoid cell lines (CCRF-CEM and MOLT-3) (Figure 3.44, 3.45, 3.49, and 3.50) and two myeloid cell lines (HL-60 and THP-1) (Figure 3.46, 3.47, 3.51, and 3.52) and the non-tumour CD133⁺ (Figure 3.48 and 3.53) for 48 h. The majority of cell types investigated showed no significant decrease in live cells or increase in the apoptotic or dead cells following inclusion of water controls or in altered pH ($P \leq 0.05$). A small but significant decrease in live cells was observed in THP-1 cells (Figure 3.52) treated with water equivalent to 12.5% and 25% PJ, and in CCRF-CEM cells treated with adjusted media to 25% (Figure 3.45). HL-60 cells also showed a small significant decrease in the number of live and increased in apoptotic cells when treated in adjusted media to 25% (Figure 3.46). However, it is noteworthy that these effects were far smaller than those seen following PJ treatment.

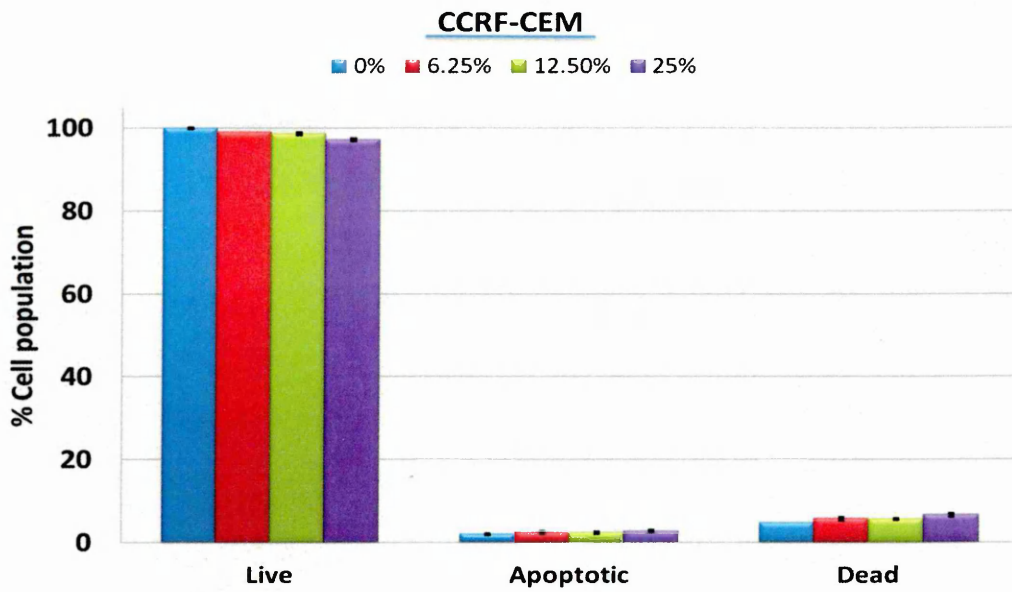


Figure 3.44: Annexin V-FITC/PI g based on flow cytometry. CCRF-CEM treated in pH adjusted media for 48 h. Mean \pm SEM. * indicates significant difference ($P \leq 0.05$) vs. untreated control. n= 3.

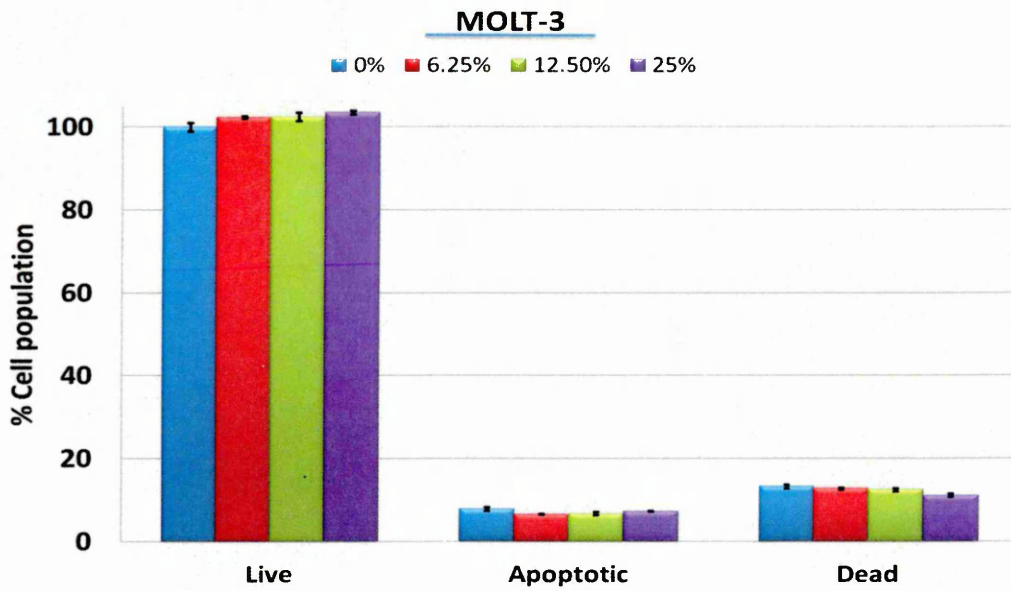


Figure 3.45: Annexin V-FITC/PI based on flow cytometry. MOLT-3 treated in pH adjusted media for 48 h. Mean \pm SEM. * indicates significant difference ($P \leq 0.05$) vs. untreated control. n= 3.

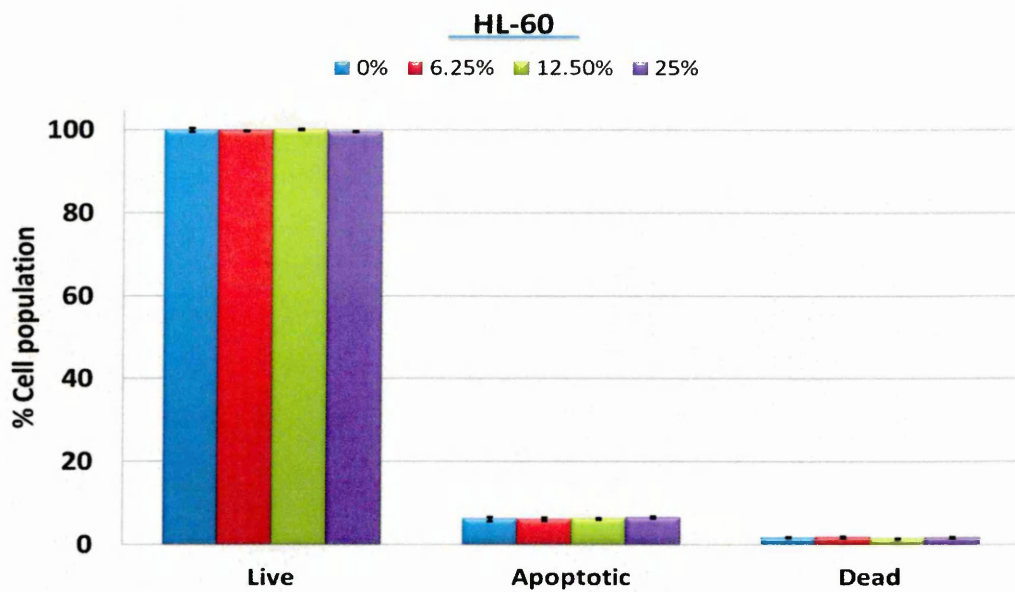


Figure 3.46: Annexin V-FITC/PI based on flow cytometry. HL-60 treated in pH adjusted media for 48 h. Mean \pm SEM. * indicates significant difference ($P \leq 0.05$) vs. untreated control. n= 3.

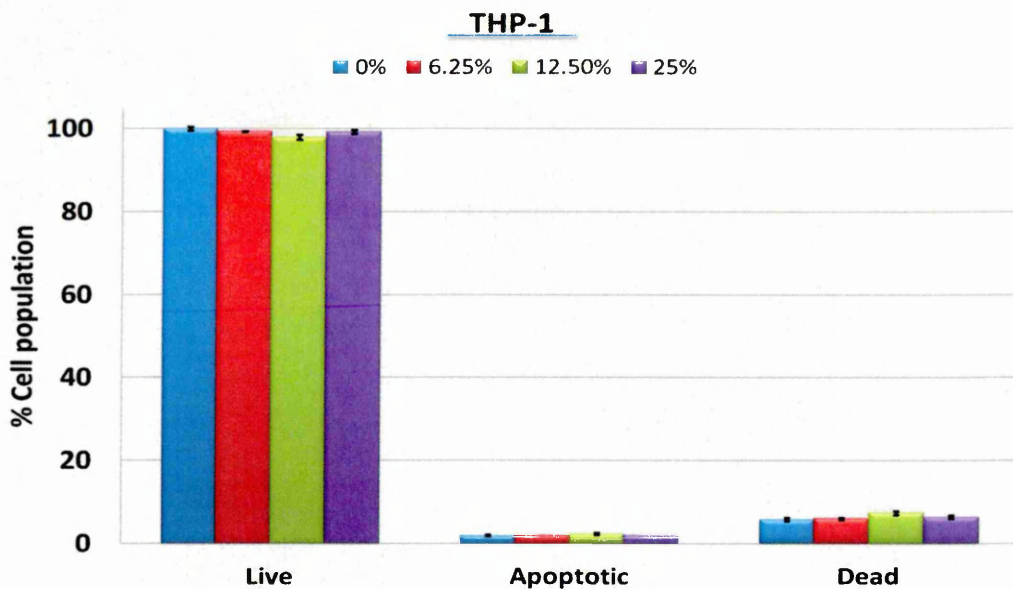


Figure 3.47: Annexin V-FITC/PI based on flow cytometry. THP-1 treated in pH adjusted media for 48 h. Mean \pm SEM. * indicates significant difference ($P \leq 0.05$) vs. untreated control. n= 3.

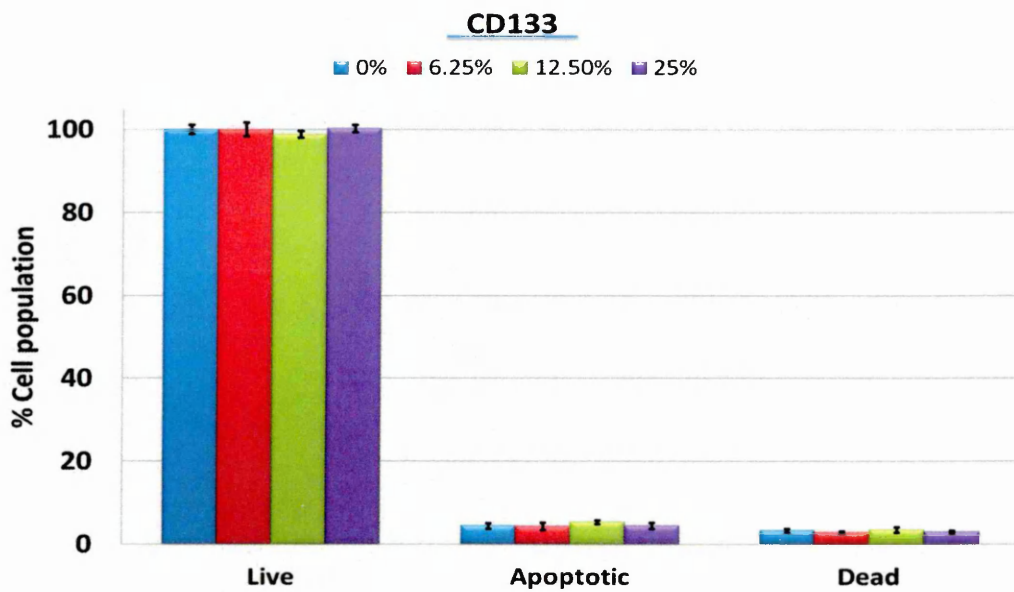


Figure 3.48: Annexin V-FITC/PI based on flow cytometry. CD133 treated in pH adjusted media for 48 h. Mean \pm SEM. * indicates significant difference ($P \leq 0.05$) vs. untreated control. n= 3.

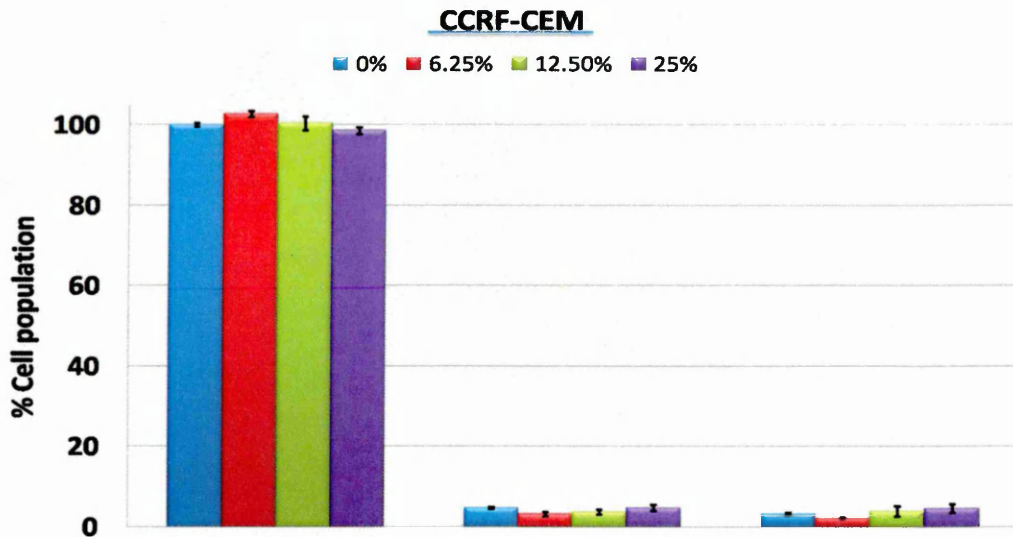


Figure 3.49: Annexin V-FITC/PI based on flow cytometry. CCRF-CEM treated in equivalent concentration of water for 48 h. Mean \pm SEM* indicates significant difference ($P \leq 0.05$) vs. untreated control. n= 3.

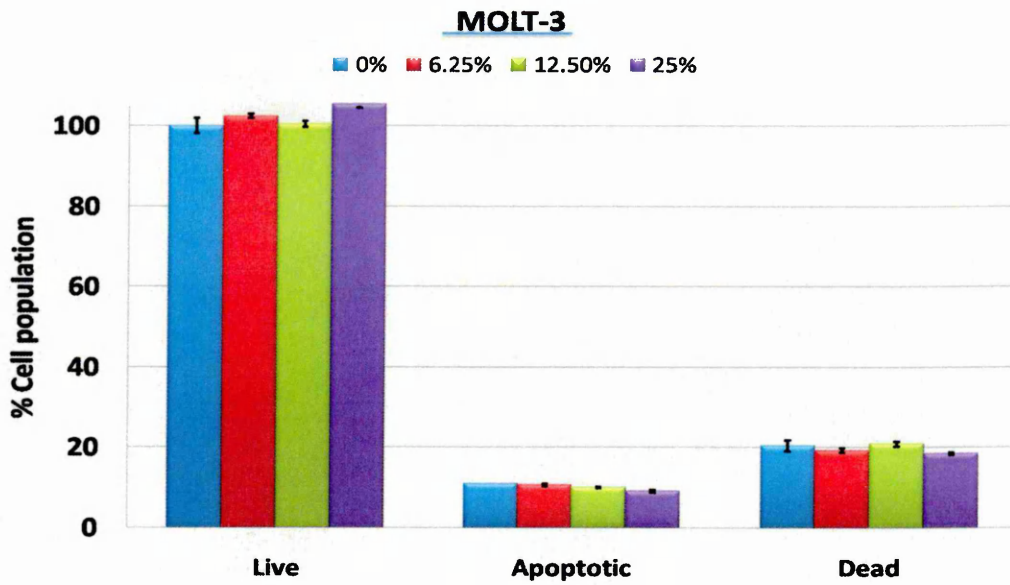


Figure 3.50: Annexin V-FITC/PI based on flow cytometry. MOLT-3 treated in with equivalent concentration of water for 48 h. Mean \pm SEM. *indicates significant difference ($P \leq 0.05$) vs. untreated control. n = 3.

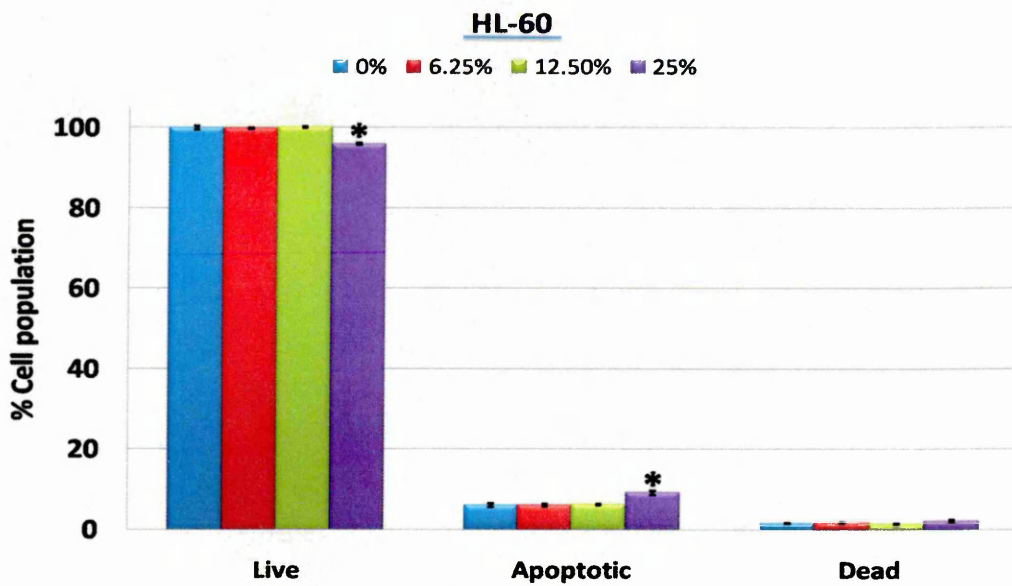


Figure 3.51: Annexin V-FITC/PI based on flow cytometry. HL-60 treated in equivalent concentration of water for 48 h. Mean \pm SEM. * indicates significant difference ($P \leq 0.05$) vs. untreated control. n = 3.

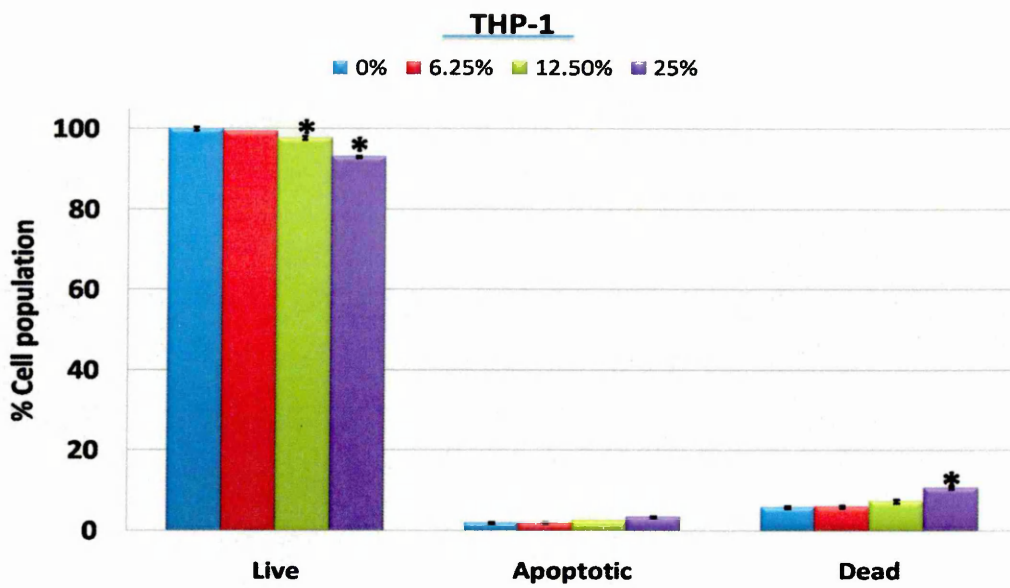


Figure 3.52: Annexin V-FITC/PI based on flow cytometry. THP-1 treated in equivalent concentration of water for 48 h. Mean \pm SEM. * indicates significant difference ($P \leq 0.05$) vs. untreated control. n= 3.

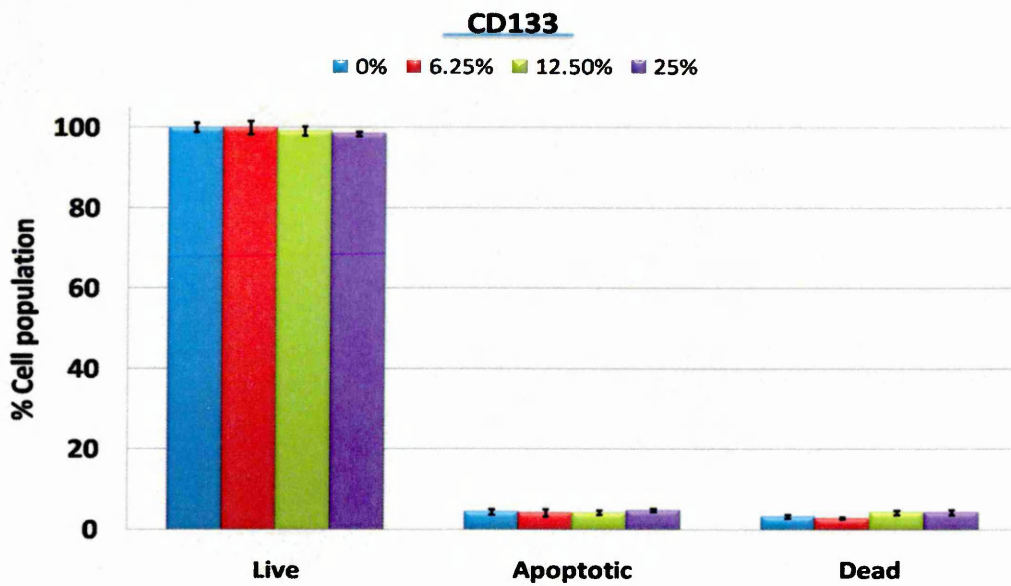


Figure 3.53: Annexin V-FITC/PI based on flow cytometry. CD133 treated in equivalent concentration of water for 48 h. Mean \pm SEM. * indicates significant difference ($P \leq 0.05$) vs. untreated control. n= 3.

3.5 Discussion

This study aimed to investigate the hypothesis that: The effect of pomegranate extracts and its purified constituents have been investigated previously using cell lines derived from solid tumours; few, however, have investigated the effect in leukaemia cells. Khan *et al.* (2009) investigated the effect of PJ on induction of apoptosis in 2 breast cancer cell lines (SUM 149 and MDA-231), together with non-tumour MCF-7 10A cells, where treatment with PJ induced apoptosis following 72 h selectively within the 2 tumour cell lines and did not affect the non-tumour MCF-7 cells. Here we also identified an increased sensitivity to PJ within the majority of leukaemia cell lines compared to non-tumour HSCs were seen. Together, these studies suggest that pomegranate extracts could hold promise for selective cancer therapies in subsets of cancer types. Seeram and his colleagues (2005) showed that both isolated constituents, such as ellagic acid and punicalagin as well as PJ induced apoptosis in 2 human colon cell cultures (HT-29 and HCT116). It has also been shown that PJ derived ellagitannins and urolithins induced apoptosis in colon cancer cell line (HT-29) following 24 h (Kasimsetty *et al.*, 2010). Induction of apoptosis, in a number of prostate cancer cells such as PC3 (Albrecht *et al.*, 2004; Malik *et al.*, 2005), DU-145 (Malik *et al.*, 2005; Hong *et al.*, 2008), LNCaP and LNCaP-AR (Hong *et al.*, 2008), and LAPC4 (Koyoma *et al.*, 2010) has also been shown. Here, PJ also induced apoptosis in a number of leukaemia cell lines. Importantly, we have shown that the response to PJ varied between leukaemia cell lines and the majority was affected to a greater extent than the non-tumour control cells. The sensitivity to chemotherapy agents often display selective targeting to either leukaemias of the lymphoid or myeloid origin; for example, phenoxodiol showed greater toxicity to lymphoid leukaemia than myeloid leukaemia (Herst *et al.*, 2009), as do extracts from carrot juice (Zaini *et al.*, 2010). Lymphoid leukaemia and myeloid leukaemia are well known to be caused by abnormalities to differential signalling pathways; for example, STATs are involved in the pathogenesis of myeloid leukaemia and act as a target for selective chemotherapy agents such as the tyrosine kinase inhibitors, which do not show any effect within lymphoid leukaemia (White and Huges, 2009). Thus, it is not surprising to see differential sensitivity patterns between cell lines derived from myeloid and lymphoid leukaemia's within the current study. Future work will focus on investigating the molecular mechanisms of PJ on these cell lines to

elucidate further the molecular targets of PJ and hence identify reasons for the selective targeting toward lymphoid leukaemia cell lines.

Interestingly, however, some of the myeloid leukaemia cell lines did show cytotoxic effects, suggesting that in certain subtypes of myeloid leukaemia PJ may still be a useful therapeutic agent. In addition to induction of apoptosis, cell cycle arrest can be a useful target for cancer therapies (Schmitt, 2007).

Here, a dose-dependent arrest of cell cycle at different phases was observed. At low doses of PJ, the majority of cells showed G_0/G_1 arrest, suggesting induction of senescence (Schmitt, 2007). G_0/G_1 arrest has been observed previously in a number of tumour cell lines following PJ treatments; for example, human lung carcinoma A549 cell line treatment with PJ for 72 h resulted in a dose-dependent arrest of cells in G_0/G_1 phase of the cell cycle (Khan *et al*, 2006b). In addition, Kasimsetty *et al*. (2010) observed a reduction in S phase and an accumulation of cells in G_0/G_1 in DU145 colon cancer cells following PJ treatment (Kasimsetty *et al*, 2010). This reduction in S phase and accumulation of cells in G_0/G_1 was also observed within the higher concentration of PJ for HL-60 and KG-1a cell lines, which were also the most sensitive myeloid cell lines. Interestingly, these 2 cell lines were the only ones investigated that at this concentration induced G_0/G_1 arrest; these 2 cell lines show myeloblast morphology unlike the other 2 myeloid cell lines that appears to affect the cell cycle response. This may be due to modulation of c-myc expression that is over expressed within HL-60 cells and inhibition of c-myc induces G_0/G_1 cell cycle arrest (Anfossi *et al*, 1989); thus it is possible the G_0/G_1 arrest observed here is due to inhibition of c-myc expression. In all other cell lines and non-tumour HSCs treated with 12.5% PJ S-phase arrest was observed, demonstrating again variability between cell lines from different leukaemia types. This effect has been observed previously in CaCo-2 cells treated with the pomegranate extracted ellagitannin: punicalagin (Herst *et al*, 2009). Kasimsetty *et al*. (2010) also evaluated the effect of PJ-derived ellagitannins (gallic acid, ellagic acid, gallagic acid, hexahydroxydiphenic, gallagylidilactone, punicalins, and punicalagins) on HT-29 colon cells, and once again S-phase arrest was observed. Differential effects on cell cycle dependent on concentration or duration has been seen in a number of

studies previously for example, Mertens-Talcott *et al.* (2003) investigated 3 polyphenolic compounds (camptothecin, ellagic acid, and quercetin) on a lymphoid leukaemia cell line (MOLT-4); they demonstrated G₀/G₁ arrest following camptothecin treatment for 12 h, but this effect was not observed at later time points, whereas treatment with a combination of ellagic acid and quercetin showed no effect following 12 h, but S-phase arrest was observed following 24 h (Mertens-Talcott *et al.*, 2003). S-phase arrest can result from 2 main causes, either an artefact of cells undergoing apoptosis within G₂/M phase thus reducing their DNA content and accumulating within the S-phase peak during cell cycle analysis. Alternatively, agents that alter cell cycle expression that control progression through S phase will result in S-phase arrest. This has been shown previously in colon cancer cells treated with 2,3-dichlorophenoxypropyl, where S-phase arrest was induced by over expression of p21 (Zhu *et al.*, 2004) or by affecting agents involved in DNA repair mechanisms such as inhibition of Poly(ADPribose) as seen following treatment of RAW 264.7, a macrophage cell line with galloytanin (Rapizzi *et al.*, 2004), which could be a mechanism induced by pomegranate extracts within our current study.

Within this study, we also investigated the overall effect of PJ on total viable cell number, which shows a combined effect of induction of apoptosis and inhibition of cellular proliferation, confirming our previous data. Decreased number of viable cells has previously been demonstrated following pomegranate extract treatments in a number of cancers. Several studies in cell culture and animal models have reported inhibition of prostate cancer by PJ (Seeram *et al.* 2005, 2007; Albrecht *et al.* 2004; Lansky (1) *et al.* 2005; Malik *et al.* 2005; Sartippour *et al.*, 2008; Retting *et al.*, 2008; Hong *et al.*, 2008; Koyoma *et al.*, 2010).

The effects of pomegranate fruit extracts on lung cancer were examined by Khan *et al.* (2007b) both *in vitro* and *in vivo*, demonstrating that Normal bronchial epithelial cells (NHBE) and human lung carcinoma A549 cells were treated with pomegranate fruit extract (50-150 µg/ml) for 72 h, showing significant decrease in cell viability in A549 cells, while treatment of NHBE cells resulted in minimal effects. Based on the results of this *in vitro* data, a study carried out in the mouse model showed that oral

administration of human acceptable dose of PJ extract to athymic mice implemented with A549 cells resulted in significant inhibition in progression of tumour growth. Human breast cancer cell lines MCF-7 and MB-MDA-231 treated with fermented pomegranate resulted in a decrease in cell viability on both cells. In other breast cancer cell lines (MDA-231 and SUM-149) pomegranate fruit extract decreased cell proliferation following 72 h. *In vitro* studies pomegranate fruit extract decreased cell viability in WA4 mouse mammary cancer cells. Seeram *et al.* (2005) reported that both isolated constituents such as ellagic acid and punicalagin as well as PJ inhibited the proliferative effects of HT29 and HCT116 colon tumour cells.

PJ investigated within this study was a total extract of all the polyphenolics and anthocyanins together with any other potential bioactive agents, rather than a pure fraction this was performed to investigate the effects of combined responses, rather than simple individual actions. Pomegranates contain a wide number of potential bioactive agents, including hydrolysable tannins (such as punicalin, punicalagin, and gallagic), and anthocyanins (such as delphinidin, cyanidin, and pelargonidin), which can often act synergistically or indeed inhibit the actions of other agents (Herst *et al*, 2009; Mertens-Talcott *et al*, 2003).

3.6 Conclusion

This study is the first to investigate the effect of PJ on 8 different leukaemia cell lines in addition to normal HSCs; we demonstrated important variations in sensitivity between different types of leukaemia cell lines and normal cells. This study suggests that the active components from PJ could have potential as agents in the treatment of certain leukaemia's, and further work will aim to identify these components.

4. Identification of potential active compounds within PJ

4.1 Introduction

We have previously shown that crude extracts of PJ induce apoptosis and inhibit cell cycle in a number of leukaemia cell lines, which demonstrated greater sensitivity than non-tumour control cells (Chapter 3) (Dahlawi *et al*, 2011).

However, to date, the compounds responsible for the anti-leukaemic properties of pomegranate remain unknown. PJ contains a number of potential active compounds including organic acids, vitamins, sugars, and phenolic components. The phenolic components include phenolic acids: principally, hydroxybenzoic acids (such as gallic acid and ellagic acid) (Amakura *et al*, 2000); hydroxycinnamic acids (such as caffeic acid and chlorogenic acid) (Elfalleh *et al*, 2011); anthocyanins, including glycosylated forms of cyanidin, delphinidin, and pelargonidin (Fanali *et al*, 2011; Krueger, 2012); and gallotannins and ellagitannins (Amakura *et al*, 2000). In addition, PJ contains glucose, fructose, water, and organic acids (including ascorbic and citric acid) (Krueger, 2012). However, the concentration and the contents of these compounds vary due to growing region, climate, cultivation practice, and storage conditions (Pande and Akoh 2009; Elfalleh *et al*, 2011; Legua *et al*, 2012).

Here, we used solid phase extraction (SPE) to fractionate PJ to determine which fractions induced apoptosis and cell cycle arrest using two lymphoid and two myeloid cell lines, which we previously demonstrated in Chapter 3 were sensitive to crude PJ. We assessed the polyphenol composition of the fractions by phenol assay and used liquid chromatography mass spectrometry (LC-MS) to identify active compounds within fractions of PJ.

4.2 Materials and Methods

4.2.1 Sample Preparation and Fraction Separation from PJ

Solid phase extraction (SPE) using Strata C18E GIGA columns (Phenomenex) were used to separate fractions from pomegranate juice extract (PJ). First, the columns were pre-equilibrated by washing with 50 mL of acetonitrile, then 50 mL of 0.1% formic acid/ultra pure water (v/v) (Sigma) PJ derived from fresh pomegranates (Sainsbury's U.K.) prepared as described in section 2.1 were sterile filtered through 0.22 μm syringe filter (Invitrogen) and diluted 1:1 with sterile distilled water, then 50 mL of this diluted juice was added to the SPE unit. The unbound compounds which passed directly through the column were collected (Fraction A: unbound Fraction). Then, 50 mL each of ultra-pure water, acetonitrile, acetone, and ethyl acetate were added to the column to collect water (Fraction B), acetonitrile (Fraction C), acetone (Fraction D), and ethyl acetate (Fraction E) fractions, respectively, as described previously (Zaini *et al*, 2012) (Figure: 4.1). Each fraction was dried using freeze drying (MODULYOD-230 freeze dryer, Thermo) at -30 to -80°C for Fractions A and B or dried under a nitrogen stream at room temperature for Fractions C, D, and E. The water, unbound, and acetonitrile fractions were dissolved in distilled water; the acetone fraction in methanol; and ethyl acetate fraction in DMSO to the required dilution (Sigma)).

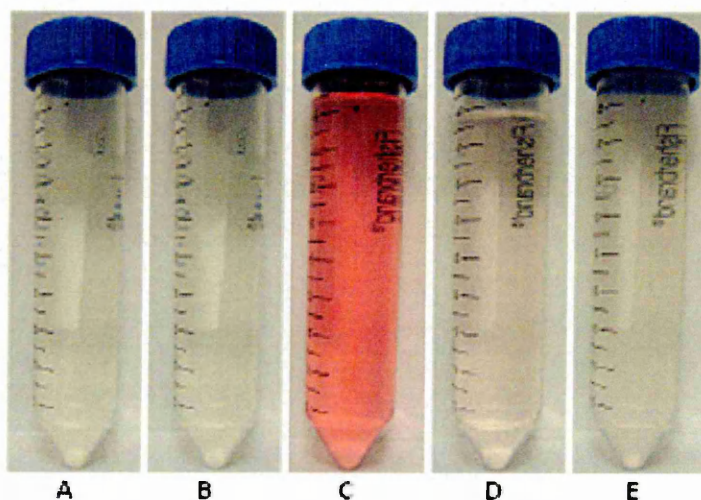


Figure 4.1: Illustrates fractions generated from PJ using SPE. A: Unbound fraction, B: water fraction, C: acetonitrile fraction, D: acetone fraction, and D: ethyl acetate fraction.

4.2.2 Cell lines and Culture

Four leukaemia cell lines were obtained from the American Type Culture Collection (ATCC; Middlesex, U.K.), which chapter 3 and Dahlawi *et al.* (2011) demonstrated differing sensitivity to PJ. Two lymphoid cell lines: CCRF-CEM and MOLT-3 and two myeloid cell lines: HL-60 and THP-1 (Section 2.2). Cell lines were maintained and cultured in RPMI 1640 medium (Invitrogen, Paisley, U.K.) supplemented with 10% (v/v) foetal bovine serum, 1.5 mmol/L L-glutamine, and 100 µg/mL penicillin/streptomycin (complete media) in a humidified atmosphere of 5% CO₂ at 37°C.

Cells were seeded in 12-well plates (Fisher Scientific) at a cell density of 0.5×10^6 cells per well and treated individually with the five fractions (unbound [i.e., compounds which passed directly through the column] and fractions eluted with water, acetonitrile, acetone, and ethyl acetate fractions) at equivalent compound weights seen in 0%, 6.25%, 12.5%, and 25% whole PJ, all treatments were performed in triplicate. Following treatment, cells were investigated for induction of apoptosis and inhibition of cell proliferation following 24, 48, and 72 h (Table 4.1).

Techniques	Treatment	Concentration	Cell lines	Time point
Cell Titer-Glo[®] Luminescent Cell Viability Assay	PJ, unbound, water, acetonitrile, acetone, and ethyl acetate fractions	6.25%, 12.5%, and 25%	CCRF-CEM, MOLT-3, HL-60, and THP-1	24, 48 and 72 hr
Cell cycle	Acetonitrile fraction	6.25%, 12.5%, and 25%	CCRF-CEM, MOLT-3, HL-60, and THP-1	48 hr
Annexin V-FITC/PI	Acetonitrile fraction	6.25%, 12.5%, and 25%	CCRF-CEM, MOLT-3, HL-60, and THP-1	24, 48 and 72 hr
NucView™ 488 Caspase-3 substrate assay	Acetonitrile fraction	6.25%, 12.5%, and 25%	CCRF-CEM, MOLT-3, HL-60, and THP-1	24, 48 and 72 hr
Hoechst 33342 and PI	Acetonitrile fraction	6.25%, 12.5%, and 25%	CCRF-CEM, MOLT-3, HL-60, and THP-1	24, 48 and 72 hr
LC-MS	PJ, unbound, water, acetonitrile, acetone, and ethyl acetate fractions			
Folin-Ciocalteu method	PJ, unbound, water, acetonitrile, acetone, and ethyl acetate fractions			

Table 4.1: Experimental design for Chapter 4.

4.2.3 Cell Viability

The effect of SPE fractions (unbound, water, acetonitrile, acetone, and ethyl acetate) on the viability of cells was determined by the Cell Titer-Glo[®] Luminescent Cell Viability Assay (Promega) which measures total adenosine triphosphate (ATP) present, indicating the number of metabolically active cells as described in section 2.3.2. Cells were seeded at 25×10^4 cells in 100 μ L of complete media and treated with each fraction at a concentration equivalent to that seen in 0%, 6.25%, 12.5%, and 25% whole PJ in white 96-well plate (Fisher Scientific) for 48 h.

4.2.4 Annexin V- FITC /PI Flow Cytometry assay

Annexin V-FITC/PI fluorescein isothiocyanate (FITC) stains were used to detect apoptosis based on flow cytometry as described in section 2.4.1. Cells were seeded at 5×10^5 cells in 100 μ L of complete media and treated with each fraction at a concentration equivalent to that seen in 0%, 6.25%, 12.5%, and 25% whole PJ in a 12-well plate (Fisher Scientific) for 24, 48, and 72 h. Data were recorded from 10,000 cells per sample and analyzed using FlowJo software (Tree Star).

4.2.5 Caspase-3 Activity

NucView[™] 488 Caspase-3 substrate (Cambridge Bioscience, Cambridge, U.K.), was used for detection of apoptosis based on flow cytometry as described in section 2.4.3. Cells were treated with PJ fractions (unbound, water, acetonitrile (ACN), acetone, and ethyl acetate) at concentrations equivalent to their component concentrations seen in 0-25% whole PJ for 48 h. Data were recorded from 10,000 cells per sample and analyzed using FlowJo software (Tree Star, Ashland, OR).

4.2.6 Hoechst 33342 and Propidium Iodide (PI) staining

Apoptotic cells can be distinguished from healthy and necrotic cells by certain morphological features which are an important tool in apoptosis research. These features include cell shrinkage, membrane blebbing, chromatin condensation and nuclear fragmentation (Kerr *et al*, 1972, Wyllie *et al*, 1980, Galluzi *et al*, 2007). In contrast necrotic cells characterised by loss of membrane integrity. Begin with swelling

of the cytoplasm and mitochondria complete necrosis with cell lysis (Galluzi *et al*, 2007). Such features can be observed under a fluorescence microscope using a DNA specific dye.

Hoechst 33342 and PI staining technique detects apoptosis based upon fluorescent detection for morphological changes in apoptotic cells. Hoechst 33342, is a cell permeable DNA stain that is excited by ultraviolet light at around 350 nm and emits blue fluorescence at 460 nm. Hoechst 33342 binds preferentially to adenine-thymine (A-T) regions of DNA. This stain binds into the minor groove of DNA and exhibits distinct fluorescence emission spectra that are dependent on dye base pair ratio. PI stain as described previously in section 2.4.1 is a red-fluorescence dye (excitation/emission 535/617), which is only permeate to dead cells. The staining pattern resulting from the simultaneous use of these dyes makes it possible to distinguish normal, apoptotic, and dead (late apoptotic and necrotic) cell populations by fluorescence microscopy (Figure 4.3).

4.2.5.1 Methodology

Hoechst 33342 and propidium iodide (PI) staining was used to observe the apoptotic/necrotic morphology of HL-60 cells. In brief, 0.25×10^5 cells/mL were seeded into 12-well plates and incubated for 24 h following treatment with the acetonitrile fractions at concentrations equivalent to component concentrations seen in 0–25% whole PJ. Then, 1 μ L of PI (50 μ g/mL) and 5 μ L of Hoechst 33258 (10 μ g/mL) stains were added to each well and incubated at 37°C for 15 min. Cells were investigated using an Olympus inverted fluorescence microscope at excitation wavelength 350 nm and 488 nm dual wavelength filter and images were captured using Q Capture-Pro 8.0 (UVP BioImaging Systems, Loughborough, U.K.).

4.2.5.2 Analysis

Cell populations (live, apoptotic & necrotic) were separated into three groups: live cells displayed low levels of fluorescence and normal morphology; apoptotic cells showed a higher level of blue fluorescence together with chromatin features of apoptosis, and dead cells displayed intense red fluorescence (Figure: 4.2). Necrotic cells is also characterized by high red fluorescence with damaged membranes display, but can be

differentiated from late apoptotic cells as mentioned in 4.2.6. (Figure4.2). Quantitative analysis of cell populations (live, apoptotic and necrotic) was performed based on counting 200 randomly-selected cells and the percentage of apoptotic features determined for each sample.

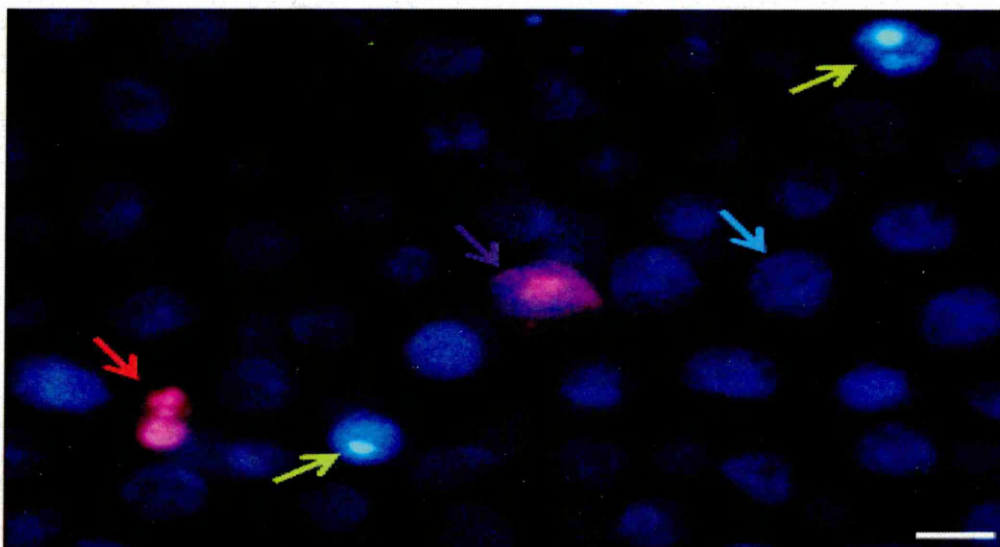


Figure 4.2: Analysis of apoptosis of HL-60 cell line using Hoechst and PI staining. Live cells indicated by blue arrow, early apoptotic cells indicated by green arrows, dead and late apoptotic cell indicated by red arrows, and necrotic cell indicated by purple arrow.

4.2.6 Cell Cycle

The cell cycle distribution of leukaemia cell lines was measured by DNA content in each cell based on flow cytometry using the PI stain as described in section 2.5. Data from 10,000 cells per sample were recorded and percentages of cells within G_0/G_1 , S, and G_2/M cell cycle phases were determined with Flow Jo software and Waston (pragmatic) analysis of cell cycle (Tree Star).

4.2.7 Liquid Chromatography Mass Spectrometry (LC-MS)

4.2.7.1 Methodology

Samples (containing 20 μg gallic acid equivalents [GAE]s by Folin assay) were analyzed on a LCQ-DECA system, comprising Surveyor autosampler, pump and photo diode array detector (PDAD), and a Thermo-Finnegan mass spectrometer iontrap (Stoke on

Trent, U.K.). The PDAD scanned three discrete channels at 280, 365, and 520 nm. Samples were eluted with a linear gradient of 5% acetonitrile (0.1% formic acid) to 30% acetonitrile (0.1% formic acid) on C18 column (Synergi Hydro C18 with polar end capping 2.0 mm × 150 mm) (Phenomenex) over 60 min at a rate of 200 µL/min. For dried fraction samples, the gradient was altered ($t = 0$, 5% acetonitrile; $t = 10$ min, 12.5% acetonitrile; and $t = 60$ min, 30% acetonitrile) to try to separate the later eluting ellagitannins. The LCQ-DECA LC-MS was fitted with an electrospray ionization interface and the samples were analyzed in positive and negative ion mode. There were two scan events: full scan analysis followed by data-dependent MS/MS of the most intense ions. The data-dependant MS/MS used collision energies (source voltage) of 45% in wideband activation mode. The MS detector was tuned against cyanidin-3-*O*-glucoside (positive mode) and against ellagic acid (negative mode).

4.2.8 Determination of Total Phenolics

The aim of this method was to determine the total polyphenol content in PJ and its fractions (unbound, water, acetonitrile, acetone, and ethyl acetate) using Half Strength Folin-Ciocalteu method (Singleton *et al*, 1999; Ainsworth *et al*, 2007).

Phenolic compounds are oxidized by Folin-Ciocalteu reagent. This reagent is formed from a mixture of phosphotungstic acid, H₃PW₁₂O₄₀, and phosphomolybdic acid, H₃PMo₁₂O₄₀, which, after oxidation of the phenols, is reduced to a mixture of blue oxides of tungsten, W₈O₂₃, and molybdenum, Mo₈O₂₃. The blue colouration produced has a maximum absorption in the region of 750 nm, and is proportional to the total quantity of phenolic compounds originally present (Ainsworth *et al*, 2007)

4.2.8.1 Methodology

The content of the total phenolics was evaluated by using the Half Strength Folin-Ciocalteu method adapted from (Deighton *et al*. 2000). First, 250 µL Folin-Ciocalteu reagent (Sigma) was added to 250 µL of each fraction (unbound, water, acetonitrile, acetone, and ethyl acetate) (1% diluted with water) and mixed gently prior to 3 minutes incubation at room temperature. Then, 250 µL of sodium carbonate solution was added to each sample, mixed well, and incubated for 1 h prior to recording at 750

nm using Ultrospec™ 2100 *pro* UV/Visible Spectrophotometer (GE Healthcare Life Science).

Triplicate samples containing a range of gallic acid contents from 0-500 µg were prepared to create standards. Total phenolics were expressed as Gallic Acid Equivalents (GAEs).

4.2.9 Statistical analysis:

Means and standard error of the mean (SEM) were calculated and a Shapiro–Wilke test (Stats Direct, Cheshire, U.K.) was used to test whether data followed a normal distribution. Data were non-parametric and thus a Kruskal–Wallis test and a Conover–Inman post hoc test were used to investigate significant differences. Results were considered statistically significant when $P \leq 0.05$.

4.3. Results:

4.3.1 Differential Effects of Pomegranate Fractions on ATP Levels

Whole PJ induced a dose-dependent inhibition of ATP levels within all four leukaemia cell lines ($P \leq 0.05$) (Figure: 4.3). The acetonitrile fraction obtained after SPE induced a significant decrease in ATP levels ($P \leq 0.05$) which showed a non-significant increase in cytotoxicity compared to the whole juice extracts mainly at the highest concentrations (25%) ($P > 0.05$) (Figure 4.3). The IC_{50} values of PJ and acetonitrile fractions for CCRF-CEM, MOLT-3, HL-60, and THP-1 cells are illustrated in Table 4.2. Low-dose treatments of leukaemia cell lines with either whole PJ or the acetonitrile fractions demonstrated dramatic reduction in ATP levels indicating decreased cell viability following 24 h treatment (Fig. 4.3). The unbound, water, acetone, and ethyl acetate SPE fractions had minimal effects on any cell line at the doses investigated (concentration equivalent to those present in 6.25%, 12.5%, and 25% whole PJ treatments) (Figure: 4.3).

	CCRF-CEM	MOLT-3	HL-60	THP-1
PJ	4.0%	4.7%	4.3%	7.0%
Acetonitrile fraction	3.1%	3.9%	3.0%	5.5%

Table 4.2: The IC_{50} of PJ and acetonitrile fractions on leukaemia cell lines (CCRF-CEM, MOLT-3, HL-60, and THP-1) following 24 h treatment. .

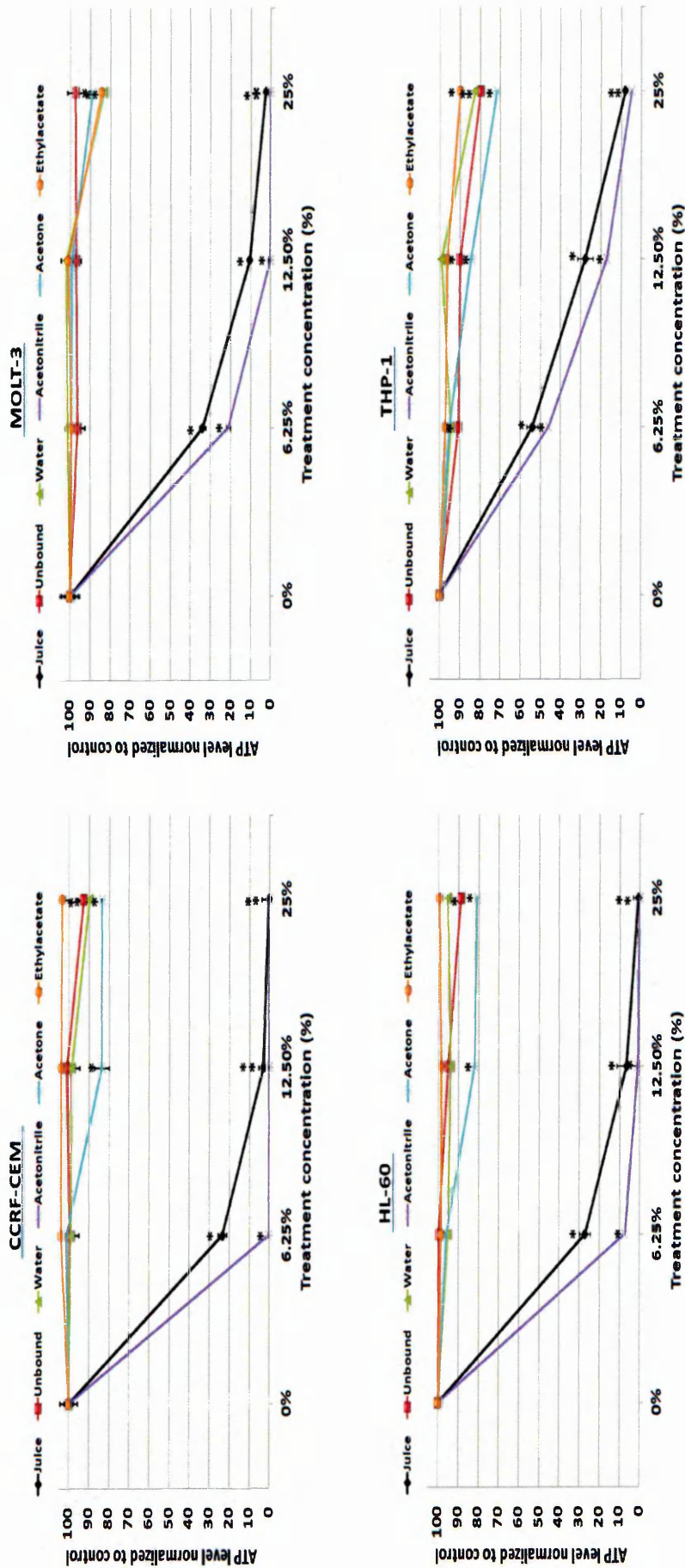


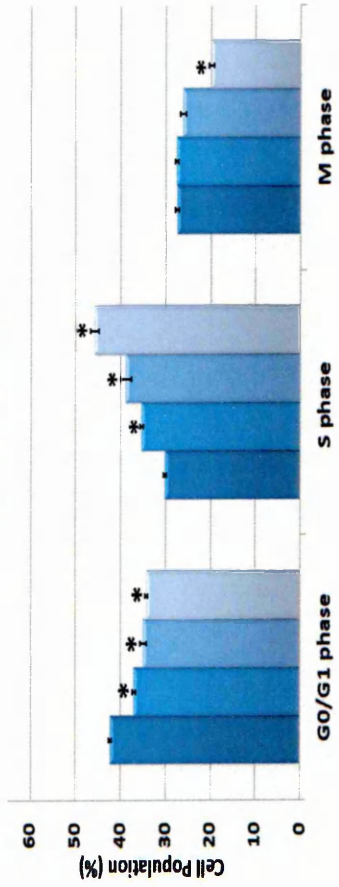
Figure 4.3: Effect of water, unbound, acetonitrile, acetone, and ethyl acetate fractions generated by SPE of PJ together with whole PJ in four leukaemia cell lines (CCRF-CEM, MOLT-3, HL-60, and THP-1). Cells were treated for 48 h with all fractions at concentrations equivalent to the concentration of compounds within 6.25%, 12.5%, and 25% whole PJ. ATP levels were investigated using the Cell Titer-Glo[®] Luminescent Cell Viability Assay to provide indication of live cell numbers. ATP levels normalized to controls and presented as means ± standard error. * indicates Significant difference ($P \leq 0.05$) vs. untreated control. n=3.

4.3.2 Effect of Acetonitrile Fraction from Pomegranate Juice on Cell Cycle Arrest within Leukaemia Cell Lines

Treatment of leukaemia cells lines with the acetonitrile fraction for 48 h demonstrated significant S phase arrest within all four cell lines ($P < 0.05$) with a corresponding significant decrease in cells within G_0/G_1 and M phases ($P < 0.05$) (Figure. 4.4).

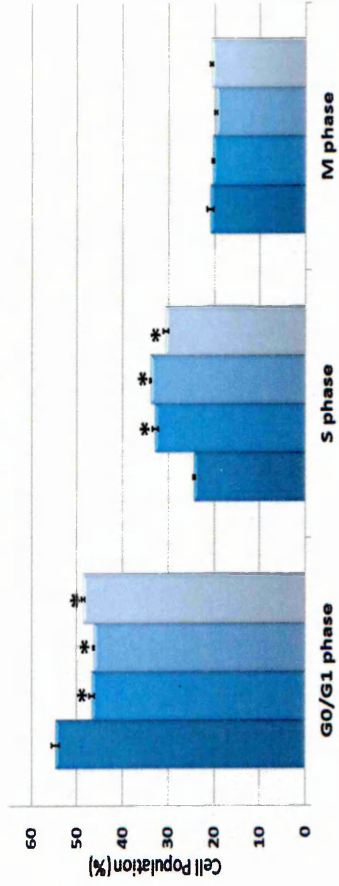
CCRF-CEM

0% 6.25% 12.50% 25%



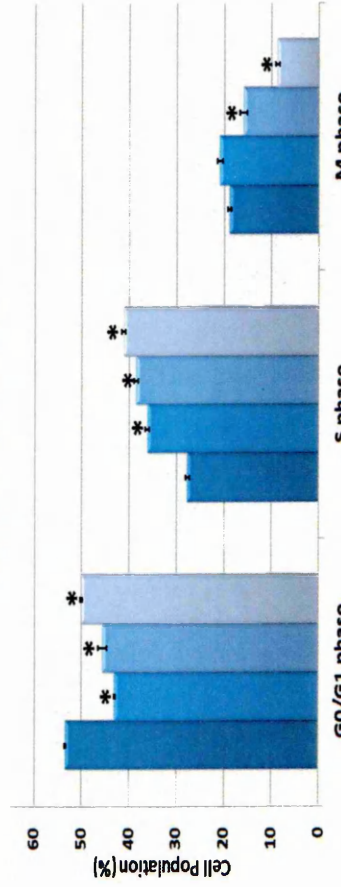
MOLT-3

0% 6.25% 12.50% 25%



HL-60

0% 6.25% 12.50% 25%



THP-1

0% 6.25% 12.50% 25%

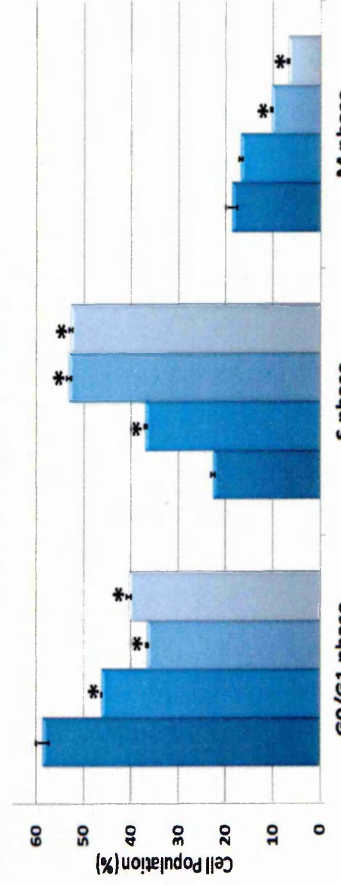


Figure 4.4: Effect of acetonitrile fraction generated by SPE of PJ on cell cycle phase distribution in four leukaemia cell lines (CCRF-CEM, MOLT-3, HL-60, and THP-1). Cells treated for 48 h with acetonitrile fraction at concentrations equivalent to those found in 6.25%, 12.5%, and 25% whole PJs. Means \pm standard error shown. * indicates significant difference ($P \leq 0.05$) vs. untreated control. n= 3.

4.3.3 Induction of Apoptosis by Acetonitrile SPE Fraction from Pomegranate Extracts within Leukaemia Cell Lines

Acetonitrile fraction induced apoptosis (determined via Annexin V/PI-FITC) in a dose-dependent manner in all four leukaemia cell lines following 24, 48, and 72 h incubation. Acetonitrile fraction showed a significant decrease in the number of live cells with a significant increase in the number of apoptotic and dead cells in CCRF-CEM cells at all concentrations following 24, 48, and 72 h ($P < 0.05$) (Figure 4.5). MOLT-3 and HL-60 cells exhibited a slight decrease in the number of live cells with a slight increase in the number of apoptotic and dead cells at 6.25% following 24 h treatment with acetonitrile fraction. However, following 48 and 72 h both cell lines significantly induced apoptosis at all concentrations ($P < 0.05$) (Figure 4.5 and 4.6). THP-1 was the least sensitive among the cell lines investigated, which illustrated only slight induction of apoptosis at the highest concentration of 25% following 24 h treatment. Following 48 and 72 h a significant decrease in the number of live cells and a significant increase in the number of live and apoptotic cells at the highest two concentrations 12.5% and 25% was seen ($P < 0.05$) (Figure: 4.6)

Induction of apoptosis by treatment with acetonitrile fraction was confirmed with induction of caspase-3 activity in all four cell lines following 24, 48, and 72 h (Figure 4.7). Results showed the same pattern of sensitivity toward acetonitrile fractions when determined with annexin V-FITC/PI (Figure 4.5 and 4.6)

Microscopic examination (Figure 4.8) also demonstrated a marked increase in the number of cells displaying apoptotic morphology (such as chromatin condensation and fragmentation), in addition to a decrease in the number of live cells displaying normal nuclear morphology in CCRF-CEM, MOLT-3, HL-60 and THP-1 cells (Figure 4.9 and 4.10). Necrotic cells were significantly increased following treatment with high concentrations (25%) in most of the cell lines.

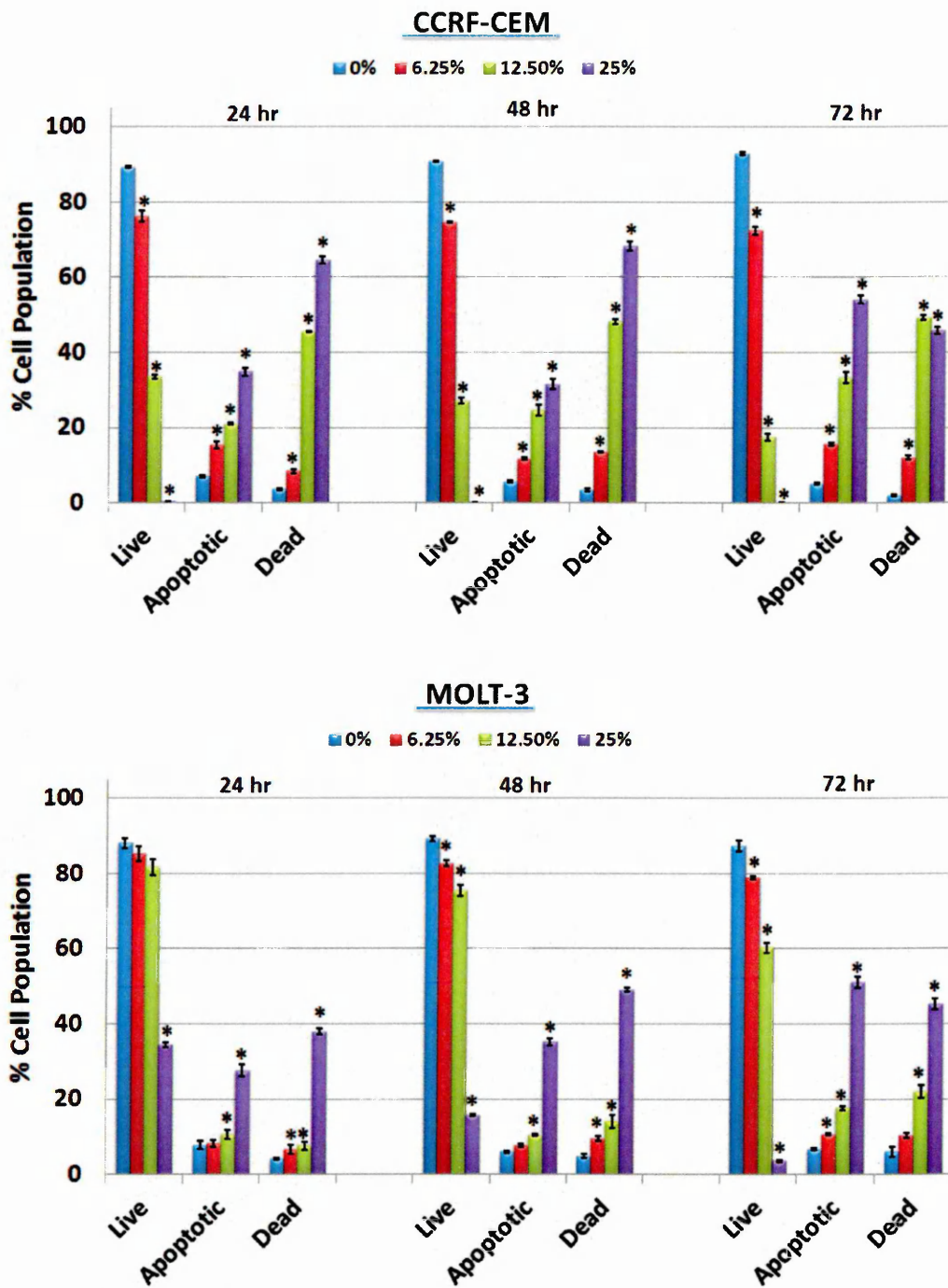


Figure 4.5: Effect of acetonitrile fraction generated by SPE of PJ on induction of apoptosis in leukaemia cell lines CCRF-CEM and MOLT-3. Cells treated for 24, 48, and 72 h with acetonitrile fraction at concentration equivalent to the concentrations of compounds found in 6.25%, 12.5%, and 25% whole PJ. Induction of apoptosis was determined by Annexin V-FITC/PI based on flow cytometry analysis. Means \pm standard error. * indicates significant difference ($P \leq 0.05$) vs. untreated control. n= 3.

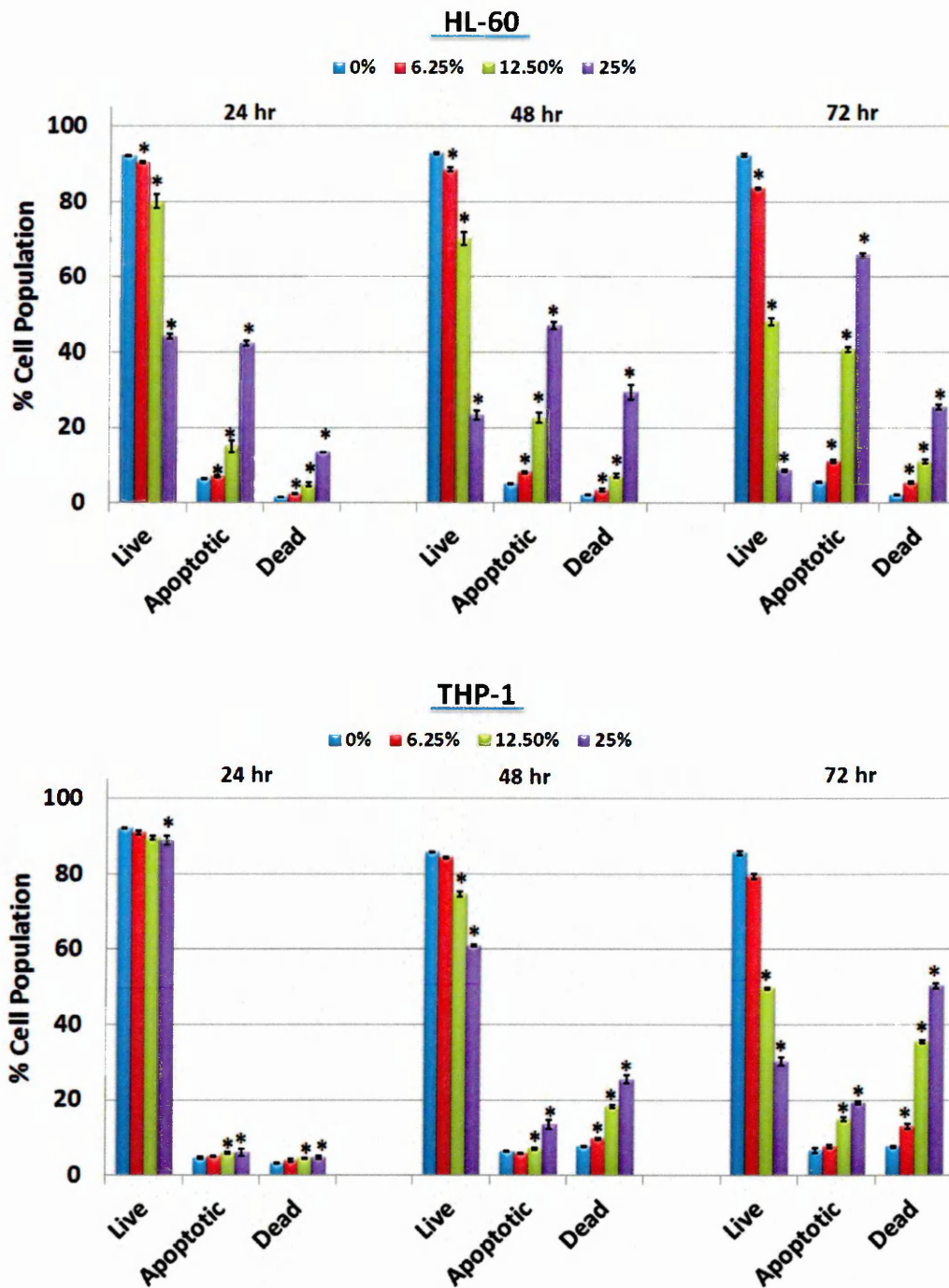


Figure 4.6: Effect of acetonitrile fraction generated by SPE of PJ on induction of apoptosis in leukaemia cell lines HL-60 and THP-1. Cells treated for 24, 48, and 72 h with acetonitrile fraction at concentration equivalent to the concentrations of compounds found in 6.25%, 12.5%, and 25% whole PJ. Induction of apoptosis was determined by Annexin V-FITC/PI based on flow cytometry analysis. Means \pm standard error. * indicates significant difference ($P \leq 0.05$) vs. untreated control. $n = 3$.

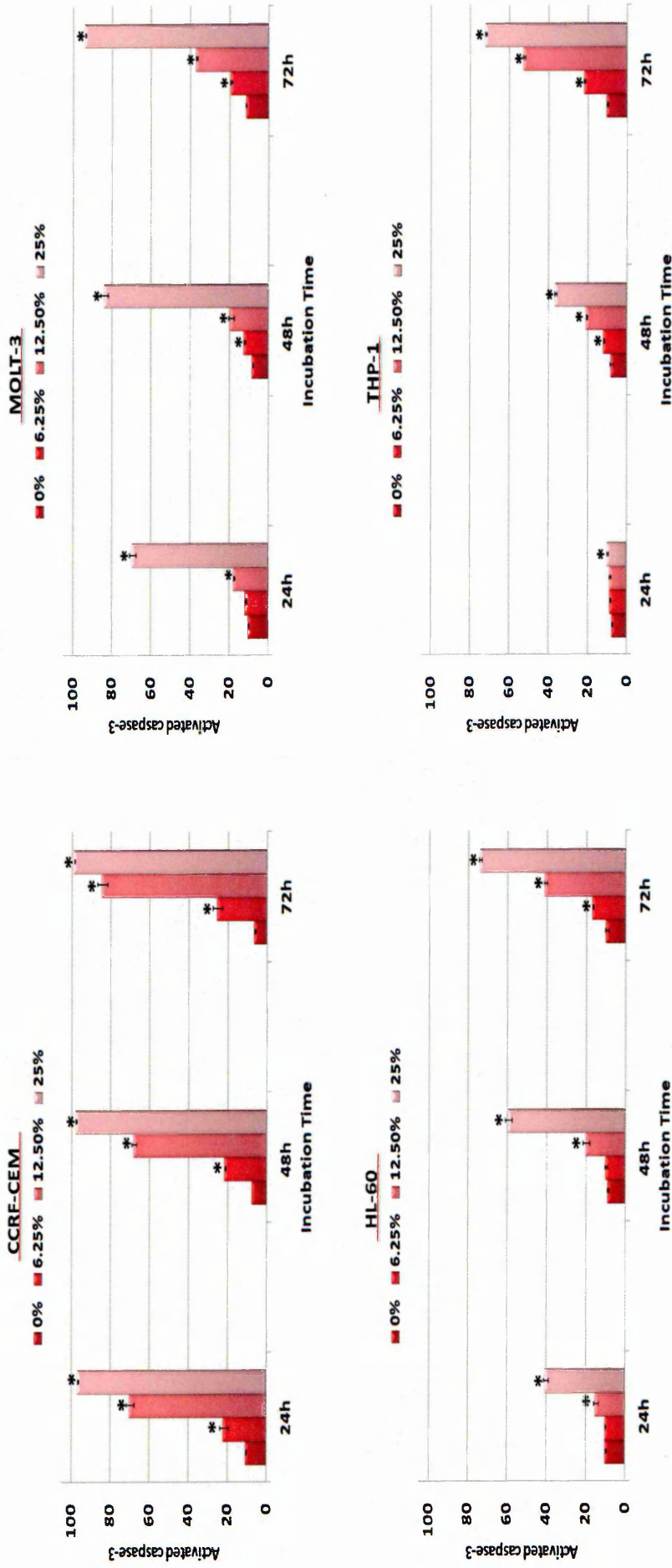


Figure 4.7: Effect of acetonitrile fraction generated by SPE of PJ on caspase-3 activation in four leukaemia cell lines (CCRF-CEM, MOLT-3, HL-60, and THP-1). Cells treated for 24; 48, and 72 h with acetonitrile fraction equivalent to the concentrations of compounds found in 6.25%, 12.5%, and 25% whole PJ. Caspase-3 activation was determined by NucView™ 488 Caspase-3 substrate based on flow cytometry analysis. Means ± standard error of the mean. * indicates significant difference ($P \leq 0.05$) vs. untreated control. n= 3.

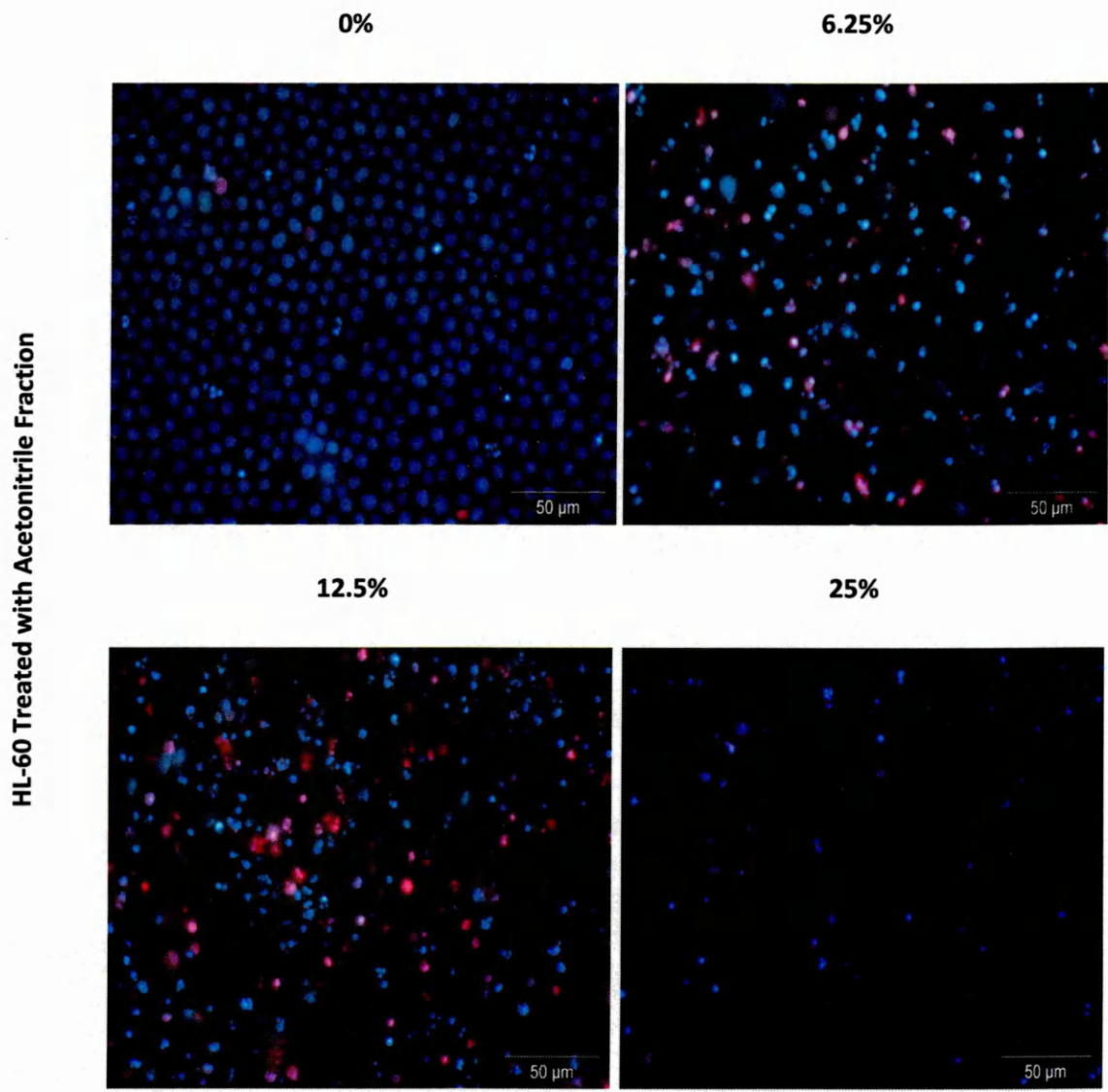


Figure 4.8: Effect of acetonitrile fraction generated by SFE of PJ on morphology of apoptotic cells in HL-60. Cells treated for 48h at concentration 6.25%, 12.5% and 25%. Apoptotic morphology was determined by Hoechst 33258 and PI staining using fluorescence microscope at magnification of x40.

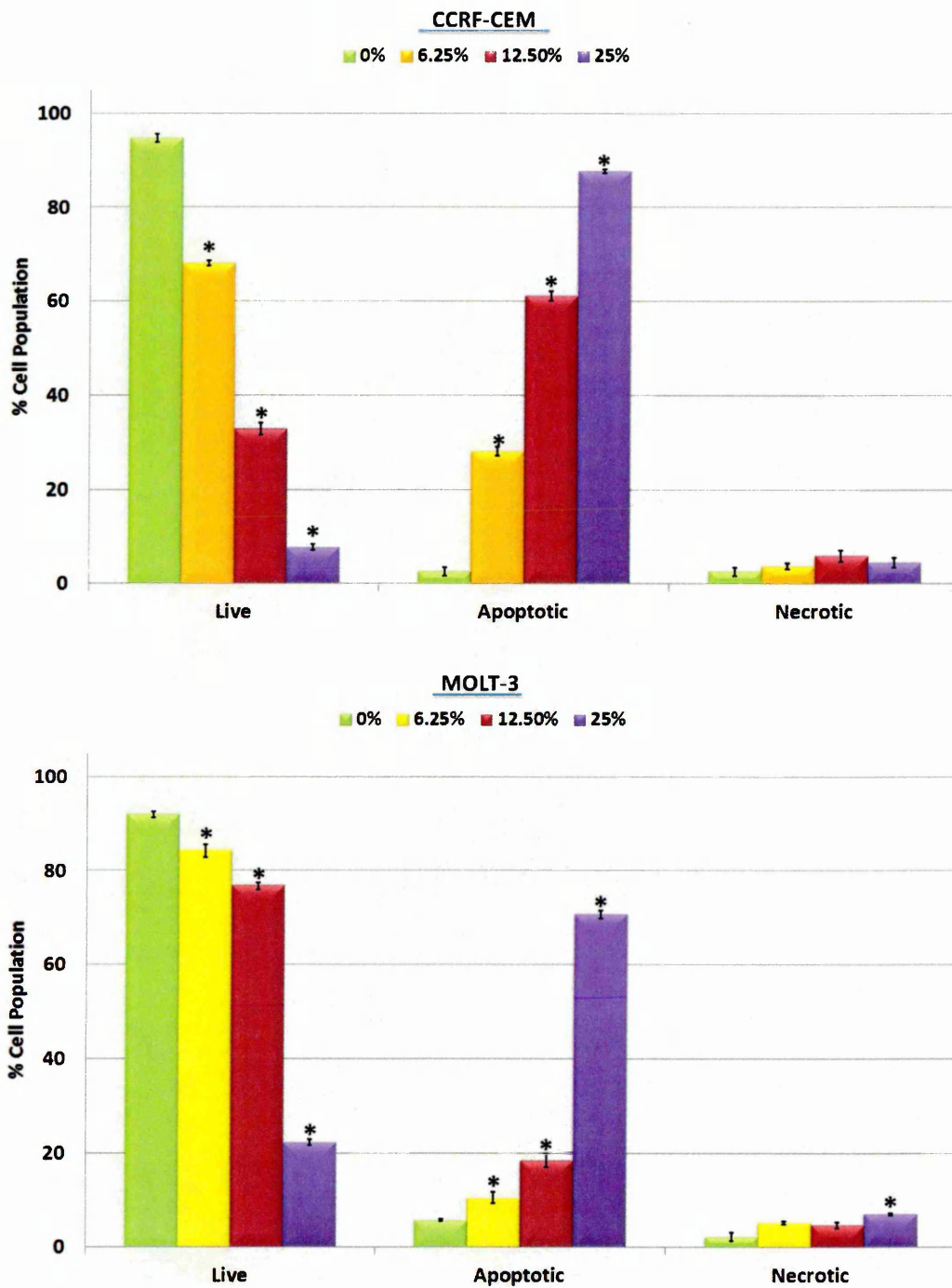


Figure 4.9: Percentage of Live, apoptotic, and necrotic in CCRF-CEM and MOLT-3 cells determined from Hoechst 33342 and PI morphological assessment following treatment with acetonitrile fraction generated by SPE of PJ at concentration 6.25%, 12.5% and 25% for 24. Mean \pm SEM. * indicates significant difference ($P \leq 0.05$) vs. untreated control. n= 3.

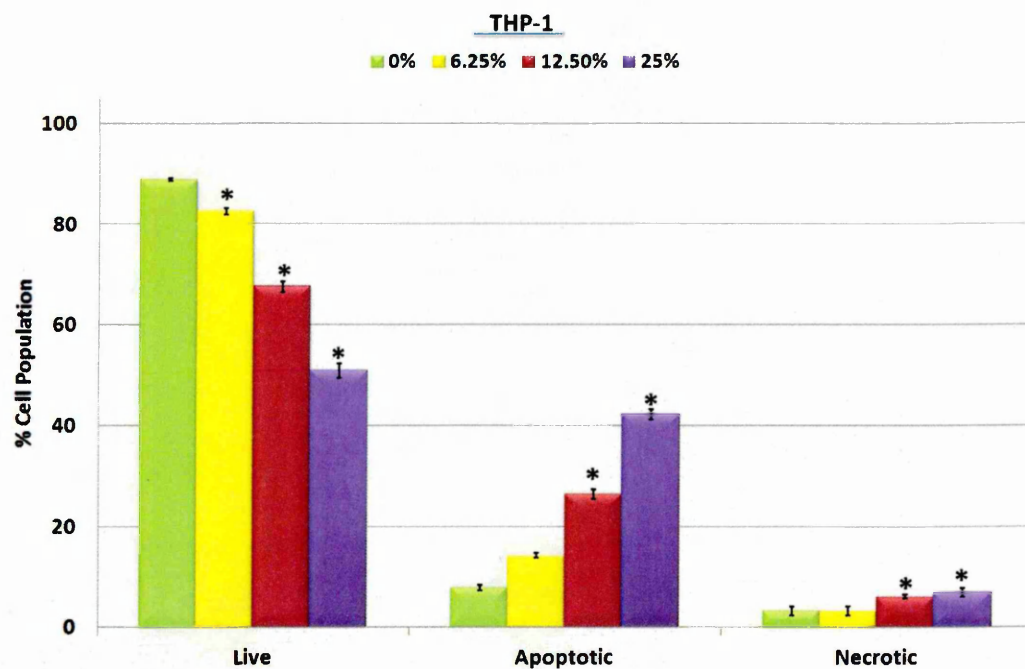
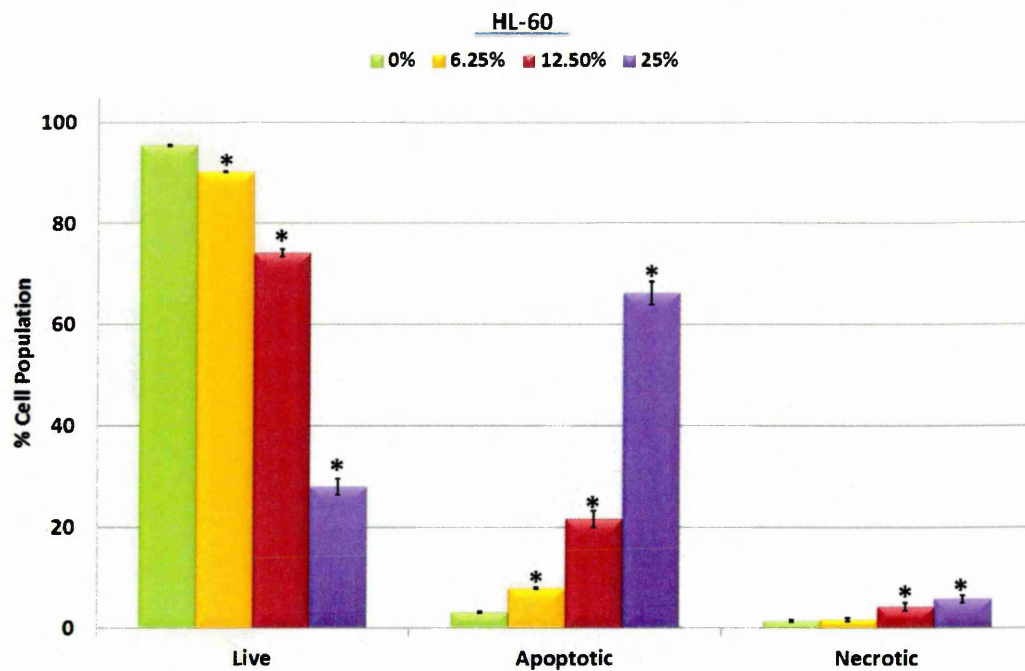


Figure 4.10: Percentage of Live, apoptotic, and necrotic in HL-60 and THP-1 cells determined from Hoechst 33258 and PI morphological assessment following treatment with acetonitrile fraction generated by SPE of PJ at concentration 6.25%, 12.5% and 25% for 24. (Mean \pm SEM, * indicates significant difference ($P \leq 0.05$) vs. untreated control. n= 3.

4.3.4 Phenolic Content of SPE Fractions

The acetonitrile fraction generated by SPE had the highest phenol content of 2696.7 μg GAE/mL, which was more than double than that seen within whole juice extracts (1236.9 μg GAE/mL), whereas the phenol content of other extracts was minor in comparison with 53.5 μg GAE/mL in the unbound fraction, 148.2 μg GAE/mL in the water fraction, 46.0 μg GAE/mL in the acetone fraction, and 5.7 μg GAE/mL in the ethyl acetate fraction (Figure: 4.11). This translated to concentrations of phenol content of 6.25% equivalent treatments containing 5.2 $\mu\text{g}/\text{mL}$ GAE within acetonitrile treatments and 2.4 $\mu\text{g}/\text{mL}$ GAE within 6.25% treatments within whole PJ. Other fractions contained negligible levels of phenols which correlated with no observable biological activity.

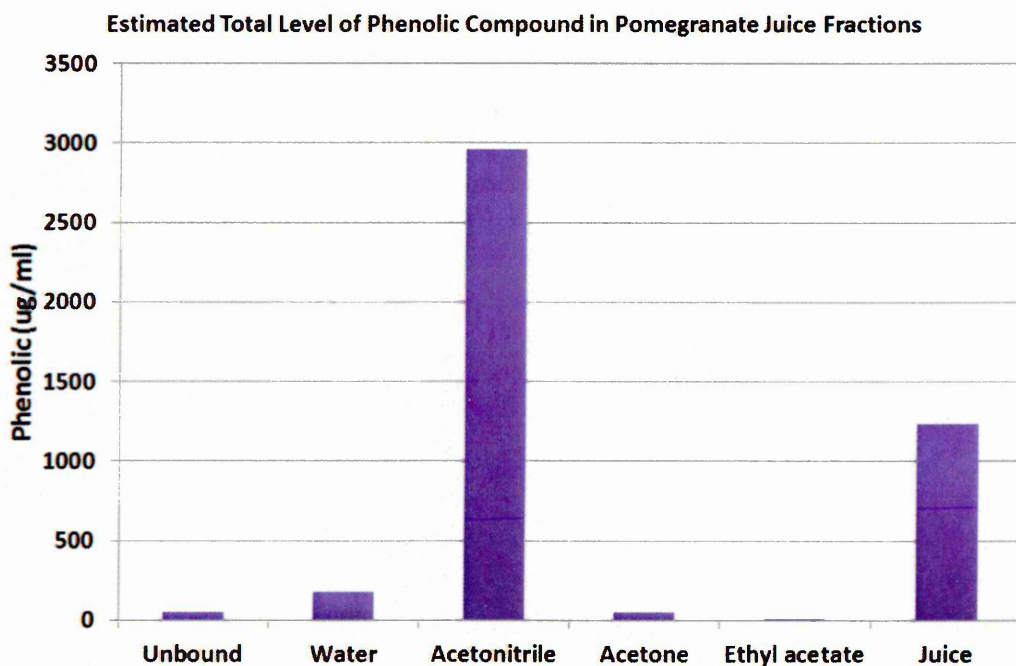


Figure 4.11: Estimated total level of phenolic compounds of PJ fractions (unbound, water, acetonitrile, acetone, and ethyl acetate) generated by SPE and whole PJ. n=3

4.3.5 LC–MS of Whole PJ and SPE Fractions

LC–MS was carried out on the whole PJ and each fraction generated from the SPE procedure on samples containing 20 µg GAE. Virtually all the material from the unbound fraction and the water fraction was not retained and eluted in the column wash (data not shown). Previous work has shown that these fractions contain organic acids, vitamin C, and sugars. The whole PJ contained peaks characteristic of phenolic components previously found in pomegranate (Fischer *et al*, 2011) and included gallotannins, ellagitannins, anthocyanins, and hydroxycinnamic acid derivatives (Figure 4.12 and Table 4.3). The acetonitrile fraction had the highest intensity of peaks but had a similar composition to the whole PJ. The acetone and ethyl acetate fractions contained lower amounts of phenolic materials but certain components were enhanced in these fractions (Figure 4.12). Comparison of whole PJ and the acetonitrile fraction (Figure 4.13) demonstrated that the acetonitrile fraction was enriched in a number of ellagitannins, ellagic acid, and hydroxycinnamic acid derivatives over the whole PJ (Figure: 4.13 and Table 4.2). However, it was clear that the acetonitrile fraction was depleted in anthocyanins compared to whole juice extracts (Figure 4.13) but all the anthocyanins in the juice were also present in the acetonitrile fraction but were eightfold lower (Figure 4.14 and Table 4.3). The anthocyanins identified within both the whole juice extracts and acetonitrile fraction included the characteristic glycosylated forms of delphinidin, cyanidin, and pelargonidin (Figure 4.14 and Table 4.3) found in pomegranate.

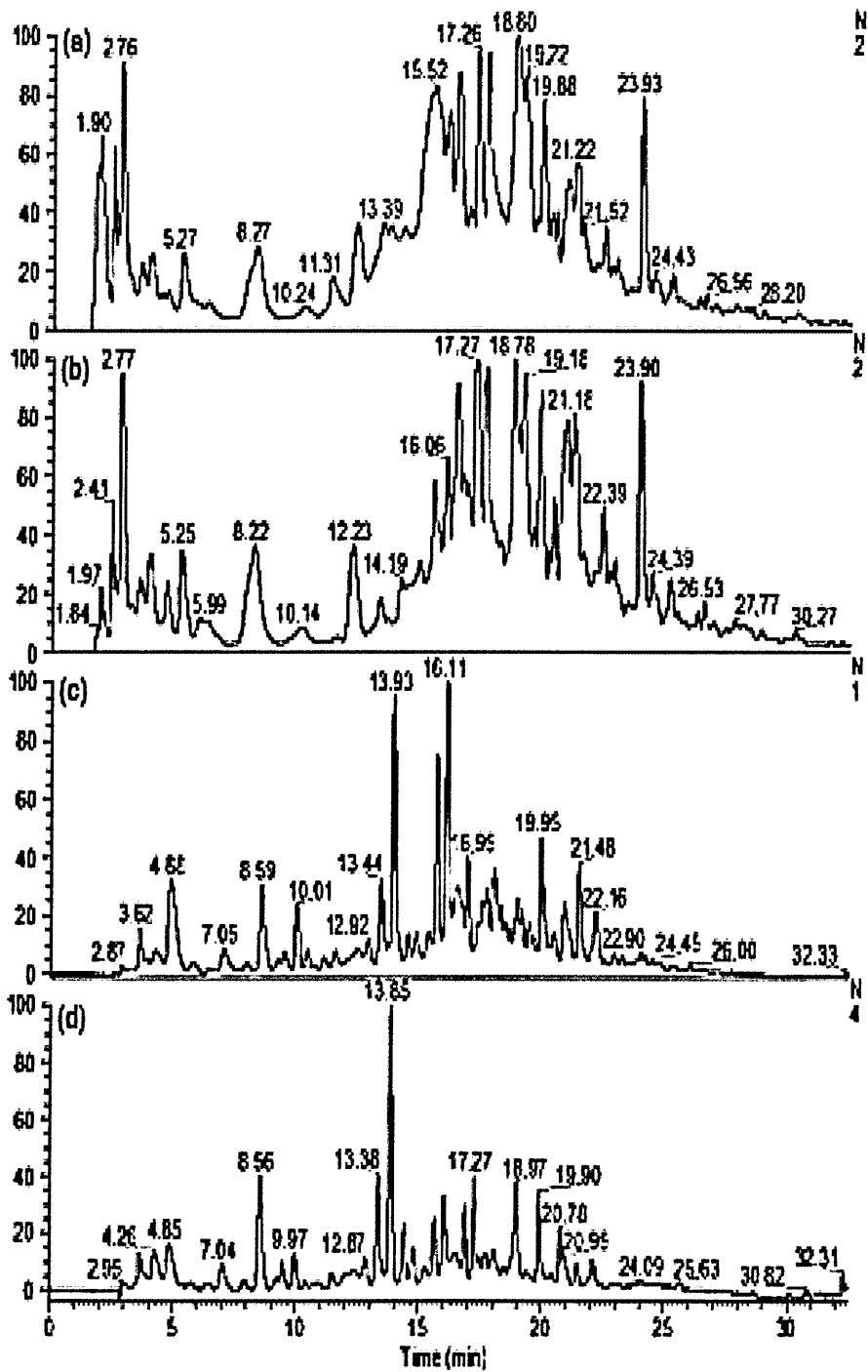


Figure 4.12: LC-MS chromatographs of whole PJ (A) and acetonitrile (B), acetone (C) and ethyl acetate fractions (D) from solid phase extraction of PJ LC-MS performed on samples containing 20 µg GAE/mL by follin assay. LC-MS, liquid chromatography mass spectrometry; PJ, pomegranate juice extract; GAE, gallic acid equivalent.

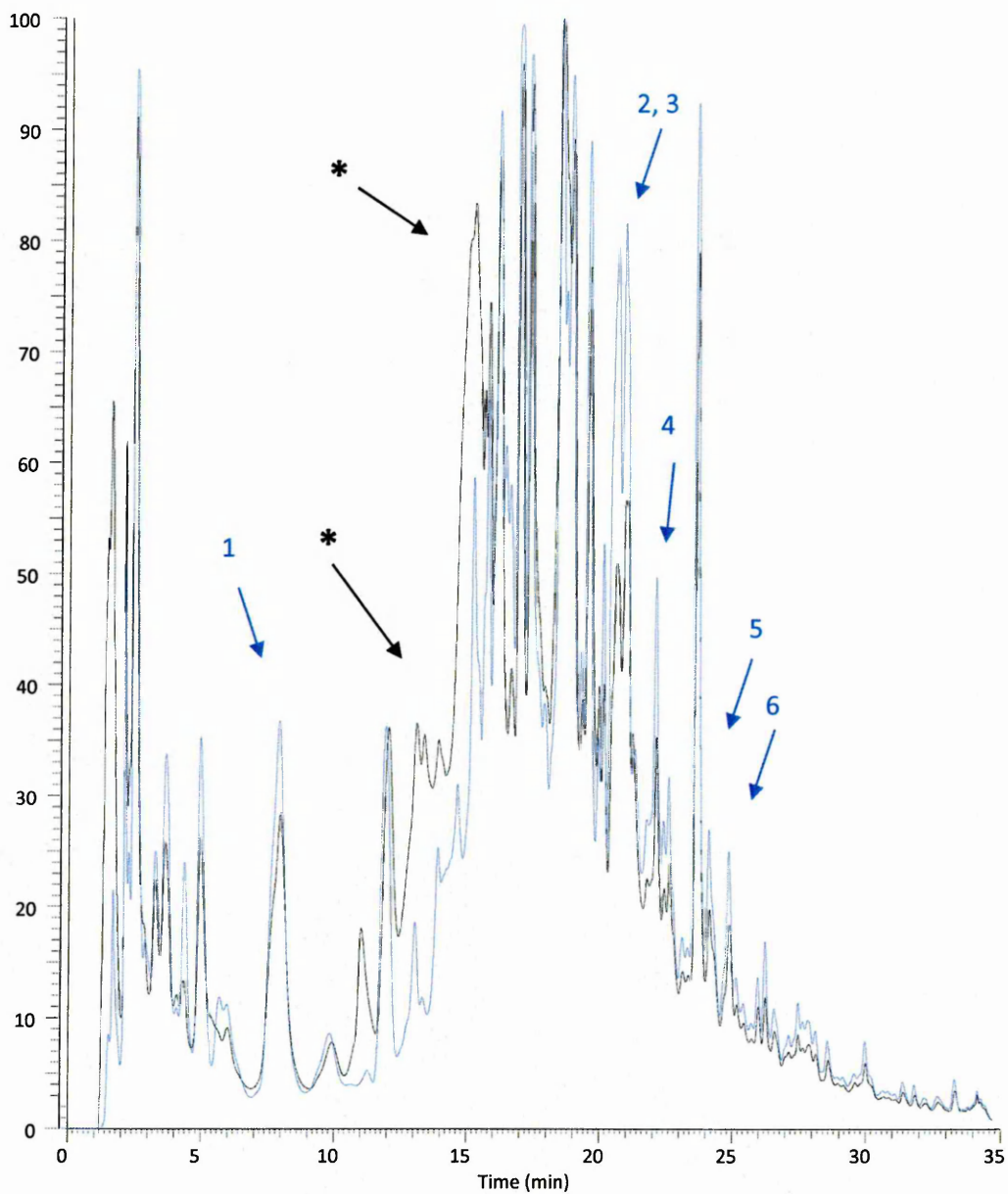


Figure 4.13: LC-MS chromatograms of whole PJ (Black) and acetonitrile solid phase fraction from PJ (Blue) demonstrating peak differences within negative ion mode. *The main peaks in juice sample that differ from the ACN fraction. The identities of peaks labelled are described in Table 4.2.

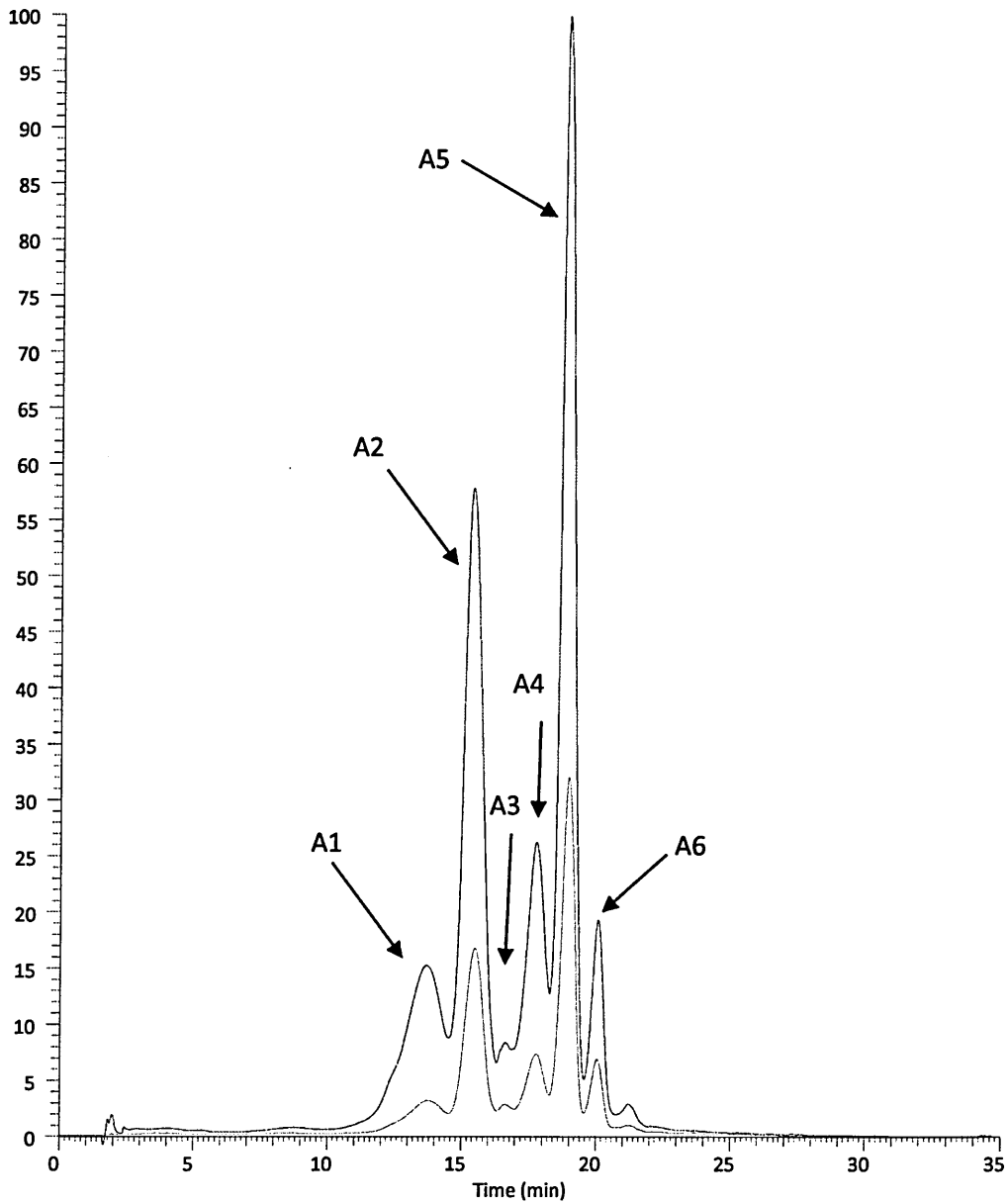


Figure 4.14: LC–MS chromatographs of whole PJ (Black) and acetonitrile solid phase fraction from PJ (Blue) demonstrating peak differences within positive ion mode. *The main peaks in juice sample that differ from the ACN fraction. The identities of peaks labelled are described in Table 4.2.

Peak	PDA <i>max</i>	<i>m/z</i> [M-H]	MS ²	Putative identity
1	275	1083	783, 481, 301	Punicalagin
2	275	1569	935, 785, 765	Sanguiin H-10 like isomer
3	275	1569	935, 785, 765	Sanguiin H-10 like isomer
4	280	1569	935, 785, 765	Sanguiin H-10 like isomer
5	275	581	301	EA derivative
6	290	507	327, 315	Methyl EA derivative
7	330	533	353	HCA derivative
A1	520	627 ⁺	303	Delphinidin-3, 5- <i>O</i> -diglucoside
A2	512	611 ⁺	287	Cyanidin-3, 5- <i>O</i> -diglucoside
A3	500	595 ⁺	271	Pelargonidin-3, 5- <i>O</i> -diglucoside
A4	520	465 ⁺	303	Delphinidin-3- <i>O</i> -glucoside
A5	515	449 ⁺	287	Cyanidin-3- <i>O</i> -glucoside
A6	500	433 ⁺	271	Pelargonidin- <i>O</i> -glucoside

Table 4.3: Putative identification of phenolic components.

4.4 Discussion

Pomegranates have been postulated by a number of groups worldwide to provide bioactive compounds with anti-cancer actions, and have been successfully used in a number of randomized clinical trials for prostate cancer (Paller *et al*, 2012). We previously demonstrated in Chapter 3 that crude pomegranate juice extract induced apoptosis and inhibited cellular proliferation inducing S phase arrest in leukemia cell lines. Here, we used SPE to separate the PJ into fractions and identified that the acetonitrile fraction contained the bioactive compounds responsible for induction of apoptosis, cell cycle arrest and inhibition of proliferation within leukemia cell lines.

LC-MS analysis confirmed that the PJ contained a mixture of gallotannins, ellagitannins, anthocyanins and hydroxycinnamic acid derivatives characteristic of pomegranate (Fischer *et al*, 2011). Importantly most of these components were recovered in the acetonitrile fraction with only a small proportion of phenolic components being identified in other fractions. The phenolic-enriched acetonitrile fraction was the most effective, and this strongly suggests that ellagitanins and other phenolic agents were responsible for its bioactive actions. Interestingly, we identified that the active acetonitrile fraction to be enriched in ellagitannins, but comparably depleted in anthocyanins.

A number of ellagitannins were identified as well as ellagic acid and hydroxycinnamic acid derivatives. Ellagitannins extracted from pomegranate have been previously shown to induce apoptosis in HL-60 cell lines (Li *et al*, 2011). We observed similar pro-apoptotic effects when we treated this cell line together with other leukemia cell lines with the ellagitannin-rich acetonitrile fraction from pomegranate juice. Similarly ellagic acid has been shown to induce apoptosis within HL-60 cell lines, together with S Phase arrest (Hagiwara *et al*, 2010). This S Phase arrest mimics that seen here following treatment with the acetonitrile fraction, and those seen previously on whole PJ (Chapter 3). In contrast, ellagic acid and caffeic acid treatment of normal human peripheral blood mononuclear cells inhibited apoptosis induced by hydrogen peroxide treatments, suggesting that these compounds have protective effects on these cells (Khanduja *et al*, 2006). This was confirmed in Chapter 3 which showed PJ showed a greater toxicity towards leukemia cell lines than non-tumour control cells. This may

suggests that the ellagitannins within PJ display protection to apoptosis in non-tumour cells, but induce apoptosis in tumour cells

Induction of apoptosis by a number of hydroxycinnamic acids have also been seen within leukaemia cell lines. Artepillin C, an extract from Brazilian propolis, has been shown to induce apoptosis and inhibit DNA synthesis resulting in S Phase arrest (Kimoto *et al*, 2001). Anthocyanins were also found in the acetonitrile fraction from PJ although at lower levels than seen in whole PJ. Anthocyanin treatments of leukaemia cell lines have also demonstrated inhibition of cell proliferation and induction of apoptosis by a number of groups worldwide (Hou *et al*, 2003, 2005; Katsuzaki *et al*, 2003; Fimognari *et al*, 2004, 2005; Hyun and Chung 2004; Chang *et al*, 2005; Xia *et al*, 2006; Feng *et al*, 2007; Lee *et al*, 2009). This could account for some of the apoptosis induction within leukaemia cells following treatment with the acetonitrile fraction from PJ. However, although treatment of U937 cells (histocytic leukemia cell lines) with cyanidin and malvinidin demonstrated G₂/M phase arrest (Hyun and Chung 2004), 50 % effectiveness was not reached until ~50 µg/mL. The acetonitrile fraction was very effective at ~50 µg GAE/mL and the anthocyanin content was less than ~5 % of the content. However, the 8-fold depletion in anthocyanin content between PJ and the acetonitrile fraction did not reduce effectiveness and this suggests that the actions of PJ may not be due to its anthocyanin content.

This study demonstrated that only the acetonitrile fraction demonstrated activity towards leukaemia cell lines suggesting the phenolic agents within pomegranate are responsible for induction of apoptosis and inhibition of cellular proliferation. The relative enrichment of ellagitannins over anthocyanins and the closer agreement on affects of cell cycle seen with ellagitannin treatment of leukemia cell lines, suggest that ellagitannins may be the major players in the anti-cancer actions of pomegranate. However, it is highly probable that a number of compounds found within the acetonitrile fraction of PJ interact with each other. Indeed synergistic actions of ellagic acid with quercetin and resveratrol have been demonstrated previously in the leukemia cell line MOLT 4 cells (Mertens-Talcott *et al*, 2003, 2005; Mertens-Talcott and Percival 2005). Seeram *et al*, (2005) found that individual treatment of human oral, colon and prostate cancer cell lines with punicalagin, ellagic acid and total

pomegranate tannins failed to induce the same toxicity as whole pomegranate extracts suggesting these agents either work synergistically or that other minor agents within PJ are responsible for the actions of pomegranate (Seeram *et al*, 2004). Conversely, our study demonstrated that treatment of leukaemia cell lines with the acetonitrile fraction from pomegranate at concentrations determined to ensure equal concentrations of agents (not just phenolics) within the fractions to those in whole PJ suggested all the toxicity seen in pomegranate juice was due to the agents seen within this acetonitrile fraction. SPE resulted in increased phenolic content of the acetonitrile fraction compared to the whole juice, which was not surprising as it is concentrated in phenolic compounds due to the loss of sugars and other compounds which are extracted in the unbound and water fractions.

Of course upon consumption of pomegranates many of the compounds identified here do not enter the blood stream within this form. For example the ellagitannins themselves do not enter the bloodstream (Seeram *et al*, 2004, 2006, 2008; Espin *et al*, 2007). As such they cannot be effective directly against leukemic cells *in vivo* if delivered via oral consumption. However these could be delivered via pharmacological means. However oral delivery could still provide bioactivity from the ellagitannins as the colonic-derived metabolites the urolithins are known to circulate in the blood stream (Seeram *et al*, 2004, 2006, 2008; Espin *et al*, 2007), accumulate at certain sites (Seeram *et al*, 2007) and are effective against cancer cell lines (Seeram *et al*, 2007; Bialonska *et al*, 2009; Kasimsetty *et al*, 2010), and thus could provide the bioactive actions of consumed pomegranates. The identification of the compounds responsible within pomegranate for the anti-cancer affects will be the next step towards understanding the role of pomegranates in cancer therapeutics.

5. Anti-proliferative activity of pomegranate pure compounds in leukaemia cell lines

5.1 Introduction

Dietary chemoprevention of cancer is increasingly considered as being an important way to reduce the risk of cancer. In the last decade pomegranate has shown promise in the prevention of cancers, as has been demonstrated in studies with extracts and/or isolated bioactive compounds (Lansky and Newman, 2007; Dahlawi *et al*, 2011, Dahlawi *et al*, 2013, Viladomiu *et al*, 2013). PJ is a rich source of many compounds belonging to different chemical classes including, organic acid and phenolic compounds such as: phenolic acids; anthocyanins; flavonoids; anthocyanins, and ellagitannins, which have been discussed previously (3.1.2.3) (Lansky and Newman, 2007; Viuda-Marrots *et al*, 2010; Viladomiu *et al*, 2013). However, the chemical composition of pomegranate can vary depending on the cultivar, growing region, climate, maturity and storage conditions and plant components (Poyrazoglu *et al*, 2002; Barzegar *et al*, 2004; Fadvi *et al*, 2005).

This study tested the hypothesis that: compounds found in the PJ have growth inhibitory properties that contribute to their protection against survival and growth of cancers.

5.2 Objective

The objective of this study was to examine the effect on cell viability of a number of pure compounds that were either identified in the acetonitrile fraction of PJ (chapter 3) (Dahlawi *et al*, 2013); were present in the other fractions of PJ or have been identified as PJ components in previous studies (Lansky and Newman, 2007, Fischer *et al*, 2011, Viladomiu *et al*, 2013). The effects of the selected compounds were studied on ATP levels in four human leukaemia cell lines and non-tumour HSCs.

Twenty six compounds (Table 5.1) representing the different classes of compounds found in PJ were screened. These included: organic acids; hydroxybenzoic acids; hydroxybenzoic acids; falavan-3-ols; ellagitannins; amino acids; indoleamines; and anthocyanins. This would enable the identification of the most active compounds in PJ for further investigation.

Chemical class	Compound name	Compound structure	References
Organic acid	Citric acid (Sigma)		Poyrazoglu <i>et al.</i> (2002).
Organic acid	Malic acid (Sigma)		Poyrazoglu <i>et al.</i> (2002).
Organic acid	Tartaric acid (Sigma)		Poyrazoglu <i>et al.</i> (2002).
Organic acid	Fumaric acid (Sigma)		Poyrazoglu <i>et al.</i> (2002).
Organic acid	Succinic acid (Sigma)		Poyrazoglu <i>et al.</i> (2002).
Organic acid	Ascorbic acid (Sigma)		Lansky and Newman, 2007
Hydroxybenzoic acid	Gallic acid (Sigma)		Amakura <i>et al.</i> (2000b), Huang <i>et al.</i> (2005), Gómez-Caravaca <i>et al.</i> (2013).
Hydroxybenzoic acid	Ellagic acid (Sigma)		Amakura <i>et al.</i> (2000), Gill <i>et al.</i> (2000), Wang <i>et al.</i> (2005), Gómez-Caravaca <i>et al.</i> (2013).

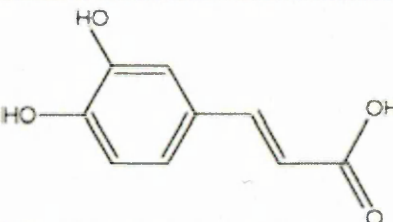
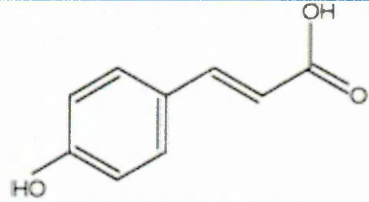
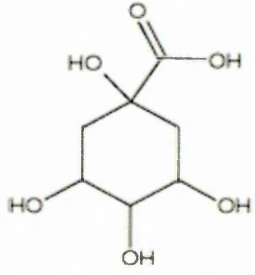
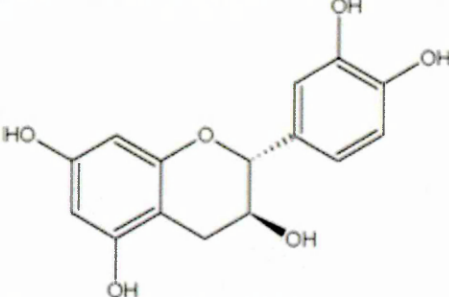
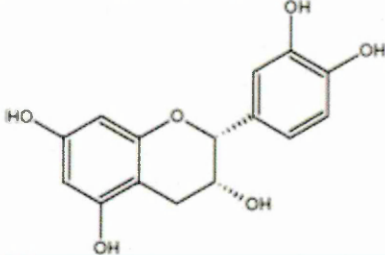
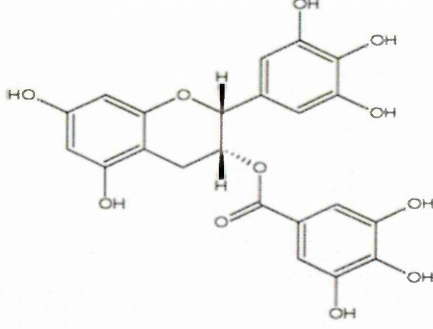
Table (continued)			
Chemical class	Compound name	Compound structure	References
Hydroxycinnamic acid	Caffeic acid (Sigma)		Artik (1998), Amakura <i>et al.</i> (2000a)
Hydroxycinnamic acid	<i>p</i> -cumaric acid		Artik (1998), Amakura <i>et al.</i> (2000a).
Cyclitol carboxylic acid	Quinic acid (Sigma)		Artik (1998), Amakura <i>et al.</i> (2000a)
Flavan-3-ols	catechin (Enzo Life Science)		de Pascual-Teresa <i>et al.</i> (2000), Gómez-Caravaca <i>et al.</i> (2013).
Flavan-3-ols	Epicatechin (Enzo Life Science)		de Pascual-Teresa <i>et al.</i> (2000), Gómez-Caravaca <i>et al.</i> (2013).
Flavan-3-ols	Epigallocatechin 3-gallate (EGCG) (Enzo Life Science)		de Pascual-Teresa <i>et al.</i> (2000).

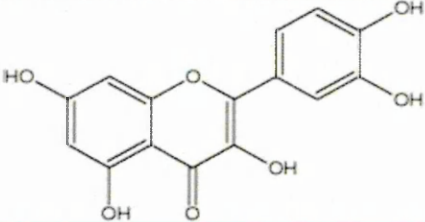
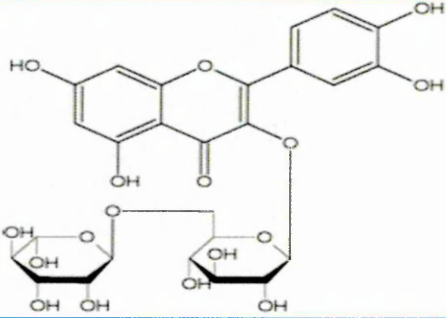
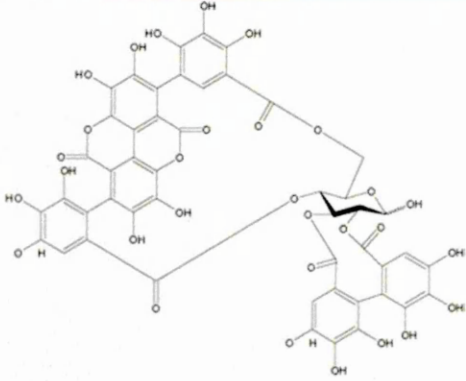
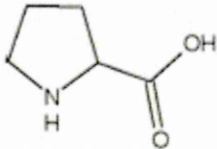
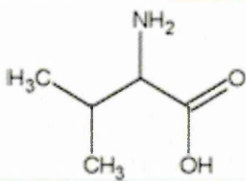
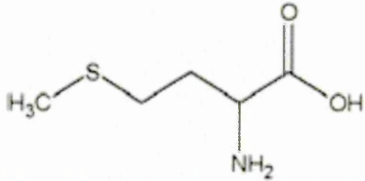
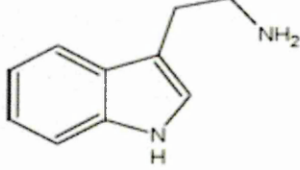
Table (continued)			
Chemical class	Compound name	Compound structure	References
Flavonols	Quercetin (Sigma)		Artik (1998); Caravaca <i>et al.</i> (2013).
Flavonols	Rutin (Enzo Life Science)		Artik (1998).
Ellagitannins	Punicalagin (Sigma)		Gill <i>et al.</i> (2000), Gómez-Caravaca <i>et al.</i> (2013). Dahlawi <i>et al.</i> (2013).
Amino acids	Proline (Sigma)		Velioglu <i>et al.</i> (1997).
Amino acids	Valine (Sigma)		Franciosi (1980).
Amino acids	Methionine (Sigma)		Franciosi (1980).
Indoleamines	Tryptamine (Enzo Life Science)		Badria (2002).

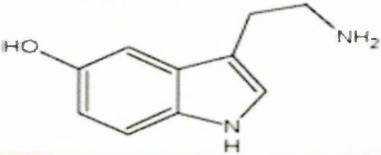
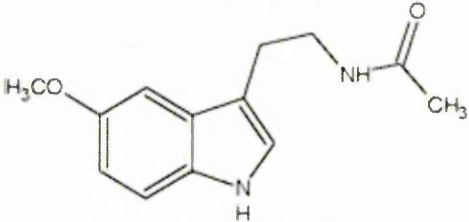
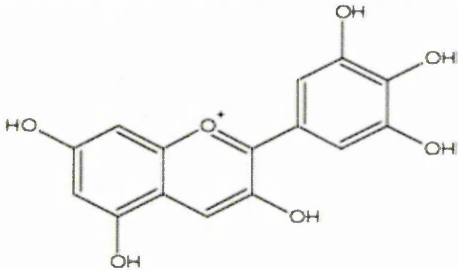
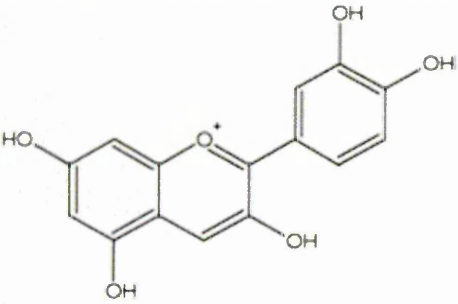
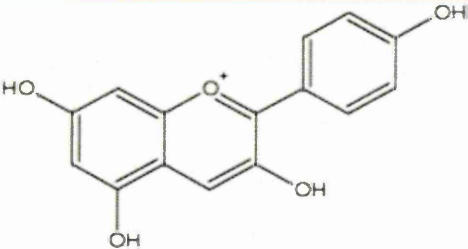
Table (continued)			
Chemical class	Compound name	Compound structure	References
Indoleamines	Serotonin (Enzo Life Science)		Badria (2002).
Indoleamines	Melatonin (Enzo Life Science)		Badria (2002).
Anthocyanidins	Delphinidin (Extrasynthese)		Hernandez et al.(1999), Gill et al.(2000), Mousavinejad et al.(2009), Gómez-Caravaca et al. (2013). Dahlawi et al.(2013)
Anthocyanidins	Cyanidin (Extrasynthese)		Hernandez et al.(1999), Gill et al.(2000), Mousavinejad et al.(2009), Gómez-Caravaca et al. (2013). Dahlawi et al. (2013).
Anthocyanidins	Pelargonidin (Extrasynthese)		Hernandez et al. (1999), Gill et al.(2000), Mousavinejad et al.(2009), Gómez-Caravaca et al. (2013). Dahlawi et al. (2013).

Table 5.1: Summarised pomegranate compounds found in PJ and their chemical structure.

5.3 Material and Methods

5.3.1 Cell Culture

Four leukaemia cell lines were obtained from the American Type Culture Collection (ATCC; Middlesex, U.K.), which have previously described to have demonstrated differing sensitivity to PJ (Chapter 3) (Dahlawi *et al*, 2011) and the acetonitrile fraction (Chapter 4) (Dahlawi *et al*, 2013). They included two lymphoid cell lines: CCRF-CEM, and MOLT-3, and two myeloid cell lines: HL-60 and THP-1 (Section 2.2). These cell lines were maintained and cultured in RPMI 1640 medium (Invitrogen, Paisley, U.K.) supplemented with 10% (v/v) foetal bovine serum, 1.5 mmol/L L-glutamine, and 100 µg/mL penicillin/streptomycin (complete media) in a humidified atmosphere of 5% CO₂ at 37°C.

5.3.2 Treatment of Cells

Cells were seeded at 25×10^4 cells in 100 µL of complete media and treated with each compound (Table 5.1) at concentrations: 0, 10, 25, 50, and 100 µM in white 96-well plates (Fisher Scientific) for 24 and 48 h. The IC₅₀ values were then determined, following assessment of cell viability using Cell Titer-Glo[®] Luminescent Cell Viability Assay (Promega) (Section 2.3.2)(Table 5.2).

Techniques	Treatment concentration	Concentration	Cell lines	Time point
Cell Titer-Glo [®] Luminescent Cell Viability Assay	26 pure compounds (Table 5.1)	10, 25, 50, and 100 µM	CCRF-CEM, MOLT-3, HL-60, and THP-1	24 and 48 hr

Table 5.2: Experimental design for Chapter 5.

5.4 Results:

5.4.1 Effect of Pomegranate Compounds in Leukaemia Cell Lines; on ATP Levels as an Indicator of Total Viable Cells

5.4.1.1 Organic acids:

The effects of the organic acids: citric acid; malic acid; tartaric acid; fumaric acid; succinic acid and ascorbic acid were investigated on four leukaemia cell lines to determine potential bioactive actions affecting cell viability and proliferation, determined via measuring total ATP levels as an indication of number of metabolically active cells.

5.4.1.1.1 Citric Acid:

Citric acid did not significantly inhibit ATP levels, in any of the four leukaemia cell lines investigated following 24 h. However after 48 h, a significant inhibition of ATP levels was observed at the two highest concentrations (50 and 100 μM) in CCRF-CEM cells. Citric acid failed to cause a 50% reduction in ATP in all four cell lines following 24 and 48 h (Figure 5.1) and no IC_{50} value could be determined.

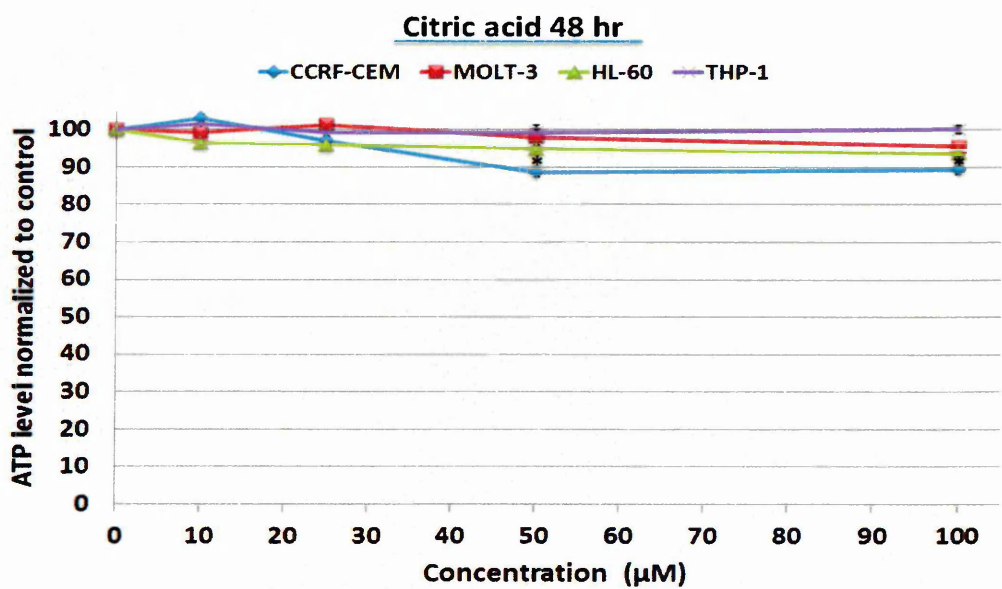
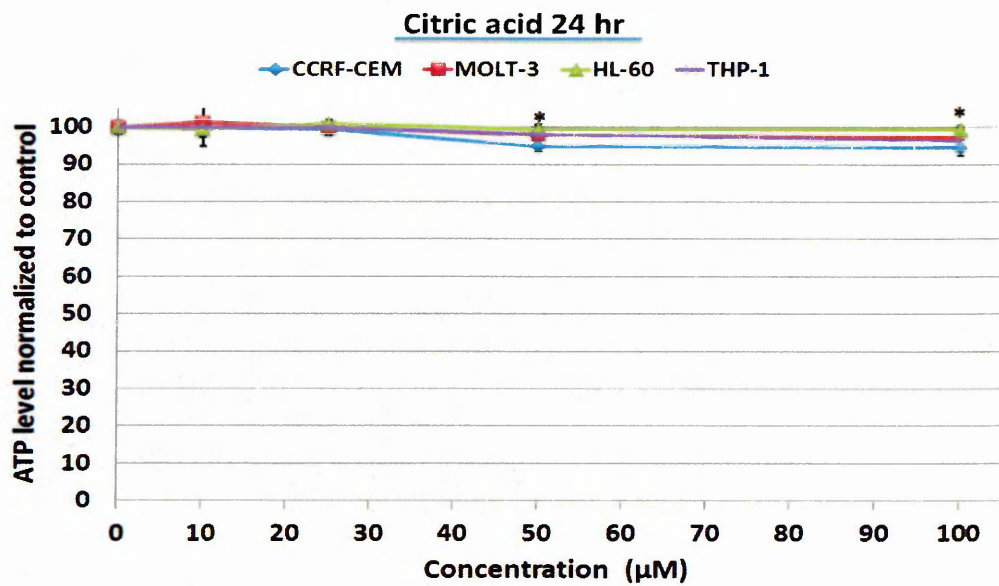


Figure 5.1: Effect of citric acid on cell proliferation at concentrations 0, 10, 25, 50, and 100 µM in CCRF-CEM, MOLT-3, HL-60, and THP-1 leukaemia cell lines following 24 and 48 h. ATP levels investigated using Cell Titer-Glo® Luminescent Cell Viability Assay to provide indication of live cell numbers. ATP levels normalized to controls and presented as means ± standard error. * indicates significant difference ($P \leq 0.05$) vs. untreated control. $n=3$.

5.4.1.1.2 Malic Acid:

Malic acid did not significantly inhibit ATP levels in any of the four leukaemia cell line investigated and failed to cause a 50% reduction in ATP in each of the four cell lines following 24 and 48 h (Figure 5.2).

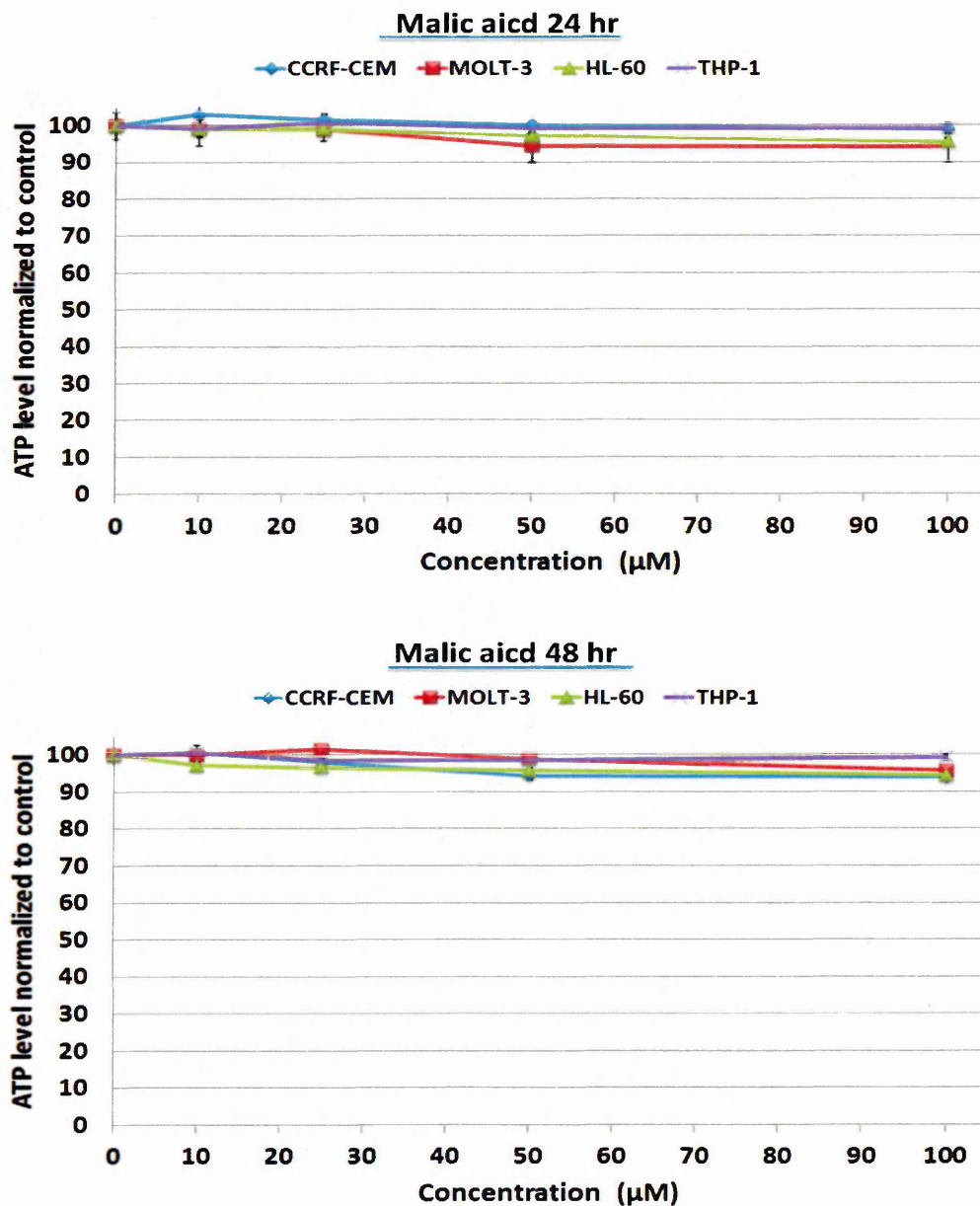


Figure 5.2: Effect of malic acid on cell proliferation at concentrations 0, 10, 25, 50, and 100 μM in CCRF-CEM, MOLT-3, HL-60, and THP-1 leukaemia cell lines following 24 and 48 h. ATP levels investigated using Cell Titer-Glo® Luminescent Cell Viability Assay to provide indication of live cell numbers. ATP levels normalized to controls and presented as means ± standard error. * indicates significant difference ($P \leq 0.05$)

5.4.1.1.3 Tartaric Acid:

Tartaric acid did not significantly inhibit ATP levels in any of the four leukaemia cell lines investigated following 24 and 48 h ($P > 0.05$). As a result, it failed to cause a 50% reduction in ATP in all four cell lines following 24 and 48 h (Figure 5.3).

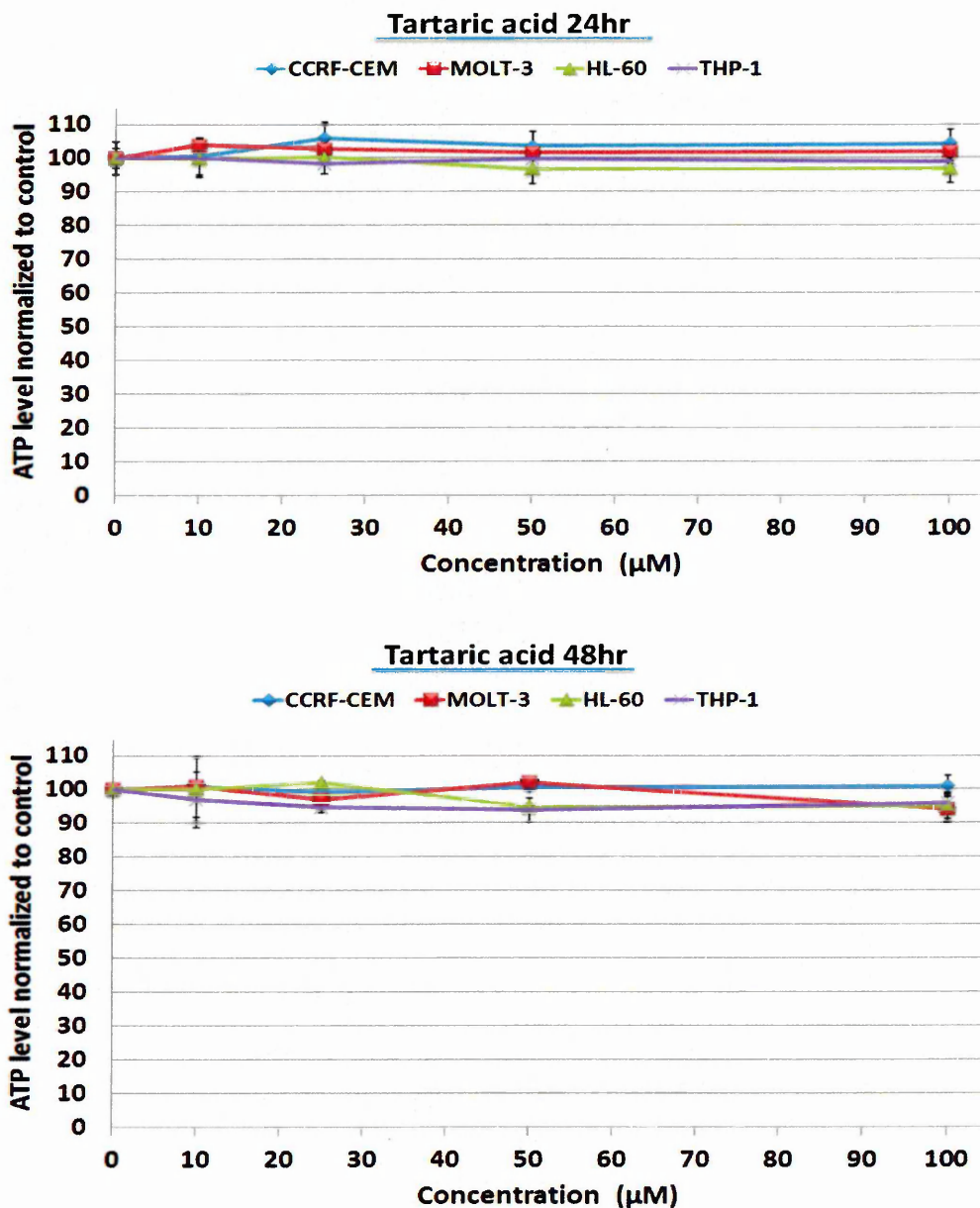


Figure 5.3: Effect of Tartaric acid on cell proliferation at concentrations 0, 10, 25, 50, and 100 μM in CCRF-CEM, MOLT-3, HL-60, and THP-1 leukaemia cell lines following 24 and 48 h. ATP levels investigated using Cell Titer-Glo® Luminescent Cell Viability Assay to provide indication of live cell numbers. ATP levels normalized to controls and presented as means ± standard error. * indicates significant difference ($P \leq 0.05$) vs. untreated control. n= 3.

5.4.1.1.4 Fumaric Acid:

Fumaric acid did not significantly inhibit ATP levels in each of the four leukaemia cell line investigated following 24 h ($P > 0.05$). Following 48 h, fumaric acid significantly inhibited ATP levels in CCRF-CEM cells only at the highest two concentrations (50 and 100 μM) ($P \leq 0.05$). However, it failed to cause a 50% reduction in ATP in any of the four cell lines following 24 and 48 h (Figure 5.4).

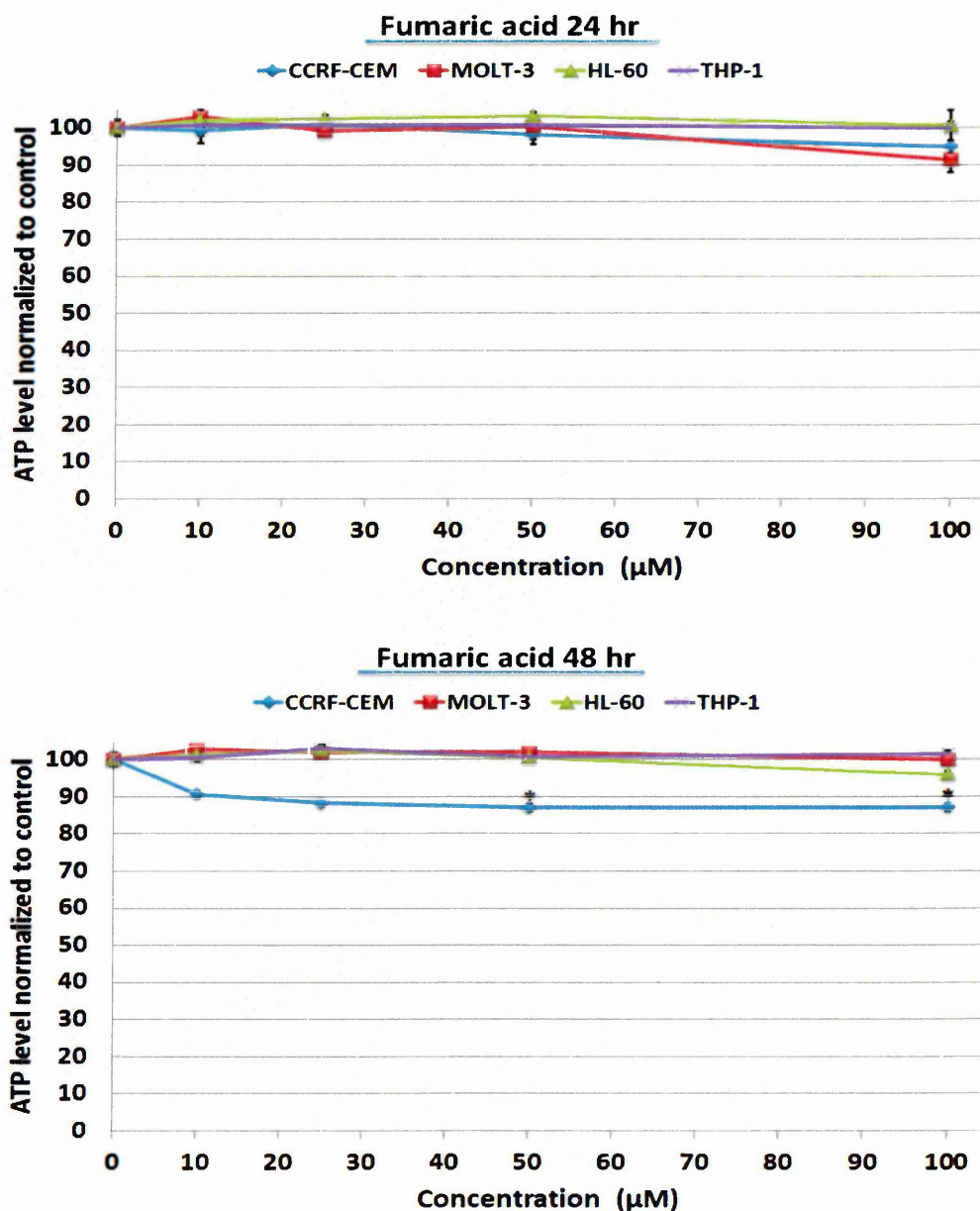


Figure 5.4: Effect of Fumaric acid on cell proliferation at concentrations 0, 10, 25, 50, and 100 μM in CCRF-CEM, MOLT-3, HL-60, and THP-1 leukaemia cell lines following 24 and 48 h. ATP levels investigated using Cell Titer-Glo[®] Luminescent Cell Viability Assay to provide indication of live cell numbers. ATP levels normalized to controls and presented as means \pm standard error. * indicates significant difference ($P \leq 0.05$) vs. untreated control. $n = 3$.

5.4.1.1.5 Succinic Acid:

Succinic acid did not significantly inhibit ATP levels in any of the four leukaemia cell lines investigated following 24 h ($P > 0.05$). Following 48 h, succinic acid significantly inhibited ATP levels in CCRF-CEM cells only following treatment with 25, 50, and 100 μM ($P \leq 0.05$). However, it failed to cause a 50% reduction in ATP in all cell lines following 24 and 48 h (Figure 5.5).

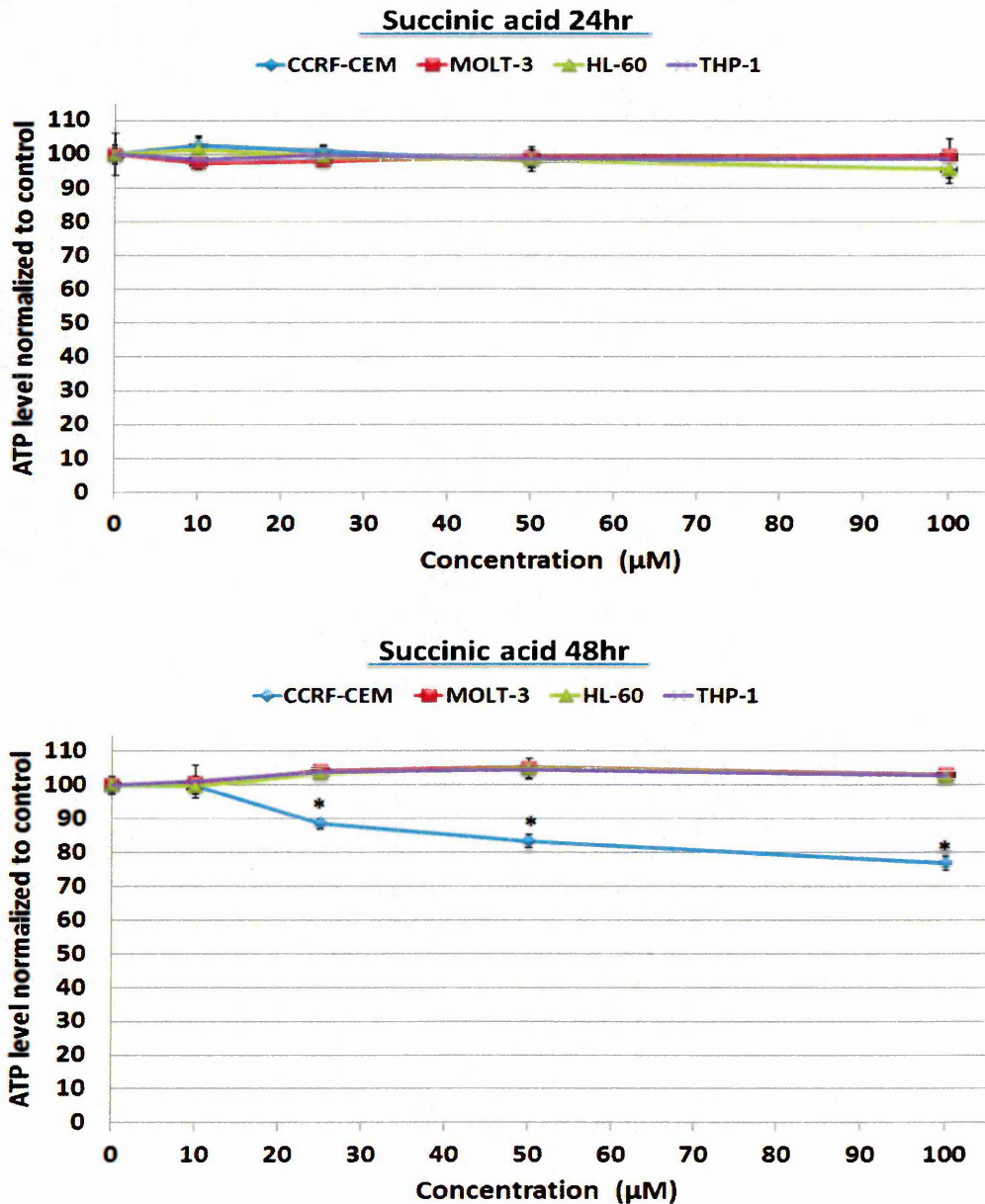


Figure 5.5: Effect of succinic acid on cell proliferation at concentrations 0, 10, 25, 50, and 100 μM in CCRF-CEM, MOLT-3, HL-60, and THP-1 leukaemia cell lines following 24 and 48 h. ATP levels investigated using Cell Titer-Glo[®] Luminescent Cell Viability Assay to provide indication of live cell numbers. ATP levels normalized to controls and presented as means \pm standard error. * indicates significant difference ($P \leq 0.05$) vs. untreated control. $n = 3$.

5.4.1.1.6 Ascorbic Acid:

Ascorbic acid showed significant inhibition on ATP levels in CCRF-CEM cells following stimulation with 25, 50, and 100 μM in a dose-dependent manner following 24 and 48 h treatments ($P \leq 0.05$). The remaining cell lines, displayed no significant inhibition of ATP levels following 24 and 48 h treatments ($P > 0.05$). Ascorbic acid caused 50% reduction in ATP levels in CCRF-CEM cells only (Figure 5.6) and the IC_{50} values following 24 and 48 h treatments were 61 and 57 μM , respectively (Figure 5.6).

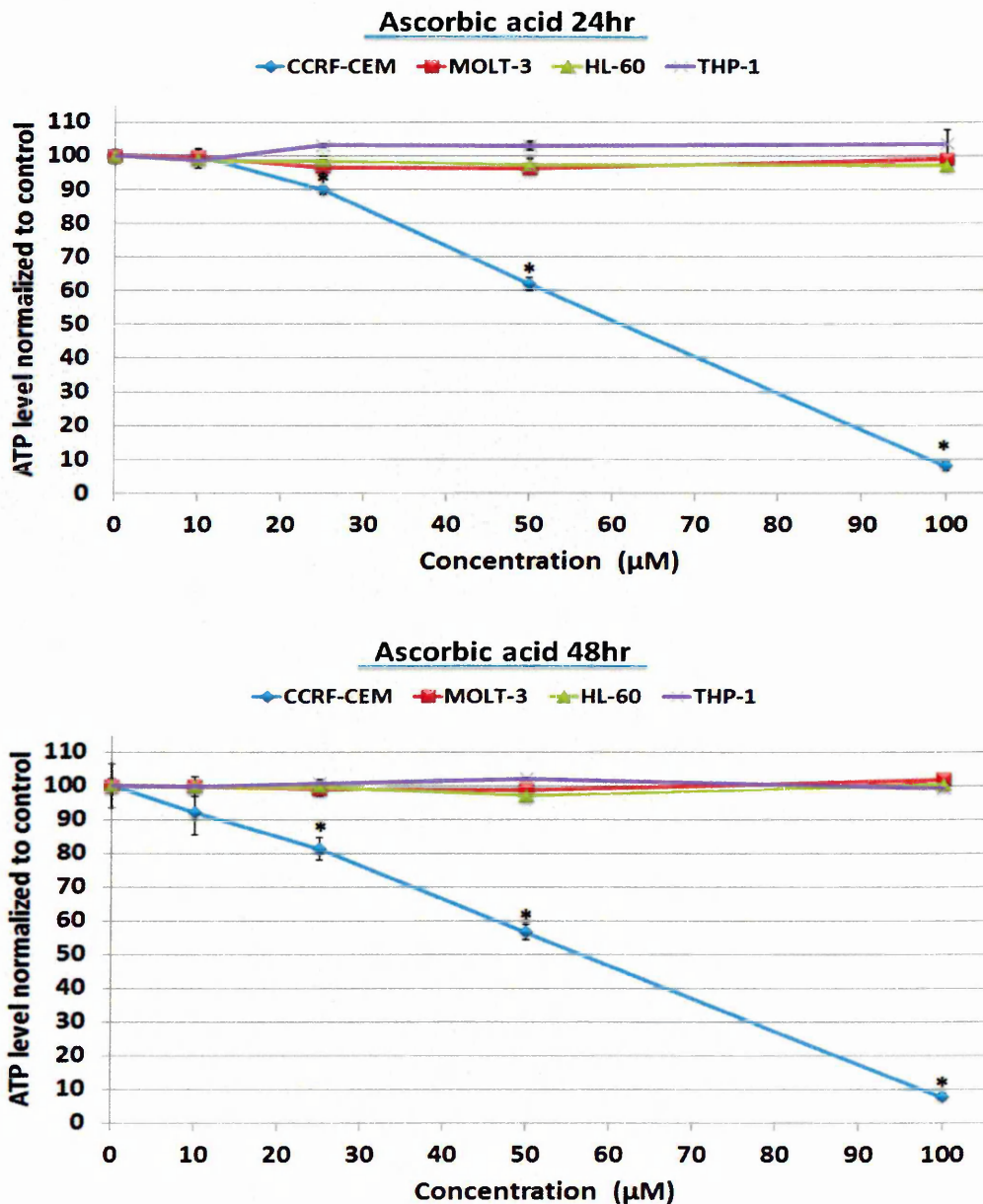


Figure 5.6: Effect of ascorbic acid on cell proliferation at concentrations 0, 10, 25, 50, and 100 μM in CCRF-CEM, MOLT-3, HL-60, and THP-1 leukaemia cell lines following 24 and 48 h. ATP levels investigated using Cell Titer-Glo[®] Luminescent Cell Viability Assay to provide indication of live cell numbers. ATP levels normalized to controls and presented as means \pm standard error. * indicates significant difference ($P \leq 0.05$) vs. untreated control. n= 3.

5.4.1.2 Phenolic Acids

A number of phenolic acid groups are found within pomegranates including: hydroxybenzoic acids and Hydroxycinnamic Acids which were investigated here for their potential bioactive actions on leukaemia cell lines.

5.4.1.2.1 Hydroxybenzoic Acids

The effects of the hydroxybenzoic acids: Gallic acid and ellagic acid were investigated on four leukaemia cell lines to determine potential bioactive actions affecting cell viability and proliferation, determined via measuring total ATP levels as an indication of number of metabolically active cells.

5.4.1.2.1.1 Gallic Acid

Gallic acid significantly inhibited ATP levels in all four leukaemia cell lines (CCRF-CEM, MOLT-3, HL-60 and THP-1) with differing sensitivity ($P \leq 0.05$) following 24 and 48 h treatments. However, it only caused a 50% reduction in ATP in CCRF-CEM, MOLT-3, and HL-60 cells following 24 and 48 h treatments. Gallic acid IC_{50} values for CCRF-CEM, MOLT-3, and HL-60 cells were 17 μ M following 24 h treatment. Following 48 h, the IC_{50} of gallic acid was 14 μ M for CCRF-CEM and 15 μ M for MOLT-3 and HL-60 was (Figure 5.7).

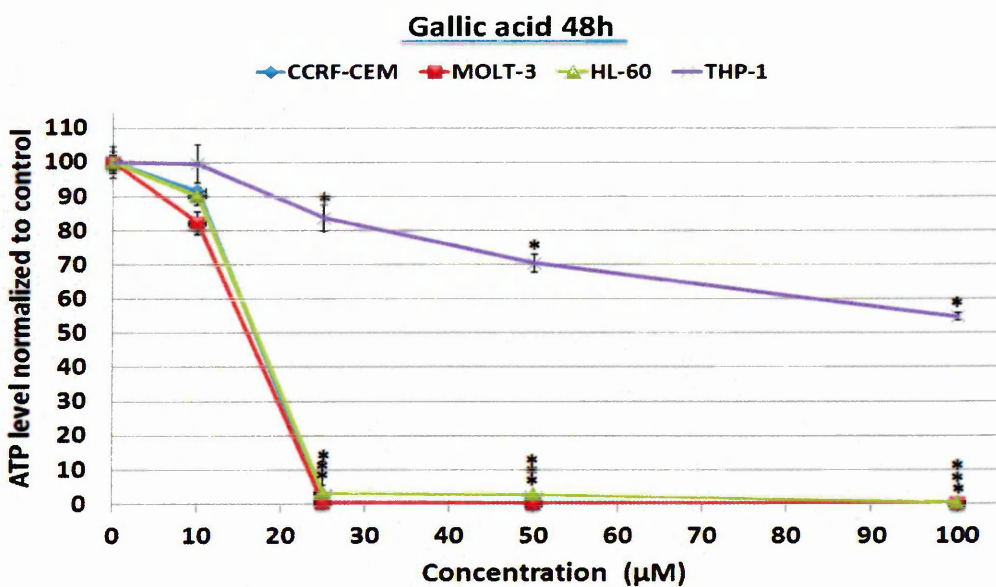
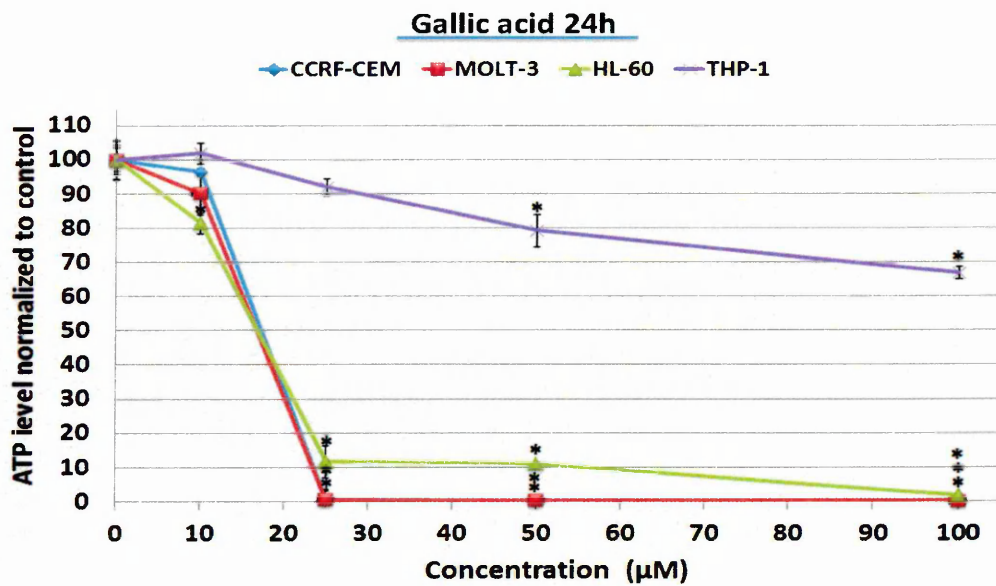


Figure 5.7: Effect of gallic acid on cell proliferation at concentrations 0, 10, 25, 50, and 100 μM in CCRF-CEM, MOLT-3, HL-60, and THP-1 leukaemia cell lines following 24 and 48 h. ATP levels investigated using Cell Titer-Glo® Luminescent Cell Viability Assay to provide indication of live cell numbers. ATP levels normalized to controls and presented as means ± standard error, * indicates significant difference ($P \leq 0.05$) vs. untreated control. n= 3.

5.4.1.2.1.2 Ellagic Acid

Ellagic acid significantly inhibited ATP levels in all four leukaemia cell lines (CCRF-CEM, MOLT-3, HL-60 and THP-1) with different sensitivity following 24 and 48 h ($P \leq 0.05$). However, it only caused a 50% reduction in ATP in MOLT-3 cells following 24 h treatments at a concentration of 98 μM . Following 48 h ellagic acid caused a 50% reduction in ATP in all four leukaemia cell lines. The IC_{50} of gallic acid for CCRF-CEM, MOLT-3, HL-60, and THP-1 cells were 40, 32, 91, and 94 μM , respectively (Figure 5.8).

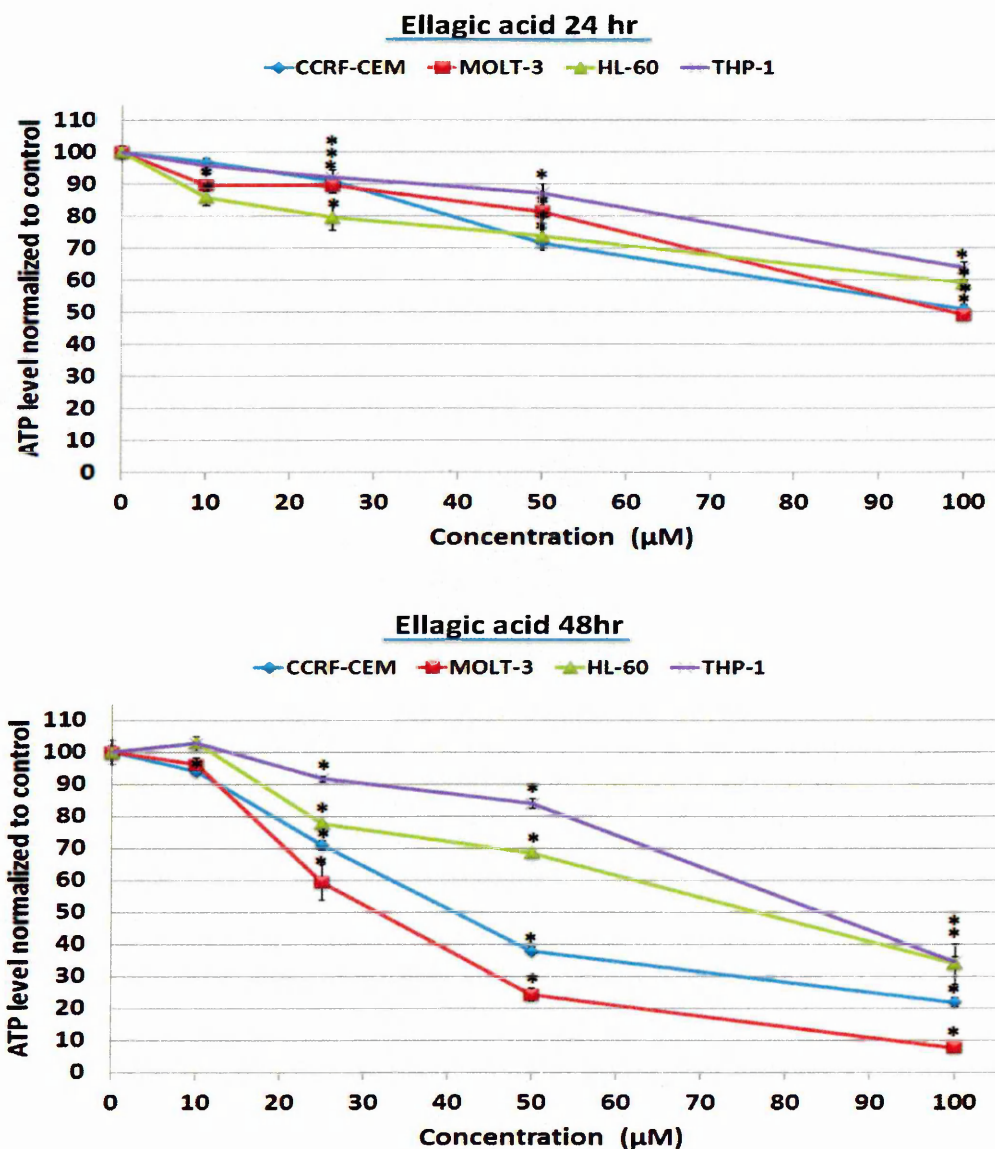


Figure 5.8: Effect of ellagic acid on cell proliferation at concentrations 0, 10, 25, 50, and 100 μM in CCRF-CEM, MOLT-3, HL-60, and THP-1 leukaemia cell lines following 24 and 48 h. ATP levels investigated using Cell Titer-Glo[®] Luminescent Cell Viability Assay to provide indication of live cell numbers. ATP levels normalized to controls and presented as means \pm standard error. * indicates significant difference ($P \leq 0.05$) vs. untreated control. n= 3.

5.4.1.2.2 Hydroxycinnamic Acids

The effects of the hydroxycinnamic acids: caffeic acid and *p*-cumaric were investigated on four leukaemia cell lines to determine potential bioactive actions affecting cell viability and proliferation, determined via measuring total ATP levels as an indication of number of metabolically active cells.

5.4.1.2.2.1 Caffeic Acid

Caffeic acid significantly inhibited ATP levels in all four cell lines, with greater sensitivity being shown by CCRF-CEM at 24 and 48 h ($P \leq 0.05$). CCRF-CEM was the only cell line to show a 50% reduction in ATP levels, with an IC_{50} value of 61 and 57 μM , at 24 and 48 h respectively (Figure 5.9).

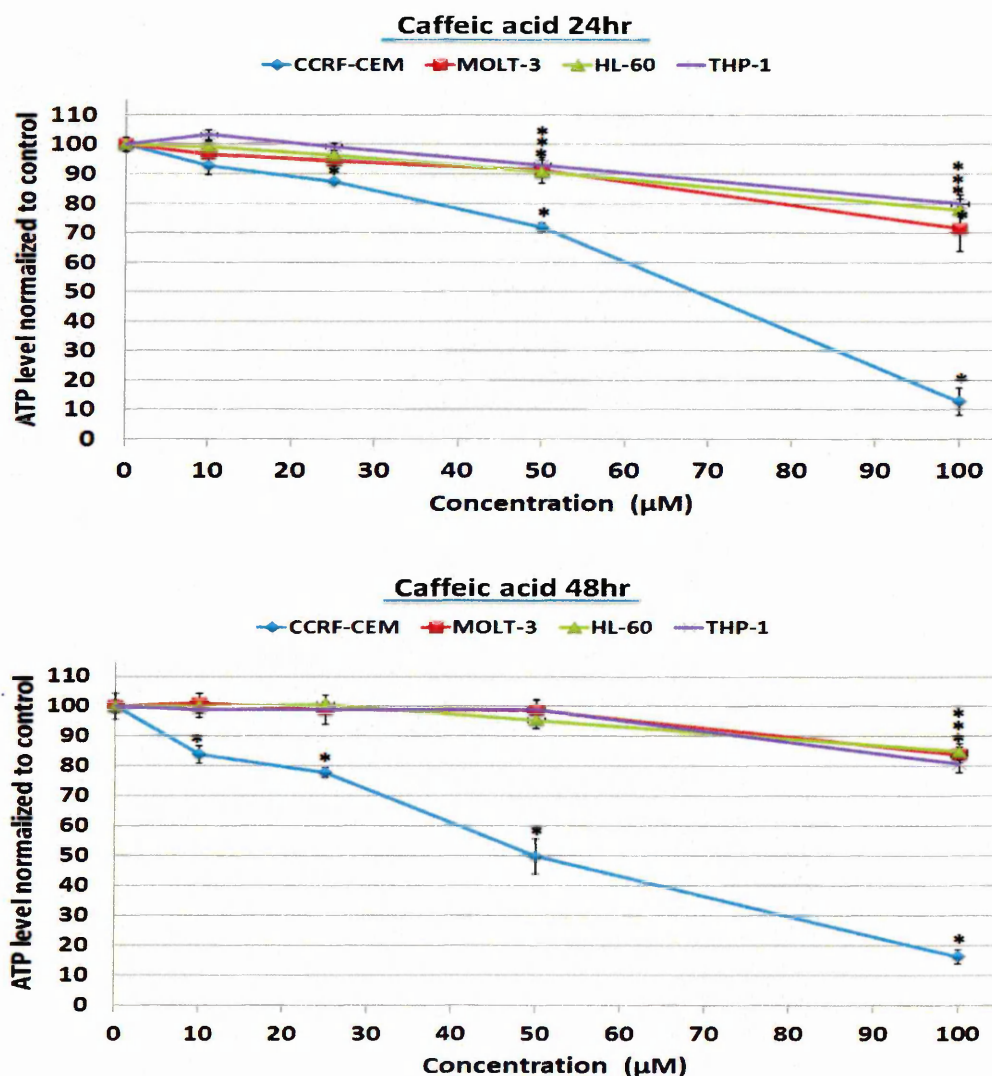


Figure 5.9: Effect of caffeic acid on cell proliferation at concentrations 0, 10, 25, 50, and 100 μM in CCRF-CEM, MOLT-3, HL-60, and THP-1 leukaemia cell lines following 24 and 48 h. ATP levels investigated using Cell Titer-Glo[®] Luminescent Cell Viability Assay to provide indication of live cell numbers. ATP levels normalized to controls and presented as means \pm standard error. * indicates significant difference ($P \leq 0.05$) vs. untreated control. $n = 3$.

5.4.1.2.2.2 *p*-cumaric Acid:

p-cumaric acid significantly inhibited ATP levels in the CCRF-CEM cells following 24 and 48 h treatment. However, it failed to cause a 50% reduction in ATP in any of the cell lines investigated following 24 and 48 h treatments (Figure 5.10).

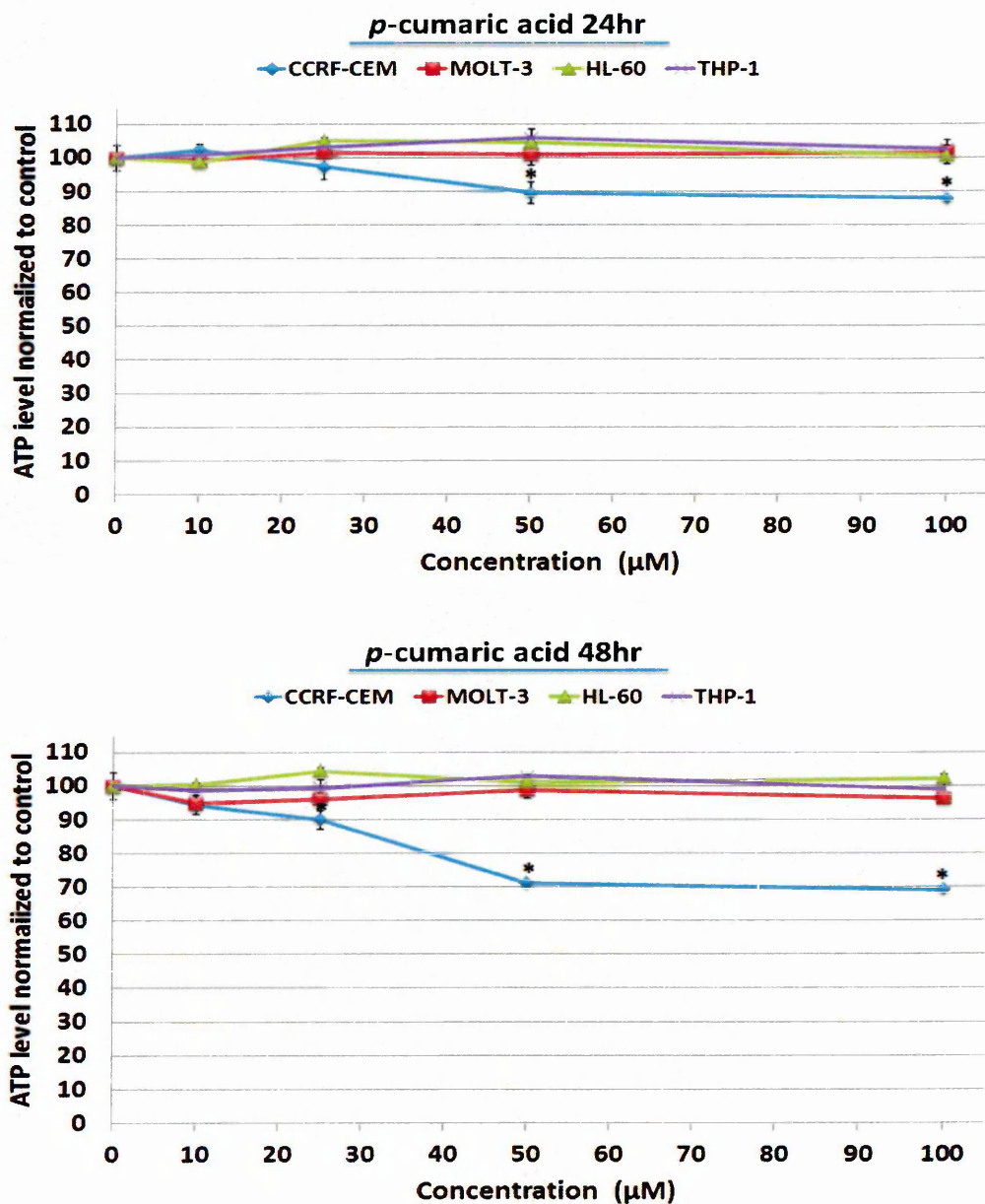


Figure 5.10: Effect of *p*-cumaric acid on cell proliferation at concentrations 0, 10, 25, 50, and 100µM in CCRF-CEM, MOLT-3, HL-60, and THP-1 leukaemia cell lines following 24 and 48 h. ATP levels investigated using Cell Titer-Glo® Luminescent Cell Viability Assay to provide indication of live cell numbers. ATP levels normalized to controls and presented as means ± standard error. * indicates significant difference ($P \leq 0.05$) vs. untreated control. n= 3.

5.4.1.3 Cyclitol Carboxylic Acid

The effects of the cyclitol carboxylic acid: Quinic acid was investigated on four leukaemia cell lines to determine potential bioactive actions affecting cell viability and proliferation, determined via measuring total ATP levels as an indication of number of metabolically active cells.

5.4.1.3.1 Quinic Acid:

Quinic acid showed no significant effect on ATP levels in any of the four leukaemia cell lines investigated, at 24 and 48 h treatments ($P \leq 0.05$). As a result, it failed to cause a 50% reduction in ATP in all four cell lines following 24 and 48 h (Figure 5.11).

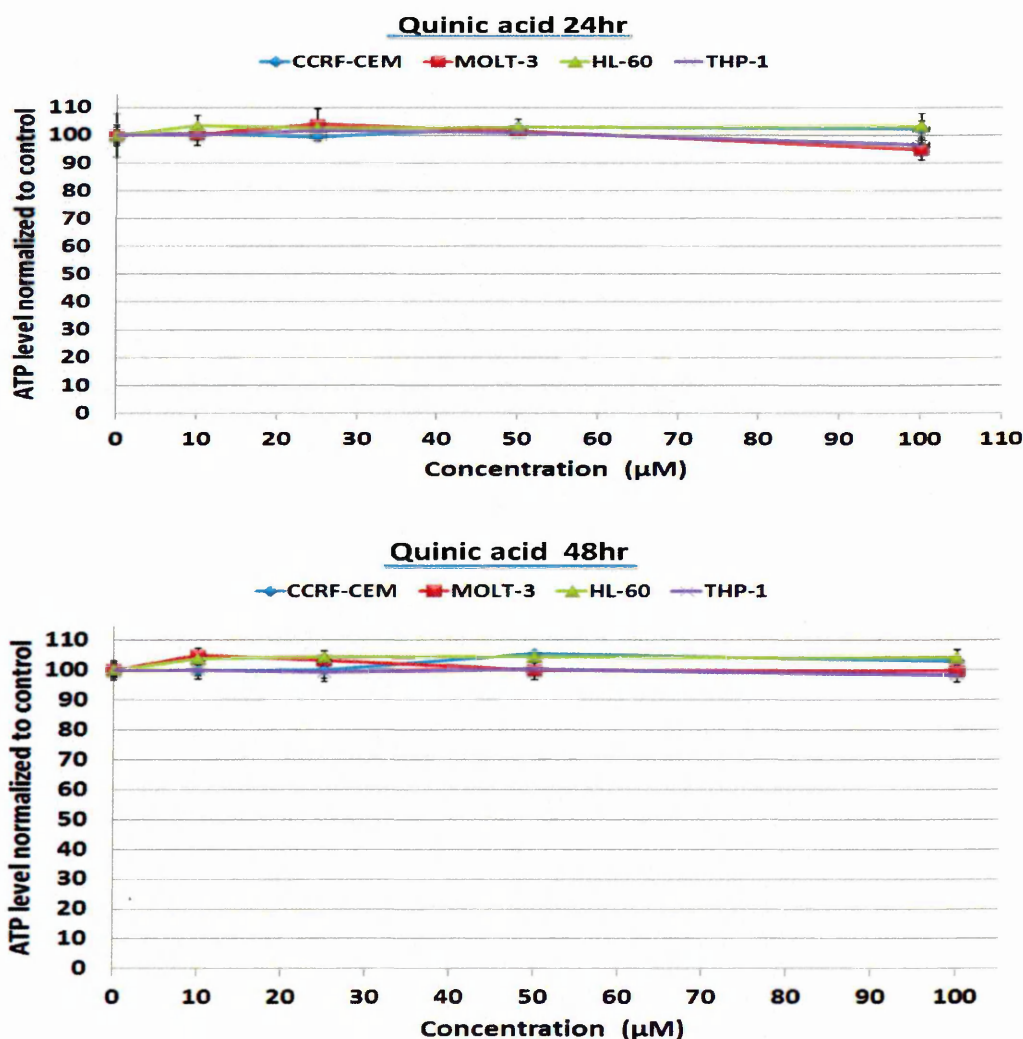


Figure 5.11: Effect of quinic acid on cell proliferation at concentrations 0, 10, 25, 50, and 100 µM in CCRF-CEM, MOLT-3, HL-60, and THP-1 leukaemia cell lines following 24 and 48 h. ATP levels investigated using Cell Titer-Glo® Luminescent Cell Viability Assay to provide indication of live cell numbers. ATP levels normalized to controls and presented as means \pm standard error. * indicates significant difference ($P \leq 0.05$) vs. untreated control. n= 3.

5.4.1.4 Flavan-3-ols

The effects of the Flavan-3-ols: catechin, epicatechin and EGCG were investigated on four leukaemia cell lines to determine potential bioactive actions affecting cell viability and proliferation, determined via measuring total ATP levels as an indication of number of metabolically active cells.

5.4.1.4.1 Catechin

Catechin showed no significant effect on ATP levels in any of the four leukaemia cell lines following 24 h treatment ($P \leq 0.05$). Following 48 h treatment, there was a significant effect on inhibition of ATP levels in CCRF-CEM, MOLT-3, and HL-60 cells following treatment with the highest two concentrations (50 and 100 μM) ($P \leq 0.05$). However, catechin failed to cause a 50% reduction in ATP in all four cell lines following 24 and 48 h (Figure 5.12).

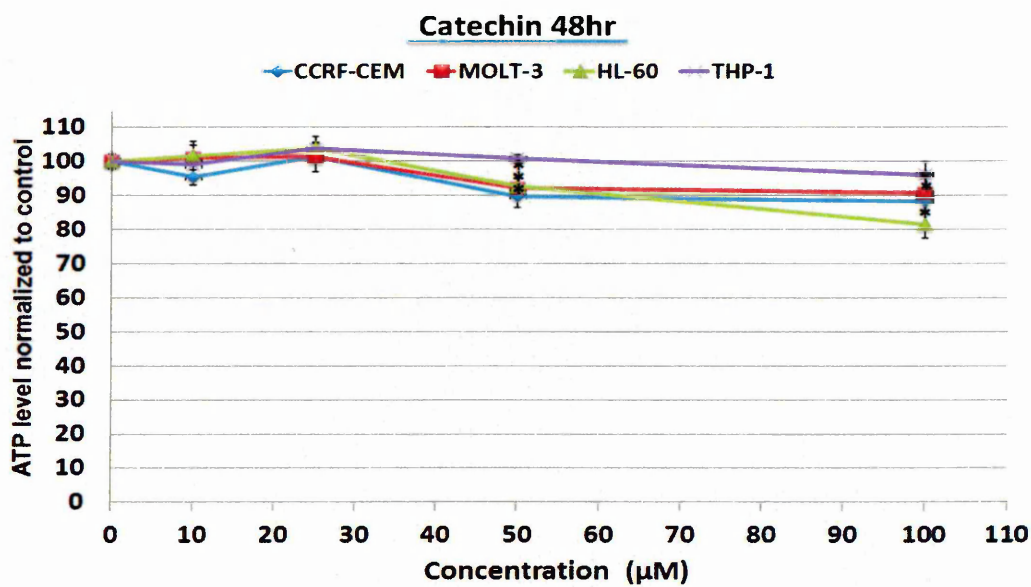
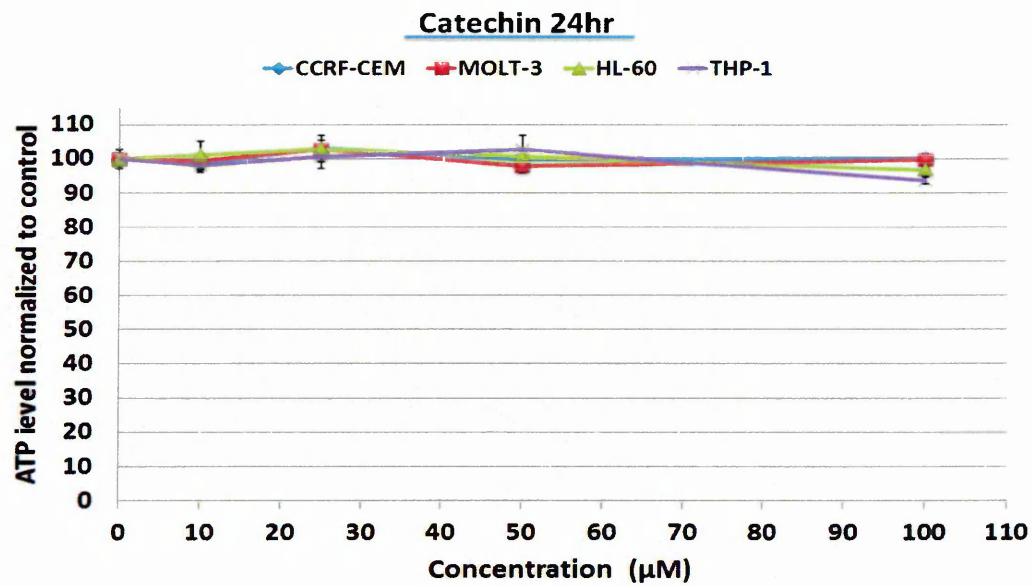


Figure 5.12: Effect of catechin on cell proliferation at concentrations 0, 10, 25, 50, and 100 μM in CCRF-CEM, MOLT-3, HL-60, and THP-1 leukaemia cell lines following 24 and 48 h. ATP levels investigated using Cell Titer-Glo[®] Luminescent Cell Viability Assay to provide indication of live cell numbers. ATP levels normalized to controls and presented as means \pm standard error. * indicates significant difference ($P \leq 0.05$) vs. untreated control. $n = 3$.

5.4.1.4.2 Epicatechin

Epicatechin treatment significantly inhibited ATP levels in all four leukaemia cell lines with different sensitivity following 24 and 48 h treatments ($P \leq 0.05$). However, epicatechin failed to cause a 50% reduction in ATP in each cell lines at 24 and 48 h (Figure 5.13).

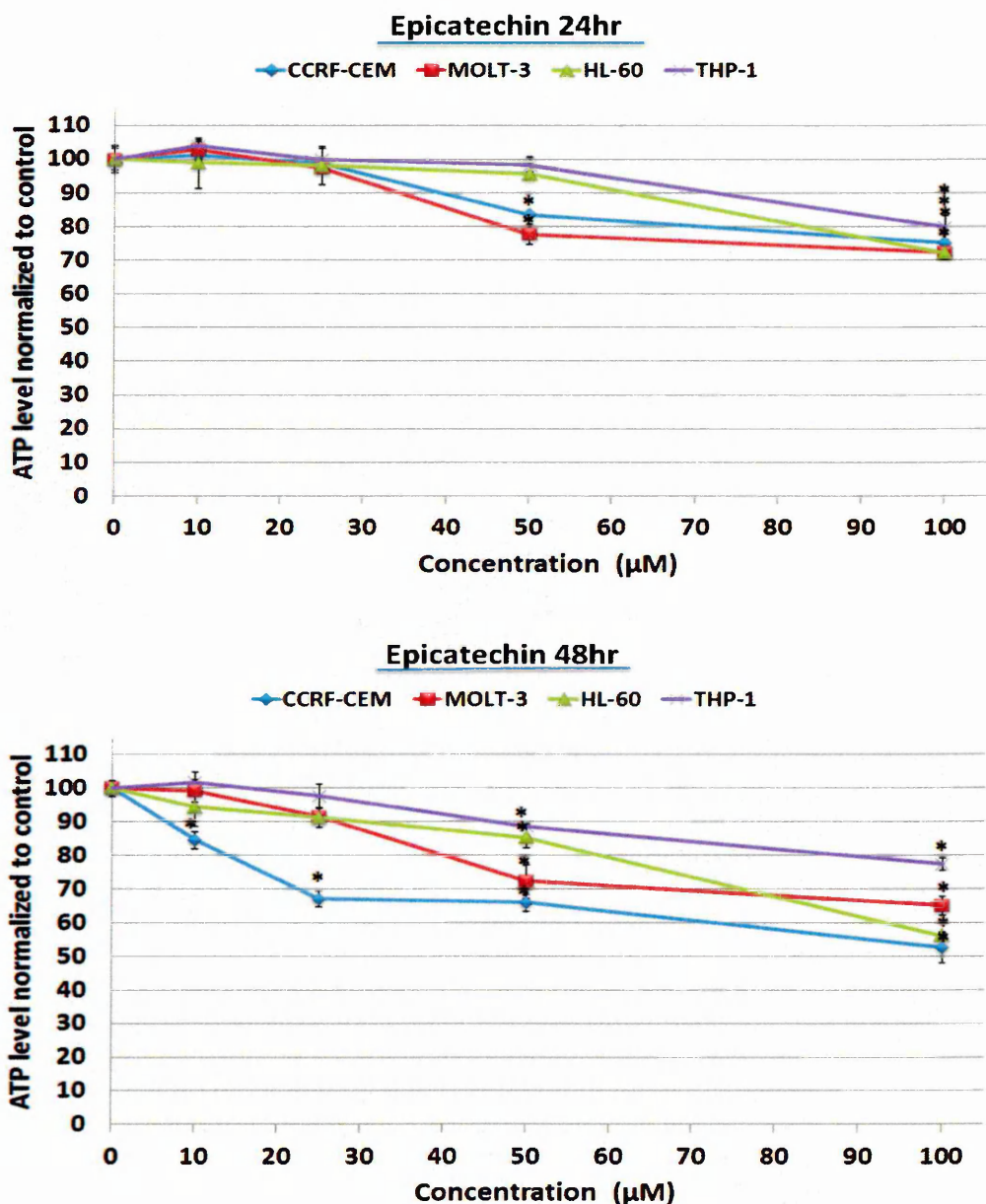


Figure 5.13: Effect of epicatechin on cell proliferation at concentrations 10, 25, 50, and 100 μM in CCRF-CEM, MOLT-3, HL-60, and THP-1 leukaemia cell lines following 24 and 48 h. ATP levels investigated using Cell Titer-Glo[®] Luminescent Cell Viability Assay to provide indication of live cell numbers. ATP levels normalized to controls and presented as means \pm standard error. * indicates significant difference ($P \leq 0.05$) vs. untreated control. $n=3$.

5.4.1.4.1 Epigallocatechin Gallate (EGCG)

Epigallocatechin gallate (EGCG) treatment of CCRF-CEM, MOLT-3, HL-60, and THP-1 cells resulted in a significant inhibition of ATP levels following 24 and 48 h incubation ($P \leq 0.05$) (Figure 5.14). Following 24 h treatment, EGCG caused a 50% reduction in ATP in CCRF-CEM, MOLT-3, and HL-60 cells at concentrations of 17, 21, and 19 μM respectively. At 48 h there was a 50% reduction in ATP in the THP-1 cells. The IC_{50} values at 48 h post-treatment with EGCG for CCRF-CEM, MOLT-3, HL-60 and THP-1 cells were 9, 15, 13, and 84 μM , respectively (Figure 5.14).

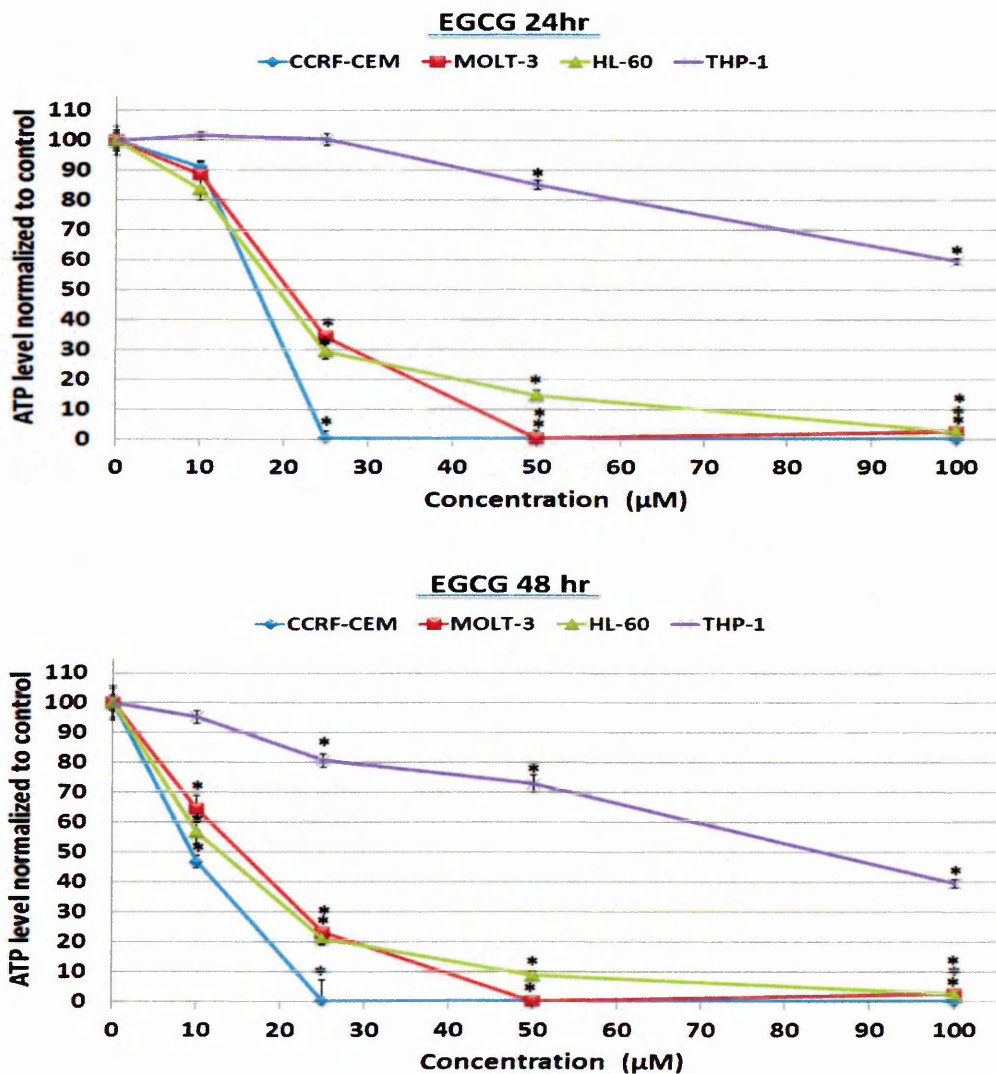


Figure 5.14: Effect of EGCG on cell proliferation at concentrations 10, 25, 50, and 100 μM in CCRF-CEM, MOLT-3, HL-60, and THP-1 leukaemia cell lines following 24 and 48 h. ATP levels investigated using Cell Titer-Glo[®] Luminescent Cell Viability Assay to provide indication of live cell numbers. ATP levels normalized to controls and presented as means \pm standard error. * indicates significant difference ($P \leq 0.05$) vs. untreated control. $n=3$.

5.4.1.5 Flavanoids

The effects of the Flavanoids: Quercetin and rutin were investigated on four leukaemia cell lines to determine potential bioactive actions affecting cell viability and proliferation, determined via measuring total ATP levels as an indication of number of metabolically active cells.

5.3.1.5.1 Quercetin

Quercetin treatment of CCRF-CEM, MOLT-3, HL-60, and THP-1 cells resulted in a significant inhibition of ATP levels following 24 and 48 h incubation ($P \leq 0.05$). The IC_{50} values at 24 h post-treatment for quercetin in CCRF-CEM, MOLT-3, HL-60, and THP-1 cells were 25, 50, 43, 23 μ M, respectively. At 48 h treatment, the IC_{50} values for CCRF-CEM, MOLT-3, HL-60, and THP-1 cells were 14.5, 29, 22.5, and 20.5 μ M, respectively (Figure 5.15).

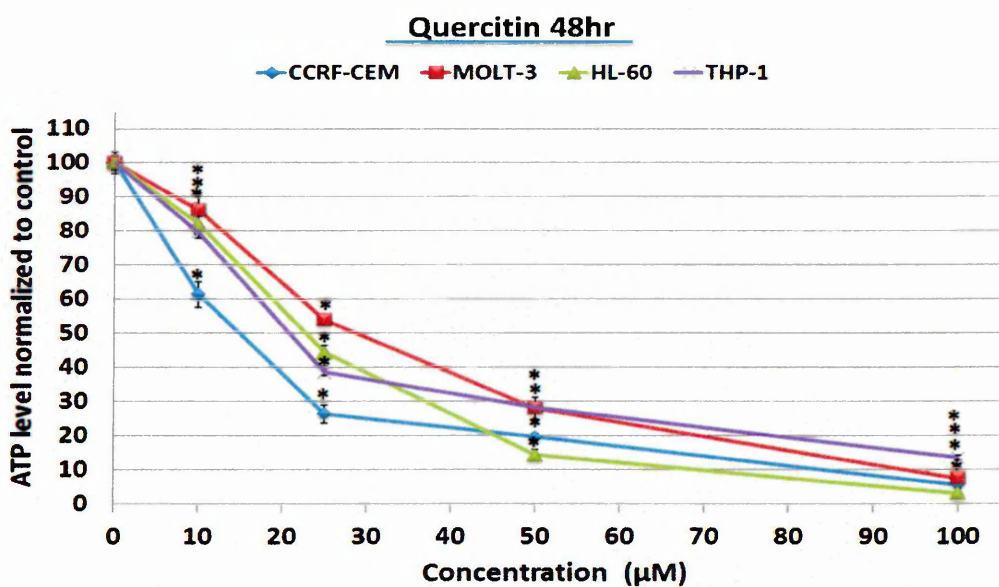
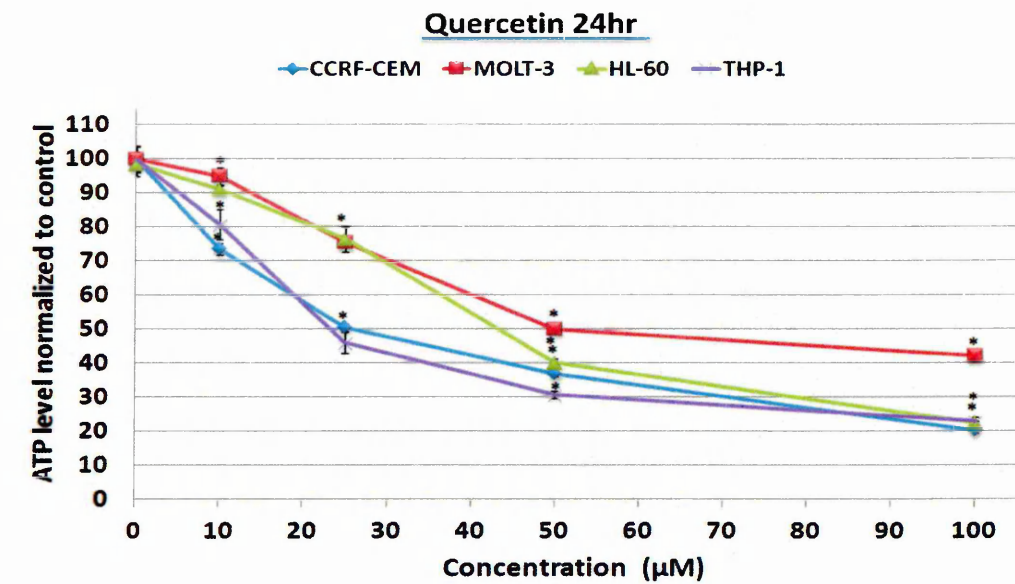


Figure 5.15: Effect of quercetin on cell proliferation at concentrations 0, 10, 25, 50, and 100 µM in CCRF-CEM, MOLT-3, HL-60, and THP-1 leukaemia cell lines following 24 and 48 h. ATP levels investigated using Cell Titer-Glo® Luminescent Cell Viability Assay to provide indication of live cell numbers. ATP levels normalized to controls and presented as means ± standard error. * indicates significant difference ($P \leq 0.05$) vs. untreated control. n= 3.

5.4.1.5.2 Rutin

Rutin did not significantly affect the ATP levels in all four leukaemia cell lines following 24 h treatment ($P > 0.05$). Rutin treatment to CCRF-CEM and HL-60 cells resulted in a significant reduction in ATP levels following 48 h treatment ($P \leq 0.05$). However, rutin failed to cause a 50% reduction in ATP in any of the cell lines (Figure 5.16).

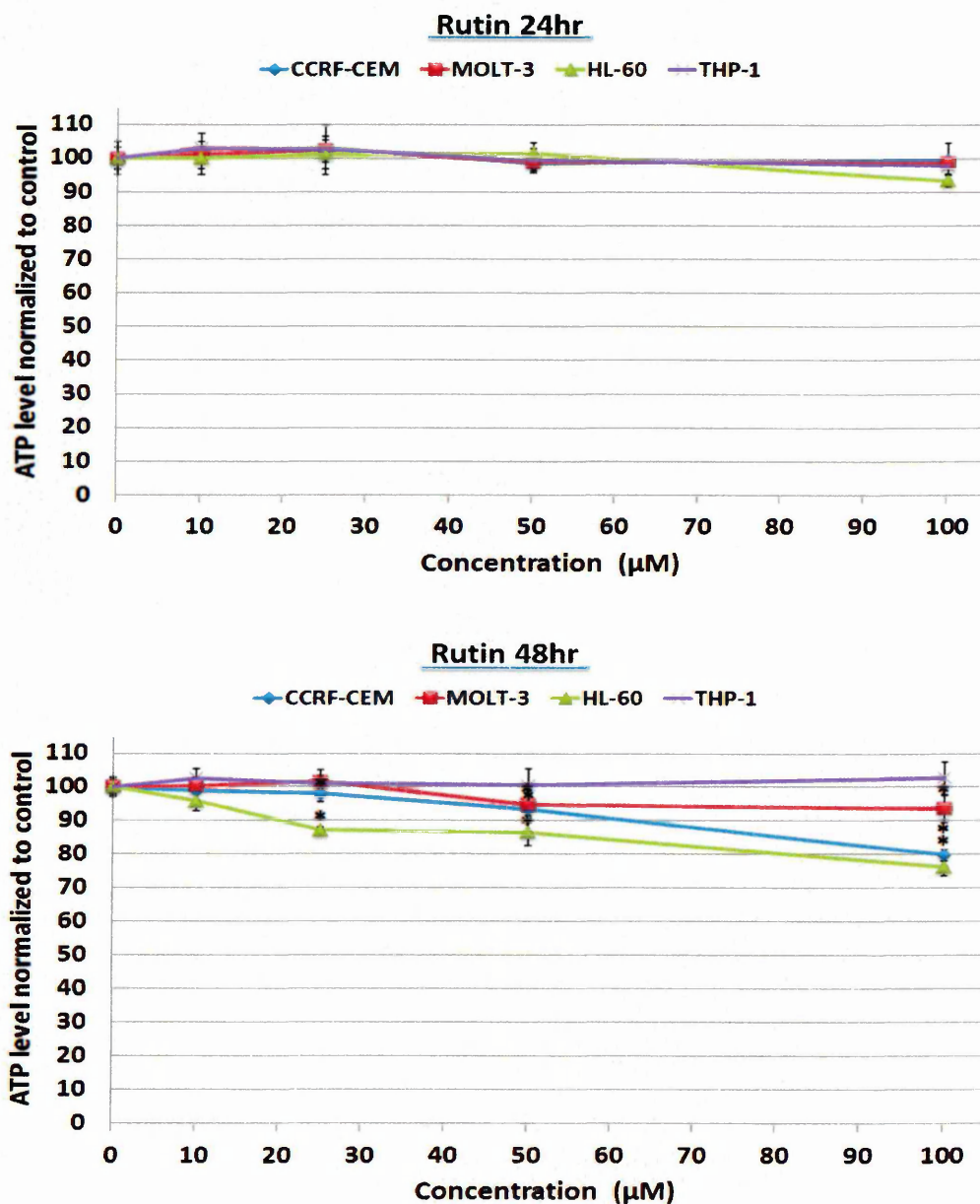


Figure 5.16: Effect of rutin on cell proliferation at concentrations 0, 10, 25, 50, and 100 µM in CCRF-CEM, MOLT-3, HL-60, and THP-1 leukaemia cell lines following 24 and 48 h. ATP levels investigated using Cell Titer-Glo® Luminescent Cell Viability Assay to provide indication of live cell numbers. ATP levels normalized to controls and presented as means \pm standard error. * indicates significant difference ($P \leq 0.05$) vs. untreated control. n= 3.

5.4.1.6 Ellagitannins

The effects of the ellagitannins: Punicalagin was investigated on four leukaemia cell lines to determine potential bioactive actions affecting cell viability and proliferation, determined via measuring total ATP levels as an indication of number of metabolically active cells.

5.4.1.6.1 Punicalagin

Punicalagin treatment of CCRF-CEM, MOLT-3, HL-60, and THP-1 cells resulted in a significant reduction in ATP levels following 24 and 48 h incubation ($P \leq 0.05$). The IC_{50} values at 24 h post-treatment with punicalagin for CCRF-CEM, MOLT-3, HL-60, and THP-1 cells were 11, 19, 17, 68 μ M, respectively. Following 48 h treatment, the IC_{50} values of punicalagin for CCRF-CEM, MOLT-3, HL-60, and THP-1 cells were 9, 14, 14, and 39 μ M, respectively (Figure 5.17).

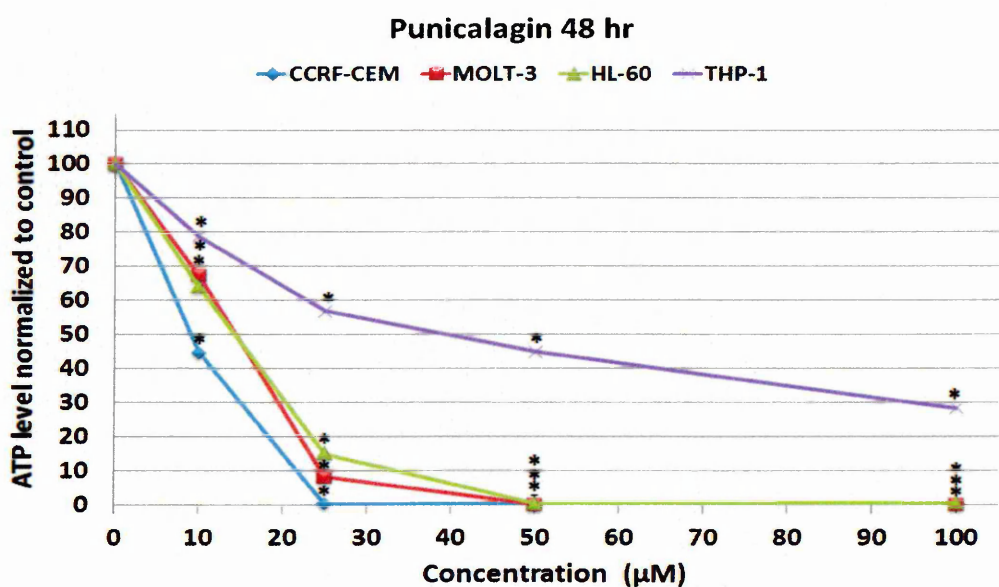
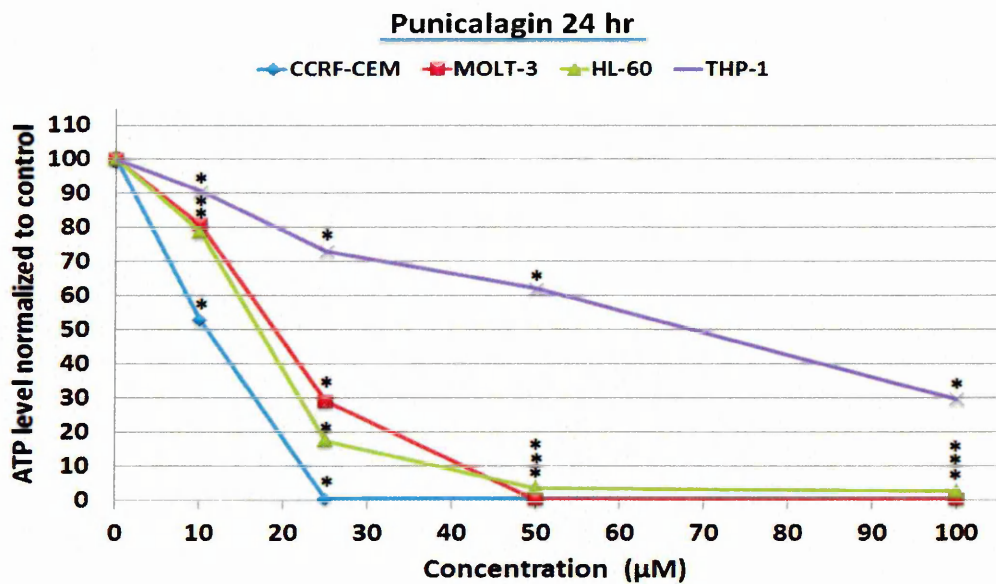


Figure 5.17: Effect of punicalagin on cell proliferation at concentrations 0, 10, 25, 50, and 100 μM in CCRF-CEM, MOLT-3, HL-60, and THP-1 leukaemia cell lines following 24 and 48 h. ATP levels investigated using Cell Titer-Glo® Luminescent Cell Viability Assay to provide indication of live cell numbers. ATP levels normalized to controls and presented as means ± standard error. * indicates significant difference ($P \leq 0.05$) vs. untreated control. n= 3.

5.4.1.7 Amino acids

The effects of the amino acids: proline; valine and methionine were investigated on four leukaemia cell lines to determine potential bioactive actions affecting cell viability and proliferation, determined via measuring total ATP levels as an indication of number of metabolically active cells.

5.4.1.7.1 Proline

Proline did not significantly reduce ATP levels, and failed to cause a 50% reduction in ATP in any of the four leukaemia cell lines investigated following 24 and 48 h treatments ($P > 0.05$) (Figure 5.18).

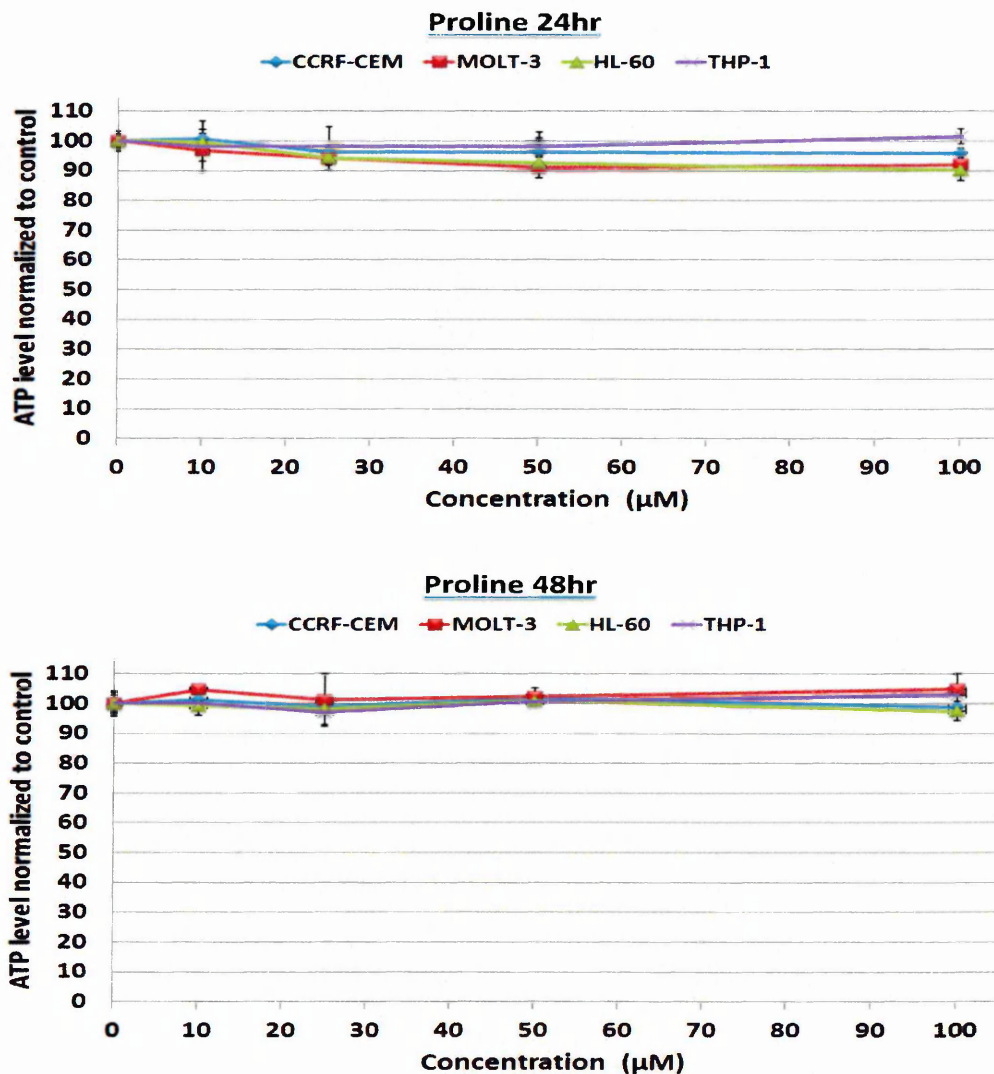


Figure 5.18: Effect of proline on cell proliferation at concentrations 0, 10, 25, 50, and 100 µM in CCRF-CEM, MOLT-3, HL-60, and THP-1 leukaemia cell lines following 24 and 48 h. ATP levels investigated using Cell Titer-Glo® Luminescent Cell Viability Assay to provide indication of live cell numbers. ATP levels normalized to controls and presented as means \pm standard error. * indicates significant difference ($P \leq 0.05$) vs. untreated control. n= 3.

5.4.1.7.2 Valine

Valine did not significantly reduce ATP levels, and failed to cause a 50% reduction in ATP in any of the four leukaemia cell lines investigated following 24 and 48 h treatments ($P > 0.05$) (Figure 5.19).

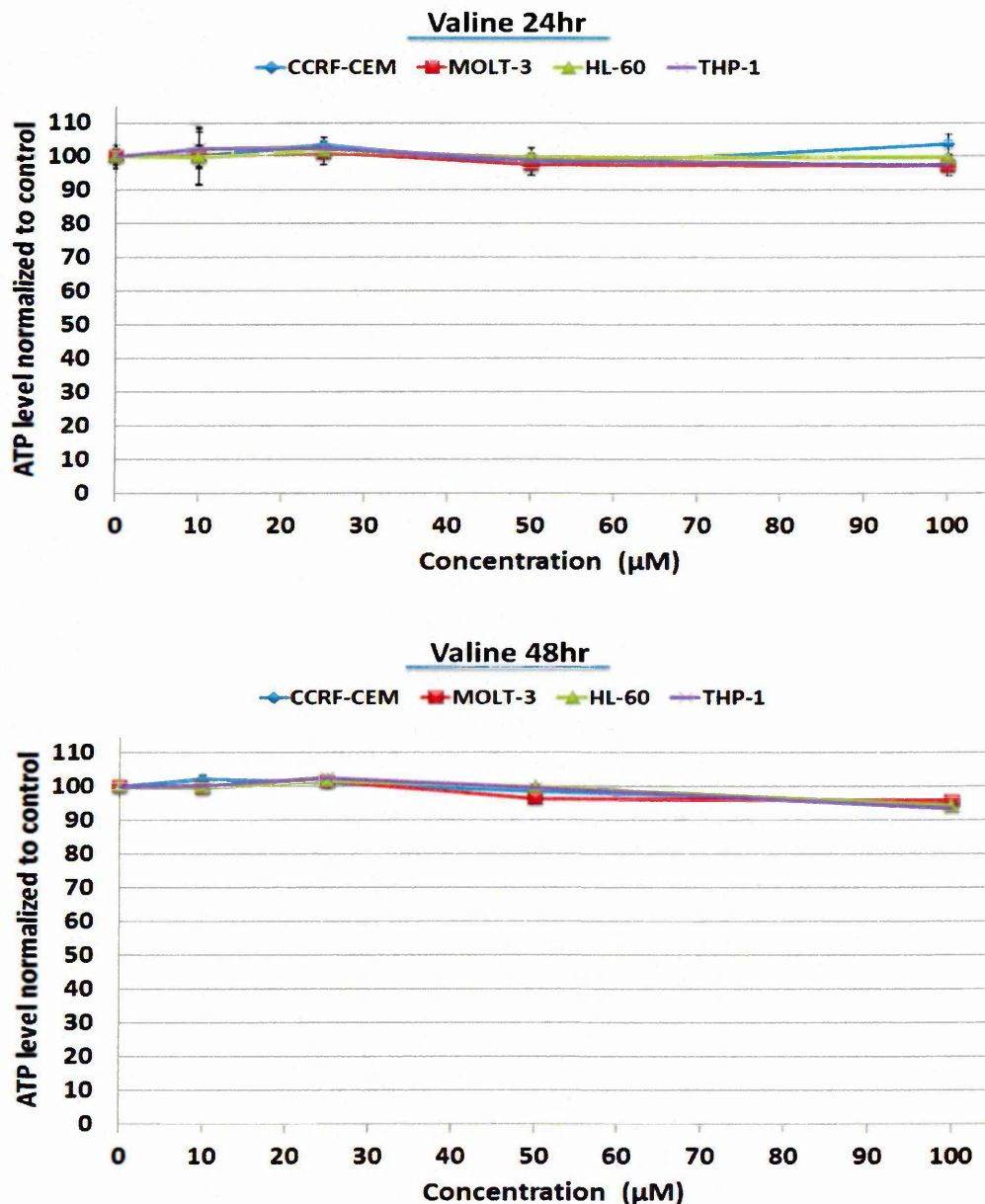


Figure 5.19: Effect of valine on cell proliferation at concentrations 0, 10, 25, 50, and 100 µM in CCRF-CEM, MOLT-3, HL-60, and THP-1 leukaemia cell lines following 24 and 48 h. ATP levels investigated using Cell Titer-Glo® Luminescent Cell Viability Assay to provide indication of live cell numbers. ATP levels normalized to controls and presented as means \pm standard error. * indicates significant difference ($P \leq 0.05$) vs. untreated control. $n=3$.

5.4.1.7.3 Methionine

Methionine showed no significant effect on inhibition of ATP levels and failed to cause a 50% reduction in ATP in any of the four leukaemia cell lines following 24 and 48 h treatments ($P > 0.05$) (Figure 5.20).

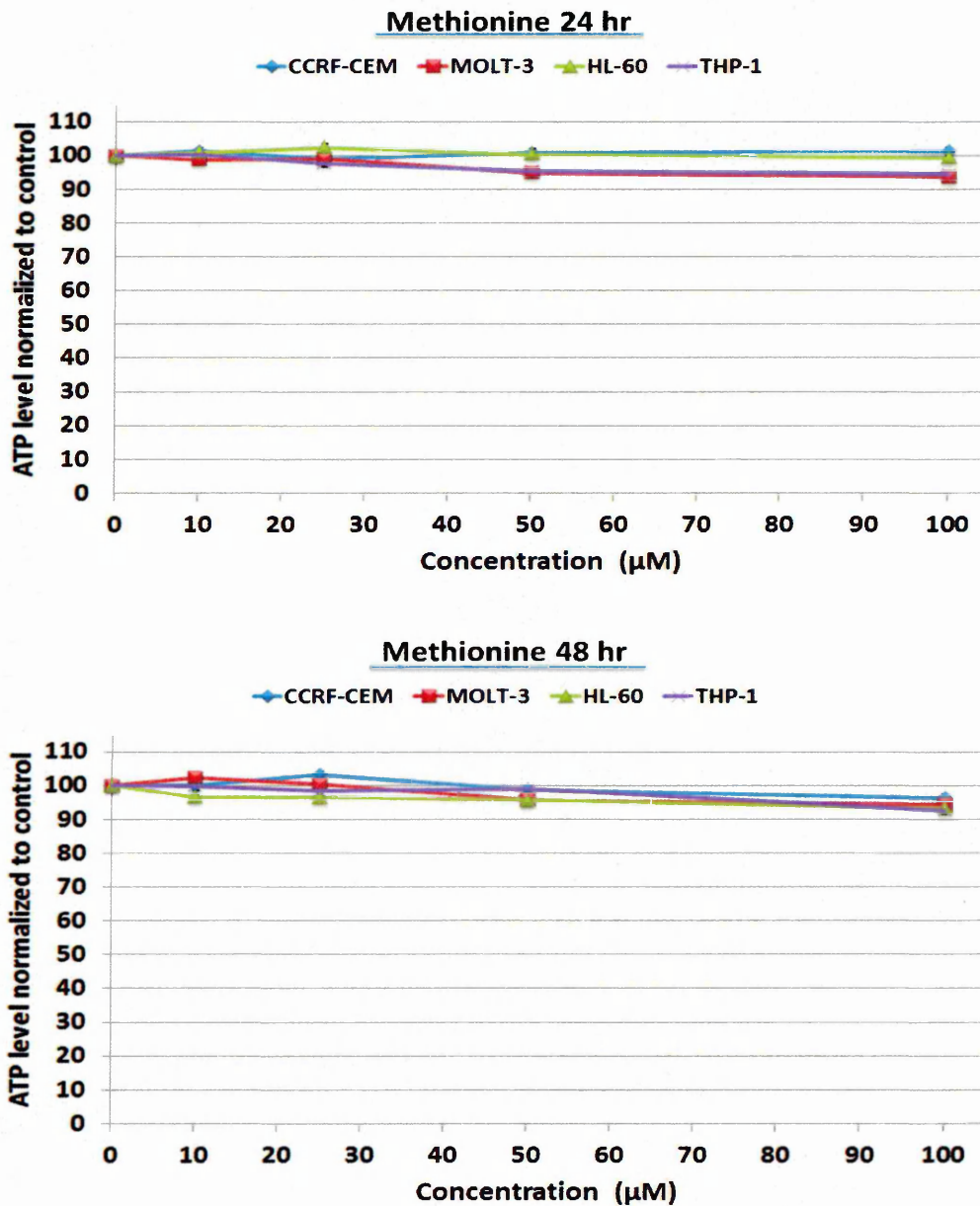


Figure 5.20: Effect of methionine on cell proliferation at concentrations 0, 10, 25, 50, and 100 μM in CCRF-CEM, MOLT-3, HL-60, and THP-1 leukaemia cell lines following 24 and 48 h. ATP levels investigated using Cell Titer-Glo[®] Luminescent Cell Viability Assay to provide indication of live cell numbers. ATP levels normalized to controls and presented as means \pm standard error. * indicates significant difference ($P \leq 0.05$) vs. untreated control. $n = 3$.

5.4.1.8 Indoleamines

The effects of the indoleamines: tryptamine; Serotonin and Melatonin were investigated on four leukaemia cell lines to determine potential bioactive actions affecting cell viability and proliferation, determined via measuring total ATP levels as an indication of number of metabolically active cells.

5.4.1.8.1 Tryptamine

Tryptamine showed no significant effect on inhibition of ATP levels and failed to cause a 50% decrease in ATP in any of the four leukaemia cell lines following 24 and 48 h treatments ($P > 0.05$) (Figure 5.21).

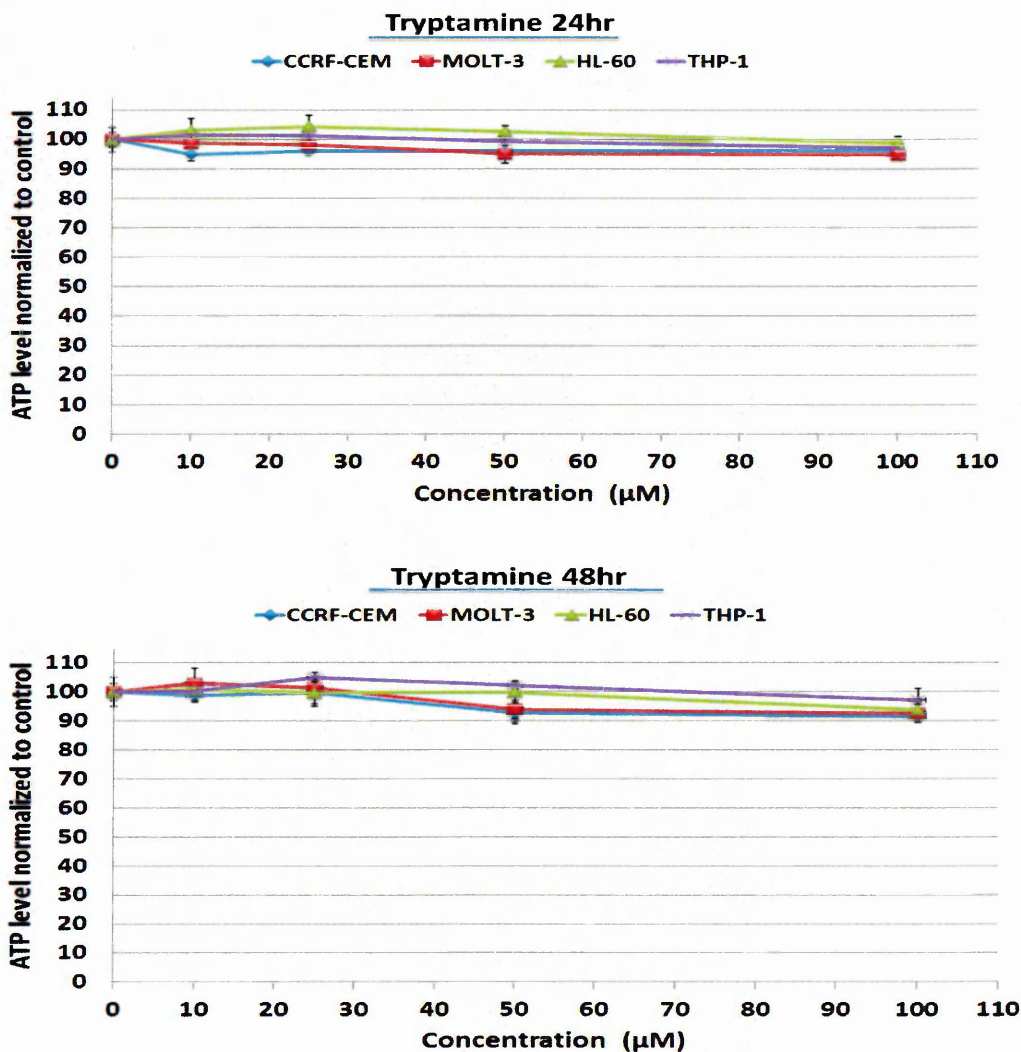


Figure 5.21: Effect of tryptamine on cell proliferation at concentrations 0, 10, 25, 50, and 100 µM in CCRF-CEM, MOLT-3, HL-60, and THP-1 leukaemia cell lines following 24 and 48 h. ATP levels investigated using Cell Titer-Glo® Luminescent Cell Viability Assay to provide indication of live cell numbers. ATP levels normalized to controls and presented as means \pm standard error. * indicates significant difference ($P \leq 0.05$) vs. untreated control. $n = 3$.

5.4.1.8.2 Serotonin

Serotonin showed significant inhibition of ATP levels in CCRF-CEM cells following 24 h treatment at concentrations of 50 and 100 μM and in MOLT-3 cells treatment at concentration of 100 μM ($P \leq 0.05$). In contrast, serotonin showed no significant effect on ATP levels in any of the four leukaemia cell lines following 48 h treatment ($P > 0.05$) (Figure 5.22).

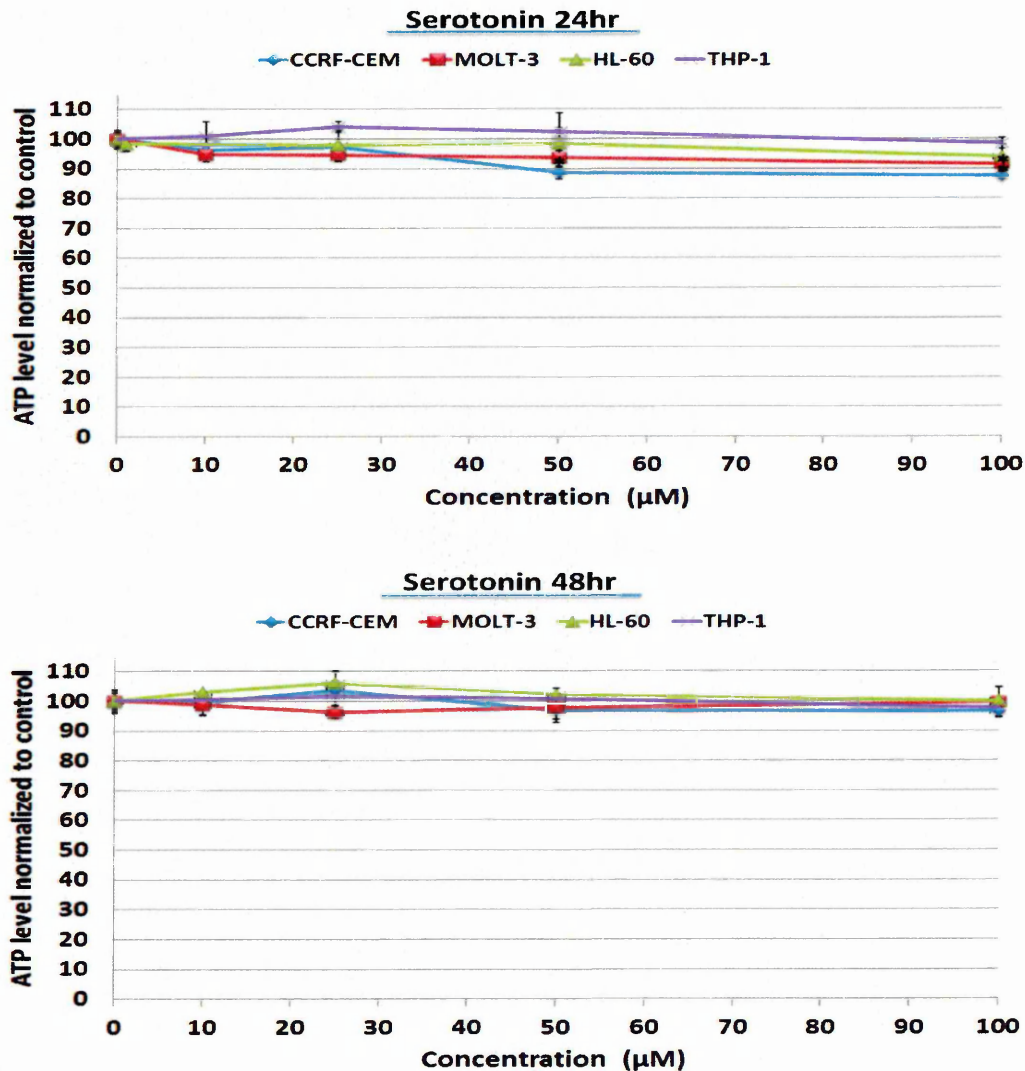


Figure 5.22: Effect of serotonin on cell proliferation at concentrations 0, 10, 25, 50, and 100 μM in CCRF-CEM, MOLT-3, HL-60, and THP-1 leukaemia cell lines following 24 and 48 h. ATP levels investigated using Cell Titer-Glo[®] Luminescent Cell Viability Assay to provide indication of live cell numbers. ATP levels normalized to controls and presented as means \pm standard error. * indicates significant difference ($P \leq 0.05$) vs. untreated control. n= 3.

5.4.1.8.3 Melatonin

Melatonin showed significant inhibition of ATP levels following 24 and 48 h treatment in the CCRF-CEM, MOLT-3, and HL-60 cell lines ($P \leq 0.05$). However, it failed to cause a 50% decrease in ATP in any of the four leukaemia cell lines (Figure 5.23).

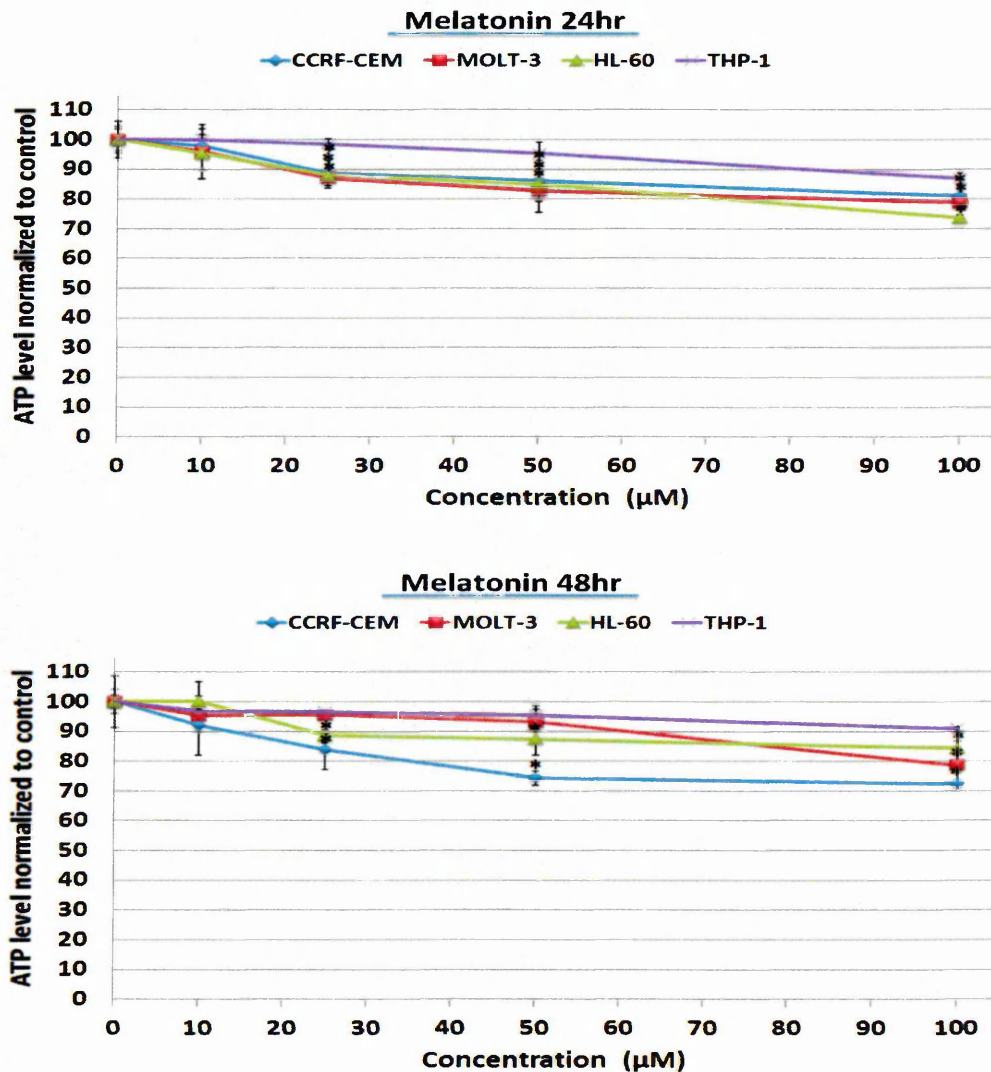


Figure 5.23: Effect of melatonin on cell proliferation at concentrations 0, 10, 25, 50, and 100 μM in CCRF-CEM, MOLT-3, HL-60, and THP-1 leukaemia cell lines following 24 and 48 h. ATP levels investigated using Cell Titer-Glo[®] Luminescent Cell Viability Assay to provide indication of live cell numbers. ATP levels normalized to controls and presented as means \pm standard error. * indicates significant difference ($P \leq 0.05$) vs. untreated control. $n = 3$.

5.4.1.9 Anthocyanins

The effects of the anthocyanins: delphinidin, cyaniding and pelargonidin were investigated on four leukaemia cell lines to determine potential bioactive actions affecting cell viability and proliferation, determined via measuring total ATP levels as an indication of number of metabolically active cells.

5.4.1.9.1 Delphinidin

Delphinidin significantly inhibited ATP levels in all four leukaemia cell lines investigated following 24 and 48 h treatment ($P \leq 0.05$). The IC_{50} values of delphinidin for CCRF-CEM, MOLT-3, HL-60, and THP-1 cells following 24 h treatments were 56, 67, 64, and 83 μ M, respectively. Following 48 h, the IC_{50} values of delphinidin for CCRF-CEM, MOLT-3, HL-60, and THP-1 were 42, 65, 60, and 78 μ M, respectively (Figure 5.24).

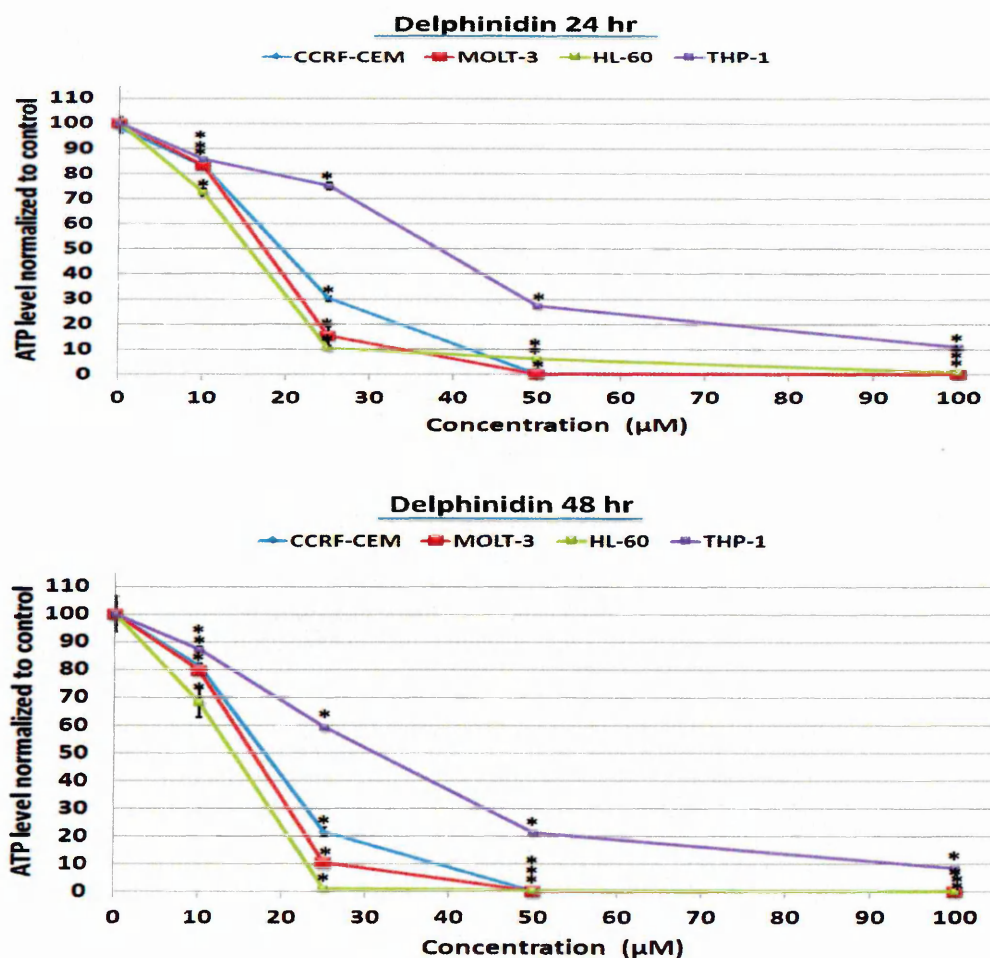


Figure 5.24: Effect of delphinidin on cell proliferation at concentrations 0, 10, 25, 50, and 100 μ M in CCRF-CEM, MOLT-3, HL-60, and THP-1 leukaemia cell lines following 24 and 48 h. ATP levels investigated using Cell Titer-Glo[®] Luminescent Cell Viability Assay to provide indication of live cell numbers. ATP levels normalized to controls and presented as means \pm standard error. * indicates significant difference ($P \leq 0.05$) vs. untreated control. n = 3.

5.4.1.9.2 Cyanidin

Cyanidin significantly inhibited ATP levels in all four leukaemia cell lines following 24 and 48 h treatment ($P \leq 0.05$). The IC_{50} values of cyanidin for CCRF-CEM, MOLT-3, HL-60, and THP-1 cells following 24 h treatments were 56, 67, 64, and 83 μM , respectively. Following 48 h, the IC_{50} values of cyanidin for CCRF-CEM, MOLT-3, HL-60, and THP-1 cells were 42, 65, 60, and 78 μM , respectively (Figure 5.25).

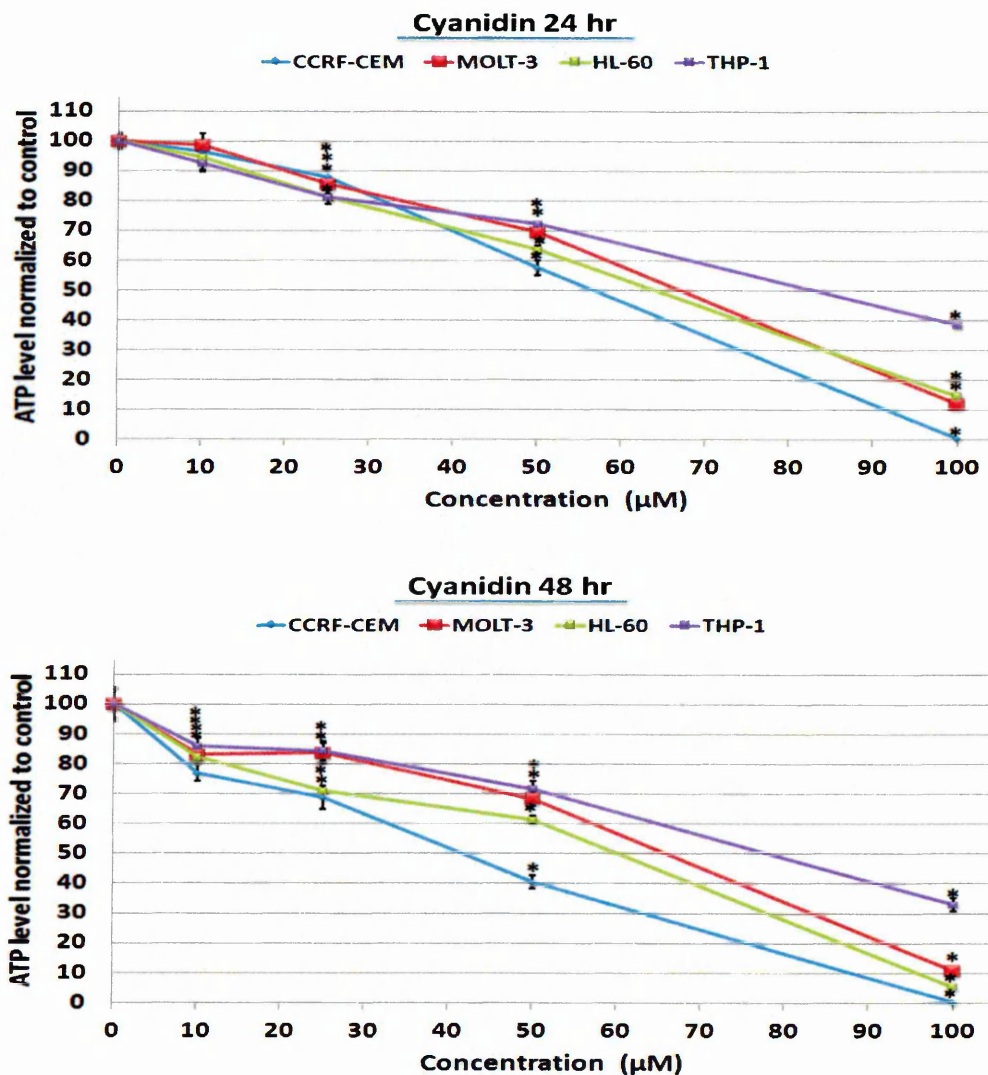


Figure 5.25: Effect of cyanidin on cell proliferation at concentrations 0, 10, 25, 50, and 100 μM in CCRF-CEM, MOLT-3, HL-60, and THP-1 leukaemia cell lines following 24 and 48 h. ATP levels investigated using Cell Titer-Glo[®] Luminescent Cell Viability Assay to provide indication of live cell numbers. ATP levels normalized to controls and presented as means \pm standard error. * indicates significant difference ($P \leq 0.05$) vs. untreated control. $n = 3$.

5.3.1.9.3 Pelargonidin

Pelargonidin significantly inhibited ATP levels in all four leukaemia cell lines following 24 and 48 h treatment ($P \leq 0.05$). Punicalagin showed similar IC_{50} value of 81 μM for each cell line at 24 h treatment. At 48 h, the IC_{50} values of pelargonidin for CCRF-CEM, MOLT-3, HL-60, and THP-1 cells were 69, 77, 74, and 82 μM , respectively (Figure 5.26).

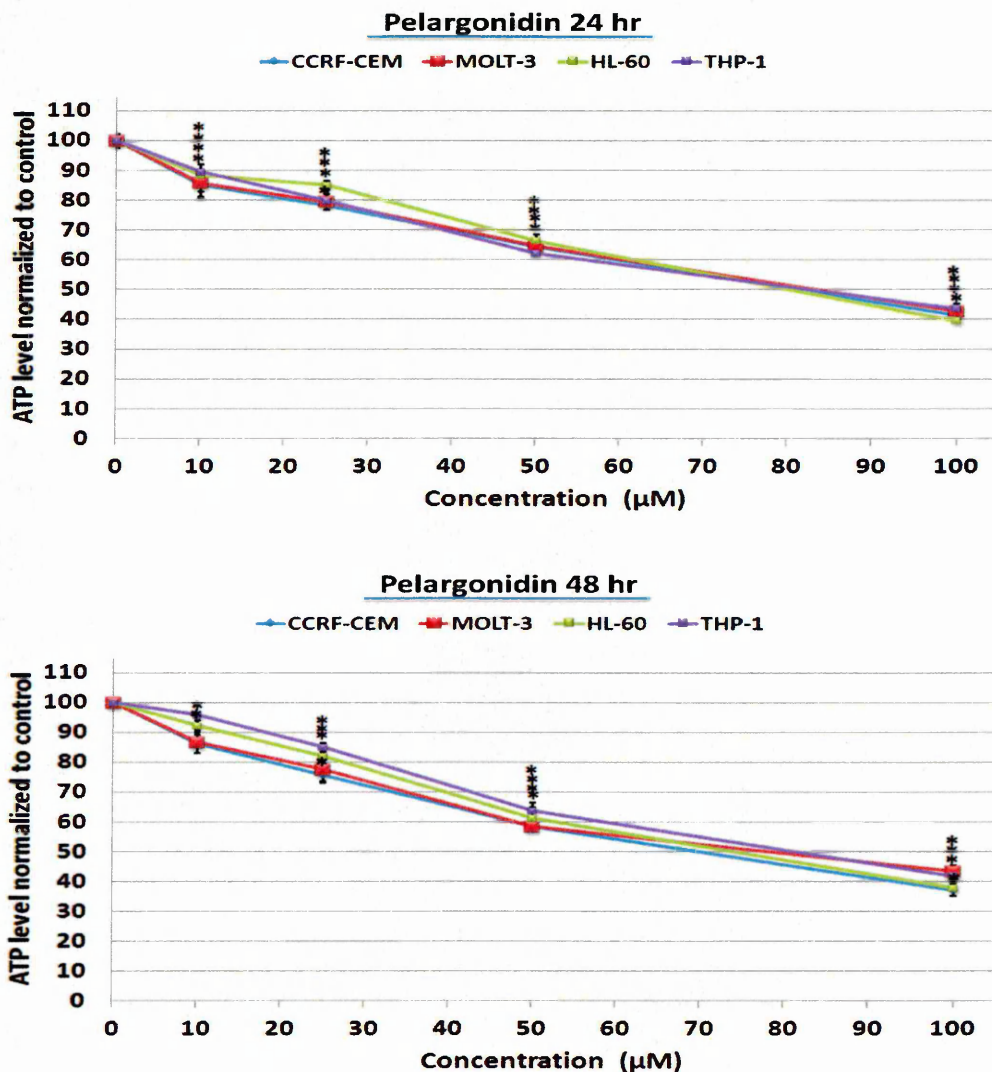


Figure 5.26: Effect of pelargonidin on cell proliferation at concentrations 0, 10, 25, 50, and 100 μM in CCRF-CEM, MOLT-3, HL-60, and THP-1 leukaemia cell lines following 24 and 48 h. ATP levels investigated using Cell Titer-Glo[®] Luminescent Cell Viability Assay to provide indication of live cell numbers. ATP levels normalized to controls and presented as means \pm standard error. * indicates significant difference ($P \leq 0.05$) vs. untreated control. $n = 3$.

5.4.2 Summary of Results

Twenty six naturally occurring pomegranate compounds exhibited selective anti-cancer activity towards the leukaemia cell lines: CCRF-CEM, MOLT-3, HL-60, and THP-1 following 24 and 48 h treatment. Only 7 out of 26 compounds induced a 50% reduction in ATP levels in 3 or more leukaemia cell lines (Table 5.3).

Chemical class	Compound name	Time point	IC ₅₀ values for each cell line			
			CCRF-CEM	MOLT-3	HL-60	THP-1
Organic acid	Citric acid	24 h	NR	NR	NR	NR
		48 h	NR	NR	NR	NR
	Malic acid	24 h	NR	NR	NR	NR
		48 h	NR	NR	NR	NR
	Tartaric acid	24 h	NR	NR	NR	NR
		48 h	NR	NR	NR	NR
	Fumaric acid	24 h	NR	NR	NR	NR
		48 h	NR	NR	NR	NR
	Succinic acid	24 h	NR	NR	NR	NR
		48 h	NR	NR	NR	NR
Ascorbic acid	24 h	61 µM	NR	NR	NR	
	48 h	57 µM	NR	NR	NR	
Hydroxybenzoic acid	Gallic acid	24 h	17 µM	17 µM	17 µM	NR
		48 h	14 µM	15 µM	15 µM	NR
	Ellagic acid	24 h	NR	98 µM	NR	NR
		48 h	40 µM	32 µM	91 µM	94 µM
Hydroxycinnamic acid	Caffeic acid	24 h	68 µM	NR	NR	NR
		48 h	64 µM	NR	NR	NR
	<i>p</i> -cumaric acid	24 h	NR	NR	NR	NR
		48 h	NR	NR	NR	NR
Cyclitol carboxylic acid	Quinic acid	24 h	NR	NR	NR	NR
		48 h	NR	NR	NR	NR
Flavan-3-ols	Catechin	24 h	NR	NR	NR	NR
		48 h	NR	NR	NR	NR
	Epicatechin	24 h	NR	NR	NR	NR
		48 h	NR	NR	NR	NR
	EGCG	24 h	17 µM	21 µM	19 µM	NR µM
		48 h	9 µM	15 µM	13 µM	84 µM
Flavonols	Quercetin	24 h	25 µM	50 µM	43 µM	23 µM
		48 h	14.5 µM	29 µM	22.5 µM	20.5 µM
	Rutin	24 h	NR	NR	NR	NR
		48 h	NR	NR	NR	NR

Table (continued)						
Chemical class	Compound name	Time point	IC ₅₀ values for each cell line			
			CCRF-CEM	MOLT-3	HL-60	THP-1
Ellagitannins	Punicalagin	24 h	11 µM	19 µM	17 µM	68 µM
		48 h	9 µM	14 µM	14 µM	39 µM
Amino acids	Proline	24 h	NR	NR	NR	NR
		48 h	NR	NR	NR	NR
	Valine	24 h	NR	NR	NR	NR
		48 h	NR	NR	NR	NR
	Methionine	24 h	NR	NR	NR	NR
		48 h	NR	NR	NR	NR
	Tryptamine	24 h	NR	NR	NR	NR
		48 h	NR	NR	NR	NR
Indoleamines	Serotonin	24 h	NR	NR	NR	NR
		48 h	NR	NR	NR	NR
	Melatonin	24 h	NR	NR	NR	NR
		48 h	NR	NR	NR	NR
Anthocyanins	Delphinidin	24 h	18.5 µM	17 µM	15 µM	76 µM
		48 h	18 µM	16 µM	14 µM	31 µM
	Cyanidin	24 h	56	67	64	83
		48 h	42	65	60	78
	Pelargonidin	24 h	81 µM	81 µM	81 µM	83 µM
		48 h	69 µM	77 µM	74 µM	82 µM

Table 5.3: IC₅₀ values of compounds found in PJ in CCRF-CEM, MOLT-3, HL-60, and THP-1 leukaemia cells following 24 and 48 h treatments. NR= IC₅₀ not reached.

5.4.3 Anti-proliferative effect of Pomegranate Compounds in Non-Tumour CD133+ HSCs

The 7 compounds that were found to cause 50% reduction in ATP in the four studied leukaemia cell lines were tested on the non-tumour CD133 + HSCs. Those compounds selected for analysis were delphinidin, cyanidin, pelargonidin, gallic acid, quercetin, EGCG, and punicalagin.

The non-tumour CD133⁺ cells less sensitive than the majority of leukaemia cell lines at all treatment doses at following 24 and 48 h (Figure 5.27). The exception was THP-1 cells when treated with gallic acid. Following 24 h treatment with gallic acid treatment at 100 µM 34% and 40% decrease in ATP levels was observed in THP-1 and CD133⁺ cells respectively. Following 48 h, gallic acid showed 40% and 52% inhibition in cell proliferation in THP-1 and CD133 + HSCs cells (Figure 5.27)

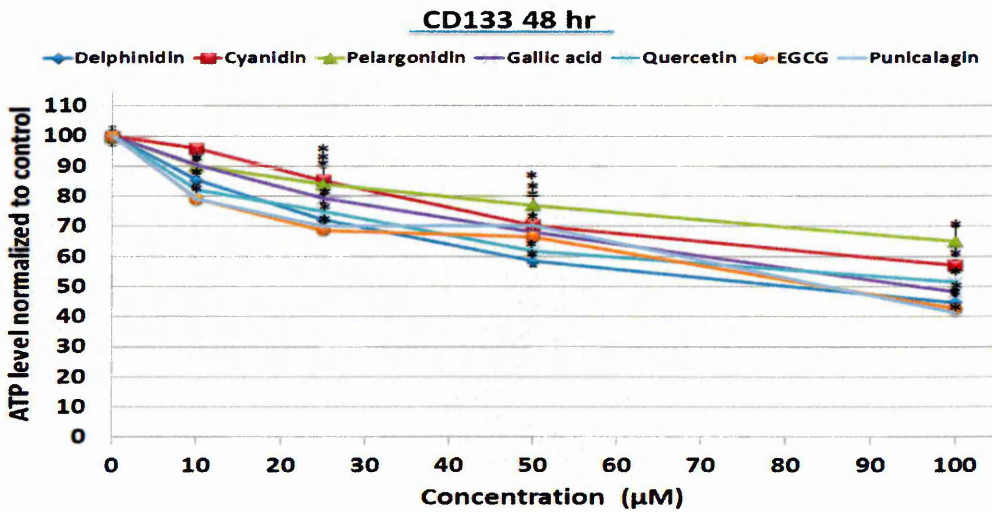
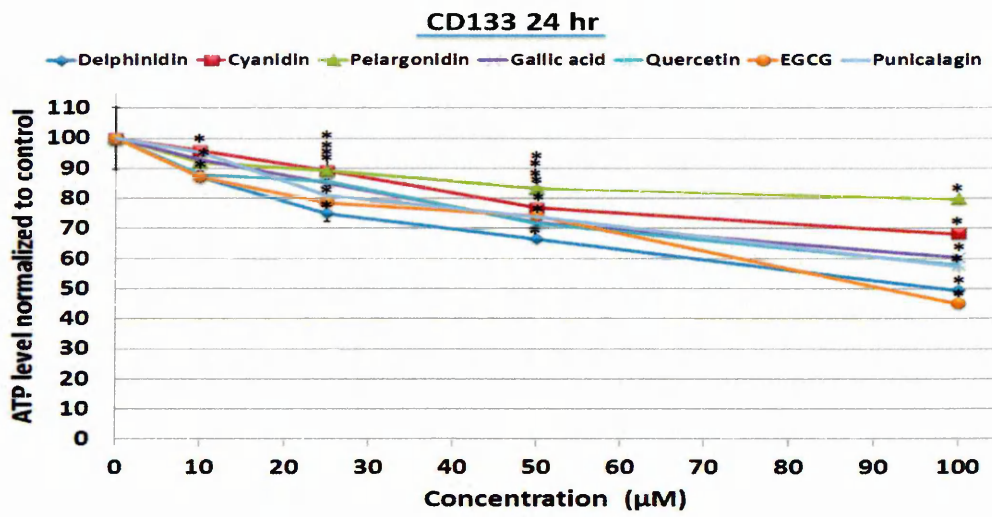


Figure 5.27: Effect of delphinidin, cyanidin, pelargonidin, gallic acid, quercetin, EGCG, and punicalagin on cell proliferation at concentrations 0, 10, 25, 50, and 100 µM in non-tumour HSC (CD133) following 24 and 48 h. ATP levels investigated using Cell Titer-Glo® Luminescent Cell Viability Assay to provide indication of live cell numbers. ATP levels normalized to controls and presented as means ± standard error. * indicates significant difference ($P \leq 0.05$) vs. untreated control. n = 3.

5.4 Discussion

The results demonstrated that 7 out of the 26 compounds found in PJ (Table 5.1): EGCG; ellagic acid; gallic acid; quercetin; delphinidin; cyanidin; pelargonidin; and punicalagin; caused a 50% reduction in ATP in leukaemia cell lines (CCRF-CEM, MOLT-3, HL-60, and THP-1). All the Organic acids, amino acids, and indoleamines compounds failed to cause a 50% reduction in ATP levels in the four leukaemia cell lines, following 24 and 48 h treatments. Suggesting that these compounds are inactive compounds and would not be of use in the treatment of leukaemia, and as such are not discussed further.

5.4.1 Phenolic Acids

The phenolic acids present in PJ are divided into two major groups: hydroxycinnamic acids and hydroxybenzoic acid, based on arrangement of the benzene ring, benzoic acids and cinnamic acids groups (Kim *et al*, 2006). These are classified as hydroxycinnamic acids including: caffeic acid and *p*-cumaric acid and hydroxybenzoic acids, which include: ellagic and gallic acids. Despite the hydroxycinnamic acid: caffeic acid, exhibiting inhibitory effects in CCRF-CEM cells, with IC₅₀ value 68 and 64 μ M following 24 and 48 h treatments, respectively. It failed to display 50% decrease in ATP levels in MOLT-3, HL-60, and THP-1 cells. Indicating that caffeic acid showed selective inhibition of ATP levels against leukaemia cell lines. This agrees with the work of Hudson *et al*. (2000) who showed the anti-proliferative effect of caffeic acid in breast cancer cell lines (MCF-7, MDA-MB-468, and HBL-100). They showed that there was a decrease in cell proliferation in MCF-7 and MDA-MB-468 cells, but not in HBL-100 cells. Other hydroxycinnamic acids such as *p*-cumaric have also failed to show an inhibition of cell proliferation in breast (MCF-7, MDA-MB-468, and HBL-100) (Hudson *et al*, 2009), colon (SW-480 and HT-29) (Hudson *et al*, 2009), and hepatoma cell lines (Yagazaki *et al*, 2000), which support our findings that the hydroxycinnamic acids are selective towards certain cancerous cell lines.

The hydroxybenzoic acids were more effective, inhibiting ATP levels in all four leukaemia cell lines to a greater extent than hydroxycinnamic acids. This has been seen in previous studies (Lapidot *et al*, 2002; Guang-Jian *et al*, 2012). Gallic acid was shown to cause a 50% reduction in ATP levels in all leukaemia cell lines, except THP-1. Generally THP-1 was the least sensitive cell line compared to other leukemic cells

when tested against PJ (Chapter 3) (Dahlawi *et al*, 2011), and the acetonitrile fraction (Chapter 4) (Dahlawi *et al*, 2013) and most of the pure PJ compounds investigated here. Gallic acid is widely used as an antioxidant in the food industry and was shown to exhibit a variety of pharmacological and biological activities, including anti-cancer properties. Previous work by Reddy *et al*. (2012) showed that gallic acid inhibited cell growth in the breast cancer cell line (MDA-MB-231), CML cell line (K562), and colon cancer cell line (COLO-205). The anti-cancer effect of gallic acid has also been demonstrated in two lung cancer cells (Calu-6 and A549), where gallic acid dose-dependently decreased the growth of Calu-6 and A549 cells following 24 h treatment (Park and You, 2010). In addition to gallic acid, ellagic acid was expressed in the acetonitrile fraction from PJ (Chapter 4) (Dahlawi *et al*, 2013), and here gallic acid significantly inhibited ATP following 24 and 48 h treatments. Mertens-Talcott *et al*. (2003) reported that treatment with ellagic acid resulted in a reduction of cell proliferation in the leukaemia cell line: MOLT-4. The anti-proliferative effect of ellagic acid was shown in several cancers cell lines including pancreatic (MIA PaCa-2; PANC-1; SW460 and SW620) (Seeram *et al*, 2005), prostate (RWPE-1; 22Rv1, DU-145, and PC3) (Seeram *et al*, 2005; Lansky (1) *et al*, 2005) and colon (HT-29 and HCT116) (Seeram *et al*, 2005) cells.

5.4.2 Flavan-3-ols

Flavan-3-ol compounds found in PJ were tested for their effect on viable cell number by measuring ATP levels of CCRF-CEM, MOLT-3, and HL-60 cell lines. Differential effects were seen where EGCG showed the most potent effects over catechin and epicatechin. Although catechin and epicatechin illustrated significant inhibitory effect on cell proliferation, they failed to induce a 50% decrease in ATP levels following 24 and 48 h treatments. Suggesting that the number of hydroxyl groups on the B ring and galloyl groups could be critical for EGCG inhibitory effects. Consistent with our results, Guang-Jian *et al* (2012) reported that EGCG has more potent anti-proliferative effect than catechin and epicatechin in two colorectal cancer cells (HCT-16 and SW-480). Similarly Yang *et al* (1998) indicated that EGCG inhibited growth of the lung cancer cell line (H441) and colon cancer cell line (HT-29), whilst epicatechin and catechin were less effective. Chung *et al* (2001) also showed that epicatechin had limited effects on prostate cancer cells (DU145) while EGCG demonstrated significant growth

suppression. However, EGCG has been shown to be the most abundant and bioactive Flavan-3-ol compounds in green tea for cancer chemoprevention (Stuart *et al*, 2006). EGCG has been shown to induce inhibition of cell growth in breast cancer cells (MDA-MB-231) (Thangapazham *et al*, 2007) and (MCF-7) (Tang *et al*, 2006) and prostate cancer cells (LnCap) (Hastak *et al*, 2005). In leukaemia, a study demonstrated a reduction in U937 and K562 cell number in response to treatment with EGCG (Nakazato *et al*, 2007).

5.4.3 Flavanoids

Quercetin and rutin belong to a class of polyphenolic flavanoid compounds. Both compounds are structurally similar; quercetin is termed the aglycone form of rutin. In rutin the hydrogen of the R-3 hydroxyl group is replaced by a disaccharide. Here, quercetin significantly inhibited ATP levels in all four leukaemia cell lines displaying 50% decrease in ATP levels. Interestingly, this study showed that quercetin has more potent inhibition in ATP levels in THP-1 cells with an IC₅₀ value of 23 µM which was lower than other the cell lines: CCRF-CEM, MOLT-3, and HL-60, with IC₅₀ values 25, 50, and 43 µM, respectively. This contradicts the sensitivity order seen following whole PJ, and fractions studied previously (Chapter 3 and 4) (Dahlawi *et al*, 2011; Dahlawi *et al*, 2013) suggesting quercetin is less likely to be the major compounds from PJ. Quercetin exerts anti-proliferative effects *in vitro* on cancer cell lines of diverse lineages, including breast cancer cells; MCF-7 (Chou *et al*, 2010; Choi *et al*, 2001), MDA-MB-231 (Chien *et al*, 2009; Jeong *et al*, 2009), SK-Br³ (Jeong *et al*, 2009), and MDA-MB-453 (Jeong *et al*, 2009), colon cancer cells: HT29 (Kim *et al*, 2005) and Caco-2 (Van Erk *et al*, 2004), and prostate cancer cells: PC-3 (Vijayababu *et al*, 2005; Aalinkeel *et al*, 2008); DU-145 and LNCap (Aalinkeel *et al*, 2008). In leukaemia cells quercetin has also been shown to inhibit cellular proliferation in cell lines including: K562, Jurkat, HL-60, U937, K562 (Kawahara *et al*, 2009; Mahbub *et al*, 2013), and MOLT-4 (Mertens-Talcott *et al*, 2003). Here, Rutin, a glycoside of quercetin, inhibited ATP levels in CCRF-CEM, MOLT-3, and HL-60 following 48 h treatment, but failed to display 50% decrease in ATP in all four leukaemia cell lines. Suggesting the sugar molecule may suppress the inhibitory effect of flavonoids toward leukaemia cell lines tested. Similarly, Kim *et al* (2005) reported that only quercetin was effective in inhibiting growth of colon cancer cells (HT-29) growth, but the glycoside rutin did not inhibit HT-29 cell growth. Kunts *et al*,

(1999) determined the growth inhibitory activity of various flavonoids, including quercetin and rutin, in two colon cancer cells (HT-29 and Caco-2) after 27 h of exposure to concentrations between 25 μM to 250 μM . Both quercetin and rutin inhibited the growth of intestinal cell lines. The IC_{50} values of quercetin for HT-29 and Caco-2 were 85 and 96 μM , respectively. Whereas, the IC_{50} value of rutin for HT-29 and Caco-2 were approximately 136 μM in both cell lines, indicating that quercetin has stronger inhibitory effect than rutin. Kim *et al*, (2005) also reported that quercetin was only effective in inhibiting growth of colon cancer cells (HT-29), but the glycoside rutin did not inhibit HT-29 cell growth. Lu *et al*, (2008) found that quercetin, not rutin, inhibited growth of human ovarian cancer cell line (OVAR-3).

5.4.4 Ellagitannins

Punicalagin is unique to pomegranate and is part of a family of ellagitannins (Tyagi *et al*, 2012). Punicalagin, which is the largest polyphenol, having a molecular weight of 1084, is reported to be the major component responsible for PJ antioxidant properties (Gil *et al*, 2000). Punicalagin was evaluated for its anti-proliferative activity against colon cancer cells (SW460, SW620, HT-29, and HCT116) and prostate cancer cells (RWPE-1 and 22Rv1), demonstrating inhibition of cell proliferation in a dose-dependent manner in all cell lines tested (Saleem *et al*, 2002). Here, punicalagin showed induction in inhibition of ATP levels in all four leukaemia cell lines (CCRF-CEM, MOLT-3, HL-60, and THP-1) following 24 and 48 h. Punicalagin was one of the most abundant compounds indicated in the effective fraction (acetonitrile fraction) showing a decrease in cell proliferation and induction of apoptosis against leukaemia cell lines (CCRF-CEM, MOLT-3, HL-60, and THP-1) (Dahlawi *et al*, 2013) (Chapter 3). Thus suggesting that punicalagin may play an important role in the efficacy of PJ toward leukaemia cells.

5.4.5 Anthocyanins

Anthocyanins are one of the groups of compounds which were detected in the acetonitrile fraction (Dahlawi *et al*, 2013) (Chapter 3). Anthocyanins are considered the largest and most important group of flavonoids present in PJ, which give the juice its red colour (Lansky and Newman, 2006; Afaq *et al*, 2005). Studies have proposed that anthocyanins are the major phytochemical group responsible for the observed anti-cancerous effects. Anthocyanins in the form of rich-extracts from fruits and vegetables have shown anti-proliferative activity toward various cancer cell types *in*

vitro. (Rodrigo *et al*, 2006; Seeram *et al*, 2006; Chen *et al*, 2005; Reddy *et al*, 2005 Zhang *et al*, 2008). Pure anthocyanins were also tested for inhibition towards the growth of cancer cell lines. Katsube *et al* (2003) found that delphinidin, cyanidin, and pelargonidin showed anti-proliferative effects in human colon cancer cells (HCT116). Cyanidin and delphinidin showed concentration-dependent growth inhibition in human hepatoma cells (HepG₂). The estimated IC₅₀ values of cyanidin and delphinidin were 18.4 and 10.8 μM, respectively (Yeh and Yen, 2005). Anthocyanins, delphinidin 3-O-β-D-glucoside and cyanidin 3-O-β-D-glucoside, from black bean seed coat and red grape skin, respectively, displayed strong inhibitory effect against human leukaemia cells (MOLT-4) (Katsuba *et al*, 2003). Here, we found that delphinidin, cyanidin and pelargonidin induced 50% inhibition in ATP levels in all four leukaemia cell lines (CCRF-CEM, MOLT-3, HL-60, and THP-1) following 24 and 48 h treatments. Delphinidin exerted the greatest inhibition among cyanidin and pelargonidin on all leukaemia cell lines, suggesting that anthocyanins appear to be affected by their chemical structures.

5.4.6 Tumour Cell Selectively

This study investigated the effects of pure compounds found in pomegranate on ATP levels in leukaemic cells. ATP levels were used as an indication of total viable cells and thus compounds resulting in decreased ATP levels could indicate agents which could either inhibit proliferation or induce cell death or both within leukaemia cell lines. Demonstrating that delphinidin, cyanidin, pelargonidin, gallic acid, quercetin, and punicalagin illustrated bioactivity against four leukaemia cell lines (CCRF-CEM, MOLT-3, HL-60, and THP-1). Interestingly, less bioactivity was observed in non-tumour cells (CD133) when treated with concentrations showing significant cytotoxicity in tumour cells, suggesting a selective cytotoxicity against leukaemia cells. Selective inhibition of proliferation in carcinoma cells of anthocyanins has been shown previously (Zhao *et al*, 2004; Ozbay and Nahta, 2011). Several studies have shown that inhibition of cell proliferation by anthocyanins or anthocyanins-rich extracts was more pronounced in carcinoma cells than non-tumour cells. Zhao *et al*. (2004) found that anthocyanin extracts inhibited the growth of colon cancer cells (HT-29) with little effects on normal colonic cell growth when added to the media in the same concentrations. In another study, although, cyanidin-3-O-β-glucopyranoside decreased cell proliferation in both transformed (Jurkat cells) and non-transformed (human lymphocytes) T cells, normal T

cells were much less sensitive to this effect than non-transformed cells. Ozbay and Nahta (2011) examined cell proliferation in response to delphinidin in 7 breast cancer cell lines (HCC1806, MDA231, MDA468, SKBR3, MDA453, BT474, and MCF-7) in addition to non-transformed breast epithelial cell line (MCF10A). In contrast to the majority of breast cancer cell lines, proliferation of non-transformed breast epithelial cell line (MCF10A) was not significantly inhibited by delphinidin except at the highest concentration. Gallic acid has been shown to inhibit the proliferation of pancreatic cancer cells (CFPAC-1 and MiaPaca-2) in a time and dose-dependent manner. Remarkably, when compared with normal human cells HL-7702, gallic acid exhibited selective cytotoxicity for cancer cells (Liu Z *et al*, 2012). Polyphenolic compounds in green tea, including EGCG, have been widely studied since they showed selective cytotoxicity to cancerous cells and not to normal cells. Ahmed *et al*, 1997 reported that delphinidin significantly decreased cell viability of human epidermal carcinoma cell line (A431) with little toxicity to normal human epidermal keratinocytes (NHEKs). The flavonoid quercetin exhibited selective toxicity, since it has been shown that quercetin significantly inhibited the growth of highly aggressive PC-3 cell line and the moderately aggressive DU-145 prostate cancer cell line, but did not affect the less aggressive LNCap prostate cancer cell or normal BG-9 fibroblast cell line (Nair *et al*, 2004). Together these studies and the findings of this study suggest natural polyphenols display selective targeting towards tumour cell lines over normal cells and thus may provide better selective therapies for cancers.

5.5 Conclusion

Among the 26 naturally occurring pomegranate compounds investigated, only seven compounds: delphinidin; cyanidin; pelargonidin; EGCG; gallic acid; ellagic acid; quercetin; and punicalagin; induced 50% decrease in ATP levels in the studied leukaemia cell lines. Of these active components only gallic acid and quercetin were not found previously in the acetonitrile fraction of PJ when analysed by MS analysis, which was shown to induce apoptosis in the studied leukaemia cell lines (Chapter 4) (Dahlawi *et al*, 2013). Future work will investigate the effect of these active components on leukaemia cell lines to investigate the ability to induce apoptosis and cell cycle arrest and indicate potential activities on inhibition of proliferation or induction of cell death.

6. Impact of Anthocyanins Chemical Structure on Induction of apoptosis and Inhibition of cell Proliferation in Leukameia cell lines

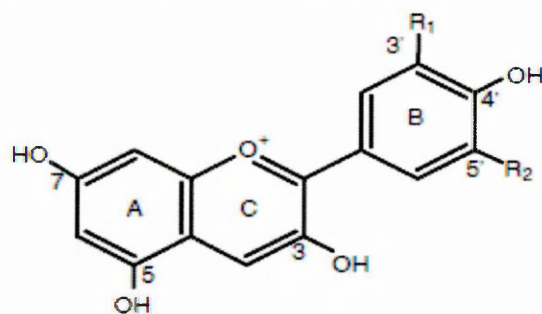
6.1 Introduction

Previously it was identified that the anthocyanins are one of most potent compounds at decreasing ATP levels in leukaemia cells.

6.1.1 Chemistry of Anthocyanins

Anthocyanins (in Greek *anthos* means flower, and *kyanos* means blue), are the largest group of water-soluble pigments in the plant kingdom (Kong *et al*, 2003). They belong to the class of flavonoid compounds and are commonly known as plant polyphenols (Kong *et al*, 2003). In contrast to other flavonoids, the anthocyanins carry a positive charge in acidic solutions (Mazza, 1995). Major sources of anthocyanins are pomegranate, berries and other fruits and the anthocyanins give them their red, blue or purple colours. Colour differences between anthocyanins are mainly determined by substitution pattern of the B ring of the glycon, the pattern of the glycosylation, and the degree and nature of esterification of the sugars with aliphatic or aromatic acids, and the presence of co-pigments (Mazza and Brouillard, 1990). One distinctive characteristic of anthocyanins is that they undergo reversible molecular transformations with changes in pH. Many anthocyanins are red in very acidic conditions and turn blue as the pH is increased (Mazza and Miniati, 1993).

The glycon or de-glycosylated forms of anthocyanins are known as anthocyanidins. Anthocyanidins are polyhydroxy and polymethoxy derivatives of 2-phenylbenzopyrylium or flavylium salts differ in the number and position of their hydroxyl and methoxyl groups on the B ring (Figure 6.1). There are 27 known anthocyanidins present in nature (Harborne and Williams, 2001), the six most common anthocyanidins are cyanidin, pelargonidin, delphinidin, malvidin, pentunidin, and peonidin (Harborne and Williams, 2001; Kong *et al*, 2003).



Anthocyanidins	R ₁	R ₂
Pelargonidin	H	H
Cyanidin	OH	H
Delphinidin	OH	OH
Peonidin	OCH ₃	H
Petunidin	OCH ₃	OH
Malvinidin	OCH ₃	OCH ₃

Figure 6.1: Basic chemical structure of common anthocyanidins.

The glycosides of the three non-methylated anthocyanidins (cyanidin, delphinidin, and pelargonidin) are the most widespread in nature being present in 80% of pigmented leaves, 69% of fruits and 50% of flowers (Kong *et al*, 2003) and were identified within Acetonitrile fraction of PJ (Chapter 4) (Dahlawi *et al*, 2013). The distribution of the six most common anthocyanidins in edible parts of plants are summarised in table 6.2.

Anthocyanidins rarely occur in their free form in nature because of their high reactivity, but are normally glycosylated with one or more sugar components which enhance their stability and solubility (Clifford, 2000; Giusti and Wrolstad, 2003). The most common sugar components which link to the anthocyanins are glucose, galactose, rhamnose, xylose, and arabinose (Kong *et al*, 2003). Anthocyanins can be glycosylated with one or more sugar units, typically up to 3, with some rare exceptions (Kong *et al*, 2003). The sugar components of anthocyanins are usually conjugated to the C3-hydroxyl group in the anthocyanidins C ring and C5 position of the A ring. Less common sites of glycosylations are the C7 position, and in rare cases glycosylation has been reported on the B ring (Kong *et al*, 2003). Several hundred anthocyanin structures are known to varying in: the basic anthocyanidin structure; the number of hydroxyl groups; the nature and the number of sugars attached to the molecule; the position of

this attachment; and the nature and number of aliphatic or aromatic acids attached to the sugars in the molecule. However, the most predominant anthocyanin is cyanidin-3-glucoside (Figure 6.1) (Mazza and Miniati, 1993).

Anthocyanidins	Percentage of abundance
Cyanidin	50%
Delphinidin	12%
Pelargonidin	12%
Petunidin	12%
Peonidin	7%
Malvinidin	7%

Table 6.1: Illustrates distribution of the six most common anthocyanidins in edible parts of plants (Kong *et al*, 2003).

6.1.2 Anthocyanins Found in Pomegranate Juice

Pomegranate juice is known to be a major source of phenolic compounds, where anthocyanins are thought to be the most important. The main anthocyanins found in the acetonitrile fraction (Chapter 4) and found in other studies are: Cyanidin-3-glucoside; cyanidin 3,5-*O*-diglucosides; delphinidin-3-glucoside; delphinidin-3,5-*O*-diglucosides; pelargonidin-3-glucoside and pelargonidin-3,5-*O*-diglucosides (Hernandez *et al*, 1999; Reed *et al*, 2005). Delphinidin has hydroxyl groups at 3', 4', and 5', cyanidin at 3' and 4' positions in the B-ring. However, pelargonidin has no orthohydroxyl substitution (Figure 6.1).

6.1.3 Anthocyanins Bioactivity

In recent years a number of studies have shown that anthocyanins exhibited a wide range of biological and pharmacological benefits such as anti-inflammatory (Wang and Mazza, 2002; Youdim *et al*, 2002), anti-microbial (Pisha and Pezzuto, 1994) and improvement of vision (Matsumoto *et al*, 2003) and neuroprotective effects (Youdim *et al*, 2002). In addition, anthocyanins have exhibited a variety of effect on cells, blood vessels (Andriambelson *et al*, 1998; Martin *et al*, 2003) and platelets that may reduce the risk of coronary heart disease (Renaud & Lorgeil 1992). They have also been found to act as antioxidants, in colon (Renis *et al*, 2008), breast (Olsson *et al*, 2004; Singletary *et al*, 2007), liver (Shish *et al*, 2007), leukaemic (Dai *et al*, 2009) and brain cell lines *in vitro* (Hogan *et al*, 2010). In these culture systems, anthocyanins have shown multiple

anti-toxic and anti-carcinogenic effects, and directly scavenged reactive oxygen species (ROS) (Singletary *et al*, 2007). Some studies reported that the glycosidic forms show a decrease in the antioxidant capacity when compared with the corresponding aglycon (Rice-Evans *et al*, 1996; Satue-Gracia *et al*, 1997; Tsuda *et al*, 1994).

Pure anthocyanins and anthocyanidins, or in the form of mixtures have demonstrated anti-proliferative and anti-apoptotic effects in breast, colon, oesophageal, uterus and prostate cancer cells (Table 6.2). Studies in human leukaemia cells have also shown they had a pro-apoptotic and anti-proliferative activity (Table 6.2). This has been confirmed in a number of animal models (Kang *et al*, 2003; Chen *et al*, 2005; Stoner *et al*, 2007).

Cell line	Substance	Mechanism	References
Prostate cancer			
Androgen refractory human PCa 22Rnu1 cells	Delphinidin	-Inhibit cell proliferation -G ₂ /M phase cell cycle arrest -cleaved Poly(ADP-ribose) polymerase; increased Bax and Bcl-2 expression; increased caspase-3 and caspase-9 activity, NF k B signalling	Hafeez <i>et al</i> (2008b)
Human PC3 cells	Delphinidin	-Inhibit cell growth -G ₂ /M phase cell cycle arrest Induced apoptosis (Phosphatidylserine exposure), cleaved poly(ADPribose) polymerase, increased Bax and decreased Bcl-2 expression, increased caspase-3 and caspase-9 activity, NF k B signalling	Hafeez <i>et al</i> (2008a)
Human androgen-dependent LNCaP cells and PC-3 cells	Anthocyanin fraction from Potatoes	- Inhibit cell growth - DNA fragmentation, cleaved poly(ADP-ribose) polymerase, cleaved caspase-3 and cleaved caspase-9 proteins and increased Bax expression,	Reddivari, <i>et al</i> (2007)
Uterus cancer			
Human HeLa S3 cells	Delphinidin	- Decreased cell viability - S phase cell cycle arrest - DNA fragmentation, phosphatidylserine exposure, mitochondrial membrane potential, poly(ADP-ribose) polymerase cleavage.	Lazze, <i>et al</i> (2004)
Esophageal cancer cells			
Rat highly tumorigenic RE-149 DHD cells	Freeze-dried black raspberries Cyanidin-3-O-rutinoside	- Inhibited cell proliferation - Caspase-3 and caspase-7 activity	Zikri, <i>et al</i> (2009)

Table (continued)			
Hepatic cancer cells			
Human hepatocellular carcinoma PLC/PRF/5 cells	Anthocyanins from the berries	- decreased cell viability -DNA fragmentation, Bcl-2 expression, Bax translocation, caspase-3 activity, cytochrome c release	Longo, et al (2008)
Human HepG2 cells	Cyanidin, delphinidin, malvidin	- Inhibited cell proliferation -DNA fragmentation and caspase-3 activity.	Yeh and Yen (2005)
Human hepatoma Hep3B	Anthocyanins extracts	- Inhibited cell proliferation - G ₀ /G ₁ phase cell cycle arrest -Induced apoptosis and decreased anti-apoptotic proteins (Bcl-2, XIAP, cIAP-1, and cIAP-2	
Mammary cancer cells			
Hormone-responsive human MCF-7 cells	Bilberry extract	- Inhibited cell proliferation - G ₂ /M phase cell cycle arrest - DNA fragmentation	Nguyen, et al (2010)
Rat mammary carcinoma cells from imethylbenz[a]anthracene-induced tumours in female c-Ha- ras transgenic rats	Cyanidin 3-O b-d -glucoside	- Inhibited cell viability - DNA fragmentation, increased caspase-3 cleavage.	Fukamachi, et al (2008)
Human estrogen dependent/ aromatase positive MCF-7 and cells and MDAMB-231 cells	Freeze-dried Jamun (<i>Eugenia jambolana</i>) fruit extract	- Inhibited cell proliferation - DNA fragmentation	Li, et al (2009).
Human EGFR positive AU-565 cells	Delphinidin	- Inhibited cell viability - DNA fragmentation, phosphatidylserine exposure, cleaved poly(ADP-ribose) polymerase, increased expression of Bax and down regulation of Bcl-2 expression, increased caspase-3 activity	Afaq, et al (2008).
Human HS578T cells	Cyanidin -3- glucoside, Peonidin 3- glucoside	- Inhibited cell viability - G ₂ /M phase cell cycle arrest. - Induced apoptosis, caspase-3 activity, cleaved poly (ADP-ribose) polymerase.	Chen, et al (2005).
Leukaemia cells			
Human promyelocytic HL-60 cells	Isolated anthocyanins from <i>Euterpe oleracea</i> Mart	- Decreased cell viability - increased caspase-3 activity	Del Pozo-Insfran, et al (2007)
Human promyelocytic HL-60 cells Human acute leukaemia T Jurkat cells	Cyanidin 3-O- b - glucopyranoside	- Induced apoptosis	Fimognari et al. (2004)

Table (continued)			
Human promyelocytic HL-60 cells	Delphinidin 3-sambubioside	- Inhibited cell proliferation -Induced apoptosis, increased caspase-3, caspase-8 and caspase-9 activity; induced mitochondrial membrane potential, cytochrome crelease, Bid truncation.	Hou <i>et al</i> (2005)
Human promyelocytic HL-60 cells	Bilberry extract, malvidin, delphinidin, cyaniding	- Induced apoptosis	Katsube <i>et al</i> (2003).
Human acute leukaemia T MOLT-4 cells Human Burkitt lymphoma Daudi cells Human T leukaemia CCRF-CEM cells	Cyanidin-3-rutinoside	- Induced apoptosis	feng <i>et al</i> (2007).
Human acute leukaemia T MOLT-4 cells	Delphinidin 3-O- β -D-glucoside petunidin 3-O- β -D-glucoside, malvidin 3-O- β -D-glucoside, cyanidin 3-O- β -D-glucoside	- Inhibited cell growth. - Induced apoptosis	Katsuzaki <i>et al</i> (2003)
Human U937 cells	Anthocyanins isolated from <i>Vitis coignetiae</i>	- Inhibited cell proliferation - Induced mitochondrial membrane potential; down-regulated of Bcl-2 expression and up regulated of Bax expression; increased caspase-3, caspase-8 and caspase-9 activity; inhibitor of apoptosis protein (IAP) activity; cleaved poly(ADP-ribose) polymerase; and induced truncated Bid translocation	Lee <i>et al</i> (2009).
Human U937 cells	Cyanidin, malvidin	- inhibited cell proliferation - G ₂ /M phase cell cycle arrest - Induced apoptosis.	Hyun and Chung (2004).
Colon cancer cells			
Human adenocarcinoma Caco-2 cells	Cabernet Sauvignon anthocyanin extract	- Inhibited cell proliferation - Increased Caspase-3 activity	Forester and Waterhouse (2010).
Human adenocarcinoma Caco-2 cells	Grape extract, anthocyanin fraction from grape extract	- Inhibited cell proliferation - Induced apoptosis	Yi (1) <i>et al</i> (2005)a
Human adenocarcinoma Caco-2 cells HT-29 cells	Anthocyanin fraction from blueberry extract	- Inhibited cell proliferation - Induced apoptosis	Yi (2) <i>et al</i> (2005) b
Human HCT-116 cells	Delphinidin	- Decreased cell viability - G ₂ /M phase cell cycle arrest - Induced apoptosis, cleavage of PARP, activation of caspases-3, -8, and -9, increase in	Yun <i>et al</i> (2009)

Table (continued)			
Human adenocarcinoma HT-29 cells	Anthocyanin fraction from Georgia-grown blueberries	- Induced apoptosis and increased caspase-3 activity	Srivastava <i>et al</i> (2007)
Gastric cells			
Human adenocarcinoma AGS cells	Malvinidin	- Inhibited cell proliferation	Shih <i>et al</i> (2005).

Table 6.2: Impact of anthocyanins in different cancer models in term of induction of apoptosis inhibition of cell proliferation and cell cycle

6.2 Objective

The aim of this study was to compare the effective properties of anthocyanins found in PJ to understand the relationship between anthocyanin chemical structures and their effects on inhibition of cell proliferation and induction of apoptosis in leukaemia cell lines.

6.3 Material and Methods

6.3.1 Cell Culture

Four leukaemia cell lines were obtained from the American Type Culture Collection (ATCC; Middlesex, U.K.), which previously demonstrated differing sensitivities to PJ (Chapter 3) (Dahlawi *et al*, 2011) and the acetonitrile fraction of PJ (chapter 4) (Dahlawi *et al*, 2013). Two lymphoid cell lines: CCRF-CEM, and MOLT-3, and two myeloid cell lines: HL-60 and THP-1 were included in this study. Cell lines were maintained and cultured in RPMI 1640 medium (Invitrogen, Paisley, U.K.) supplemented with 10% (v/v) foetal bovine serum, 1.5 mmol/L L-glutamine, and 100 µg/mL penicillin/streptomycin (complete media) in a humidified atmosphere of 5% CO₂ at 37°C (Section 2.2).

6.3.2 Treatment of Cells

Cell lines were treated with: Cyanidin; cyanidin 3-glucoside; cyanidin 3,5-diglucosides; delphinidin; delphinidin 3-glucoside; delphinidin 3,5-diglucosides; pelargonidin; pelargonidin 3-glucoside and pelargonidin 3,5-diglucosides at concentrations between 0 - 100 µM for 24 h. All compounds were purchased from Extrasynthese and were dissolved in 100% methanol. Following treatments, induction of apoptosis and cell

cycle arrest was determined and mechanisms of apoptosis induction by delphinidin investigated (Table 6.3).

Techniques	Treatment	Concentration	Cell lines	Time point
Cell Titer-Glo[®] Luminescent Cell Viability Assay	Cyanidin; cyanidin 3-glucoside; cyanidin 3,5-diglucosides; delphinidin; delphinidin 3-glucoside; delphinidin 3,5-diglucosides; pelargonidin; pelargonidin 3-glucoside and pelargonidin 3,5-diglucosides	0, 10, 25, 50, and 100 μ M	CCRF-CEM, MOLT-3, HL-60, and THP-1	24 hr
Annexin V-FITC/PI	Cyanidin; cyanidin 3-glucoside; cyanidin 3,5-diglucosides; delphinidin; delphinidin 3-glucoside; delphinidin 3,5-diglucosides; pelargonidin; pelargonidin 3-glucoside and pelargonidin 3,5-diglucosides	0, 10, 25, 50, 75, and 100 μ M	CCRF-CEM, MOLT-3, HL-60, and THP-1	24 hr
NucView[™] 488 Caspase-3 substrate assay	Cyanidin; cyanidin 3-glucoside; cyanidin 3,5-diglucosides; delphinidin; delphinidin 3-glucoside; delphinidin 3,5-diglucosides; pelargonidin; pelargonidin 3-glucoside and pelargonidin 3,5-diglucosides	0, 10, 25, 50, 75, and 100 μ M	CCRF-CEM, MOLT-3, HL-60, and THP-1	24 hr
DAPI staining	Delphinidin	0, 25, 50, 100 μ M	CCRF-CEM, MOLT-3, HL-60, and THP-1	24 hr
Cell cycle	Delphinidin	0, 25, 50, 100 μ M	CCRF-CEM, MOLT-3, HL-60, and THP-1	24 hr
The Caspase-8 and 9 Glo[™] Assays	Delphinidin	50 μ M	MOLT-3 and HL-60	3, 6, and 24 hr
ICC (Cytochrome C and SMAC/ Diablo)	Delphinidin	50 μ M	MOLT-3 and HL-60	3, 6, and 24 hr
qRT-PCR (Bax, Bad, Bcl-2, and Bcl-xl)	Delphinidin	50 μ M	MOLT-3 and HL-60	6 hr

Table 6.3: Experimental design for chapter 6.

6.3.3 Cell Viability

The effect of cyanidin, cyanidin 3-glucooside, cyanidin 3,5-diglucosides, delphinidin, delphinidin 3-glucooside, delphinidin 3,5-diglucosides, pelargonidin, pelargonidin 3-glucooside and pelargonidin 3,5-diglucosides on cell viability was determined by the Cell Titer-Glo[®] Luminescent Cell Viability Assay as described previously (2.3.2). Cells were seeded at 25×10^4 cells in 100 μ L of complete media and treated with each compound at 0, 10, 25, 50, and 100 μ M, in white 96-well plates (Fisher Scientific) for 24 h.

6.3.4 Annexin V- FITC /PI Flow Cytometry Assay

Annexin V-FITC/PI and flow cytometry were used to detect levels of apoptosis as described previously (section 2.4.1). Cells were seeded at 5×10^5 cells in 100 μ L of complete media and treated with cyanidin, cyanidin 3-glucooside, cyanidin 3,5-diglucosides, delphinidin, delphinidin 3-glucooside, delphinidin 3,5-diglucosides, pelargonidin, pelargonidin 3-glucooside and pelargonidin 3,5-diglucosides at concentration of 0, 10, 25, 50, 75, and 100 μ M in 12-well plate (Fisher Scientific) for 24 h. Data were recorded from 10,000 cells per sample and analyzed using FlowJo software (Tree Star).

6.3.5 Caspase-3 Activity

NucView[™] 488 Caspase-3 substrate assay (Cambridge Bioscience) and flow cytometry were used to determine induction of caspase-3 (Section 2.4.3). Cells were treated with cyanidin, delphinidin, and pelargonidin at concentrations of 0, 10, 25, 50, 75, and 100 μ M for 24 h. Data were recorded from 10,000 cells per sample and analyzed using FlowJo software (Tree Star, Ashland, OR).

6.3.6 DAPI Stain

Following treatment with delphinidin at concentrations of 0, 25, 50, 100 μ M for 24 h at a cell density of 5×10^4 per well, cells were stained with DAPI to observe apoptotic morphology changes (Section 2.4.2). Cells were investigated using Olympus BX60 fluorescence microscope using UV light at excitation wavelength 350 nm. Quantitative analysis of cell populations (live & apoptotic) was performed based on counting of 200

randomly-selected cells and the percentage of apoptotic features determined for each sample.

6.3.7 Cell Cycle

The cell cycle distribution of leukaemia cell lines was measured by flow cytometry in PI stained cells (Section 2.5). Cells were treated with delphinidin at concentrations 0, 25, 50, and 100 μM for 24 h. Data from 10,000 cells per sample were recorded and percentages of cells within G_0/G_1 , S, and G_2/M cell cycle phase were determined with FlowJo software and Waston (pragmatic) analysis of cell cycle (Tree Star).

6.3.8 Caspase-8 and -9

The Caspase-Glo™ Assays use the luminogenic caspase-8 tetrapeptide substrate (Z-LETD-aminoluciferin) or caspase-9 tetrapeptide substrate (Z-LEHD-aminoluciferin) and a stable luciferase in proprietary buffers. In the absence of active caspases, the caspase substrates do not produce light. Upon cleavage of the substrates by the respective caspases, aminoluciferin is liberated and can contribute to the generation of light in a luminescence reaction (Figure 6.2). The resulting luminescent signal is directly proportional to the amount of caspase activity present in the sample. Figure 6.2:

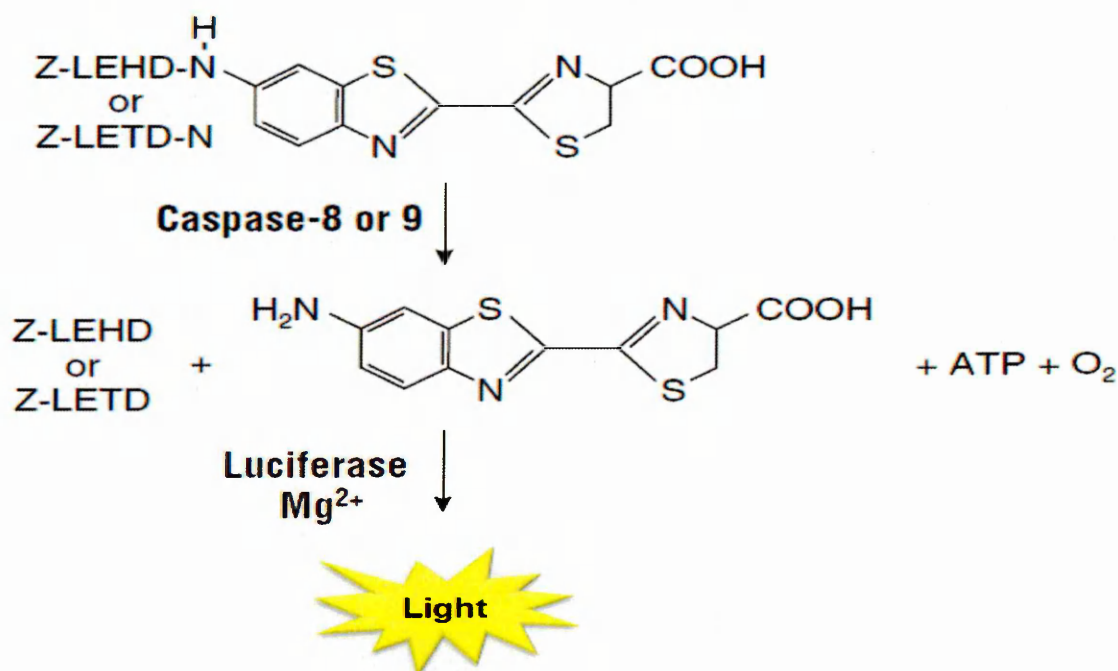


Figure 6.2: Caspase-8 or -9 cleavage of the pro-luminogenic substrates containing LETD or LEHD, respectively. Following caspase cleavage, a substrate for luciferase (aminoluciferin) is released, resulting in the luciferase reaction and production of light.

6.3.8.1 Methodology

Cells were plated at a cell density of 2.5×10^4 cells per well in a white 96 well culture plate and then treated with 50 μ M delphinidin for 3,6 and 24 h. Following treatment Caspase-8 and 9 activity was measured by using Caspase-Glo™ 8 and 9 assays as per manufactures industry. MG-132 (30 μ l) inhibitor was added to Caspase-Glo™ 8 and 9 reagents to reduce nonspecific background activity. One hundred microliters of Caspase-Glo™ 8 and 9 reagents were added to each sample, mixed well for 30 seconds on an orbital shaker at 400 rpm. The plate was allowed to incubate at room temperature for 1 h prior to luminescence detection using Wallac 1420 luminescence detector (PerkinElmer, Waltham, USA). Control wells were prepared containing medium and treatments without cells to obtain a value for background luminescence.

6.3.8.2 Analysis

Background readings were subtracted from all test measurements. The average luminescence readings were calculated and all treated samples were normalized to controls.

6.3.8.3 Statistical Analysis:

Average and Standard error of the mean (SEM) were calculated and Stats Direct was used to test whether data followed a normal distribution using a Shapiro Wilke test. Data did not follow a normal distribution, thus Kruskal-Wallis and Conover-Inman post hoc tests were used to investigate significant differences. Results were considered statistically significant when $P \leq 0.05$.

6.3.9 Immunocytochemistry

Immunocytochemistry (ICC) is a method used to identify the presence of a specific protein within cells by using a specific antibody, which binds to it and allows visualization and examination of the target protein under the light microscope. Here we used an indirect method for ICC (Figure 6.3) to detect the expression of cytochrome C and SMAC/Diablo using specific antibodies (Table 6.4).

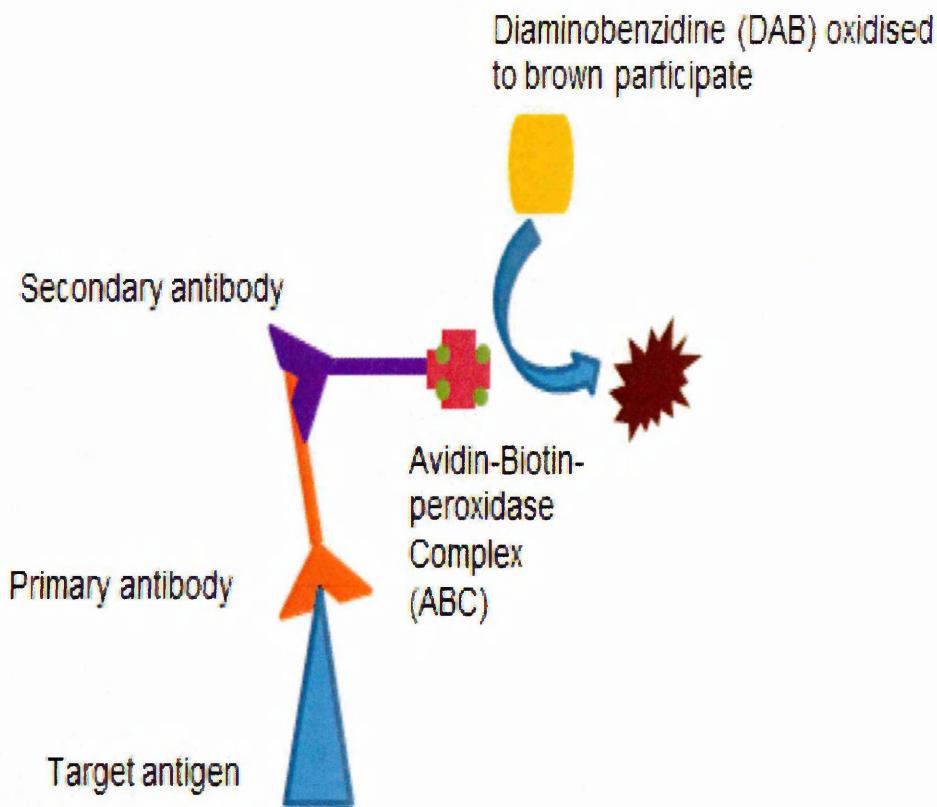


Figure 6.3: Illustration of the indirect method of immunocytochemistry.

	Description	Dilution	Species reactivity
Cytochrome C	mouse monoclonal	1: 200	Human (Abcam, ab13575)
SMAC/ Diablo	rabbit monoclonal	1: 100	human (Abcam ab32023)

Table 6.4: The source and dilution factors used for the primary antibodies.

6.3.9.1 Method

Following treatment of MOLT-3 and HL-60 cells with 50 μ M delphinidin, cells were incubated for 3, 6 and 24 h and cells were then transferred to eppendorf tubes and centrifuged for 5 minutes at 400 g at 4°C. The supernatant was removed, and cells washed in 100 μ l DPBS and resuspended in 100 μ l 4% (w/v) paraformaldehyde/DPBS and stored at 4°C for 20 minutes. Cells were then washed with DPBS and 40,000 cells / slide were transferred to slides via a 20 minute cytospin at 1000 rpm (Shandon Cytospin 3 Centrifuge) (Thermo Fisher Scientific). Samples were air dried and then washed in IMS for 5 minutes. To block any endogenous peroxidase activity within the cells, a hydrogen peroxidase (H_2O_2) block (containing 9 mL 30% H_2O_2 , 291 IMS and 5

drops of HCL) was applied for 30 minutes followed by 5 minutes wash in deionized water and two washes in 1X TBS (Tris Buffered Saline) (20 mM Tris base (Fisher Scientific) 150 mM NaCl (Fisher Scientific) pH 7.6) for 5 minutes. In a humid chamber, 100 µl of proteinase K (10 µg/mL) was applied to each slide to lightly digest the cellular membrane to retrieve the antigens. Slides were then washed in triplicate with 1X TBS for 5 minutes. The serum of the secondary antibodies at 25% v/v in 1% w/v BSA in PBS was freshly prepared and added to each slide and incubated for 45 minutes at RT. The primary antibodies (Table 6.4) were prepared with suitable serum species and 100 µl was added in a humid chamber and incubated overnight at 4°C.

Following overnight incubation, cytopins were washed with 1X TBS three times for 5 minutes and secondary antibodies (Table 6.5) were added and incubated for 30 minutes at RT followed by 5 minutes wash with 1X TBS in triplicate. A drop of Avidin-Biotin-peroxidase Complex (ABC) was added to each slide for 30 minutes in the wet box on the orbital shaker followed by 5 minutes wash in triplicate with 1X TBS. Then 3,3'-Diaminobenzidine (DAB) was added for 20 minutes at RT followed by 5 minutes washing in running tap water. Slides were counterstained in haematoxylin for 45 seconds then washed in running tap water for 5 minutes. Finally, cells were dehydrated in IMS and cleared in Sub-X prior to mounting in pertex.

	Description	Dilution	
Cytochrome C	rabbit anti-mouse	1: 400	Abcam (Ab 87032)
SMAC/ Diablo	goat anti-rabbit	1: 300	Abcam (Ab 97049)

Table 6.5: The source and dilution factors used for the secondary antibodies.

6.3.9.2 Analysis

Slides were examined using Olympus light microscope (X100). Images were captured using Q Capture Pro 8.0 (UVP BioImaging Systems). Quantitative analysis of cells (active and non-active) (Figure 6.4) was performed based on counting of 200 randomly selected cells and the percentage of cells with active staining determined for each sample (untreated control cells and cells treated with delphinidin).

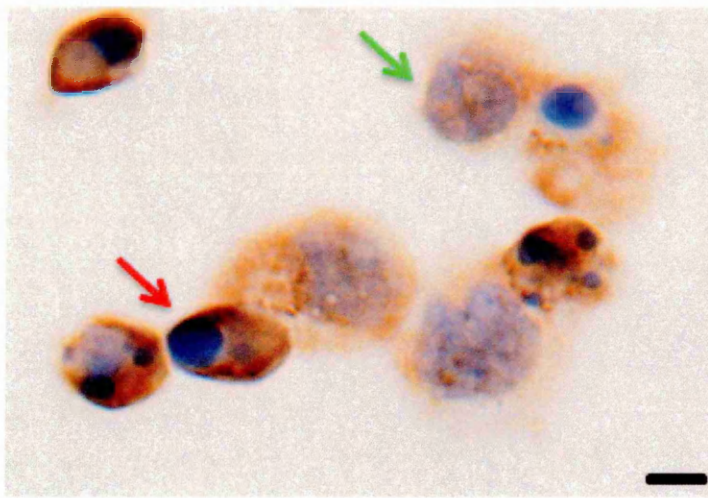


Figure 6.4: Illustrates analysis of cytochrome C expression in HL-60 cells following treatment with delphinidin for 3 h using Olympus light microscope (X100). Cells were divided into two groups: active and non-active. Active cells indicated by red arrows. Non-active cells indicated by green arrows.

6.3.9.3 Statistical Analysis

Average and Standard error of the mean (SEM) was calculated and Shapiro Wilke test using Stats Direct was used to analyse whether data followed a normal distribution. Data did not follow a normal distribution, thus a Kruskal-Wallis and Conover-Inman post hoc test was used to investigate statistical significance. Results of treated cells were normalized to the control (untreated cells) where control = 100%. Results were considered statistically significant when $P \leq 0.05$.

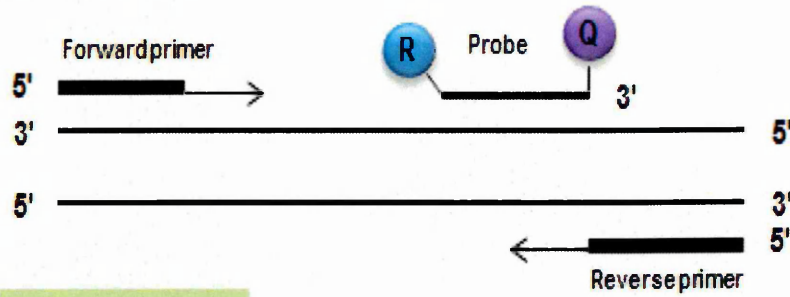
6.3.10 Quantitative Real Time Polymerase Chain Reaction (qRT-PCR)

Real-time PCR (Figure 6.5) is widely used to detect and quantify gene expression. It involves reverse transcription (RT) of mRNA into cDNA followed by PCR to amplify a specific target cDNA molecule, which is quantified in real-time by the accumulation of fluorescence after each amplification cycle (Orlando *et al*, 1998, Bustin, 2000).

Step:1:

A reporter (R) and a quencher (Q) are attached to the 5' and 3' ends of taqMan probe

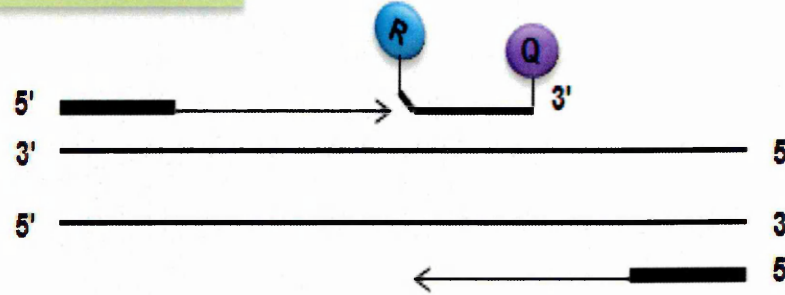
Polymerisation



Step: 2

When both labels are attached to the probe, reporter dye emission is quenched.

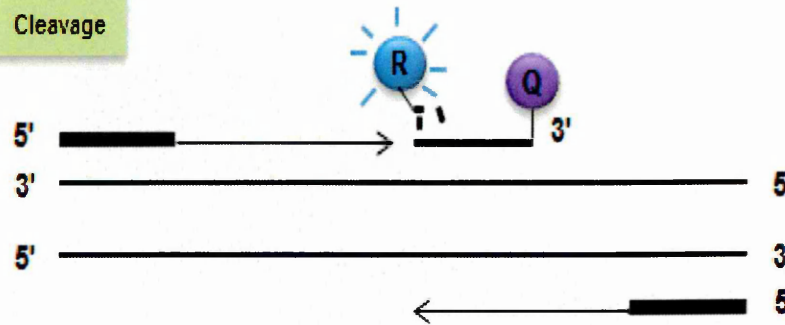
Strand displacement



Step:3

During each extension cycle, Taq polymerase cleaves the reporter dye from the probe.

Cleavage



Step:4

Once separated from the quencher, the reporter dye emits its characteristic fluorescence.

Polymerisation completed

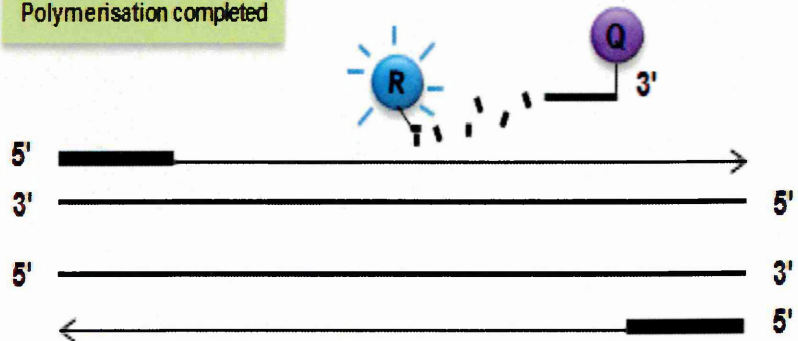


Figure 6.5: Illustration of how TaqMan reagent works. Modified from Applied Biosystems.

As amplification proceeds, the fluorescence amplification is captured by the instrument after every cycle, and is translated in a RT-PCR graph. With RT-PCR there are three amplification stages: 1) lag phase; 2) exponential; 3) plateau (Figure 6.6). In the exponential phase, the reagents are in abundance and the PCR products double every cycle. In the plateau phase, the reagents are depleted and PCR reaction stops. RT-PCR focuses on the exponential phase because it provides the most precise and accurate data for quantitation. Within the exponential phase, a threshold is set, the PCR cycle at which the sample reaches this threshold is called cycle threshold (C_t). The C_t value is used in downstream quantitation and depends on the amount of target, the larger the amount of template in the reaction the fewer amplification cycles to form a significant fluorescent signal. In contrast a small amount of target will require more amplification cycles for the fluorescent signal to generate a detectable fluorescence signal (Figure 6.6).

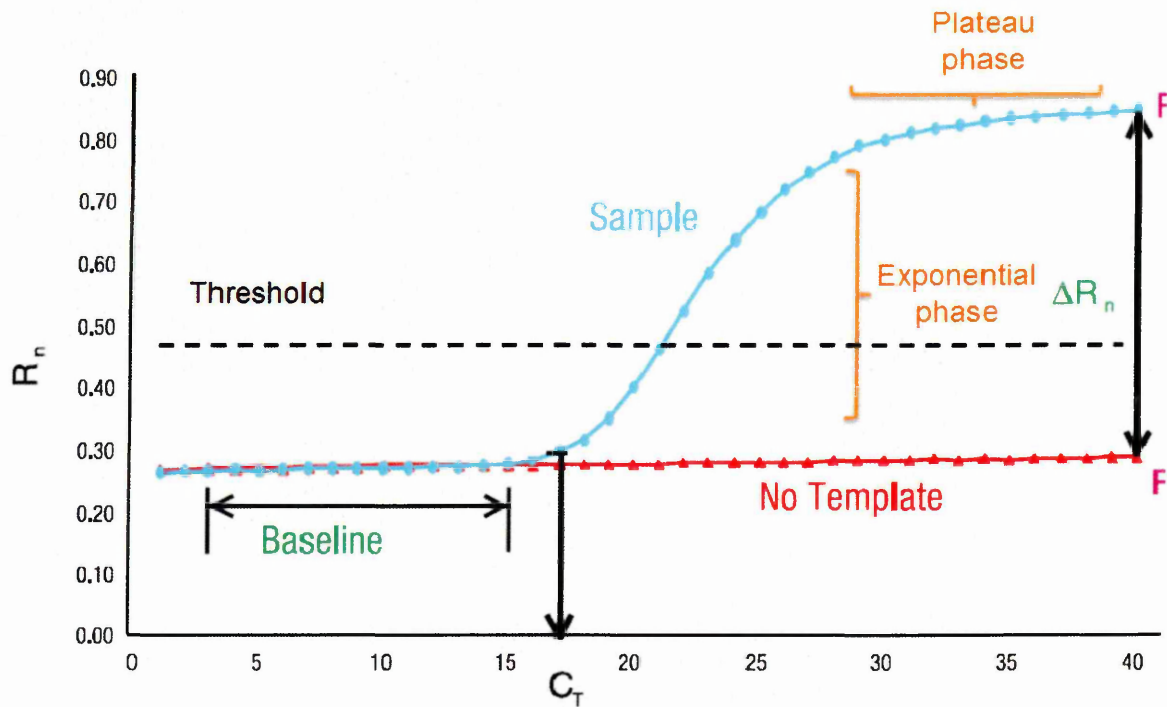


Figure 6.6: Illustrates qRT-PCR amplification plot.

6.3.10.1 Methodology

6.3.10.1.1 RNA Extraction

Following treatment with 50 μM of delphinidin on two leukaemia cell lines (MOLT-3 and HL-60), cell number was determined using an Invitrogen Countess automated cell counter (Invitrogen) incorporating Trypan Blue (Sigma) to distinguish live and dead cells (Section 2.3.1). Cell suspension aliquots containing 1×10^5 live cells were transferred to RNase free 1.5mL tubes and centrifuged at 400g for 10 minutes to recover cells. Supernatant was removed and the remaining cell pellet re-suspended in 1mL Trizol (Ambion) and incubated at room temperature for 5 minutes. Chloroform (Sigma) was added at a rate of 200 μL per tube; samples were mixed by vortexing for 15 seconds and incubated at room temperature for 3 minutes prior to centrifugation at 12,000g for 15 minutes at 4°C. Following centrifugation the upper aqueous phase (RNA containing) was removed to a fresh 1.5mL tube and 500 μL isopropanol (Sigma) added. RNA samples were incubated for 10 minutes at room temperature and then at -80°C for 1 hour to precipitate RNA. Samples were thawed on ice and centrifuged at 12,000g for 30 minutes at 4°C to collect RNA precipitate. The resulting cell pellet was resuspended in 500 μL of 80% ethanol and centrifuged at 7,500 g for 15 minutes. Then samples were air dried on ice for 30 minutes. RNA samples were eluted in 14 μL sterile deionized water and used immediately for cDNA synthesis.

6.3.10.1.2 cDNA Synthesis

RNA samples were converted to cDNA using Moloney Murine Leukaemia Virus (MMLV) reverse transcriptase (Biolin) prior to carrying out real-time quantitative polymerase chain reaction (qPCR). Fourteen microliters of RNA samples were incubated at 60°C for 5 minutes to denature RNA. RT mastermix was added immediately at a rate of 36 μL per 14 μL RNA sample (Table 6.6).

For 1 reaction		14 μL RNA
Deoxynucleotide triphosphates (dNTPs)	40mM (Biolin)	1.5 μL
Random Hexamers (AB)		1.0 μL
Bioscript 5x RT Buffer (Biolin)		5.0 μL
Bioscript RT Enzyme (Biolin)		0.5 μL
Sterile distilled H ₂ O		28 μL
		36.0 μL

Table 6.6: RT Mastermix.

Samples were incubated at 42°C for 1 h to permit cDNA synthesis, then 10 minutes at 80°C to inactivate RT enzyme. cDNA samples were diluted 1:10 by addition of sterile deionised water and stored at -20°C for use in qPCR.

6.3.10.1.3 qPCR cDNA from Directly Extracted HL-60 and MOLT-3 cells

Taqman PCR was performed on cDNA samples from directly extracted HL-60 and MOLT-3 cells. Glyceraldehyde-3-phosphate dehydrogenase (GAPDH), was used in all experiments to normalise for variations in total RNA in each sample.

2 µL sample cDNA was loaded in duplicate into 96-well FAST PCR plates (Applied Biosystems). Real-Time PCR mastermix was added at a rate of 8 µL per well (Table 6.7).

For 1 reaction	µL
Taqman Gene Expression Assay	0.5 µL
2x Taqman Fast MasterMix (Applied Biosystems)	5.0 µL
Sterile deionised water	2.5 µL
	8.0 µL

Table 6.7: Real-Time PCR Mastermix.

Separate reaction mastermixes were prepared and loaded for glyceraldehyde 3-phosphate dehydrogenase (GAPDH) and each target gene assay. Plates were sealed with adhesive film and ran on an Applied Biosystems, StepOnePlus Real-Time PCR machine on FAST programme incorporating 50 cycles of denaturation at 95°C for 1 second followed by annealing and extension at 60°C for 20 seconds.

6.3.10.4 Analysis of qRT-PCR

Real-time PCR data is expressed as an amplification plot (Figure 6.6) for each individual target detected. Baseline was set 2 cycles prior to the first visible amplification individually for each target detected. Thresholds were set within the exponential phase of the amplification plot and maintained across all samples investigated. Measured C_T values were then exported to an excel file where analysis by $2^{-\Delta\Delta C_T}$ method (Livak and Schmittgen, 2001) was performed to determine target mRNA expression relative to internal reference gene and basal expression. Briefly analysis was performed by: Arithmetical mean C_T values of internal reference gene and target gene sample duplicates were calculated.

Arithmetical mean of the 2 internal reference genes was calculated to generate 'mean reference' value for each sample.

ΔC_T values were calculated using the equation:

$$\Delta C_T = C_T(\text{target}) - C_T(\text{mean reference})$$

Arithmetical mean ΔC_T and standard error of the mean (ΔC_T SE) for each triplicate data set (untreated control and treatment group) was calculated

$\Delta\Delta C_T$ values were calculated using the equation:

$$\Delta\Delta C_T = C_T(\text{target}) - C_T(\text{mean reference})$$

Target gene expression, relative to internal reference gene and basal expression was calculated using the equation:

$$\text{Relative gene expression} = 2^{-\Delta\Delta C_T}$$

Relative gene expression was represented graphically and error bars representing standard error of ΔC_T values for each triplicate data set were calculated using the equations:

$$\text{Positive Error Bar} = 2^{(-\Delta C_T + \Delta SE)} - 2^{-\Delta C_T}$$

$$\text{Negative Error Bar} = 2^{-\Delta C_T} - 2^{(-\Delta C_T - \Delta SE)}$$

6.3.10.3 Statistical Analysis

In order to perform statistical analysis on RT-PCR data, $2^{-\Delta\Delta C_T}$ was calculated for each sample and control versus treated groups compared using a Mann Whitney U test. Results were considered statistically significant when $P \leq 0.05$. To generate error bar to control data, each control replicate is normalized against control average to enable spread of data to be shown as error bars.

6.4 Results

6.4.1 Effect of Anthocyanidins and Anthocyanins on ATP Levels as an Indicator of Total Viable Cells

To test whether anthocyanidins and anthocyanins found in PJ are effective in suppressing ATP levels of human leukaemia cell lines, the effects on ATP levels were investigated to indicate potential action on inhibiting proliferation or induction of apoptosis of cyanidin, cyanidin-3-*O*-glucoside, cyanidin-3,5-*O*-diglucosides, delphinidin, delphinidin-3-*O*-glucoside, delphinidin-3,5-*O*-diglucosides, pelargonidin, pelargonidin-3-*O*-glucoside and pelargonidin-3,5-*O*-diglucosides on CCRF-CEM, MOLT-3, HL-60 and THP-1 cells.

Delphinidin, Delphinidin-3-*O*-glucoside, and delphinidin-3,5-di-*O*-glucose significantly ($P \leq 0.05$) inhibited ATP levels in CCRF-CEM cells at all concentrations (10, 25, 50, 100 μM) in a dose-dependent manner following 24 h treatment. The IC_{50} values of delphinidin, delphinidin-3-*O*-glucoside, and delphinidin-3,5-di-*O*-glucose for CCRF-CEM cells at 24 h treatments were 20, 35, and 41 μM respectively (Figure 6.7) (Table 6.8).

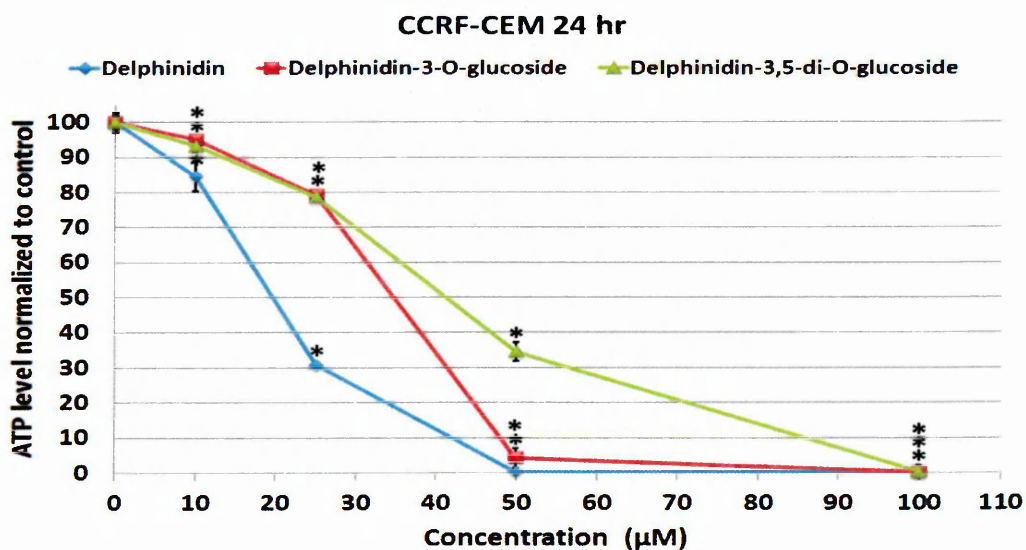


Figure 6.7: Effect of Delphinidin, Delphinidin-3-*O*-glucoside, and delphinidin-3,5-di-*O*-glucose on ATP levels proliferation at concentrations 10, 25, 50, and 100 μM on CCRF-CEM leukaemia cell line. ATP levels investigated using Cell Titer-Glo[®] Luminescent Cell Viability Assay to provide indication of live cell numbers. ATP levels normalized to controls and presented as means \pm standard error. * indicates significant difference ($P \leq 0.05$) vs. untreated control. $n = 3$.

Delphinidin and delphinidin-3-*O*-glucoside treatment in MOLT-3 cells resulted in a significant ($P \leq 0.05$) inhibition of ATP levels at all concentrations (10 to 100 μM) in a dose-dependent manner, while delphinidin-3,5-di-*O*-glucose showed significant ($P \leq 0.05$) decrease in ATP levels only at 25, 50, 100 μM . The IC_{50} values at 24 h post treatment with delphinidin, delphinidin-3-*O* glucoside, and delphinidin-3,5-di-*O*-glucose for MOLT-3 cells were 17, 34, 44 μM respectively (Figure 6.8) (Table 6.8).

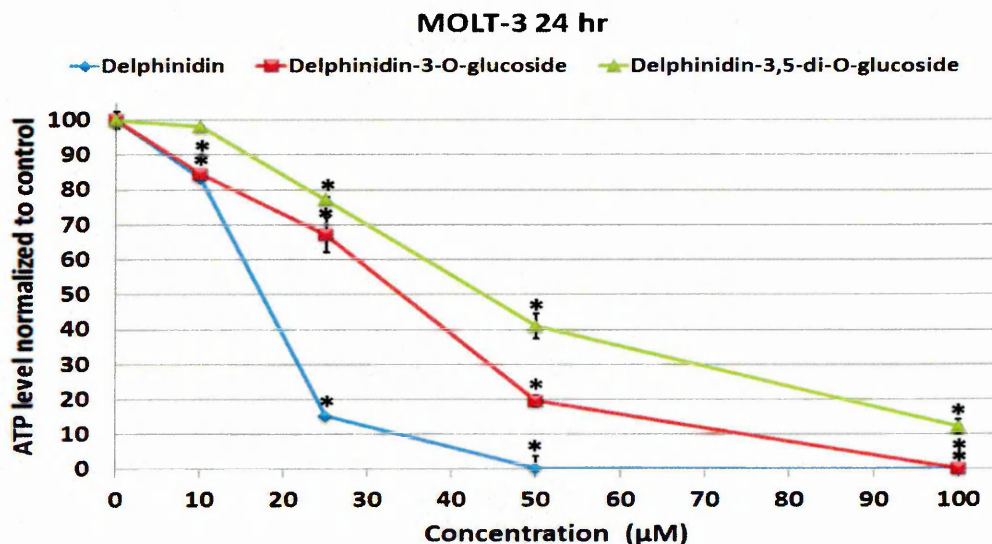


Figure 6.8: Effect of Delphinidin, Delphinidin-3-*O*-glucoside, and delphinidin-3,5-di-*O*-glucose on ATP levels at concentrations 10, 25, 50, and 100 μM on MOLT-3 leukaemia cell line. ATP levels investigated using Cell Titer-Glo[®] Luminescent Cell Viability Assay to provide indication of live cell numbers. ATP levels normalized to controls and presented as means \pm standard error. * indicates significant difference ($P \leq 0.05$) vs. untreated control. $n = 3$.

Delphinidin, Delphinidin-3-*O*-glucoside, and delphinidin-3,5-di-*O*-glucose significantly ($P \leq 0.05$) inhibited ATP levels in HL-60 cells at all concentrations (10, 25, 50, 100 μM) in a dose-dependent manner following 24 h treatment. The IC_{50} values of delphinidin, Delphinidin-3-*O*-glucoside, and delphinidin-3,5-di-*O*-glucose for HL-60 cells at 24 h treatments were 16, 19, and 34 μM respectively (Figure 6.9) (Table 6.8).

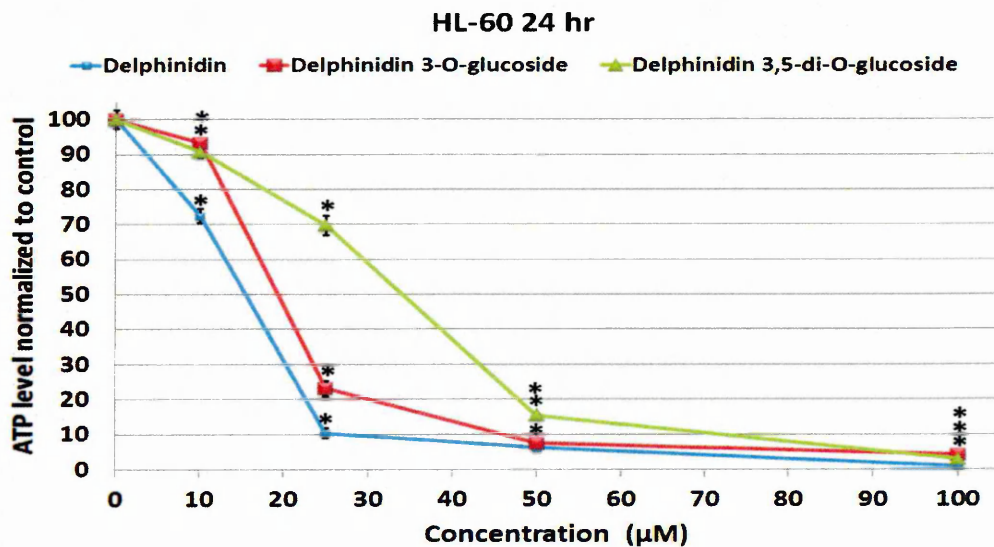


Figure 6.9: Effect of Delphinidin, Delphinidin-3-*O*-glucoside, and delphinidin-3,5-di-*O*-glucose on ATP levels at concentrations 10, 25, 50, and 100 μM on HL-60 leukaemia cell line. ATP levels investigated using Cell Titer-Glo[®] Luminescent Cell Viability Assay to provide indication of live cell numbers. ATP levels normalized to controls and presented as means \pm standard error. * indicates significant difference ($P \leq 0.05$) vs. untreated control. n= 3.

The ATP levels in THP-1 cells was also significantly ($P \leq 0.05$) inhibited in a dose-dependent manner by delphinidin, delphinidin-3-*O*-glucoside, and delphinidin-3,5-di-*O*-glucose following 24 h treatment. The IC_{50} values of delphinidin, delphinidin-3-*O*-glucoside, and delphinidin-3,5-di-*O*-glucose for THP-1 cells was found to be 38, 63, and 74 μ M respectively (Figure 6.10) (Table 6.8).

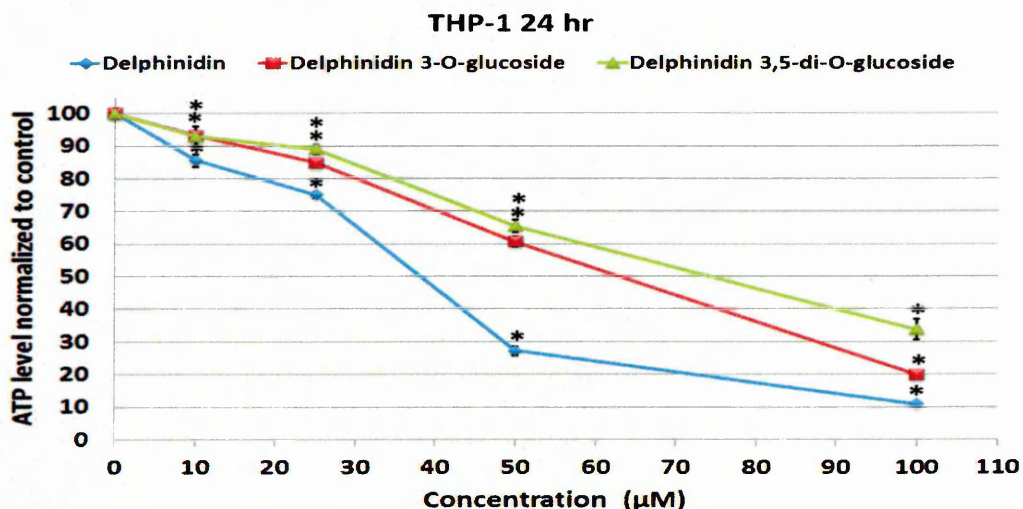


Figure 6.10: Effect of Delphinidin, Delphinidin-3-*O*-glucoside, and delphinidin-3,5-di-*O*-glucose on ATP levels at concentrations 10, 25, 50, and 100 μ M on THP-1 leukaemia cell line. ATP levels investigated using Cell Titer-Glo[®] Luminescent Cell Viability Assay to provide indication of live cell numbers. ATP levels normalized to controls and presented as means \pm standard error. * indicates significant difference ($P \leq 0.05$) vs. untreated control. n= 3.

Cyanidin and cyanidin-3-*O*-glucoside significantly ($P \leq 0.05$) inhibited ATP levels in CCRF-CEM cells at all concentrations (10, 25, 50, and 100 μM) in a dose-dependent manner following 24 h treatment. The IC_{50} values of cyanidin and cyanidin-3-*O*-glucoside for CCRF-CEM cells at 24 h were 75 and 87 μM respectively. Although cyanidin-3,5-di-*O*-glucose exhibited a significant decrease in ATP levels of CCRF-CEM cells, it failed to display 50% growth inhibition (Figure 6.11) (Table 6.8).

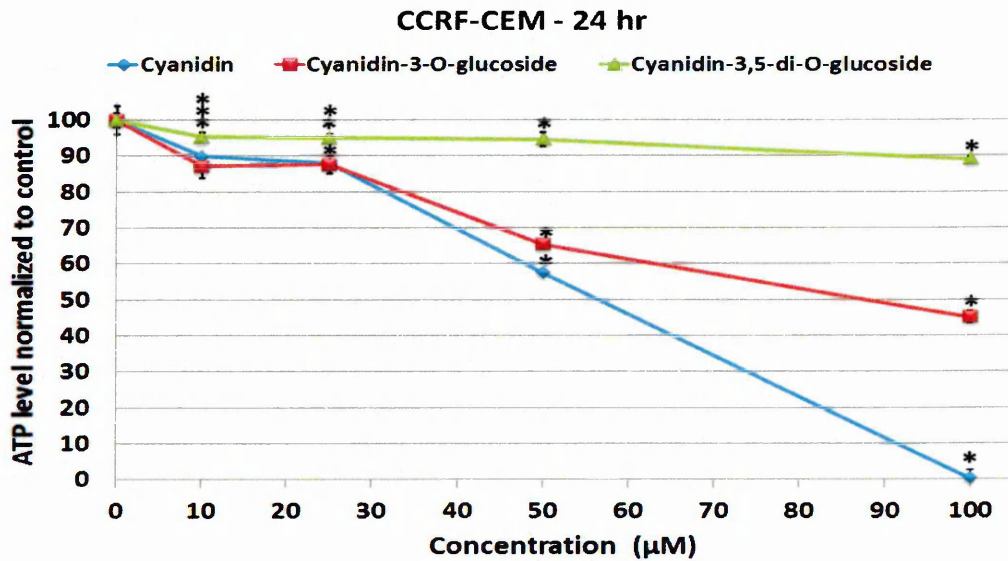


Figure 6.11: Effect of cyanidin, cyanidin-3-*O*-glucoside, and cyanidin -3,5-di-*O*-glucose on ATP levels at concentrations 10, 25, 50, and 100 μM on CCRF-CEM leukaemia cell line. ATP levels investigated using Cell Titer-Glo[®] Luminescent Cell Viability Assay to provide indication of live cell numbers. ATP levels normalized to controls and presented as means \pm standard error. * indicates significant difference ($P \leq 0.05$) vs. untreated control. $n = 3$.

Cyanidin and cyanidin-3-*O*-glucoside significantly ($P \leq 0.05$) inhibited ATP levels in MOLT-3 cells at all concentrations (10, 25, 50, and 100 μM) in a dose-dependent manner following 24 h treatment. The IC_{50} values of cyanidin and cyanidin-3-*O*-glucoside for MOLT-3 cells were 67 and 88 μM respectively. Although cyanidin -3,5-di-*O*-glucose showed significant decrease in ATP in MOLT-3 cells at 50 and 100 μM , it failed to display 50% growth inhibition (Figure 6.12) (Table 6.8).

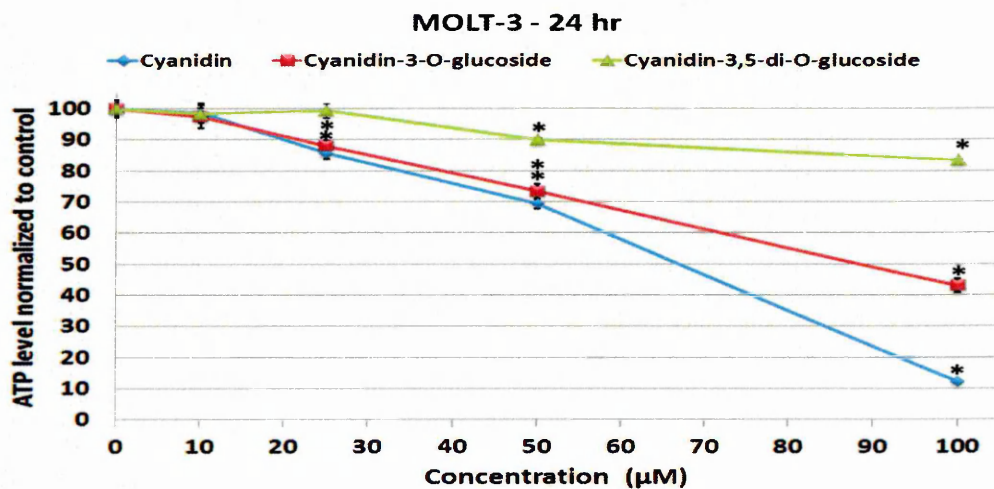


Figure 6.12: Effect of cyanidin, cyanidin-3-*O*-glucoside, and cyanidin -3,5-di-*O*-glucose on ATP levels at concentrations 10, 25, 50, and 100 μM on MOLT-3 leukaemia cell line. ATP levels investigated using Cell Titer-Glo[®] Luminescent Cell Viability Assay to provide indication of live cell numbers. ATP levels normalized to controls and presented as means \pm standard error. * indicates significant difference ($P \leq 0.05$) vs. untreated control. $n = 3$.

Cyanidin significantly ($P \leq 0.05$) inhibited ATP levels in HL-60 cells at all concentrations (10, 25, 50, 100 μM) in a dose-dependent manner, while cyanidin-3-*O*-glucoside displayed significant ($P \leq 0.05$) decrease at 25, 50, and 100 μM following 24 h treatment. The IC_{50} values cyanidin and cyanidin-3-*O*-glucoside for HL-60 cells were 64 and 70 μM , respectively. Cyanidin-3,5-di-*O*-glucose showed a decrease in ATP in HL-60 cells at the highest two concentrations (50 and 100 μM), but not significantly and failed to display 50% growth inhibition (Figure 6.13) (Table 6.8).

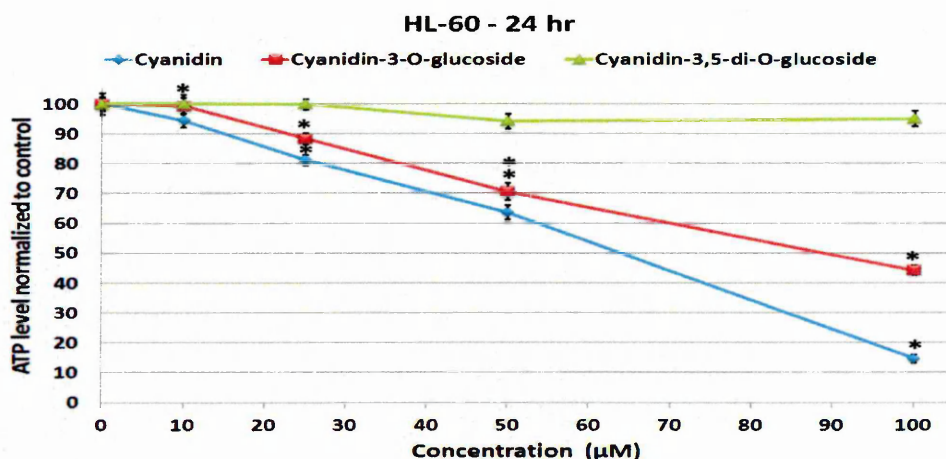


Figure 6.13: Effect of cyanidin, cyanidin-3-*O*-glucoside, and cyanidin -3,5-di-*O*-glucose on ATP levels at concentrations 10, 25, 50, and 100 μM on HL-60 leukaemia cell line. ATP levels investigated using Cell Titer-Glo[®] Luminescent Cell Viability Assay to provide indication of live cell numbers. ATP levels normalized to controls and presented as means \pm standard error. * indicates significant difference ($P \leq 0.05$) vs. untreated control. n= 3.

Cyanidin significantly ($P \leq 0.05$) inhibited ATP levels in THP-1 cells at all concentrations (10, 25, 50, 100 μM) in a dose-dependent manner, while cyanidin-3-*O*-glucoside displayed significant ($P \leq 0.05$) decrease at 25, 50, and 100 μM following 24 h treatment. The IC_{50} values of cyanidin and cyanidin-3-*O*-glucoside for THP-1 cells were 83 and 90 μM , respectively. Cyanidin -3,5-di-*O*-glucose showed only a significant decrease in ATP levels in THP-1 cells at highest concentration (100 μM), and failed to display 50% growth inhibition (Figure 6.14) (Table 6.8).

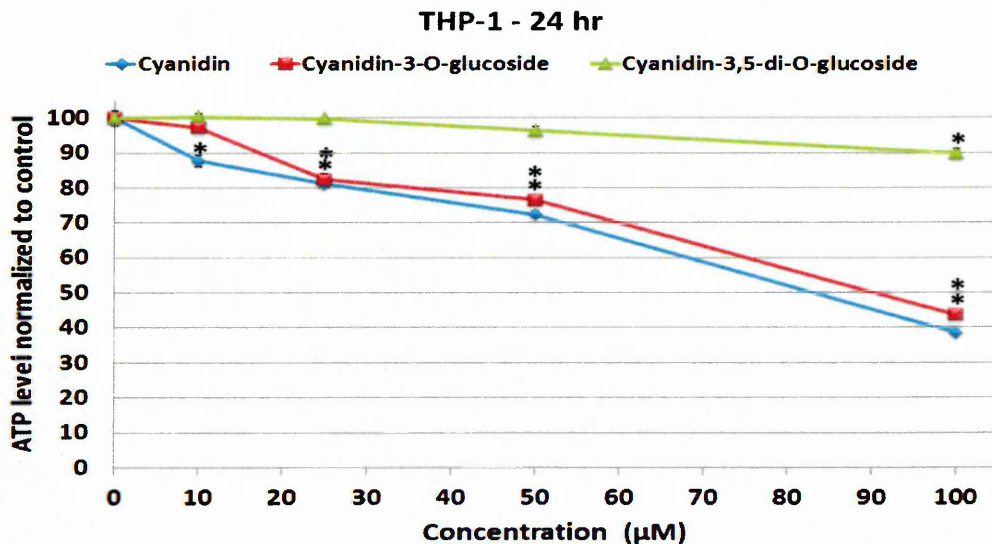


Figure 6.14: Effect of cyanidin, cyanidin-3-*O*-glucoside, and cyanidin -3,5-di-*O*-glucose on ATP levels at concentrations 10, 25, 50, and 100 μM on THP-1 leukaemia cell line. ATP levels investigated using Cell Titer-Glo[®] Luminescent Cell Viability Assay to provide indication of live cell numbers. ATP levels normalized to controls and presented as means \pm standard error. * indicates significant difference ($P \leq 0.05$) vs. untreated control. n= 3.

Pelargonidin and pelargonidin-3-*O*-glucoside significantly ($P \leq 0.05$) inhibited ATP levels in CCRF-CEM cells at 10, 25, 50, 100 μM in a dose-dependent manner ($P \leq 0.05$), while pelargonidin -3,5-di-*O*-glucose did not show a significant ($P > 0.05$) decrease at all concentrations following 24 h treatment. Pelargonidin induced IC_{50} in CCRF-CEM cells at 81 μM . In contrast, pelargonidin-3-*O*-glucoside and pelargonidin-3,5-di-*O*-glucose failed to display 50% decrease in ATP levels in CCRF-CEM cells (Figure 6.15) (Table 6.8).

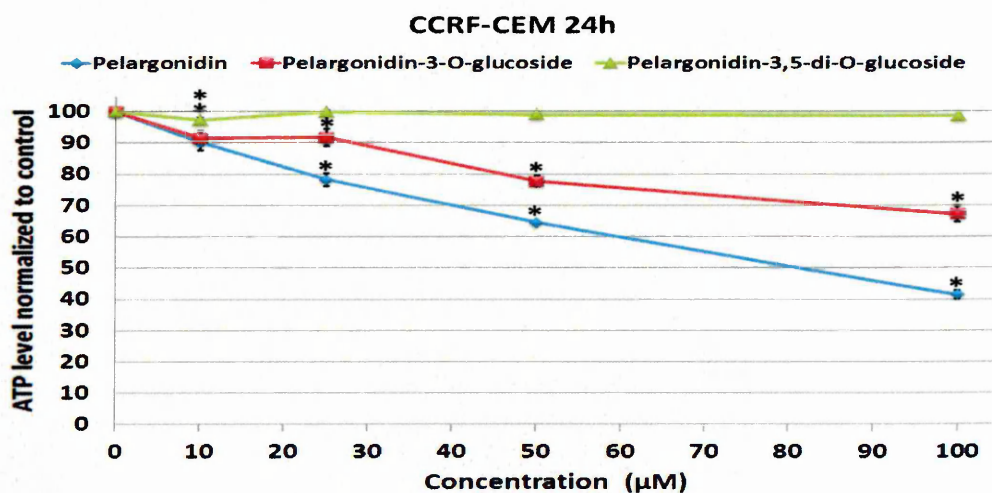


Figure 6.15: Effect of pelargonidin, pelargonidin-3-*O*-glucoside, and pelargonidin -3,5-di-*O*-glucose on ATP levels at concentrations 10, 25, 50, and 100 μM on CCRF-CEM leukaemia cell line. ATP levels investigated using Cell Titer-Glo[®] Luminescent Cell Viability Assay to provide indication of live cell numbers. ATP levels normalized to controls and presented as means \pm standard error. * indicates significant difference ($P \leq 0.05$) vs. untreated control. $n = 3$.

Pelargonidin and pelargonidin-3-*O*-glucoside significantly ($P \leq 0.05$) inhibited ATP levels in MOLT-3 cells at 25, 50, 100 μM in a dose-dependent manner, while pelargonidin-3,5-di-*O*-glucose showed significant decrease at only 50 and 100 μM following 24 h treatment ($P \leq 0.05$). Pelargonidin induced IC_{50} in MOLT-3 cells at 83 μM . In contrast, pelargonidin-3-*O*-glucoside and pelargonidin-3-*O*-glucoside failed to display 50% decrease in ATP levels in MOLT-3 cells (Figure 6.16) (Table 6.8).

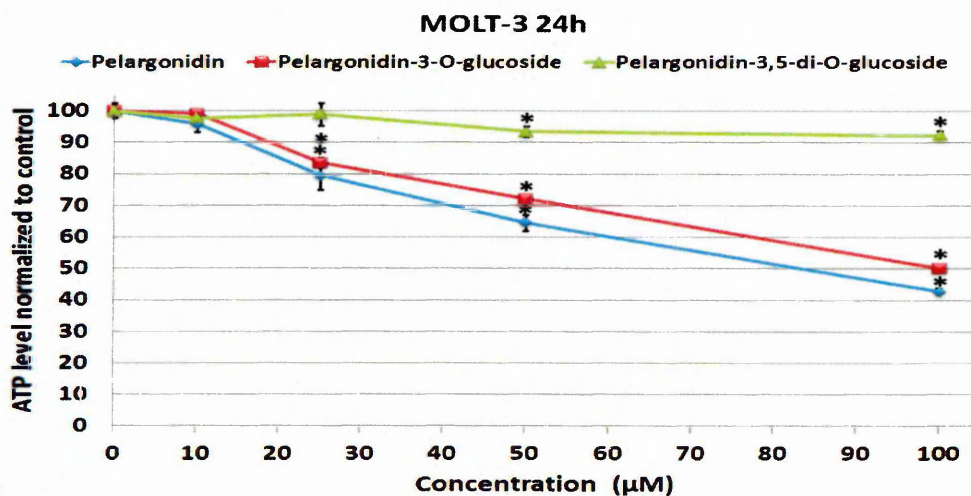


Figure 6.16: Effect of pelargonidin, pelargonidin-3-*O*-glucoside, and pelargonidin -3,5-di-*O*-glucose on ATP levels at concentrations 10, 25, 50, and 100 μM on MOLT-3 leukaemia cell line. ATP levels investigated using Cell Titer-Glo[®] Luminescent Cell Viability Assay to provide indication of live cell numbers. ATP levels normalized to controls and presented as means \pm standard error. * indicates significant difference ($P \leq 0.05$) vs. untreated control. $n = 3$.

Pelargonidin and pelargonidin-3-*O*-glucoside significantly ($P \leq 0.05$) inhibited ATP levels in HL-60 cells at 25, 50 and 100 μM in a dose-dependent manner, while pelargonidin -3,5-di-*O*-glucose did not show a significant ($P \leq 0.05$) decrease at all concentrations following 24 h treatment. Pelargonidin and pelargonidin-3-*O*-glucoside displayed IC_{50} against HL-60 cells at 81 and 98 μM . In contrast, pelargonidin -3,5-di-*O*-glucose failed to display 50% decrease in ATP levels in HL-60 cells (Figure 6.17) (Table 6.8).

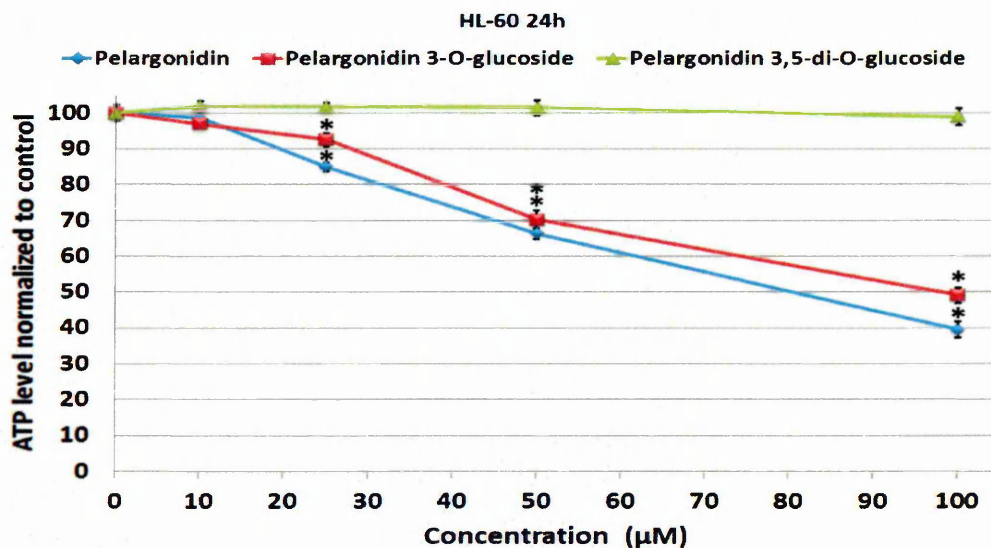


Figure 6.17: Effect of pelargonidin, pelargonidin-3-*O*-glucoside, and pelargonidin -3,5-di-*O*-glucose on ATP levels at concentrations 10, 25, 50, and 100 μM on HL-60 leukaemia cell line. ATP levels investigated using Cell Titer-Glo[®] Luminescent Cell Viability Assay to provide indication of live cell numbers. ATP levels normalized to controls and presented as means \pm standard error. * indicates significant difference ($P \leq 0.05$) vs. untreated control. $n = 3$.

Pelargonidin and pelargonidin-3-*O*-glucoside significantly ($P \leq 0.05$) inhibited ATP levels in THP-1 cells at 10, 25, 50, 100 μM in a dose-dependent manner, while pelargonidin -3,5-di-*O*-glucose did not show significant decrease at any concentration following 24 h treatment ($P > 0.05$). Pelargonidin displayed IC_{50} against THP-1 cells of 83 μM . In contrast, pelargonidin-3-*O*-glucoside and pelargonidin-3-*O*-glucoside failed to display 50% decrease in ATP levels in THP-1 cells (Figure 6.18) (Table 6.8).

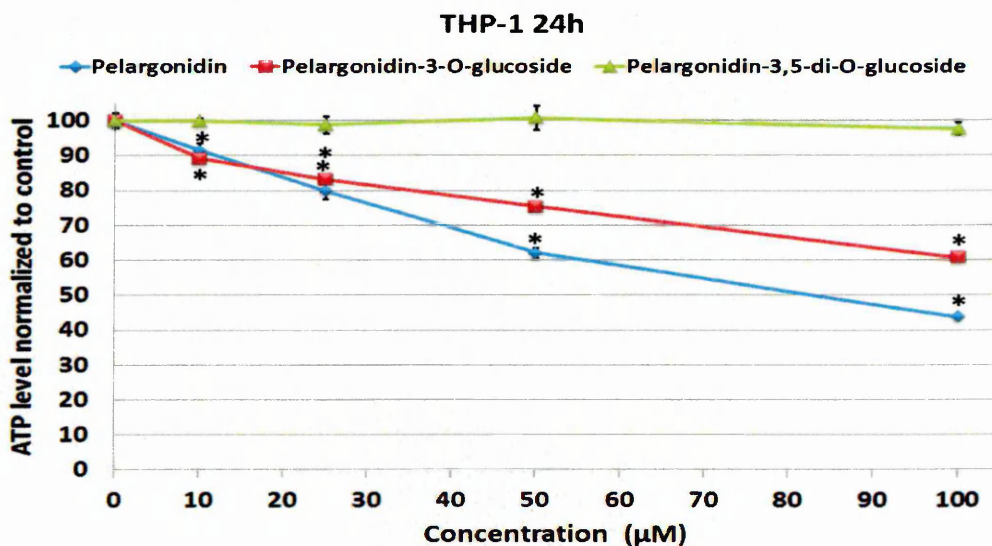


Figure 6.18: Effect of pelargonidin, pelargonidin-3-*O*-glucoside, and pelargonidin -3,5-di-*O*-glucose on ATP levels at concentrations 10, 25, 50, and 100 μM on THP-1 leukaemia cell line. ATP levels investigated using Cell Titer-Glo[®] Luminescent Cell Viability Assay to provide indication of live cell numbers. ATP levels normalized to controls and presented as means \pm standard error. * indicates significant difference ($P \leq 0.05$) vs. untreated control. $n = 3$.

Compounds	CCRF-CEM	MOLT-3	HL-60	THP-1
Delphinidin	20 μ M	17 μ M	16 μ M	38 μ M
Delphinidin-3-O-glucoside	35 μ M	34 μ M	19 μ M	63 μ M
Delphinidin-3,5-O-diglucosie	41 μ M	44 μ M	34 μ M	74 μ M
Cyanidin	57 μ M	67 μ M	64 μ M	83 μ M
Cyanidin-3-O-glucoside	87 μ M	88 μ M	70 μ M	90 μ M
Cyanidin-3,5-O-diglucosie	NR	NR	NR	NR
Pelargonidin	81 μ M	83 μ M	81 μ M	83 μ M
Pelargonidin-3-O-glucoside	NR	NR	98 μ M	NR
Pelargonidin-3,5-O-diglucosie	NR	NR	NR	NR

Table 6.8: The IC₅₀ of anthocyanins and anthocyanidins on leukaemia cell lines (CCRF-CEM, MOLT-3, HL-60, and THP-1) following 24 h treatment. NR= not reached.

6.4.2 Effect of anthocyanidins and anthocyanins found in PJ on induction of cell death

Delphinidin, delphinidin-3-O-glucoside, and delphinidin-3,5-di-O-glucose showed a significant ($P \leq 0.05$) increase in the number of apoptotic and dead cells and significant ($P \leq 0.05$) decrease in the number of live cells in CCRF-CEM, MOLT-3 (Figure 6.19), HL-60, and THP-1 cells (Figure 6.20) with different sensitivity between these cells following 24 h treatment. Delphinidin exhibited potent induction of apoptosis in all cells compared to delphinidin-3-O-glucoside, and delphinidin-3,5-di-O-glucose which had less effect on the induction of apoptosis ($P > 0.05$).

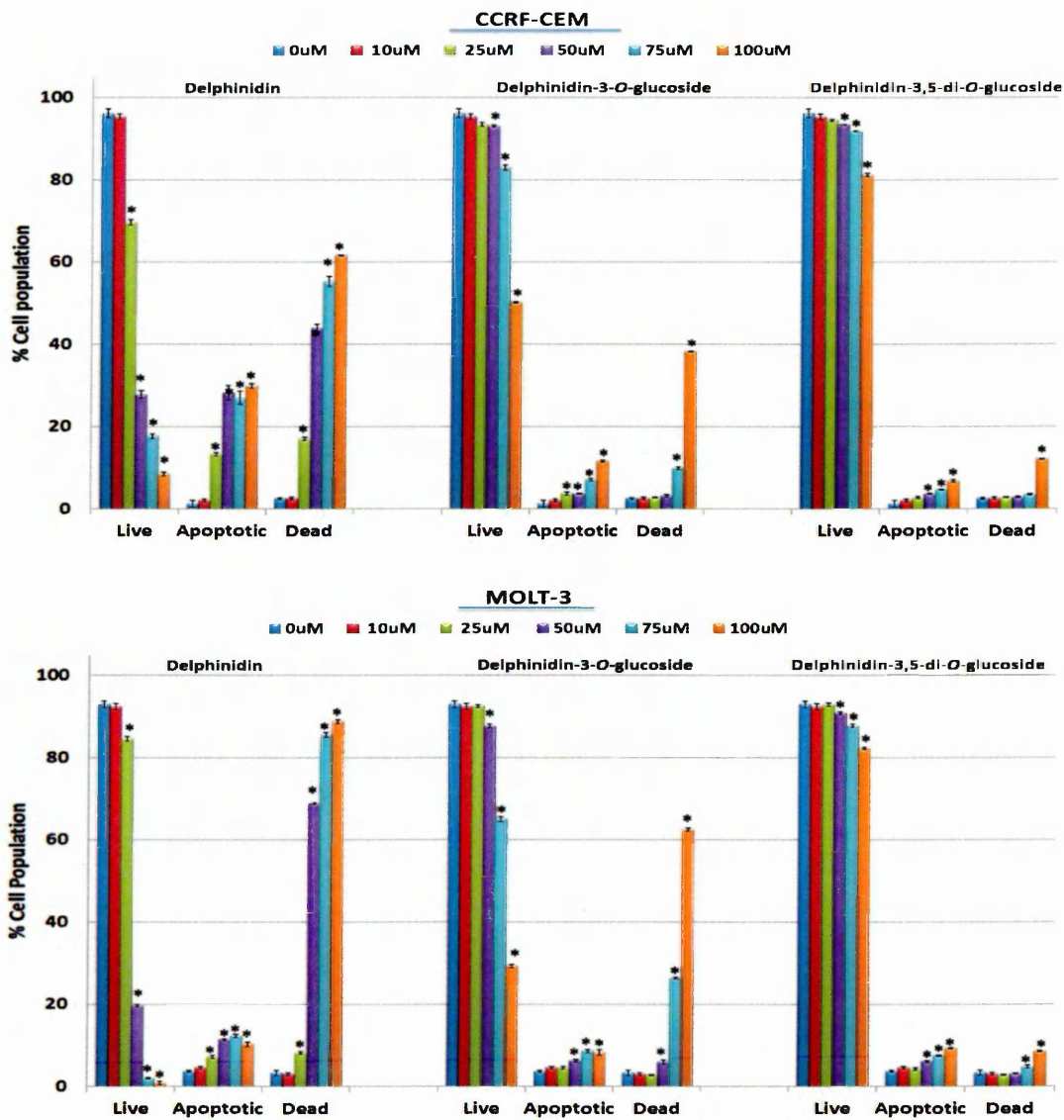


Figure 6.19: Annexin V-FITC/ PI based on flow cytometry following treatment with delphinidin, delphinidin-3-O-glucoside, and delphinidin-3,5-di-O-glucose (0, 10, 25, 50, 75, and 100 μ M) for 24 h on CCRF-CEM and MOLT-3. * indicates significant difference ($P \leq 0.05$) vs. untreated control. n= 3.

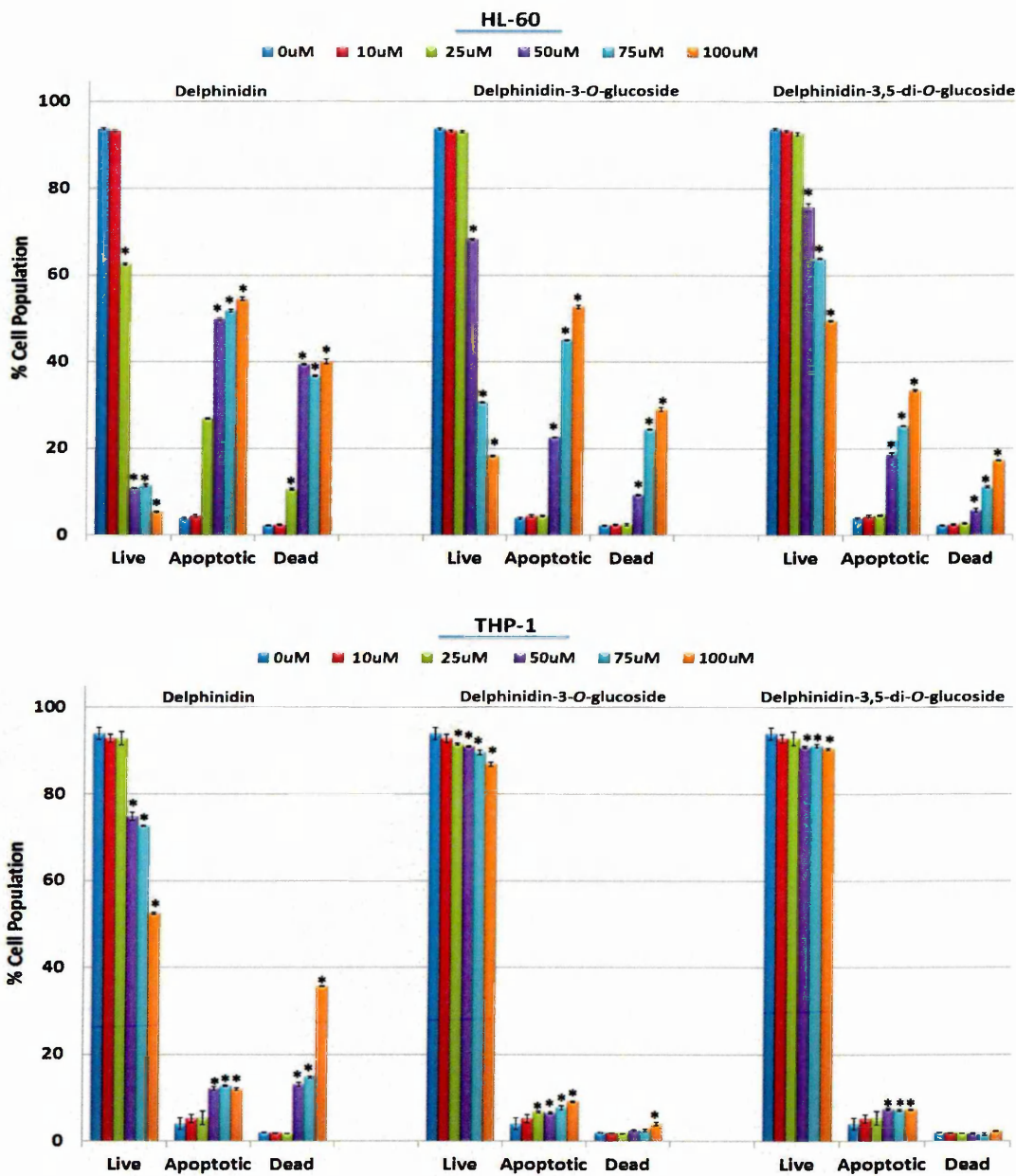


Figure 6.20: Annexin V-FITC/ PI based on flow cytometry following treatment with delphinidin, delphinidin-3-O-glucoside, and delphinidin-3,5-di-O-glucoside (0, 10, 25, 50, 75, and 100 μM) for 24 h on HL-60 and THP-1 Mean ± SEM. * indicates significant difference ($P \leq 0.05$) vs. untreated control. n= 3.

Cyanidin, cyanidin-3-*O*-glucoside, and cyanidin -3,5-di-*O*-glucose showed a significant increase in the number of apoptotic and dead cells and significant decrease in the number of live cells in CCRF-CEM cells following 24 h treatment ($P \leq 0.05$) (Figure 6.21). Cyanidin illustrated potent induction of apoptosis compared to cyanidin-3-*O*-glucoside and cyanidin-3,5-di-*O*-glucose on CCRF-CEM cells. Cyanidin induced apoptosis in MOLT-3 (Figure 6.21) and HL-60 cells (Figure 6.22), while cyanidin treatment of THP-1 cells failed to induce apoptosis. Cyanidin-3-*O*-glucoside and cyanidin -3,5-di-*O*-glucose did not show any effect on induction of apoptosis in MOLT-3, HL-60, and THP-1 cells (Figure 6.21 and 6.22).

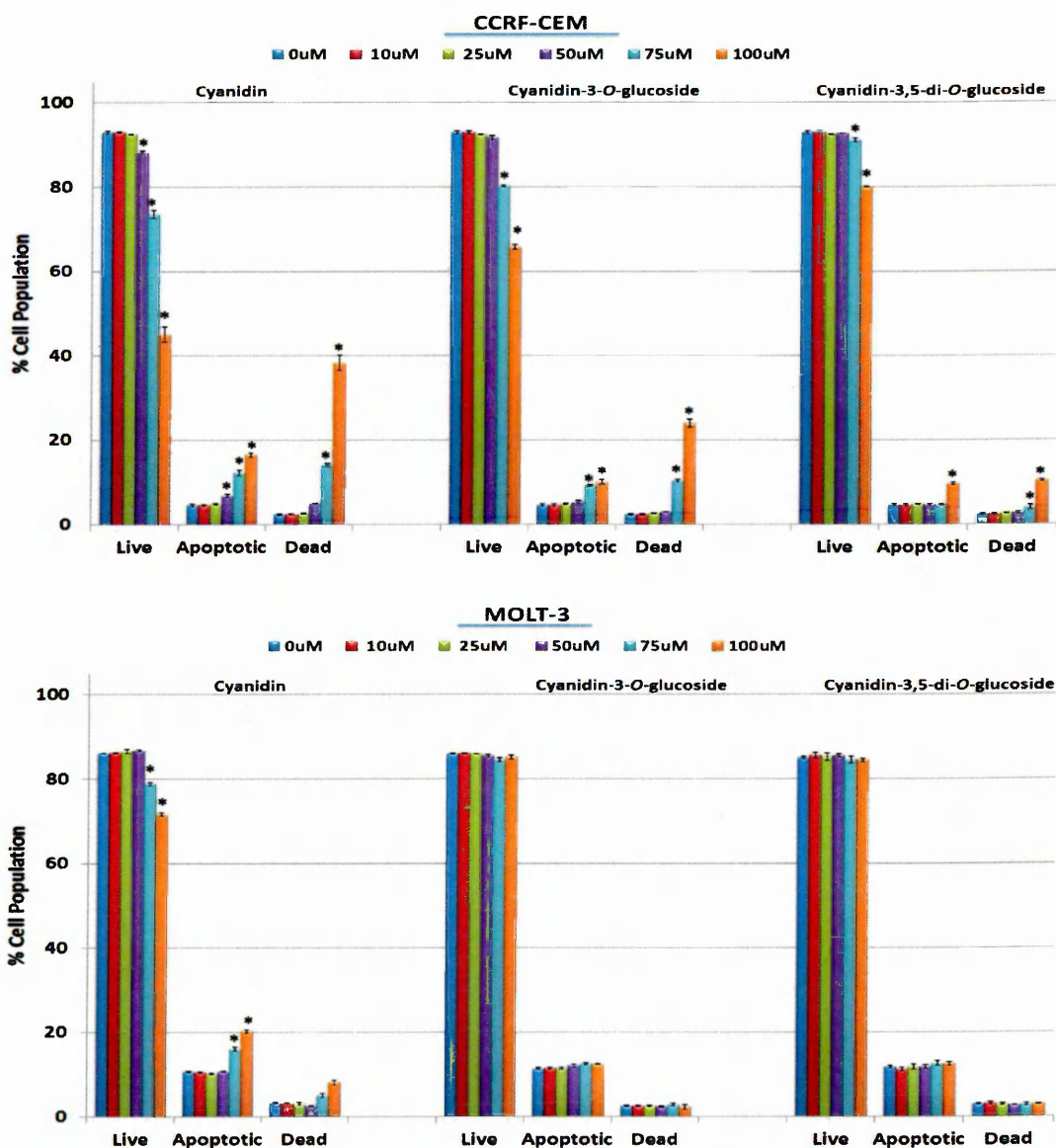


Figure 6.21: Annexin V-FITC/ PI based on flow cytometry following treatment with cyanidin, cyanidin-3-*O*-glucoside, and cyanidin-3,5-di-*O*-glucose (0, 10, 25, 50, 75, and 100 μM) for 24 h on CCRF-CEM and MOLT-3. Mean \pm SEM. * indicates significant difference ($P \leq 0.05$) vs. untreated control. $n = 3$.

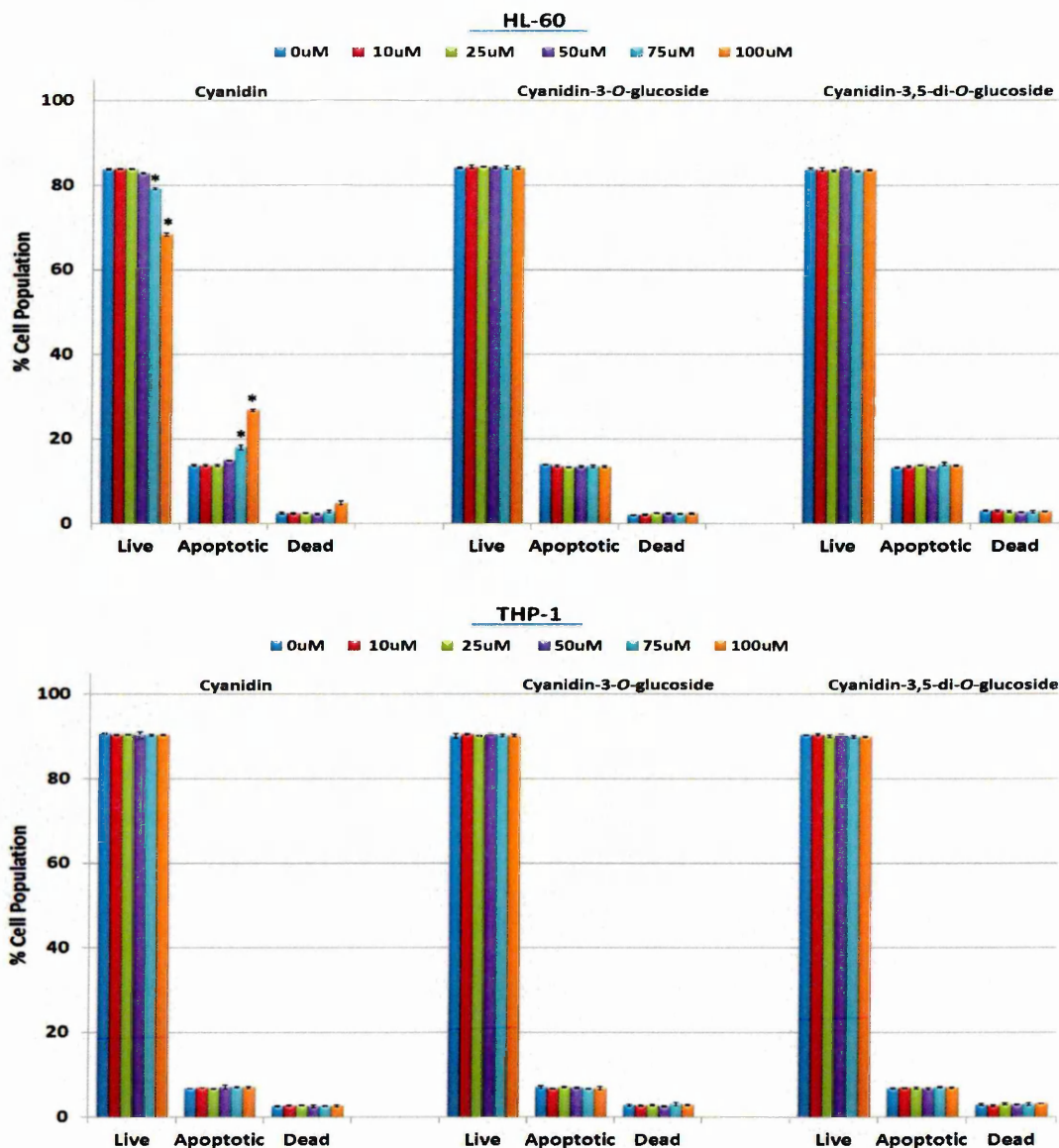


Figure 6.22: Analysis of Annexin V-FITC/ PI based on flow cytometry following treatment with cyanidin, cyanidin-3-*O*-glucoside, and cyanidin-3,5-di-*O*-glucose (0, 10, 25, 50, 75, and 100 μM) for 24 h on HL-60 and THP-1. Mean ± SEM. * indicates significant difference ($P \leq 0.05$) vs. untreated control. n= 3.

Pelargonidin slightly induced apoptosis, but this failed to reach significance in CCRF-CEM, MOLT-3, and HL-60 cells, and failed to induce apoptosis on THP-1 cells (Figure 6.23 and 6.24). Pelargonidin, Pelargonidin-3-*O*-glucoside, and pelargonidin-3,5-di-*O*-glucose did not show any effect on induction of apoptosis in any of the cells lines investigated (Figure 6.23 and 6.24).

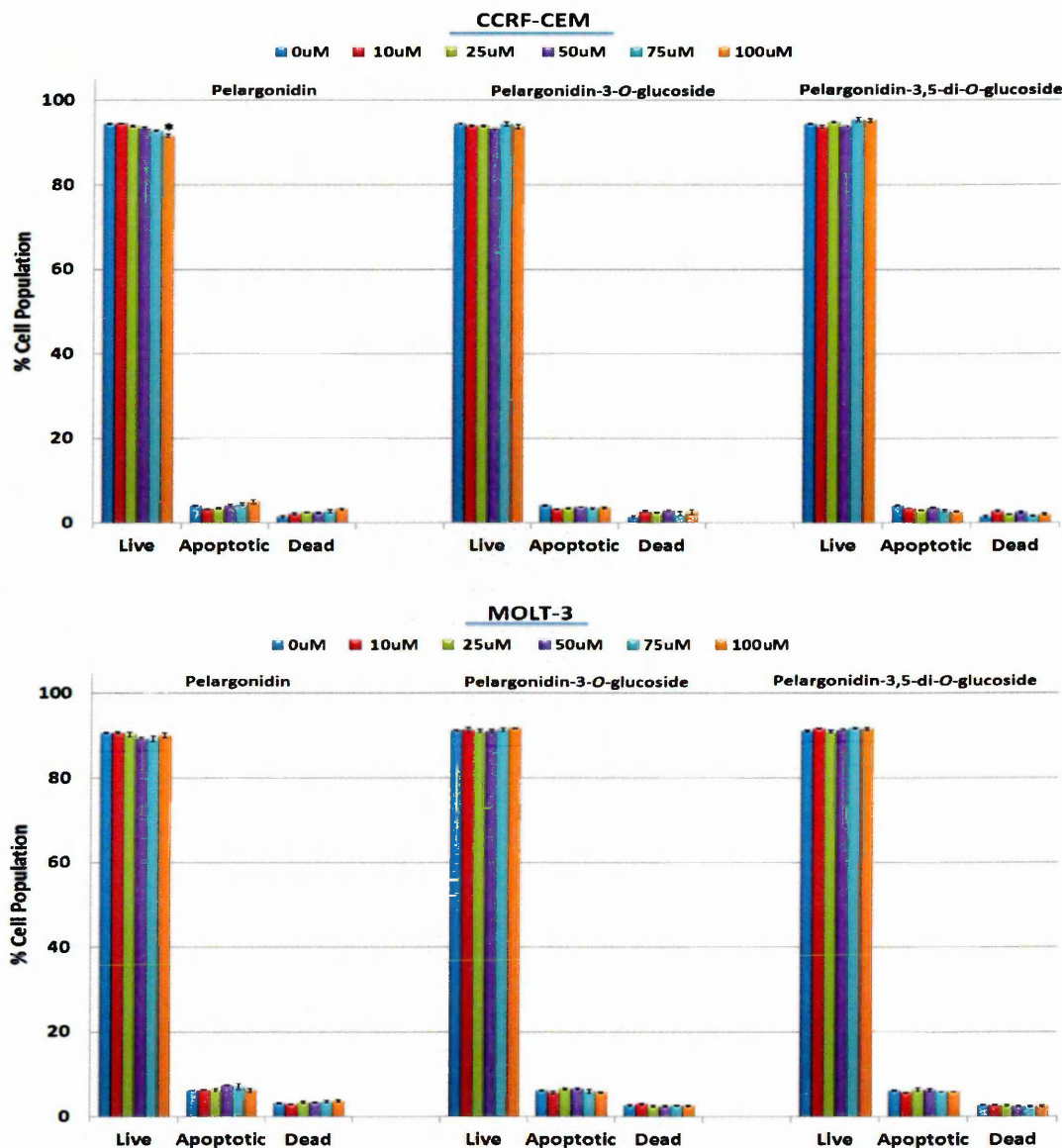


Figure 6.23: Annexin V-FITC/ PI based on flow cytometry following treatment with pelargonidin, pelargonidin -3-*O*-glucoside, and pelargonidin-3,5-di-*O*-glucose (0, 10, 25, 50, 75, and 100 μM) for 24 h on CCRF-CEM and MOLT-3. Mean ± SEM. * indicates significant difference ($P \leq 0.05$) vs. untreated control. n= 3.

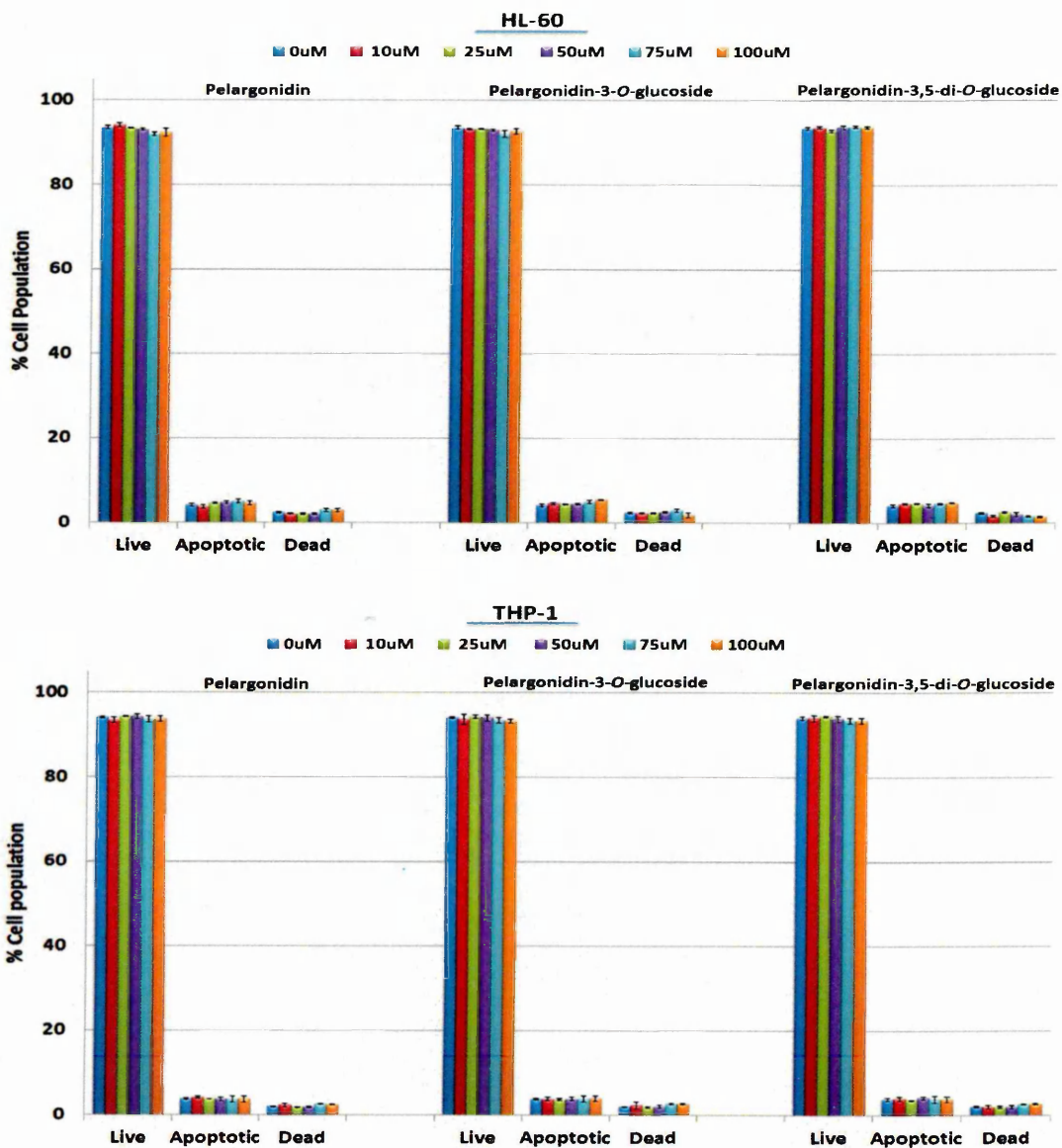


Figure 6.24: Annexin V-FITC/ PI based on flow cytometry following treatment with pelargonidin, pelargonidin -3-O-glucoside, and pelargonidin-3,5-di-O-glucose (0, 10, 25, 50, 75, and 100 μ M) for 24 h on HL-60 and THP-1. Mean \pm SEM. * indicates significant difference ($P \leq 0.05$) vs. untreated control. n= 3.

6.4.3 Effect of Anthocyanidins (Delphinidin, Cyanidin, and Pelargonidin) on Caspase-3 Activity

Caspase-3 activation plays a central role during the apoptotic process. Induction of apoptosis by treatment with delphinidin, cyanidin, and pelargonidin was confirmed with induction of caspase-3 activity in all four cell lines following 24 h. In CCRF-CEM, MOLT-3, and HL-60 cells a significant increase in the number of cells with active caspase-3 was observed at concentrations 25, 50, 75 and 100 μM delphinidin ($P \leq 0.05$). While, in THP-1 the number of cells with active caspase-3 was observed at concentrations 50, 75, and 100 μM delphinidin, with no significant effect seen following 25 μM treatment with delphinidin ($P \leq 0.05$) (Figure 6.25).

Cyanidin induced apoptosis with different sensitivity in CCRF-CEM, MOLT-3, HL-60 and THP-1 cells, cyanidin failed to induce apoptosis at all concentrations (Figure 6.25). Pelargonidin failed to induce apoptosis in all four leukaemia cell lines (Figure 6.25).

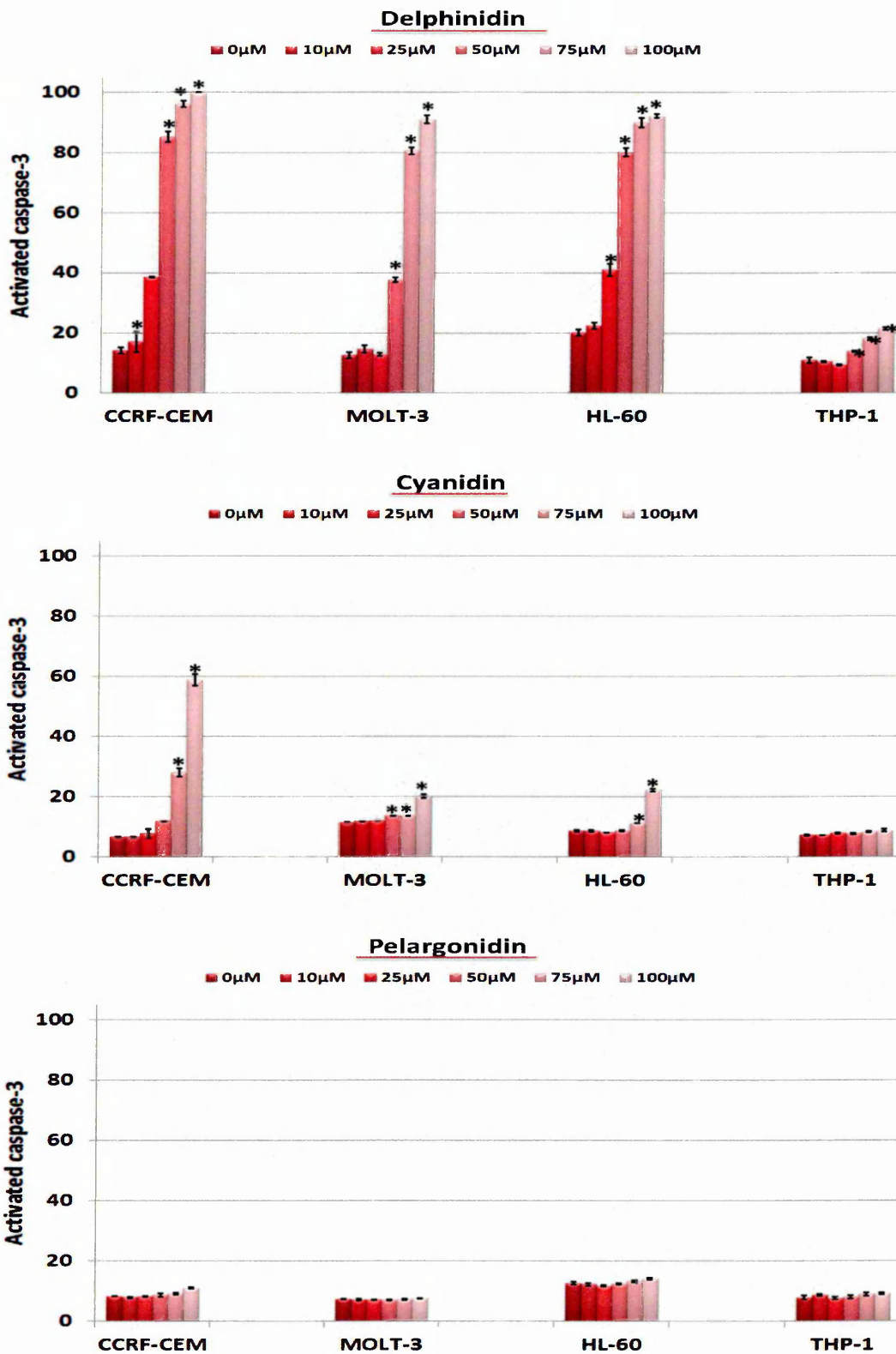


Figure 6.25: Effect of delphinidin, cyanidin, and pelargonidin on caspase-3 activation in four leukaemia cell lines (CCRF-CEM, MOLT-3, HL-60, and THP-1). Cells treated for 24 at concentrations 10, 25, 50 and 100 μM. Caspase-3 activation was determined by NucView™ 488 Caspase-3 substrate based on flow cytometry analysis. Mean ± SEM. * indicates significant difference ($P < 0.05$) vs. untreated control. n = 3.

6.4.4 Effect of Delphinidin on Induction of Apoptosis Using DAPI for Morphology Assessment

To confirm the results of annexin V/PI-FITC and caspase-3 activity, we examined the effect of delphinidin on leukaemia cell lines (CCRF-CEM, MOLT-3, HL-60, and THP-1) on apoptotic morphology using DAPI stain at concentrations (25, 50, and 100 μM) following 24 h treatments.

In all cell lines, untreated cells (0 μM) exhibited intact cells, but delphinidin-treated cells showed significant nuclear fragmentation, which is a typical marker of apoptosis. The induction of apoptosis cell death was accompanied by characteristic morphology and structural changes, including a condensed and fragmented nuclear structure and decreased cell size (Figure 6.27 and 6.29).

Differential responses between cells lines was observed following delphinidin treatment at different concentrations as was observed with annexin V-FITC /PI and caspase-3 activity assessment. Treatment of CCRF-CEM and HL-60 cells with delphinidin resulted in a significant increase in the number of apoptotic cells at all concentrations 25, 50, and 100 μM (Figure 6.26 and 6.28), while in MOLT-3 and THP-1 cells a significant increase in the number of apoptotic cells was only observed following 50 and 100 μM ($P \leq 0.05$) (Figure 6.27 and 6.29).

CCRF-CEM

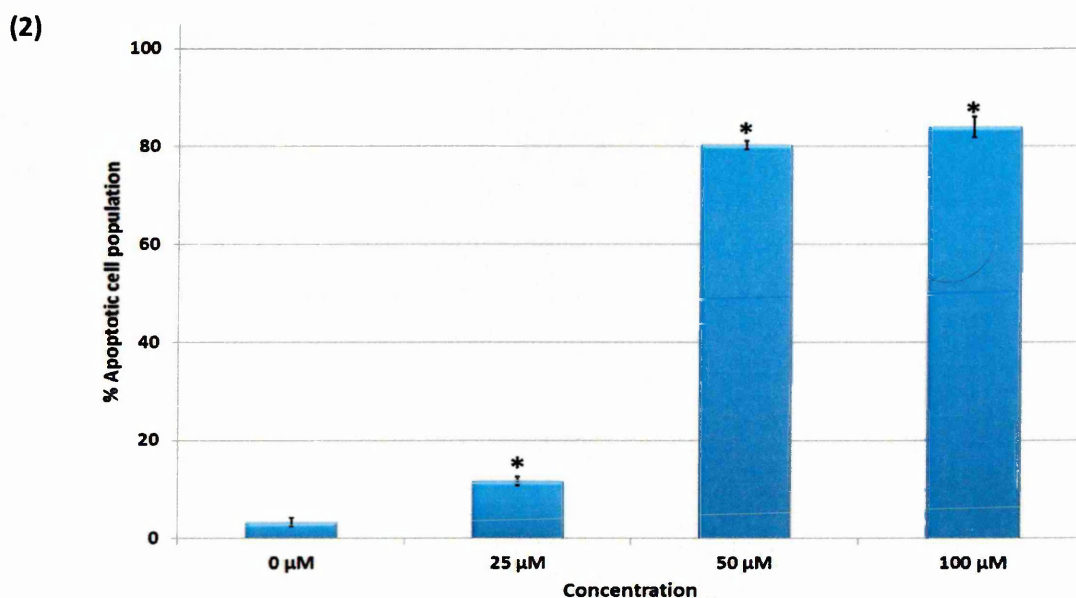
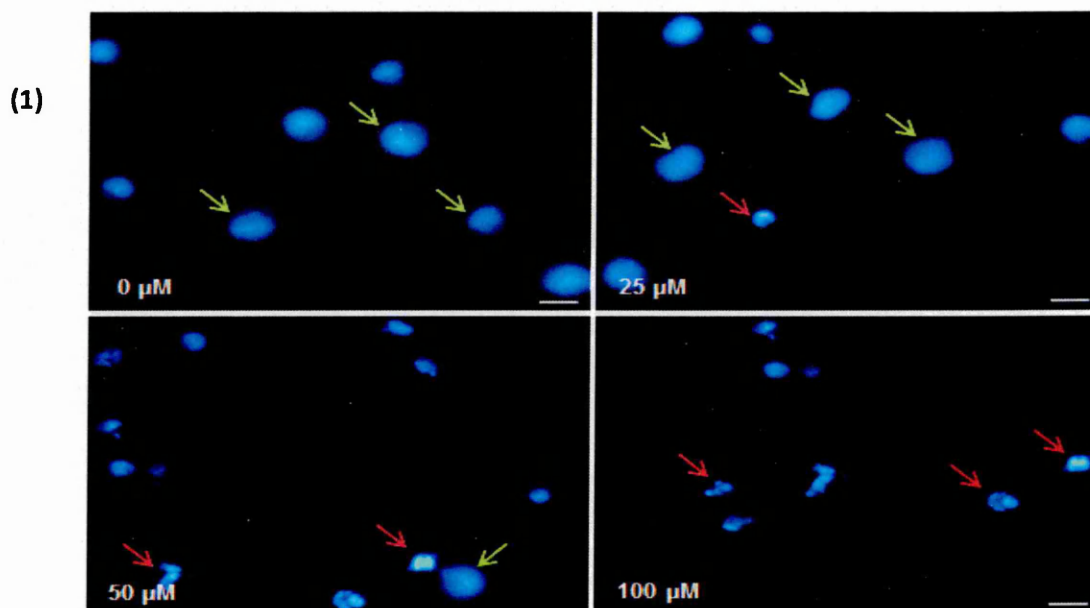


Figure 6.26: (1) Morphological staining analysis of CCRF-CEM with DAPI treated with delphinidin 25, 50, and 100 μM for 24 h. Live cells are indicated by the green arrows, and apoptotic cells are indicated by the red arrows. **(2)** Percentage of apoptotic cells determined from DAPI morphological assessment following treatment with delphinidin at concentration 25, 50, and 100 μM for 24 h. * indicates significant difference ($P \leq 0.05$) vs. untreated control. Scale bar = 12.5 μm . n= 3.

MOLT-3

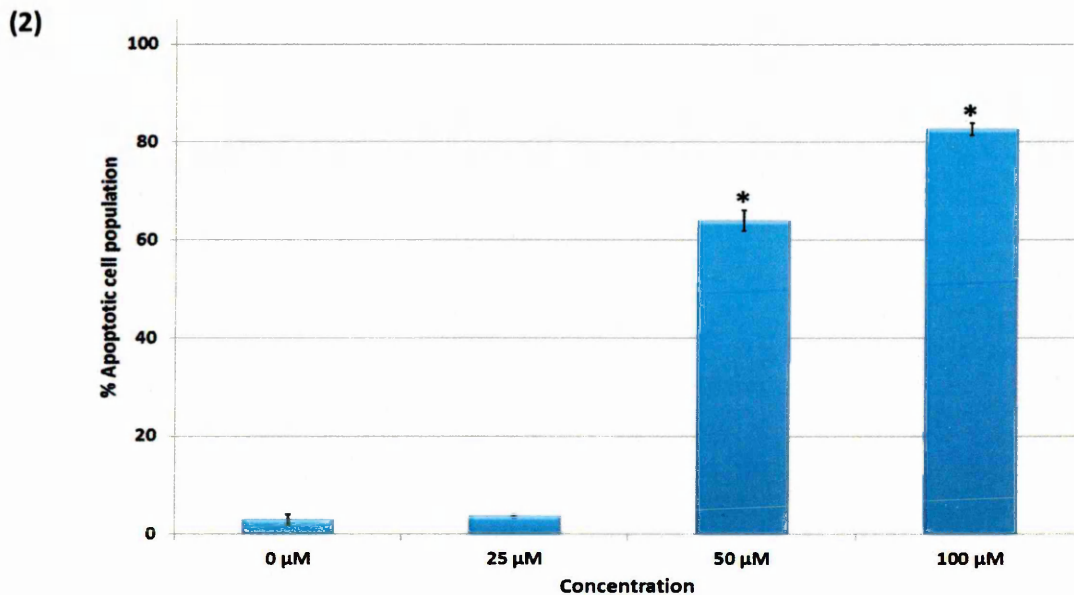
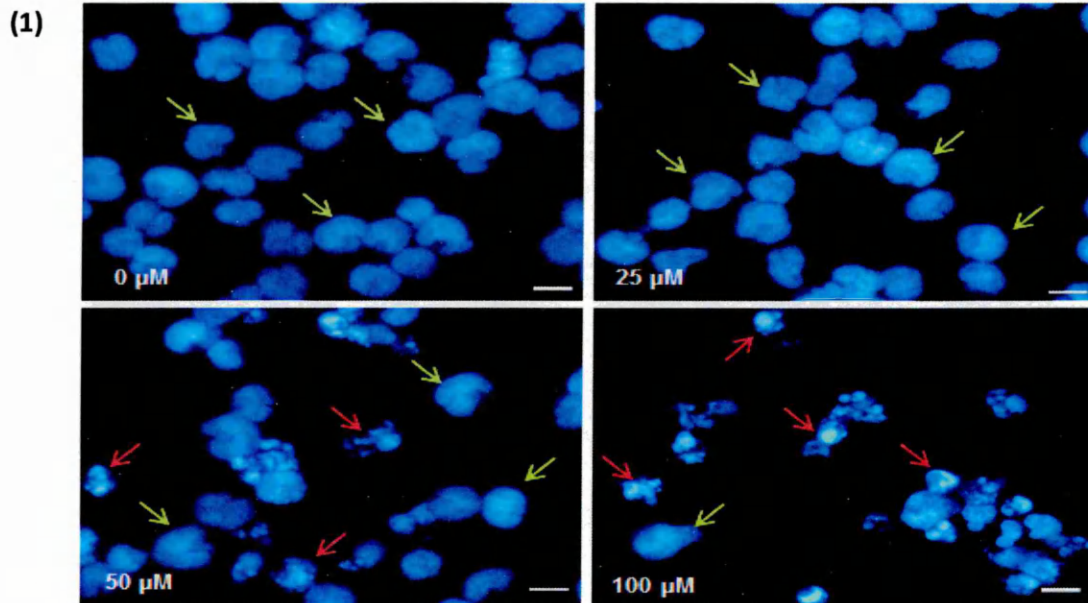


Figure 6.27: (1) Morphological staining analysis of MOLT-3 with DAPI treated with delphinidin 25, 50, and 100 μM for 24 h. Live cells are indicated by the green arrows, and apoptotic cells are indicated by the red arrows. **(2)** Percentage of apoptotic cells determined from DAPI morphological assessment following treatment with delphinidin at concentration 25, 50, and 100 μM for 24 h. * indicates significant difference ($P \leq 0.05$) vs. untreated control. Scale bar = 12.5 μm . $n=3$.

HL-60

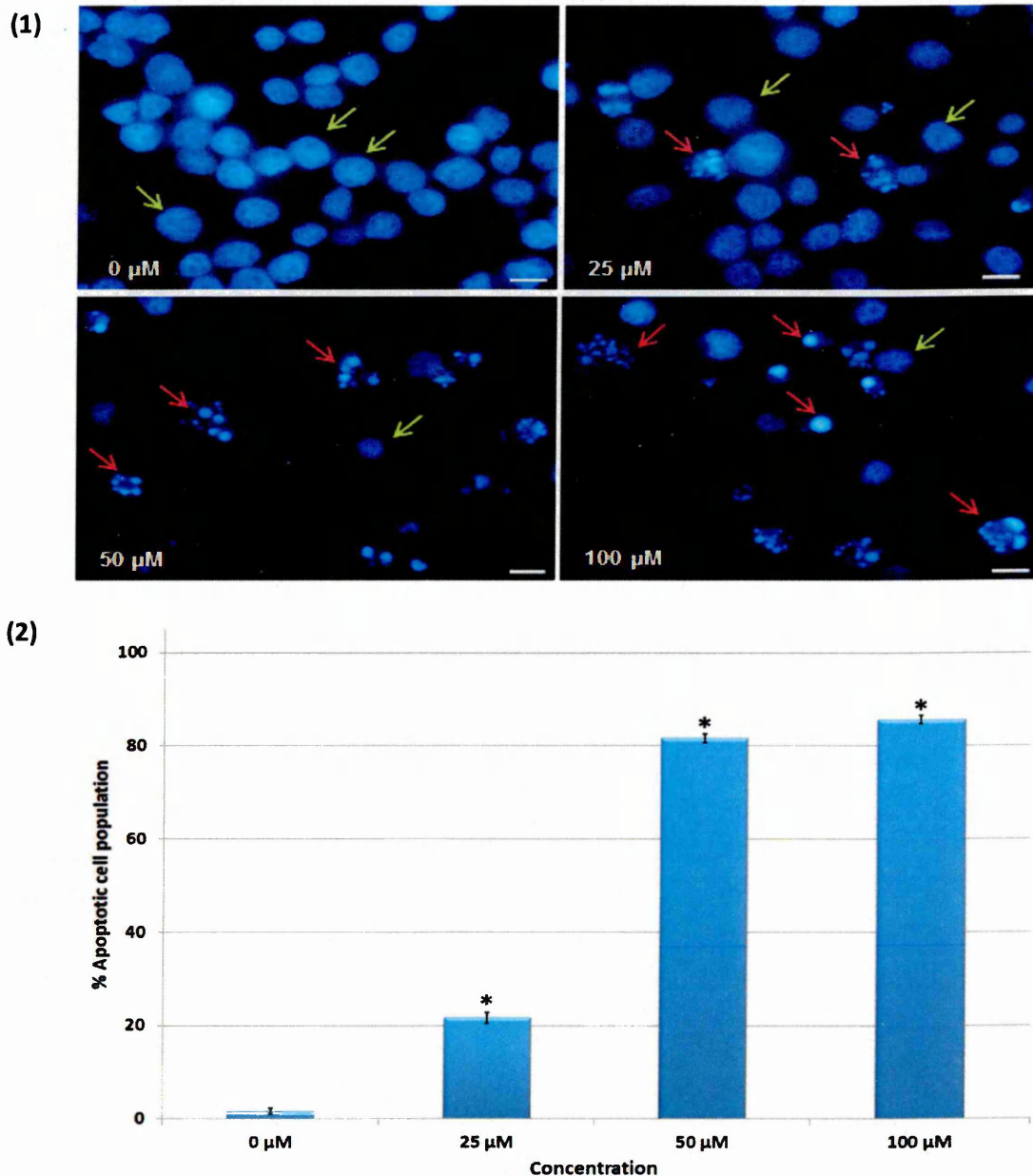
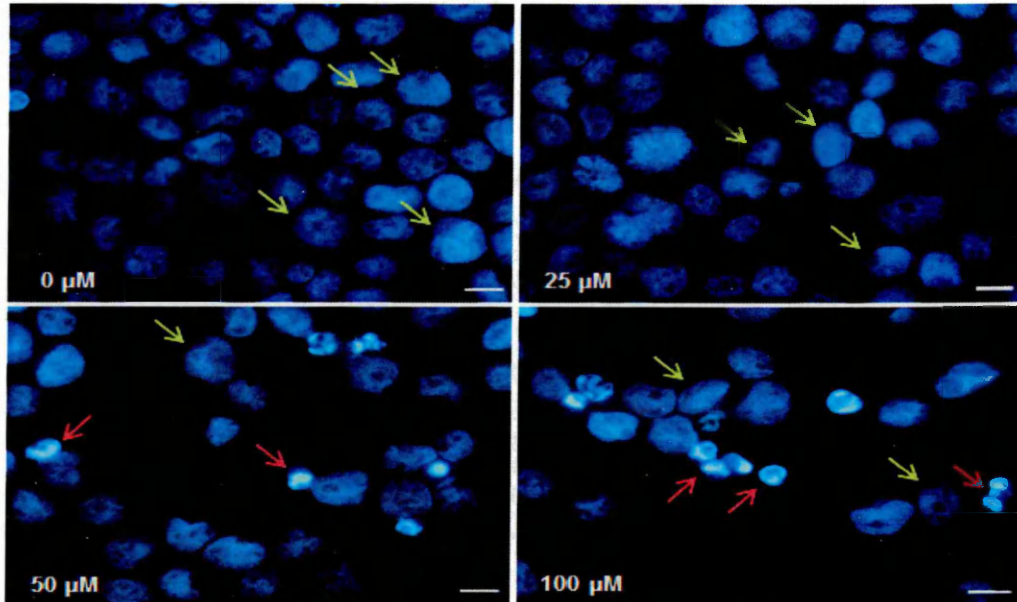


Figure 6.28: (1) Morphological staining analysis of HL-60 with DAPI treated with delphinidin 25, 50, and 100 μM for 24 h. Live cells are indicated by the **green arrows**, and apoptotic cells are indicated by the **red arrows**. **(2)** Percentage of apoptotic cells determined from DAPI morphological assessment following treatment with delphinidin at concentration 25, 50, and 100 μM for 24 h. * indicates significant difference ($P \leq 0.05$) vs. untreated control. Scale bar = 12.5 μm . n = 3.

THP-1

(1)



(2)

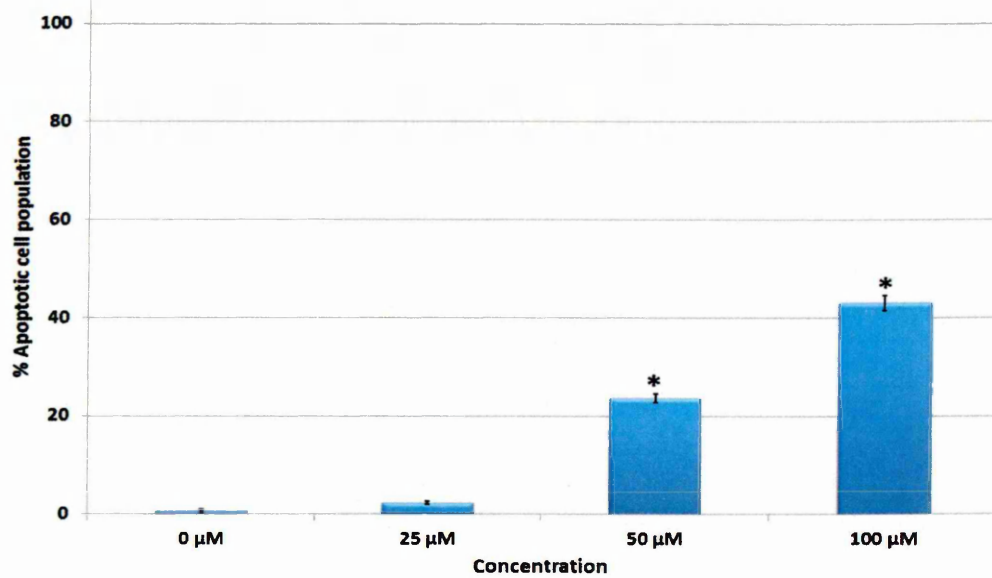


Figure 6.29: (1) Morphological staining analysis of THP-1 with DAPI treated with delphinidin 25, 50, and 100 μM for 24 h. Live cells are indicated by the green arrows, and apoptotic cells are indicated by the red arrows. **(2)** Percentage of apoptotic cells determined from DAPI morphological assessment following treatment with delphinidin at concentration 25, 50, and 100 μM for 24 h. * indicates significant difference ($P \leq 0.05$) vs. untreated control. Scale bar = 12.5 μm. n = 3.

6.4.5 Effect of Delphinidin on Cell Cycle Arrest within Leukaemia Cell

Lines

To evaluate the effect of delphinidin treatment on the distribution of cells in phases of cell cycle, DNA cell cycle analysis by flow cytometry was performed. Delphinidin treatment at concentrations 25, 50, and 100 μM resulted in a dose-dependent accumulation of cells in S phase, in all leukaemia cell lines (CCRF-CEM, MOLT-3, HL-60, and THP-1).

CCRF-CEM cells showed a significant accumulation of cells in S phase, and a significant ($P \leq 0.05$) decrease in the G_0/G_1 phase, at all delphinidin concentrations (25, 50, and 100 μM) at 24 h (Figure 6.30). MOLT-3 cells exhibited similar pattern as CCRF-CEM cells, however, the significant accumulation of cells at S phase was only seen at concentrations of 50 and 100 μM of delphinidin following 24 h treatments (Figure 6.30). The myeloid cell lines HL-60 and THP-1, showed a significant ($P \leq 0.05$) accumulation of cells in S phase corresponding with a decrease in the G_0/G_1 and M phases following treatment with delphinidin for 24 h (Figure 6.30).

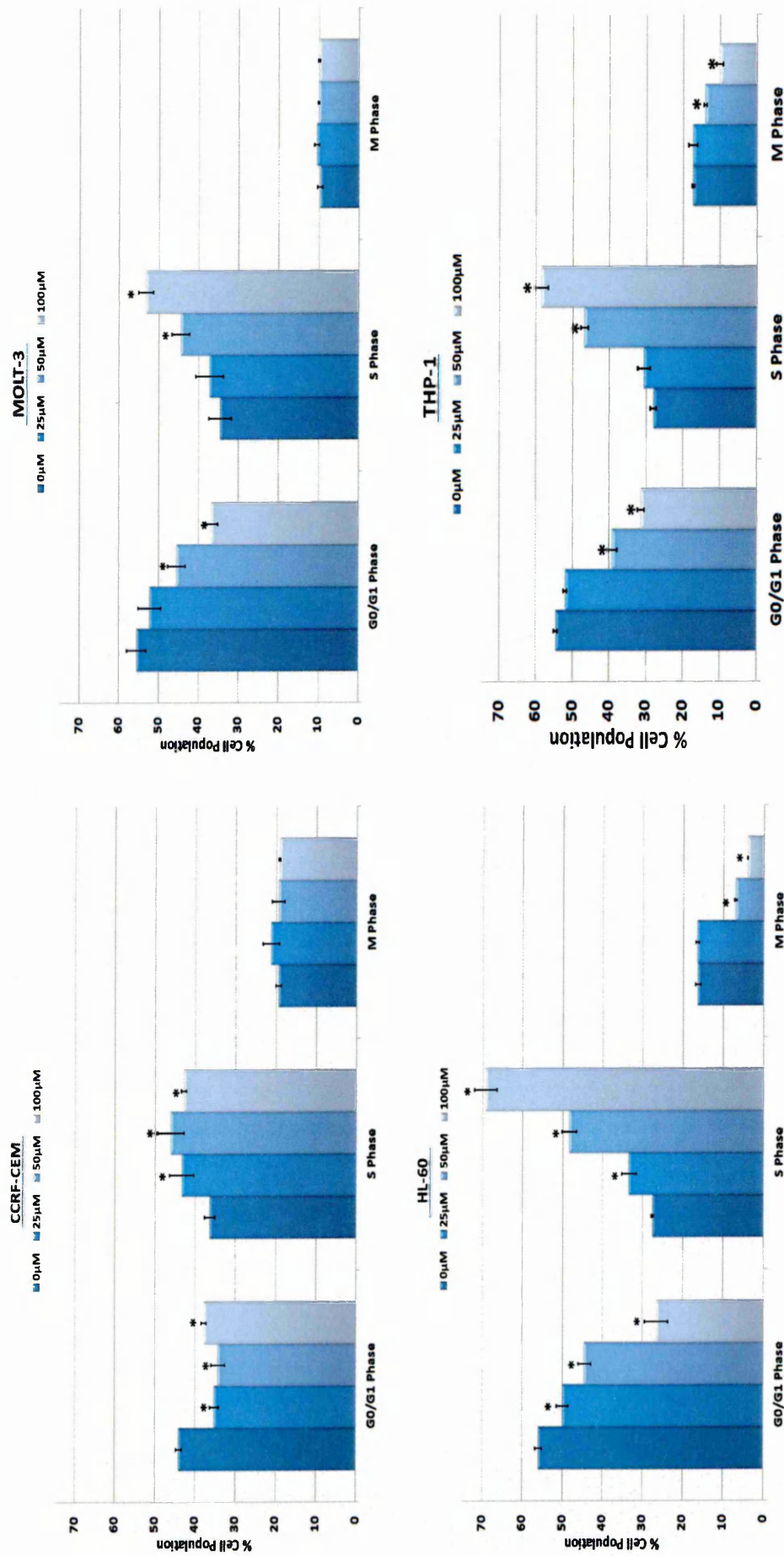


Figure 6.30: Analysis of cell cycle based on flow cytometry using FlowJo software following treatment with delphinidin at concentration 25, 50, and 100 μM for 24 h incubation on four leukaemia cell lines (CCRF-CEM, MOLT-3, HL-60, and THP-1). Mean ± SEM. * indicates significant difference ($P \leq 0.05$) vs. untreated control. n=3.

6.4.6 Effect of Delphinidin on Activities of Caspase-8 and -9 in HL-60 and MOLT-3

In order to determine whether delphinidin activated the intrinsic or extrinsic pathway levels of caspase-8 and -9 were determined using Caspase-Glo™ 8 and 9 assays. In HL-60 cells, there was a significant time-dependent increase in caspase-8 and -9 when treated with 25 and 50 μ M (Figure 6.31). There was at least a 2-fold increase in caspase-8 and -9 activity between 3 and 6 h incubation. After 24 h, there was a decrease in both caspase-8 and -9 (Figure 6.31).

In MOLT-3 cells, delphinidin failed to stimulate both caspase-8 and -9, at 3 h incubation. At 6 h, there was increase in caspase-8 and -9 activity but was only following treatment with 25 μ M concentration. When a 50 μ M of delphinidin treatment was used more than 3.5 fold increase in both caspases. At 24 h, a decrease in both caspases was observed (Figure 6.32).

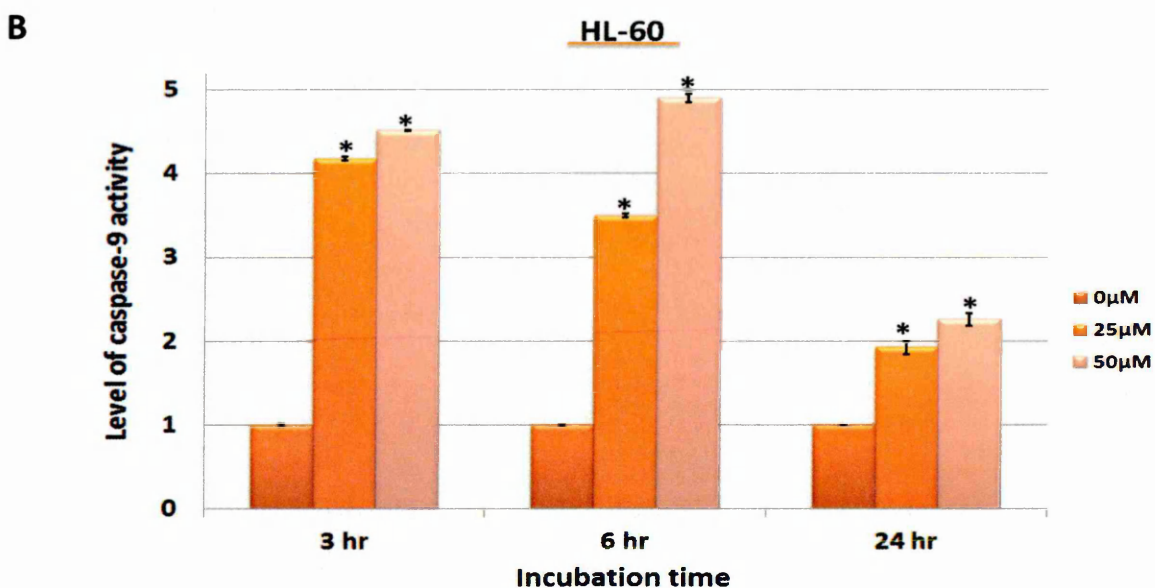
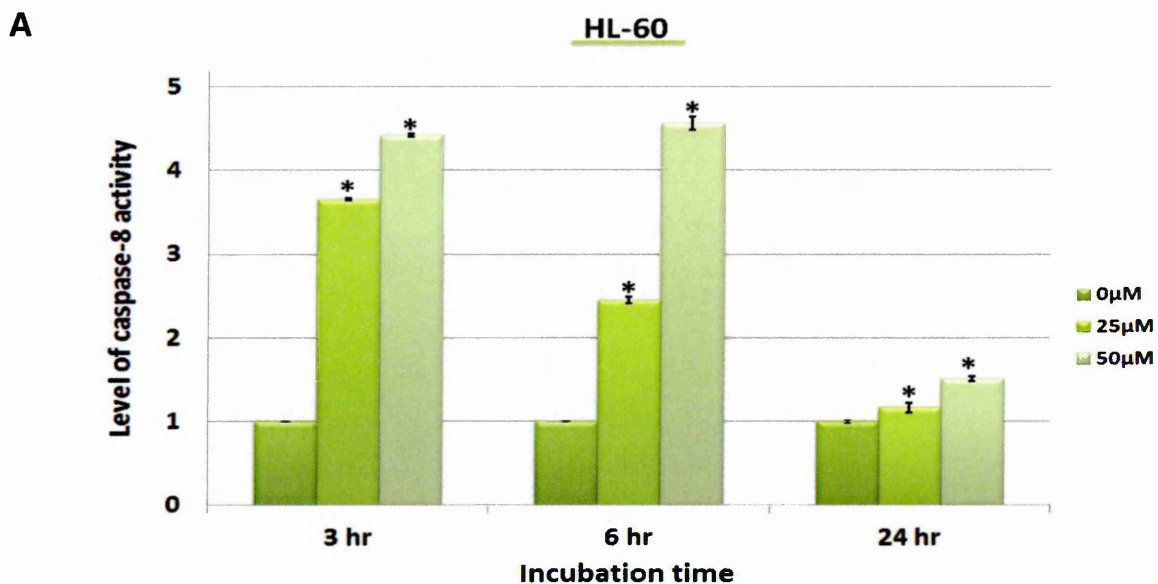


Figure 6.31: Effect of delphinidin on activation of caspase-8 (A) and caspase-9 (B). HL-60 cells were treated with delphinidin at concentration 25 and 50 μM for 3, 6, and 24 h. Caspase-8 and -9 activities were investigated using Caspase-Glo™ 8 and 9 Assays. Level of both caspases activities normalized to control and presented as means ± standard error. * indicates significant difference ($P \leq 0.05$) vs. untreated control. n= 3.

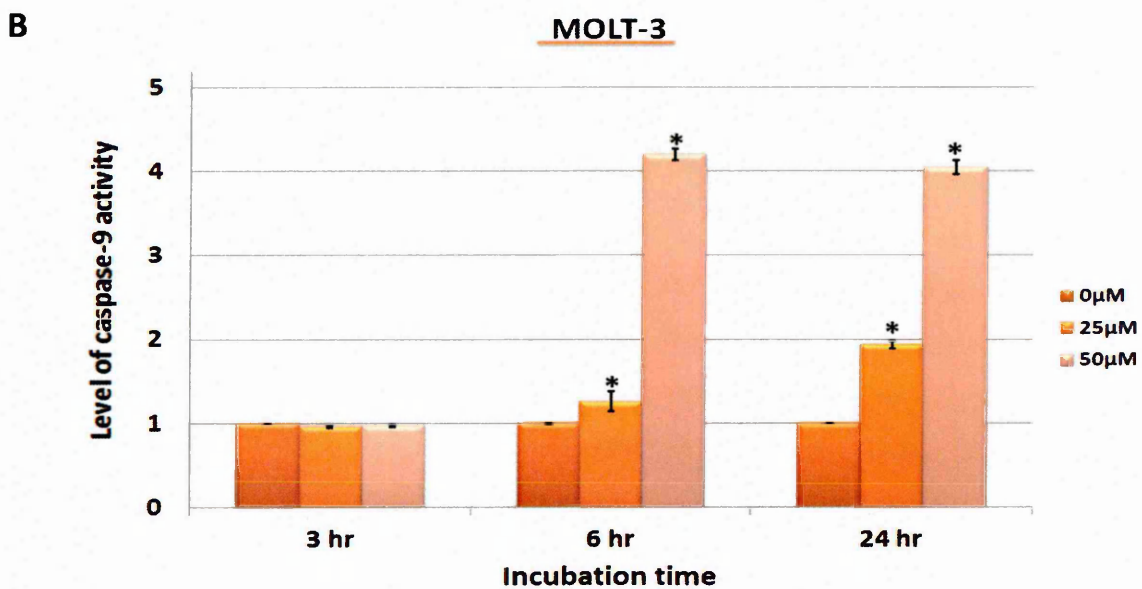
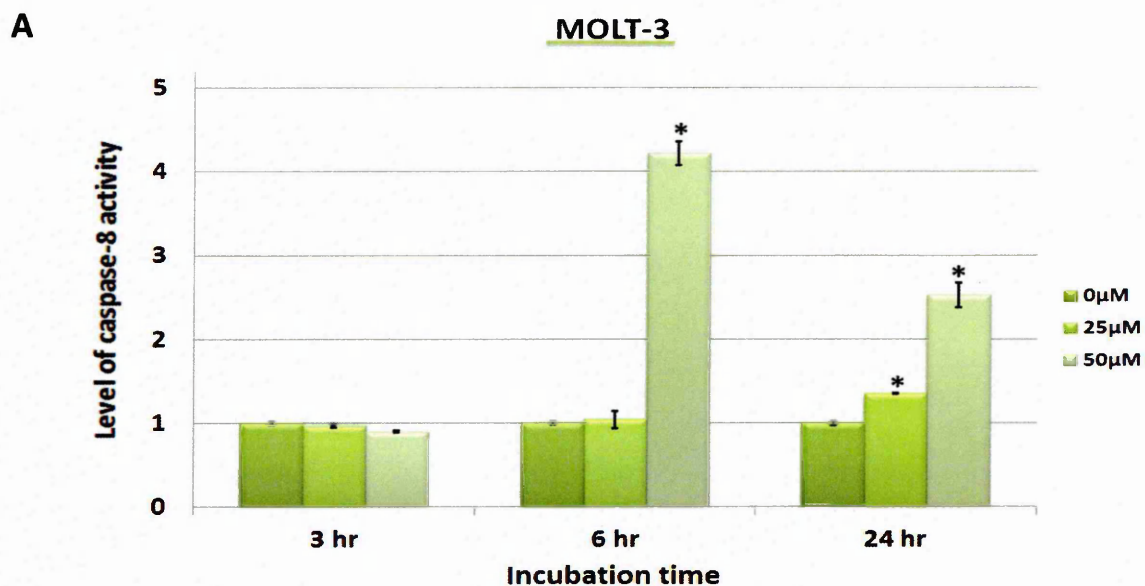


Figure 6.32: Effect of delphinidin on activation of caspase-8 (A) and caspase-9 (B). MOLT-3 cells were treated with delphinidin at concentration 25 and 50 μM for 3, 6, and 24 h. Caspase-8 and -9 activities were investigated using Caspase-Glo™ 8 and 9 Assays. Level of both caspases activities normalized to control and presented as means ± standard error. * indicates significant difference ($P \leq 0.05$) vs. untreated control. n= 3.

6.4.7 Effect of Delphinidin on Expression of Cytochrome C in HL-60 and MOLT-3 Cells

Cytochrome *c* is normally expressed in the cells binding to the inner membrane of the mitochondria. In response to pro-apoptotic stimuli it is released from the mitochondria to the cytosol. Thus, when using a specific antibody it is possible to demonstrate the expression, and translocation of cytochrome *c* as a dark brown staining. In cells with inactive cytochrome *c* this appears as a pale brown colour.

The number of cells displaying active cytochrome *c* was significantly ($P \leq 0.05$) increased in HL-60 cells following 3, 6, and 24 h in a dose dependent manner (Figure 6.33 and 6.37). In MOLT-3 cells the number of active cytochrome *c* cells was significantly ($P \leq 0.05$) increased after 6 and 24 h treatment, with 50 μM delphinidin (Figure 6.34 and 6.37).

6.4.8 Effect of Delphinidin on Expression of Smac/Diablo in HL-60 and MOLT-3 Cells

Smac/Diablo is a mitochondrial pro-apoptotic protein, which is found in an inactive form within normal cells, within active cells an increased intensity was seen indicating the release from the mitochondrial membrane.

Smac/Diablo immunopositivity was also significantly increased following 3, 6, and 24 h treatment with 50 μM of delphinidin ($P \leq 0.05$). At 6 h, there was a 44% increase in Smac/Diablo activity, this was greater than that seen in controls and the earlier 1 and 3 h time points (Figure 6.35 and 6.38). In MOLT-3 cells the number of active Smac/Diablo cells was also significantly increased after 6 and 24 h treatment with 50 μM delphinidin (Figure 6.36 and 6.38) ($P \leq 0.05$).

Cytochrome C

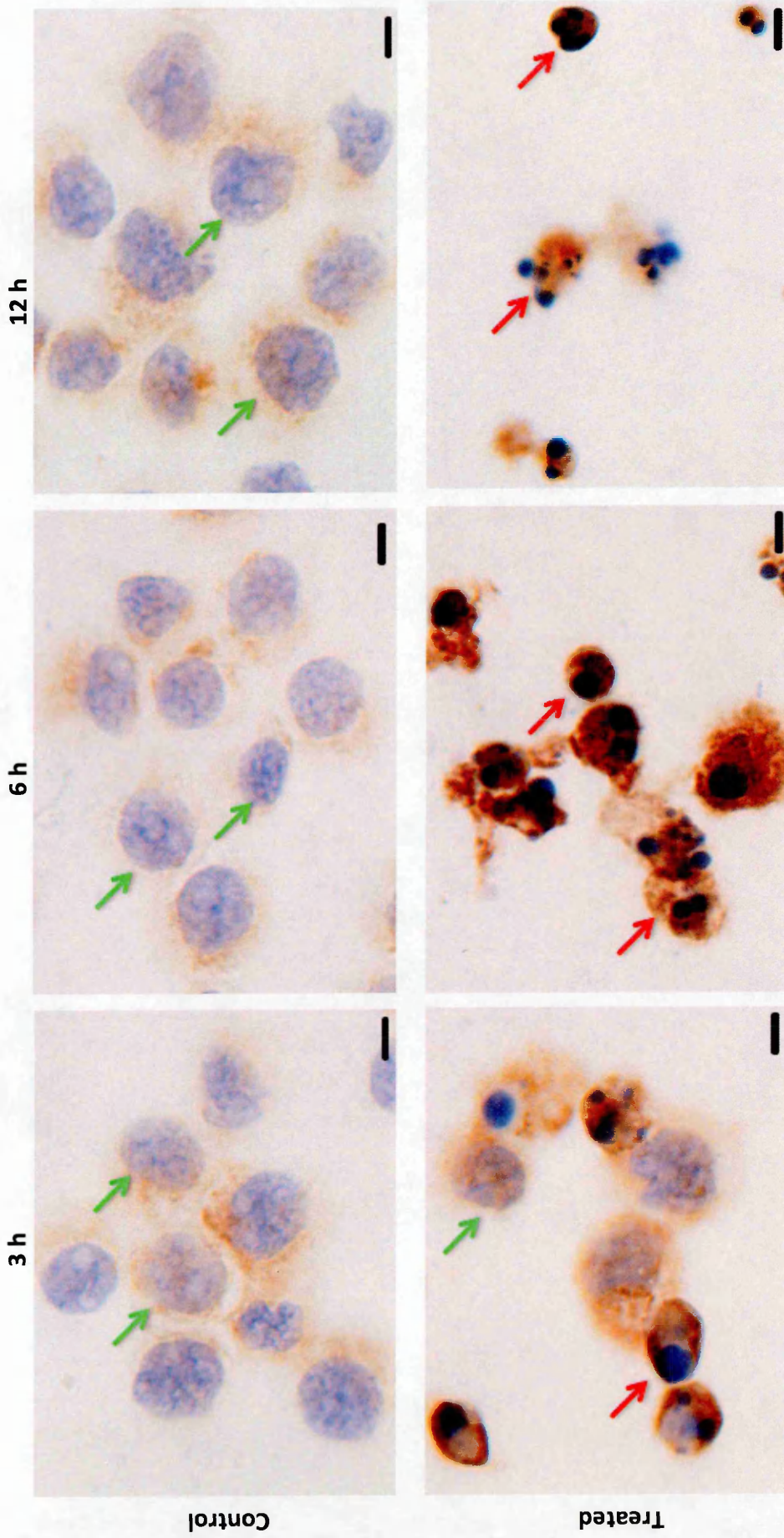


Figure 6.33: Effect of delphinidin (50 μM) on the expression of cytochrome C on HL-60 leukaemia cells following 3, 6, and 24 h treatment. The result of untreated cells was normalized to 1. Results were significant to the control sample when $P \leq 0.05$. Active cells indicated by **green arrows**. Inactive cells indicated by **red arrows**. Scale bar = 12.5 μm . n = 3.

Cytochrome C

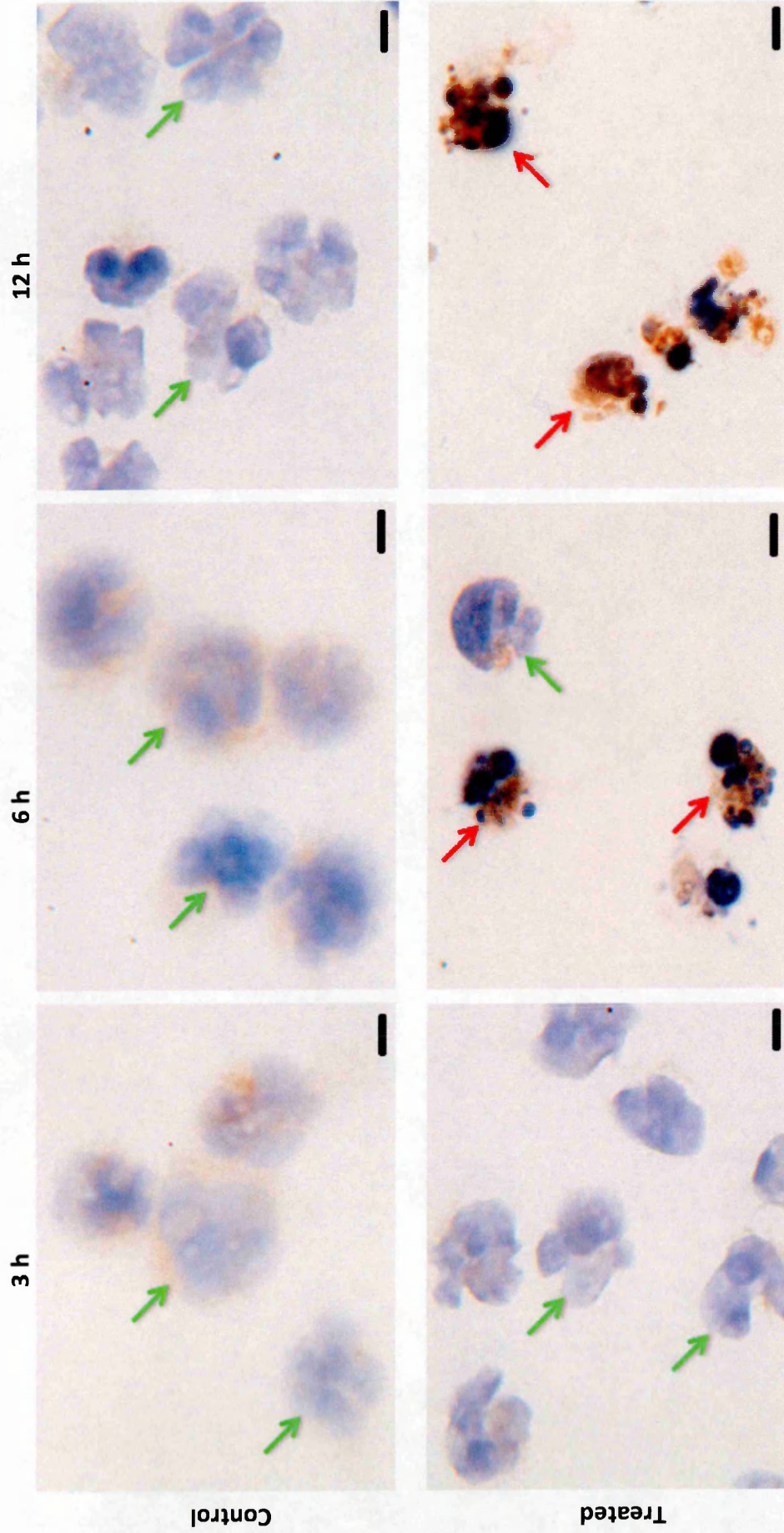


Figure 6.34: Effect of delphinidin (50 μM) on the expression of cytochrome C on MOLT-3 leukaemia cells following 3, 6, and 24 h treatment. The result of untreated cells was normalized to 1. Results were significant to the control sample when $P \leq 0.05$. Active cells indicated by **green arrows**. Inactive cells indicated by **red arrows**. Scale bar = 12.5 μm . n= 3.

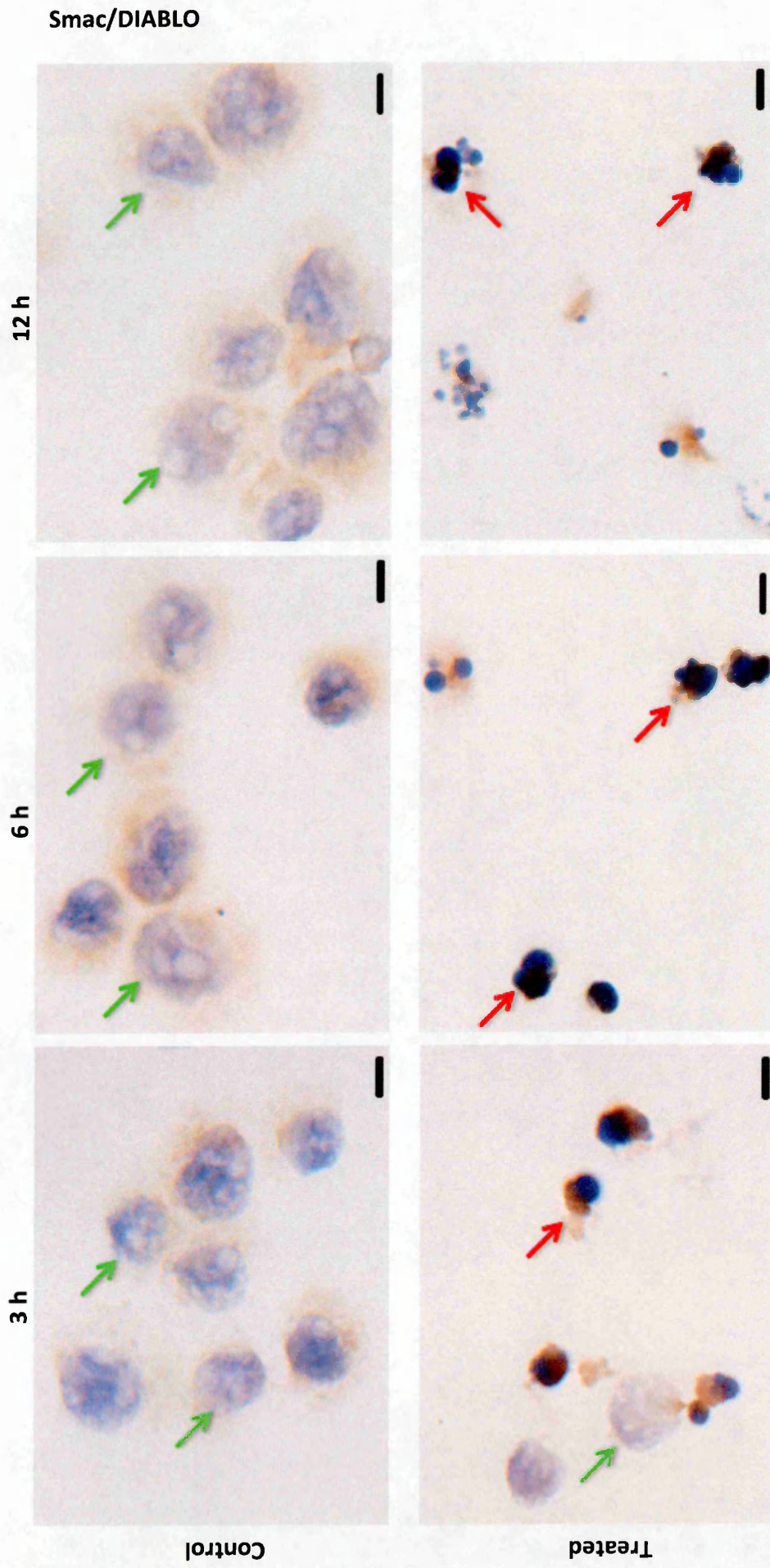


Figure 6.35: Morphological analysis of effect of delphinidin (50 μM) on the expression of SMAC/DIABLO on HL-60 leukaemia cells following 3,6, and 24 h treatment. The result of untreated cells was normalized to 1. Results were significant to the control sample when $P \leq 0.05$. Active cells indicated by **red arrows**. Inactive cells indicated by **green arrows**. Scale bar = 12.5 μm . $n=3$.

Smac/DIABLO

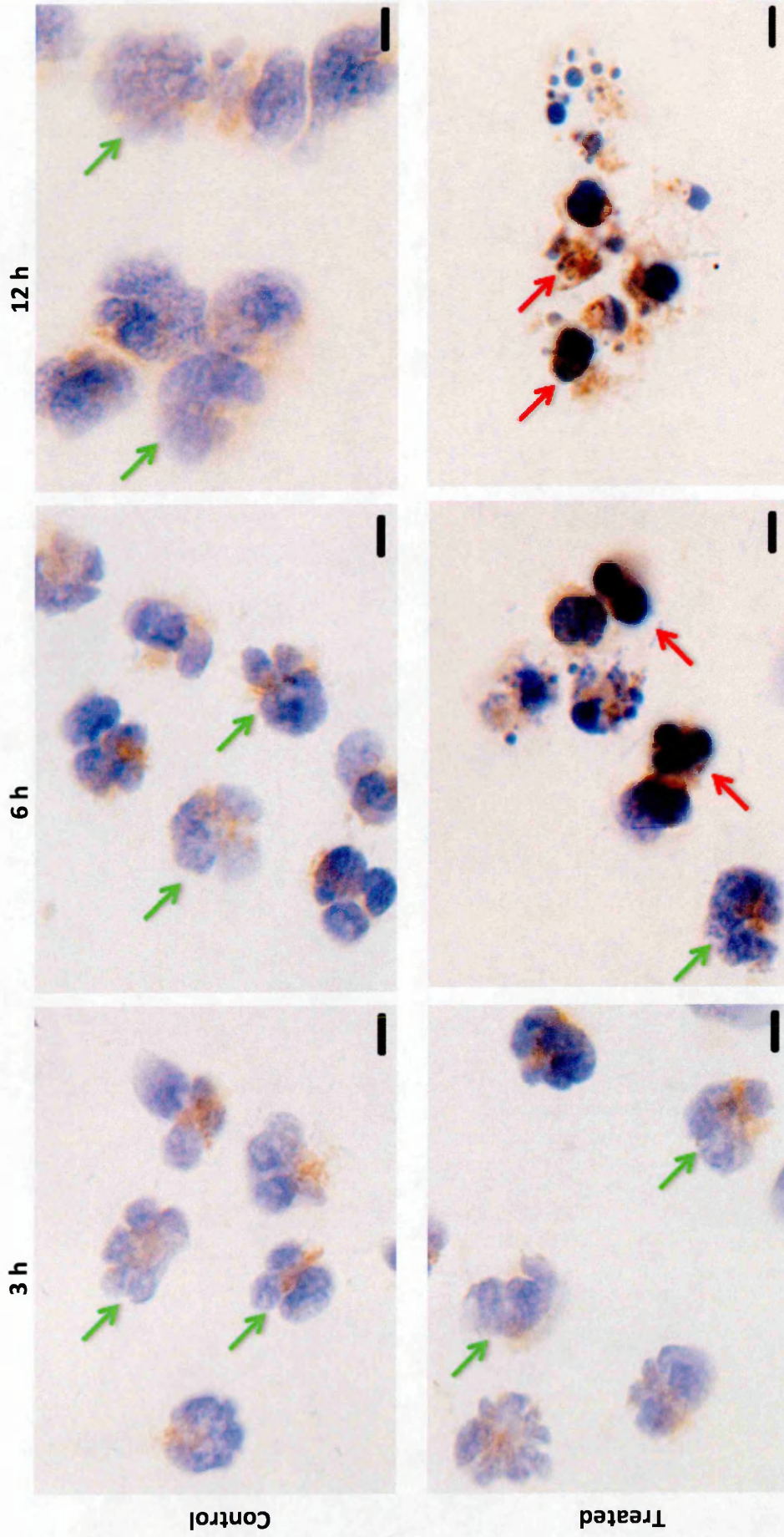


Figure 6.36: Effect of delphinidin (50 μ M) on the expression of Smac/DIABLO on MOLT-3 leukaemia cells following 3, 6, and 24 h treatment. The result of untreated cells was normalized to 1. Results were significant to the control sample when $P \leq 0.05$. Active cells indicated by **red arrows**. Inactive cells indicated by **green arrows**. Scale bar = 12.5 μ m. n=3.

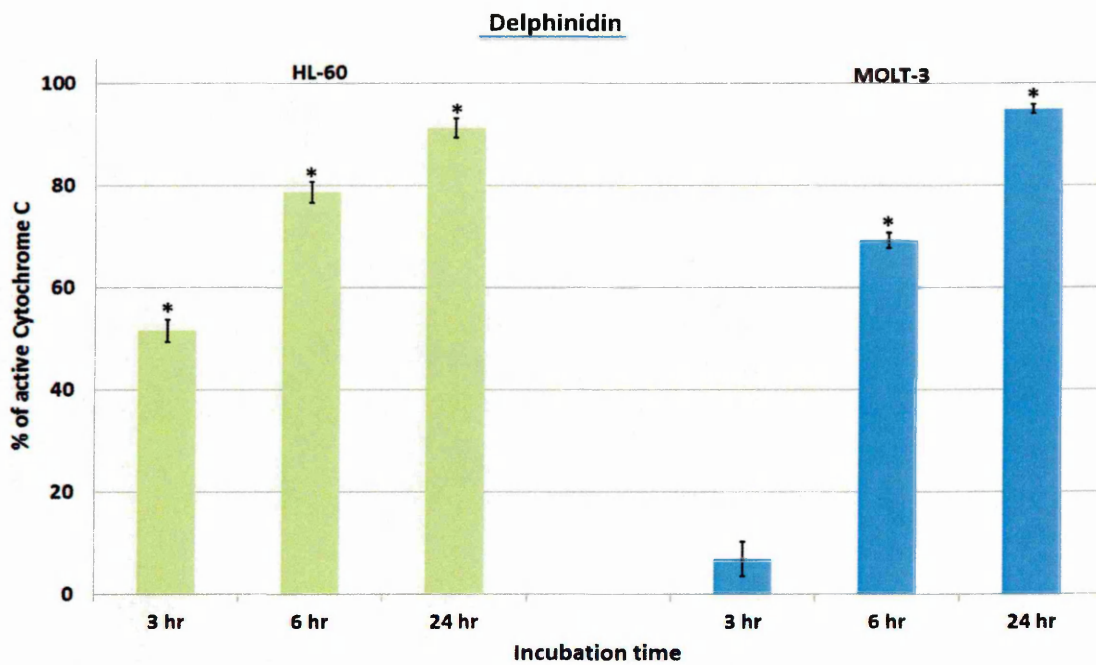


Figure 6.37: Percentage of active cytochrome C in HL-60 and MOLT-3 cells determined from ICC morphological assessment following treatment with delphinidin at 50 μ M for 3, 6, and 24 h normalized to untreated controls. Mean \pm SEM. * indicates significant difference ($P \leq 0.05$) vs. untreated control. n= 3.

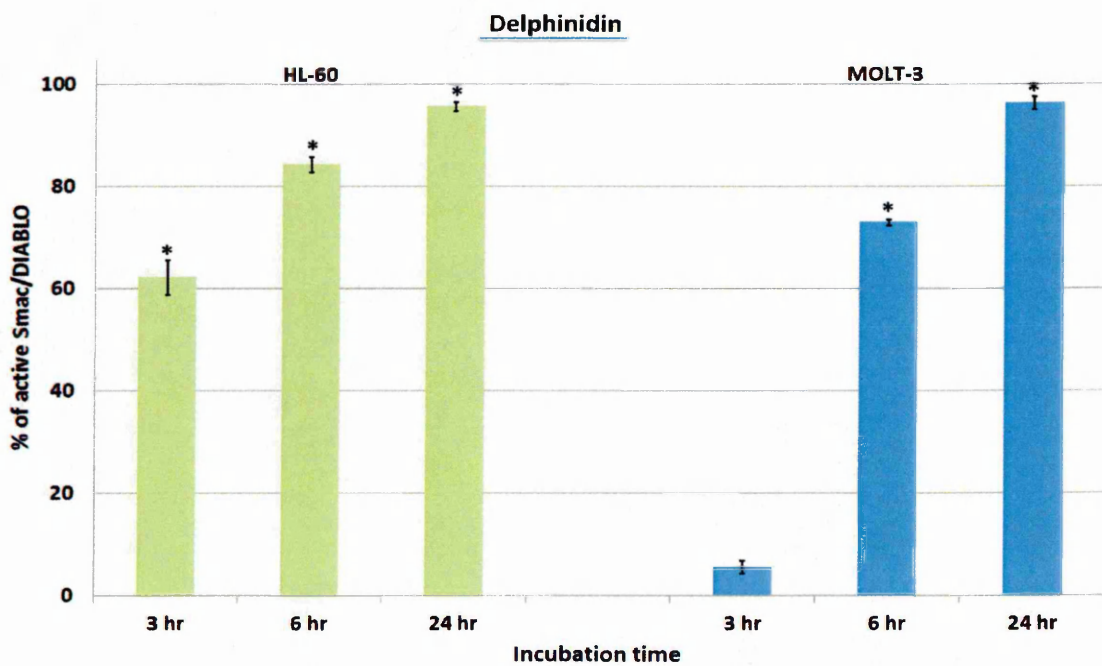


Figure 6.38: Percentage of active Smac/DIABLO in HL-60 and MOLT-3 cells determined from ICC morphological assessment following treatment with delphinidin at 50 μ M for 3, 6, and 24 h normalized to untreated controls. Mean \pm SEM. * indicates significant difference ($P \leq 0.05$) vs. untreated control. n= 3.

6.4.9 Effect of Delphinidin on the Expression of Pro-Apoptotic Proteins (BAX and BAD) and Anti-Apoptotic Proteins (Bcl-2 and Bcl-xl)

The effect of delphinidin on the mRNA expression of pro-apoptotic proteins (BAX and BAD) and anti-apoptotic proteins (Bcl-2 and Bcl-xl) on two leukaemia cell lines (HL-60 and MOLT-3) was investigated. Delphinidin (50 μ M) up-regulated the mRNA expression of Bax and Bad (4.6-fold and 4.4-fold respectively) on HL-60 cells following 6 h treatment. In addition, mRNA expression for Bcl-2 and Bcl-xl were significantly down-regulated (6.2-fold and 6.6-fold respectively) in HL-60 cells following treatment with 50 μ M delphinidin for 6 h (Figure 6.39).

Similarly in MOLT-3 cells treatment with delphinidin (50 μ M) resulted in up-regulated of the mRNA expression of BAX and BAD (4.1-fold and 3.5-fold respectively) and down-regulated the mRNA expression of Bcl-2 and Bcl-xl (5.8-fold and 5.6-fold respectively) following 6 h treatment (Figure 6.40).

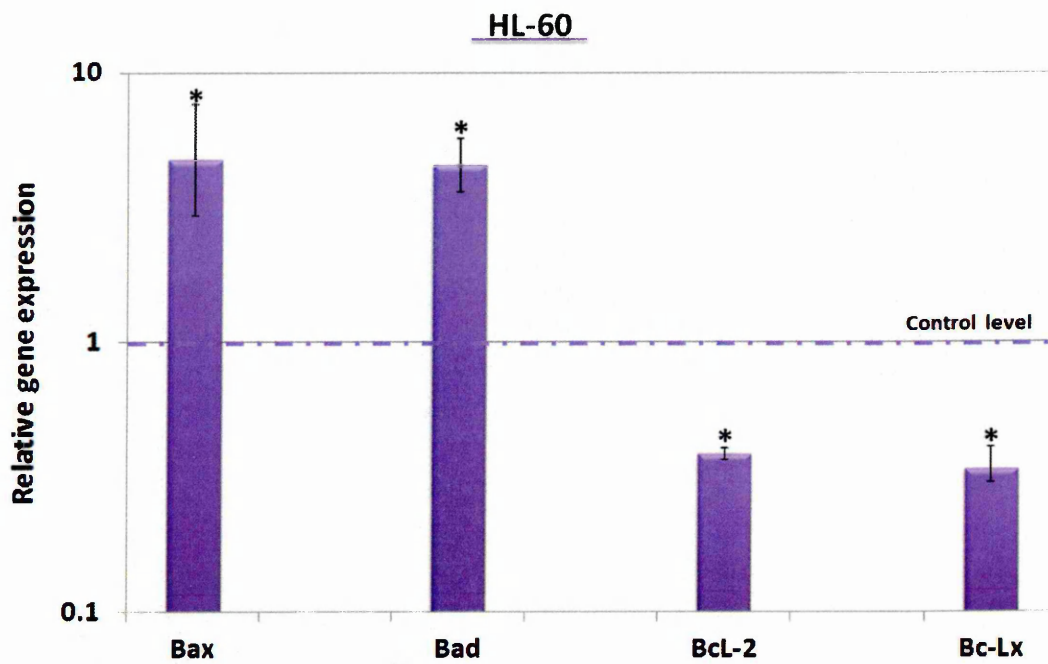


Figure 6.39: Effect of delphinidin (50 μ M) on the mRNA expression of pro-apoptotic protein (BAX and BAD) and anti-apoptotic proteins (Bcl-2 and Bcl-xl) on HL-60 leukaemia cells following 6 h treatment. The result of untreated cells was normalized to 1. Results were significant to the control sample when $P \leq 0.05$. $n = 3$.

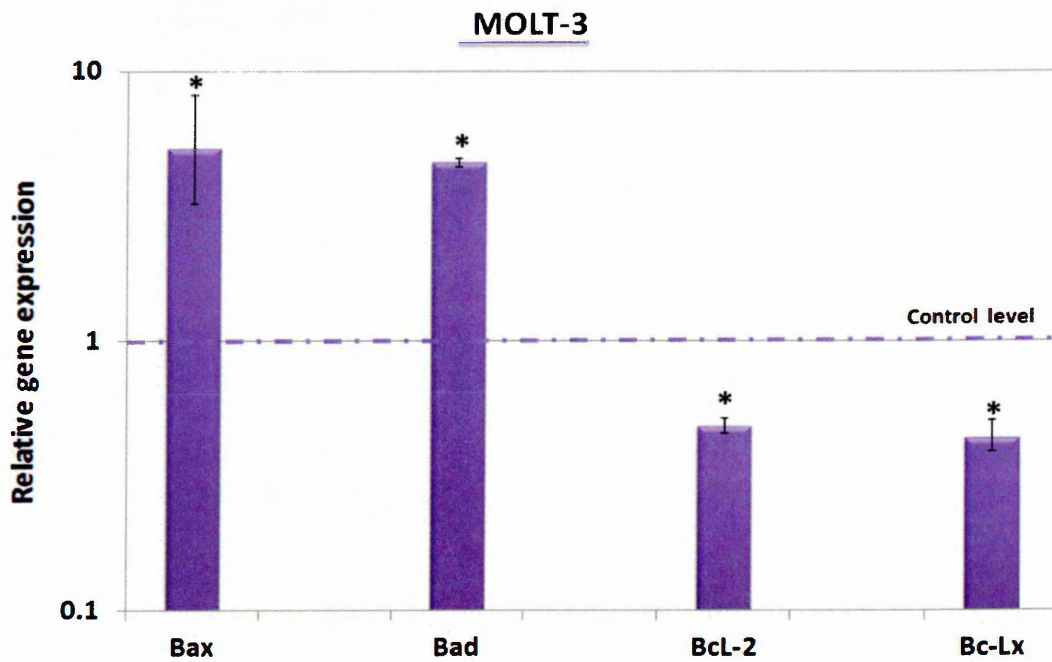


Figure 6.40: Effect of delphinidin (50 μ M) on the mRNA expression of pro-apoptotic protein (BAX and BAD) and anti-apoptotic proteins (Bcl-2 and Bcl-xl) on MOLT-3 leukaemia cells following 6 h treatment. The result of untreated cells was normalized to 1. Results were significant to the control sample when $P \leq 0.05$. $n = 3$.

6.5 Discussion:

This study showed for the first time that delphinidin, cyanidin, and pelargonidin, were capable of reducing ATP levels in all four leukaemia cell lines investigated.

Delphinidin was the most potent anthocyanins studied, suggesting that its ortho-hydroxyphenyl structure is critical for its activity. Consistent with our results Katsube *et al*, (2003) demonstrated that anthocyanidins could reduce cell proliferation of HCT116 colon cell line. Their anti-proliferative effects in order of effectiveness were: delphinidin > cyanidin > peonidin > pelargonidin > malvinidin in HCT116 cells. Similarly, six anthocyanidins were shown to inhibit TPA-induced JB6 mouse epidermal cell transformation and AP-1 transcription activity (Hou *et al*, 2004). Delphinidin was shown to be the most effective having a greater activity than petunidin, cyanidin, pelargonidin, malvinidin, and peonidin (Hou *et al*, 2004). It was concluded that the ortho-dihydroxyphenyl structure at the B-ring found in delphinidin was essential for apoptosis (Hou *et al*, 2003). Meiers *et al*. (2001) reported that cyanidin and delphinidin contain hydroxyl groups, whilst malvinidin did not. Cyanidin and delphinidin induced higher inhibitory effects on the growth of human vulva carcinoma cell line A431 *in vitro* (Meiers *et al*, 2001).

6.5.1 Delphinidin is the most active Anthocyanin on Leukaemia Cells

Delphinidin showed the greatest induction of apoptosis compared with cyanidin and pelargonidin in all four leukaemia cell lines (CCRF-CEM, MOLT-3, HL-60, and THP-1). However, there was differential sensitivity shown between them. Similarly delphinidin induced apoptosis in HepG2 cells more effectively than cyanidin (Yeh and Yen, 2005). Delphinidin has also been shown to induce apoptosis in different cancer cell lines including breast (AU-565 cells) (Afaq *et al*, 2008); prostate (PC3 cells (Hafeez *et al*, 2008a) and PCa 22Rnu1 cells (Hafeez *et al*, 2008b)); colon (HCT-116 cells) (Yun *et al*, 2009); liver (HepG2 cells) (Yeh and Yen, 2005); uterus (Hela S3 cells) (Lazze *et al*, 2004) and leukaemia (HL-60 cells).

Here, cyanidin inhibited cell proliferation in all four leukaemia cell lines (CCRF-CEM, MOLT-3, HL-60, and THP-1), but only induced apoptosis in CCRF-CEM, MOLT-3, and HL-60 at high concentrations and failed to induce apoptosis in THP-1 cells. Several studies have reported that cyanidin in different forms (cyanidin-rutinoside, cyanidin-3-O- β -glucopyranoside and cyanidin-3-O- β -D-glucopyranoside) induced apoptosis in

oesophageal (Zikri *et al*, 2009) liver (Longo *et al*, 2008), and 6 leukaemia cell lines: (HL-60 (Feng *et al*, 2007; Fimograni *et al*, 2004); MOLT-4 (Katsuzaki *et al*, 2003); U937 (Hyun and Chung, 2004) and Jurkat cells (Fimognari *et al*, 2004)). In contrast Annalucia *et al*, (2004) demonstrated cyanidin-3-O- β -glucopyranoside failed to induce apoptosis but did decrease cellular proliferation.

Pelargonidin failed to induce apoptosis in all four leukaemia cell lines. Similarly, Katsub *et al* (2003) reported that pelargonidin failed to induce apoptosis in colon cancer cells HCT-116 (Katsub *et al*, 2003). Yeh and Yen (2005) showed that delphinidin and cyanidin induced apoptosis in HepG2 cells whilst pelargonidin did not induce apoptosis.

6.5.2 Effect of Sugar Molecules

This study showed that the anthocyanidins exhibited greater anti-proliferative and pro-apoptotic effects than their glycosylated counterparts: the anthocyanins. Shish *et al* (2005) also reported that cyanidin and pelargonidin show stronger inhibitory effects on human gastric adenocarcinoma than their glycosidic forms: cyanidin-3-glucose and pelargonidin-3-glucose. The current study also showed the number of glucoside groups affected their activity, with mono-glycoside being more potent inhibitors of cellular proliferation and inducers of apoptosis than di-glycosides. This result agrees with previous work (Chapter 5), which showed that rutin illustrated less inhibitory effect on ATP levels than its aglycon form, quercetin. This data suggests that glycosylation of the anthocyanins inhibit their biological activities. Few studies have been conducted to investigate the relationship between structure and function of glycosylated anthocyanins. Jing *et al*. (2008) studied the relationship between chemical characteristics of anthocyanins and their biological activity. Demonstrating that anthocyanins with structure properties of mono-glycoside were stronger inhibitors of cell proliferation in HT-29 colon cells than their tri-glycosylated counterparts (Jing *et al*, 2008). Similarly it has been found that cyanidin and pelargonidin showed greater anti-proliferative capabilities than cyanidin-3-glucoside and pelargonidin-3-glucose on human gastric adenocarcinoma AGS cells (Shish *et al*, 2005). Koide *et al*. (1997) reported that an extract containing mostly cyanidin-glucoside and cyanidin-rhamnoside was more effective in suppressing the HCT15 colon cells growth *in vitro* than the extract rich in cyanidin-rhamnoside, suggesting that anthocyanin chemical structure has an effect on inhibiting cell growth (Koide *et al*, 1997).

The results indicated that potency of cancer chemoprevention of anthocyanins including inhibition of ATP levels and induction of apoptosis is associated with the number of hydroxyl groups on the B-ring and sugar units. These factors have also been reported to have an effect on antioxidant activity which plays an important role in cancer treatment (Kahkonen and Heinonen, 2002). Noda *et al* (2002) reported that delphinidin has more potent antioxidant activity than cyanidin and pelargonidin. In addition, studies suggest that glycosidic forms generally display a decrease in the antioxidant capacity when compared with the corresponding aglycon. This may be due to the steric hindrance conferred by the bulky sugars (Satue-Garcia *et al*, 1997; Tsuda *et al*, 1994).

Delphinidin was the most potent compound inhibiting cell proliferation and inducing apoptosis in a dose dependent manner to a greater extent than cyanidin and pelargonidin and thus was selected for further investigation.

6.5.3 Regulation of Cell Cycle by Delphinidin

Studies have shown the involvement of cell cycle regulation in inhibiting cell growth. Here, delphinidin treatment of CCRF-CEM, MOLT-3, HL-60 and THP-1 cells resulted in arrest of cells in S phase. Similarly, Lazze, *et al.*, (2004) showed that exposure of human uterus cancer cells (Hela S3) to delphinidin caused S phase arrest. Whilst G₂/M phase arrest has been shown in breast cancer cells (MCF-7) (Nguyen *et al*, 2010; Chen *et al*, 2005) and (HS578T), and colon cancer cells (HCT-116) (Yun *et al*, 2009). Previously S phase arrest was also observed following treatment with PJ (Chapter 3) (Dahlawi *et al*, 2011) and acetonitrile fractions (Chapter 4) (Dahlawi *et al*, 2013) in the same cell lines tested here, indicating that delphinidin may be one of the major components in PJ.

6.5.4 Molecular Mechanism of Apoptosis Induction by Delphinidin

Here, caspase-3 activity was increased in all four leukaemia cell lines following treatment with delphinidin. This finding is supported by the work of Hou *et al.* (2005) who showed that treatment with delphinidin-3-sambubioside at a concentration of 100 µM induced caspase-3 activity in human promyelocytic HL-60 cells. Delphinidin has also been shown to induce caspase-3 in human colon (HCT-116) (Yun *et al*, 2009), breast (Human EGFR positive AU-565) (Afaq *et al*, 2008), and prostate (Androgen refractory human PCa 22Rnu 1) (Hafeez *et al*, 2008b), (PC3), and (human androgen-dependent LNCaP) (Hafeez *et al*, 2008b) cancer cell lines.

Delphinidin was shown here to induce activation of both caspase-8 and -9 in MOLT-3 and HL-60 cells, suggesting activation of both intrinsic and extrinsic apoptosis pathways by delphinidin. This has also been reported in delphinidin-3-sambubioside treated HL-60 cells (Hou *et al*, 2005) and delphinidin treated colon cancer cells (HCT-116) (Yun *et al*, 2009). In addition the current study showed that delphinidin treatment increased the expression of cytochrome *c* in HL-60 and MOLT-3 cells. Consistent with our results, Hou *et al* (2005) reported that cytochrome *c* release was observed in HL-60 cells following treatment with delphinidin-3-sambubioside. Release of cytochrome *c* was also observed in leukaemia cells (HL-60) and in hepatic cancer cells (PLC/PRF/5) following treatment with a mixture of anthocyanins (Change *et al*, 2005; Longo *et al*, 2008).

In addition, delphinidin treatment of MOLT-3 and HL-60 cells caused release of Smac/Diablo from the mitochondria. Khan *et al*. (2008) found that flavonoid treatment, fisetin, resulted in inhibition of IAP and induction of apoptosis via Smac/Diablo in prostate cancer cells (LNCaP).

A decrease in Bcl-2 and Bcl-Xl and an increase in Bax and Bad mRNA in MOLT-3 and HL-60 cells following treatment with delphinidin was also seen further supporting the activation of the intrinsic pathway of apoptosis.

The activation of both intrinsic and extrinsic apoptosis by delphinidin has also been shown in breast cancer cells (MCF-7) Kue *et al*, (2004). Together with studies showing intrinsic and extrinsic apoptosis by anthocyanins extracted from different fruits (Change *et al*, 2005; Reddivari *et al*, 2007).

6.6 Conclusion

Anthocyanins activity was found to be dependent on the ortho-hydroxyphenyl structure and the most potent glycosidic form of the anthocyanins with proliferation and apoptosis effects seen in anthocyanins with greatest hydroxyl groups and least glycosidic form, namely delphinidin. Delphinidin induced apoptosis through intrinsic and extrinsic pathways. Suggesting that delphinidin may have potential for use as a chemotherapeutic agent against leukaemia.

7. Induction of apoptosis and cell cycle arrest following stimulation with EGCG, Gallic acid, quercetin and punicalagin.

7.1 Introduction

Pomegranates have been shown to be a rich source of a wide variety of bioactive compounds amongst these compounds, EGCG; gallic acid; quercetin and punicalagin were identified as demonstrating potent decreases in ATP levels in leukaemia cell lines (Chapter 5). To determine whether the decrease in ATP levels by these compounds was due to apoptosis or cell cycle arrest these agents were investigated further.

EGCG is a flavan-3-ol and is the major polyphenolic agent in green tea, which has been shown to have potential as a chemopreventive agent for a number of cancers (Cimino *et al*, 2012). Previously EGCG was shown to be the most potent compound among other flavan-3-ol agents tested (Chapter 5). *In vitro* EGCG induces apoptosis and cell cycle arrest in many cancer cells without affecting normal cells (Paschtka *et al*, 1998; Ahmad *et al*, 2000; Ahn *et al*, 2003; Salucci *et al*, 2002; Hastak *et al*, 2005; hangapazham *et al*, 2007; Tang *et al*, 2007; Adhami *et al*, 2007), although to date there are limited studies on its effects on leukaemia cells.

Quercetin is a flavonol and is found in a variety of fruits and vegetables (Chen *et al*, 2007). Numerous reports on the potential anti-cancer effects of quercetin have been published (Nair *et al*, 2004; Vijayababu *et al*, 2005; Granado-Serrano *et al*, 2006; Jeong *et al*, 2009; Chien *et al*, 2009; Jung *et al*, 2010; Jung *et al*, 2010). The cancer-preventive effects have been attributed to cell cycle arrest, inhibition of proliferation and induction of apoptosis (Nair *et al*, 2004; Vijayababu *et al*, 2005; Granado-Serrano *et al*, 2006; Jeong *et al*, 2009; Chien *et al*, 2009; Jung *et al*, 2010; Jung *et al*, 2010).

Gallic acid is a naturally occurring plant phenolic acid, and has been reported to have potential anti-cancer activities (Weng and Yen 2012). *In vitro* and *in vivo* studies using gallic acid have shown anti-cancer activities in several types of cancer cell lines including: colon, lung, and prostate cancer cell lines (Yoshioka *et al*, 2000; Veluri *et al*, 2006; Ji *et al*, 2009). In addition gallic acid displays selectivity towards tumour cells with lower toxicity seen in normal cells (Veluri *et al*, 2006; Bernhaus *et al*, 2009). Gallic acid can induce apoptosis and results in cell cycle arrest (Kaur *et al*, 2009; You and Park, 2010; Ou *et al*. 2010; Locatelli *et al*, 2012).

Punicalagin, an ellagitannin is found in pomegranates, strawberries, raspberries, almonds, and walnuts (Amakura et al, 2000; Clifford and Scalbert, 2000). In PJ, punicalagin is believed to be responsible for more than 50% of its antioxidant activity (Gil et al, 2000). Our previous work (Chapter 4) (Dahlawi et al, 2013) has identified punicalagin as one of the most abundant compounds within acetonitrile fraction, and we have shown it induces a potent inhibition of ATP levels indicating decreases in live cell numbers (Chapter 5). However, to date, few studies have investigated the effect of punicalagin as pure agent in cancer cell lines (Larrosa et al, 2005; Seeram et al, 2005).

The present chapter will focus on the potential chemopreventive activities of EGCG, quercetin, gallic acid and punicalagin. Testing the hypothesis that: these agents induce apoptosis and cell cycle arrest in leukaemia cell lines.

7.2 Materials and Methods

7.2.1 Cell Culture

Four leukaemia cell lines were used in this study. These were selected as they were shown to have sensitivity to PJ (Dahlawi et al, 2011) (chapter 3) and to the acetonitrile fraction of PJ (Dahlawi et al, 2013) (Chapter 4). They included two lymphoid cell lines: CCRF-CEM and MOLT-3 and two myeloid cell lines: HL-60 and THP-1. Cell lines were maintained and cultured in RPMI 1640 medium (Invitrogen, Paisley, U.K.) supplemented with 10% (v/v) foetal bovine serum, 1.5 mmol/L L-glutamine, and 100 µg/mL penicillin/streptomycin (complete media) in a humidified atmosphere of 5% CO₂ at 37°C.

7.2.2 Treatment of Cells

Cells were treated with EGCG, gallic acid, quercetin, and punicalagin at dose of 0 – 100 µM for 24 h and induction of apoptosis and cell cycle arrest investigated (Table 7.1).

Techniques	Treatment	Concentration	Cell lines	Time point
Annexin V-FITC/PI	EGCG, gallic acid, quercetin, and punicalagin	0, 10, 25, 50, 75, and 100 μ M	CCRF-CEM, MOLT-3, HL-60, and THP-1	24 hr
NucView™ 488 Caspase-3 substrate assay	EGCG, gallic acid, quercetin, and punicalagin	0, 10, 25, 50, 75, and 100 μ M	CCRF-CEM, MOLT-3, HL-60, and THP-1	24 hr
DAPI staining	EGCG, gallic acid, quercetin, and punicalagin	0, 25, 50, 100 μ M	CCRF-CEM, MOLT-3, HL-60, and THP-1	24 hr
Cell cycle	EGCG, gallic acid, quercetin, and punicalagin	0, 25, 50, 100 μ M	CCRF-CEM, MOLT-3, HL-60, and THP-1	24 hr

Table 7.1: Experimental design for chapter 7.

7.2.3 Annexin V- FITC /PI Flow Cytometry Assay

Flow cytometry of Annexin V-FITC /PI was used to detect apoptosis as described previously (section 2.4.1). Cells were seeded at 5×10^5 cells in 1 ml of complete media in a 6-well plate (Fisher Scientific) and treated with EGCG, gallic acid, quercetin, and punicalagin at a concentration of 0, 10, 25, 50, 75, and 100 μ M for 24 h. Data were recorded from 10,000 cells per sample and analyzed using FlowJo software (Tree Star).

7.2.4 Caspase-3 Activity

NucView™ 488 Caspase-3 substrate was used to detect caspase-3 activity as described in section 2.4.3. Cells were treated with EGCG, gallic acid, quercetin, and punicalagin at concentrations 0, 10, 25, 50, 75, and 100 μ M for 24 h. Data were recorded from 10,000 cells per sample and analyzed using FlowJo software (Tree Star).

7.2.5 DAPI Stain

Following treatment with EGCG, gallic acid, quercetin, and punicalagin at concentrations of 0, 25, 50, 100 for 24 h at cell density 5×10^4 cells per well, cells were stained with DAPI to observe apoptotic morphology as described previously (section 2.4.2). Cells were examined using an Olympus BX60 fluorescence microscope using UV light at excitation wavelength 350 nm. Quantitative analysis of cell populations (live & apoptotic) was performed based on counting of 200 randomly-selected cells and the percentage of apoptotic features determined for each sample.

7.2.6 Cell Cycle

The cell cycle distribution of leukaemia cell lines was measured by the DNA contents in each cell based on flow cytometry using PI stain as described previously in section 2.5. Cells were treated with EGCG, gallic acid, quercetin, and punicalagin at concentrations of 0, 25, 50, and 100 μ M for 24 h. Data from 10,000 cells per sample were recorded and percentages of cells within G₀/G₁, S, and G₂/M cell cycle phase were determined with FlowJo software and Waston (pragmatic) analysis of cell cycle (Tree Star).

7.3 Results

7.3.1 EGCG

7.3.1.1 Effect of EGCG on Induction of Apoptosis

7.3.1.1.1 Annexin V-FITC/PI Based on Flow Cytometry

EGCG treatment of CCRF-CEM, MOLT-3, HL-60, and THP-1 cells resulted in a significant increase in the number of apoptotic and dead cells and a decrease in the number of live cells following 24 h incubation at concentrations: 25, 50, 75, and 100 μM ($P \leq 0.05$). At the lowest concentration (10 μM) of EGCG no significant induction of apoptosis was observed in all four cell lines. THP-1 was the least sensitive among the cell lines investigated, which illustrated only slight decrease in the number of live cells and increase in the number of apoptotic and dead cells (Figure 7.1).

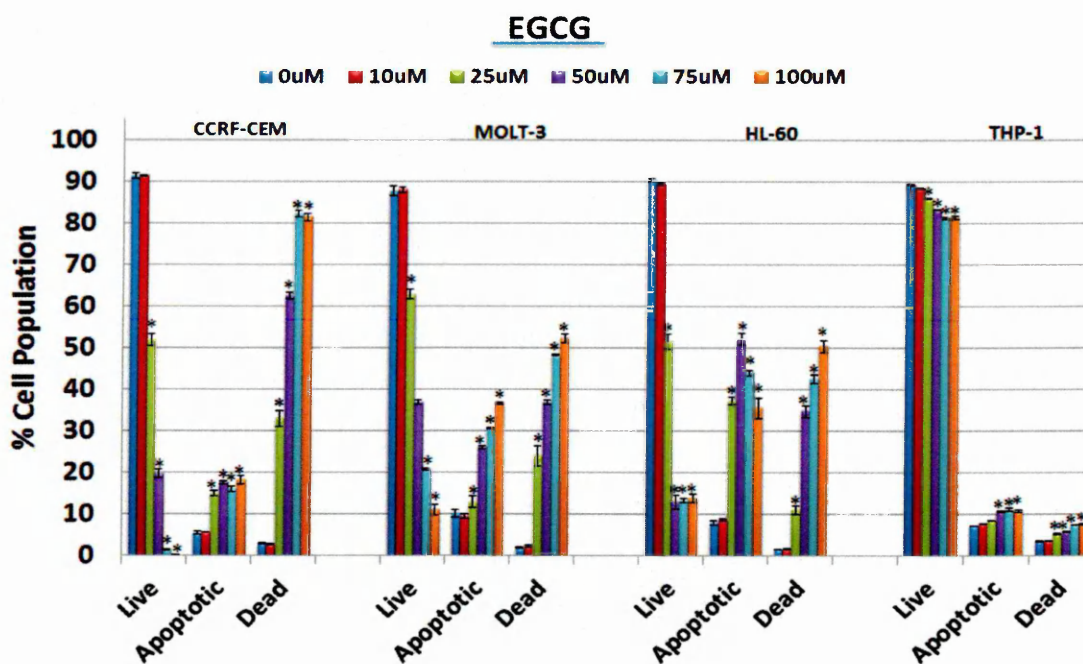


Figure 7.1: Annexin V-FITC/ PI based on flow cytometry following treatment with EGCG (0, 10, 25, 50, 75, and 100 μM) for 24 h on CCRF-CEM, MOLT-3, HL-60, and THP-1. Mean \pm SEM. * indicates significant difference ($P \leq 0.05$) vs. untreated control. n= 3.

7.3.1.1.2 Caspase-3 Activity:

EGCG at treatment dose of 25, 50, 75, and 100 μM significantly increased caspase-3 activity in all four leukaemia cell lines (CCRF-CEM, MOLT-3, HL-60 and THP-1) with different sensitivity following 24 h treatment ($P \leq 0.05$). In CCRF-CEM cells, following 100 μM of EGCG caspase-3 activity was increased to 98% of cells positive as compared to 8% in untreated controls cells. In HL-60 and MOLT-3 cells caspase-3 activity was increased to 88% and 78% of cells positive respectively. THP-1 cells were the least sensitive cell lines, with only 16% of cells positive for caspase-3 activity following 100 μM of EGCG for 24 h compared to 7.5% in control cells (Figure 7.2).

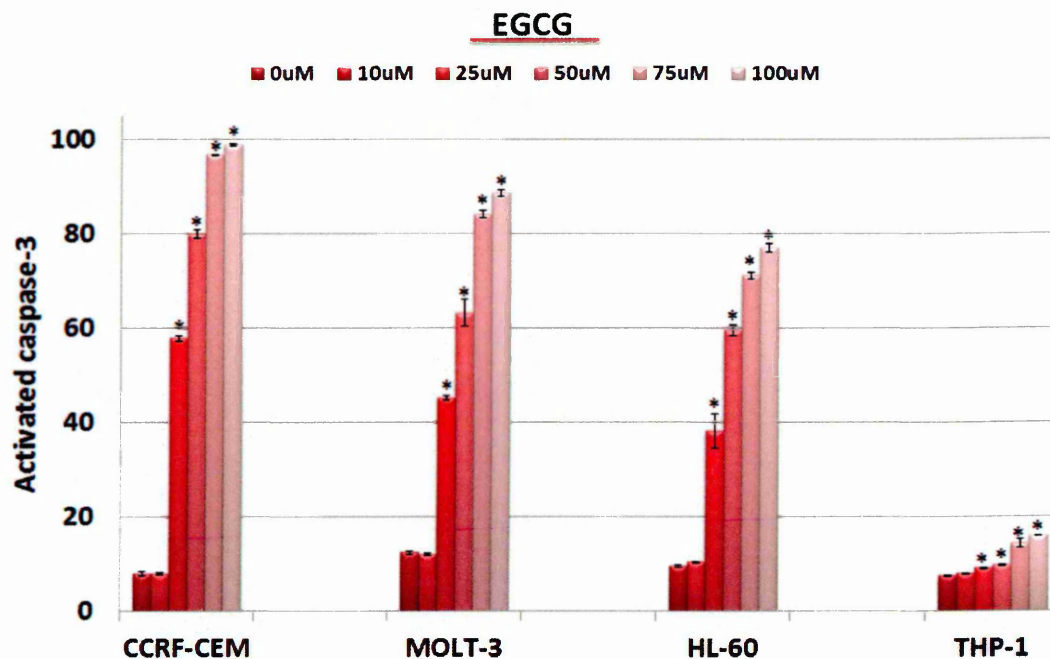


Figure 7.2: Effect of EGCG on caspase-3 activation in four leukaemia cell lines (CCRF-CEM, MOLT-3, HL-60, and THP-1). Cells treated for 24 h at concentrations 10, 25, 50, 75 and 100 μM . Caspase-3 activation was determined by NucView™ 488 Caspase-3 substrate based on flow cytometry analysis. Mean \pm SEM. * indicates significant difference ($P \leq 0.05$) vs. untreated control. n= 3.

7.3.1.1.3 DAPI for Morphological Assessment:

The EGCG-treated cells showed significant increase in the number of apoptotic cells in all four leukaemia cell lines tested (CCRF-CEM, MOLT-3, HL-60, and THP-1) at all concentrations 25, 50, 100 μM following 24 h treatment ($P \leq 0.05$) (Figure 7.3-7.6).

CCRF-CEM

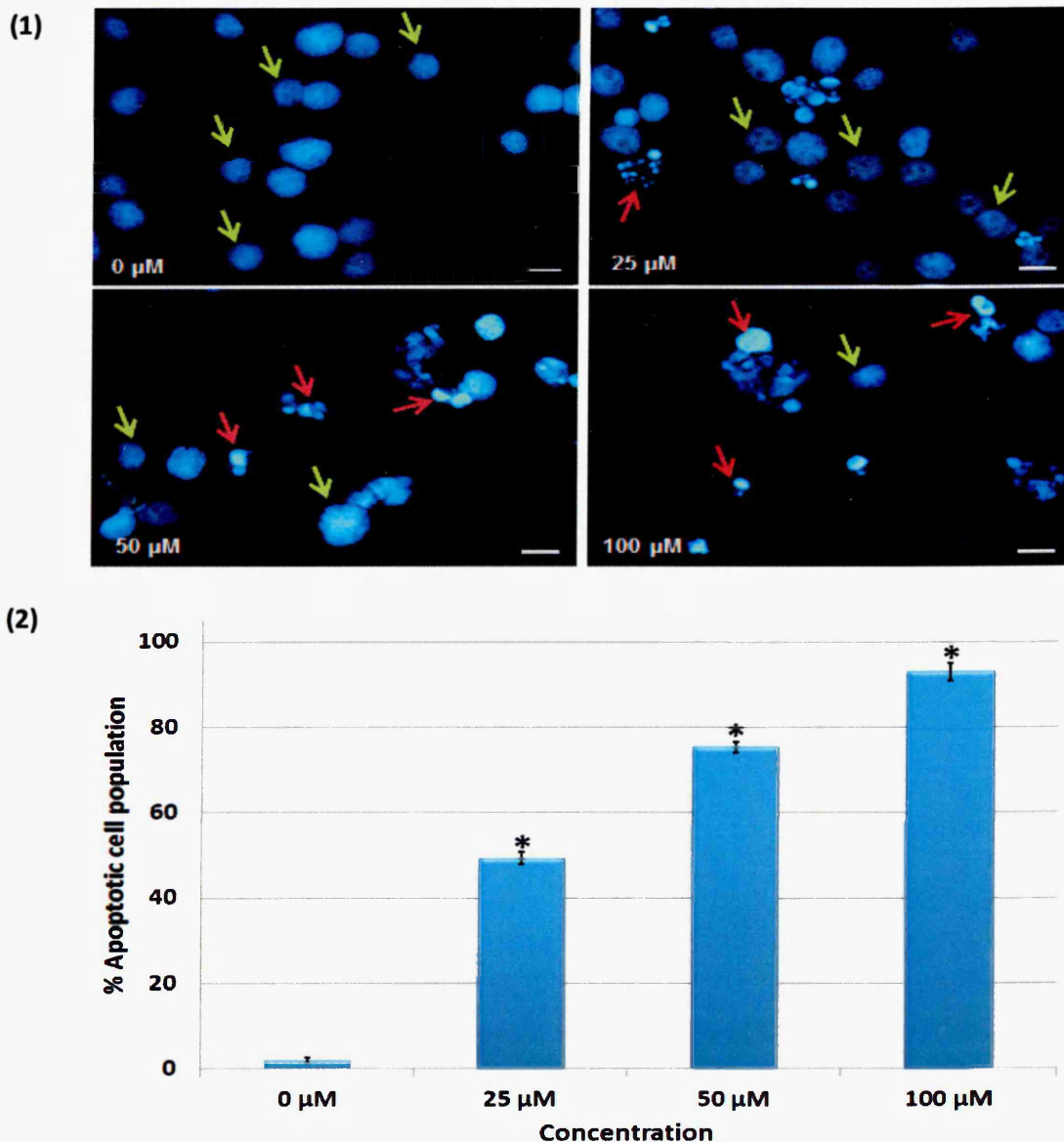


Figure 7.3: (1) DAPI Morphological staining analysis of CCRF-CEM with DAPI treated with EGCG at concentrations 25, 50, and 100 μM for 24 h. Live cells are indicated by the **green arrows**, and apoptotic cells are indicated by the **red arrows**. (2) Percentage of apoptotic cells determined from DAPI morphological assessment following treatment with delphinidin at 25, 50, and 100 μM for 24 h. Mean \pm SEM. * indicates significant difference ($P \leq 0.05$) vs. untreated control. Scale bar= 12.5 μm . n= 3.

MOLT-3

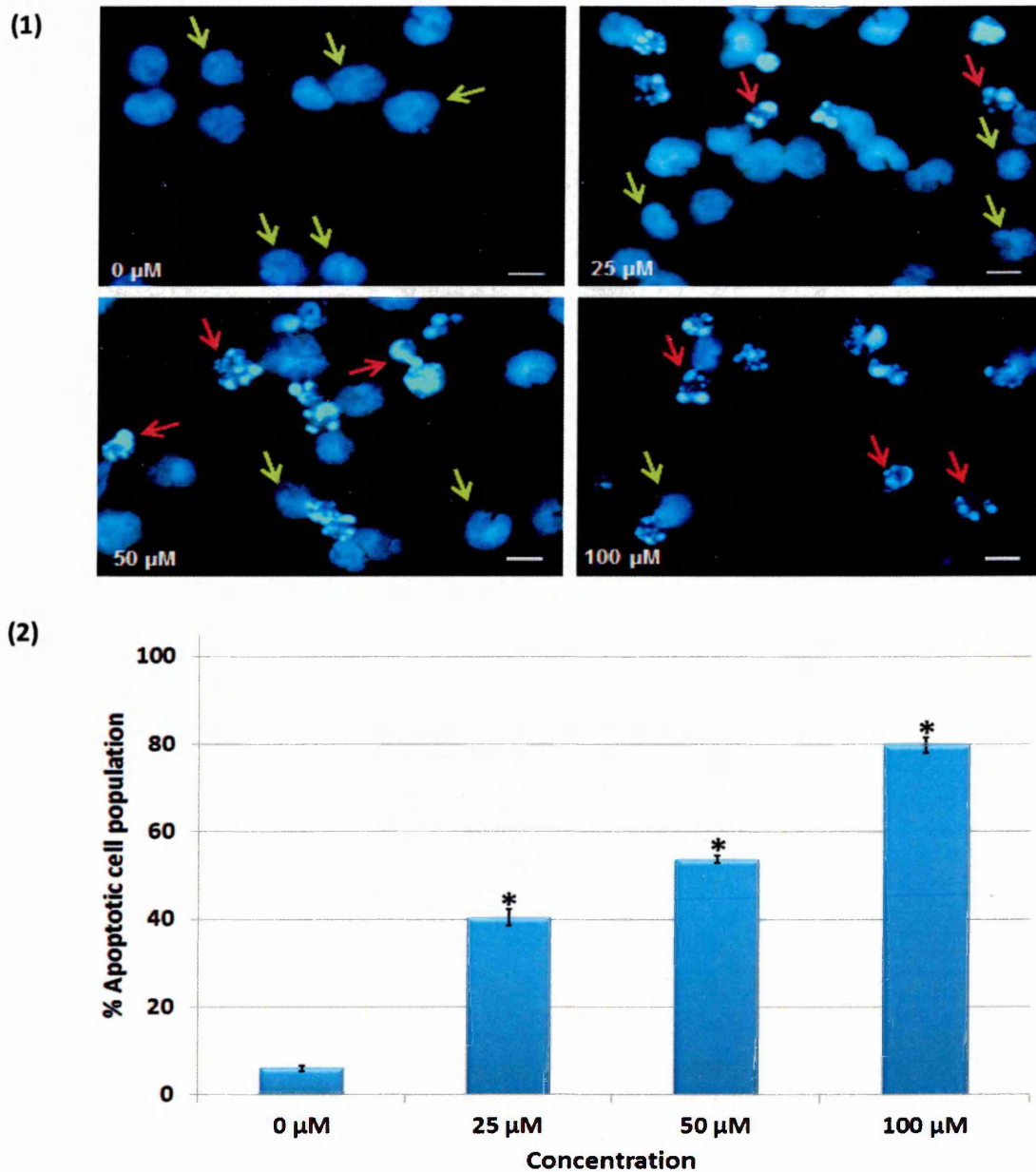


Figure 7.4: (1) Morphological staining analysis of MOLT-3 with DAPI treated with EGCG at concentrations 25, 50, and 100 μM for 24 h. Live cells are indicated by the green arrows, and apoptotic cells are indicated by the red arrows. **(2)** Percentage of apoptotic cells determined from DAPI morphological assessment following treatment with delphinidin at 25, 50, and 100 μM for 24 h. Mean \pm SEM. * indicates significant difference ($P \leq 0.05$) vs. untreated control. Scale bar= 12.5 μm . n= 3.

HL-60

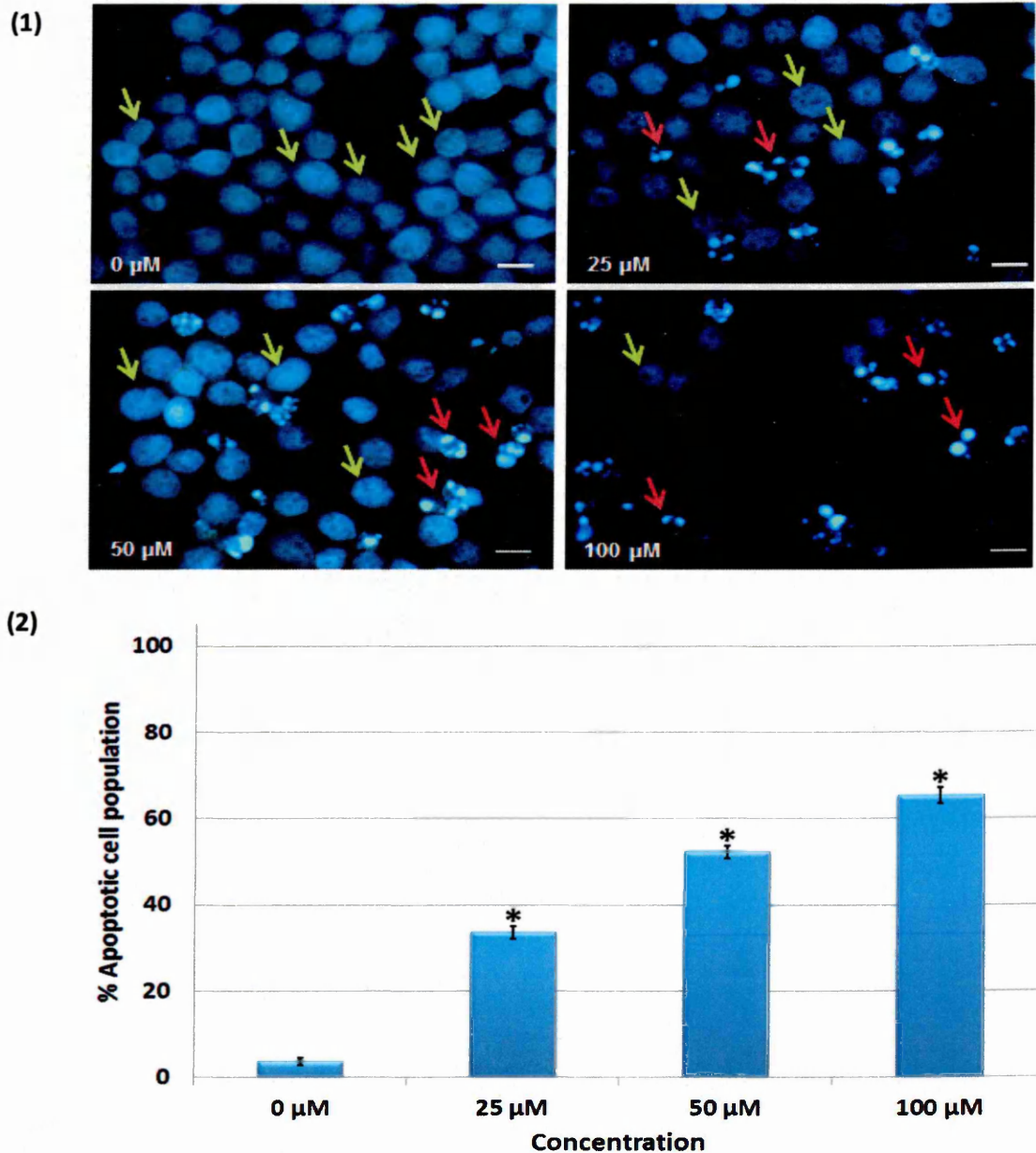


Figure 7.5: (1) Morphological staining analysis of HL-60 with DAPI treated with EGCG at concentrations 25, 50, and 100 μM for 24 h. Live cells are indicated by the green arrows, and apoptotic cells are indicated by the red arrows. **(2)** Percentage of apoptotic cells determined from DAPI morphological assessment following treatment with delphinidin at 25, 50, and 100 μM for 24 h. Mean \pm SEM. * indicates significant difference ($P \leq 0.05$) vs. untreated control. Scale bar= 12.5 μm . n= 3.

THP-1

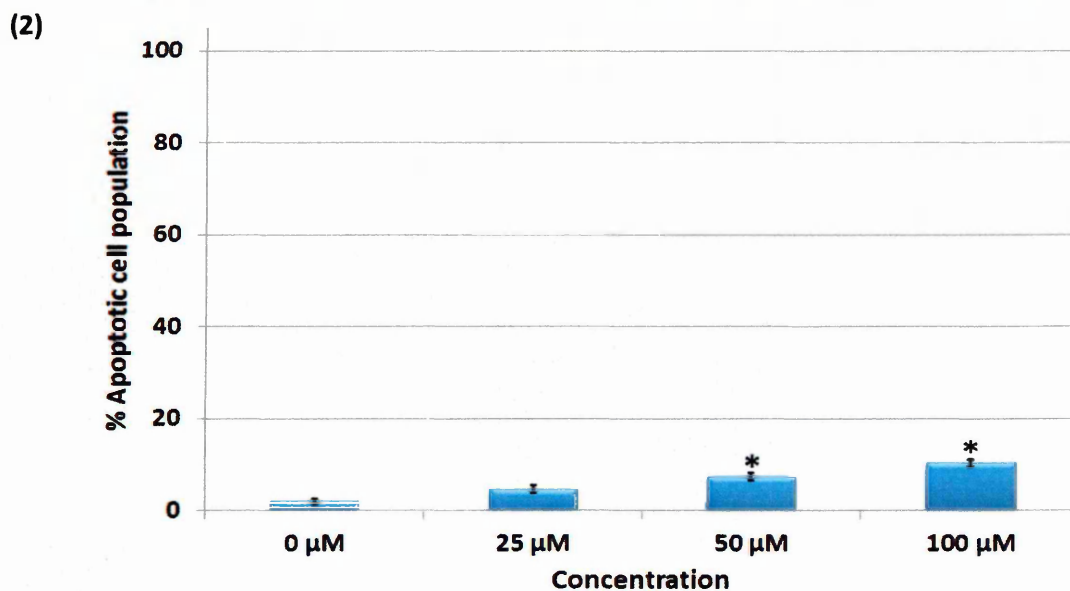
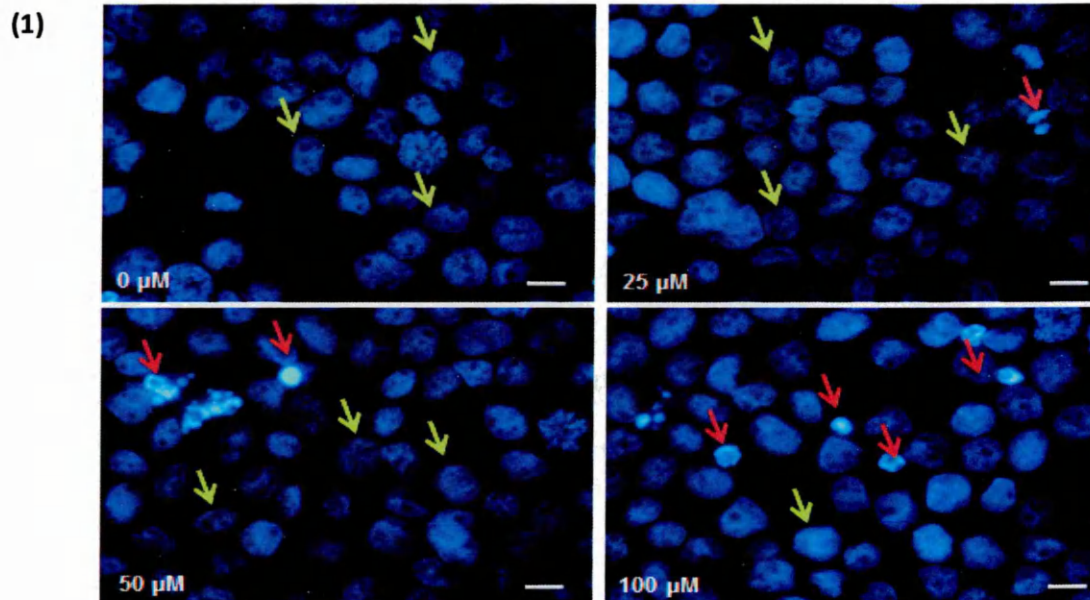


Figure 7.6: (1) Morphological staining analysis of THP-1 with DAPI treated with EGCG at concentrations 25, 50, and 100 μM for 24 h. Live cells are indicated by the green arrows, and apoptotic cells are indicated by the red arrows. **(2)** Percentage of apoptotic cells determined from DAPI morphological assessment following treatment with delphinidin at 25, 50, and 100 μM for 24 h. Mean \pm SEM. * indicates significant difference ($P \leq 0.05$) vs. untreated control. Scale bar= 12.5 μm . n= 3.

7.3.1.2 Effect of EGCG on Cell Cycle:

EGCG showed significant accumulation of cells in G_0/G_1 phase corresponding with a significant decrease in S and M phases in CCRF-CEM, MOLT-3, and HL-60 cell lines following 24 h treatment with concentration of 25, 50, and 100 μM ($P \leq 0.05$) (Figure 7.7). In THP-1 cells G_0/G_1 phase arrest was observed, but this failed to reach significance ($P > 0.05$) (Figure 7.7).

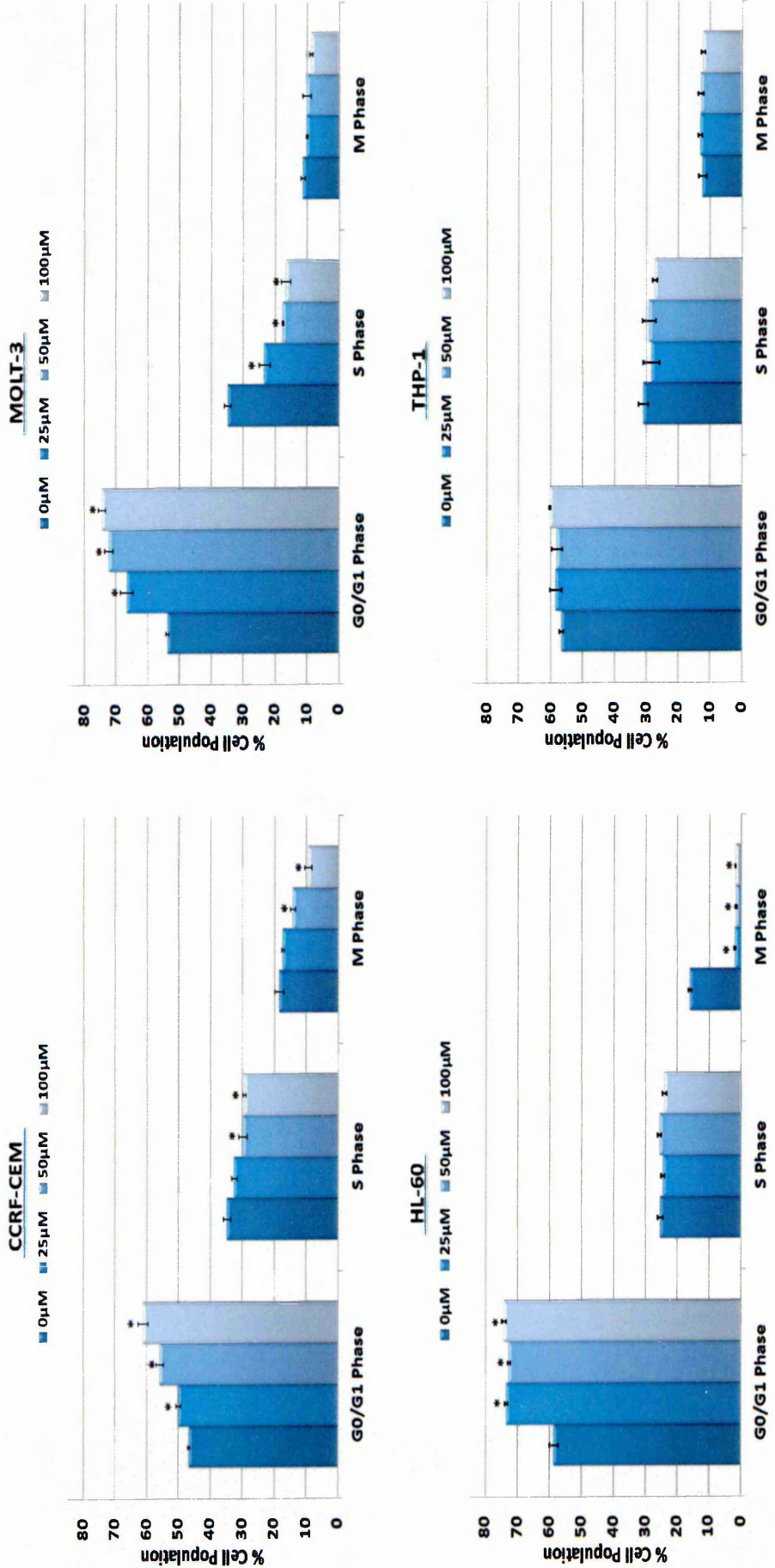


Figure 7.7: Cell cycle based on flow cytometry using FlowJo software following treatment with EGCG at concentration 25, 50, and 100 μM for 24 h incubation on four leukaemia cell lines (CCRF-CEM, MOLT-3, HL-60, AND THP-1. Mean ± SEM. * indicates significant difference ($P \leq 0.05$) vs. untreated control. n= 3.

7.3.2 Gallic acid

7.3.2.1 Effect of Gallic Acid on Induction of Apoptosis

7.3.2.1.1 Annexin V-FITC/PI Based on Flow Cytometry

Gallic acid treatment of CCRF-CEM, MOLT-3, HL-60, and THP-1 cells resulted in a significant increase in the number of apoptotic and dead cells and decrease in the number of live cells following 24 h incubation at concentrations: 25, 50, 75, and 100 μM ($P \leq 0.05$). At the lowest concentration (10 μM) of gallic acid no significant induction of apoptosis was observed in all four cell lines ($P > 0.05$) (Figure 7.8). THP-1 was the least sensitive among the cell lines investigated, which illustrated significant decrease in the number of live cells and increase in the number of apoptotic and dead cells at concentration 50, 75, and 100 μM , but the effects seen were lower than that observed in the other cell lines (Figure 7.8).

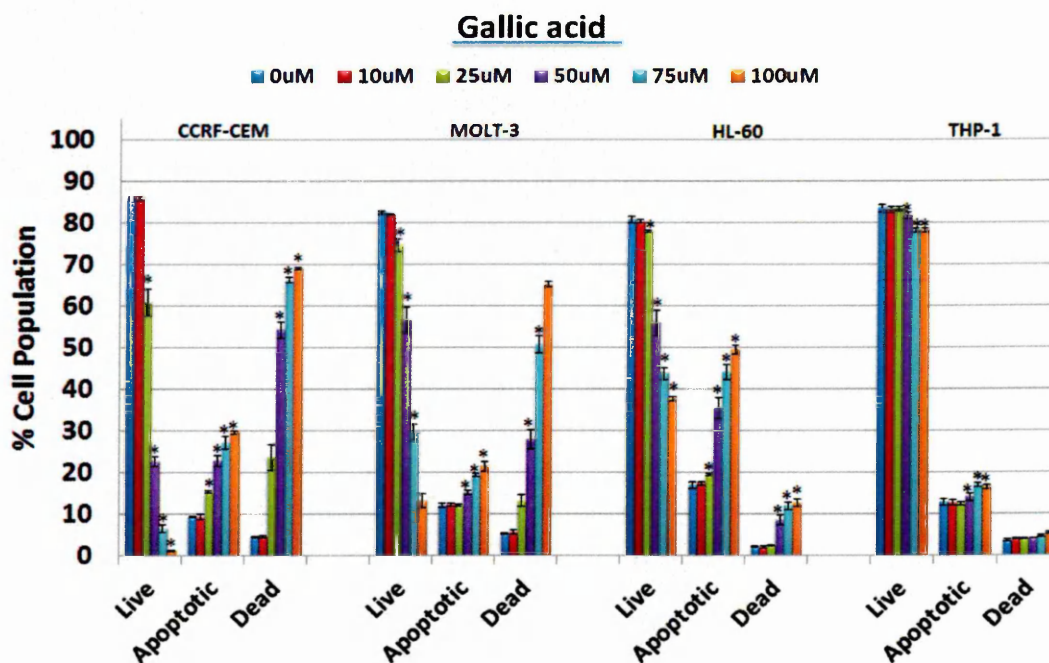


Figure 7.8: Annexin V-FITC/ PI based on flow cytometry following treatment with gallic acid (0, 10, 25, 50, 75, and 100 μM) for 24 h on CCRF-CEM, MOLT-3, HL-60, and THP-1. Mean \pm SEM. * indicates significant difference ($P \leq 0.05$) vs. untreated control. $n = 3$.

7.3.2.1.2 Caspase-3 Activity:

Gallic acid showed a significant increase in caspase-3 activity in CCRF-CEM, MOLT-3, and HL-60 cells, but failed to induce apoptosis in THP-1 cells ($P \leq 0.05$) (Figure 7.9).

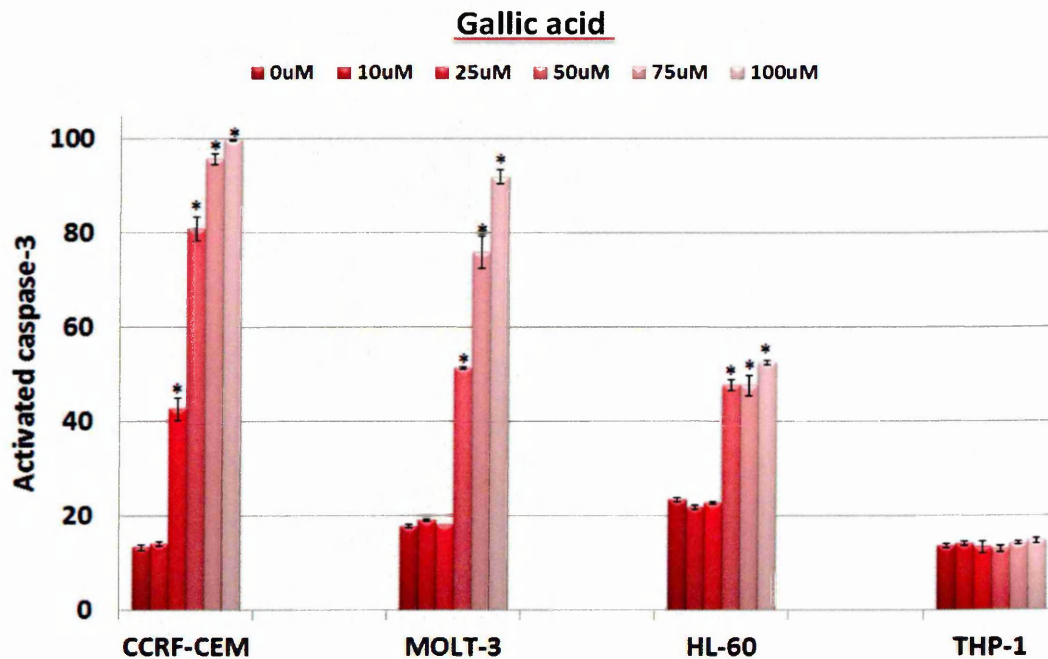


Figure 7.9: Effect of gallic acid on caspase-3 activation in four leukaemia cell lines (CCRF-CEM, MOLT-3, HL-60, and THP-1). Cells treated for 24 at concentrations of 10, 25, 50, 75 and 100 μ M. Caspase-3 activation was determined by NucView™ 488 Caspase-3 substrate assay based on flow cytometry analysis. Mean \pm SEM. * indicates significant difference ($P \leq 0.05$) vs. untreated control. n= 3.

7.3.1.1.3 DAPI for Morphological Assessment:

Gallic acid showed a significant increase the number of apoptotic cells at all concentrations in CCRF-CEM and HL-60 cells following 24 h treatment ($P \leq 0.05$) (Figure 7.10-7.11). In MOLT-3, a significant increase in the number of apoptotic cells was observed at 50 and 100 μM . THP-1 cells were the least sensitive with only a small but significant increase in the number of apoptotic cells at high concentration 100 μM following 24 h treatment ($P \leq 0.05$) (Figure 7.13).

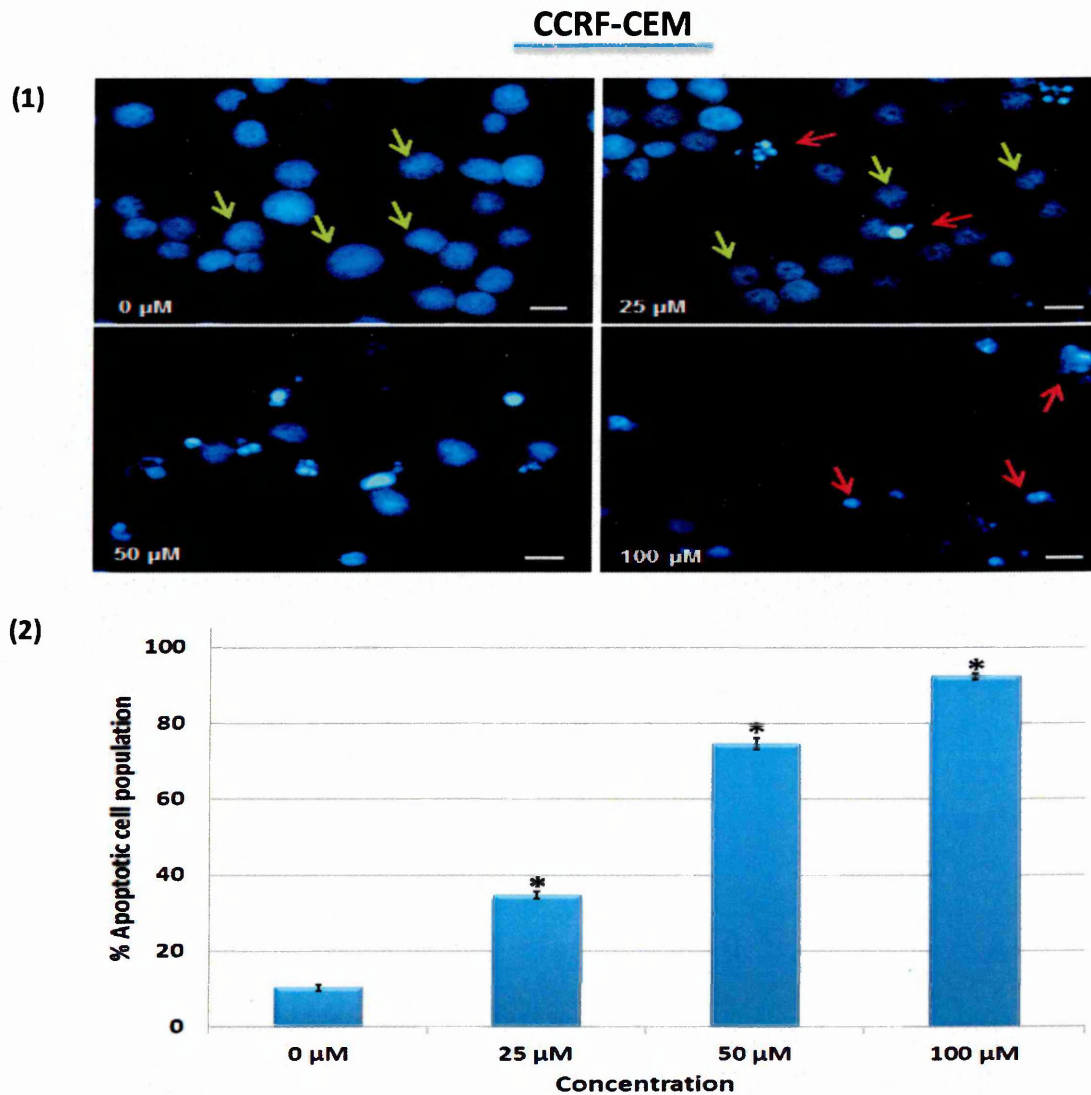
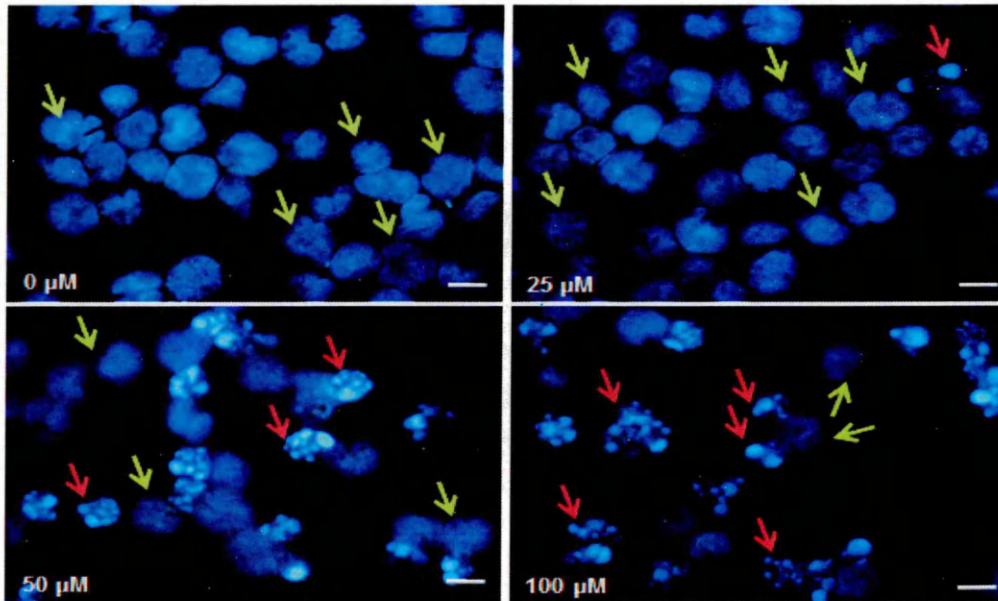


Figure 7.10: (1) Morphological staining analysis of CCRF-CEM with DAPI treated with gallic acid at concentrations 25, 50, and 100 μM for 24 h. Live cells are indicated by the green arrows, and apoptotic cells are indicated by the red arrows. **(2)** Percentage of apoptotic cells determined from DAPI morphological assessment following treatment with delphinidin at 25, 50, and 100 μM for 24 h. Mean \pm SEM. * indicates significant difference ($P \leq 0.05$) vs. untreated control. Scale bar= 12.5 μm . n= 3.

MOLT-3

(1)



(2)

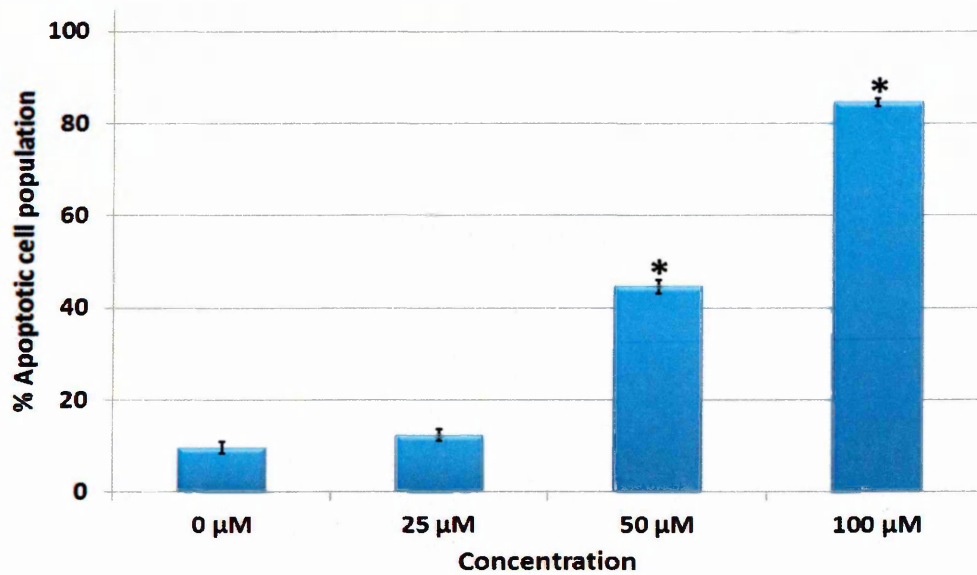


Figure 7.11: (1) Morphological staining analysis of MOLT-3 with DAPI treated with gallic acid at concentrations 25, 50, and 100 μM for 24 h. Live cells are indicated by the green arrows, and apoptotic cells are indicated by the red arrows. **(2)** Percentage of apoptotic cells determined from DAPI morphological assessment following treatment with delphinidin at 25, 50, and 100 μM for 24 h. Mean ± SEM. * indicates significant difference ($P \leq 0.05$) vs. untreated control. Scale bar= 12.5 μm. n= 3.

HL-60

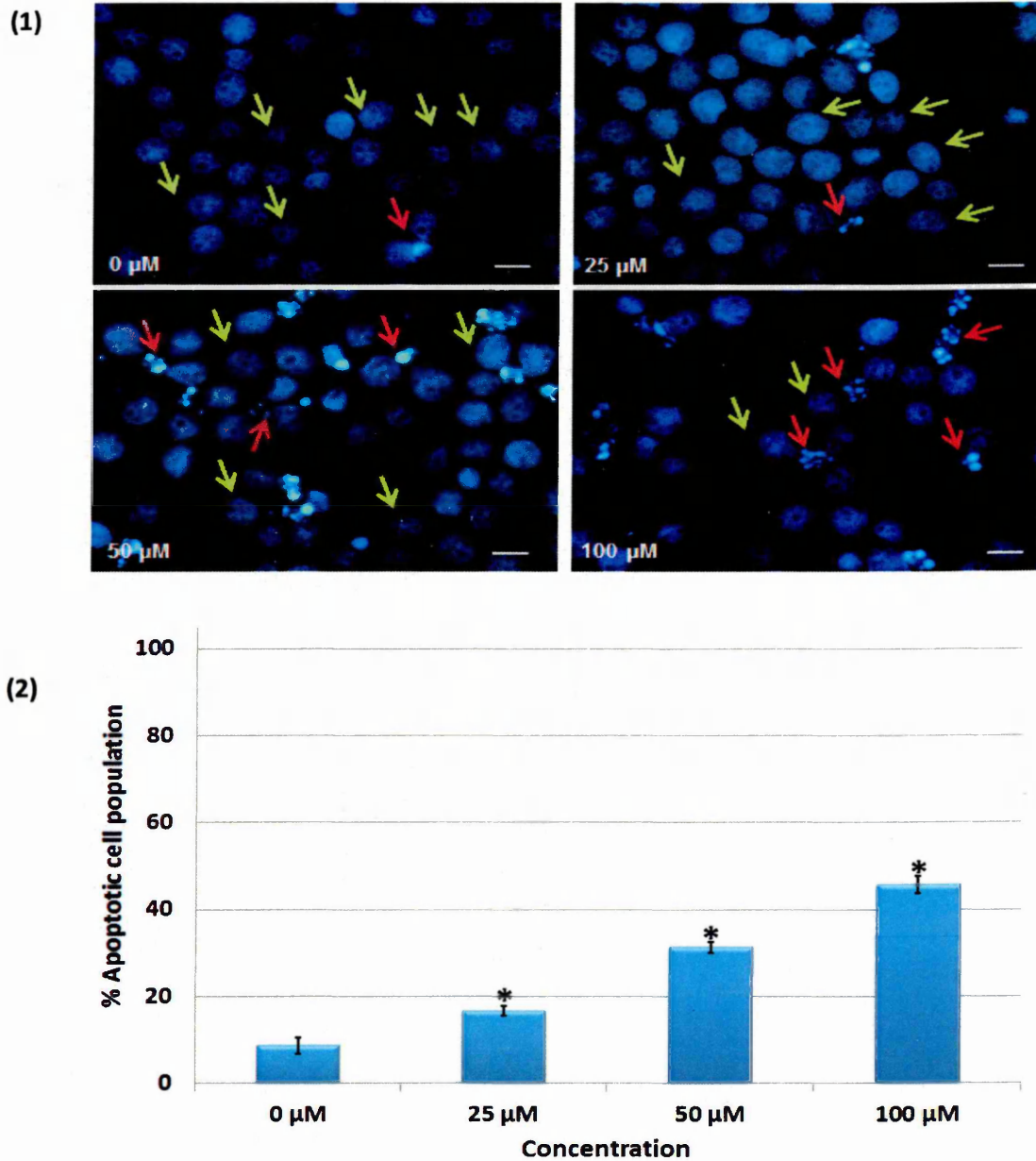


Figure 7.12: (1) Morphological staining analysis of HL-60 with DAPI treated with gallic acid at concentrations 25, 50, and 100 μM for 24 h. Live cells are indicated by the green arrows, and apoptotic cells are indicated by the red arrows. **(2)** Percentage of apoptotic cells determined from DAPI morphological assessment following treatment with delphinidin at 25, 50, and 100 μM for 24 h. Mean \pm SEM. * indicates significant difference ($P \leq 0.05$) vs. untreated control. Scale bar= 12.5 μm . n= 3.

THP-1

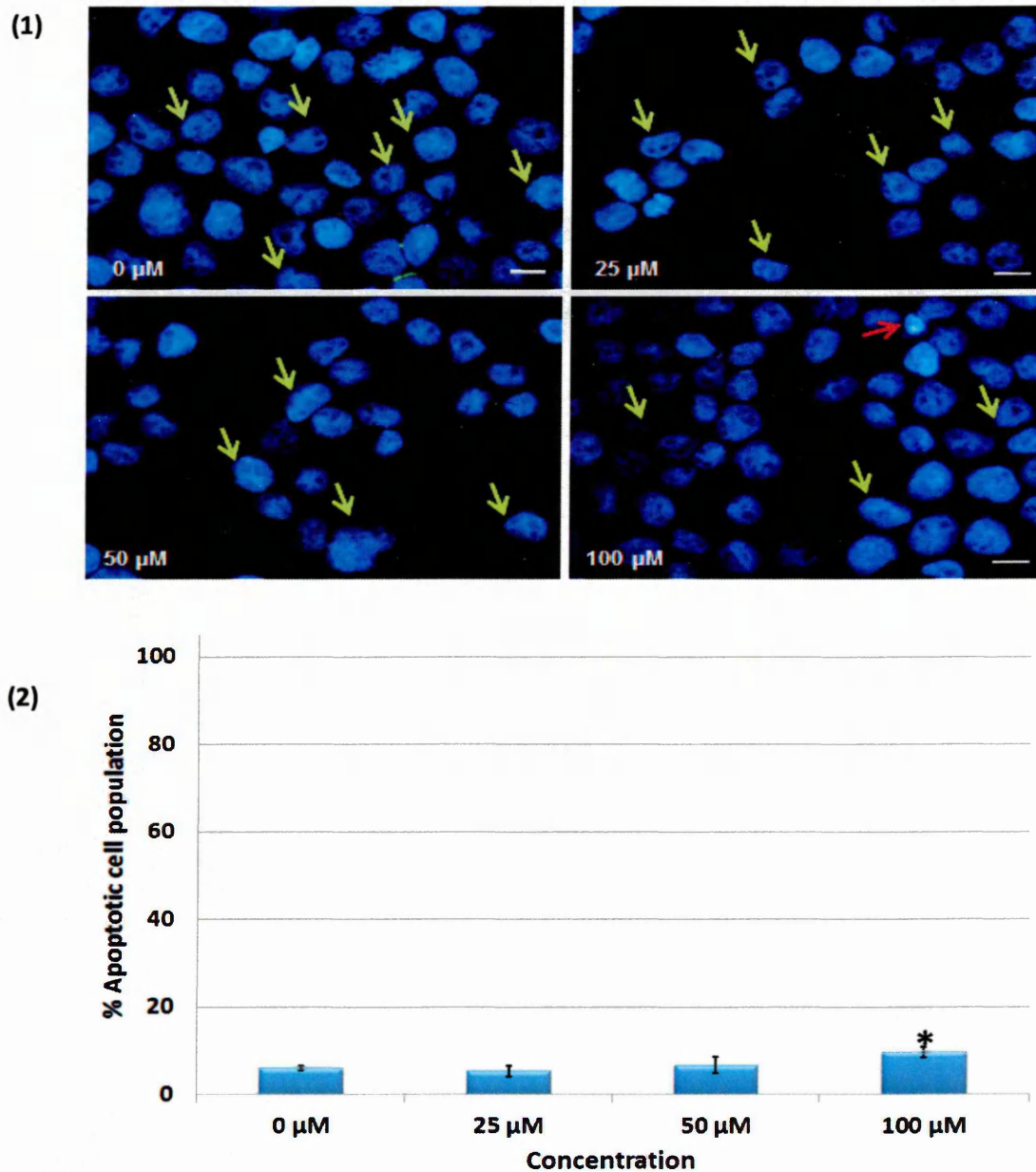


Figure 7.13: (1) Morphological staining analysis of THP-1 with DAPI treated with gallic acid at concentrations 25, 50, and 100 μM for 24 h. Live cells are indicated by the green arrows, and apoptotic cells are indicated by the red arrows. **(2)** Percentage of apoptotic cells determined from DAPI morphological assessment following treatment with delphinidin at 25, 50, and 100 μM for 24 h. Mean \pm SEM. * indicates significant difference ($P \leq 0.05$) vs. untreated control. Scale bar= 12.5 μm . n= 3.

7.3.2.2 Effect of Gallic Acid on Cell Cycle

Gallic acid induced a significant accumulation of cells in S phase corresponding with a significant decrease in G₀/G₁ phase in CCRF-CEM and MOLT-3 and M phase in HL-60 cells at concentrations of 25, 50, 100 μM following 24 h treatment ($P \leq 0.05$) (Figure 7.14). Gallic acid treatment to THP-1 cells resulted in a significant accumulation of cells in S phase, but only at 50 and 100 μM corresponding with decrease in G₀/G₁ phase following 24 h incubation ($P \leq 0.05$) (Figure 7.14).

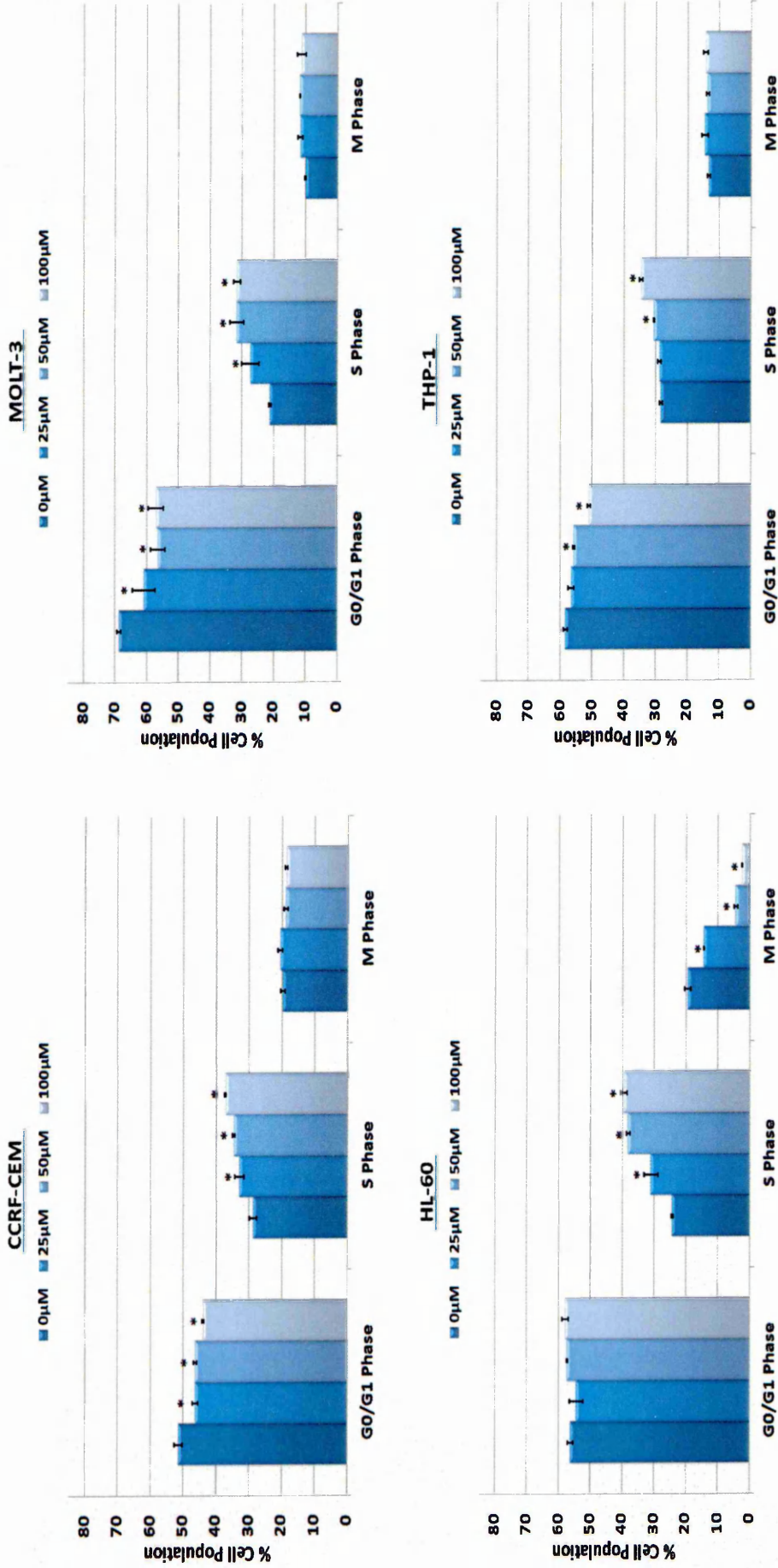


Figure 7.14: Cell cycle based on flow cytometry using FlowJo software following treatment with gallic acid at concentration 25, 50, and 100 μM for 24 h incubation in four leukaemia cell lines (CCRF-CEM, MOLT-3, HL-60, AND THP-1). Mean ± SEM. * indicates significant difference ($P \leq 0.05$) vs. untreated control. n= 3.

7.3.3 Quercetin

7.3.3.1 Effect of Quercetin on Induction of Apoptosis

7.3.3.1.1 Annexin V-FITC/PI based on flow cytometry

Quercetin showed a significant increase in the number of apoptotic and dead cells and a decrease in the number of live cells following 24 h treatment in all four leukaemia cell lines (CCRF-CEM, MOLT-3, HL-60, and THP-1) ($P \leq 0.05$) (Figure 7.15). Quercetin illustrated potent induction of apoptosis compared to EGCGC, gallic acid, and punicalagin in THP-1 cells.

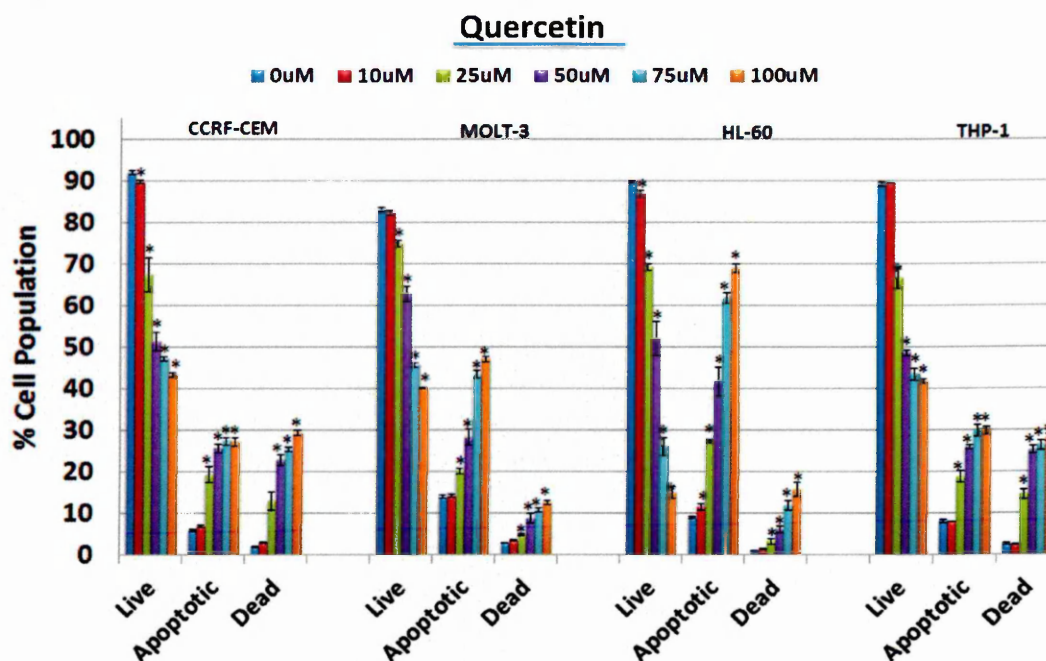


Figure 7.15: Annexin V-FITC/ PI based on flow cytometry following treatment with quercetin (0, 10, 25, 50, 75, and 100 μM) for 24 h on CCRF-CEM and MOLT-3. Mean \pm SEM. * indicates significant difference ($P \leq 0.05$) vs. untreated control. $n = 3$.

7.3.3.1.2 Caspase-3 Activity

Quercetin significantly increased caspase-3 activity in all four leukaemia cell lines (CCRF-CEM, MOLT-3, HL-60 and THP-1) with different sensitivity following 24 h treatment with CCRF-CEM being the least sensitive cells. Notably, quercetin illustrated potent increase in caspase-3 activity compared to EGCG, gallic acid, and punicalagin in THP-1 cells (Figure 7.16).

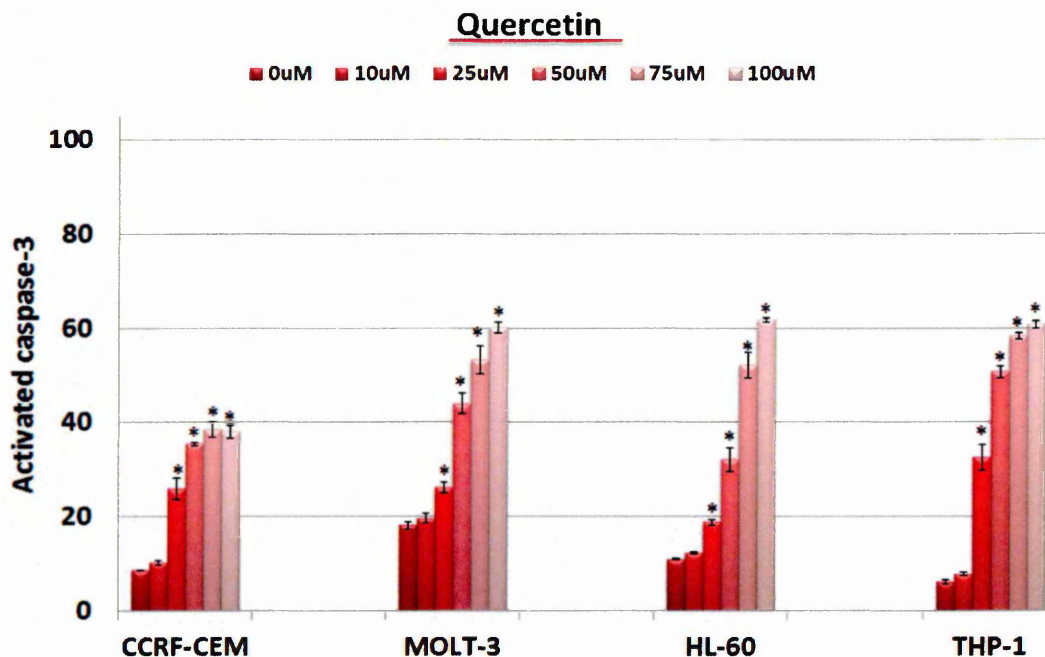


Figure 7.16: Effect of punicalagin on caspase-3 activation in four leukaemia cell lines (CCRF-CEM, MOLT-3, HL-60, and THP-1). Cells treated for 24h at concentrations 10, 25, 50, 75 and 100 μ M. Caspase-3 activation was determined by NucView™ 488 Caspase-3 substrate based on flow cytometry analysis. Mean \pm SEM. * indicates significant difference ($P \leq 0.05$) vs. untreated control. n= 3.

7.3.3.1.3 DAPI for Morphological Assessment

Quercetin-treated cells showed a significant increase in the number of apoptotic cells displaying condensed and fragmented nuclear structure and a decrease in cell size which are markers of apoptosis in CCRF-CEM, MOLT-3, HL-60 and THP-1 cells at all concentrations: 25; 50; 100 μM following 24 h treatment ($P \leq 0.05$) (7.17-7.20). However, quercetin illustrated potent increase in the number of apoptotic cells compared to EGCGC, gallic acid, and punicalagin in THP-1 cells as was observed with annexin V-FITC/PI and caspase-3 activity assessments (7.15 and 7.16).

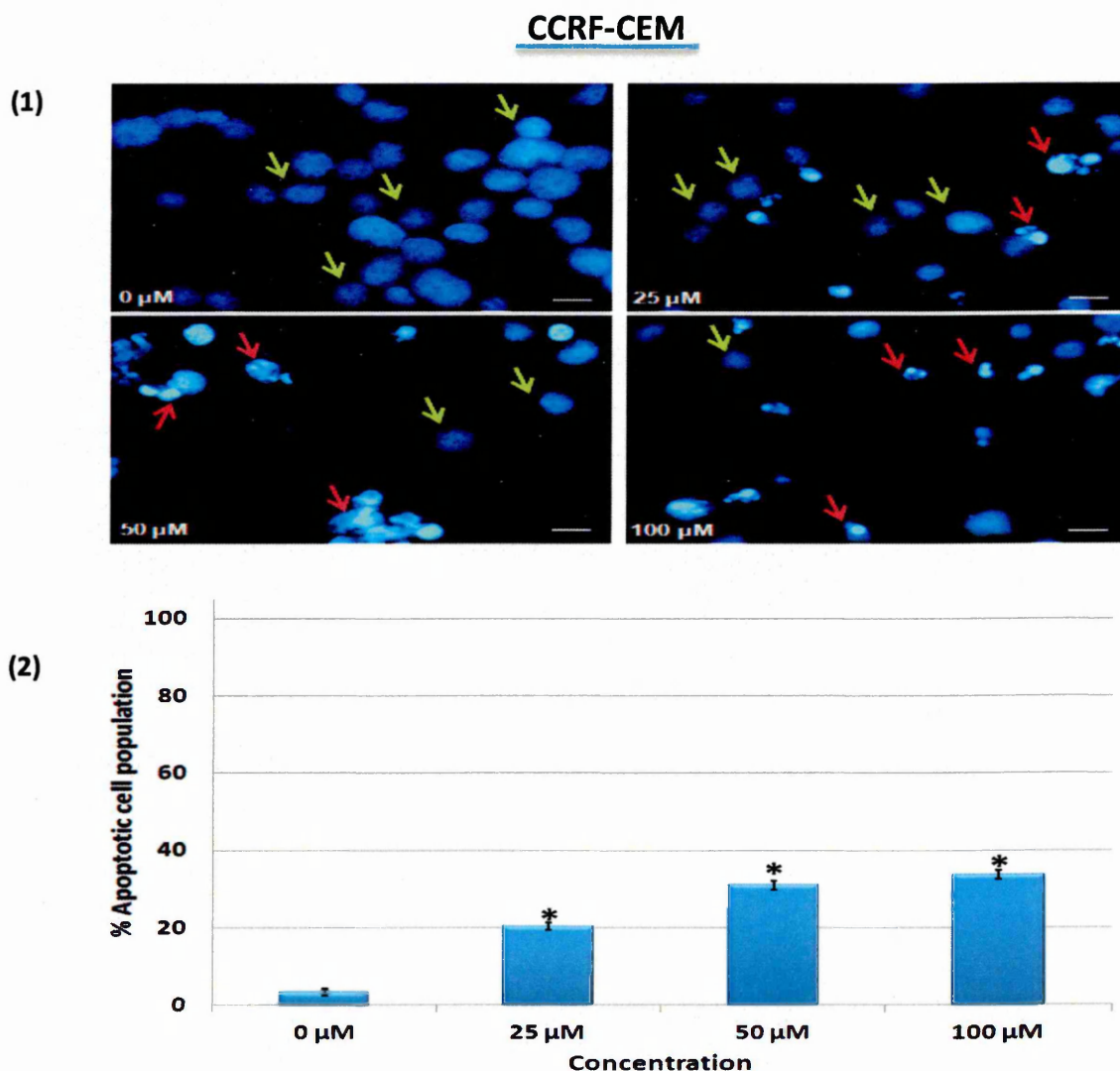
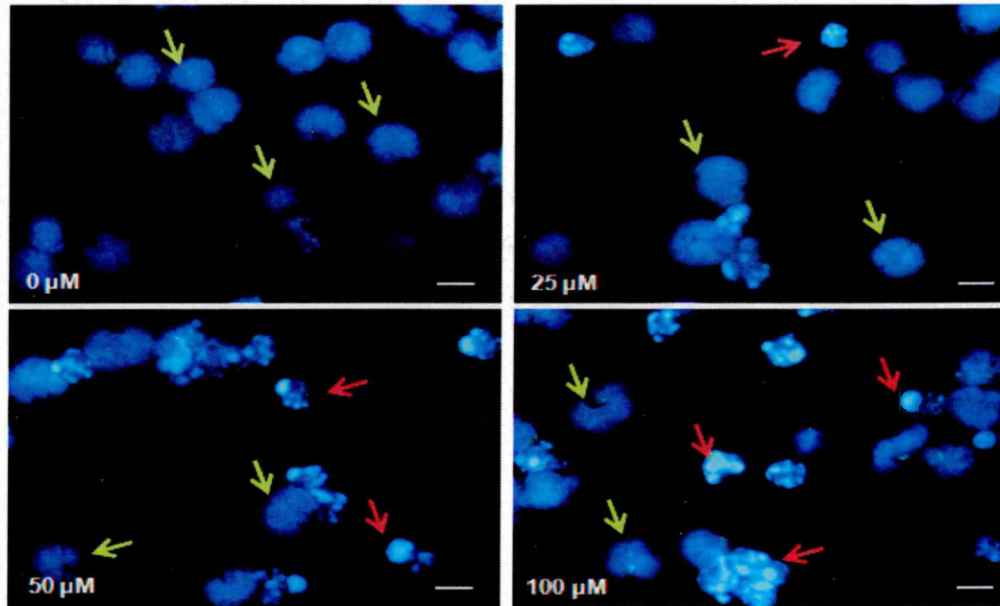


Figure 7.17: (1) Morphological staining analysis of CCRF-CEM with DAPI treated with quercetin at concentrations 25, 50, and 100 μM for 24 h. Live cells are indicated by the green arrows, and apoptotic cells are indicated by the red arrows. (2) Percentage of apoptotic cells determined from DAPI morphological assessment following treatment with delphinidin at 25, 50, and 100 μM for 24 h. Mean \pm SEM. * indicates significant difference ($P \leq 0.05$) vs. untreated control. Scale bar= 12.5 μm . n= 3.

MOLT-3

(1)



(2)

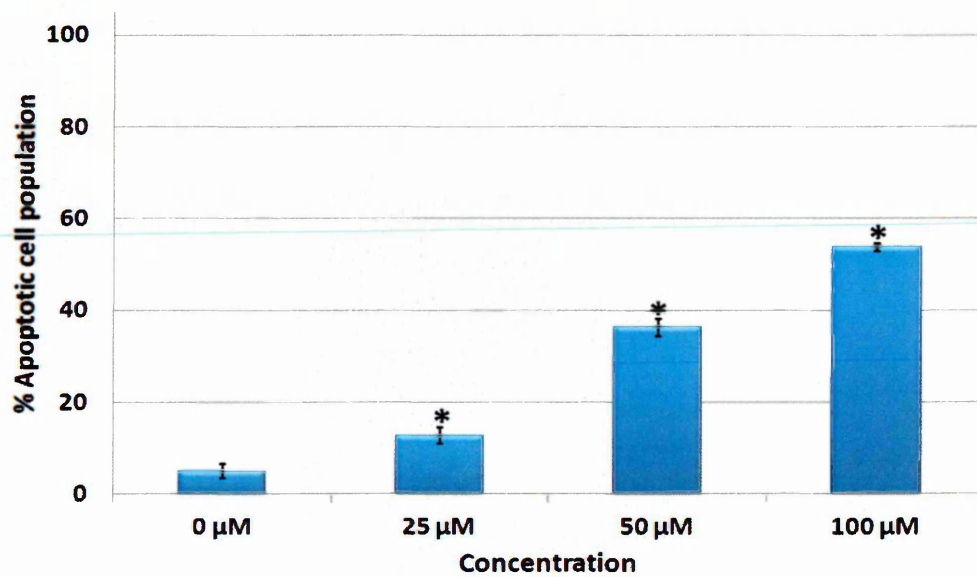


Figure 7.18: (1) Morphological staining analysis of MOLT-3 with DAPI treated with quercetin at concentrations 25, 50, and 100 μM for 24 h. Live cells are indicated by the green arrows, and apoptotic cells are indicated by the red arrows. **(2)** Percentage of apoptotic cells determined from DAPI morphological assessment following treatment with delphinidin at 25, 50, and 100 μM for 24 h. Mean ± SEM. * indicates significant difference ($P \leq 0.05$) vs. untreated control. Scale bar= 12.5 μm. n= 3.

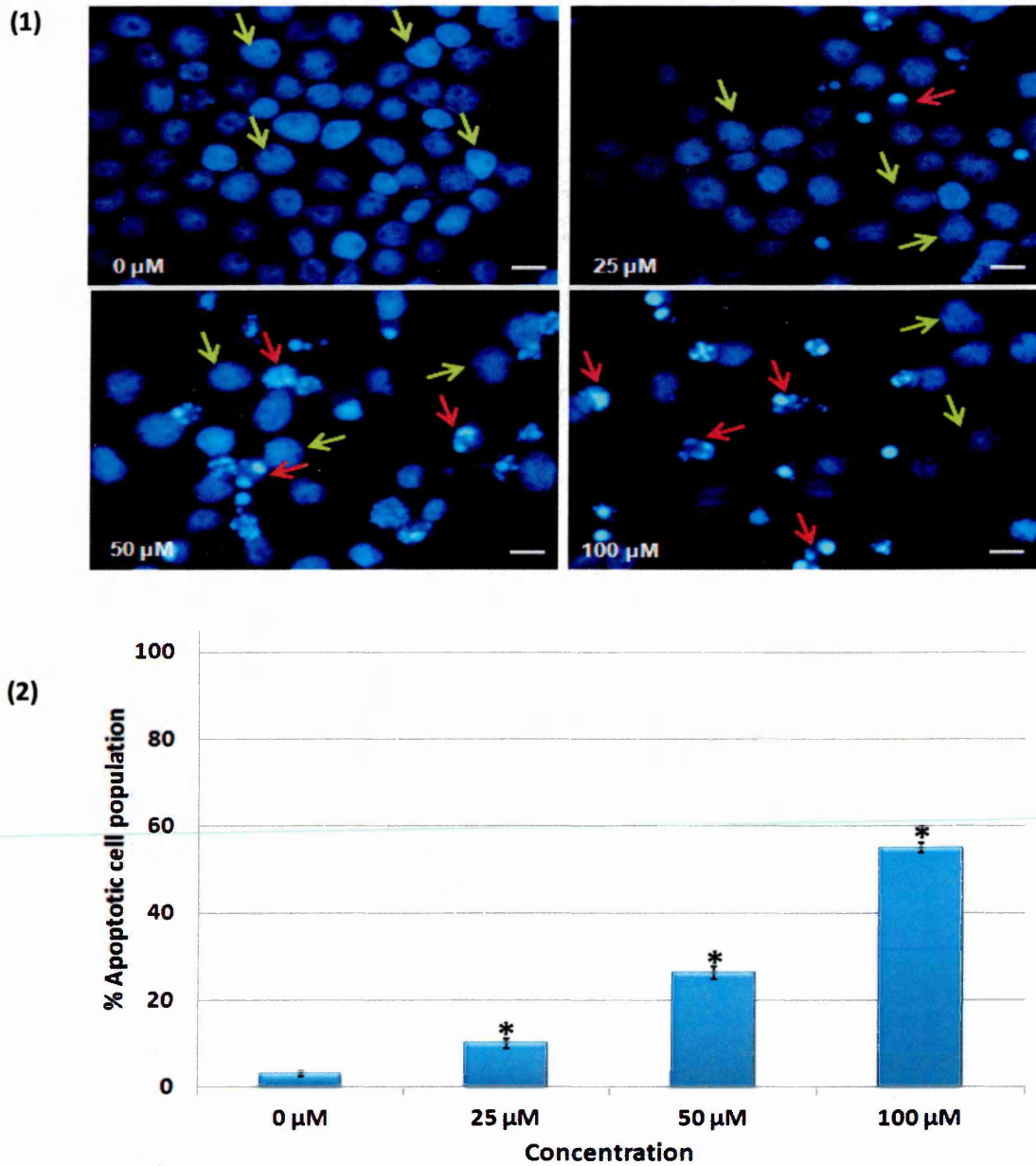
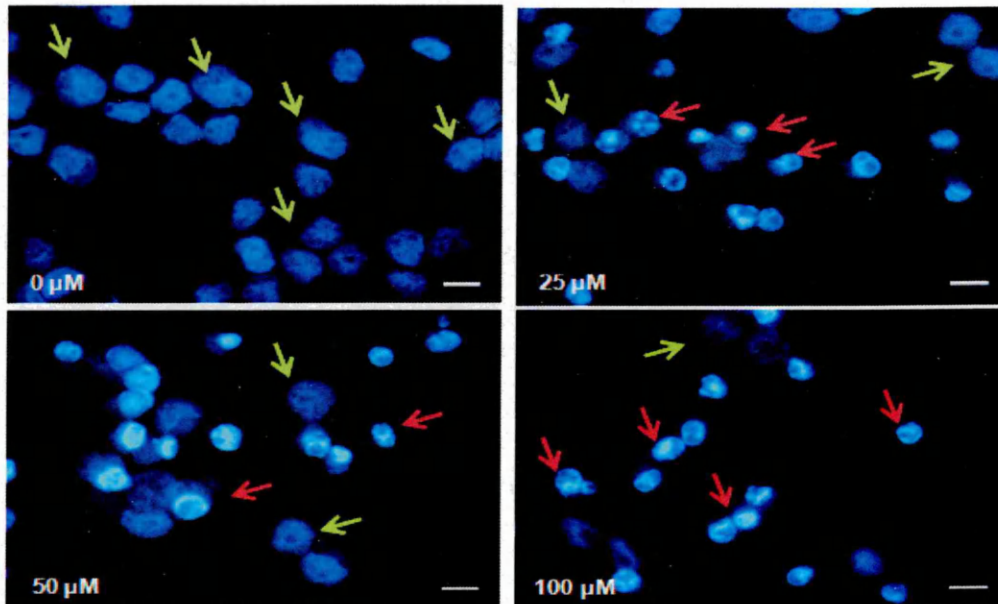


Figure 7.19: (1) Morphological staining analysis of HL-60 with DAPI treated with quercetin at concentrations 25, 50, and 100 μM for 24 h. Live cells are indicated by the green arrows, and apoptotic cells are indicated by the red arrows. **(2)** Percentage of apoptotic cells determined from DAPI morphological assessment following treatment with delphinidin at 25, 50, and 100 μM for 24 h. Mean ± SEM. * indicates significant difference ($P \leq 0.05$) vs. untreated control. Scale bar= 12.5 μm. n= 3.

THP-1

(1)



(2)

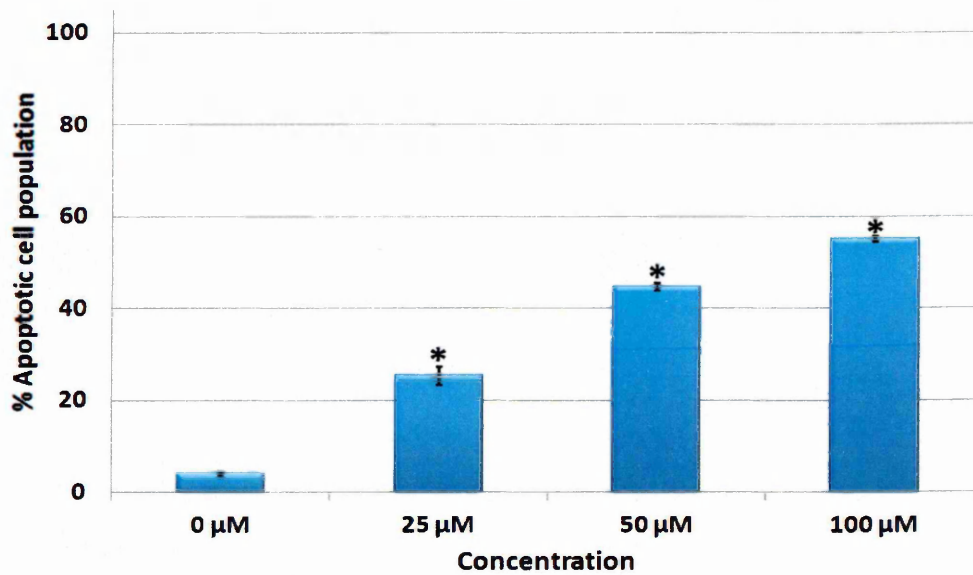


Figure 7.20: (1) Morphological staining analysis of THP-1 with DAPI treated with quercetin at concentrations 25, 50, and 100 μM for 24 h. Live cells are indicated by the green arrows, and apoptotic cells are indicated by the red arrows. **(2)** Percentage of apoptotic cells determined from DAPI morphological assessment following treatment with delphinidin at 25, 50, and 100 μM for 24 h. Mean ± SEM. * indicates significant difference ($P \leq 0.05$) vs. untreated control. Scale bar= 12.5 μm. n= 3.

7.3.3.2 Effect of Quercetin on Cell Cycle

Quercetin treatment of CCRF-CEM, MOLT-3, HL-60, and THP-1 cells resulted in a significant accumulation of cells in S phase in all four leukaemia cell lines corresponding with a significant decrease in G₀/G₁ and M phase at concentrations: 25; 50 and 100 µM following 24 h treatment ($P < 0.05$) (Figure 7.21).

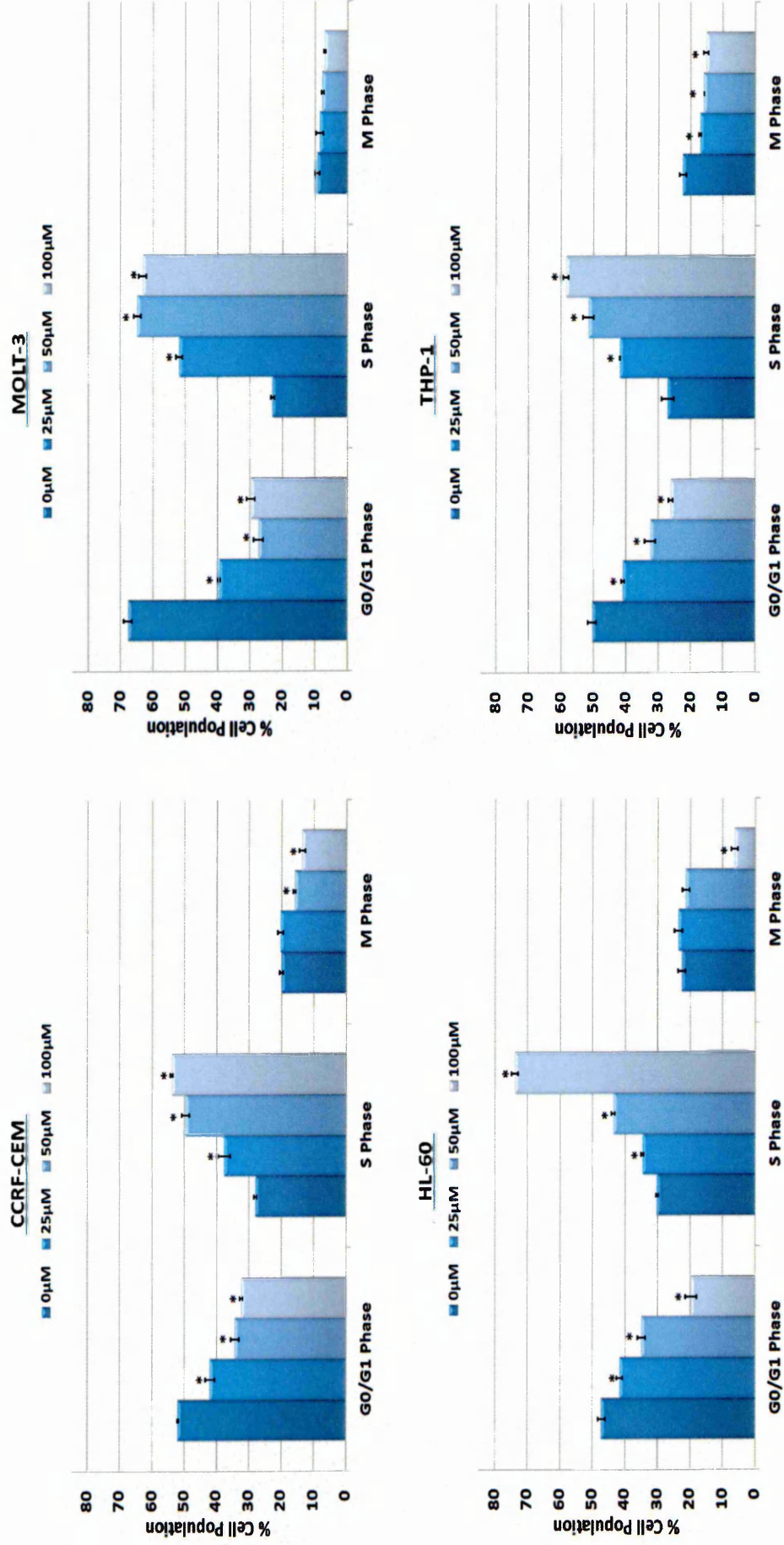


Figure 7.21: Cell cycle based on flow cytometry using FlowJo software following treatment with quercetin at concentration 25, 50, and 100 μM for 24 h incubation on four leukaemia cell lines (CCRF-CEM, MOLT-3, HL-60, AND THP-1). Mean ± SEM. * indicates significant difference ($P \leq 0.05$) vs. untreated control. n=3.

7.3.4 Punicalagin

7.3.4.1 Effect of Punicalagin on Induction of Apoptosis

7.3.4.1.1 Annexin V-FITC/PI Based on Flow Cytometry

Punicalagin significantly increased the number of apoptotic and dead cells and decreased the number of live cells following 24 h treatment in all four leukaemia cell lines (CCRF-CEM, MOLT-3, HL-60, and THP-1) at concentrations of 10, 25, 50, 75, and 100 μM ($P \leq 0.05$) (Figure 7.55). THP-1 was the least sensitive among the cell lines investigated, which illustrated small, but significant decrease in the number of live cell and an increase in the number of apoptotic and dead cells at all concentrations (Figure 7.22).

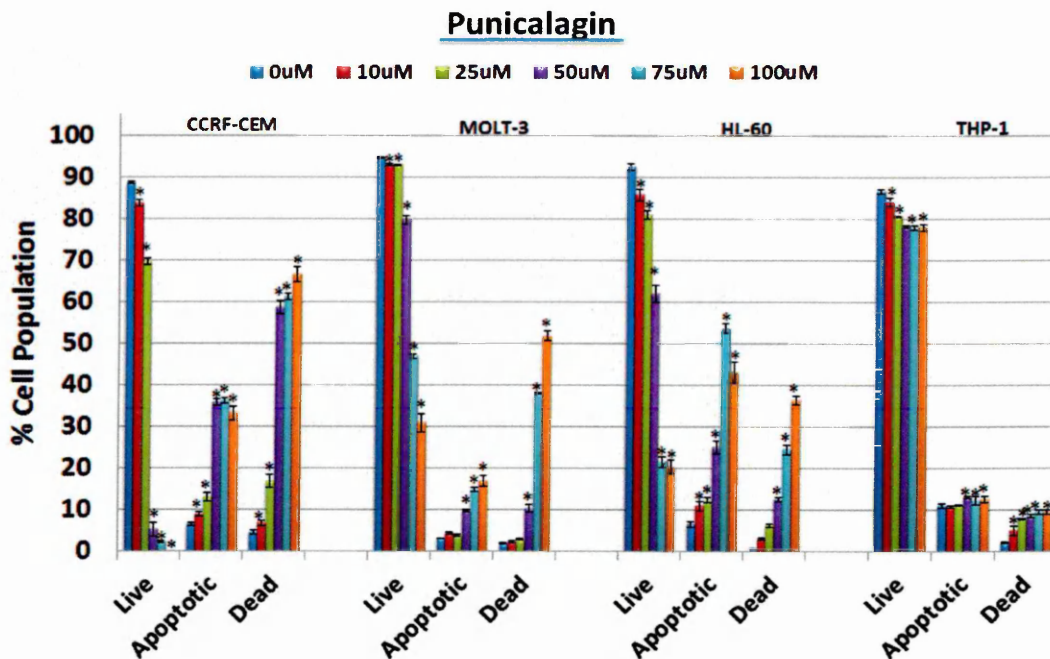


Figure 7.22: Annexin V-FITC/ PI based on flow cytometry following treatment with punicalagin (0, 10, 25, 50, 75, and 100 μM) for 24 h on CCRF-CEM and MOLT-3. Mean \pm SEM. * indicates significant difference ($P \leq 0.05$) vs. untreated control. $n = 3$.

7.3.4.1.2 Caspase-3 Activity

Punicalagin significantly increased caspase-3 activity in all four leukaemia cell lines (CCRF-CEM, MOLT-3, HL-60 and THP-1) with different sensitivity following 24 h treatment ($P < 0.05$) (Figure 7.23). Punicalagin was considerably less effective towards THP-1 cells with only 19% of cells positive for caspase-3 activity at 100 μM following 24 h incubation compared to 10% in control cells (Figure 7.23).

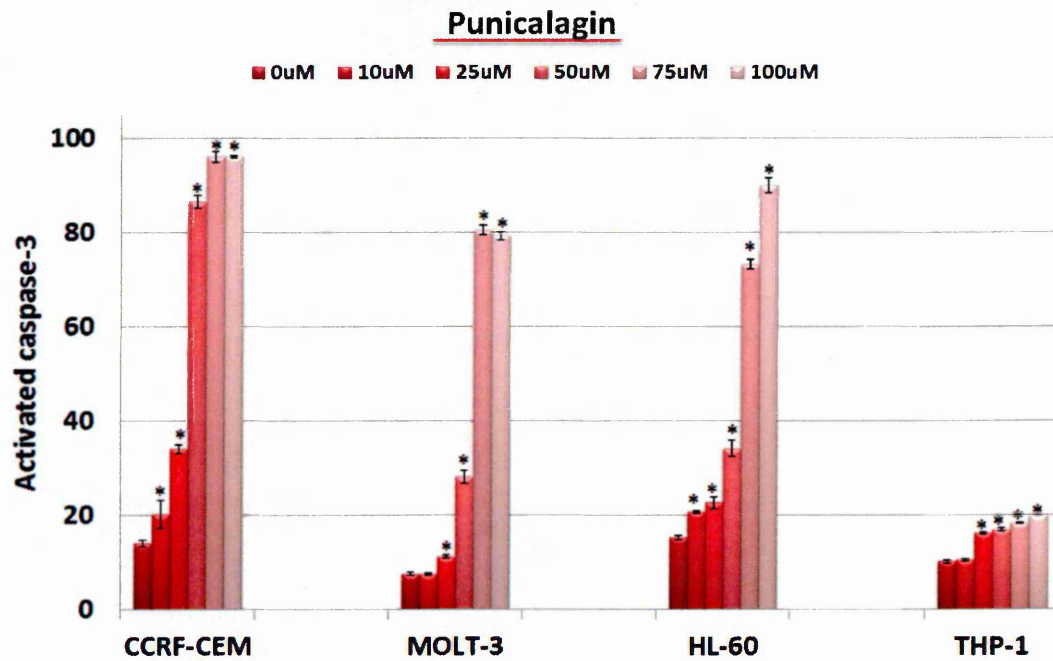


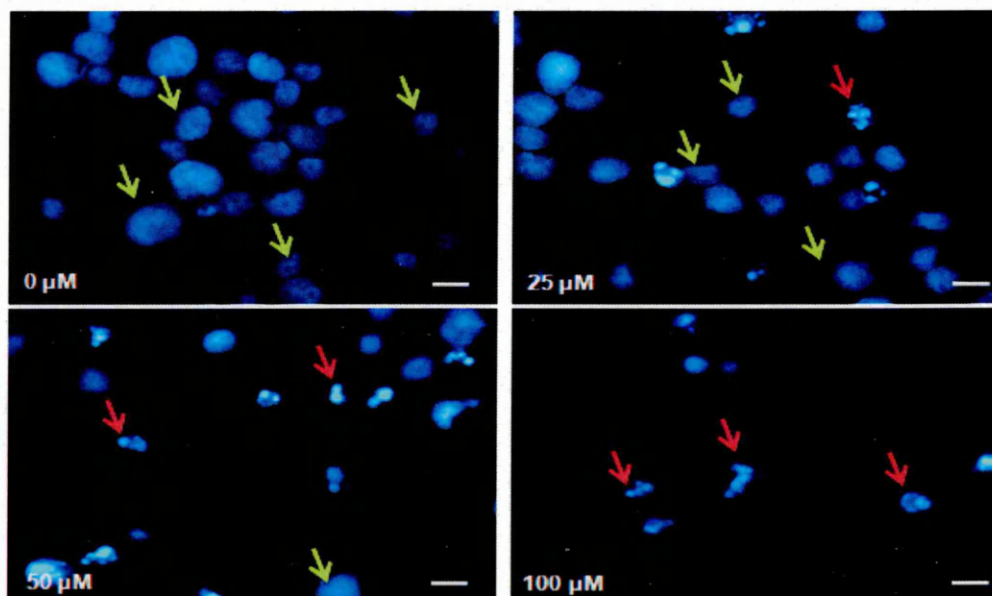
Figure 7.23: Effect of punicalagin on caspase-3 activation in four leukaemia cell lines (CCRF-CEM, MOLT-3, HL-60, and THP-1). Cells treated for 24h at concentrations of 10, 25, 50, 75 and 100 μM . Caspase-3 activation was determined by NucView™ 488 Caspase-3 substrate based on flow cytometry analysis. Means \pm standard error of the mean. *Significant difference ($P \leq 0.05$). n= 3.

7.3.4.1.3 DAPI for Morphological Assessment

Punicalagin showed a significant increase in the number of apoptotic cells in all four leukaemia cell lines tested (CCRF-CEM, MOLT-3, HL-60 and THP-1) at all concentrations following 24 h treatment ($P \leq 0.05$) (Figure 7.24-7.27).

CCRF-CEM

(1)



(2)

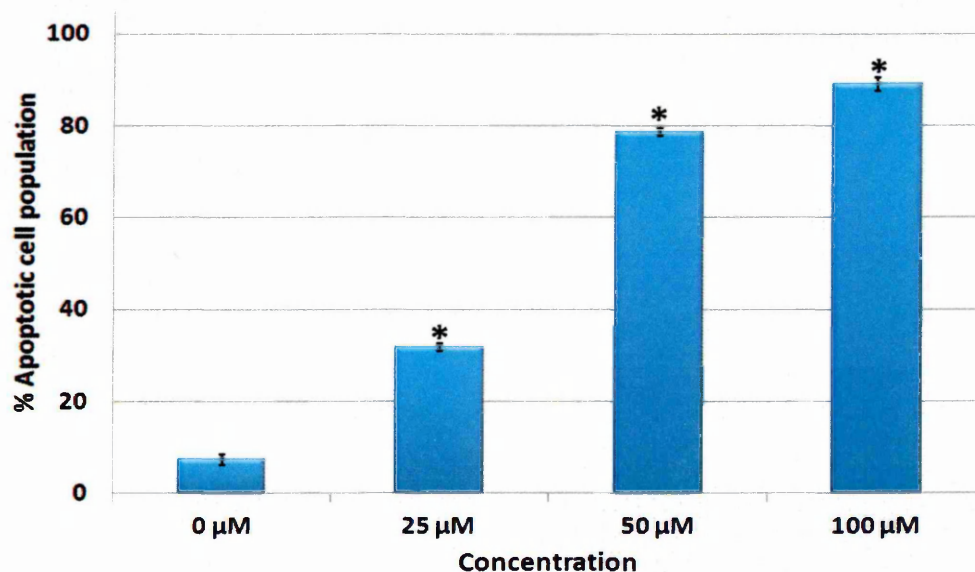


Figure 7.24: (1) Morphological staining analysis of CCRF-CEM with DAPI treated with punicalagin at concentrations 25, 50, and 100 μM for 24 h. Live cells are indicated by the green arrows, and apoptotic cells are indicated by the red arrows. (2) Percentage of apoptotic cells determined from DAPI morphological assessment following treatment with delphinidin at 25, 50, and 100 μM for 24 h. Mean \pm SEM. * indicates significant difference ($P \leq 0.05$) vs. untreated control. Scale bar= 12.5 μm. n= 3.

MOLT-3

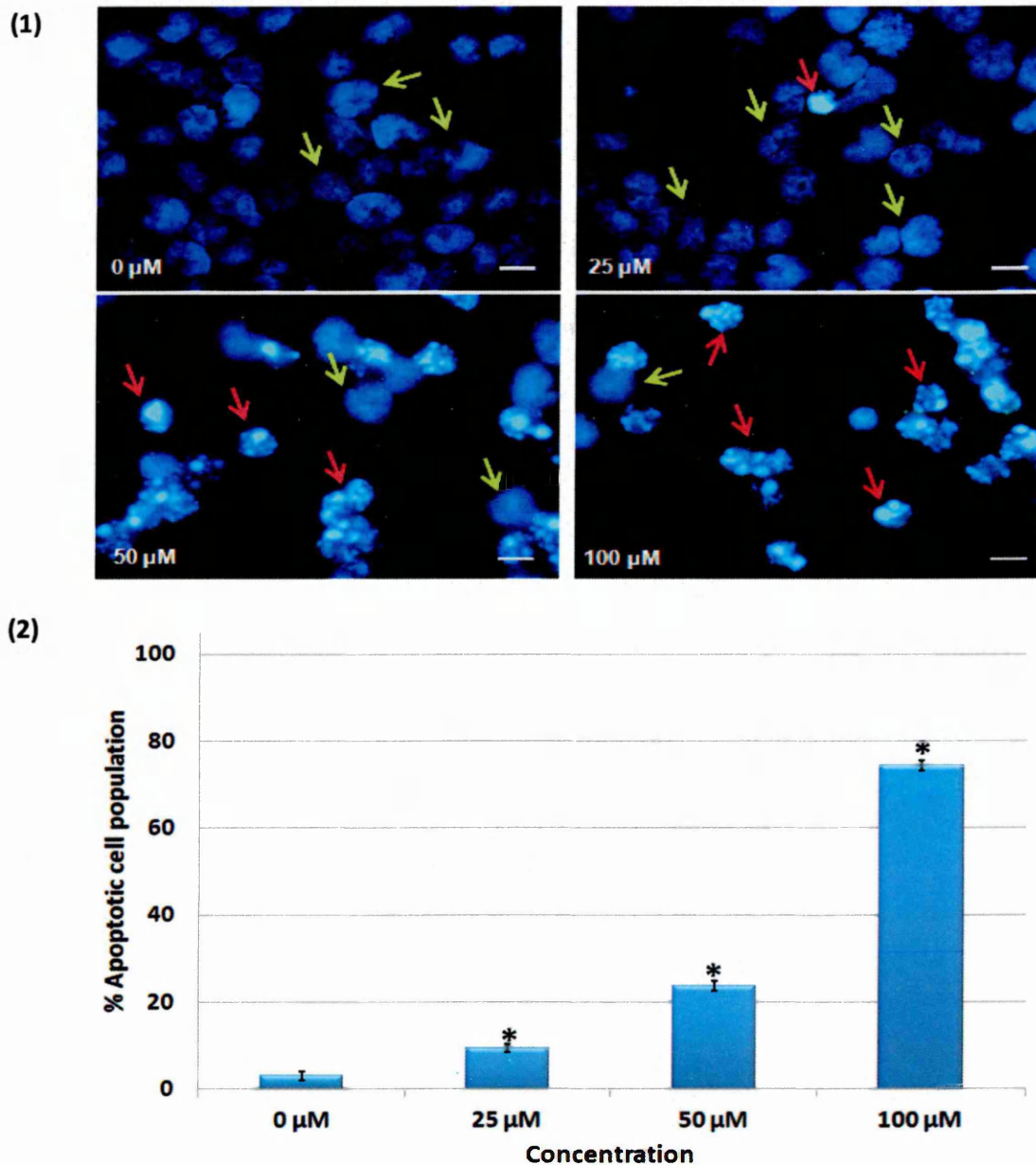
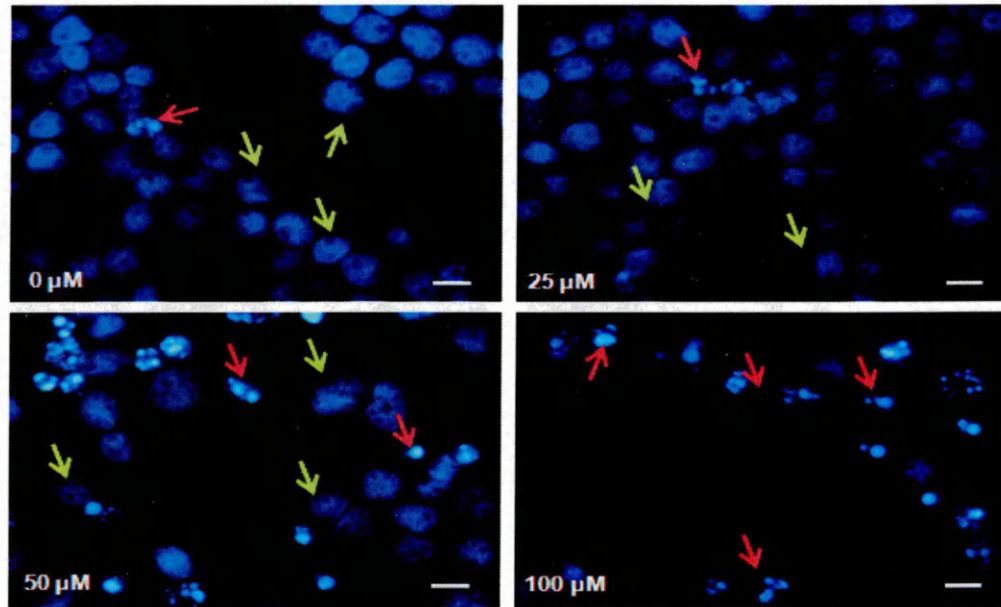


Figure 7.25: (1) Morphological staining analysis of MOLT-3 with DAPI treated with punicalagin at concentrations 25, 50, and 100 μM for 24 h. Live cells are indicated by the green arrows, and apoptotic cells are indicated by the red arrows. **(2)** Percentage of apoptotic cells determined from DAPI morphological assessment following treatment with delphinidin at 25, 50, and 100 μM for 24 h. Mean \pm SEM. * indicates significant difference ($P \leq 0.05$) vs. untreated control. Scale bar= 12.5 μm . n= 3.

HL-60

(1)



(2)

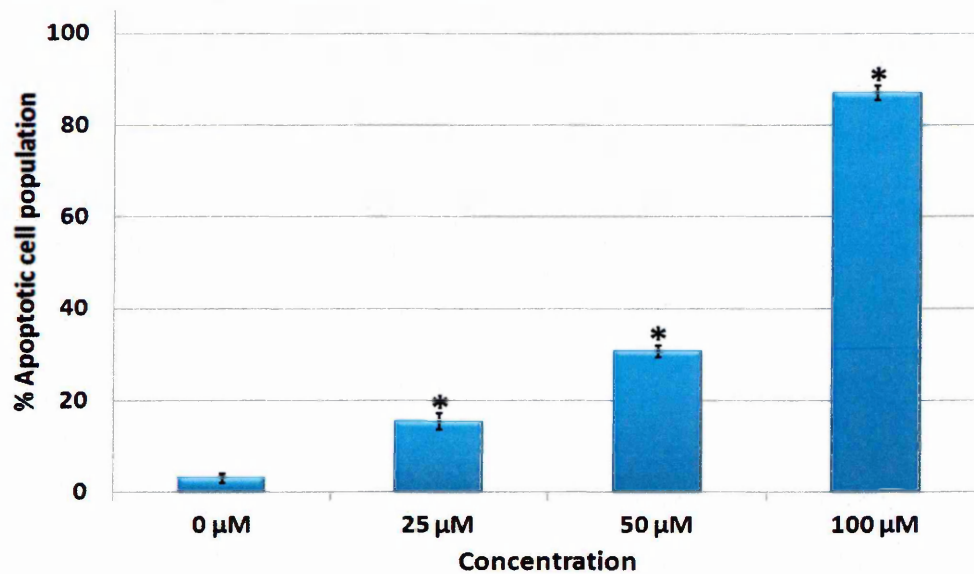
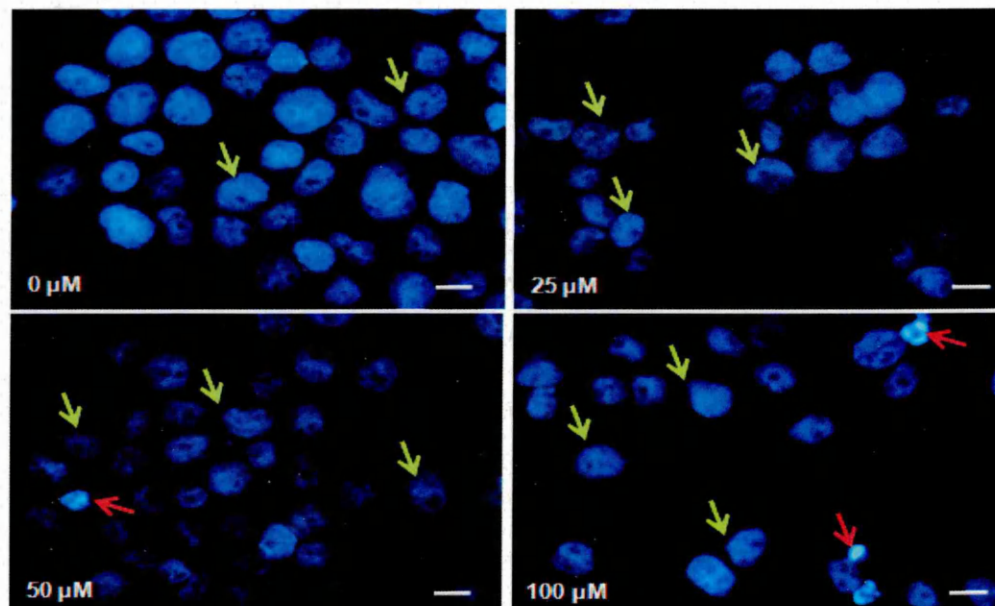


Figure 7.26: (1) Morphological staining analysis of HL-60 with DAPI treated with punicalagin at concentrations 25, 50, and 100 μM for 24 h. Live cells are indicated by the green arrows, and apoptotic cells are indicated by the red arrows. **(2)** Percentage of apoptotic cells determined from DAPI morphological assessment following treatment with delphinidin at 25, 50, and 100 μM for 24 h. Mean ± SEM. * indicates significant difference ($P \leq 0.05$) vs. untreated control. Scale bar= 12.5 μm. n= 3.

THP-1

(1)



(2)

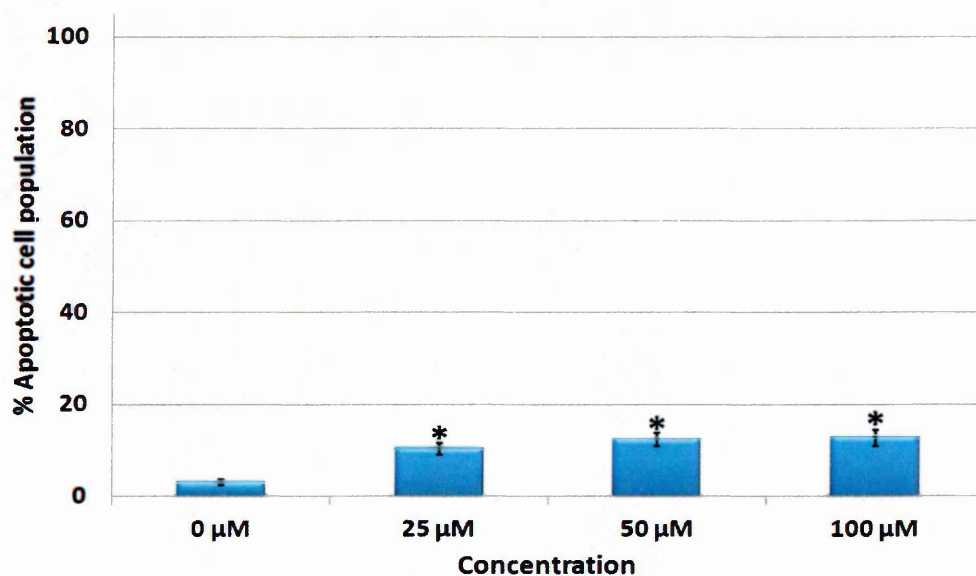


Figure 7.27: (1) Morphological staining analysis of THP-1 with DAPI treated with punicalagin at concentrations 25, 50, and 100 μM for 24 h. Live cells are indicated by the green arrows, and apoptotic cells are indicated by the red arrows. **(2)** Percentage of apoptotic cells determined from DAPI morphological assessment following treatment with delphinidin at 25, 50, and 100 μM for 24 h. Mean ± SEM. * indicates significant difference ($P \leq 0.05$) vs. untreated control. Scale bar= 12.5 μm. n= 3.

7.3.4.2 Effect of Punicalagin on Cell Cycle

Punicalagin showed a significant accumulation of cells in S phase corresponding with a significant decrease in G₀/G₁ phase in CCRF-CEM, MOLT-3 and HL-60 cells at all concentrations following 24 h treatment ($P < 0.05$) (Figure 7.28). Punicalagin treatment of THP-1 cells resulted in a significant accumulation of cells in S phase only following 100 μM stimulation corresponding with decrease in G₀/G₁ phase following 24 h incubation ($P < 0.05$) (Figure 7.28).

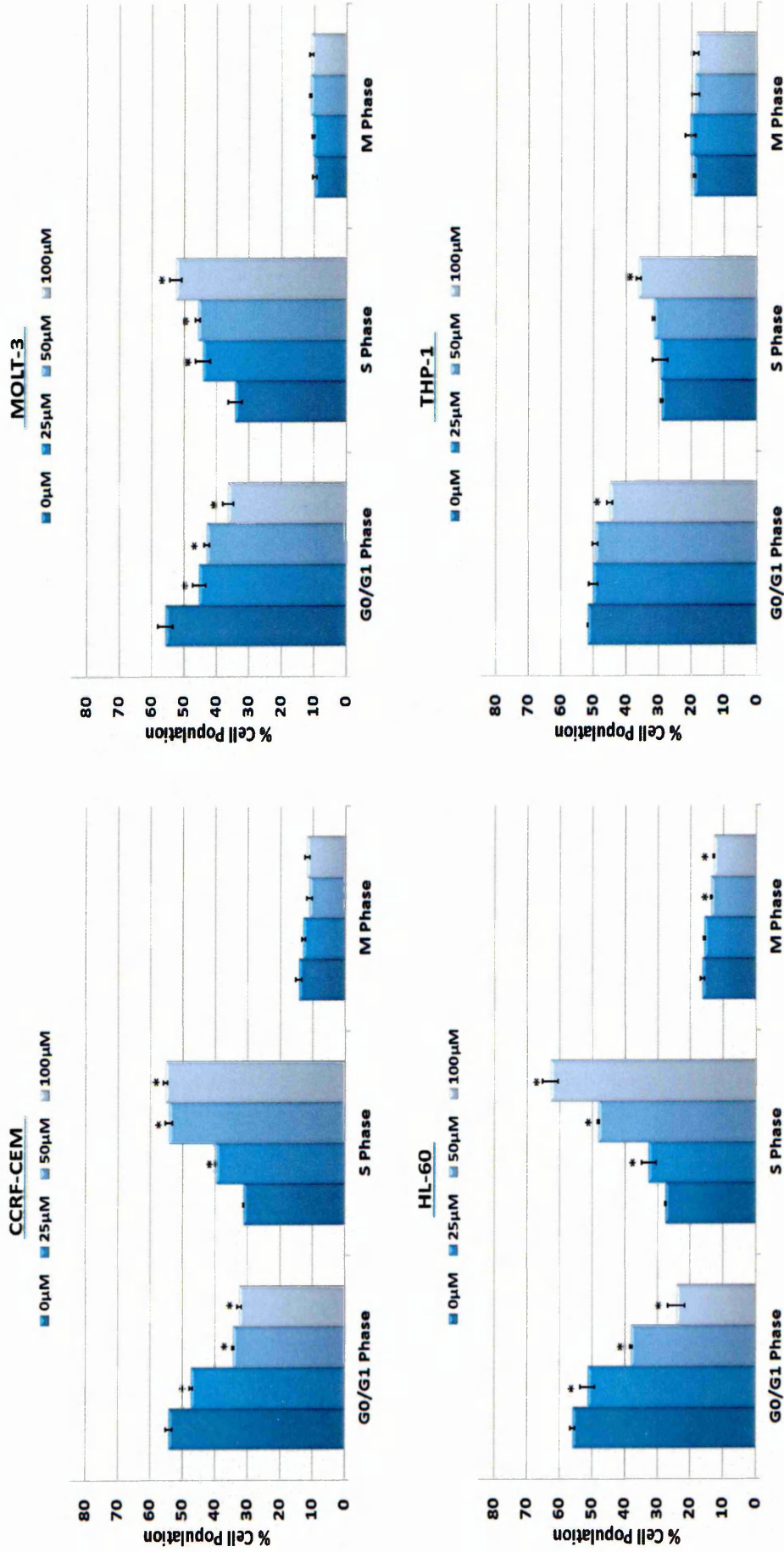


Figure 7.28: Cell cycle based on flow cytometry using FlowJo software following treatment with punicalagin at concentration 25, 50, and 100 μM for 24 h incubation on four leukaemia cell lines (CCRF-CEM, MOLT-3, HL-60, AND THP-1). Mean ± SEM. * indicates significant difference ($P \leq 0.05$) vs. untreated control. n= 3.

7.4 Discussion

EGCG, gallic acid, quercetin, and punicalagin significantly induced apoptosis determined by AV/PI, caspase-3 activity and DAPI morphology in all leukaemia cell lines. Moreover, S phase arrest was observed following treatment with gallic acid, quercetin, and punicalagin, and in G_0/G_1 following treatment with EGCG for 24 h.

7.4.1 EGCG

A number of laboratory studies *in vivo* and *in vitro* have demonstrated the inhibitory action of green tea rich in EGCG as having anti-carcinogenic activities. Previously (Chapter 5), EGCG induced a potent decrease in ATP level. Here, its effect on induction of apoptosis and cell cycle regulation showed promising results in all four leukaemia cell lines tested. Using annexin V/PI-FITC based on flow cytometry and DAPI morphological assessment a significant induction of apoptosis in leukaemia cell lines was observed. In addition, caspase-3 which plays an important role in apoptosis increased in most cell lines. This is consistent with Nakazato *et al.* (2007) who showed that EGCG induced apoptosis in four human leukaemia cell lines HL-60, U937, KG-1a, and K562 following 24 h treatment. In addition many studies have verified this observation in several cell types (Khan (3) *et al.*, 2006). In breast cancer EGCG induced apoptosis in several cell lines including MCF-7 and MDA-MB-231 by regulating pro- and anti-apoptotic proteins including Bcl-2, Bcl-XL, and Bax (Thangapazham *et al.*, 2007; Tang *et al.*, 2007). In prostate cancer, induction of apoptosis was identified in different cell lines (LNCap, PC-3 and DU145) (Paschtka *et al.*, 1998; Hastak *et al.*, 2005) in response to treatment with EGCG, which was also shown to be mediated via altered expression of the Bcl-2 family, which triggered the activation of initiator caspase-8 and -9 followed by activation of effector caspase-3 (Hastak *et al.*, 2005). Qanungo *et al.* (2005) observed that the anti-proliferative action of EGCG on pancreatic cancer cells was mediated through induction of apoptosis as evident from nuclear condensation, caspase-3 activation and PARP cleavage. In addition he reported that induction of apoptosis in pancreatic cells following treatment with EGCG was accompanied by cell cycle arrest at G_0/G_1 . Here G_0/G_1 arrest was also observed in all four leukaemia cell lines tested following treatment with EGCG. Similarly, Nakazato *et al.* (2005) investigated the effect of EGCG in four human myeloid leukaemia cell lines (K562, U937,

HL-60, and KU812) at a concentration of 100 μ M for 24 h. Following treatment with EGCG increased the population of G_0/G_1 phase with a reduction of cells in S phase. This observation may indicate that EGCG is not one of major compounds present in PJ, as the current study has shown that PJ (Chapter 3) and acetonitrile fraction (Chapter 4) induce S phase arrest. However, G_0/G_1 arrest following EGCG was also identified in many cancer cell lines including prostate (DU145 and LNCap) (Gupta *et al*, 2000), cervical (CaSKi) (Ahn *et al*, 2003), breast (MDA-MB-231 and MCF-10A), human epidermal carcinoma (A431) (Ahmad *et al*, 2000). Other studies reported M Phase arrest following treatment with 50 and 100 μ M EGCG cancer cells such as lung cells (PC-9) (Okabe *et al*, 1997) and colon cells (Caco2) (Salucci *et al*, 2002) indicating that effect of EGCG on cell cycle may depend on cell type and tumour origin.

7.4.2 Gallic Acid

Gallic acid is well known to possess anti-oxidant and pro-oxidant properties in a concentration dependent manner which varies according to the presence of metal ions (Locatelli *et al*, 2012). This pro-oxidant property of gallic acid has been suggested as the trigger for apoptosis in cancer cell lines, however, it has also been shown to regulate Fas/FasL, p53, and Bcl-2 family leading to activation of the caspase cascade (Veluri *et al*, 2006; Ji *et al*, 2009; Verma *et al*, 2013). Gallic acid has been shown to induce apoptosis in several cancer cell lines including: stomach (KATO III) (Yoshioka *et al*, 2000); colon (COLO 205 and HT-29) (Yoshioka *et al*, 2000; Bernhaus *et al*, 2009); prostate (DU145 and 22Rv1) (Veluri *et al*, 2006; Kaur *et al*, 2009); lung (Calu-6, A459, and NCI-H460) (Ji *et al*, 2009; You and Park, 2010) and cervical cancer cell lines (Hela) (You *et al*, 2010). Here gallic acid significantly induced apoptosis and increased caspase-3 activity in CCRF-CEM, MOLT-3, and HL-60 cells, while had no effect on THP-1 cells.

In terms of cell cycle, gallic acid has been shown to inhibit proliferation of cancer cells by inhibiting cell cycle progression at different stages of the cell cycle. Here, gallic acid treatment resulted in an increase in the number of cells in S phase. This arrest was also detected in prostate cancer cells (DU145) (Agarwal (1) *et al*, 2006). In contrast, Hsu *et al*. (2001) found that gallic acid induced significant M phase arrest in breast cancer cells

(MCF-7). Ou *et al.* (2010) also reported that exposure of human bladder carcinoma cell lines (TSGH-8301) to gallic acid resulted in significant increase M phase cells, which was accompanied by a decrease in G₀/G₁ phase cells.

7.4.3 Quercetin

Here, quercetin significantly induced apoptosis and increased caspase-3 activity in all four leukaemia cell lines following 24 h treatment. Interestingly quercetin showed a potent effect in THP-1 cells comparing to other agents tested (EGCG, gallic acid, punicalagin). This confirms the effect of quercetin on ATP seen previously (Chapter 5). However these responses are inconsistent with the sensitivity of cell lines following treatment with PJ and acetonitrile fraction (Chapter 3 and 4) (Dahlawi *et al.*, 2011; Dahlawi *et al.*, 2013) indicating that quercetin is less likely to be one of the major bioactive compounds from PJ. However as quercetin is found in greater abundance in the peel from the pomegranate rather than the arils (Poyrazoglu *et al.*, 2002), it is possible that limited quantities of quercetin were seen in the PJ used in this study, which were isolated from the edible part of the pomegranate, the arils. This is further supported by the lack of quercetin identified during LC/MS analysis of whole PJ and the acetonitrile fractions in Chapter 4. A number of studies have shown that quercetin can induce cell death by an apoptotic mechanism in cancer cell lines including breast (MCF-7) (Chou *et al.*, 2010) and (MDA-MB-231) (Chien *et al.*, 2009), lung (A549) (Nguyen *et al.*, 2004), colon (HT29 and SW480) (Kim *et al.*, 2005), and prostate (DU-145) (Kim *et al.*, 2008; Jung *et al.*, 2010) (PC-3) (Vijayababu *et al.*, 2005; Kim *et al.*, 2008; Jung *et al.*, 2010; Senthilkumar *et al.*, 2010;) (LNCaP) (Lee *et al.*, 2008; Jung *et al.*, 2010) and more recently in leukaemia cell lines (Mahbub *et al.*, 2013). Some evidence has also been reported which indicates quercetin can modulate a number of key elements linked to the apoptosis including: activation of caspase-3, -8, and -9, release cytochrome *c* and cleavage PARP in cervical cells (Hela) (Bishayee *et al.*, 2013) breast (MDA-MB-231) (Chien *et al.*, 2009), prostate (DU-145) (Kim *et al.*, 2008) and regulation of Bcl-2 family proteins (Vijayababu *et al.*, 2005; Kim *et al.*, 2005; Kim *et al.*, 2008; Jung *et al.*, 2010).

In addition to the effects on apoptosis it was also found that quercetin induced accumulation in S phase in all four leukaemia cell lines tested. This S arrest was also seen

in human leukaemia cells (MOLT-4) treated with quercetin (Mertens *et al*, 2004) and colon cancer cell lines (SW480 and T84) (Richter *et al*, 1999). In contrast, quercetin has also been shown to induce M phase arrest in human leukaemia cells (U937) (Lee *et al.*, (2006); oesophageal squamous cell carcinoma (KYSE-510) (Zhang *et al*, 2009); lung (NCI-H209); and prostate cancer cells (PC-3 and DU-145) (Nair *et al*, 2004; Vijayababu *et al*, 2005; Senthilkumar *et al*, 2010). Conversely G_0/G_1 arrest has also been shown in breast (SKBr3, MDA-MB-435 and MDA-MB-231) (Jeong *et al*, 2009); liver (HepG2) (Mu *et al*, 2007) and liposacroma cell line (SW827) (Robaszkiewicz *et al*, 2007) cell lines. Suggesting that depending on cell type and tumour origin quercetin was found to arrest cell cycle at G_0/G_1 , S, or M phase.

7.4.4 Punicalagin

Punicalagin significantly induced apoptosis with an increase in caspase-3 activity in all four leukaemia cell lines following 24 h treatment, however there is limited work on the effect of punicalagin on cancer cell lines, with the majority of studies focusing on colon cancers. Seeram *et al.* (2005) reported that punicalagin exhibited apoptotic activity in HT-29 and HCT116 colon cells. In another study, Caco-2 underwent apoptosis upon treatment with punicalagin after 24 h through Bcl-xl down-regulation with mitochondrial release of cytochrome c into the cytosol, and activation of initiator caspase-9 and effector caspase-3 (Larrosa *et al*, 2005). In addition, the same study found that punicalagin treatment resulted in S phase arrest following 100 μ M treatment, which is consistent with our results where S phase arrest was also seen. However, punicalagin is unique to pomegranate and was one of agents detected in the acetonitrile fraction (Chapter 4) which induced apoptosis and S phase arrest.

7.5 Conclusion

All selected compounds (EGCG, gallic acid, quercetin, and punicalagin which showed 50% reduction in ATP levels (Chapter 5) induced apoptosis and resulted in cell cycle arrest in the majority of the leukaemia cell lines. EGCG induced apoptosis in leukaemia cell lines with sensitivity matching of PJ. However EGCG was found to induce G_0/G_1 cell arrest in contrast to the S phase arrest seen following PJ and ACN fraction of PJ. Suggesting EGCG was not the main bioactive component in PJ. Gallic acid induced apoptosis in CCRF-CEM,

MOLT-3, and HL-60 cells only and caused S phase arrest with sensitivity levels matching those seen following PJ and ACN fraction treatment. Suggesting gallic acid may be one of the bioactive compounds found in PJ, although MS analysis of his study failed to identify this as one of the key peaks. Quercetin induced apoptosis and S phase arrest in leukaemia cell lines. Although the order of sensitivity did not match that of PJ and ACN fraction as THP-1 cells displayed greatest sensitivity to quercetin compared to being the least sensitive following PJ whilst CCRF-CEM cells were the least sensitive to quercetin but most sensitive to PJ. Suggesting quercetin is not the main bioactive agent in the PJ studied here. Punicalagin induced apoptosis and S phase arrest with sensitivity levels matching those seen following PJ and acetonitrile fraction treatments. Suggests punicalagin may be one of the bioactive compounds found in PJ. Importantly MS analysis of the PJ used in this study identified punicalagin as one of the major components of the acetonitrile fraction of PJ. Interestingly to date punicalagin has only been associated from pomegranate.

8.1 Key Findings

This study demonstrated for the first time that PJ displayed potential anti-cancer effects through induction of apoptosis, inhibition of cellular proliferation and arrest of cell cycle in four myeloid and four lymphoid human leukaemia cell lines. In addition, induction of apoptosis and inhibition of cellular proliferation was dose and time dependant. Interestingly, different degrees of cytotoxicity between leukaemia cell lines were identified, where most of the lymphoid leukaemia cells were more sensitive than the myeloid cell lines. In addition PJ treatments induced cell cycle arrest in different phases which was dependant on the type of cells investigated (myeloid/lymphoid), dose and incubation times. These differential sensitivity patterns seen within myeloid and lymphoid cell lines could be due to different cellular origin, genetic abnormalities and or expression of differential proteins by different types of cells. Importantly, PJ showed a lower level of cytotoxicity against normal HSCs than the effects seen in the majority of leukaemia cells.

Further SPE of PJ demonstrated bioactive compounds were found in the acetonitrile fraction which showed highest phenolic content suggesting polyphenols were the active component. Further analysis of the bioactive acetonitrile fraction using mass spectrometry identified a number of compounds including: the anthocyanins: cyanidin-3-glucoside; cyanidin 3,5-*O*-diglucosides; delphinidin-3-glucoside; delphinidin-3,5-*O* diglucosides; pelargonidin-3-glucoside and pelargonidin-3,5-*O*-diglucosides; ellagitannins including punicalagin and phenolic acids including ellagic acid.

Comparison of IC_{50} (determined as 50% decrease in ATP levels) was used to determine the most effective compounds from PJ. Seven key polyphenols were identified as potent compounds including: delphinidin; pelargonidin; cyanidin; quercetin; EGCG; gallic acid and punicalagin.

Interestingly of the anthocyanins investigated, delphinidin was more potent than cyanidin and pelargonidin suggesting the activity of the anthocyanins was related to the number of hydroxyl groups. In addition anthocyanidins which lacked sugar molecules displayed greater toxicity toward leukaemia cells than their glycosylated forms.

The mechanisms of apoptosis for delphinidin were determined demonstrating delphinidin induced both caspase-8 and -9 in leukaemia cell lines, suggesting delphinidin activated both intrinsic and extrinsic pathways. Delphinidin also modulated expression of Bcl-2 family proteins resulting in decreased expression of anti-apoptotic proteins: Bcl-2 and Bcl-xl, and increased pro-apoptotic proteins: Bax and Bad. In addition treatment of leukaemia cells with delphinidin resulted in increased expression of cytochrome C and Smac/Diablo

Quercetin induced apoptosis and S phase arrest in leukaemia cell lines. Although the order of sensitivity did not match that of PJ and ACN fraction as THP-1 cells displayed greatest sensitivity to quercetin compared to being the least sensitive following PJ whilst CCRF-CEM was the least sensitive to quercetin but most sensitive to PJ. Suggesting quercetin was not the main bioactive agent found in PJ. EGCG also induced apoptosis in leukaemia cell lines with sensitivity which matched that seen following PJ treatments. However EGCG was found to induce G₀/G₁ cell arrest in contrast to the S phase arrest seen following PJ and ACN fraction of PJ. Suggesting EGCG was not the main bioactive component in PJ.

Gallic acid induced apoptosis and S phase arrest with sensitivity levels matching those seen following PJ and ACN fraction treatment. Suggesting gallic acid may be one of the bioactive compounds found in PJ, although MS analysis of the PJ used in this study failed to identify gallic acid as a major component.

Punicalagin induced apoptosis and S phase arrest with sensitivity levels matching those seen following PJ and acetonitrile fraction treatments. Suggesting punicalagin may be one of the bioactive compounds found in PJ. Importantly MS analysis of the PJ used in this study identified punicalagin as one of the major components of the acetonitrile fraction of PJ. Interestingly to date punicalagin has only been associated from pomegranate, suggesting this could be a novel bioactive agent only sourced from pomegranates.

8.2 Future Directions

In order to test the efficiency and safety of PJ and its bioactive compounds on human health, further studies are required including *in vitro* and *in vivo* studies. These phases are

essential to approve the clinical use of these agents in general population prior to being used as a novel treatment for leukaemia

8.2.1 *In vitro* Studies

8.2.1.1 Investigation into the Mechanisms of Induction of Apoptosis

Experimental data obtained from this study has indicated that delphinidin, punicalagin, gallic acid, EGCG, and quercetin can induce apoptosis in leukaemia cell lines. Considering their beneficial effects in induction of apoptosis in prevention of leukaemia or as novel potential therapeutic agents more research is required to determine their mechanism of action in induction of apoptosis in leukaemia cell lines. Thus it is important to investigate their mechanistic effects on a number of pro- and anti-apoptotic proteins, caspase activation and other apoptotic proteins (Table 1.2 and 1.3). Mechanistic study by Larrosa *et al.* (2006) found that both punicalagin and ellagic acid induce apoptosis in human colon cancer cell line (Caco-2) as evidenced by an increase in cytochrome *c* release, decrease Bcl-xl, and increased caspase-3 and -9 expression. As such further investigations within leukaemia cell lines will aid in the identification of new therapeutic agents for the treatment of leukaemia.

8.2.1.2 Investigation into Cell Cycle Regulatory Proteins

This study showed that PJ and its bioactive compounds induce cell cycle arrest in different phases in leukaemia cell lines investigated, with the majority of agents inducing S phase arrest. Understanding the effects on progression of cell cycle is essential for the rational design of novel drugs to prevent abnormal cellular proliferation seen during cancer. The progression of cell cycle is regulated by the actions of protein kinase complexes composed of cyclin and cyclin-dependent kinases (CDK) (Table 1.1) in addition to other key regulators including CDK inhibitors and retinoblastoma (Section 1.1.1.2.3 and 1.1.1.2.4). Thus it is important to investigate the effect of PJ and its bioactive compounds on the activities of protein kinases and cell cycle regulators. Vicinanza *et al.* (2013) found that ellagic acid induced S phase which was associated with a decrease in cyclin B1 and cyclin

D1 in prostate cancer cell lines (DU-145 and PC-3). Whilst quercetin has been shown to down-regulate cyclin B1 and CK1 and increase the levels of CDK inhibitors, including: p53; p21^{CIP1/waf1}; and p27^{kip1} in human breast cancer cell lines (SK-Br3, MDA-MB-453, and MDA-MB-231 (Jeong et al, 2009; Jae-Hoon *et al*, 2009; Chou et al, 2010; Choi et al,)

8.2.1.3 Using Pomegranate Compounds in Combination

Although natural compounds naturally occur in combinations as seen within the PJ used within the current study, little information is available regarding possible additive or synergistic interactions between compounds naturally occurring. Synergism is important as it allows lower and potentially safer doses of each compound to generate the desired effect. Thus the identification of potential interactions between natural compounds may give information regarding the efficiency of compounds contained in foods in cancer prevention. Mertens-Talcott *et al.* (2006) reported that ellagic acid and quercetin interact synergistically with resveratrol in the induction of apoptosis and cause transient cell cycle arrest in human leukaemia cells (MOLT-4). In addition the effects of quercetin, kaempferol, and catechin in combination in breast cancer cell line (MDA-MB-231) synergistically inhibited cell proliferation and induce apoptosis (Schlachterman *et al*, 2008)

8.2.1.4 Investigating the Effect of Pomegranate Compounds in Combination with Chemotherapy

Despite recent advances in cancer treatment, most of the current chemotherapy agents cause severe side effects in addition to high failure rates resulting in patient relapse following single agent therapies. Thus searching for safer and better drugs to eliminate side effects and prevent relapse are important. Punicalagin, delphinidin, gallic acid, quercetin, and EGCG are polyphenols which induce apoptosis and cell cycle arrest in leukaemia cell lines. However, using combinations of these compounds with chemotherapy drugs may open new avenues for the discovery of ideal drug combinations for leukaemia therapy. A number of studies *in vitro* have used polyphenols in combination with chemotherapy agents, demonstrating promising results in cancer treatment. Kubato *et al.*, (2003) showed that combined effects in lung cancer cell lines of resveratrol and paclitaxel (an essential chemotherapeutic agent against lung cancer) significantly enhanced the effect of paclitaxel. Lev-Ari *et al.* (2009) reported that combined celecoxim

(chemotherapy agent that used for colon cancer) and curcumin (a natural compound) showed synergistic inhibition of growth of colon cancer cell lines: HT-29 and SW480 cells. In prostate cancer, lycopene (natural compound) synergistically enhanced the anti-proliferative effect of docetaxel (chemotherapeutic drug that clinically used to treat patients with advanced prostate cancer) (Tang *et al*, 2011).

8.2.1.5 Measuring Reactive Oxygen Species (ROS)

ROS are considered to be an important preventive biomarker and may be a crucial target for anti-cancer therapies by ameliorating oxidative stress and thus DNA damage (Valko *et al*, 2007; Lambert *et al*, 2010). Therefore it is important to measure ROS level in leukaemia cell lines following treatment with PJ and its bioactive compounds. Two studies have shown that treatment of cancer cells with extracted and purified anthocyanins resulted in an accumulation of ROS and subsequent induction of apoptosis (Feng *et al*, 2007; Hou *et al*, 2005). EGCG has also been shown to induce ROS generation in a number of cancer cell lines including leukaemia (Jurkat) (Nakagawa, 2004), colon (HT-29) (Nie *et al*, 2002), and lung (H1299) (Li *et al*, 2010) cancer.

8.2.2 In vivo Studies

Most of the medicines that are used to treat animals are the same as those developed to treat human patients (Wienkers and Heath, 2005; Steele and Lubet, 2010). Although pomegranate products have shown promising anti-tumour activities in various organs of animals including: skin (CD1 mice) (Afaq *et al*, 2005), prostate (Athymic nude mice) (Malik *et al*, 2005), lung (Athymic nude mice) (Khan (2) *et al*, 2006), and colon (F344 rats) (Seeram *et al*, 2005), the chemo preventive potential of pomegranate has not been investigated against the pre-clinical model of leukaemia. Thus, in order to justify the non-toxicity of the PJ and its effective compounds on human health and for predicting therapeutic responses in leukaemic patients, the effects of these agents in treatment of animal models to determine the effective doses and administration schedules of these compounds would need to be performed prior to clinical trials to investigate their use as potential chemo preventive and anti-leukaemic agents.

8.2.3 Clinical Trials

Following investigation of the effect of PJ and its bioactive compounds *in vitro* and *in vivo*, the next step would be to examine the efficacy and safety in humans. Human clinical trials to date have involved consumption of a normal amount of PJ or a concentrated liquid or powder that is equivalent in polyphenolic content to an 8 oz serving of pomegranate juice (Johanningsmeier and Harris, 2011). In these studies no side effects were indicated and it is generally considered safe to consume the fresh fruit and juice of pomegranate, and indeed is a natural component of many normal diets.

PJ has been taken forward to phase II clinical trials, particularly in prostate cancers (Pantuck *et al*, 2006). In a phase II clinical trial, 46 men with rising prostate-specific antigen (PSA) levels following treatment for prostate cancer, were given 8 ounces of PJ daily during disease progression, PJ consumption significantly delayed the rise in PSA, increased the PSA doubling time from 15 months to 54 months based on baseline versus post-treatment measurements (Pantuck *et al*, 2006). In addition, analysis of plasma levels before and after treatment with PJ exhibited the treated subject plasma to have higher antioxidant and anti-proliferative activities (Pantuck *et al*, 2006). Thus the expansion to clinical trials in patients with leukaemia would be an essential step towards developing the use of pomegranate extracts in the treatment of leukaemia.

8.3 Final Conclusions

Together this study has shown that PJ is a rich source of bioactive compounds which could hold promise for treatment of leukaemia. The most promising compounds found with PJ were delphinidin, gallic acid, and punicalagin. Further investigation into these agents in the treatment and prevention of leukaemia are essential to develop these potential agents as future treatments.

Appendixes

Company	Location
ATCC	Middlesex, UK
Becton Dickinson BD	Oxford, UK
Cambridge Biosciences	Cambridge, UK
Enzo Life Sciences	Exeter, UK
Extrasynthese	Genay, France
Fisher Scientific	Leicestershire, UK
Fisher Scientific	Loughborough, UK
GE healthcare	Buckinghamshire, UK
Invitrogen	Paisley, UK
LONZA	Slough, UK
Olympus	Essex, UK
Promega	Southampton, UK
R&D Systems	Abingdon, UK
Roche	Burgess Hill, West Sussex, UK
Sigma	Poole, UK
Tree Star	Ashland, OR, USA
Applied Bioscience	Cheshire, UK
Phenomenex	Hartsfield, UK
Cambridge Bioscience	Cambridge, UK
Invitrogen	Paisley, UK
Ambion	Cambridgeshire, UK
Bioline	London, UK
Abcam	Cambridge, UK

Referances

- Adams, J.M., 2003. Ways of dying: multiple pathways to apoptosis. *Genes Dev.* 17, 2481-2495.
- Adams, L.S., Seeram, N.P., Aggarwal, B.B., Takada, Y., Sand, D., Heber, D., 2006. Pomegranate juice, total pomegranate ellagitannins, and punicalagin suppress inflammatory cell signaling in colon cancer cells. *J. Agric. Food Chem.* 54, 980-985.
- Adams, L.S., Zhang, Y., Seeram, N.P., Heber, D., Chen, S., 2010. Pomegranate Ellagitannin-Derived Compounds Exhibit Antiproliferative and Antiaromatase Activity in Breast Cancer Cells *In vitro*. *Cancer Prevention Research* 3, 108-113.
- Adhami, V.M., Malik, A., Zaman, N., Sarfaraz, S., Siddiqui, I.A., Syed, D.N., Afaq, F., Pasha, F.S., Saleem, M., Mukhtar, H., 2007. Combined inhibitory effects of green tea polyphenols and selective cyclooxygenase-2 inhibitors on the growth of human prostate cancer cells both *in vitro* and *in vivo*. *Clinical Cancer Research* 13, 1611-1619.
- Afaq, F., Saleem, M., Krueger, C.G., Reed, J.D., Mukhtar, H., 2004. Anthocyanin-and hydrolyzable tannin-rich pomegranate fruit extract modulates MAPK and NF- κ B pathways and inhibits skin tumorigenesis in CD-1 mice. *International Journal of Cancer* 113, 423-433.
- Afaq, F., Zaid, M.A., Khan, N., Dreher, M., Mukhtar, H., 2009. Protective effect of pomegranate-derived products on UVB-mediated damage in human reconstituted skin. *Exp. Dermatol.* 18, 553-561.
- Afaq, F., Zaman, N., Khan, N., Syed, D.N., Sarfaraz, S., Zaid, M.A., Mukhtar, H., 2008. Inhibition of epidermal growth factor receptor signaling pathway by delphinidin, an anthocyanidin in pigmented fruits and vegetables. *International Journal of Cancer* 123, 1508-1515.
- Agarwal, C., Tyagi, A., Agarwal, R., 2006. Gallic acid causes inactivating phosphorylation of cdc25A/cdc25C-cdc2 via ATM-Chk2 activation, leading to cell cycle arrest, and induces apoptosis in human prostate carcinoma DU145 cells. *Molecular cancer therapeutics* 5, 3294-3302.
- Aggarwal, B.B., Shishodia, S., 2006. Molecular targets of dietary agents for prevention and therapy of cancer. *Biochem. Pharmacol.* 71, 1397-1421.
- Ahmad, N., Cheng, P., Mukhtar, H., 2000. Cell cycle dysregulation by green tea polyphenol epigallocatechin-3-gallate. *Biochem. Biophys. Res. Commun.* 275, 328-334.
- Ahmed, S., Wang, N., Hafeez, B.B., Cheruvu, V.K., Haqqi, T.M., 2005. Punica granatum L. extract inhibits IL-1 β -Induced expression of matrix metalloproteinases by inhibiting the activation of MAP kinases and NF- κ B in human chondrocytes *in vitro*. *J. Nutr.* 135, 2096-2102.
- Ahn, W.S., Huh, S.W., Bae, S., Lee, I.P., Lee, J.M., Namkoong, S.E., Kim, C.K., Sin, J., 2003. A major constituent of green tea, EGCG, inhibits the growth of a human cervical cancer cell line, CaSki cells, through apoptosis, G1 arrest, and regulation of gene expression. *DNA Cell Biol.* 22, 217-224.
- Ainsworth, E.A., Gillespie, K.M., 2007. Estimation of total phenolic content and other oxidation substrates in plant tissues using Folin-Ciocalteu reagent. *Nature Protocols* 2, 875-877.
- Akan, I., Akan, S., Akca, H., Savas, B., Ozben, T., 2005. Multidrug resistance-associated protein 1 (MRP1) mediated vincristine resistance: effects of N-acetylcysteine and Buthionine sulfoximine. *Cancer Cell Int* 5, 22-30.
- Albrecht, M., Jiang, W., Kumi-Diaka, J., Lansky, E.P., Gommersall, L.M., Patel, A., Mansel, R.E., Neeman, I., Geldof, A.A., Campbell, M.J., 2004. Pomegranate extracts potently suppress

proliferation, xenograft growth, and invasion of human prostate cancer cells. *Journal of medicinal food* 7, 274-283.

Alegre, M.L., Frauwirth, K.A., Thompson, C.B., 2001. T-cell regulation by CD28 and CTLA-4. *Nature Reviews Immunology* 1, 220-228.

Alitheen, N., Yeap, S., Faujan, N., Ho, W., Beh, B., Mashitoh, A., *Leukemia and Therapy. American Journal of Immunology* 7.

Amakura, Y., Okada, M., Tsuji, S., Tonogai, Y., 2000. Determination of phenolic acids in fruit juices by isocratic column liquid chromatography. *Journal of Chromatography A* 891, 183-188.

American Cancer Society [online]. Last accessed May 22 2013 at: <http://www.cancer.org/>

Amigou, A., Sermage-Faure, C., Orsi, L., Leverger, G., Baruchel, A., Bertrand, Y., Nelken, B., Robert, A., Michel, G., Margueritte, G., 2011. Road traffic and childhood leukemia: The ESCALE Study (SFCE). *Environ. Health Perspect.* 119, 566.

Andersson, L.C., Nilsson, K., Gahmberg, C.G., 1979. K562—a human erythroleukemic cell line. *International Journal of Cancer* 23, 143-147.

Andriambeloson, E., Magnier, C., Haan-Archipoff, G., Lobstein, A., Anton, R., Beretz, A., Stoclet, J.C., Andriantsitohaina, R., 1998. Natural dietary polyphenolic compounds cause endothelium-dependent vasorelaxation in rat thoracic aorta. *J. Nutr.* 128, 2324-2333.

Appelbaum, F.R., Gundacker, H., Head, D.R., Slovak, M.L., Willman, C.L., Godwin, J.E., Anderson, J.E., Petersdorf, S.H., 2006. Age and acute myeloid leukemia. *Blood* 107, 3481-3485.

Artik, N., 1998. Determination of phenolic compounds in pomegranate juice by using HPLC. *Fruit Processing* 8, 492-499.

Ashkenazi, A., 2008. Targeting the extrinsic apoptosis pathway in cancer. *Cytokine Growth Factor Rev.* 19, 325-331.

Ashkenazi, A., Dixit, V.M., 1998. Death receptors: signaling and modulation. *Science* 281, 1305-1308.

Asiedu, C., Biggs, J., Lilly, M., Kraft, A.S., 1995. Inhibition of leukemic cell growth by the protein kinase C activator bryostatin 1 correlates with the dephosphorylation of cyclin-dependent kinase 2. *Cancer Res.* 55, 3716-3720.

Aviram, M., Dornfeld, L., Rosenblat, M., Volkova, N., Kaplan, M., Coleman, R., Hayek, T., Presser, D., Fuhrman, B., 2000. Pomegranate juice consumption reduces oxidative stress, atherogenic modifications to LDL, and platelet aggregation: studies in humans and in atherosclerotic apolipoprotein E-deficient mice. *Am. J. Clin. Nutr.* 71, 1062-1076.

Azadzoi, K.M., Schulman, R.N., Aviram, M., Siroky, M.B., 2005. Oxidative stress in arteriogenic erectile dysfunction: prophylactic role of antioxidants. *J. Urol.* 174, 386-393.

Badria, F.A., 2002. Melatonin, serotonin, and tryptamine in some Egyptian food and medicinal plants. *Journal of medicinal food* 5, 153-157.

Barcellona, M.L., Cardiel, G., Gratton, E., 1990. Time-resolved fluorescence of DAPI in solution and bound to polydeoxynucleotides. *Biochem. Biophys. Res. Commun.* 170, 270-280.

Barzegar, M., Fadavi, A., Azizi, M., 2004. An investigation on the physico-chemical composition of various pomegranates (*Punica granatum L.*) grown in Yazd. *Iranian Journal of Food Science and Technology* .

- Ben Nasr, C., Ayed, N., Metche, M., 1996. Quantitative determination of the polyphenolic content of pomegranate peel. *Zeitschrift für Lebensmitteluntersuchung und-Forschung A* 203, 374-378.
- Benitez, D.A., Pozo-Guisado, E., Alvarez-Barrientos, A., Fernandez-Salguero, P.M., Castellon, E.A., 2007. Mechanisms involved in resveratrol-induced apoptosis and cell cycle arrest in prostate cancer-derived cell lines. *J. Androl.* 28, 282.
- Bernasconi, N.L., Traggiai, E., Lanzavecchia, A., 2002. Maintenance of serological memory by polyclonal activation of human memory B cells. *Science Signalling* 298, 2199.
- Bernhaus, A., Fritzer-Szekeres, M., Grusch, M., Saiko, P., Krupitza, G., Venkateswarlu, S., Trimurtulu, G., Jaeger, W., Szekeres, T., 2009. Digalloylresveratrol, a new phenolic acid derivative induces apoptosis and cell cycle arrest in human HT-29 colon cancer cells. *Cancer Lett.* 274, 299-304.
- Biondi, A., Cimino, G., Pieters, R., Pui, C.H., 2000. Biological and therapeutic aspects of infant leukemia. *Blood* 96, 24-33.
- Biotium [online]. Last accessed February 30 2013 at: http://www.biotium.com/product/product_info/newproduct/nucview.asp
- Bishayee, K., Ghosh, S., Mukherjee, A., Sadhukhan, R., Mondal, J., Khuda-Bukhsh, A., 2013. Quercetin induces cytochrome-c release and ROS accumulation to promote apoptosis and arrest the cell cycle in G2/M, in cervical carcinoma: signal cascade and drug-DNA interaction. *Cell Prolif.* 46, 153-163.
- Blagosklonny, M.V., 2011. Cell cycle arrest is not senescence. *Aging (Albany NY)* 3, 94.
- Boatright, K.M., Salvesen, G.S., 2003. Mechanisms of caspase activation. *Curr. Opin. Cell Biol.* 15, 725-731.
- Boffetta, P., Couto, E., Wichmann, J., Ferrari, P., Trichopoulos, D., Bueno-de-Mesquita, H.B., van Duijnhoven, F.J.B., Büchner, F.L., Key, T., Boeing, H., 2010. Fruit and vegetable intake and overall cancer risk in the European Prospective Investigation into Cancer and Nutrition (EPIC). *J. Natl. Cancer Inst.* 102, 529-537.
- Bouillet, P., Strasser, A., 2002. BH3-only proteins—evolutionarily conserved proapoptotic Bcl-2 family members essential for initiating programmed cell death. *J. Cell. Sci.* 115, 1567-1574.
- Boxem, M., Srinivasan, D.G., van den Heuvel, S., 1999. The *Caenorhabditis elegans* gene *ncc-1* encodes a *cdc2*-related kinase required for M phase in meiotic and mitotic cell divisions, but not for S phase. *Development.* 126, 2227-2239.
- Boxem, M., van den Heuvel, S., 2001. *lin-35* Rb and *cki-1* Cip/Kip cooperate in developmental regulation of G1 progression in *C. elegans*. *Development* 128, 4349-4359.
- Brady, H.J.M., 2003. Apoptosis and leukaemia. *Br. J. Haematol.* 123, 577-585.
- Brusselmans, K., De Schrijver, E., Heyns, W., Verhoeven, G., Swinnen, J.V., 2003. Epigallocatechin-3-gallate is a potent natural inhibitor of fatty acid synthase in intact cells and selectively induces apoptosis in prostate cancer cells. *International journal of cancer* 106, 856-862.
- Buffler, P.A., Kwan, M.L., Reynolds, P., Urayama, K.Y., 2005. Environmental and genetic risk factors for childhood leukemia: appraising the evidence. *Cancer Invest.* 23, 60-75.
- Burkhardt, D.L., Sage, J., 2008. Cellular mechanisms of tumour suppression by the retinoblastoma gene. *Nature Reviews Cancer* 8, 671-682.
- Calame, K.L., 2001. Plasma cells: finding new light at the end of B cell development. *Nat. Immunol.* 2, 1103-1108.

Campo, E., Swerdlow, S.H., Harris, N.L., Pileri, S., Stein, H., Jaffe, E.S., 2011. The 2008 WHO classification of lymphoid neoplasms and beyond: evolving concepts and practical applications. *Blood* 117, 5019-5032.

Cancer research UK [online]. Last accessed May 22 2013 at: <http://www.cancerresearchuk.org/cancer-info/cancerstats/incidence/uk-cancer-incidence-statistics>

Carlson, B.A., Dubay, M.M., Sausville, E.A., Brizuela, L., Worland, P.J., 1996. Flavopiridol induces G1 arrest with inhibition of cyclin-dependent kinase (CDK) 2 and CDK4 in human breast carcinoma cells. *Cancer Res.* 56, 2973-2978.

Castonguay, A., Gali, H., Perchellet, E., Gao, X., Boukharta, M., Jalbert, G., Okuda, T., Yoshida, T., Hatano, T., Perchellet, J., 1997. Antitumorigenic and antipromoting activities of ellagic acid, ellagitannins and oligomeric anthocyanin and procyanidin. *Int. J. Oncol.* 10, 367-373.

Cerdá (1), B., Cerón, J.J., Tomás-Barberán, F.A., Espín, J.C., 2003. Repeated oral administration of high doses of the pomegranate ellagitannin punicalagin to rats for 37 days is not toxic. *J. Agric. Food Chem.* 51, 3493-3501.

Cerdá (2), B., Llorach, R., Cerón, J.J., Espín, J.C., Tomás-Barberán, F.A., 2003. Evaluation of the bioavailability and metabolism in the rat of punicalagin, an antioxidant polyphenol from pomegranate juice. *Eur. J. Nutr.* 42, 18-28.

César de Souza Vasconcelos, Laurylene, Sampaio, M.C.C., Sampaio, F.C., Higino, J.S., 2003. Use of *Punica granatum* as an antifungal agent against candidosis associated with denture stomatitis. *Mycoses* 46, 192-196.

Chan, S., Lee, M.C., Tan, K.O., Yang, L., Lee, A.S., Flotow, H., Fu, N.Y., Butler, M.S., Soejarto, D.D., Buss, A.D., 2003. Identification of chelerythrine as an inhibitor of BclXL function. *J. Biol. Chem.* 278, 20453-20456.

Chandramohan Reddy, T., Bharat Reddy, D., Aparna, A., Arunasree, K.M., Gupta, G., Achari, C., Reddy, G., Lakshminpathi, V., Subramanyam, A., Reddanna, P., 2012. Anti-leukemic effects of gallic acid on human leukemia K562 cells: Downregulation of COX-2, inhibition of BCR/ABL kinase and NF- κ B inactivation. *Toxicology in vitro* 26, 396-405.

Cheah, Y.H., Nordin, F.J., Sarip, R., Tee, T.T., Azimahtol, H., Sirat, H.M., Rashid, B., Abdullah, N.R., Ismail, Z., 2009. Combined xanthorrhizol-curcumin exhibits synergistic growth inhibitory activity via apoptosis induction in human breast cancer cells MDA-MB-231. *Cancer Cell Int* 9.

Chen, C., Zhou, J., Ji, C., 2010. Quercetin: a potential drug to reverse multidrug resistance. *Life Sci.* 87, 333-338.

Chen, H., Hsieh, W., Chang, W., Chung, J., 2004. Aloe-emodin induced *in vitro* G2/M arrest of cell cycle in human promyelocytic leukemia HL-60 cells. *Food and chemical toxicology* 42, 1251-1257.

Chen, P., Chu, S., Chiou, H., Chiang, C., Yang, S., Hsieh, Y., 2005. Cyanidin 3-glucoside and peonidin 3-glucoside inhibit tumor cell growth and induce apoptosis *in vitro* and suppress tumor growth *in vivo*. *Nutr. Cancer* 53, 232-243.

Chien, S., Wu, Y., Chung, J., Yang, J., Lu, H., Tsou, M., Wood, W., Kuo, S., Chen, D., 2009. Quercetin-induced apoptosis acts through mitochondrial-and caspase-3-dependent pathways in human breast cancer MDA-MB-231 cells. *Hum. Exp. Toxicol.* 28, 493-503.

Choi, E.J., Kim, G., 2008. Daidzein causes cell cycle arrest at the G1 and G2/M phases in human breast cancer MCF-7 and MDA-MB-453 cells. *Phytomedicine* 15, 683-690.

- Choi, E.J., Kim, G., 2009. Apigenin induces apoptosis through a mitochondria/caspase-pathway in human breast cancer MDA-MB-453 cells. *Journal of clinical biochemistry and nutrition* 44, 260.
- Choi, J., Kim, J., Lee, J., Kang, C., Kwon, H., Yoo, Y., Kim, T., Lee, Y., Lee, S., 2001. Induction of cell cycle arrest and apoptosis in human breast cancer cells by quercetin. *Int. J. Oncol.* 19, 837-844.
- Choi, S., Singh, S.V., 2005. Bax and Bak Are Required for Apoptosis Induction by Sulforaphane, a Cruciferous Vegetable-Derived Cancer Chemopreventive Agent. *Cancer Res.* 65, 2035-2043.
- Chou, C., Wu, Y., Wang, Y., Chou, M., Kuo, S., Chen, D., 2009. Capsaicin-induced apoptosis in human breast cancer MCF-7 cells through caspase-independent pathway. *Oncol. Rep.* 21, 665-671.
- Chou, C., Yang, J., Lu, H., Ip, S., Lo, C., Wu, C., Lin, J., Tang, N., Chung, J., Chou, M., 2010. Quercetin-mediated cell cycle arrest and apoptosis involving activation of a caspase cascade through the mitochondrial pathway in human breast cancer MCF-7 cells. *Arch. Pharm. Res.* 33, 1181-1191.
- Chung, C., Jiang, Y., Cheng, D., Birt, D., 2007. Impact of adenomatous polyposis coli (APC) tumor suppressor gene in human colon cancer cell lines on cell cycle arrest by apigenin. *Mol. Carcinog.* 46, 773-782.
- Chung, L., Cheung, T., Kong, S., Fung, K., Choy, Y., Chan, Z., Kwok, T., 2001. Induction of apoptosis by green tea catechins in human prostate cancer DU145 cells. *Life Sci.* 68, 1207-1214.
- Cimino, S., Sortino, G., Favilla, V., Castelli, T., Madonia, M., Sansalone, S., Russo, G.I., Morgia, G., 2012. Polyphenols: key issues involved in chemoprevention of prostate cancer. *Oxidative medicine and cellular longevity.*
- Clément, M.V., Hirpara, J.L., Chawdhury, S.H., Pervaiz, S., 1998. Chemopreventive agent resveratrol, a natural product derived from grapes, triggers CD95 signaling-dependent apoptosis in human tumor cells. *Blood* 92, 996-1002.
- Clifford, M.N., 2000. Anthocyanins—nature, occurrence and dietary burden. *J. Sci. Food Agric.* 80, 1063-1072.
- Clifford, M.N., Scalbert, A., 2000. Ellagitannins—nature, occurrence and dietary burden. *J. Sci. Food Agric.* 80, 1118-1125.
- Cory, S., Adams, J.M., 2002. The Bcl2 family: regulators of the cellular life-or-death switch. *Nature Reviews Cancer* 2, 647-656.
- Crouch, S., Kozlowski, R., Slater, K., Fletcher, J., 1993. The use of ATP bioluminescence as a measure of cell proliferation and cytotoxicity. *J. Immunol. Methods* 160, 81-88.
- Cruz, J.C., Tsai, L.H., 2004. Cdk5 deregulation in the pathogenesis of Alzheimer's disease. *Trends Mol. Med.* 10, 452-458.
- Dahlawi, H., Jordan-Mahy, N., Clench, M.R., Le Maitre, C.L., 2012. Bioactive actions of pomegranate fruit extracts on leukemia cell lines *in vitro* hold promise for new therapeutic agents for leukemia. *Nutr. Cancer* 64, 100-110.
- Dahlawi, H., Jordan-Mahy, N., Clench, M., McDougall, G.J., Maitre, C.L., 2013. Polyphenols are responsible for the proapoptotic properties of pomegranate juice on leukemia cell lines. *Food Science & Nutrition.*
- Dai, J., Gupte, A., Gates, L., Mumper, R., 2009. A comprehensive study of anthocyanin-containing extracts from selected blackberry cultivars: extraction methods, stability, anticancer properties and mechanisms. *Food and chemical toxicology* 47, 837-847.

- Dai, Y., Grant, S., 2003. Cyclin-dependent kinase inhibitors. *Current opinion in pharmacology* 3, 362.
- Davidson, M.H., Maki, K.C., Dicklin, M.R., Feinstein, S.B., Witchger, M., Bell, M., McGuire, D.K., Provost, J., Liker, H., Aviram, M., 2009. Effects of consumption of pomegranate juice on carotid intima-media thickness in men and women at moderate risk for coronary heart disease. *Am. J. Cardiol.* 104, 936-942.
- de Pascual-Teresa, S., Santos-Buelga, C., Rivas-Gonzalo, J.C., 2000. Quantitative analysis of flavan-3-ols in Spanish foodstuffs and beverages. *J. Agric. Food Chem.* 48, 5331-5337.
- Dean, M., Fojo, T., Bates, S., 2005. Tumour stem cells and drug resistance. *Nature Reviews Cancer* 5, 275-284.
- Debatin, K., 2004. Apoptosis pathways in cancer and cancer therapy. *Cancer Immunology, Immunotherapy* 53, 153-159.
- Deep, G., Agarwal, R., 2007. Chemopreventive efficacy of silymarin in skin and prostate cancer. *Integrative Cancer Therapies* 6, 130-145.
- Degterev, A., Lugovskoy, A., Cardone, M., Mulley, B., Wagner, G., Mitchison, T., Yuan, J., 2001. Identification of small-molecule inhibitors of interaction between the BH3 domain and Bcl-xL. *Nat. Cell Biol.* 3, 173-182.
- Del Pozo-Insfran, D., Percival, S.S., Talcott, S.T., 2006. Açai (*Euterpe oleracea* Mart.) polyphenolics in their glycoside and aglycone forms induce apoptosis of HL-60 leukemia cells. *J. Agric. Food Chem.* 54, 1222-1229.
- Deschler, B., Lübbert, M., 2006. Acute myeloid leukemia: epidemiology and etiology. *Cancer* 107, 2099-2107.
- Dimova, D.K., Stevaux, O., Frolov, M.V., Dyson, N.J., 2003. Cell cycle-dependent and cell cycle-independent control of transcription by the *Drosophila* E2F/RB pathway. *Genes Dev.* 17, 2308-2320.
- Dombret, H., Chastang, C., Fenaux, P., Reiffers, J., Bordessoule, D., Bouabdallah, R., Mandelli, F., Ferrant, A., Auzanneau, G., Tilly, H., 1995. A controlled study of recombinant human granulocyte colony-stimulating factor in elderly patients after treatment for acute myelogenous leukemia. *N. Engl. J. Med.* 332, 1678-1683.
- Donaldson, M.S., 2004. Nutrition and cancer: a review of the evidence for an anti-cancer diet. *Nutr J* 3, 19.
- Dorai, T., Aggarwal, B.B., 2004. Role of chemopreventive agents in cancer therapy. *Cancer Lett.* 215, 129-140.
- Drexler, H.G., Uphoff, C.C., 2002. Mycoplasma contamination of cell cultures: incidence, sources, effects, detection, elimination, prevention. *Cytotechnology* 39, 75-90.
- Du, G., Zhang, Z., Wen, X., Yu, C., Calway, T., Yuan, C., Wang, C., 2012. Epigallocatechin Gallate (EGCG) Is the Most Effective Cancer Chemopreventive Polyphenol in Green Tea. *Nutrients* 4, 1679-1691.
- Duorakova, H., Valicek, L., Reichelova, M., 2007. Detection of mycoplasma contamination in cell cultures and bovine sera. *Vet Med-Czech* 50, 262-268.
- E Mendoza, E., Burd, R., 2011. Quercetin as a systemic chemopreventative agent: structural and functional mechanisms. *Mini reviews in medicinal chemistry* 11, 1216-1221.

- Eden, T., 2010. Aetiology of childhood leukaemia. *Cancer Treat. Rev.* 36, 286-297.
- Elmore, S., 2007. Apoptosis: a review of programmed cell death. *Toxicol. Pathol.* 35, 495-516.
- Enari, M., Sakahira, H., Yokoyama, H., Okawa, K., Iwamatsu, A., Nagata, S., 1998. A caspase-activated DNase that degrades DNA during apoptosis, and its inhibitor ICAD. *Nature* 391, 43-50.
- Estrov, Z., Thall, P.F., Talpaz, M., Estey, E.H., Kantarjian, H.M., Andreeff, M., Harris, D., Van, Q., Walterscheid, M., Kornblau, S.M., 1998. Caspase 2 and caspase 3 protein levels as predictors of survival in acute myelogenous leukemia. *Blood* 92, 3090-3097.
- Fabiani, R., De Bartolomeo, A., Rosignoli, P., Servili, M., Montedoro, G., Morozzi, G., 2002. Cancer chemoprevention by hydroxytyrosol isolated from virgin olive oil through G1 cell cycle arrest and apoptosis. *European journal of cancer prevention* 11, 351-358.
- Fadavi, A., Barzegar, M., Azizi, M., Bayat, M., 2005. Note. Physicochemical composition of ten pomegranate cultivars (*Punica granatum* L.) grown in Iran. *Food Sci. Technol. Int.* 11, 113-119.
- Fadeel, B., Orrenius, S., 2005. Apoptosis: a basic biological phenomenon with wide-ranging implications in human disease. *J. Intern. Med.* 258, 479-517.
- Fadok, V.A., Voelker, D.R., Campbell, P.A., Cohen, J.J., Bratton, D.L., Henson, P.M., 1992. Exposure of phosphatidylserine on the surface of apoptotic lymphocytes triggers specific recognition and removal by macrophages. *The Journal of Immunology* 148, 2207-2216.
- Fainstein, E., Marcelle, C., Rosner, A., Canaani, E., Gale, R., Dreazen, O., Smith, S., Croce, C., 1987. A new fused transcript in Philadelphia chromosome positive acute lymphocytic leukaemia. *Nature* 330, 386-388.
- Farkas, D., Greenblatt, D.J., 2008. Influence of fruit juices on drug disposition: discrepancies between *in vitro* and clinical studies.
- Ferbeyre, G., De Stanchina, E., Lin, A.W., Querido, E., McCurrach, M.E., Hannon, G.J., Lowe, S.W., 2002. Oncogenic ras and p53 cooperate to induce cellular senescence. *Mol. Cell. Biol.* 22, 3497-3508.
- Fernandes-Alnemri, T., Litwack, G., Alnemri, E.S., 1994. CPP32, a novel human apoptotic protein with homology to *Caenorhabditis elegans* cell death protein Ced-3 and mammalian interleukin-1 beta-converting enzyme. *J. Biol. Chem.* 269, 30761-30764.
- Fimognari, C., Berti, F., Cantelli-Forti, G., Hrelia, P., 2004. Effect of cyanidin 3-O- β -glucopyranoside on micronucleus induction in cultured human lymphocytes by four different mutagens. *Environ. Mol. Mutagen.* 43, 45-52.
- Fischer, P.M., Gianella-Borradori, A., 2003. CDK inhibitors in clinical development for the treatment of cancer. *Expert Opin. Investig. Drugs* 12, 955-970.
- Foley, G.E., Lazarus, H., Farber, S., Uzman, B.G., Boone, B.A., McCarthy, R.E., 1965. Continuous culture of human lymphoblasts from peripheral blood of a child with acute leukemia. *Cancer* 18, 522-529.
- Forester, S.C., Waterhouse, A.L., 2010. Gut metabolites of anthocyanins, gallic acid, 3-O-methylgallic acid, and 2, 4, 6-trihydroxybenzaldehyde, inhibit cell proliferation of Caco-2 cells. *J. Agric. Food Chem.* 58, 5320-5327.
- Frawley, D., Lad, V., 1986. *The yoga of herbs.*

- Fuhrman, B., Volkova, N., Aviram, M., 2010. Pomegranate juice polyphenols increase recombinant paraoxonase-1 binding to high-density lipoprotein: studies *in vitro* and in diabetic patients. *Nutrition* 26, 359.
- Fukamachi, K., Imada, T., Ohshima, Y., Xu, J., Tsuda, H., 2008. Purple corn color suppresses Ras protein level and inhibits 7, 12-dimethylbenz [a] anthracene-induced mammary carcinogenesis in the rat. *Cancer science* 99, 1841-1846.
- Zaini, RG, Brandt, K., R Clench, M., L Le Maitre, C., 2012. Effects of bioactive compounds from carrots (*Daucus carota* L.), polyacetylenes, beta-carotene and lutein on human lymphoid leukaemia cells. *Anti-Cancer Agents in Medicinal Chemistry-Anti-Cancer Agents* 12, 640-652.
- Gabrilovich, D.I., Nagaraj, S., 2009. Myeloid-derived suppressor cells as regulators of the immune system. *Nature Reviews Immunology* 9, 162-174.
- Gallagher, R., Collins, S., Trujillo, J., McCredie, K., Ahearn, M., Tsai, S., Metzgar, R., Aulakh, G., Ting, R., Ruscetti, F., 1979. Characterization of the continuous, differentiating myeloid cell line (HL-60) from a patient with acute promyelocytic leukemia. *Blood* 54, 713-733.
- Galluzzi, L., Larochette, N., Zamzami, N., Kroemer, G., 2006. Mitochondria as therapeutic targets for cancer chemotherapy. *Oncogene* 25, 4812-4830.
- Galluzzi, L., Maiuri, M., Vitale, I., Zischka, H., Castedo, M., Zitvogel, L., Kroemer, G., 2007. Cell death modalities: classification and pathophysiological implications. *Cell Death & Differentiation* 14, 1237-1243.
- Garrido, C., Galluzzi, L., Brunet, M., Puig, P., Didelot, C., Kroemer, G., 2006. Mechanisms of cytochrome c release from mitochondria. *Cell Death & Differentiation* 13, 1423-1433.
- Ghobrial, I.M., Witzig, T.E., Adjei, A.A., 2005. Targeting apoptosis pathways in cancer therapy. *CA: A Cancer Journal for Clinicians* 55, 178-194.
- Giacinti, C., Giordano, A., 2006. RB and cell cycle progression. *Oncogene* 25, 5220-5227.
- Gil, M.I., Tomás-Barberán, F.A., Hess-Pierce, B., Holcroft, D.M., Kader, A.A., 2000. Antioxidant activity of pomegranate juice and its relationship with phenolic composition and processing. *J. Agric. Food Chem.* 48, 4581-4589.
- Giralt, S.A., Champlin, R.E., 1994. Leukemia relapse after allogeneic bone marrow transplantation: a review. *Blood* 84, 3603-3612.
- Giusti, M.M., Wrolstad, R.E., 2003. Acylated anthocyanins from edible sources and their applications in food systems. *Biochem. Eng. J.* 14, 217-225.
- Gómez-Caravaca, A.M., Verardo, V., Toselli, M., Segura-Carretero, A., Fernandez-Gutierrez, A., Caboni, M.F., 2013. Determination of the major phenolic compounds in pomegranate juices by HPLC-DAD-ESI-MS. *J. Agric. Food Chem.* .
- Gottesman, M.M., 2002. Mechanisms of cancer drug resistance. *Annu. Rev. Med.* 53, 615-627.
- Gottesman, M.M., Fojo, T., Bates, S.E., 2002. Multidrug resistance in cancer: role of ATP-dependent transporters. *Nature Reviews Cancer* 2, 48-58.
- Gözlekçi, Ş., Saraçoğlu, O., Onursal, E., Özgen, M., 2011. Total phenolic distribution of juice, peel, and seed extracts of four pomegranate cultivars. *Pharmacognosy magazine* 7, 161.
- Gralnick, H.R., Galton, D., CATOVSKY, D., SULTAN, C., BENNETT, J.M., 1977. Classification of acute leukemia. *Ann. Intern. Med.* 87, 740-753.

- Granado-Serrano, A.B., Martín, M.A., Bravo, L., Goya, L., Ramos, S., 2006. Quercetin induces apoptosis via caspase activation, regulation of Bcl-2, and inhibition of PI-3-kinase/Akt and ERK pathways in a human hepatoma cell line (HepG2). *J. Nutr.* 136, 2715-2721.
- Greaves, M., 1997. Aetiology of acute leukaemia. *The Lancet* 349, 344-349.
- Guo, J., Xiao, B., Liu, D., Grant, M., Zhang, S., Lai, Y., Guo, Y., Liu, Q., 2004. Biphasic effect of daidzein on cell growth of human colon cancer cells. *Food and chemical toxicology* 42, 1641-1646.
- Gupta, S., Ahmad, N., Nieminen, A., Mukhtar, H., 2000. Growth inhibition, cell-cycle dysregulation, and induction of apoptosis by green tea constituent (-)-epigallocatechin-3-gallate in androgen-sensitive and androgen-insensitive human prostate carcinoma cells. *Toxicol. Appl. Pharmacol.* 164, 82-90.
- Häcker, G., 2000. The morphology of apoptosis. *Cell Tissue Res.* 301, 5-17.
- Hafeez, B.B., Siddiqui, I.A., Asim, M., Malik, A., Afaq, F., Adhami, V.M., Saleem, M., Din, M., Mukhtar, H., 2008. A dietary anthocyanidin delphinidin induces apoptosis of human prostate cancer PC3 cells *in vitro* and *in vivo*: involvement of nuclear factor- κ B signaling. *Cancer Res.* 68, 8564-8572.
- Hallek, M., Cheson, B.D., Catovsky, D., Caligaris-Cappio, F., Dighiero, G., Döhner, H., Hillmen, P., Keating, M.J., Montserrat, E., Rai, K.R., 2008. Guidelines for the diagnosis and treatment of chronic lymphocytic leukemia: a report from the International Workshop on Chronic Lymphocytic Leukemia updating the National Cancer Institute-Working Group 1996 guidelines. *Blood* 111, 5446-5456.
- Halvorsen, B.L., Holte, K., Myhrstad, M.C., Barikmo, I., Hvattum, E., Remberg, S.F., Wold, A., Haffner, K., Baugerød, H., Andersen, L.F., 2002. A systematic screening of total antioxidants in dietary plants. *J. Nutr.* 132, 461-471.
- Hanahan, D., Weinberg, R.A., 2011. Hallmarks of cancer: the next generation. *Cell* 144, 646-674.
- Harborne, J.B., Williams, C.A., 2001. Anthocyanins and other flavonoids. *Nat. Prod. Rep.* 18, 310-333.
- Harbour, J.W., Dean, D.C., 2000. Rb function in cell-cycle regulation and apoptosis. *Nat. Cell Biol.* 2, E65-E67.
- Hastak, K., Agarwal, M.K., Mukhtar, H., Agarwal, M.L., 2005. Ablation of either p21 or Bax prevents p53-dependent apoptosis induced by green tea polyphenol epigallocatechin-3-gallate. *The FASEB journal* 19, 789-791.
- Havell, E.A., Fiers, W., North, R.J., 1988. The antitumor function of tumor necrosis factor (TNF), I. Therapeutic action of TNF against an established murine sarcoma is indirect, immunologically dependent, and limited by severe toxicity. *J. Exp. Med.* 167, 1067-1085.
- Hegde, V.V.L., Mahesh, P.A., Venkatesh, Y.P., 2002. Anaphylaxis Caused by Mannitol in Pomegranate. *Allergy & Clinical Immunology International-Journal of the World Allergy Organization* 14, 37-39.
- Heinrichs, A., 2008. Cell division: Back and forth. *Nature Reviews Molecular Cell Biology* 9, 740-741.
- Hernandez, F., Melgarejo, P., Tomas-Barberan, F., Artes, F., 1999. Evolution of juice anthocyanins during ripening of new selected pomegranate (*Punica granatum*) clones. *European Food Research and Technology* 210, 39-42.

- Hiddemann, W., Kern, W., Schoch, C., Fonatsch, C., Heinecke, A., Wörmann, B., Büchner, T., 1999. Management of acute myeloid leukemia in elderly patients. *Journal of Clinical Oncology* 17, 3569-3576.
- Hill, M.M., Adrain, C., Duriez, P.J., Creagh, E.M., Martin, S.J., 2004. Analysis of the composition, assembly kinetics and activity of native Apaf-1 apoptosomes. *EMBO J.* 23, 2134-2145.
- Hoffmann, P.R., Ogden, C.A., Leverrier, Y., Bratton, D.L., Daleke, D.L., Ridley, A.J., Fadok, V.A., Henson, P.M., 2001. Phosphatidylserine (PS) induces PS receptor-mediated macropinocytosis and promotes clearance of apoptotic cells. *J. Cell Biol.* 155, 649-660.
- Hofseth, L.J., Hussain, S.P., Harris, C.C., 2004. p53: 25 years after its discovery. *Trends Pharmacol. Sci.* 25, 177-181.
- Hogan, S., Chung, H., Zhang, L., Li, J., Lee, Y., Dai, Y., Zhou, K., 2010. Antiproliferative and antioxidant properties of anthocyanin-rich extract from açai. *Food Chem.* 118, 208-214.
- Holdenrieder, S., Stieber, P., 2004. Apoptotic markers in cancer. *Clin. Biochem.* 37, 605-617.
- Hong, M.Y., Seeram, N.P., Heber, D., 2008. Pomegranate polyphenols down-regulate expression of androgen-synthesizing genes in human prostate cancer cells overexpressing the androgen receptor. *J. Nutr. Biochem.* 19, 848-855.
- Hora, J.J., Maydew, E.R., Lansky, E.P., Dwivedi, C., 2003. Chemopreventive effects of pomegranate seed oil on skin tumor development in CD1 mice. *Journal of medicinal food* 6, 157-161.
- Hou, D., Tong, X., Terahara, N., Luo, D., Fujii, M., 2005. Delphinidin 3-sambubioside, Hibiscus, anthocyanin, induces apoptosis in human leukemia cells through reactive oxygen species-mediated mitochondrial pathway. *Arch. Biochem. Biophys.* 440, 101-109.
- Hsu, A., Bray, T.M., Helferich, W.G., Doerge, D.R., Ho, E., 2010. Differential effects of whole soy extract and soy isoflavones on apoptosis in prostate cancer cells. *Exp. Biol. Med.* 235, 90-97.
- Hsu, J., Kao, S., Ou, T., Chen, Y., Li, Y., Wang, C., 2011. Gallic acid induces G2/M phase arrest of breast cancer cell MCF-7 through stabilization of p27Kip1 attributed to disruption of p27Kip1/Skp2 complex. *J. Agric. Food Chem.* 59, 1996-2003.
- Huang, T.H., Peng, G., Kota, B.P., Li, G.Q., Yamahara, J., Roufogalis, B.D., Li, Y., 2005. Anti-diabetic action of *Punica granatum* flower extract: Activation of PPAR- γ and identification of an active component. *Toxicol. Appl. Pharmacol.* 207, 160-169.
- Hudson, E.A., Dinh, P.A., Kokubun, T., Simmonds, M.S., Gescher, A., 2000. Characterization of potentially chemopreventive phenols in extracts of brown rice that inhibit the growth of human breast and colon cancer cells. *Cancer Epidemiology Biomarkers & Prevention* 9, 1163-1170.
- Huh, S.W., Bae, S.M., Kim, Y.W., Lee, J.M., Namkoong, S.E., Lee, I.P., Kim, S.H., Kim, C.K., Ahn, W.S., 2004. Anticancer effects of (-)-epigallocatechin-3-gallate on ovarian carcinoma cell lines. *Gynecol. Oncol.* 94, 760.
- Hui, A.M., Li, X., Makuuchi, M., Takayama, T., Kubota, K., 1999. Over-expression and lack of retinoblastoma protein are associated with tumor progression and metastasis in hepatocellular carcinoma. *International journal of cancer* 84, 604-608.
- Hwang, E.S., Bowen, P.E., 2004. Cell cycle arrest and induction of apoptosis by lycopene in LNCaP human prostate cancer cells. *Journal of medicinal food* 7, 284-289.
- Hwang, J., Ha, J., Park, I., Lee, S., Baik, H.W., Kim, Y.M., Park, O.J., 2007. Apoptotic effect of EGCG in HT-29 colon cancer cells via AMPK signal pathway. *Cancer Lett.* 247, 115-121.

- Hyun, J.W., Chung, H.S., 2004. Cyanidin and malvidin from *Oryza sativa* cv. Heuginjubyeo mediate cytotoxicity against human monocytic leukemia cells by arrest of G2/M phase and induction of apoptosis. *J. Agric. Food Chem.* 52, 2213-2217.
- Jacks, T., Fazeli, A., Schmitt, E.M., Bronson, R.T., Goodell, M.A., Weinberg, R.A., 1992. Effects of an Rb mutation in the mouse. *Nature* 359, 295-300.
- Jeong, J., An, J.Y., Kwon, Y.T., Rhee, J.G., Lee, Y.J., 2009. Effects of low dose quercetin: Cancer cell-specific inhibition of cell cycle progression. *J. Cell. Biochem.* 106, 73-82.
- Jeune, M.L., Kumi-Diaka, J., Brown, J., 2005. Anticancer activities of pomegranate extracts and genistein in human breast cancer cells. *Journal of medicinal food* 8, 469-475.
- Ji, B., Hsu, W., Yang, J., Hsia, T., Lu, C., Chiang, J., Yang, J., Lin, C., Lin, J., Suen, L.W., 2009. Gallic acid induces apoptosis via caspase-3 and mitochondrion-dependent pathways *in vitro* and suppresses lung xenograft tumor growth *in vivo*. *J. Agric. Food Chem.* 57, 7596-7604.
- Johanningsmeier, S.D., Harris, G.K., 2011. Pomegranate as a functional food and nutraceutical source. *Annual review of food science and technology* 2, 181-201.
- Joza, N., Susin, S.A., Daugas, E., Stanford, W.L., Cho, S.K., Li, C.Y.J., Sasaki, T., Elia, A.J., Cheng, H.Y.M., Ravagnan, L., 2001. Essential role of the mitochondrial apoptosis-inducing factor in programmed cell death. *Nature* 410, 549-554.
- Juliusson, G., Billström, R., Gruber, A., Hellström-Lindberg, E., Höglund, M., Karlsson, K., Stockelberg, D., Wahlin, A., Åström, M., Arnesson, C., 2005. Attitude towards remission induction for elderly patients with acute myeloid leukemia influences survival. *Leukemia* 20, 42-47.
- Jung, Y., Heo, J., Lee, Y.J., Kwon, T.K., Kim, Y., 2010. Quercetin enhances TRAIL-induced apoptosis in prostate cancer cells via increased protein stability of death receptor 5. *Life Sci.* 86, 351-357.
- Junttila, M.R., Evan, G.I., 2009. p53 a Jack of all trades but master of none. *Nature Reviews Cancer* 9, 821-829.
- Jurenka, J., 2008. Therapeutic applications of pomegranate (*Punica granatum* L.): a review. *Alternative medicine review* 13, 128-144.
- Kähkönen, M.P., Heinonen, M., 2003. Antioxidant activity of anthocyanins and their aglycons. *J. Agric. Food Chem.* 51, 628-633.
- Kakizuka, A., Miller Jr, W., Umesono, K., Warrell Jr, R., Frankel, S., Murty, V., Dmitrovsky, E., Evans, R., 1991. Chromosomal translocation t (15; 17) in human acute promyelocytic leukemia fuses RAR alpha with a novel putative transcription factor, PML. *Cell* 66, 663.
- Kang, S., Seeram, N.P., Nair, M.G., Bourquin, L.D., 2003. Tart cherry anthocyanins inhibit tumor development in *Apc⁺ Min^{-/-}* mice and reduce proliferation of human colon cancer cells. *Cancer Lett.* 194, 13-19.
- Kangas, L., Grönroos, M., Nieminen, A., 1984. Bioluminescence of cellular ATP: a new method for evaluating cytotoxic agents *in vitro*. *Med. Biol.* 62, 338.
- Kantarjian, H.M., O'Brien, S., Cortes, J.E., Giralto, S.A., Rios, M.B., Shan, J., Giles, F.J., Thomas, D.A., Faderl, S., De Lima, M., 2002. Imatinib mesylate therapy for relapse after allogeneic stem cell transplantation for chronic myelogenous leukemia. *Blood* 100, 1590-1595.
- Kasimsetty, S.G., Bialonska, D., Reddy, M.K., Thornton, C., Willett, K.L., Ferreira, D., 2009. Effects of pomegranate chemical constituents/intestinal microbial metabolites on CYP1B1 in 22Rv1 prostate cancer cells. *J. Agric. Food Chem.* 57, 10636-10644.

- Katsube, N., Iwashita, K., Tsushida, T., Yamaki, K., Kobori, M., 2003. Induction of apoptosis in cancer cells by bilberry (*Vaccinium myrtillus*) and the anthocyanins. *J. Agric. Food Chem.* 51, 68-75.
- Katsuzaki, H., Hibasami, H., Ohwaki, S., Ishikawa, K., Imai, K., Date, K., Kimura, Y., Komiya, T., 2003. Cyanidin 3-O-beta-D-glucoside isolated from skin of black Glycine max and other anthocyanins isolated from skin of red grape induce apoptosis in human lymphoid leukemia Molt 4B cells. *Oncol. Rep.* 10, 297.
- Katz, S.R., Newman, R.A., Lansky, E.P., 2007. *Punica granatum*: heuristic treatment for diabetes mellitus. *Journal of medicinal food* 10, 213-217.
- Kaur, M., Velmurugan, B., Rajamanickam, S., Agarwal, R., Agarwal, C., 2009. Gallic acid, an active constituent of grape seed extract, exhibits anti-proliferative, pro-apoptotic and anti-tumorigenic effects against prostate carcinoma xenograft growth in nude mice. *Pharm. Res.* 26, 2133-2140.
- Kawahara, T., Kawaguchi-Ihara, N., Okuhashi, Y., Itoh, M., Nara, N., Tohda, S., 2009. Cyclopamine and quercetin suppress the growth of leukemia and lymphoma cells. *Anticancer Res.* 29, 4629-4632.
- Kawakami, K., Futami, H., Takahara, J., Yamaguchi, K., 1996. UCN-01, 7-hydroxyl-staurosporine, inhibits kinase activity of cyclin-dependent kinases and reduces the phosphorylation of the retinoblastoma susceptibility gene product in A549 human lung cancer cell line. *Biochem. Biophys. Res. Commun.* 219, 778-783.
- Kerr, J.F., Wyllie, A.H., Currie, A.R., 1972. Apoptosis: a basic biological phenomenon with wide-ranging implications in tissue kinetics. *Br. J. Cancer* 26, 239.
- Key, T., 2010. Fruit and vegetables and cancer risk. *Br. J. Cancer* 104, 6-11.
- Khan (1), N., Afaq, F., Mukhtar, H., 2006. Apoptosis by dietary factors: the suicide solution for delaying cancer growth. *Carcinogenesis* 28, 233-239.
- Khan (2), N., Hadi, N., Afaq, F., Syed, D.N., Kweon, M., Mukhtar, H., 2006. Pomegranate fruit extract inhibits prosurvival pathways in human A549 lung carcinoma cells and tumor growth in athymic nude mice. *Carcinogenesis* 28, 163-173.
- Khan (3), N., Afaq, F., Saleem, M., Ahmad, N., Mukhtar, H., 2006. Targeting multiple signaling pathways by green tea polyphenol (-)-epigallocatechin-3-gallate. *Cancer Res.* 66, 2500-2505.
- Khan, G.N., Gorin, M.A., Rosenthal, D., Pan, Q., Bao, L.W., Wu, Z.F., Newman, R.A., Pawlus, A.D., Yang, P., Lansky, E.P., 2009. Pomegranate fruit extract impairs invasion and motility in human breast cancer. *Integrative Cancer Therapies* 8, 242-253.
- Khan, N., Afaq, F., Kweon, M., Kim, K., Mukhtar, H., 2007. Oral consumption of pomegranate fruit extract inhibits growth and progression of primary lung tumors in mice. *Cancer Res.* 67, 3475-3482.
- Khan, N., Afaq, F., Syed, D.N., Mukhtar, H., 2008. Fisetin, a novel dietary flavonoid, causes apoptosis and cell cycle arrest in human prostate cancer LNCaP cells. *Carcinogenesis* 29, 1049-1056.
- Kim, N.D., Mehta, R., Yu, W., Neeman, I., Livney, T., Amichay, A., Poirier, D., Nicholls, P., Kirby, A., Jiang, W., 2002. Chemopreventive and adjuvant therapeutic potential of pomegranate (*Punica granatum*) for human breast cancer. *Breast Cancer Res. Treat.* 71, 203-217.
- Kim, W.K., Bang, M.H., Kim, E.S., Kang, N.E., Jung, K.C., Cho, H.J., Park, J.H., 2005. Quercetin decreases the expression of ErbB2 and ErbB3 proteins in HT-29 human colon cancer cells. *J. Nutr. Biochem.* 16, 155-162.

- Kim, Y., Lee, D., Jeong, J., Guo, Z.S., Lee, Y.J., 2008. Quercetin augments TRAIL-induced apoptotic death: involvement of the ERK signal transduction pathway. *Biochem. Pharmacol.* 75, 1946-1958.
- Kischkel, F.C., Lawrence, D.A., Chuntharapai, A., Schow, P., Kim, K.J., Ashkenazi, A., 2000. Apo2L/TRAIL-dependent recruitment of endogenous FADD and caspase-8 to death receptors 4 and 5. *Immunity* 12, 611.
- Koeffler, H., Billing, R., Lusa, A., Sparkes, R., Golde, D., 1980. An undifferentiated variant derived from the human acute myelogenous leukemia cell line (KG-1). *Blood* 56, 265-273.
- Koeffler, H.P., 1983. Induction of differentiation of human acute myelogenous leukemia cells: therapeutic implications. *Blood* 62, 709-721.
- Kohn, H., Suzuki, R., Yasui, Y., Hosokawa, M., Miyashita, K., Tanaka, T., 2004. Pomegranate seed oil rich in conjugated linolenic acid suppresses chemically induced colon carcinogenesis in rats. *Cancer science* 95, 481-486.
- Kondo, M., 2010. Lymphoid and myeloid lineage commitment in multipotent hematopoietic progenitors. *Immunol. Rev.* 238, 37-46.
- Kondo, M., Wagers, A.J., Manz, M.G., Prohaska, S.S., Scherer, D.C., Beilhack, G.F., Shizuru, J.A., Weissman, I.L., 2003. Biology of hematopoietic stem cells and progenitors: implications for clinical application. *Annu. Rev. Immunol.* 21, 759-806.
- Kong, J., Chia, L., Goh, N., Chia, T., Brouillard, R., 2003. Analysis and biological activities of anthocyanins. *Phytochemistry* 64, 923-933.
- Korpál, M., Kang, Y., 2010. Targeting the transforming growth factor- β signalling pathway in metastatic cancer. *Eur. J. Cancer* 46, 1232-1240.
- Koyama, S., Cobb, L.J., Mehta, H.H., Seeram, N.P., Heber, D., Pantuck, A.J., Cohen, P., 2010. Pomegranate extract induces apoptosis in human prostate cancer cells by modulation of the IGF-IGFBP axis. *Growth Hormone & IGF Research* 20, 55-62.
- Krug, U., Ganser, A., Koeffler, H.P., 2002. Tumor suppressor genes in normal and malignant hematopoiesis. *Oncogene* 21, 3475.
- Kubota, T., Uemura, Y., Kobayashi, M., Taguchi, H., 2002. Combined effects of resveratrol and paclitaxel on lung cancer cells. *Anticancer Res.* 23, 4039-4046.
- Lacour, B., Guyot-Goubin, A., Guissou, S., Bellec, S., Désandes, E., Clavel, J., 2010. Incidence of childhood cancer in France: national children cancer registries, 2000-2004. *European Journal of Cancer Prevention* 19, 173.
- Lambert, J.D., Elias, R.J., 2010. The antioxidant and pro-oxidant activities of green tea polyphenols: a role in cancer prevention. *Arch. Biochem. Biophys.* 501, 65.
- Langley, P., 2000. Why a pomegranate? *BMJ* 321, 1153-1154.
- Lansky, E.P., Harrison, G., Froom, P., Jiang, W.G., 2005. Pomegranate (*Punica granatum*) pure chemicals show possible synergistic inhibition of human PC-3 prostate cancer cell invasion across Matrigel™. *Invest. New Drugs* 23, 121-122.
- Lansky, E.P., Jiang, W., Mo, H., Bravo, L., Froom, P., Yu, W., Harris, N.M., Neeman, I., Campbell, M.J., 2005. Possible synergistic prostate cancer suppression by anatomically discrete pomegranate fractions. *Invest. New Drugs* 23, 11-20.
- Lansky, E.P., Newman, R.A., 2007. *Punica granatum* (pomegranate) and its potential for prevention and treatment of inflammation and cancer. *J. Ethnopharmacol.* 109, 177-206.

- Lapidot, T., Walker, M.D., Kanner, J., 2002. Antioxidant and prooxidant effects of phenolics on pancreatic β -cells *in vitro*. *J. Agric. Food Chem.* 50, 7220-7225.
- Larrosa, M., Tomás-Barberán, F.A., Espín, J.C., 2006. The dietary hydrolysable tannin punicalagin releases ellagic acid that induces apoptosis in human colon adenocarcinoma Caco-2 cells by using the mitochondrial pathway. *J. Nutr. Biochem.* 17, 611-625.
- Larsen, B.D., Rampalli, S., Burns, L.E., Brunette, S., Dilworth, F.J., Megeney, L.A., 2010. Caspase 3/caspase-activated DNase promote cell differentiation by inducing DNA strand breaks. *Proceedings of the National Academy of Sciences* 107, 4230-4235.
- Laughlin, M.J., Eapen, M., Rubinstein, P., Wagner, J.E., Zhang, M., Champlin, R.E., Stevens, C., Barker, J.N., Gale, R.P., Lazarus, H.M., 2004. Outcomes after transplantation of cord blood or bone marrow from unrelated donors in adults with leukemia. *N. Engl. J. Med.* 351, 2265-2275.
- Lazzè, M.C., Savio, M., Pizzala, R., Cazzalini, O., Perucca, P., Scovassi, A.I., Stivala, L.A., Bianchi, L., 2004. Anthocyanins induce cell cycle perturbations and apoptosis in different human cell lines. *Carcinogenesis* 25, 1427-1433.
- Lee, S.H., Park, S.M., PARK, S.M., Park, J.H., Shin, D.Y., Kim, G.Y., Ryu, C.H., Shin, S.C., Jung, J.M., Kang, H.S., 2009. Induction of apoptosis in human leukemia U937 cells by anthocyanins through down-regulation of Bcl-2 and activation of caspases. *Int. J. Oncol.* 34, 1077-1083.
- Leopold, L.H., Willemze, R., 2002. The treatment of acute myeloid leukemia in first relapse: a comprehensive review of the literature. *Leuk. Lymphoma* 43, 1715-1727.
- Lessene, G., Czabotar, P.E., Colman, P.M., 2008. BCL-2 family antagonists for cancer therapy. *Nature Reviews Drug Discovery* 7, 989-1000.
- Lev-Ari, S., Strier, L., Kazanov, D., Madar-Shapiro, L., Dvory-Sobol, H., Pinchuk, I., Marian, B., Lichtenberg, D., Arber, N., 2005. Celecoxib and curcumin synergistically inhibit the growth of colorectal cancer cells. *Clinical Cancer Research* 11, 6738-6744.
- Levin, G.M., 1994. Pomegranate (*Punica granatum*) plant genetic resources in Turkmenistan. *Bulletin des Ressources Phytogenétiques* .
- LGC Standard [online]. Last accessed February 30 2013 at: http://www.lgcstandards-atcc.org/Products/Cells%20and%20Microorganisms/Cell%20Lines/Human.aspx?geo_country=gb
- Li, G., Chen, Y., Hou, Z., Xiao, H., Jin, H., Lu, G., Lee, M., Liu, B., Guan, F., Yang, Z., 2010. Pro-oxidative activities and dose-response relationship of (-)-epigallocatechin-3-gallate in the inhibition of lung cancer cell growth: a comparative study *in vivo* and *in vitro*. *Carcinogenesis* 31, 902-910.
- Li, L., Adams, L.S., Chen, S., Killian, C., Ahmed, A., Seeram, N.P., 2009. Eugenia jambolana Lam. berry extract inhibits growth and induces apoptosis of human breast cancer but not non-tumorigenic breast cells. *J. Agric. Food Chem.* 57, 826-831.
- Li, L.Y., Luo, X., Wang, X., 2001. Endonuclease G is an apoptotic DNase when released from mitochondria. *Nature* 412, 95-99.
- Li, T.E.M.A.O., Chen, G.W.E.I., Su, C.C., Lin, J.G., Yeh, C.C., Cheng, K.C.H.U., Chung, J.G., 2005. Ellagic acid induced p53/p21 expression, G1 arrest and apoptosis in human bladder cancer T24 cells. *Anticancer Res.* 25, 971-979.
- Lim, D.Y., Jeong, Y., Tyner, A.L., Park, J.H.Y., 2007. Induction of cell cycle arrest and apoptosis in HT-29 human colon cancer cells by the dietary compound luteolin. *American Journal of Physiology-Gastrointestinal and Liver Physiology* 292, G66-G75.

- Liscovitch, M., Lavie, Y., 2002. Cancer multidrug resistance: a review of recent drug discovery research. *IDrugs* 5, 349-355.
- Liu, C., Wang, Y., Xie, S., Zhou, Y., Ren, X., Li, X., Cai, Y., 2010. Liquiritigenin induces mitochondria-mediated apoptosis via cytochrome c release and caspases activation in heLa Cells. *Phytotherapy Research* 25, 277-283.
- Liu, E., Wu, J., Cao, W., Zhang, J., Liu, W., Jiang, X., Zhang, X., 2007. Curcumin induces G2/M cell cycle arrest in a p53-dependent manner and upregulates ING4 expression in human glioma. *J. Neurooncol.* 85, 263-270.
- Liu, Z., Li, D., Yu, L., Niu, F., 2012. Gallic Acid as a Cancer-Selective Agent Induces Apoptosis in Pancreatic Cancer Cells. *Chemotherapy* 58, 185-194.
- Locatelli, C., Filippin-Monteiro, F.B., Creczynski-Pasa, T.B., 2012. Alkyl esters of gallic acid as anticancer agents: A review. *Eur. J. Med. Chem.*
- Locatelli, F., Nöllke, P., Zecca, M., Korthof, E., Lanino, E., Peters, C., Pession, A., Kabisch, H., Uderzo, C., Bonfim, C.S., 2005. Hematopoietic stem cell transplantation (HSCT) in children with juvenile myelomonocytic leukemia (JMML): results of the EWOG-MDS/EBMT trial. *Blood* 105, 410-419.
- Locksley, R.M., Killeen, N., Lenardo, M.J., 2001. The TNF and TNF receptor superfamilies: integrating mammalian biology. *Cell* 104, 487-501.
- Longo, L., Platini, F., Scardino, A., Alabiso, O., Vasapollo, G., Tessitore, L., 2008. Autophagy inhibition enhances anthocyanin-induced apoptosis in hepatocellular carcinoma. *Molecular cancer therapeutics* 7, 2476-2485.
- Longtin, R., 2003. The Pomegranate: Nature's Power Fruit? *J. Natl. Cancer Inst.* 95, 346-348.
- Lorenzo, H.K., Susin, S.A., 2004. Mitochondrial effectors in caspase-independent cell death. *FEBS Lett.* 557, 14-20.
- Losiewicz, M.D., Carlson, B.A., Kaur, G., Sausville, E.A., Worland, P.J., 1994. Potent inhibition of CDC2 kinase activity by the flavonoid L86-8275. *Biochem. Biophys. Res. Commun.* 201, 589-595.
- Lowenberg, B., Downing, J.R., Burnett, A., 1999. Acute myeloid leukemia. *N. Engl. J. Med.* 341, 1051-1062.
- Löwenberg, B., van Putten, W., Theobald, M., Gmür, J., Verdonck, L., Sonneveld, P., Fey, M., Schouten, H., de Greef, G., Ferrant, A., 2003. Effect of priming with granulocyte colony-stimulating factor on the outcome of chemotherapy for acute myeloid leukemia. *N. Engl. J. Med.* 349, 743-752.
- Lozzio, C.B., Lozzio, B.B., 1975. Human chronic myelogenous leukemia cell-line with positive Philadelphia chromosome. *Blood* 45, 321-334.
- Luo, H., Jiang, B., King, S.M., Chen, Y.C., 2008. Inhibition of cell growth and VEGF expression in ovarian cancer cells by flavonoids. *Nutr. Cancer* 60, 800-809.
- Luqmani, Y., 2008. Mechanisms of drug resistance in cancer chemotherapy. *Medical principles and practice* 14, 35-48.
- Lymphoma and Myeloma Society [online]. Last accessed May 22 2013 at: <http://www.lls.org/diseaseinformation/getinformationsupport/factsstatistics/>
- Mahbub, A., Le Maitre, C., Haywood-Small, S., McDougall, G., Cross, N., Mahy, N., 2013. Differential effects of polyphenols on proliferation and apoptosis in human myeloid and lymphoid leukemia cell lines. *Anti-cancer agents in medicinal chemistry. Ahead of Press.*

- Malik, A., Afaq, F., Sarfaraz, S., Adhami, V.M., Syed, D.N., Mukhtar, H., 2005. Pomegranate fruit juice for chemoprevention and chemotherapy of prostate cancer. *Proc. Natl. Acad. Sci. U. S. A.* 102, 14813-14818.
- Malik, A., Mukhtar, H., 2006. Extra View Prostate Cancer Prevention Through Pomegranate Fruit. *Cell Cycle* 5, 371-373.
- Malinge, S., Ben-Abdelali, R., Settegrana, C., Radford-Weiss, I., Debre, M., Beldjord, K., Macintyre, E.A., Villeval, J.L., Vainchenker, W., Berger, R., 2007. Novel activating JAK2 mutation in a patient with Down syndrome and B-cell precursor acute lymphoblastic leukemia. *Blood* 109, 2202-2204.
- Manohar, M., Fatima, I., Saxena, R., Chandra, V., Sankhwar, P.L., Dwivedi, A., 2012. (-)-Epigallocatechin-3-gallate induces apoptosis in human endometrial adenocarcinoma cells via ROS generation and p38 MAP kinase activation. *J. Nutr. Biochem.* .
- Mansour, M., Linch, D., Foroni, L., Goldstone, A., Gale, R., 2006. High incidence of Notch-1 mutations in adult patients with T-cell acute lymphoblastic leukemia. *Leukemia* 20, 537-539.
- Mars, M., 2000. Pomegranate plant material: Genetic resources and breeding, a review. P.Melgarejo-Moreno, JJ Mart í nez-Nicol á s, and J.Mart í nez Tome [eds.], *Production, processing and marketing of pomegranate in the Mediterranean region: Advances in research and technology*. Options Mediterraneennes Serie A 42, 55-62.
- Martin, K.R., 2006. Targeting apoptosis with dietary bioactive agents. *Exp. Biol. Med.* 231, 117-129.
- Martin, S., Giannone, G., Andriantsitohaina, R., Carmen Martinez, M., 2003. Delphinidin, an active compound of red wine, inhibits endothelial cell apoptosis via nitric oxide pathway and regulation of calcium homeostasis. *Br. J. Pharmacol.* 139, 1095-1102.
- Matsumoto, H., Nakamura, Y., Tachibanaki, S., Kawamura, S., Hirayama, M., 2003. Stimulatory effect of cyanidin 3-glycosides on the regeneration of rhodopsin. *J. Agric. Food Chem.* 51, 3560-3563.
- Mazza, G., Brouillard, R., 1990. The mechanism of co-pigmentation of anthocyanins in aqueous solutions. *Phytochemistry* 29, 1097-1102.
- Mazza, G., Francis, F., 1995. Anthocyanins in grapes and grape products. *Critical Reviews in Food Science & Nutrition* 35, 341-371.
- Mazza, G., Miniati, E., 1993. *Anthocyanins in Fruits, Vegetables, and Grains*. CRC Press.
- McClue, S.J., Blake, D., Clarke, R., Cowan, A., Cummings, L., Fischer, P.M., MacKenzie, M., Melville, J., Stewart, K., Wang, S., 2002. *In vitro* and *in vivo* antitumor properties of the cyclin dependent kinase inhibitor CYC202 (R-roscovitine). *International Journal of Cancer* 102, 463-468.
- Meeran, S.M., Katiyar, S.K., 2007. Grape seed proanthocyanidins promote apoptosis in human epidermoid carcinoma A431 cells through alterations in Cdk1-Cdk-cyclin cascade, and caspase-3 activation via loss of mitochondrial membrane potential. *Exp. Dermatol.* 16, 405-415.
- Meeran, S.M., Katiyar, S.K., 2008. Cell cycle control as a basis for cancer chemoprevention through dietary agents. *Frontiers in bioscience: a journal and virtual library* 13, 2191.
- Mehta, R., Lansky, E., 2004. Breast cancer chemopreventive properties of pomegranate (*Punica granatum*) fruit extracts in a mouse mammary organ culture. *European journal of cancer prevention* 13, 345-348.
- Meirow, D., Nugent, D., 2001. The effects of radiotherapy and chemotherapy on female reproduction. *Hum. Reprod. Update* 7, 535-543.

- Mertens-Talcott, S.U., Percival, S.S., 2005. Ellagic acid and quercetin interact synergistically with resveratrol in the induction of apoptosis and cause transient cell cycle arrest in human leukemia cells. *Cancer Lett.* 218, 141-151.
- Mertens-Talcott, S.U., Talcott, S.T., Percival, S.S., 2003. Low Concentrations of Quercetin and Ellagic Acid Synergistically Influence Proliferation, Cytotoxicity and Apoptosis in MOLT-4 Human Leukemia Cells-. *J. Nutr.* 133, 2669-2674.
- Minowada, J., Ohnuma, T., Moore, G., 1972. Rosette-forming human lymphoid cell lines. I. Establishment and evidence for origin of thymus-derived lymphocytes. *J. Natl. Cancer Inst.* 49, 891-895.
- Mirdehghan, S.H., Rahemi, M., 2007. Seasonal changes of mineral nutrients and phenolics in pomegranate (*Punica granatum L.*) fruit. *Scientia horticulturae* 111, 120-127.
- Miura, T., Mattson, M.P., Rao, M.S., 2004. Cellular lifespan and senescence signaling in embryonic stem cells. *Aging cell* 3, 333-343.
- Miyoshi, N., Nakamura, Y., Ueda, Y., Abe, M., Ozawa, Y., Uchida, K., Osawa, T., 2003. Dietary ginger constituents, galanals A and B, are potent apoptosis inducers in Human T lymphoma Jurkat cells. *Cancer Lett.* 199, 113-119.
- Mohan, A., Narayanan, S., Sethuraman, S., Maheswari Krishnan, U., 2013. Combinations of Plant Polyphenols Anti-Cancer Molecules: A Novel Treatment Strategy for Cancer Chemotherapy. *Anti-Cancer Agents in Medicinal Chemistry-Anti-Cancer Agents* 13, 281-295.
- Mohan, K., Gunasekaran, P., Varalakshmi, E., Hara, Y., Nagini, S., 2007. *In vitro* evaluation of the anticancer effect of lactoferrin and tea polyphenol combination on oral carcinoma cells. *Cell Biol. Int.* 31, 599-608.
- Mousavinejad, G., Emam-Djomeh, Z., Rezaei, K., Khodaparast, M.H.H., 2009. Identification and quantification of phenolic compounds and their effects on antioxidant activity in pomegranate juices of eight Iranian cultivars. *Food Chem.* 115, 1274-1278.
- Mu, C., Jia, P., Yan, Z., Liu, X., Li, X., Liu, H., 2007. Quercetin induces cell cycle G1 arrest through elevating Cdk inhibitors p21 and p27 in human hepatoma cell line (HepG2). *Methods Find. Exp. Clin. Pharmacol.* 29, 179-184.
- Mullighan, C.G., Goorha, S., Radtke, I., Miller, C.B., Coustan-Smith, E., Dalton, J.D., Girtman, K., Mathew, S., Ma, J., Pounds, S.B., 2007. Genome-wide analysis of genetic alterations in acute lymphoblastic leukaemia. *Nature* 446, 758-764.
- Nagata, S., 1997. Apoptosis by Death Factor Review. *Cell* 88, 392.
- Nair, H.K., Rao, K.V., Aalinkeel, R., Mahajan, S., Chawda, R., Schwartz, S.A., 2004. Inhibition of prostate cancer cell colony formation by the flavonoid quercetin correlates with modulation of specific regulatory genes. *Clin. Diagn. Lab. Immunol.* 11, 63-69.
- Nakagawa, H., Hasumi, K., Woo, J., Nagai, K., Wachi, M., 2004. Generation of hydrogen peroxide primarily contributes to the induction of Fe (II)-dependent apoptosis in Jurkat cells by (-)-epigallocatechin gallate. *Carcinogenesis* 25, 1567-1574.
- Nakazato, T., Ito, K., Ikeda, Y., Kizaki, M., 2005. Green tea component, catechin, induces apoptosis of human malignant B cells via production of reactive oxygen species. *Clinical cancer research* 11, 6040-6049.

- Nakazato, T., Sagawa, M., Yamato, K., Xian, M., Yamamoto, T., Suematsu, M., Ikeda, Y., Kizaki, M., 2007. Myeloperoxidase Is a Key Regulator of Oxidative Stress–Mediated Apoptosis in Myeloid Leukemic Cells. *Clinical Cancer Research* 13, 5436-5445.
- Nam, S., Smith, D.M., Dou, Q.P., 2001. Tannic acid potently inhibits tumor cell proteasome activity, increases p27 and Bax expression, and induces G1 arrest and apoptosis. *Cancer Epidemiology Biomarkers & Prevention* 10, 1083-1088.
- Naqvi, S., Khan, M., Vohora, S., 1991. Anti-bacterial, anti-fungal and anthelmintic investigations on Indian medicinal plants. *Fitoterapia* 62, 221-228.
- Narayanan, B.A., Geoffroy, O., Willingham, M.C., Re, G.G., Nixon, D.W., 1999. p53/p21 (WAF1/CIP1) expression and its possible role in G1 arrest and apoptosis in ellagic acid treated cancer cells. *Cancer Lett.* 136, 215-221.
- Neame, P.B., Soamboonsrup, P., Browman, G.P., Meyer, R.M., Bengler, A., Wilson, W., Walker, I.R., Saeed, N., McBride, J.A., 1986. Classifying acute leukemia by immunophenotyping: a combined FAB-immunologic classification of AML. *Blood* 68, 1355-1362.
- Neuhouser, M.L., 2004. Review: Dietary flavonoids and cancer risk: Evidence from human population studies. *Nutr. Cancer* 50, 1-7.
- Neurath, A.R., Strick, N., Li, Y., Debnath, A.K., 2004. Punica granatum (Pomegranate) juice provides an HIV-1 entry inhibitor and candidate topical microbicide. *BMC infectious diseases* 4, 41.
- Nguyen, T., Tran, E., Nguyen, T., Do, P., Huynh, T., Huynh, H., 2004. The role of activated MEK-ERK pathway in quercetin-induced growth inhibition and apoptosis in A549 lung cancer cells. *Carcinogenesis* 25, 647-659.
- Nguyen, V., Tang, J., Oroudjev, E., Lee, C.J., Marasigan, C., Wilson, L., Ayoub, G., 2010. Cytotoxic effects of bilberry extract on MCF7-GFP-tubulin breast cancer cells. *Journal of Medicinal Food* 13, 278-285.
- Nicholson, D.W., Ali, A., Thornberry, N.A., Vaillancourt, J.P., Ding, C.K., Gallant, M., Gareau, Y., Griffin, P.R., Labelle, M., Lazebnik, Y.A., 1995. Identification and inhibition of the ICE/CED-3 protease necessary for mammalian apoptosis.
- Nie, G., Cao, Y., Zhao, B., 2002. Protective effects of green tea polyphenols and their major component, (–)-epigallocatechin-3-gallate (EGCG), on 6-hydroxydopamine-induced apoptosis in PC12 cells. *Redox report* 7, 171-177.
- Nielsen, L., Papoutsakis, E., Miller, W., 1998. Modeling ex vivo hematopoiesis using chemical engineering metaphors. *Chemical engineering science* 53, 1913-1925.
- Norbury, C.J., Hickson, I.D., 2001. Cellular responses to DNA damage. *Annu. Rev. Pharmacol. Toxicol.* 41, 367-401.
- Nucifora, G., Rowley, J., 1995. AML1 and the 8; 21 and 3; 21 translocations in acute and chronic myeloid leukemia. *Blood* 86, 1-14.
- Nunez, R., 2001. DNA measurement and cell cycle analysis by flow cytometry. *Curr. Issues Mol. Biol.* 3, 67-70.
- O'Brien, S., Moore, J.O., Boyd, T.E., Larratt, L.M., Skotnicki, A., Koziner, B., Chanan-Khan, A.A., Seymour, J.F., Bociek, R.G., Pavletic, S., 2007. Randomized phase III trial of fludarabine plus cyclophosphamide with or without oblimersen sodium (Bcl-2 antisense) in patients with relapsed or refractory chronic lymphocytic leukemia. *Journal of clinical oncology* 25, 1114-1120.

- Okabe, S., Suganuma, M., Hayashi, M., Sueoka, E., Komori, A., Fujiki, H., 1997. Mechanisms of Growth Inhibition of Human Lung Cancer Cell Line, PC-9, by Tea Polyphenols. *Cancer Science* 88, 639-643.
- Olsson, M.E., Gustavsson, K., Andersson, S., Nilsson, Å., Duan, R., 2004. Inhibition of cancer cell proliferation *in vitro* by fruit and berry extracts and correlations with antioxidant levels. *J. Agric. Food Chem.* 52, 7264-7271.
- Oltersdorf, T., Elmore, S.W., Shoemaker, A.R., Armstrong, R.C., Augeri, D.J., Belli, B.A., Bruncko, M., Deckwerth, T.L., Dinges, J., Hajduk, P.J., 2005. An inhibitor of Bcl-2 family proteins induces regression of solid tumours. *Nature* 435, 677-681.
- Ou, T., Wang, C., Lee, Y., Wu, C., Lee, H., 2010. Gallic acid induces G2/M phase cell cycle arrest via regulating 14-3-3 β release from Cdc25C and Chk2 activation in human bladder transitional carcinoma cells. *Molecular nutrition & food research* 54, 1781-1790.
- Oudard, S., Carpentier, A., Banu, E., Fauchon, F., Celerier, D., Poupon, M.F., Dutrillaux, B., Andrieu, J.M., Delattre, J.Y., 2003. Phase II study of lonidamine and diazepam in the treatment of recurrent glioblastoma multiforme. *J. Neurooncol.* 63, 81-86.
- Owen, R.G., Treon, S.P., Al-Katib, A., Fonseca, R., Greipp, P.R., McMaster, M.L., Morra, E., Pangalis, G.A., Miguel, J.F.S., Branagan, A.R., 2003. Clinicopathological definition of Waldenstrom's macroglobulinemia: consensus panel recommendations from the Second International Workshop on Waldenstrom's Macroglobulinemia. 30, 110-115.
- Ozben, T., 2006. Mechanisms and strategies to overcome multiple drug resistance in cancer. *FEBS Lett.* 580, 2903-2909.
- Pacheco-Palencia, L.A., Noratto, G., Hingorani, L., Talcott, S.T., Mertens-Talcott, S.U., 2008. Protective effects of standardized pomegranate (*Punica granatum* L.) polyphenolic extract in ultraviolet-irradiated human skin fibroblasts. *J. Agric. Food Chem.* 56, 8434-8441.
- Pantuck, A.J., Leppert, J.T., Zomorodian, N., Aronson, W., Hong, J., Barnard, R.J., Seeram, N., Liker, H., Wang, H., Elashoff, R., 2006. Phase II study of pomegranate juice for men with rising prostate-specific antigen following surgery or radiation for prostate cancer. *Clinical Cancer Research* 12, 4018-4026.
- Paschka, A.G., Butler, R., Young, C.Y., 1998. Induction of apoptosis in prostate cancer cell lines by the green tea component,(-)-epigallocatechin-3-gallate. *Cancer Lett.* 130, 1-7.
- Passegué, E., Jamieson, C.H.M., Ailles, L.E., Weissman, I.L., 2003. Normal and leukemic hematopoiesis: are leukemias a stem cell disorder or a reacquisition of stem cell characteristics? *Proc. Natl. Acad. Sci. U. S. A.* 100, 11842-11849.
- Pavia, M., Pileggi, C., Nobile, C.G.A., Angelillo, I.F., 2006. Association between fruit and vegetable consumption and oral cancer: a meta-analysis of observational studies. *Am. J. Clin. Nutr.* 83, 1126-1134.
- Pham, N.A., Jacobberger, J.W., Schimmer, A.D., Cao, P., Gronda, M., Hedley, D.W., 2004. The dietary isothiocyanate sulforaphane targets pathways of apoptosis, cell cycle arrest, and oxidative stress in human pancreatic cancer cells and inhibits tumor growth in severe combined immunodeficient mice. *Molecular cancer therapeutics* 3, 1239-1248.
- Pietras, K., Östman, A., 2010. Hallmarks of cancer: interactions with the tumor stroma. *Exp. Cell Res.* 316, 1324-1331.

- Pineiro, R., Iglesias, M., Gualillo, O., Kelly, P., Dieguez, C., Lago, F., 2004. GH prevents apoptosis in cardiomyocytes cultured *in vitro* through a calcineurin-dependent mechanism. *J. Endocrinol.* 180, 325-335.
- Pisha, E., Pezzuto, J., 1994. Fruits and vegetables containing compounds that demonstrate pharmacological activity in humans. *Economic and Medicinal Plant Research* 6, 189-189.
- Poyrazoğlu, E., Gökmen, V., Artık, N., 2002. Organic Acids and Phenolic Compounds in Pomegranates (*Punica granatum* L.) Grown in Turkey. *Journal of Food Composition and Analysis* 15, 567-575.
- Pozo-Guisado, E., Merino, J.M., Mulero-Navarro, S., Lorenzo-Benayas, M.J., Centeno, F., Alvarez-Barrientos, A., Salguero, P.M.F., 2005. Resveratrol-induced apoptosis in MCF-7 human breast cancer cells involves a caspase-independent mechanism with downregulation of Bcl-2 and NF- κ B. *International journal of cancer* 115, 74-84.
- Puente, X.S., Pinyol, M., Quesada, V., Conde, L., Ordóñez, G.R., Villamor, N., Escaramis, G., Jares, P., Beà, S., González-Díaz, M., 2011. Whole-genome sequencing identifies recurrent mutations in chronic lymphocytic leukaemia. *Nature* 475, 101-105.
- Qanungo, S., Das, M., Haldar, S., Basu, A., 2005. Epigallocatechin-3-gallate induces mitochondrial membrane depolarization and caspase-dependent apoptosis in pancreatic cancer cells. *Carcinogenesis* 26, 958-967.
- Qian, Y., Luckey, C., Horton, L., Esser, M., Templeton, D., 1992. Biological function of the retinoblastoma protein requires distinct domains for hyperphosphorylation and transcription factor binding. *Mol. Cell. Biol.* 12, 5363-5372.
- Ralstin, M.C., Gage, E.A., Yip-Schneider, M.T., Klein, P.J., Wiebke, E.A., Schmidt, C.M., 2006. Parthenolide cooperates with NS398 to inhibit growth of human hepatocellular carcinoma cells through effects on apoptosis and G0-G1 cell cycle arrest. *Molecular cancer research* 4, 387-399.
- Redd, W.H., Montgomery, G.H., DuHamel, K.N., 2001. Behavioral intervention for cancer treatment side effects. *J. Natl. Cancer Inst.* 93, 810-823.
- Reddy, M.K., Alexander-Lindo, R.L., Nair, M.G., 2005. Relative inhibition of lipid peroxidation, cyclooxygenase enzymes, and human tumor cell proliferation by natural food colors. *J. Agric. Food Chem.* 53, 9268-9273.
- Reed, J.D., Krueger, C.G., Vestling, M.M., 2005. MALDI-TOF mass spectrometry of oligomeric food polyphenols. *Phytochemistry* 66, 2248-2263.
- Ren, Y., Savill, J., 1998. Apoptosis: the importance of being eaten. *Cell Death Differ.* 5, 563.
- Renaud, S., de Lorgeril, M., 1992. Wine, alcohol, platelets, and the French paradox for coronary heart disease. *The Lancet* 339, 1523-1526.
- Renis, M., Calandra, L., Scifo, C., Tomasello, B., Cardile, V., Vanella, L., Bei, R., Fauci, L.L., Galvano, F., 2008. Response of cell cycle/stress-related protein expression and DNA damage upon treatment of CaCo2 cells with anthocyanins. *Br. J. Nutr.* 100, 27-35.
- Rettig, M.B., Heber, D., An, J., Seeram, N.P., Rao, J.Y., Liu, H., Klatte, T., Belldegrun, A., Moro, A., Henning, S.M., 2008. Pomegranate extract inhibits androgen-independent prostate cancer growth through a nuclear factor- κ B-dependent mechanism. *Molecular cancer therapeutics* 7, 2662-2671.
- Reuter, S., Eifes, S., Dicato, M., Aggarwal, B.B., Diederich, M., 2008. Modulation of anti-apoptotic and survival pathways by curcumin as a strategy to induce apoptosis in cancer cells. *Biochem. Pharmacol.* 76, 1340-1351.

- Rice-Evans, C.A., Miller, N.J., Paganga, G., 1996. Structure-antioxidant activity relationships of flavonoids and phenolic acids. *Free radical biology and medicine* 20, 933-956.
- Richter, M., Ebermann, R., Marian, B., 1999. Quercetin-induced apoptosis in colorectal tumor cells: possible role of EGF receptor signaling. *Nutr. Cancer* 34, 88-99.
- Robaszkiewicz, A., Balcerczyk, A., Bartosz, G., 2007. Antioxidative and prooxidative effects of quercetin on A549 cells. *Cell Biol. Int.* 31, 1245-1250.
- Rodrigo, K.A., Rawal, Y., Renner, R.J., Schwartz, S.J., Tian, Q., Larsen, P.E., Mallery, S.R., 2006. Suppression of the tumorigenic phenotype in human oral squamous cell carcinoma cells by an ethanol extract derived from freeze-dried black raspberries. *Nutr. Cancer* 54, 58-68.
- Rodriguez, M., Schaper, J., 2005. Apoptosis: measurement and technical issues. *J. Mol. Cell. Cardiol.* 38, 15-20.
- Rosenblat, M., Aviram, M., 2006. Antioxidative properties of pomegranate: *In vitro* studies. *Pomegranates: Ancient Roots to Modern Medicine*. New York, NY: Taylor and Francis Group, 31-43.
- Rossi, G., Pelizzari, A., Bellotti, D., Tonelli, M., Barlati, S., 2000. Cytogenetic analogy between myelodysplastic syndrome and acute myeloid leukemia of elderly patients. *Leukemia: official journal of the Leukemia Society of America, Leukemia Research Fund, UK* 14, 636.
- Roy, A.M., Baliga, M.S., Katiyar, S.K., 2005. Epigallocatechin-3-gallate induces apoptosis in estrogen receptor-negative human breast carcinoma cells via modulation in protein expression of p53 and Bax and caspase-3 activation. *Molecular cancer therapeutics* 4, 81-90.
- Saelens, X., Festjens, N., Walle, L.V., Van Gurp, M., Van Loo, G., Vandenabeele, P., 2004. Toxic proteins released from mitochondria in cell death. *Oncogene* 23, 2861-2874.
- Salucci, M., Stivala, L., Maiani, G., Bugianesi, R., Vannini, V., 2002. Flavonoids uptake and their effect on cell cycle of human colon adenocarcinoma cells (Caco2). *Br. J. Cancer* 86, 1645-1651.
- Sánchez, A.M., Malagarie-Cazenave, S., Olea, N., Vara, D., Chiloeches, A., Díaz-Laviada, I., 2007. Apoptosis induced by capsaicin in prostate PC-3 cells involves ceramide accumulation, neutral sphingomyelinase, and JNK activation. *Apoptosis* 12, 2013-2024.
- Saraste, A., Pulkki, K., 2000. Morphologic and biochemical hallmarks of apoptosis. *Cardiovasc. Res.* 45, 528-537.
- Sartippour, M.R., Seeram, N.P., Rao, J.Y., Moro, A., Harris, D.M., Henning, S.M., Firouzi, A., Rettig, M.B., Aronson, W.J., Pantuck, A.J., 2008. Ellagitannin-rich pomegranate extract inhibits angiogenesis in prostate cancer *in vitro* and *in vivo*. *Int. J. Oncol.* 32, 475-480.
- Saruwatari, A., Okamura, S., Nakajima, Y., Narukawa, Y., Takeda, T., Tamura, H., 2008. Pomegranate juice inhibits sulfoconjugation in Caco-2 human colon carcinoma cells. *Journal of medicinal food* 11, 623-628.
- Satomi, Y., Nishino, H., Shibata, S., 2005. Glycyrrhetic acid and related compounds induce G1 arrest and apoptosis in human hepatocellular carcinoma HepG2. *Anticancer Res.* 25, 4043-4047.
- Satué-Gracia, M.T., Heinonen, M., Frankel, E.N., 1997. Anthocyanins as antioxidants on human low-density lipoprotein and lecithin-liposome systems. *J. Agric. Food Chem.* 45, 3362-3367.
- Schlachterman, A., Valle, F., Wall, K.M., Azios, N.G., Castillo, L., Morell, L., Washington, A.V., Cubano, L.A., Dharmawardhane, S.F., 2008. Combined resveratrol, quercetin, and catechin treatment reduces breast tumor growth in a nude mouse model. *Translational oncology* 1, 19.

- Schneider, U., Schwenk, H., Bornkamm, G., 1977. Characterization of EBV-genome negative "null" and "T" cell lines derived from children with acute lymphoblastic leukemia and leukemic transformed non-Hodgkin lymphoma. *International journal of cancer* 19, 621-626.
- Schwartz, G.K., Shah, M.A., 2005. Targeting the cell cycle: a new approach to cancer therapy. *Journal of Clinical Oncology* 23, 9408-9421.
- Seeram, N.P., Adams, L., Henning, S.M., Niu, Y., Zhang, Y., Nair, M.G., Heber, D., 2005. *In vitro* antiproliferative, apoptotic and antioxidant activities of punicalagin, ellagic acid and a total pomegranate tannin extract are enhanced in combination with other polyphenols as found in pomegranate juice.
- Seeram, N.P., Adams, L.S., Zhang, Y., Lee, R., Sand, D., Scheuller, H.S., Heber, D., 2006. Blackberry, black raspberry, blueberry, cranberry, red raspberry, and strawberry extracts inhibit growth and stimulate apoptosis of human cancer cells *in vitro*. *J. Agric. Food Chem.* 54, 9329-9339.
- Seeram, N.P., Aronson, W.J., Zhang, Y., Henning, S.M., Moro, A., Lee, R., Sartippour, M., Harris, D.M., Rettig, M., Suchard, M.A., 2007. Pomegranate ellagitannin-derived metabolites inhibit prostate cancer growth and localize to the mouse prostate gland. *J. of Agricultural and Food Chemistry* 55, 7732-7737.
- Seeram, N.P., Aviram, M., Zhang, Y., Henning, S.M., Feng, L., Dreher, M., Heber, D., 2008. Comparison of antioxidant potency of commonly consumed polyphenol-rich beverages in the United States. *J. Agric. Food Chem.* 56, 1415-1422.
- Senthilkumar, K., Elumalai, P., Arunkumar, R., Banudevi, S., Gunadharini, N.D., Sharmila, G., Selvakumar, K., Arunakaran, J., 2010. Quercetin regulates insulin like growth factor signaling and induces intrinsic and extrinsic pathway mediated apoptosis in androgen independent prostate cancer cells (PC-3). *Mol. Cell. Biochem.* 344, 173-184.
- Seppi, A., Franciosi, A., 1980. Chemical composition of pomegranate juice (*punica granatum*): amino acid content. *Rivista della Societa Italiana di Scienza dell'Alimentazione* 9.
- Serafino, A., Sinibaldi-Vallebona, P., Lazzarino, G., Tavazzi, B., Rasi, G., Pierimarchi, P., Andreola, F., Moroni, G., Galvano, G., Galvano, F., 2004. Differentiation of human melanoma cells induced by cyanidin-3-O- β -glucopyranoside. *The FASEB journal* 18, 1940-1942.
- Shariat, S.F., Desai, S., Song, W., Khan, T., Zhao, J., Nguyen, C., Foster, B.A., Greenberg, N., Spencer, D.M., Slawin, K.M., 2001. Adenovirus-mediated Transfer of Inducible Caspases A Novel "Death Switch" Gene Therapeutic Approach to Prostate Cancer. *Cancer Res.* 61, 2562-2571.
- Sherr, C.J., McCormick, F., 2002. The RB and p53 pathways in cancer. *Cancer cell* 2, 103-112.
- Shih, P., Yeh, C., Yen, G., 2005. Effects of anthocyanidin on the inhibition of proliferation and induction of apoptosis in human gastric adenocarcinoma cells. *Food and chemical toxicology* 43, 1557-1566.
- Shim, E.Y., Walker, A.K., Shi, Y., Blackwell, T.K., 2002. CDK-9/cyclin T (P-TEFb) is required in two postinitiation pathways for transcription in the *C. elegans* embryo. *Genes Dev.* 16, 2135-2146.
- Shin, D.Y., Ryu, C.H., Lee, W.S., Kim, D.C., Kim, S.H., Hah, Y., Lee, S.J., Shin, S.C., Kang, H.S., Choi, Y.H., 2009. Induction of apoptosis and inhibition of invasion in human hepatoma cells by anthocyanins from meoru. *Ann. N. Y. Acad. Sci.* 1171, 137-148.
- Shukla, S., Gupta, S., 2008. Apigenin-induced prostate cancer cell death is initiated by reactive oxygen species and p53 activation. *Free Radical Biology and Medicine* 44, 1833-1845.

- Siegel, R., Naishadham, D., Jemal, A., 2012. Cancer statistics, 2012. *CA: a cancer journal for clinicians* 62, 10-29.
- Singh, M., Arseneault, M., Sanderson, T., Murthy, V., Ramassamy, C., 2008. Challenges for research on polyphenols from foods in Alzheimer's disease: bioavailability, metabolism, and cellular and molecular mechanisms. *J. Agric. Food Chem.* 56, 4855-4873.
- Singleton, K.W., Jung, K., Giusti, M., 2007. Anthocyanin-rich grape extract blocks breast cell DNA damage. *Journal of medicinal food* 10, 244-251.
- Singleton, V.L., Orthofer, R., Lamuela-Raventos, R.M., 1999. [14] Analysis of total phenols and other oxidation substrates and antioxidants by means of folin-ciocalteu reagent. *Meth. Enzymol.* 299, 152-178.
- Skubitz, K.M., Pessano, S., Bottero, L., Ferrero, D., Rovera, G., August, J., 1983. Human granulocyte surface molecules identified by murine monoclonal antibodies. *The Journal of Immunology* 131, 1882-1888.
- Srivastava, A., Akoh, C.C., Fischer, J., Krewer, G., 2007. Effect of anthocyanin fractions from selected cultivars of Georgia-grown blueberries on apoptosis and phase II enzymes. *J. Agric. Food Chem.* 55, 3180-3185.
- Stevaux, O., Dyson, N.J., 2002. A revised picture of the E2F transcriptional network and RB function. *Curr. Opin. Cell Biol.* 14, 684-691.
- Stoner, G.D., Wang, L., Zikri, N., Chen, T., Hecht, S.S., Huang, C., Sardo, C., Lechner, J.F., 2007. Cancer prevention with freeze-dried berries and berry components. 17, 403-410.
- Sun, J., Hai Liu, R., 2006. Cranberry phytochemical extracts induce cell cycle arrest and apoptosis in human MCF-7 breast cancer cells. *Cancer Lett.* 241, 124-134.
- Suzuki, Y., Nakabayashi, Y., Takahashi, R., 2001. Ubiquitin-protein ligase activity of X-linked inhibitor of apoptosis protein promotes proteasomal degradation of caspase-3 and enhances its anti-apoptotic effect in Fas-induced cell death. *Proceedings of the National Academy of Sciences* 98, 8662-8667.
- Syed, D.N., Malik, A., Hadi, N., Sarfaraz, S., Afaq, F., Mukhtar, H., 2007. Photochemopreventive Effect of Pomegranate Fruit Extract on UVA-mediated Activation of Cellular Pathways in Normal Human Epidermal Keratinocytes. *Photochem. Photobiol.* 82, 398-405.
- Takasawa, R., Tanuma, S., 2003. Sustained release of Smac/DIABLO from mitochondria commits to undergo UVB-induced apoptosis. *Apoptosis* 8, 291-299.
- Tang, J.L., Yeh, S.H., Chen, P.J., Lin, M.T., Tien, H.F., Chen, Y.C., 1992. Inactivation of the retinoblastoma gene in acute myelogenous leukaemia. *Br. J. Haematol.* 82, 502-507.
- Tang, L., Jin, T., Zeng, X., Wang, J., 2005. Lycopene inhibits the growth of human androgen-independent prostate cancer cells *in vitro* and in BALB/c nude mice. *J. Nutr.* 135, 287-290.
- Tang, Y., Parmakhtiar, B., Simoneau, A.R., Xie, J., Fruehauf, J., Lilly, M., Zi, X., 2011. Lycopene enhances docetaxel's effect in castration-resistant prostate cancer associated with insulin-like growth factor I receptor levels. *Neoplasia (New York, NY)* 13, 108.
- Tang, Y., Zhao, D.Y., Elliott, S., Zhao, W., Curiel, T.J., Beckman, B.S., Burow, M.E., 2007. Epigallocatechin-3 gallate induces growth inhibition and apoptosis in human breast cancer cells through survivin suppression. *Int. J. Oncol.* 31, 705.

- Terret, C., Zanetta, S., Roche, H., Schellens, J., Faber, M., Wanders, J., Ravic, M., Droz, J., 2003. Phase I clinical and pharmacokinetic study of E7070, a novel sulfonamide given as a 5-day continuous infusion repeated every 3 weeks in patients with solid tumours. A study by the EORTC Early Clinical Study Group (ECSG). *Eur. J. Cancer* 39, 1097-1104.
- Tezcan, F., Gültekin-Özğüven, M., Diken, T., Özçelik, B., Erim, F.B., 2009. Antioxidant activity and total phenolic, organic acid and sugar content in commercial pomegranate juices. *Food Chem.* 115, 873-877.
- Thangapazham, R.L., Passi, N., Maheshwari, R.K., 2007. Green tea polyphenol and epigallocatechin gallate induce apoptosis and inhibit invasion in human breast cancer cells. *Cancer biology & therapy* 6, 1938-1943.
- Thoennissen, N., O'Kelly, J., Lu, D., Iwanski, G., La, D., Abbassi, S., Leiter, A., Karlan, B., Mehta, R., Koeffler, H., 2009. Capsaicin causes cell-cycle arrest and apoptosis in ER-positive and-negative breast cancer cells by modulating the EGFR/HER-2 pathway. *Oncogene* 29, 285-296.
- Toi, M., Bando, H., Ramachandran, C., Melnick, S.J., Imai, A., Fife, R.S., Carr, R.E., Oikawa, T., Lansky, E.P., 2003. Preliminary studies on the anti-angiogenic potential of pomegranate fractions *in vitro* and *in vivo*. *Angiogenesis* 6, 121-128.
- Tran, H.N.A., Bae, S., Song, B., Lee, B., Bae, Y., Kim, Y., Lansky, E.P., Newman, R.A., 2010. Pomegranate (*punica granatum*) seed linolenic acid isomers: concentration-dependent modulation of estrogen receptor activity. *Endocr. Res.* 35, 1-16.
- Tsuchiya, S., Yamabe, M., Yamaguchi, Y., Kobayashi, Y., Konno, T., Tada, K., 1980. Establishment and characterization of a human acute monocytic leukemia cell line (THP-1). *International journal of cancer* 26, 171-176.
- Tsuda, T., Watanabe, M., Ohshima, K., Norinobu, S., Choi, S., Kawakishi, S., Osawa, T., 1994. Antioxidative activity of the anthocyanin pigments cyanidin 3-O- β -D-glucoside and cyanidin. *J. Agric. Food Chem.* 42, 2407-2410.
- Türk, G., Sönmez, M., Çeribaslı, A.O., Yüce, A., Atessahin, A., 2010. Attenuation of cyclosporine A-induced testicular and spermatozoal damages associated with oxidative stress by ellagic acid. *Int. Immunopharmacol.* 10, 177-182.
- Valko, M., Leibfritz, D., Moncol, J., Cronin, M.T., Mazur, M., Telser, J., 2007. Free radicals and antioxidants in normal physiological functions and human disease. *Int. J. Biochem. Cell Biol.* 39, 44-84.
- Van Den Heuvel, S., 2005. Cell-cycle regulation.
- Van Der Eb, Marjolijn M, Pietersen, A.M., Speetjens, F.M., Kuppen, P.J., van de Velde, Cornelis JH, Noteborn, M.H., Hoeben, R.C., 2002. Gene therapy with apoptin induces regression of xenografted human hepatomas. *Cancer Gene Ther.* 9, 53-61.
- Van Engeland, M., Nieland, L.J., Ramaekers, F.C., Schutte, B., Reutelingsperger, C.P., 1998. Annexin V-affinity assay: a review on an apoptosis detection system based on phosphatidylserine exposure. *Cytometry* 31, 1-9.
- Van Erk, M.J., Roepman, P., van der Lende, Ted R, Stierum, R.H., Aarts, J., van Bladeren, P.J., van Ommen, B., 2005. Integrated assessment by multiple gene expression analysis of quercetin bioactivity on anticancer-related mechanisms in colon cancer cells *in vitro*. *Eur. J. Nutr.* 44, 143-156.

- Van Loo, G., Van Gurp, M., Depuydt, B., Srinivasula, S., Rodriguez, I., Alnemri, E., Gevaert, K., Vandekerckhove, J., Declercq, W., Vandenabeele, P., 2002. The serine protease Omi/HtrA2 is released from mitochondria during apoptosis. Omi interacts with caspase-inhibitor XIAP and induces enhanced caspase activity. *Cell Death Differ.* 9, 20.
- Vander Heiden, M.G., Cantley, L.C., Thompson, C.B., 2009. Understanding the Warburg effect: the metabolic requirements of cell proliferation. *Science Signaling* 324, 1029.
- Vardiman, J.W., 2010. The World Health Organization (WHO) classification of tumors of the hematopoietic and lymphoid tissues: an overview with emphasis on the myeloid neoplasms. *Chem. Biol. Interact.* 184, 16-20.
- Vardiman, J.W., Thiele, J., Arber, D.A., Brunning, R.D., Borowitz, M.J., Porwit, A., Harris, N.L., Le Beau, M.M., Hellström-Lindberg, E., Tefferi, A., 2009. The 2008 revision of the World Health Organization (WHO) classification of myeloid neoplasms and acute leukemia: rationale and important changes. *Blood* 114, 937-951.
- Vaskivuo, T., 2002. Regulation of apoptosis in the female reproductive system. *Apoptosis* 2, 1.
- Veluri, R., Singh, R.P., Liu, Z., Thompson, J.A., Agarwal, R., Agarwal, C., 2006. Fractionation of grape seed extract and identification of gallic acid as one of the major active constituents causing growth inhibition and apoptotic death of DU145 human prostate carcinoma cells. *Carcinogenesis* 27, 1445-1453.
- Verma, S., Singh, A., Mishra, A., 2013. Gallic acid: Molecular rival of cancer. *Environ. Toxicol. Pharmacol.* .
- Vermes, I., Haanen, C., Steffens-Nakken, H., Reutellingsperger, C., 1995. A novel assay for apoptosis flow cytometric detection of phosphatidylserine expression on early apoptotic cells using fluorescein labelled annexin V. *J. Immunol. Methods* 184, 39-51.
- Vermeulen, K., Bockstaele, D.R., Berneman, Z.N., 2005. Apoptosis: mechanisms and relevance in cancer. *Ann. Hematol.* 84, 627-639.
- Vermeulen, K., Van Bockstaele, D.R., Berneman, Z.N., 2003. The cell cycle: a review of regulation, deregulation and therapeutic targets in cancer. *Cell Prolif.* 36, 131-149.
- Vicinanza, R., Zhang, Y., Henning, S.M., Heber, D., 2013. Pomegranate Juice Metabolites, Ellagic Acid and Urolithin A, Synergistically Inhibit Androgen-Independent Prostate Cancer Cell Growth via Distinct Effects on Cell Cycle Control and Apoptosis. *Evidence-Based Complementary and Alternative Medicine* 2013.
- Vijayababu, M., Kanagaraj, P., Arunkumar, A., Ilangovan, R., Aruldhas, M., Arunakaran, J., 2005. Quercetin-induced growth inhibition and cell death in prostatic carcinoma cells (PC-3) are associated with increase in p21 and hypophosphorylated retinoblastoma proteins expression. *J. Cancer Res. Clin. Oncol.* 131, 765-771.
- Vijayababu, M.R., Arunkumar, A., Kanagaraj, P., Arunakaran, J., 2006. Effects of quercetin on insulin-like growth factors (IGFs) and their binding protein-3 (IGFBP-3) secretion and induction of apoptosis in human prostate cancer cells. *Journal of carcinogenesis* 5, 10.
- Viladomiu, M., Hontecillas, R., Lu, P., Bassaganya-Riera, J., 2013. Preventive and Prophylactic Mechanisms of Action of Pomegranate Bioactive Constituents. *Evidence-Based Complementary and Alternative Medicine* 2013.

- Viuda-Martos, M., Fernández-López, J., Pérez-Álvarez, J., 2010. Pomegranate and its many functional components as related to human health: A Review. *Comprehensive Reviews in Food Science and Food Safety* 9, 635-654.
- Vos, S.D., Miller, C.W., Takeuchi, S., Gombart, A.F., Cho, S.K., Koeffler, H.P., 2006. Alterations of CDKN2 (p16) in non-small cell lung cancer. *Genes, Chromosomes and Cancer* 14, 164-170.
- Waheed, S., Siddique, N., Rahman, A., Zaidi, J., Ahmad, S., 2004. INAA for dietary assessment of essential and other trace elements in fourteen fruits harvested and consumed in Pakistan. *J. Radioanal. Nucl.* 260, 523-531.
- Walch, J., Tettenborn, B., Weber, J., Hundsberger, T., 2013. Radiation-Induced Cavernoma after Total Body Irradiation and Haematopoietic Stem Cell Transplantation in an Adult Patient Suffering from Acute Myeloid Leukaemia. *Case reports in neurology* 5, 91-97.
- Wang, C., Youle, R.J., 2009. The role of mitochondria in apoptosis*. *Annu. Rev. Genet.* 43, 95-118.
- Wang, J., Mazza, G., 2002. Inhibitory effects of anthocyanins and other phenolic compounds on nitric oxide production in LPS/IFN- γ -activated RAW 264.7 macrophages. *J. Agric. Food Chem.* 50, 850-857.
- Wang, R., Xie, W., Zhang, Z., Xing, D., Ding, Y., Wang, W., Ma, C., Du, L., 2004. Bioactive Compounds from the Seeds of *Punica granatum* (Pomegranate). *J. Nat. Prod.* 67, 2096-2098.
- Wang, W., Heideman, L., Chung, C.S., Pelling, J.C., Koehler, K.J., Birt, D.F., 2000. Cell-Cycle Arrest at G2/M and Growth Inhibition by Apigenin in Human Colon Carcinoma Cell Lines. *Mol. Carcinog.* 28, 102-110.
- Weng, A.P., Ferrando, A.A., Lee, W., Morris IV, J.P., Silverman, L.B., Sanchez-Irizarry, C., Blacklow, S.C., Look, A.T., Aster, J.C., 2004. Activating mutations of NOTCH1 in human T cell acute lymphoblastic leukemia. *Science Signalling* 306, 269.
- Weng, C., Yen, G., 2012. Chemopreventive effects of dietary phytochemicals against cancer invasion and metastasis: Phenolic acids, monophenol, polyphenol, and their derivatives. *Cancer Treat. Rev.* 38, 76-87.
- Wenzel, U., Herzog, A., Kuntz, S., Daniel, H., 2004. Protein expression profiling identifies molecular targets of quercetin as a major dietary flavonoid in human colon cancer cells. *Proteomics* 4, 2160-2174.
- Wikenheiser-Brokamp, K.A., 2006. Retinoblastoma regulatory pathway in lung cancer. *Curr. Mol. Med.* 6, 783.
- Wyllie, A.H., 1980. Cell death: the significance of apoptosis. *Int. Rev. Cytol.* 68, 251.
- Xavier, C.P., Lima, C.F., Preto, A., Seruca, R., Fernandes-Ferreira, M., Pereira-Wilson, C., 2009. Luteolin, quercetin and ursolic acid are potent inhibitors of proliferation and inducers of apoptosis in both KRAS and BRAF mutated human colorectal cancer cells. *Cancer Lett.* 281, 162-170.
- Yagasaki, K., Miura, Y., Okauchi, R., Furuse, T., 2000. Inhibitory effects of chlorogenic acid and its related compounds on the invasion of hepatoma cells in culture. *Cytotechnology* 33, 229-235.
- Yang, G., Liao, J., Kim, K., Yurkow, E.J., Yang, C.S., 1998. Inhibition of growth and induction of apoptosis in human cancer cell lines by tea polyphenols. *Carcinogenesis* 19, 611-616.
- Yang, J.H., Hsia, T.C., Kuo, H.M., Chao, P.D.L., Chou, C.C., Wei, Y.H., Chung, J.G., 2006. Inhibition of lung cancer cell growth by quercetin glucuronides via G2/M arrest and induction of apoptosis. *Drug Metab. Disposition* 34, 296-304.

- Yang, K.M., Pyo, J.O., Kim, G., Yu, R., Han, I.S., Ju, S.A., Kim, W.H., Kim, B., 2009. Capsaicin induces apoptosis by generating reactive oxygen species and disrupting mitochondrial transmembrane potential in human colon cancer cell lines. *Cell. Mol. Biol. Lett.* 14, 497-510.
- Yeh, C., Yen, G., 2005. Induction of apoptosis by the Anthocyanidins through regulation of Bcl-2 gene and activation of c-Jun N-terminal kinase cascade in hepatoma cells. *J. Agric. Food Chem.* 53, 1740-1749.
- Yi (1), W., Fischer, J., Akoh, C.C., 2005. Study of anticancer activities of muscadine grape phenolics *in vitro*. *J. Agric. Food Chem.* 53, 8804-8812.
- Yi (2), W., Fischer, J., Krewer, G., Akoh, C.C., 2005. Phenolic compounds from blueberries can inhibit colon cancer cell proliferation and induce apoptosis. *J. Agric. Food Chem.* 53, 7320-7329.
- Yip, K., Reed, J., 2008. Bcl-2 family proteins and cancer. *Oncogene* 27, 6398-6406.
- Yoshioka, K., Kataoka, T., Hayashi, T., Hasegawa, M., Ishi, Y., Hibasami, H., 2000. Induction of apoptosis by gallic acid in human stomach cancer KATO III and colon adenocarcinoma COLO 205 cell lines. *Oncol. Rep.* 7, 1221-1224.
- You, B.R., Moon, H.J., Han, Y.H., Park, W.H., 2010. Gallic acid inhibits the growth of HeLa cervical cancer cells via apoptosis and/or necrosis. *Food and Chemical Toxicology* 48, 1334-1340.
- You, B.R., Park, W.H., 2010. Gallic acid-induced lung cancer cell death is related to glutathione depletion as well as reactive oxygen species increase. *Toxicology in vitro* 24, 1356-1362.
- Youdim, K., Shukitt-Hale, B., Martin, A., Wang, H., Denisova, N., Bickford, P., Joseph, J., 2000. Short-term dietary supplementation of blueberry polyphenolics: beneficial effects on aging brain performance and peripheral tissue function. *Nutr. Neurosci.* 3, 383-397.
- Youdim, K.A., McDonald, J., Kalt, W., Joseph, J.A., 2002. Potential role of dietary flavonoids in reducing microvascular endothelium vulnerability to oxidative and inflammatory insults. *J. Nutr. Biochem.* 13, 282-288.
- Yun, J., Afaq, F., Khan, N., Mukhtar, H., 2009. Delphinidin, an anthocyanidin in pigmented fruits and vegetables, induces apoptosis and cell cycle arrest in human colon cancer HCT116 cells. *Mol. Carcinog.* 48, 260-270.
- Zaffaroni, N., Daidone, M.G., 2002. Survivin expression and resistance to anticancer treatments: perspectives for new therapeutic interventions. *Drug resistance updates* 5, 65-72.
- Zaid, M.A., Afaq, F., Syed, D.N., Dreher, M., Mukhtar, H., 2007. Inhibition of UVB-mediated Oxidative Stress and Markers of Photoaging in Immortalized HaCaT Keratinocytes by Pomegranate Polyphenol Extract POMx. *Photochem. Photobiol.* 83, 882-888.
- Zangemeister-Wittke, U., Leech, S.H., Olie, R.A., Simões-Wüst, A.P., Gautschi, O., Luedke, G.H., Natt, F., Häner, R., Martin, P., Hall, J., 2000. A novel bispecific antisense oligonucleotide inhibiting both bcl-2 and bcl-xL expression efficiently induces apoptosis in tumor cells. *Clinical cancer research* 6, 2547-2555.
- Zenz, T., Eichhorst, B., Busch, R., Denzel, T., Häbe, S., Winkler, D., Bühler, A., Edelmann, J., Bergmann, M., Hopfinger, G., 2010. TP53 mutation and survival in chronic lymphocytic leukemia. *Journal of Clinical Oncology* 28, 4473-4479.
- Zhang, Q., Zhao, X., Wang, Z., 2009. Cytotoxicity of flavones and flavonols to a human esophageal squamous cell carcinoma cell line (KYSE-510) by induction of G₂/M arrest and apoptosis. *Toxicology in vitro* 23, 797-807.

Zhang, Y., Seeram, N.P., Lee, R., Feng, L., Heber, D., 2008. Isolation and identification of strawberry phenolics with antioxidant and human cancer cell antiproliferative properties. *J. Agric. Food Chem.* 56, 670-675.

Zhao, Z., Zuber, J., Diaz-Flores, E., Lintault, L., Kogan, S.C., Shannon, K., Lowe, S.W., 2010. p53 loss promotes acute myeloid leukemia by enabling aberrant self-renewal. *Genes Dev.* 24, 1389-1402.

Zikri, N.N., Riedl, K.M., Wang, L., Lechner, J., Schwartz, S.J., Stoner, G.D., 2009. Black raspberry components inhibit proliferation, induce apoptosis, and modulate gene expression in rat esophageal epithelial cells. *Nutr. Cancer* 61, 816-826.

Zou, C., Liu, H., Feugang, J.M., Hao, Z., Chow, H.H.S., Garcia, F., 2010. Green tea compound in chemoprevention of cervical cancer. *International journal of gynecological cancer: official journal of the International Gynecological Cancer Society* 20, 617.